Biochemical Engineering and Biotechnology

Ghasem D. Najafpour

BIOCHEMICAL ENGINEERING
AND BIOTECHNOLOGY

This page intentionally left blank

BIOCHEMICAL ENGINEERING AND BIOTECHNOLOGY

GHASEM D. NAJAFPOUR

Professor of Chemical Engineering
Noshirvani Institute of Technology
University of Mazandaran
Babol, Iran

ELSEVIER

Amsterdam · Boston · Heidelberg · London · New York · Oxford
Paris · San Diego · San Francisco · Singapore · Sydney · Tokyo

Elsevier
Radarweg 29, PO Box 211, 1000 AE Amsterdam, The Netherlands
The Boulevard, Langford Lane, Kidlington, Oxford OX5 1GB, UK

First edition 2007

Library of Congress Cataloging-in-Publication Data
A catalog record for this book is available from the Library of Congress

British Library Cataloguing in Publication Data
A catalogue record for this book is available from the British Library

ISBN-13: 978-0-444-52845-2
ISBN-10: 0-444-52845-8

Printed and bound in The Netherlands

07 08 09 10 11 10 9 8 7 6 5 4 3 2 1

Preface

In the new millennium, extensive application of bioprocesses has created an environment for many engineers to expand knowledge of and interest in biotechnology. Microorganisms produce alcohols and acetone, which are used in industrial processes. Knowledge related to industrial microbiology has been revolutionised by the ability of genetically engineered cells to make many new products. Genetic engineering and gene mounting has been developed in the enhancement of industrial fermentation. Finally, application of biochemical engineering in biotechnology has become a new way of making commercial products.

This book demonstrates the application of biological sciences in engineering with theoretical and practical aspects. The seventeen chapters give more understanding of the knowledge related to the specified field, with more practical approaches and related case studies with original research data. It is a book for students to follow the sequential lectures with detailed explanations, and solves the actual problems in the related chapters.

There are many graphs that present actual experimental data, and figures and tables, along with sufficient explanations. It is a good book for those who are interested in more advanced research in the field of biotechnology, and a true guide for beginners to practise and establish advanced research in this field. The book is specifically targeted to serve as a useful text for college and university students; it is mostly recommended for undergraduate courses in one or two semesters. It will also prove very useful for research institutes and postgraduates involved in practical research in biochemical engineering and biotechnology.

This book has suitable biological science applications in biochemical engineering and the knowledge related to those biological processes. The book is unique, with practical approaches in the industrial field. I have tried to prepare a suitable textbook by using a direct approach that should be very useful for students in following the many case studies. It is unique in having solved problems, examples and demonstrations of detailed experiments, with simple design equations and required calculations. Several authors have contributed to enrich the case studies.

During the years of my graduate studies in the USA at the University of Oklahoma and the University of Arkansas, the late Professor Mark Townsend gave me much knowledge and assisted me in my academic achievements. I have also had the opportunity to learn many things from different people, including Professor Starling, Professor C.M. Sliepcevich and Professor S. Ellaison at the University of Oklahoma. Also, it is a privilege to acknowledge Professor J.L. Gaddy and Professor Ed Clausen, who assisted me at the University of Arkansas. I am very thankful for their courage and the guidance they have given me. My vision in research and my success are due to these two great scholars at the University of Arkansas: they are always remembered.

This book was prepared with the encouragement of distinguished Professor Gaddy, who made me proud to be his student. I also acknowledge my Ph.D. students at the University of Science Malaysia: Habibouallah Younesi and Aliakbar Zinatizadeh, who have assisted me in drawing most of the figures. I am very thankful to my colleagues who have contributed to some parts of the chapters: Dr M. Jahanshahi, from the University of Mazandaran, Iran, and Dr Nidal Hilal from the University of Nottingham, UK. Also special thanks go to Dr H. Younesi, Dr W.S. Long, Associate Professor A.H. Kamaruddin, Professor S. Bhatia, Professor A.R. Mohamed and Associate Professor A.L. Ahmad for their contribution of case studies.

I acknowledge my friends in Malaysia: Dr Long Wei Sing, Associate Professor Azlina Harun Kamaruddin and Professor Omar Kadiar, School of Chemical Engineering and School of Industrial Technology, the Universiti Sains Malaysia, for editing part of this book. I also acknowledge my colleague Dr Mohammad Ali Rupani, who has edited part of the book. Nor should I forget the person who has accelerated this work and given lots of encouragement: *Deirdre Clark* at Elsevier.

G. D. NAJAFPOUR
Professor of Chemical Engineering
University of Mazandaran, Babol, Iran

Table of Contents

This page intentionally left blank

CHAPTER 1

Industrial Microbiology

1.1 INTRODUCTION

Microorganisms have been identified and exploited for more than a century. The Babylonians and Sumerians used yeast to prepare alcohol. There is a great history beyond fermentation processes, which explains the applications of microbial processes that resulted in the production of food and beverages. In the mid-nineteenth century, Louis Pasteur understood the role of microorganisms in fermented food, wine, alcohols, beverages, cheese, milk, yoghurt and other dairy products, fuels, and fine chemical industries. He identified many microbial processes and discovered the first principal role of fermentation, which was that microbes required substrate to produce primary and secondary metabolites, and end products.

In the new millennium, extensive application of bioprocesses has created an environment for many engineers to expand the field of biotechnology. One of the useful applications of biotechnology is the use of microorganisms to produce alcohols and acetone, which are used in the industrial processes. The knowledge related to industrial microbiology has been revolutionised by the ability of genetically engineered cells to make many new products. Genetic engineering and gene mounting have been developed in the enhancement of industrial fermentation. Consequently, biotechnology is a new approach to making commercial products by using living organisms. Furthermore, knowledge of bioprocesses has been developed to deliver fine-quality products.

Application of biological sciences in industrial processes is known as bioprocessing. Nowadays most biological and pharmaceutical products are produced in well-defined industrial bioprocesses. For instance, bacteria are able to produce most amino acids that can be used in food and medicine. There are hundreds of microbial and fungal products purely available in the biotechnology market. Microbial production of amino acids can be used to produce L-isomers; chemical production results in both D- and L-isomers. Lysine and glutamic acid are produced by *Corynebacterium glutamicum*. Another food additive is citric acid, which is produced by *Aspergillus niger*. Table 1.1 summarises several widespread applications of industrial microbiology to deliver a variety of products in applied industries.

The growth of cells on a large scale is called industrial fermentation. Industrial fermentation is normally performed in a bioreactor, which controls aeration, pH and temperature. Microorganisms utilise an organic source and produce primary metabolites such as ethanol,

TABLE 1.1. *Industrial products produced by biological processes*[12]

Fermentation product	Microorganism	Application
Ethanol (non-beverage)	*Saccharomyces cerevisiae*	Fine chemicals
2-Ketogluconic acid	*Pseudomonas* sp.	Intermediate for D-araboascorbic acid
Pectinase, protease	*Aspergillus niger, A. aureus*	Clarifying agents in fruit juice
Bacterial amylase	*Bacillus subtilis*	Modified starch, sizing paper
Bacterial protease	*B. subtilis*	Desizing fibres, spot remover
Dextran	*Leuconostoc mesenteroides*	Food stabilizer
Sorbose	*Gluconobacter suboxydans*	Manufacturing of ascorbic acid
Cobalamin (vitamin B_{12})	*Streptomyces olivaceus*	Food supplements
Glutamic acid	*Brevibacterium* sp.	Food additive
Gluconic acid	*Aspergillus niger*	Pharmaceutical products
Lactic acid	*Rhizopus oryzae*	Foods and pharmaceuticals
Citric acid	*Aspergillus niger* or *A. wentii*	Food products, medicine
Acetone-butanol	*Clostridium acetobutylicum*	Solvents, chemical intermediate
Insulin, interferon	Recombinant *E. coli* Baker's yeast	Human therapy
Yeast and culture starter	*Lactobacillus bulgaricus* Lactic acid bacteria	Cheese and yoghurt production
Microbial protein (SCP)	*Candida utilis* *Pseudomonas methylotroph*	Food supplements
Penicillin	*Penicillium chrysogenum*	Antibiotics
Cephalosporins	*Cephalosparium acremonium*	Antibiotics
Erythromycin	*Streptomyces erythreus*	Antibiotics

which are formed during the cells' exponential growth phase. In some bioprocesses, yeast or fungi are used to produce advanced valuable products. Those products are considered as secondary metabolites, such as penicillin, which is produced during the stationary phase. Yeasts are grown for wine- and bread-making. There are other microbes, such as *Rhizobium*, *Bradyrhizobium* and *Bacillus thuringiensis*, which are able to grow and utilise carbohydrates and organic sources originating from agricultural wastes. Vaccines, antibiotics and steroids are also products of microbial growth.

1.2 PROCESS FERMENTATION

The term 'fermentation' was obtained from the Latin verb '*fervere*', which describes the action of yeast or malt on sugar or fruit extracts and grain. The 'boiling' is due to the production of carbon dioxide bubbles from the aqueous phase under the anaerobic catabolism of carbohydrates in the fermentation media. The art of fermentation is defined as the chemical transformation of organic compounds with the aid of enzymes. The ability of yeast to make alcohol was known to the Babylonians and Sumerians before 6000 BC. The Egyptians discovered the generation of carbon dioxide by brewer's yeast in the preparation

of bread. The degradation of carbohydrates by microorganisms is followed by glycolytic or Embden–Myerhof–Parnas pathways.[1,2] Therefore the overall biochemical reaction mechanisms to extract energy and form products under anaerobic conditions are called fermentation processes. In the process of ethanol production, carbohydrates are reduced to pyruvate with the aid of nicotinamide adenine dinucleotide (NADH); ethanol is the end product. Other fermentation processes include the cultivation of acetic acid bacteria for the production of vinegar. Lactic acid bacteria preserve milk; the products are yoghurt and cheese. Various bacteria and mold are involved in the production of cheese. Louis Pasteur, who is known as the father of the fermentation process, in early nineteenth century defined fermentation as life without air. He proved that existing microbial life came from pre-existing life. There was a strong belief that fermentation was strictly a biochemical reaction. Pasteur disproved the chemical hypothesis. In 1876, he had been called by distillers of Lille in France to investigate why the content of their fermentation product turned sour.[3] Pasteur found under his microscope the microbial contamination of yeast broth. He discovered organic acid formation such as lactic acid before ethanol fermentation. His greatest contribution was to establish different types of fermentation by specific microorganisms, enabling work on pure cultures to obtain pure product. In other words, fermentation is known as a process with the existence of strictly anaerobic life: that is, life in the absence of oxygen. The process is summarised in the following steps:

- Action of yeast on extracts of fruit juice or, malted grain. The biochemical reactions are related to generation of energy by catabolism of organic compounds.
- Biomass or mass of living matter, living cells in a liquid solution with essential nutrients at suitable temperature and pH leads to cell growth. As a result, the content of biomass increases with time.

In World War I, Germany was desperate to manufacture explosives, and glycerol was needed for this. They had identified glycerol in alcohol fermentation. Neuberg discovered that the addition of sodium bisulphate in the fermentation broth favored glycerol production with the utilization of ethanol. Germany quickly developed industrial-scale fermentation, with production capacity of about 35 tons per day.[3] In Great Britain, acetone was in great demand; it was obtained by anaerobic fermentation of acetone–butanol using *Clostridium acetobutylicum*.

In large-scale fermentation production, contamination was major problem. Microorganisms are capable of a wide range of metabolic reactions, using various sources of nutrients. That makes fermentation processes suitable for industrial applications with inexpensive nutrients. Molasses, corn syrup, waste products from crystallisation of sugar industries and the wet milling of corn are valuable broth for production of antibiotics and fine chemicals. We will discuss many industrial fermentation processes in the coming chapters. It is best to focus first on the fundamental concepts of biochemical engineering rather than the applications.

There are various industries using biological processes to produce new products, such as antibiotics, chemicals, alcohols, lipid, fatty acids and proteins. Deep understanding of bioprocessing may require actual knowledge of biology and microbiology in the applications of the above processes. It is very interesting to demonstrate bench-scale experiments and

make use of large-scale advanced technology. However, application of the bioprocess in large-scale control of microorganisms in 100,000 litres of media may not be quite so simple to manage. Therefore trained engineers are essential and highly in demand; this can be achieved by knowledge enhancement in the sheathe bioprocesses. To achieve such objectives we may need to explain the whole process to the skilled labour and trained staff to implement bioprocess knowhow in biotechnology.

1.3 APPLICATION OF FERMENTATION PROCESSES

Man has been using the fermentative abilities of microorganisms in various forms for many centuries. Yeasts were first used to make bread; later, use expanded to the fermentation of dairy products to make cheese and yoghurt. Nowadays more than 200 types of fermented food product are available in the market. There are several biological processes actively used in the industry, with high-quality products such as various antibiotics, organic acids, glutamic acid, citric acid, acetic acid, butyric and propionic acids. Synthesis of proteins and amino acids, lipids and fatty acids, simple sugar and polysaccharides such as xanthan gum, glycerol, many more fine chemicals and alcohols are produced by bioprocesses with suitable industrial applications. The knowledge of bioprocessing is an integration of biochemistry, microbiology and engineering science applied in industrial technology. Application of viable microorganisms and cultured tissue cells in an industrial process to produce specific products is known as bioprocessing. Thus fermentation products and the ability to cultivate large amounts of organisms are the focus of bioprocessing, and such achievements may be obtained by using vessels known as fermenters or bioreactors. The cultivation of large amounts of organisms in vessels such as fermenters and bioreactors with related fermentation products is the major focus of bioprocess.

A bioreactor is a vessel in which an organism is cultivated and grown in a controlled manner to form the by-product. In some cases specialised organisms are cultivated to produce very specific products such as antibiotics. The laboratory scale of a bioreactor is in the range 2–100 litres, but in commercial processes or in large-scale operation this may be up to 100 m^3.[4,5] Initially the term ‘fermenter’ was used to describe these vessels, but in strict terms fermentation is an anaerobic process whereas the major proportion of fermenter uses aerobic conditions. The term ‘bioreactor’ has been introduced to describe fermentation vessels for growing the microorganisms under aerobic or anaerobic conditions.

Bioprocess plants are an essential part of food, fine chemical and pharmaceutical industries. Use of microorganisms to transform biological materials for production of fermented foods, cheese and chemicals has its antiquity. Bioprocesses have been developed for an enormous range of commercial products, as listed in Table 1.1. Most of the products originate from relatively cheap raw materials. Production of industrial alcohols and organic solvents is mostly originated from cheap feed stocks. The more expensive and special bioprocesses are in the production of antibiotics, monoclonal antibodies and vaccines. Industrial enzymes and living cells such as baker’s yeast and brewer’s yeast are also commercial products obtained from bioprocess plants.

TABLE 1.2. *Products and services by biological processes*

Sector	Product and service	Remark
Chemicals	Ethanol, acetone, butanol	Bulk
	Organic acids (acetic, butyric, propionic and citric acids)	
	Enzymes	Fine
	Perfumeries	
	Polymers	
Pharmaceuticals	Antibiotics	
	Enzymes	
	Enzyme inhibitors	
	Monoclonal antibodies	
	Steroids	
	Vaccines	
Energy	Ethanol (gasohol)	Non-sterile
	Methane (biogas)	
Food	Diary products (cheese, yoghurts, etc.)	Non-sterile
	Baker's yeast	
	Beverages (beer, wine)	
	Food additives	
	Amino acids	
	Vitamin B	
	Proteins (SCP)	
Agriculture	Animal feeds (SCP)	Non-sterile
	Waste treatment	
	Vaccines	
	Microbial pesticides	
	Mycorrhizal inoculants	

1.4 BIOPROCESS PRODUCTS

Major bioprocess products are in the area of chemicals, pharmaceuticals, energy, food and agriculture, as depicted in Table 1.2. The table shows the general aspects, benefits and application of biological processes in these fields.

Most fermented products are formed into three types. The main categories are now discussed.

1.4.1 Biomass

The aim is to produce biomass or a mass of cells such as microbes, yeast and fungi. The commercial production of biomass has been seen in the production of baker's yeast, which is used in the baking industry. Production of single cell protein (SCP) is used as biomass enriched in protein.[6] An algae called *Spirulina* has been used for animal food in some countries. SCP is used as a food source from renewable sources such as whey, cellulose, starch, molasses and a wide range of plant waste.

1.4.2 Cell Products

Products are produced by cells, with the aid of enzymes and metabolites known as cell products. These products are categorised as either extracellular or intracellular. Enzymes are one of the major cell products used in industry. Enzymes are extracted from plants and animals. Microbial enzymes, on the other hand, can be produced in large quantities by conventional techniques. Enzyme productivity can be improved by mutation, selection and perhaps by genetic manipulation. The use of enzymes in industry is very extensive in baking, cereal making, coffee, candy, chocolate, corn syrup, dairy product, fruit juice and beverages. The most common enzymes used in the food industries are amylase in baking, protease and amylase in beef product, pectinase and hemicellulase in coffee, catalase, lactase and protease in dairy products, and glucose oxidase in fruit juice.

1.4.3 Modified Compounds (Biotransformation)

Almost all types of cell can be used to convert an added compound into another compound, involving many forms of enzymatic reaction including dehydration, oxidation, hydroxylation, amination, isomerisation, etc. These types of conversion have advantages over chemical processes in that the reaction can be very specific, and produced at moderate temperatures. Examples of transformations using enzymes include the production of steroids, conversion of antibiotics and prostaglandins. Industrial transformation requires the production of large quantities of enzyme, but the half-life of enzymes can be improved by immobilisation and extraction simplified by the use of whole cells.

In any bioprocess, the bioreactor is not an isolated unit, but is as part of an integrated process with upstream and downstream components. The upstream consists of storage tanks, growth and media preparation, followed by sterilisation. Also, seed culture for inoculation is required upstream, with sterilised raw material, mainly sugar and nutrients, required for the bioreactor to operate. The sterilisation of the bioreactor can be done by steam at 15 pounds per square inch guage (psig), 121 °C or any disinfectant chemical reagent such as ethylene oxide. The downstream processing involves extraction of the product and purification as normal chemical units of operation.[7] The solids are separated from the liquid, and the solution and supernatant from separation unit may go further for purification after the product has been concentrated.

1.5 PRODUCTION OF LACTIC ACID

Several carbohydrates such as corn and potato starch, molasses and whey can be used to produce lactic acid. Starch must first be hydrolysed to glucose by enzymatic hydrolysis; then fermentation is performed in the second stage. The choice of carbohydrate material depends upon its availability, and pretreatment is required before fermentation. We shall describe the bioprocess for the production of lactic acid from whey.

Large quantities of whey constitute a waste product in the manufacture of dairy products such as cheese. From the standpoint of environmental pollution it is considered a major problem, and disposal of untreated wastes may create environmental disasters. It is desirable

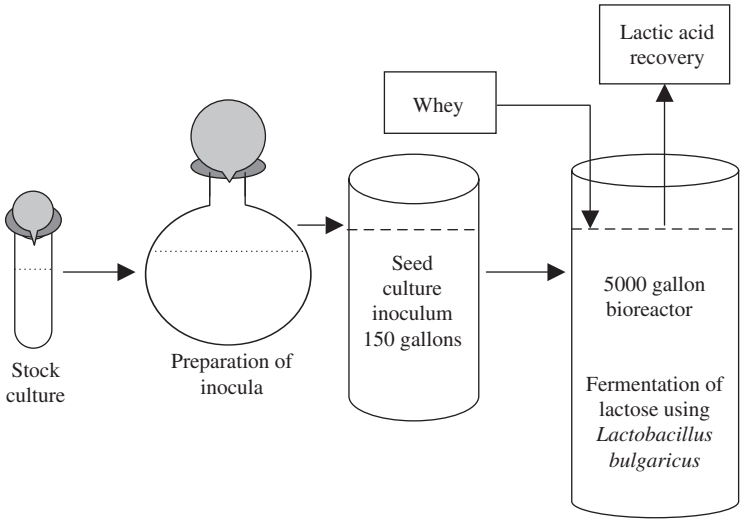

FIG. 1.1. Production of lactic acid from whey.

to use whey to make some more useful product. Whey can be converted from being a waste product to something more desirable that can be used for the growth of certain bacteria, because it contains lactose, nitrogenous substances, vitamins and salts. Organisms can utilise lactose and grow on cheese wastes; the most suitable of them are *Lactobacillus* species such as *Lactobacillus bulgaricus*, which is the most suitable species for whey. This organism grows rapidly, is homofermentative and thus capable of converting lactose to the single end-product of lactic acid. Stock cultures of the organism are maintained in skimmed milk medium. The 3–5% of inoculum is prepared and transferred to the main bioreactor, and the culture is stored in pasteurised, skimmed milk at an incubation temperature of 43 °C. During fermentation, pH is controlled by the addition of slurry of lime to neutralise the product to prevent any product inhibition. The accumulation of lactic acid would retard the fermentation process because of the formation of calcium lactate. After 2 days of complete incubation, the material is boiled to coagulate the protein, and then filtered. The solid filter cake is a useful, enriched protein product, which may be used as an animal feed supplement. The filtrate containing calcium lactate is then concentrated by removing water under vacuum, followed by purification of the final product. The flow diagram for this process is shown in Figure 1.1.

1.6 PRODUCTION OF VINEGAR

The sugars in fruits such as grapes are fermented by yeasts to produce wines. In wine-making, lactic acid bacteria convert malic acid into lactic acid in malolactic fermentation in fruits with high acidity. *Acetobacter* and *Gluconobacter* oxidise ethanol in wine to acetic acid (vinegar).

The word ‘wine’ is derived from the French term ‘vinaigre’ meaning ‘sour wine’. It is prepared by allowing a wine to get sour under controlled conditions. The production of vinegar involves two steps of biochemical changes:

(1) Alcoholic fermentation in fermentation of a carbohydrate.
(2) Oxidation of the alcohol to acetic acid.

There are several kinds of vinegar. The differences between them are primarily associated with the kind of material used in the alcoholic fermentation, e.g. fruit juices, sugar and hydrolysed starchy materials. Based on US Department of Agriculture (USDA) definitions, there are a few types of vinegar: vinegar, cider vinegar, apple vinegar. The products are made by the alcoholic and subsequent acetous fermentations of the apple juice. The acetic acid content is about 5%. Yeast fermentation is used for the production of alcohol. The alcohol is adjusted to 10–13%, then it is exposed to acetic acid bacteria (*Acetobacter* species), whereby oxygen is required for the oxidation of alcohol to acetic acid. The desired temperature for *Acetobacter* is 15–34 °C. The reaction is:

$$C_6H_{12}O_6 \xrightarrow{\textit{Zymomonas mobilis}} 2CH_3CH_2OH + 2CO_2 \quad (1.6.1)$$

$$2CH_3CH_2OH + 2O_2 \xrightarrow{\textit{Acetobacter}\ \text{sp.}} 2CH_3COOH + 2H_2O \quad (1.6.2)$$

1.7 PRODUCTION OF AMINO ACIDS (LYSINE AND GLUTAMIC ACID) AND INSULIN

Many microorganisms can synthesise amino acids from inorganic nitrogen compounds. The rate and amount of some amino acids may exceed the cells’ need for protein synthesis, where the excess amino acids are excreted into the media. Some microorganisms are capable of producing certain amino acids such as lysine, glutamic acid and tryptophan.

1.7.1 Stepwise Amino Acid Production

One of the commercial methods for production of lysine consists of a two-stage process using two species of bacteria. The carbon sources for production of amino acids are corn, potato starch, molasses, and whey. If starch is used, it must be hydrolysed to glucose to achieve higher yield. *Escherichia coli* is grown in a medium consisting of glycerol, corn-steep liquor and di-ammonium phosphate under aerobic conditions, with temperature and pH controlled.

- Step 1: Formation of diaminopimelic acid (DAP) by *E. coli*.
- Step 2: Decarboxylation of DAP by *Enterobacter aerogenes*.

E. coli can easily grow on corn steep liquor with phosphate buffer for an incubation period of 3 days. Lysine is an essential amino acid for the nutrition of humans, which is used as a

supplementary food with bread and other foodstuffs. This amino acid is a biological product which is also used as a food additive and cereal protein.

Many species of microorganisms, especially bacteria and fungi, are capable of producing large amounts of glutamic acid. Glutamic acid is produced by microbial metabolites of *Micrococcus, Arthrobacter*, and *Brevibacterium* by the Krebs cycle. Monosodium glutamate is known as a flavour-enhancing amino acid in food industries. The medium generally used consists of carbohydrate, peptone, inorganic salts and biotin. The concentration of biotin has a significant influence on the yield of glutamic acid. The α-ketoglutaric acid is an intermediate in the Krebs cycle and is the precursor of glutamic acid. The conversion of α-ketoglutaric acid to glutamic acid is accomplished in the presence of glutamic acid dehydrogenase, ammonia and nicotinamide adenine dinucleotide dehydrogenase ($NADH_2$). The living cells assimilate nitrogen by incorporating it into ketoglutaric acid, then to glutamic acid and glutamine. Therefore glutamic acid is formed by the reaction between ammonia and α-ketoglutaric acid in one of the tricarboxylic acid (TCA) cycle or Krebs cycle intermediates.[2,9]

1.7.2 Insulin

Insulin is one of the important pharmaceutical products produced commercially by genetically engineered bactera. Before this development, commercial insulin was isolated from animal pancreatic tissue. Microbial insulin has been available since 1982. The human insulin gene is introduced into a bacterium like *E. coli*. Two of the major advantages of insulin production by microorganisms are that the resultant insulin is chemically identical to human insulin, and it can be produced in unlimited quantities.

1.8 ANTIBIOTICS, PRODUCTION OF PENICILLIN

The commercial production of penicillin and other antibiotics are the most dramatic in industrial microbiology. The annual production of bulk penicillin is about 33 thousand metric tonnes with annual sales market of more than US$400 million.[8] The worldwide bulk sales of the four most important groups of antibiotics, penicillins, cephalosporins, tetracyclines and erythromycin, are US$4.2 billion per annum.[10]

The mold isolated by Alexander Fleming in early 1940s was *Penicillium notatum*, who noted that this species killed his culture of *Staphylococcus aureus*. The production of penicillin is now done by a better penicillin-producing mould species, *Penicillium chrysogenum*. Development of submerged culture techniques enhanced the cultivation of the mould in large-scale operation by using a sterile air supply.

- Streptomycin produced by *Actinomycetes*
- Molasses, corn steep liquor, waste product from sugar industry, and wet milling corn are used for the production of penicillin
- *Penicillium chrysogenum* can produce 1000 times more penicillin than Fleming's original culture[8]

- The major steps in the commercial production of penicillin are:
  (1) Preparation of inoculum.
  (2) Preparation and sterilisation of the medium.
  (3) Inoculation of the medium in the fermenter.
  (4) Forced aeration with sterile air during incubation.
  (5) Removal of mould mycelium after fermentation.
  (6) Extraction and purification of the penicillin.

1.9 PRODUCTION OF ENZYMES

Many moulds synthesise and excrete large quantities of enzymes into the surrounding medium. Enzymes are proteins; they are denatured by heat and extracted or precipitated by chemical solvents like ethanol and by inorganic salts like ammonium sulphate.[11] Coenzymes are also proteins combined with low molecular mass organics like vitamin B. It is industrially applicable and economically feasible to produce, concentrate, extract and purify enzymes from cultures of moulds such as *Aspergillus*, *Penicillium*, *Mucor* and *Rhizopus*. Mould enzymes such as amylase, invertase, protease, and pectinase are useful in the processing or refining of a variety of materials. Amylases hydrolyse starch to dextrin and sugars. They are used in preparing sizes and adhesives, desizing textile, clarifying fruit juices, manufacturing pharmaceuticals and other purposes. Invertase hydrolyses sucrose to form glucose and fructose (invert sugar). It is widely used in candy making and the production of non-crystallizable

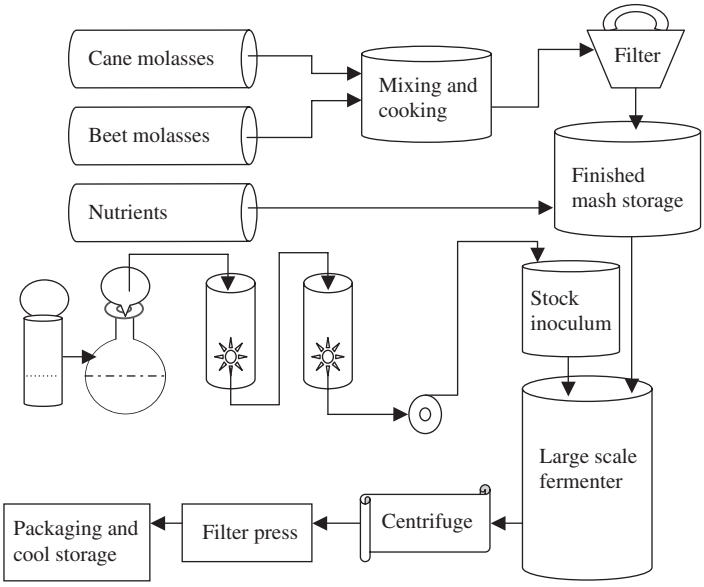

FIG. 1.2. Commercial production of baker's yeast.

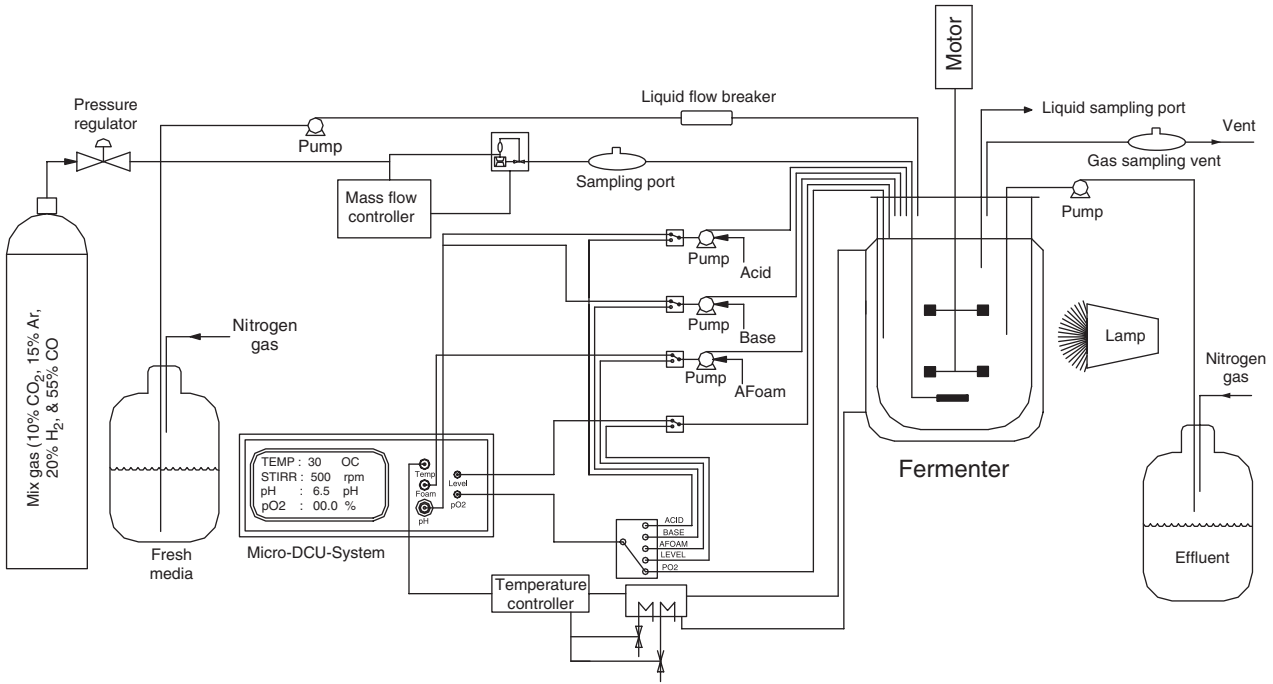

FIG. 1.3. One complete set of fermenters with all accessory controlling units.

syrup from sucrose, which is partly hydrolysed by this enzyme. The proteolytic enzymes such as protease are used for bating in leather processing to obtain fine texture. Protease is also used in the manufacture of liquid glue, degumming of silks and clarification of beer protein. It is used in laundry detergents and as an adjunct with soaps. Pectinase is used in the clarification of fruit juice and to hydrolyse pectins in the retting of flax for the manufacture of linen. Apoenzyme is the protein portion of the enzyme, which is inactive. The reaction between low molecular mass coenzymes and apoenzyme gives active holoenzyme:

$$\text{Apoenzyme} + \text{coenzyme} \rightarrow \text{holoenzyme (active)} \qquad (1.9.1)$$

1.10 PRODUCTION OF BAKER'S YEAST

The use of yeast as a leavening agent in baking dates back to the early histories of the Egyptians, Greeks and Romans. In those days, leavened bread was made by mixing some leftover dough from the previous batch of bread with fresh dough. In modern baking, pure cultures of selected strains of *Saccharomyces cerevisiae* are mixed with the bread dough to bring about desired changes in the texture and flavour of the bread. Characteristics of *S. cerevisiae* strains are selected for commercial production of baker's yeast. It has the ability to ferment sugar in the dough vigorously and rapidly. The selected strains must be stable and produce carbon dioxide, which results from the fermentation process for leavening or rising the dough. The quality of the bread depends on the selected strain of yeast, the incubation period and the choice of raw materials. Sugars in the bread dough are fermented by yeast to ethanol and CO_2; whereby the CO_2 causes the bread to rise.

In the manufacture of baker's yeast, the stock strain is inoculated into a medium that containing molasses and corn steep liquor. The pH of the medium is adjusted to be slightly acidic at pH 4–5. The acidic pH may retard the bacterial growth. The inoculated medium is aerated during the incubation period. At the end, the cells are harvested by centrifuging out the fermentation broth, and they are recovered by filter press. A small amount of vegetable oil is added to act as plasticiser, and then the cell mass is moulded into blocks. The process is shown in Figure 1.2.

A full set of bioreactors with pH and temperature controllers are shown in Figure 1.3. The complete set of a 25 litre fermenter with all the accessory controlling units creates a good opportunity to control suitable production of biochemical products with variation of process parameters. Pumping fresh nutrients and operating in batch, fed batch and continuous mode are easy and suitable for producing fine chemicals, amino acids, and even antibiotics.

REFERENCES

1. Aiba, S., Humphrey, A.E. and Millis, N.F., "Biochemical Engineering", 2nd edn. Academic Press, New York, 1973.
2. Baily, J.E. and Ollis, D.F., "Biochemical Engineering Fundamentals", 2nd edn. McGraw-Hill, New York, 1986.
3. Demain, A.L. and Solomon, A.N. *Sci. Am.* **245**, 67 (1981).

4. Ghose, T.K., “Bioprocess Computation in Biotechnology”, vol. 1. Ellis Horwood Series in Biochemistry and Biotechnology, New York, 1990.
5. Scragg, A.H., “Bioreactors in Biotechnology, A Practical Approach”. Ellis Horwood Series in Biochemistry and Biotechnology, New York, 1991.
6. Bradford, M.M., *J. Analyt. Biochem.* **72**, 248 (1976).
7. Doran, P.M., “Bioprocess Engineering Principles”. Academic Press, New York, 1995.
8. Pelczar, M.J., Chan, E.C.S. and Krieg, N.R., “Microbiology”. McGraw-Hill, New York, 1986.
9. Shuler, M.L. and Kargi, F., “Bioprocess Engineering, Basic Concepts”. Prentice-Hall, New Jersey, 1992.
10. Aharonowitz, Y. and Cohen, G., *Sci. Am.* **245**, 141 (1981).
11. Thomas, L.C. and Chamberlin, G.J., “Colorimetric Chemical Analytical Methods”. Tintometer Ltd, Salisbury, United Kingdom, 1980.
12. Phaff, H.J., *Sci. Am.* **245**, 77 (1981).

CHAPTER 2

Dissolved Oxygen Measurement and Mixing

2.1 INTRODUCTION

In biochemical engineering processes, measurement of dissolved oxygen (DO) is essential. The production of SCP may reach a steady-state condition by keeping the DO level constant, while the viable protein is continuously harvested. The concentration of protein is proportional to oxygen uptake rate. Control of DO would lead us to achieve steady SCP production. Variation of DO may affect retention time and other process variables such as substrate and product concentrations, retention time, dilution rate and aeration rate. Microbial activities are monitored by the oxygen uptake rate from the supplied air or oxygen.

Microbial cells in the aerobic condition take up oxygen from the gas and then liquid phases. The rate of oxygen transfer from the gas phase to liquid phase is important. At high cell densities, the cell growth is limited by the availability of oxygen in the medium. The growth of aerobic bacteria in the fermenter is then controlled by the availability of oxygen, substrate, energy sources and enzymes. Air has to be supplied for aerobic process in order to enhance the cell growth. Oxygen limitation may cause a reduction in the growth rate. The supplied oxygen from the gas phase has to penetrate into the microorganism. Several steps are required in order to let such a phenomenon take place. The oxygen first must travel through the gas–liquid interface, then the bulk of liquid and finally into the microbial cell.

The solubility of air in water at 10 °C and under atmospheric conditions is 11.5 ppm; as the temperature is increased to 30 °C, the solubility of air drops to 8 ppm. The solubility of air decreases to 7 ppm at 40 °C. Availability of oxygen in the fermentation broth is higher than the air, if pure oxygen is used. The solubility of pure oxygen in water at 10 °C and 1 atm pressure is 55 ppm. As the temperature increases to 30 °C, the solubility of pure oxygen drops to 38.5 ppm. The solubility of pure oxygen decreased to 33.7 ppm at 40 °C. The above data show that in case of high oxygen demand for SCP production, oxygen drastically depletes in 12–24 hours of incubation. Therefore pure oxygen is commonly used to enhance oxygen availability in the fermentation media.

2.2 MEASUREMENT OF DISSOLVED OXYGEN CONCENTRATIONS

The concentration of dissolved oxygen in a fermenter is normally measured with a dissolved oxygen electrode, known as a DO probe. There are two types in common use: galvanic

electrodes and polarographic electrodes. In both probes, there are membranes that are permeable to oxygen. Oxygen diffuses through the membrane and reaches to cathode, where it reacts to produce a current between anode and cathode proportional to the oxygen partial pressure in the fermentation broth. The electrolyte solutions in the electrode take part in the reactions and must be located in the bulk of liquid medium.

There several DO probes available. Some well-known branded fermenters, like New Brunswick, Bioflo series and the B. Braun Biotstat B fermenters are equipped with a DO meter. This unit has a 2 litre fermentation vessel equipped with DO meter and pH probe, antifoam sensor and level controllers for harvesting culture. The concentration of DO in the media is a function of temperature. The higher operating temperature would decrease the level of DO. A micro-sparger is used to provide sufficient small air bubbles. The air bubbles are stabilized in the media and the liquid phase is saturated with air. The availability of oxygen is major parameter to be considered in effective microbial cell growth rate.

2.3 BATCH AND CONTINUOUS FERMENTATION FOR PRODUCTION OF SCP

The fermentation vessel is a jacketed vessel with a defined working volume. The media are made of phosphate buffer at neutral pH with 3.3 g KH_2PO_4 and 0.3 g Na_2HPO_4, 1 g yeast extract and 30 g glucose in 1 litre of distilled water. The media should be sterilised in a 20 litres carboy. The fermentation vessel with a working volume of 2 litres may have 500 ml media initially sterilised by stream under 15 psig and 121 °C. The seed culture is transferred to the fermentation vessel with filtered and pressurized air; the production of SCP is monitored by pumping fresh nutrients and supplying air. Continuous culture with constant volume and controlled dilution rate is conducted in SCP production, as fresh and sterilised media are pumped into the culture vessel. It is desirable to control pH, temperature and aeration with a constant air flow rate. The most common continuous culture system is the chemostat. The word chemostat refers to the constant chemical environment at steady-state condition.[1] Another continuous culture vessel is the turbidostat, where the cell concentration in the culture vessel is kept constant by monitoring cell optical density. The chemostat experiment is carried out for 24 hours at a constant temperature of 32 °C, and by controlling pH and monitoring DO concentration. The medium consists of an excess amount of nutrients which is required to synthesise the desired concentration of SCP. The growth-limiting nutrient controls the steady-state SCP production rate. The data for optical density, DO level, cell dry weight and measurements of protein and carbohydrates are carried out at 8, 12, 16 and 24 hours in batch mode. The continuous operation is extended for another 24 hours to monitor all parameters and measure SCP. The results should be compared with batch-wise production. The expected results for reduction of sugar in real experiments are similar, as shown in Figure 2.1. The data plotted in Figure 2.1 were obtained by aeration of pharmaceutical wastewater. A well-known reagent for determination of carbohydrates dinitrosalicylic acid (DNS), was used to reduce the organic chemicals in the above wastewater for the course of 3 days incubation.[2,3] The method of measurement will be discussed in the

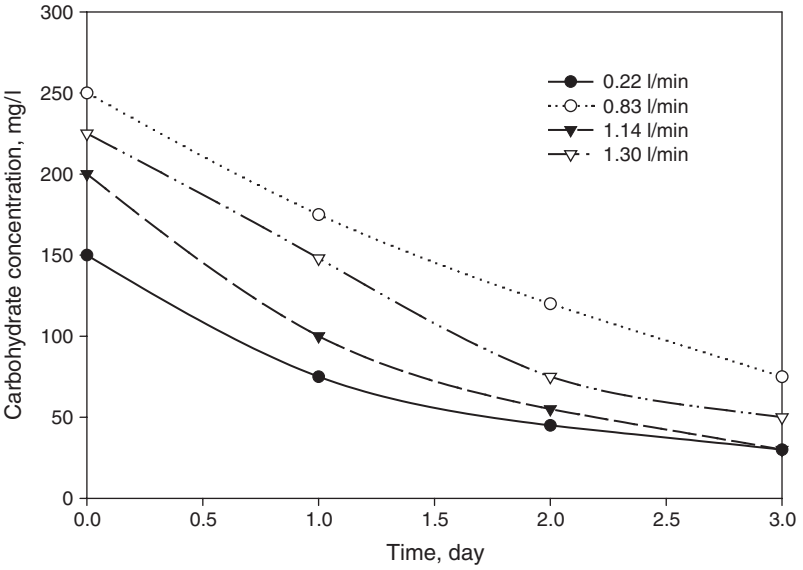

FIG. 2.1. Reduction of carbohydrate in an aeration tank at various air flow rates.

following sections. If the above experiments are conducted, they may lead us to a new set of data that are totally different from Figure 2.1, and only the reduction trend would be about the same. SCP production has to be determined by experimentation, and research is needed to obtain the data. Maximum carbohydrate reduction took place after 24 hours of aeration. Since the carbon source was initially quite low, the rate of biomass production was not appreciable.

Figure 2.2 shows the cell density and DO level in a pilot-scale aeration vessel. The role of dissolved oxygen in the treatment system is absolutely vital. Therefore the DO level must be maintained at not less than 3–4 ppm in the wastewater for effective aeration. SCP production is very oxygen-dependent. The results would be very satisfactory if pure oxygen is used.

2.3.1 Analytical Methods for Measuring Protein Content of Baker's Yeast (SCP)

Protein concentration can be determined using a method introduced by Bradford,[4] which utilises Pierce reagent 23200 (Piece Chemical Company, Rockford, IL, USA) in combination with an acidic Coomassie Brilliant Blue G-250 solution to absorb at 595 nm when the reagent binds to the protein. A 20 mg/l bovine serum albumin (Piece Chemical Company, Rockford, IL, USA) solution will be used to prepare a standard calibration curve for determination of protein concentration. The sample for analysis of SCP is initially homogenised or vibrated in a sonic system to break down the cell walls.

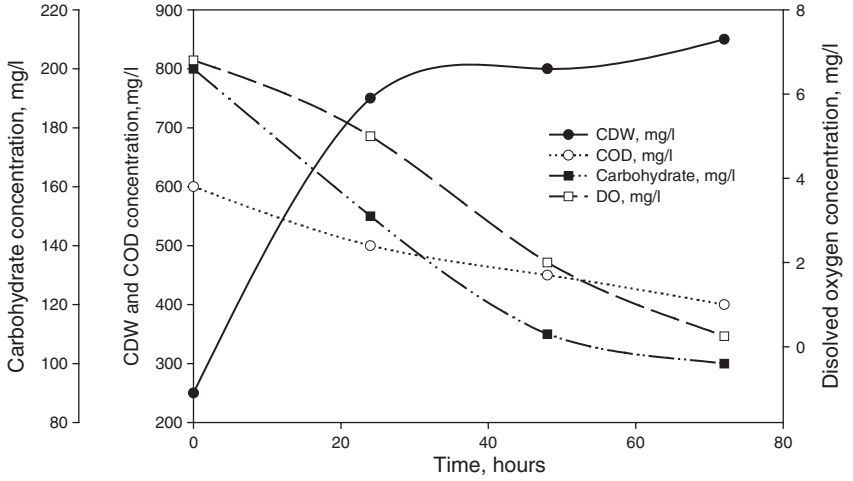

FIG. 2.2. COD, cell dry weight (CDW), carbohydrate and dissolved oxygen concentrations in a 15 litres aeration tank at an air flow rate of 5 litres/min.

2.3.2 Seed Culture

How do we start the real experiment? A 100 ml seed culture is prepared in advance. A 100 ml media consists of 0.1 g yeast extract and 1 g glucose with 0.33 g KH_2PO_4 and 0.03 g Na_2HPO_4. It is sterilised, then the microorganism, *Saccharomyces cerevisiae* (ATCC 24860), on a YM slant tube used as stock culture is transferred to the sterile cooled media.[5] The inoculated media is incubated and harvested after 24 hours. The first stage of the work is the batch experiment, which is then changed to a continuous experimental run with glucose as carbon source and the microorganism, *S. cerevisiae,* as an organism sensitive to aeration. The last stage demonstrates how agitation plays an important role in the mass transfer process.

2.4 BATCH EXPERIMENT FOR PRODUCTION OF BAKER'S YEAST

The fermentation vessel is a jacketed vessel with working volume of 2 litres. The media is made of phosphate buffer at neutral pH with 3.3 g KH_2PO_4 and 0.3 g Na_2HPO_4, 1 g yeast extract and 50 g glucose in 1 litre of distilled water. The media should be sterilised in a 20 litre carboy. The fermentation vessel with 500 ml media is initially sterilised under 15 psig steam at 121 °C for 20 min.[6] The seed culture is transferred to the fermentation vessel and feed is gradually pumped in at a flow rate of 350 ml h^{-1}. The filtered pure oxygen or pressurised air is continuously supplied. The production of baker's yeast should be monitored for 48 hours by batch experiment at a constant temperature of 32 °C, controlling pH and monitoring DO level. Sufficient air is blown at a flow rate of 2000 ml min^{-1} (1 vvm).[7,8] Data collection for optical density, DO level, cell dry weight, protein and carbohydrates is done at 6, 12, 18, 24, 36 and 48 hours in batch mode as projected in Table 2.1.

TABLE 2.1. *Batch production of baker's yeast with air flow rate of 1 vvm and an agitation speed of 350 rpm*

Time, hours	DO, mg/l	Optical density, absorbance, $\lambda_{520,nm}$	Cell dry weight, mg/ml	Protein concentration, g/l	Sugar concentration, g/l	Yield, $Y_{X/S}$
0	7.9	0.00	0.00	0.00	32.0	–
6	5.6	0.28	0.14	0.83	30.0	0.42
12	4.1	0.50	0.29	4.75	21.0	0.43
18	2.4	1.55	1.10	8.90	13.0	0.47
24	1.5	2.00	1.45	11.15	5.0	0.41
36	1.1	4.20	2.00	11.95	1.7	0.40
48	0.2	4.45	2.65	12.35	0.5	0.39

TABLE 2.2. *Effect of aeration rate on baker's yeast production*

Air flow rate, ml/min	DO, mg/l	Optical density, absorbance, $\lambda_{520,nm}$	Cell dry weight, mg/ml	Protein concentration, mg/l	Sugar concentration, g/l
50	2	0.2	0.26	1300	16.8
100	4	0.45	0.59	1450	14.5
200	6	0.69	1.24	2500	13.9
500	7.7	1/10 diluted 0.72	3.95	3000	12.5
1000	8	1/10 diluted 0.74	4.63	3100	9.8
1500	8	1/10 diluted 0.77	4.68	3350	8.6
2000	8	1/10 diluted 0.79	4.75	4800	6.7

2.5 OXYGEN TRANSFER RATE (OTR)

Once batch mode studies are completed and the required data are collected, without dismantling the bioreactor, liquid media is prepared with 33 g KH_2PO_4 and 3 g Na_2HPO_4, 10 g yeast extract and 500 g glucose in 10 litres of distilled water. The liquid media can be sterilised in an autoclave at 121 °C, 15 psig for 20 min. The liquid media is cooled down to room temperature with air flow rate of 100 ml min^{-1}. The fluid residence time of 10 hours is expected to give maximum cell optical density. Otherwise, the effect of media flow rate has to be carried out separately. This is the basic assumption made in this experiment. The aim of this set of experiments is to determine a suitable air flow rate with variation from 0.025 to 1 vvm. Table 2.2 shows the data collected in a continuous mode of operation for 3.5 days using isolated strains from the waste stream of a food processing plant. The time intervals for sampling are 12 hours. The steady-state condition of the system may be reached at about 10 hours. If any samples are taken at shorter time intervals, steady-state condition did not reach then overlapping in the experimental condition may occurs.

2.6 RESPIRATION QUOTIENT (RQ)

Measurements of inlet and outlet gas compositions of a culture vessel have been considered as an indicator for cell activities in the fermentation broth. The continuous monitoring of gas analysis would lead us to understand the oxygen consumption rate and carbon dioxide production, which originate from catabolism of carbon sources. Respiration is a sequence of biochemical reactions resulting in electrons from substances that are then transferred to an exogenous electron accepting terminal. Respiration in a cell is an energy-delivery process in which electrons are generated from oxidation of substrate and transferred through a series of oxidation–reduction reactions to electron acceptor terminals. In biosynthesis, the end products result from a respiration process. Since oxidation of carbonaceous substrate ends with carbon dioxide and water molecules, the molar ratio of carbon dioxide generated from oxidation–reduction to oxygen supplied is known as the respiration quotient:

$$\mathrm{RQ} = \frac{\mathrm{d}C_{\mathrm{CO}_2}/\mathrm{d}t}{\mathrm{d}C_{\mathrm{O}_2}/\mathrm{d}t} = \frac{\mathrm{d}C_{\mathrm{CO}_2}}{\mathrm{d}C_{\mathrm{O}_2}} \tag{2.6.1}$$

There are several methods to monitor the off-gas analysis. Online gas chromatography is commonly used. The daily operation for inlet and outlet gases is balanced to project growth in the bioprocess. High operating cost is the disadvantage of the online system.

For an online bioreactor a few important process variables should be monitored continuously. The off-gas analysis provides the most reliable information for growth activities. Measurement of oxygen and carbon dioxide in the off-gas is a fairly standard procedure used for a pilot-scale bioreactor. Knowing air flow rate and exit gas compositions or having a simple material balance can quantify oxygen uptake rate (OUR) and carbon dioxide production rate (CPR), which would lead us to a value for RQ. The three indicators for growth can be correlated and give cell growth rate. From RQ the metabolic activity of the bioprocess and the success of a healthy operation can be predicted. The off-gas analysis will show the specific CO_2 production rate, which is used to calculate oxygen consumption rate.

2.7 AGITATION RATE STUDIES

In the following experiment we shall assume that the optimum air flow rate of 0.5 vvm is desired. This means for an aeration vessel with a 2 litre working volume, the experiment requires 1000 ml air per minute. The rest of process parameters and media conditions remain unchanged. Another 10 litres of fresh aseptic media must be prepared. The operation is continued for 3.5 days at an agitation speed from 100 to 700 rpm; samples are drawn at intervals of 12 hours. Table 2.3 shows the effect of agitation rate on cell dry weight and protein production using a starchy wastewater stream. The active strain was isolated from a food-processing plant.

TABLE 2.3. *Effect of agitation rate on baker's yeast production*

Agitation rate, rpm	DO, mg/l	Optical density, absorbance, $\lambda_{520,nm}$	Cell dry weight, mg/ml	Protein concentration, mg/l	Sugar concentration, g/l
100	2	1/10 diluted 0.22	0.29	1250	15.5
200	3	1/10 diluted 0.36	0.46	1360	14.7
300	5	1/10 diluted 0.45	0.59	1450	13.6
400	6	1/10 diluted 0.65	0.85	1850	12.1
500	8	1/10 diluted 0.79	1.12	2150	11.5
600	8	1/10 diluted 0.82	1.16	2250	10.8
700	8	1/10 diluted 0.83	1.19	2300	8.4

Example 2.1: Calculate Cell Density in an Aerobic Culture

A strain of *Azotobacter vinelandii* was cultured in a 15 m^3 stirred fermenter for the production of alginate. Under current conditions the mass transfer coefficient, $k_L a$, is 0.18 s^{-1}. Oxygen solubility in the fermentation broth is approximately 8×10^{-3} kg m^{-3}.[9] The specific oxygen uptake rate is 12.5 mmol g^{-1} h^{-1}. What is the maximum cell density in the broth? If copper sulphate is accidentally added to the fermentation broth, which may reduce the oxygen uptake rate to 3 mmol g^{-1} h^{-1} and inhibit the microbial cell growth, what would be the maximum cell density in this condition?

The oxygen uptake rate (OUR) is defined as:[10]

$$\text{OUR} = (q_{O_2})(x) = k_L a(C^*_{AL} - C_{AL}) \tag{E.2.1}$$

Solution

We make an assumption based on the fact that all of the dissolved oxygen in the fermentation broth is used or taken by microorganisms. In this case the DO goes to zero. The value for C_{AL} can be zero since it is not given in the problem statement. Also the cell density has to be maximised. Therefore the above assumption is valid. In the above equation x represented the cell density, that is:

$$x_{max} = \frac{k_L a C^*_{AL}}{q_{O_2}} \tag{E.2.2}$$

Substituting values into (E.2.2), the maximum biomass production is calculated as follows:

$$x_{max} = \frac{(0.18\ s^{-1})(8\times10^{-3}\ kg/m^3)}{(12.5\ mmol/g-h)(1\ h/3600\ s)(1\ mol/1000\ mmol)(32\ g/1\ mol)(1\ kg/1000\ g)}$$

$$= 12960\ g/m^3 \text{ or } 2.96\ g\ l^{-1}$$

Let us assume the solubility of oxygen does not affect on C^*_{AL} or $k_L a$, the factor affected on the oxygen uptake rate that is 12.5/3 = 4.167, then x_{max} is:

$$x_{max} = (12.96)(4.167) = 54\,g\,l^{-1}$$

To achieve the calculated cell densities, other conditions must be favourable, such as substrate concentration and sufficient time.

2.8 NOMENCLATURE

C^*_{AL}	Equilibrium concentration of A at the liquid phase, mmol/g
C_{AL}	Concentration of A at liquid phase, mmol/g
CPR	Carbon dioxide production rate, mmol/g·s
$k_L a$	Mass transfer coefficient at liquid phase, s^{-1}
OUR	Oxygen uptake rate, mmol/g·s
RQ	Respiration quotient, mmol CO_2/mmol O_2
x	Biomass concentration, mg/l
x_{max}	The maximum biomass production, s^{-1}
q_{O_2}	Specific oxygen uptake rate, s^{-1}

REFERENCES

1. Wang, D.I.C. Cooney, C.L. Deman, A.L. Dunnill, P. Humphrey, A.E. and Lilly, M.D., "Fermentation and Enzyme Technology". John Wiley & Sons, New York, 1979.
2. Miller, G.L., *Analyt. Chem*. **31**, 426 (1959).
3. Thomas, L.C. and Chamberlin, G.J., "Colorimetric Chemical Analytical Methods". Tintometer Ltd, Salisbury, United Kingdom, 1980.
4. Bradford, M.M., *J. Analyt. Biochem*. **72**, 248 (1976).
5. Pelczar, M.J. Chan, E.C.S. and Krieg, N.R., "Microbiology". McGraw Hill, New York, 1986.
6. Scragg, A.H., "Bioreactors in Biotechnology, A Practical Approach". Ellis Horwood Series in Biochemistry and Biotechnology, New York, 1991.
7. Ghose, T.K., "Bioprocess Computation in Biotechnology", vol. 1. Ellis Horwood Series in Biochemistry and Biotechnology, New York, 1990.
8. Doran, P.M., "Bioprocess Engineering Principles". Academic Press, New York, 1995.
9. Shuler, M.L. and Kargi, F., "Bioprocess Engineering, Basic Concepts". Prentice Hall, New Jersey, 1992.
10. Baily, J.E. and Ollis, D.F., "Biochemical Engineering Fundamentals", 2nd edn. McGraw-Hill, New York, 1986.

CHAPTER 3

Gas and Liquid System (Aeration and Agitation)

3.1 INTRODUCTION

In the biochemical engineering profession, there are various bioprocesses actively involved in the synthesis and production of biological products. Understanding of all the processes may require basic knowledge of biology, biochemistry, biotechnology, and real knowledge of engineering processes. Transfer of oxygen is a major concern in many bioprocesses that require air for microbial growth such as single cell protein and production of antibiotics. Agitation in a fermentation unit is directly related to oxygen transported from the gas phase to liquid phase followed by oxygen uptake by the individual microbial cell. The activities of microorganisms are monitored by the utilisation of oxygen from the supplied air and the respiration quotient. The primary and secondary metabolites in a bioprocess can be estimated based on projected pathways for production of intracellular and extracellular by-products. In the previous chapter, dissolved oxygen was discussed; in this chapter, mechanisms of oxygen transport are focused on. The details of process operation are also discussed in this chapter.

3.2 AERATION AND AGITATION

Aeration and agitation are implemented in most fermentation processes. The word 'aerobe' refers to the kind of microorganism that needs molecular oxygen for growth and metabolism. 'Aerobic' is the condition of living organisms surviving only in the presence of molecular oxygen. Aerobic bacteria require oxygen for growth and can be incubated to be grown in atmospheric air. Oxygen is a strong oxidising agent which has the ability to accept electrons for yielding energy, a process known as respiration. A bioreactor is a reaction vessel in which an organism is cultivated in a controlled manner to produce cell bodies and/or product. Initially the term 'fermenter' was used to describe these vessels, but in strict terms, fermentation is an anaerobic process whereas the major proportion of fermenters use aerobic processes. Thus, in general terms, 'bioreactor' means a vessel in which organisms are grown under aerobic or anaerobic conditions. If a bioreactor or a reaction vessel operates under aerating conditions, the system is called an aerobic bioreactor. Sterile air is supplied

as a source of intake for respiration of microorganisms. The oxygen is dissolved in the liquid phase. The microorganisms consume the oxygen that is dissolved in the liquid media.

Growth of the aerobic bacteria in the fermenter is controlled by the availability of substrate, energy and enzymes. Microbial cultures are always known as heterogeneous systems, as cells are solid and nutrients are in the liquid phase. If the process is aerobic, air has to be supplied to enhance cell growth, otherwise the limited dissolved oxygen is used up and then oxygen limitation may cause a decrease in the growth rate. The rate of reaction depends on substrate concentration and product presence. High concentrations of substrate and product may cause growth inhibition, as the microorganisms are intoxicated at high levels of substrate or product; such phenomena may easily happen in batch culture. The aerobic activity depends upon the local bulk oxygen concentration, the oxygen diffusion coefficient and the respiration rate of microbes in the aerobic region. The transfer of oxygen from the gas to the microorganism takes place in several steps. The oxygen must first travel through the gas–liquid interface, then the bulk of liquid and finally into the microbial cell.[1]

3.3 EFFECT OF AGITATION ON DISSOLVED OXYGEN

Aerobic bacteria are easily grown at a small scale in tubes and flasks by incubating the media under normal atmospheric conditions. In large-scale operations, the media has to be exposed to air, and sufficient air must be present for respiration of all living microorganisms. The indication of availability of oxygen in the liquid phase is to measure the amount of dissolved oxygen. DO probes are available on the market, and most fermenters are equipped with a DO meter. For aerobic fermentation, the bioreactor must be equipped with a DO meter. The level of DO in the media is a function of temperature. Higher operating temperatures decrease the level of DO. To have sufficient oxygen, an air sparger is required to purge compressed air or pressured air to be bubbled into the media. The availability of oxygen is a major parameter to be considered for effective microbial cell growth rate.

3.4 AIR SPARGER

Air under pressure is supplied through a tube end consists of an ‘O’ ring with very fine holes or orifices. The size of bubbles depends on the size of hole and type of sparger. For very fine bubbles with effective gas dispersion, a micro-sparger is used in the fermenter. A micro-sparger is in fact a highly porous ceramic material and is used instead of a gas sparger. The size of bubbles affects the mass transfer process. Smaller bubble size provides more surface area for gas exposure, so a better oxygen transfer rate is obtained. The size of gas bubbles and their dispersion throughout the tank are critical to bioreactor performance. Although a sparging ring will initially provide smaller size and better gas distribution with sufficient agitation, micro-spargers are often used because the porous media provides an extensive number of fine and uniform bubbles. They are also resistant to plugging of biomass on the outer surface of the sparger. Gas dispersion is not mainly related to the sparger, but rather it is dependent on the type of impeller used for agitation. Agitation

creates uniformity of gas bubbles in the entire media by placing the agitator in the appropriate position. A few sets of impellers are used to ensure the even distribution of the gas in the fermentation broth. Very high agitation may cause high shear forces, which may damage the cell wall and cause cell rupture. If the propagating cells such as animal cells and plant tissue cultures are shear-sensitive, special configurations of impellers are required. A wide variety of impellers are available; other shapes of impellers related to mixing and agitation of bioreactors are discussed in the literature.[2] In this book, the term 'bioreactor' will be used because of its global applications.

3.5 OXYGEN TRANSFER RATE IN A FERMENTER

The molar flux of oxygen is generalised in a simple equation, with the concentration gradient as the major driving force in the transfer of oxygen from gas and liquid interface to the bulk of liquid. The rate of oxygen transfer in a fermenter broth is influenced by several physical and chemical parameters that change either k_L, or the value of interfacial area of bubbles (a) or the concentration gradient known as the driving force for the mass transfer. At low concentrations of the soluble gas, the molar flux of oxygen transported to the fermentation media is:[3]

$$N_A = k_L a\,(C^*_{AL} - C_{AL}) \tag{3.5.1}$$

where N_A is the oxygen flux in kmol m^{-2} s^{-1}, k_L is the liquid side mass transfer coefficient in ms^{-1}, $C_{AL}{}^*$ is the oxygen concentration in equilibrium with the liquid phase at the interface in kmol/m^3, C_{AL} is the oxygen concentration in the bulk of liquid in kmol m^{-3}, and a is the interfacial area in surface area of bubbles per unit volume of broth (m^2 m^{-3}). The dissolved oxygen can be measured at one or several points in the vessel, depending on vessel size, using a dissolved oxygen probe. In the large bioreactor, the partial pressure of oxygen in the gas will fall as it passes through the fermentation broth.

$$P_{\text{log mean}} = \frac{P_{\text{in}} - P_{\text{out}}}{\ln (P_{\text{in}}/P_{\text{out}})} \tag{3.5.2}$$

The equilibrium concentration is evaluated from Henry's law.[3,4] The equilibrium concentration of oxygen is calculated by the ratio of mean value of pressure over Henry's law constant, H.

$$C^* = \frac{P_{\text{log mean}}}{H} \tag{3.5.3}$$

This is the most accurate method of measuring the mass transfer coefficient and it can be used in the actual fermentation system. It depends on accurate oxygen analyses and

accurate measurement of temperature and pressure. For bubble sizes of 2–3 mm diameter in the fermentation broth, the mass transfer coefficient is about 3×10^{-4} to 4×10^{-4} m s^{-1}.

3.5.1 Mass Transfer in a Gas–Liquid System

Oxygen transfer at low concentrations is proportional to the oxygen concentration gradient existing on the interface of the gas and liquid bulk phase.

$$N_A = k_L(C_i - C_L) \tag{3.5.1.1}$$

where N_A is oxygen flux in kmol m^{-2} s^{-1}, k_L is the mass transfer coefficient in liquid side in m/s, C_i is oxygen concentration at the interface in kmol m^{-3}, and C_L is oxygen concentration in the bulk of the liquid. The molar flux of oxygen in the gas phase to liquid phase is also stated as:

$$N_a = k_g(P_{O_2} - P_{O_2,i}) \tag{3.5.1.2}$$

where k_g is the mass transfer coefficient at the gas side in kmol m^{-2} atm^{-1}s^{-1}, $P_{O_{2,i}}$ is the oxygen partial pressure at the interface in atm, and P_{O_2} is the oxygen partial pressure at the bulk of gas phase in atmospheres. It is impossible to measure the interface concentration by the molar flux with knowing the mass transfer coefficient.

$$N_A = K_L(C^* - C_L) \tag{3.5.1.3}$$

where K_L is the overall mass transfer coefficient, then, Henry's law is

$$P = HC^* \tag{3.5.1.4}$$

$$\frac{1}{K_L} = \frac{1}{k_L} + \frac{1}{HK_g} \tag{3.5.1.5}$$

For slightly soluble gases, H is defined as a large value (4.2×10^4 bar mol^{-1}; that is the mole fraction of oxygen in H_2O). The liquid phase controls, $k_L = K_L$. For the oxygen transfer rate, the interface area is important. For oxygen bubbles, the surface area of bubbles is defined as:

$$a = \frac{\text{surface area of bubbles}}{\text{volume}}\left(\frac{\text{m}^2}{\text{m}^3}\right) \tag{3.5.1.6}$$

By multiplying both sides of (3.5.1.5) with (3.5.1.6), the following equation results:

$$-r_A = K_L a(C^* - C_L) \tag{3.5.1.7}$$

where, $-r_A$ is the consumption rate of substrate A in mol l^{-1} s^{-1}.

3.6 MASS TRANSFER COEFFICIENTS FOR STIRRED TANKS

Agitation of fermentation broth creates a uniform distribution of air in the media. Once you mix a solution, you exert an energy into the system. Increasing power input reduces the bubble size and this in turn increases the interfacial area. Therefore the mass transfer coefficient would be a function of power input per unit volume of fermentation broth, which is also affected by the gas superficial velocity.[2,3] The general correlation is expected to be as follows:

$$K_L a = \alpha \left(\frac{P_g}{V_L}\right)^y (v_g)^z \tag{3.6.1}$$

where $K_L a$ is the volumetric mass transfer coefficient in s^{-1}; α is proportionality factor, as a constant; P_g is the agitator power under gassing conditions in W; V_L is the liquid volume without gassing in m^3; v_g is the gas superficial velocity in m/s; and y and z are empirical constants. The mass transfer coefficient for coalescing air–water dispersion is:

$$K_L a = 2.6 \times 10^{-2} \left(\frac{P_g}{V_L}\right)^{0.4} (v_g)^{0.5} \tag{3.6.2}$$

The above correlation is valid for a bioreactor size of less than 3000 litres and a gassed power per unit volume of 0.5–10 kW. For non-coalescing (non-sticky) air–electrolyte dispersion, the exponent of the gassed power per unit volume in the correlation of mass transfer coefficient changes slightly. The empirical correlation with defined coefficients may come from the experimental data with a well-defined bioreactor with a working volume of less than 5000 litres and a gassed power per unit volume of 0.5–10 kW. The defined correlation is:

$$K_L a = 2 \times 10^{-3} \left(\frac{P_g}{V_L}\right)^{0.7} (v_g)^{0.5} \tag{3.6.3}$$

In general, coalescing systems are those where the water is relatively pure; non-coalescing systems are those where a small amount of electrolytes is in the system. These correlations

do not take into account either the non-Newtonian behaviour of biological fluids or the effect of antifoam and the presence of solids. A correlation may be applied to a non-Newtonian filamentous fermentation in the form:[2]

$$K_L a = \alpha \left(\frac{P_g}{V_L} \right)^{0.33} (v_g)^{0.56} \tag{3.6.4}$$

Comparing this with the equation for Newtonian fluids shows that the oxygen transfer coefficient for non-Newtonian fluids is less sensitive to power input changes. Thus, more power input is required to reach the same mass transfer coefficient value than in a Newtonian fluid.

The addition of antifoam has a significant effect on the value of the mass transfer coefficient. The antifoam reduces the interfacial free energy at the interface between air and water. Therefore the surface tension and the bubble size are reduced, leading to higher values of interfacial area per unit volume (a). However, k_L may decrease owing to liquid movement near the interface. This means that the mobility of the liquid could decrease at the interface, and a film of liquid generates a resistance between the liquid and gas systems. Figure 3.1 shows the linear dependency of the mass transfer coefficient with the air flow rate, as volume of air per volume of liquid media per minute. It is customary for fermentation to be shown in vvm (l l^{-1} min^{-1}) for 10, 100 and 1000 litres fermenters. A higher mass transfer coefficient can be obtained as the air flow rate is increased.

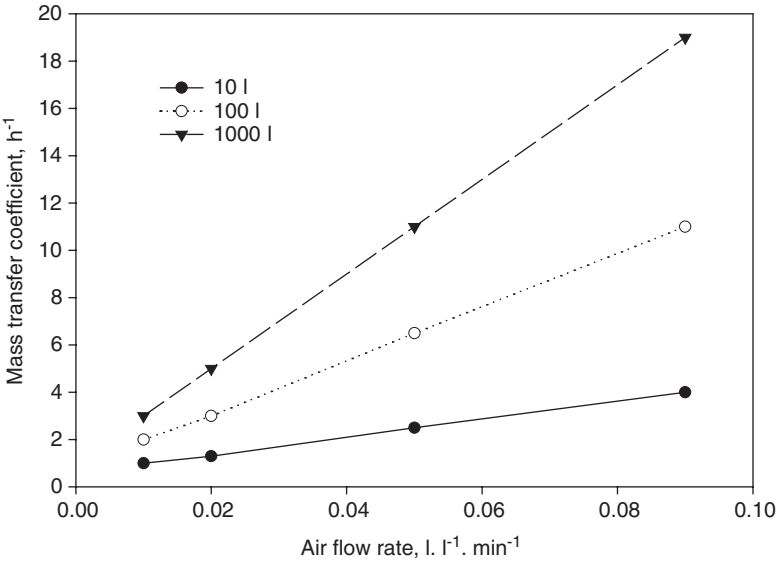

FIG. 3.1. Effect of air flow rate on oxygen transfer coefficients, $K_L a$.
(l. l^{-1}. min^{-1} = liters of air per liter of liquid per min)

3.7 GAS HOLD-UP

Most laboratory fermenters operate with a stirrer power between 10 and 20 kW/m^3, whereas large bioreactors operate at 0.5–5 kW/m^3. Virtually all large-scale operations and commercial-size continuous stirred tank reactors (CSTRs) operate mostly in a free bubble-rise regime. The most important property of air bubbles in the fermenters is their size. If the gas is dispersed into many small bubbles rather than a few large ones, more interfacial area per unit volume results. Small bubbles have a slow rising velocity. Consequently, they stay longer in contact with the liquid, which allows more time for oxygen to dissolve. The fraction of the fluid volume occupied by gas is called gas hold-up: that is, the volume fraction of gas phase to total gas–liquid volume. Small bubbles lead to higher gas hold-up, which is defined by the following equation:[4,5]

$$\varepsilon = \frac{V_G}{V_L + V_G} \tag{3.7.1}$$

where ε is the gas hold-up, V_G is the volume of gas bubbles in the reactor in m^3 and V_L is the volume of liquid in the fermenter in m^3. The bubble surface area is defined as

$$a = \frac{6\varepsilon}{d} \tag{3.7.2}$$

where d is the bubble diameter.

3.8 AGITATED SYSTEM AND MIXING PHENOMENA

Mixing is a physical operation which creates uniformities in fluids and eliminates any concentration and temperature gradients. If a system is perfectly mixed, there is homogeneous distribution of system properties. Mixing is one of the most important operations in bioprocessing. Efficient liquid mixing is essential in a bioreactor to maintain not only a uniform dissolved oxygen concentration, but also a uniform liquid concentration. To create an optimal environment in the bioreactor, agitation is required for cells to have access to all the substrates including oxygen in aerobic culture. Another aspect of an agitated system is uniform heat transfer. Most bioreactors must be able to operate at a constant uniform temperature. A jacketed system for cooling, or a cooling coil, is provided for sufficient heat transfer. The objectives of agitation and effective mixing are to circulate the fluid for sufficient time, to disperse the gas bubbles in the liquid, to have small bubbles with high interfacial area, and to maintain uniform conditions for mass and heat transfer operations.

3.9 CHARACTERISATION OF AGITATION

The following treatment of agitation is restricted to fluids that approximate to Newtonian fluids. As mixing is a complex process, the variables involved are considered together in a

dimensionless group known as the Reynolds number (*Re*). *Re* is used to characterise the behaviour of flow:

$$Re = \frac{D_i^2 N \rho}{\mu} = \frac{\text{inertia forces}}{\text{viscous forces}} \tag{3.9.1}$$

where D_i is the impeller diameter in m, N is the rotational speed of impellers in round per second (rps), ρ is the fluid density in kg/m^3, and μ is the viscosity of the fluid in kg m^{-1} s^{-1}. Fully turbulent flow exists above a Reynolds number of 10^4, whereas fully laminar flow exists below 100; in between is the transitional region. Another group of dimensionless variables that are used to characterise mixing in a vessel is the Froude number (*Fr*), which takes gravitational forces into account:

$$Fr = \frac{N^2 D_i}{g} = \frac{\text{inertia forces}}{\text{gravity forces}} \tag{3.9.2}$$

where g is gravitational acceleration in m/s^2. A third group, which is related to energy required by the agitator, is the power number. This shows the power consumption for stirring. The power consumption is related to fluid properties, the density and viscosity of the fluid, the stirrer rotation rate and the impeller diameter. Several well-known studies have shown the relation between power number and Reynolds number; the laminar region is a straight line but it depends on the shape of the impellers.[2,4,5] Marine propellers require less energy compared with flat blade turbine disks. The power in the turbulent region is proportional to $N_i^3 D_i^5$; therefore the power number is the ratio of power for the aerated fluid and the non-aerated powered system, which is:

$$N_{\text{Po}} = \frac{P}{N^3 D_i^5 \rho} \tag{3.9.3}$$

where N_{Po} is agitator power in W. The power number for laminar flow is proportional to the inverse of the Reynolds number, $N_{\text{Po}} \approx k_1/Re_i$; for turbulent flow the agitation power is proportional to $K_2 N^3 D_i^5 \rho$, where units for agitation power are in W, kW or hp.

3.10 TYPES OF AGITATOR

There are four types of agitator commonly used in the bioreactors:

- Turbine disk (Rushton)
- Turbine inclined blades
- Propeller, marine type
- Intermig

These types of agitator are used in low-viscosity systems ($\mu < 50$ kg m^{-1} s^{-1}) with high rotational speed. The typical tip speed velocity for turbine and intermig is in the region of 3 m s^{-1} a propeller rotates faster. These impellers are classified as remote clearance type, having diameters in the range 25–67% of the tank diameter.

The most common type of agitator is turbine. It consists of several short blades mounted on a central shaft. The diameter of a turbine is normally 35–45% of the tank diameter. There are four to six blades for perfect mixing. Turbines with flat blades give radial flow. This is good for gas dispersion in the media, where the gas is introduced just below the impeller, is drawn up to the blades and broken up into uniform fine bubbles.

The propeller agitator with three blades rotates at relatively high speeds of 60–300 rps; high efficient mixing is obtained. The generated flow pattern is axial flow since the fluid moves axially down to the centre and up the side of the tank.

The intermig agitator is the most recently developed agitator. This is an axial pumping impeller in which the blades are mounted with an angle opposite each other. Comparing a disk turbine agitator with an intermig agitator, this type results in a more uniform energy transfer to the fluid in the vessel. Therefore this type of agitator requires less power and less air input to obtain the same degree of mixing and the same mass transfer coefficient.

3.11 GAS–LIQUID PHASE MASS TRANSFER

There is always a limit to the liquid phase oxygen transfer for high cell density because mass transfer is limited. Actual cases are:

- In a large-scale fermenter for penicillin production; or
- In extracellular biopolymers such as xantham gum;
- In wastewater treatment with an activated sludge system

Gas and liquid systems are explained by solubility. The solubility of oxygen at room temperature is about 10 ppm; therefore the concentration of oxygen is 10 ppm (oxygen flux, N_A). The solubility of oxygen at 0 °C is double that at 35 °C. Also, the solubility decreases if the electrolyte concentration is increased. The concentrations of oxygen in the gas phase and liquid phase are related to each other by the Raoult–Dalton equilibrium law.

$$\overline{P_{Ag}} = y_A P_A = x_{AL} H_A \tag{3.11.1}$$

The above relation is rewritten in terms of concentration:

$$HC_{l,i} = C_{g,i} \tag{3.11.2}$$

Based on film theory, the oxygen flux in the gas film is equal to flux in the liquid film:

$$N_A = K_g (C_g - C_{g,i}) = K_l (C_{l,i} - C_l) \tag{3.11.3}$$

where C_{li} is oxygen concentration at interface. Let us define C_l^* oxygen concentration at equilibrium with the liquid phase. Henry's law in terms of oxygen concentration at equilibrium is

$$HC_l^* = C_g \tag{3.11.4}$$

The molar flux in terms of equilibrium concentration is:

$$N_A = K_L (C_l^* - C_l) \tag{3.11.5}$$

where K_L is the overall mass transfer coefficient. If we simplify all the resistances in liquid and gas phases, then the resistances in series are written as:

$$\frac{1}{K_L} = \frac{1}{k_l} + \frac{1}{H}\frac{1}{k_g} \tag{3.11.6}$$

If k_g is larger than k_l, then the resistance to mass transfer lies on the liquid film side.

Oxygen absorption rate is:

$$\mathrm{Q_{O_2}} = (\text{flux})\left(\frac{\text{interfacial area}}{\text{volume}}\right)$$

$$\mathrm{Q_{O_2}} = k_l(C_l^* - C_l)\left(\frac{A}{V}\right) \tag{3.11.7}$$

The interfacial area per unit volume and $a' = A/V$ is incorporated into (3.11.7):

$$\mathrm{Q_{O_2}} = k_L a'(C_l^* - C_l) \tag{3.11.8}$$

The minimum oxygen utilisation rate is $x\mu_{\max}/Y_{\mathrm{O_2}}$. If the system is mass-transfer limited, C_l approaches zero. Then the amount of oxygen absorbed is exactly equal to the amount of oxygen consumed. Equation (3.11.8) leads to the following:

$$k_l a'(C_l^* - C_l) = \frac{x\mu}{Y_{\mathrm{O_2}}} \tag{3.11.9}$$

Using the Monod rate for the specific growth rate in (3.11.9), it is reduced to following equation:

$$k_l a'(C_l^* - C_l) = \frac{x}{Y_{\mathrm{O_2}}}\left(\frac{\mu_{\max} C_l}{K_{\mathrm{O_2}} + C_l}\right) \tag{3.11.10}$$

Rearranging (3.11.10) yields the following equation:

$$Y_{O_2} k_l a'(C_l^* - C_l) = x\mu_{max}\left(\frac{C_l}{K_{O_2} + C_l}\right) \tag{3.11.11}$$

if $C_l < C_l^*$, then the concentration profile for oxygen in the liquid phase is:

$$C_l = C_l^*\left[\frac{Y_{O_2} K_{O_2} k_l a'/x\mu_{max}}{1 - Y_{O_2} C_l^* k_l a'/x\mu_{max}}\right] \tag{3.11.12}$$

Example 1.1 Effect of Carbon Source in Penicillin Production

The carbon source affects oxygen demand. In penicillin production, oxygen demand for glucose is 4.9 mol l^{-1} h^{-1}. The lactose concentration is 6.7 mol l^{-1} h^{-1}, sucrose is 13.4 mol l^{-1} h^{-1}. The yield of oxygen per mole of carbon source for CH_4 is $Y_{O_2/C} = 1.34$, $Y_{O_2/C}$ for Paraffins = 1, and $Y_{O_2/C}$ for hydrocarbon $(CH_2O)_n = 0.4$. The mass transfer coefficient $k_l a$ is for gas–liquid reactions, and the film thickness where the mass transfer takes place is δ

$$\delta \times \text{rate}\,|_{film} < k_l(C_l^* - C) \tag{E1}$$

The film thickness of the mass transfer is given

$$\delta = \frac{D_{O_2}}{k_l} \tag{E2}$$

and the reaction rate is based on elementary rate that means rate is proportional to substrate concentration to definite exponent.

$$-r_A = k_r(C^*)^\alpha \tag{E3}$$

Substituting the rate expression into (E1) leads to an inequality for mass transfer coefficient in the liquid phase:

$$k_r(C^*)^\alpha \times \frac{D_{O_2}}{k_l} < k_l(C^* - C) \tag{E4}$$

By rearranging (E4), then solving for k_l, we obtain

$$k_l > \left[\frac{k_r (C^*)^{\alpha} D_{O_2}}{C^* - C} \right]^{\frac{1}{2}} \tag{E5}$$

For $C < C^*$, (E5) is simplified and the above inequality becomes

$$k_l > \left[k_r (C^*)^{\alpha - 1} D_{O_2} \right]^{\frac{1}{2}} \tag{E6}$$

Given a value for $\alpha = 0.5$

$$k_l > \left[\frac{k_r (C^*)^{\alpha} D_{O_2}}{C^* - C} \right]^{\frac{1}{2}} \tag{E7}$$

The mass transfer coefficient is calculated for a given diffusivity coefficient and reaction rate constant at the equilibrium concentration of oxygen. When oxygen is continuously transported and removed from the liquid phase we may write:

$$\overline{Q}_{O_2} = [F_{g,in} \times \overline{P}_{O_2} - F_{g,out} \overline{P}_{O_2,out}]/VRT \tag{E8}$$

where F_g is the volumetric oxygen flow rate and $\overline{P}_{O_2}$ is the partial pressure of oxygen. Using the ideal gas law ($PV = nRT$), we then solve for moles of oxygen utilised in the bioreactor. The moles of gas transferred are calculated by the ideal gas law:

$$n_A = \frac{P_A V}{RT} = \frac{F_A}{V} \tag{E9}$$

3.11.1 Oxygen Transport

Molar transformation of oxygen is proportional to the concentration gradient of oxygen at the gas–liquid interface and oxygen dissolved in the bulk liquid phase:

$$N_{O_2} = N_A = k_l (C_i^* - C_l) \tag{3.11.1.1}$$

where N_{O_2} is oxygen flux in kmol/m^2 s, k_l is the liquid side mass transfer coefficient in m/s, C_i^* is the oxygen concentration at interface in kmol m^{-3}, and C_l is the oxygen concentration

in the bulk of liquid. The molar transformation of oxygen in the gas phase is proportional to the pressure gradient:

$$N_{O_2} = k_g(P_{O_2} - P_i^*) \tag{3.11.1.2}$$

where k_g is the gas side mass transfer coefficient in kmol m^{-2}·s, P_i^* is the interfacial partial pressure of oxygen, P_{O_2} is the partial pressure of oxygen in bulk gas. The resistances in series are explained earlier (3.11.6) which are associated with Henry's law. For the slightly soluble gas, H is greater than 4×10^4 bar·mol^{-1}, the mass transfer coefficient for gas phase, k_g, is large, and we may neglect the resistance created by the gas film; then it would be a perfect assumption to state $K_L = k_l$. The interfacial surface area created by the gas bubbles is:

$$a_i = \frac{\text{surface area of gas bubbles}}{V_L} (\text{m}^2 \cdot \text{m}^{-3}) \tag{3.11.1.3}$$

The molar flux is given by Equation 3.5.1

Gas hold-up is defined as H_o = Bubble volume/Reactor volume, which is the volume of gas per unit volume of reactor. Assume the system is an agitated vessel. Let us use Richard's data to define gas hold-up:[3]

$$\left(\frac{P}{V}\right)^{0.4} (V_S)^{0.5} = 7.63h + 2.37 \tag{3.11.1.4}$$

where P is power in hp, V is ungassed liquid volume in m^3, V_S is gas superficial velocity in $m.h^{-1}$ and h is the volume void fraction.

Example 2 Calculated Gas Hold-up

Calculate the gas hold-up for an agitated and aerated system with power input of 18 hp in an 80 m^3 vessel with gas superficial velocity of 2.6 m·min^{-1}.

$$\left(\frac{18}{80}\right)^{0.4} (2.6 \times 60\,\text{min/h})^{0.5} = 7.63H + 2.37 \tag{E1}$$

The gas hold-up can be defined by the above definition using the gas height per volume, where H is 0.6 m for aeration

$$H_o = \frac{V_g}{V_g + V_L} = \frac{0.6}{0.6 + 6.5} = 0.085 \tag{E2}$$

The calculated gas hold-up is 8.5%.

3.11.2 Diameter of Gas Bubble Formed D_0

As gas flows with fixed volumetric flow rate through an orifice gas sparger, bubbles are formed with diameter D_0. Analysis of bubble formation is based on the balance of buoyant force, as the bubbles leave the orifice and rise through the media $(\pi\Delta\rho g D_o^3)/6$ with rest of the forces resulting from the surface tension, $\pi\sigma d$.

Buoyant force = rest of force

$$\frac{\pi g \Delta P D_0^{\ 3}}{6} = \pi\sigma d \tag{3.11.2.1}$$

$$D = \left[\frac{6\sigma d}{g\Delta\rho}\right]^{\frac{1}{3}} \tag{3.11.2.2}$$

The interfacial area:

$$a = H\left(\frac{6}{D}\right) \tag{3.11.2.3}$$

Bubble residence time

$$t_b = \frac{H_L}{u_t} = \frac{\text{Height of liquid}}{\text{Gas terminal velocity}} \tag{3.11.2.4}$$

The terminal velocity for rising bubbles is

$$u_t = \frac{D\Delta\rho^2 g}{18\mu} \tag{3.11.2.5}$$

Using the following equation:

$$a' = \frac{1}{V}(nF_0)(t_b)\left(\frac{6}{D}\right) \tag{3.11.2.6}$$

where a' is the interfacial area per unit volume of liquid.

$$a' = \frac{nF_0(\mu_L/u_t)\times 6}{VD} \tag{3.11.2.7}$$

The oxygen utilisation balanced with growth gives:

$$Y_{O_2} k_L a'(C_l^* - C_l) = x\mu = x\frac{\mu_{max} C_l}{K_{O_2} + C_l} \tag{3.11.2.8}$$

given $K_S = K_{O_2}$

$$\mu = \frac{1}{x}\frac{dx}{dt} = \frac{\mu_{max} C_l}{Y_{O_2}(K_{O_2} + C_l)} \tag{3.11.2.9}$$

Useful equations similar to (3.11.12) for $C_l < C_l^*$ are sobtained.

$$C_l = C_l^* \left[\frac{Y_{O_2} K_{O_2} k_l a'/x\mu_{max}}{1 - Y_{O_2} K_{O_2} k_l a'/x\mu_{max}} \right] \tag{3.11.2.10}$$

Example 3 Calculation of Cell Density in Aerobic Culture

A strain of *Azotobacter vinelandii* is cultured in a 15 m^3 stirred fermenter for production of alginate. Under current conditions the mass transfer coefficient, $k_L a$, is 0.25 s^{-1}. Oxygen solubility in the fermentation broth is approximately 8.5×10^{-3} kg m^{-3}. The specific oxygen uptake rate is 15 mmol·g^{-1}·h^{-1}. What is the maximum cell density in the broth? If copper sulphate is accidentally added to the fermentation broth, which may reduce the oxygen uptake rate to 1.5 mmol/g h and inhibit the microbial cell growth, what would be the maximum cell density in such a case?

The oxygen uptake rate is defined as:

$$\text{OUR} = (q_{O_2})(x) = k_L a(C_{AL}^* - C_{AL}) \tag{3.11.2.11}$$

Solution

We assume all the dissolved oxygen in the fermentation broth is used or taken by microorganisms. In this case the DO is zero or the value for C_{AL} is zero since it is not given in the problem statement. Also the cell density has to be maximised; therefore the above assumption is valid. In the above equation x represents cell density, which is

$$x_{max} = \frac{k_L a C_{AL}^*}{q_{O_2}} \tag{3.11.2.12}$$

$$x_{max} = \frac{(0.25\ s^{-1})(8.5 \times 10^{-3}\ kg/m^3)}{(15\,mmol/g{\cdot}h)(1\,h/3600\,s)(1\,mol/1000\,mmol)(32\,g/1\,mol)(1\,kg/1000\,g)}$$

$$= 15937.5\,g/m^3 = 15.94\,g/l$$

Let us assume the solubility of oxygen does not affect on C^*_{AL} or k_La. The factor affected by OUR is

$$15/1.5 = 10$$

then x_{max} is:

$$x_{max} = (15.94)(10) = 159.4\ \text{g}\cdot\text{l}^{-1}$$

To achieve the calculated cell densities all other conditions must be favourable, such as substrate concentration and sufficient time.

Example 4 Oxygen Requirements for Activated Sludge in an Aerated Bioreactor

Oxygen balance for an aerated system with activated sludge is defined by a dynamic model:

$$V\frac{dC_{O_2}}{dt} = aF(S_o - S) + bV \tag{3.11.2.13}$$

The substrate in this equation is represented by biological oxygen demand (BOD), where V is the reactor volume, X is the cell density or sludge concentration, a is a constant in kg O_2 kg^{-1} BOD, b is also a constant in kg O_2 kg^{-1} MLSS, and F is the fresh feed flow rate in m^3 h^{-1}. MLSS is the mixed liquor suspended solid in mg·l^{-1} and BOD is 0.4 kg/kg MLSS. The constants for $a = 0.5$ and $b = 0.4$ are given. For a flow rate of 100 m^3·h^{-1} and initial substrate S_o is 20,000 ppm in an aeration tank volume of V = 10 m^3, what would be the BOD concentration if an oxygen rate of 2 m^3 h^{-1} is supplied, and what would be the leaving substrate concentration, S?

$$X = \frac{X_m S}{K_M + S} \quad \text{and} \quad \mu = \frac{\mu_M XS}{K_M + S} \tag{3.11.2.14}$$

Given $X = 0.5$ g/g BOD

Oxygen flow rate supplied in 2 m^3 h^{-1}:

$$\text{OTR} = (2\text{m}^3/\text{h})\left(\frac{1\ \text{kg mole}}{22.4\ \text{m}^3}\middle|\frac{32\ \text{kg}}{1\ \text{MW}}\right) = 2.86\ \text{kg/h}$$

$$S_o = 0.02\ \text{kg m}^{-3}$$

Plug in values into Equation (3.11.2.13)

$$2.86 = 0.5 \times 100 \times (0.02 - \text{S}) + 0.4 \times 0.5 \times 10$$

$$S = 0.003\ \text{kg m}^{-3}$$

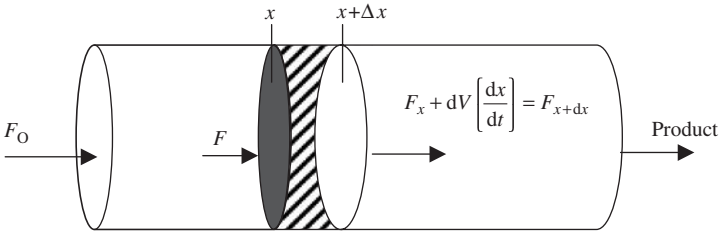

FIG. 3.2. Schematic diagram of plug flow reactor.

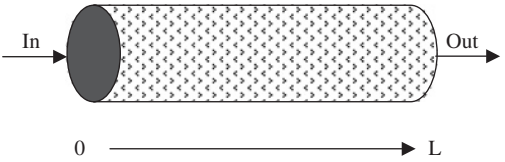

FIG. 3.3. Schematic diagram of plug flow bioreactor.

For a plug flow system we can define all the conditions in inlet and outlet streams as shown in Figure 3.2.

The residence time for an ideal plug flow system is stipulated as:

$$t_p = \int_{x1}^{x2} \frac{dx}{(dx/dt)} = \int_0^{xA} \frac{dx_A}{-r_A} \tag{3.11.2.15}$$

Generally residence time is obtained by division of working volume by volumetric flow rate.

$$\tau = \frac{V}{F} \tag{3.11.2.16}$$

The differential form shows the changes occurring along the length of tubular reactor. The plug flow bioreactor as the substrate and the product formed along the length of the tubular bioreactor is shown in Figure 3.3.

$$d\tau = \frac{dV}{F} = \frac{dx}{\left(\frac{dx}{dt}\right)} \tag{3.11.2.17}$$

The concentration profiles for substrate, product and biomass in a plug flow system are shown in Figure 3.4.

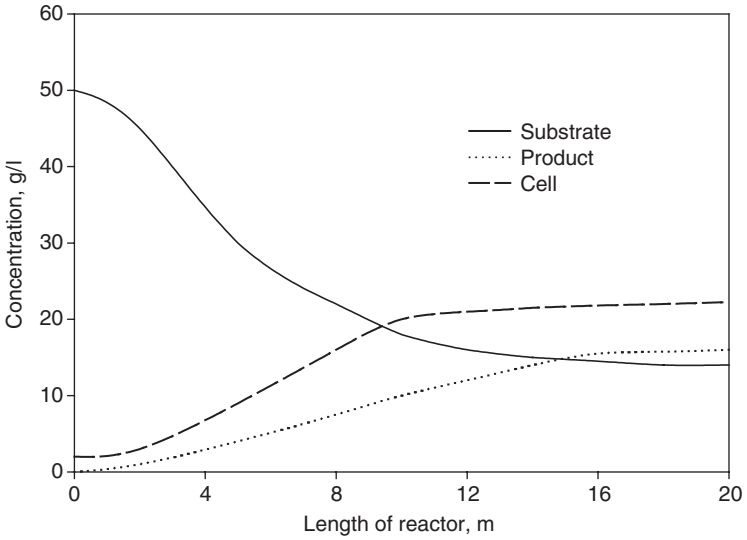

FIG. 3.4. Substrate, product and cell concentration versus length of plug flow bioreactor.

For CSTR the design equation is given below:

$$\tau_m = \frac{C_{Ao} x_A}{-r_A} \tag{3.11.2.18}$$

The rate model for a biological process is given by a Monod rate model

$$-r_A = \frac{v_{\max} SX}{K_M + S} \tag{3.11.2.19}$$

Bioreactor with the assumption of tank diameter is equal to the height of the liquid ($D_t = H$). Assume steady-state condition, no cell accumulation and no death rate:

$$\frac{F}{V}(x_0 - x) + r_x \frac{V}{v} = 0 \tag{3.11.2.20}$$

(Flow rate) (Cell in − Cell out) + Rate of cell generation = 0

Let us define μ, which is known as specific growth rate

$$\mu = \frac{r_x}{x} \tag{3.11.2.21}$$

Dilution rate is defined as the number of tank volume pass through per unit time, $D = F/V$. The residence time is defined as the time required for one unit volume of reactor to be replaced by the flow rate, $\tau = V/\nu$. When feed is sterile, there is no cell entering the bioreactor, which means $x_0 = 0$, the rate may be simplified and reduced to:

$$D_x = r_x \tag{3.11.2.22}$$

Steady-state material balance is used for cell mass.

$$\frac{F}{V}x_0 = \frac{F}{V}x - x\left(\frac{r_x}{x}\right). \tag{3.11.2.23}$$

Substituting dilution rate and specific rate into (3.11.2.23) leads to a useful relation:

$$Dx_0 = (D-\mu)(x) \tag{3.11.2.24}$$

For the case of sterile feed, (3.11.2.24) reduces to:

$$(D-\mu) = 0 \quad \text{or} \quad D = \mu \tag{3.11.2.25}$$

The general balance equation is given below:

$$V_R \frac{\mathrm{d}C_i}{\mathrm{d}t} = F(t)[C_{if} - C_i] + r_{fi} \tag{3.11.2.26}$$

At unsteady-state conditions, the change of concentration with respect to time is detectable, $\mathrm{d}S/\mathrm{d}t \neq 0$ but for steady-state conditions the leaving substrate may be constant. For a plug flow bioreactor we can treat it like a batch system.

The cell balance is:

$$-\frac{\mathrm{d}C_A}{\mathrm{d}t} = -r_A \tag{3.11.2.27}$$

The change of cell density with respect to time is given as follows:

$$\frac{\mathrm{d}x}{\mathrm{d}t} = \frac{r_x}{x}x = \mu x \tag{3.11.2.28}$$

Substituting the specific growth rate into (3.11.2.28) leads to the following differential equation.

$$\frac{\mathrm{d}x}{\mathrm{d}t} = \left(\frac{\mu_{\max} S}{K_S + S}\right) X \tag{3.11.2.29}$$

when dilution rate reaches the maximum specific rate ($D = \mu_{\max}$) wash out phenomena may take place.

Balance for S:

$$-\frac{\mathrm{d}S}{\mathrm{d}t} = \frac{X}{Y}\left(\frac{\mu_{\max} S}{K_S + S}\right) \tag{3.11.2.30}$$

For sterile media in a chemostat,

$$D_{in} = \frac{\mu_{\max} S_0}{K_S + S_0} \tag{3.11.2.31}$$

The substrate concentration is defined as

$$S = \frac{DK_S}{\mu_{\max} - D} \quad \text{and} \quad Y = \frac{X}{S_0 - S} \tag{3.11.2.32}$$

The biomass is calculated using (3.11.2.32):

$$X = Y(S_0 - S) = Y\left(S_0 - \frac{DK_S}{\mu_{\max} - D}\right) \tag{3.11.2.33}$$

Yield of biomass is defined as:

$$Y = \frac{\text{mass of cells formed}}{\text{mass of substrate consumed}}$$

Monod rate equation, $\mu = \dfrac{\mu_{\max} S}{K_S + S}$, is used to substitute into mass balance.

Substituting S into X, the following equation is obtained:

$$Dx_0 + \left(\frac{\mu_{\max} S}{K_S + S} - D\right) X = 0 \tag{3.11.2.34}$$

At steady state, the mass balance for S, $\frac{dS}{dt} = 0$, results in the following equation:

$$D(S_0 - S) = \left(\frac{\mu_{max} S}{K_S + S}\right)\frac{X}{Y} \tag{3.11.2.35}$$

The rate equation is incorporated

$$D(S_0 - S) = \frac{r_x}{Y} \tag{3.11.2.36}$$

3.12 NOMENCLATURE

N_A	Oxygen flux, kmol m^{-2} s^{-1}
k_L	Mass transfer coefficient, m/s
C^*_{AL}	Oxygen concentration in equilibrium with liquid phase at the interface, kmol/m^3
C_{AL}	Oxygen concentration in the bulk of liquid, kmol/m^3
a	Interfacial area in surface area of bubbles per unit volume of broth, m^2/m^3
$P_{O_2,i}$	Oxygen partial pressure at the interface, atm
H	Henry's law constant, atm
P_{O_2}	Oxygen partial pressure at the bulk of gas phase, atm
$-r_A$	Consumption rate of substrate A, mol l^{-1} s^{-1}
P_g	Agitator power under gassing conditions, W
V_L	Liquid volume without gassing, m^3
v_g	Gas superficial velocity, m/s
d	Bubble diameter, mm
ε	Gas hold-up, m^3/m^3
V_G	Volume of gas bubbles in the reactor, m^3
V_L	Volume of liquid in the fermenter, m^3
D_i	Impeller diameter, m
C_{li}	Oxygen concentration at interface, mmol·l^{-1}
C_l*	Oxygen concentration at equilibrium with liquid phase, mmol·l^{-1}
μ	Specific growth rate, h^{-1}
μ	Growth rate, g·l^{-1}·h^{-1}
N	Rotational speed of impellers in round per second, rps
ρ	Fluid density, kg/m^3
μ	Viscosity of the fluid, kg m^{-1} s^{-1}
Re	Reynolds number, dimensionless number
Fr	Froude number, dimensionless number
g	Gravitational acceleration, m/s^2
N_{Po}	Agitator power, W
k_g	Mass transfer coefficient in gas phase, h^{-1}

k_l Mass transfer coefficient in liquid phase, h^{-1}
Q_{O_2} Oxygen absorption rate, $mol \cdot l^{-1} \cdot h^{-1}$
Y Yield, $g \cdot g^{-1}$
y Mole fraction in gas phase
C_l^* Oxygen concentration at equilibrium with liquid phase, $mmol \cdot l^{-1}$
μ_{max} Specific growth rate, h^{-1}
μ Growth rate, $g \cdot l^{-1} \cdot h^{-1}$
D Dilution rate, h^{-1}
F Flow rate, $m^3 \cdot h^{-1}$
x Biomass concentration, $g \cdot l^{-1}$
τ Retention time, min
ν Volumetric flow rate, $ml \cdot min^{-1}$
C_i Concentration of i, $mg \cdot l^{-1}$
S Substrate concentration, $g \cdot l^{-1}$
S_0 Initial substrate concentration, $g \cdot l^{-1}$
x_A Conversion factor
H_o Gas hold-up

REFERENCES

1. Baily, J.E. and Ollis, D.F., "Biochemical Engineering Fundamentals", 2nd edn. McGraw-Hill, New York, 1986.
2. Scragg, A.H., "Bioreactors in Biotechnology, A Practical Approach". Ellis Horwood Series in Biochemistry and Biotechnology, New York, 1991.
3. Wang, D.I.C., Cooney, C.L., Deman, A.L., Dunnill, P., Humphrey, A.E. and Lilly, M.D., "Fermentation and Enzyme Technology". John Wiley & Sons, New York, 1979.
4. Doran, P.M., "Bioprocess Engineering Principles". Academic Press, New York, 1995.
5. Shuler, M.L. and Kargi, F., "Bioprocess Engineering, Basic Concepts". Prentice Hall, New Jersey, 1992.

3.13 CASE STUDY: OXYGEN TRANSFER RATE MODEL IN AN AERATED TANK FOR PHARMACEUTICAL WASTEWATER

Abstract

The treatment of pharmaceutical non-penicillin wastewater was conducted using the biological aerobic process. Oxygen transfer rate played the major role in reducing the organic pollutants of the wastewater by removing gases, oils, volatile acids and odour. The microbe used in the experiment was an ethanol producer, a type of fungus isolated from the wastewater. The optical density, COD and concentration of chemicals equivalent to carbohydrate were measured for a duration of 3–4 days aeration. Thus, the propagation of bacteria was monitored and growth rate determined. Oxygen transfer rate and mass transfer coefficient were affected by airflow rate, bubble size and agitation rate. Dissolved oxygen was shown as an indicator of microbial growth and limitation of mass transfer. The dissolved oxygen

was about 7.89 ppm from the starting point; it then dropped to 2 ppm by the end of the first day. After the second day of aeration the oxygen depletion was obviously determined since the DO meter showed 0.14 ppm. Aeration rate was 0.2–1.3 litres per minute for a working volume of 3 litres and 5–10 litres per minute for a 15 litre aerated tank. Maximum optical density was obtained with high aeration rate by the first day of aeration, 0.95 $g \cdot l^{-1}$; as the aeration was reduced the cell propagation also reduced, and the maximum cell growth was obtained by the end of the 3-day aeration with minimum air flow rate. The maximum COD and carbohydrate reduction was 58% and 90% respectively with 1.15 litre/min airflow rate in the 3 litre aeration system. The bubble size affected the mass transfer coefficient ($K_L \cdot a$). As the surface of gas exposure to liquid increased, S_1, the mass transfer coefficient, increased. As the dissolved oxygen rate dropped, $K_L \cdot a$ also decreased. $K_L \cdot a$ for the 5 and 10 $l \cdot min^{-1}$ airflow rate for a 15 litres aerated tank was 0.06 h^{-1} and 0.4 h^{-1} respectively.

3.13.1 Introduction

Aerobic wastewater treatment processes remove dissolved and colloidal organic matter in industrial wastewater. The growth and propagation of the microorganisms consume oxygen in the liquid phase. This causes the dissolved oxygen to be depleted when the microorganisms are in the exponential growth phase. However, the specific oxygen uptake of bacteria increases only slightly with increasing oxygen concentration above a certain critical concentration. To achieve the optimum oxygen transfer rate (OTR) several parameters such as airflow rate, bubble size, nature of the wastewater, agitation rate, temperature, reaction rate and propagation of the microorganisms, which influence the mass transfer rate, have to be considered.

The activated sludge process for domestic wastewater treatment was introduced to the world in 1914.[1] Since then, many studies have been conducted to improve the oxygen transfer efficiency. Among the aeration devices introduced have been a porous diffuser, a filter type diffuser, a mechanical aeration device, an orifice type diffuser and a fine-pore air diffuser. The aeration market is in a substantial state of flux in the USA today. Emphasis on high efficiency has led many intensive research programmes to aim at the evaluation of the design, operation and control processes to improve overall system performance.

The transfer of oxygen from the gas phase to the microorganism takes place in several steps. Firstly, the oxygen must travel through the gas to the gas–liquid interface, then through the bulk liquid, and finally into the microorganisms. Some researchers believe that oxygen transfer occurs significantly during bubble formation when the interfacial area exposed to the liquid is constantly renewed. On the other hand, there are other researchers who believe that significant oxygen transfer occurs during the bubble's ascent. However, it is well understood that regardless of where the transfer occurs, the rate of transfer is proportional to the contact time and area of contact between the liquid and the gas. It is found that the overall gas transfer coefficient, $K_L \cdot a$, increases while bubble size decreases down to a diameter of 2.2 mm; further reduction in bubble size results in a decrease of $K_L \cdot a$, although smaller bubbles may increase oxygen transfer efficiency.[2]

Modelling oxygen transport in the aeration system is important as it can be used as a reference for overall process performance improvement as well as process design and simulation. The oxygen transfer process mentioned above is based on the concentration gradient between

the oxygen concentration in the gas phase and in the organism. The basic model for oxygen transfer in a dispersed gas–liquid system is given by Equation (3.11.2.6).[3] For the gas side, mass transfer can be similarly defined in terms of the gas partial pressure, explained in (3.11.2.16).

Since it is usually impossible to measure the local and interface concentrations everywhere in a bioreactor, average values of the concentrations or dominant bulk concentrations and overall mass transfer coefficients are used. To know the total oxygen transfer rate in a vessel, the total surface area available for the oxygen transfer has to be determined. Thus an overall mass transfer coefficient incorporating the surface area of the bubble is used, namely $N_A = K_L{\cdot}a\ (C^* - C)$. The $K_L{\cdot}a$ value is dependent on the physicochemical properties of the bioreactor media, the physical properties of the bioreactor and the operating conditions of the vessel. The magnitude of $K_L{\cdot}a$ can be controlled by the agitation rate and the airflow rate. Oxygen is a substrate, which enhances microbial growth; however, above a certain concentration, the microbial growth becomes independent of the oxygen concentration.

In a short time period, the dynamic model shown in Equation (3.13.1.1) at quasi-steady-state condition, OTR to microbial cells would be equal to oxygen molar flow transfer to the liquid phase.[4]

$$\frac{\mathrm{d}C}{\mathrm{d}t} = K_L.a(C^* - C) - Q_{\mathrm{O}_2} X \tag{3.13.1.1}$$

At steady-state condition the oxygen concentration profile would be an exponential model:

$$\frac{C - C^*}{C_O - C^*} = \mathrm{e}^{-K_L \cdot at} \tag{3.13.1.2}$$

In reality, oxygen concentration never reaches the concentration defined in the proposed model, since the microbial activities at optimal and maximum cell density would reach the point where oxygen depletion takes place.[5]

The mass transfer, $K_L{\cdot}a$ for a continuous stirred tank bioreactor can be correlated by power input per unit volume, bubble size, which reflects the interfacial area and superficial gas velocity.[3,6] The general form of the correlations for evaluating $K_L{\cdot}a$ is defined as a polynomial equation given by (3.6.1).

The mass transfer coefficient is expected to relate gas power per unit volume and gas terminal velocity. Measurement of gas bubble velocity is troublesome in the experimental stage of aeration. Extensive research has been conducted for an explanation of the above correlation. Gas–liquid mass transfer in low viscosity fluids in agitated vessels has been reviewed and summarised as stated in (3.5.1.7)–(3.6.2):[3]

a) For coalescing air–water dispersion, when liquid is relatively pure, the mass transfer coefficient was estimated from (3.6.2) for the defined range power per unit volume:

$$V_L \leqslant 2.6\ \mathrm{m}^3;\ 500 < P_g/V_L < 10000 \tag{3.13.1.3}$$

b) For non-coalescing air–electrolyte dispersion, when there is a small amount of electrolyte in the system, the mass transfer coefficient may be correlated using (3.6.3), with the following condition for liquid volume and power per unit volume:

$$V_L \leqslant 4\ \mathrm{m}^3; 500 < P_g/V_L < 10000 \qquad (3.13.1.3)$$

The above correlations may not be valid for non-Newtonian behaviour of biological fluids, nor for the effect of antifoam or the presence of solids. A correlation proposed in the literature as stated in (3.6.4)[3] may be true for aerobic non-Newtonian fluid filamentous media of fermentation broth.

The industrial wastewater used in the experiment is considered as having non-coalescing air electrolyte dispersion. Thus the equations discussed above would be used as a theoretical model for the estimation of oxygen transfer rate in the liquid phase, and compared with the experimental data obtained.

3.13.2 Material and Method

The non-penicillin wastewater from a pharmaceutical company was collected and used in the batch aeration wastewater treatment experiment. The pharmaceutical wastewater had a clear orange colour, strong odour, contained toxic chemicals and had a COD value in the range of 3000–30,000 mg per litre. The pH of the wastewater was neutralised and monitored for each experimental run, as the bacteria would have a higher rate of propagation at neutral pH.

Two different sizes of aerated tank with working volumes of 3 and 15 litres were used. An aeration pump model 8500, 6W, with low, medium and high rates of oxygenation was used for the small tank. A gas flow meter, Cole Parmer 0–70 ml/min model 6G08 R4 was used for setting the desired airflow rate. Air bubbles entered the bottom of the tank through a gas sparger and maintained the wastewater as highly aerated. A stirrer Cafamo digital model RZR2000 in the range of 100–600 rpm was used for complete aeration in the small aeration tank. Also, a 15 litres aeration unit, model TR01 with a stirrer model RW20DZM.n, 72W, KIKA from Labortechnik, Malaysia, was used for the large aeration tank. A high-shear dispersing impeller with diameter 82 mm was used in the large system. A dissolved oxygen meter model HI9145 microprocessor, Hanna Instrument, Portugal, was used to detect and measure the amount of dissolved oxygen in the large aeration tank.

The fungus isolated from the wastewater was used as a seed culture. The media for seed culture as a starter of each experimental run was prepared by using 1.0 g of glucose and 1.0 g of peptone in 100 ml of distilled water. The nutrients and minerals were obtained from Merck. The media was sterilised in an autoclave at 121 °C, 15 psig steam pressure for 20 minutes.

Periodic samples were taken at the starting point after introducing the inocula, on the first, second and third day of each experimental run. The optical cell density, COD, carbohydrate concentration and dissolved oxygen were monitored for various air flow rates. The COD was measured by the closed reflux colorimetric method at 600 nm with a spectrophotometer using potassium dichromate as a reducing reagent.[7] All organic chemicals

that were present in the wastewater could be detected as equivalent to carbohydrates by a chemical reducing agent 3,5-dinitrosalycilic acid (DNS) which was detected by the spectrophotometer at 540 nm wavelength.[8,9]

3.13.3 Results and Discussion

An experimental run had been conducted to study the effect of airflow rate in the 3 litres aeration wastewater treatment tank. Nutrients were added in the treatment tank to ensure sufficient bacterial growth. In each experiment, the cell optical density, COD and the concentration of chemicals equivalent to carbohydrates were monitored for the duration of aeration.

Based on the experimental results shown in Figure 3.5, the COD curves showed sharp reduction in the first day of the treatment and the rates were gradually reduced when the aeration was extended until the third day. The data show that higher reduction of COD was achieved with the higher airflow rate. An airflow rate of 1.3 litres/min yielded the highest percentage of COD reduction, about 58%. On the other hand, the percentage of carbohydrate consumption also presented the similar trend with the airflow rate. Reduction of chemical equivalent to carbohydrate for the small aeration tank with airflow rates of 0.22, 0.83 and 1.3 litres/min was shown in the previous chapter, Figure 2.1. The highest percentage of carbohydrate reduction, i.e. 90%, was obtained with an airflow rate of 1.3 litres/min. The results indicated that the aerobic wastewater treatment process with the airflow rate of 0.22 to 1.14 litres/min was under oxygen transfer limitation; further process improvement can be achieved by increasing the airflow rate.

Further experiments were conducted in a large aeration tank, 15 litres batch system to study the dry weight cell density, COD, carbohydrate, dissolved oxygen and oxygen transfer modelling. Two different airflow rates, 5 and 10 litres/min, were applied. However,

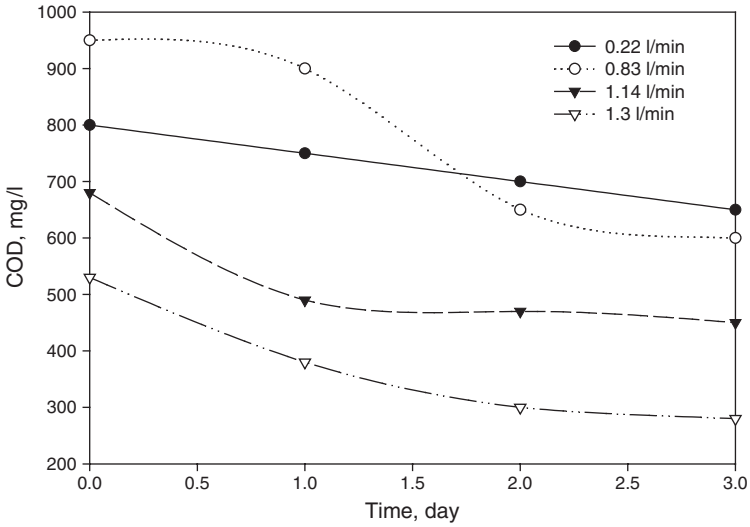

FIG. 3.5. COD reduction for small aeration tank with various airflow rates.

owing to the failure and operation limitation of the system, the system could only operate for 8 hours a day. The COD, dry cell weight, carbohydrate and dissolved oxygen concentrations for the experimental run with an airflow rate of 5 litres/min are presented in Figure 2.2 (Chapter 2).

It was expected that the dissolved oxygen for the 5 litres/min system would decrease with time as the system was running in an oxygen-limited condition. The concentration of the oxygen approached zero per cent on the third day of the experiment. Even though the system was running in an oxygen transfer limiting condition, the microbes achieved maximal growth at 24 hours. The reduction of COD and carbohydrate were 40% and 74% respectively. The experimental results showed that the system required more aeration. Therefore an airflow rate of 5 litres/min was not sufficient and the calculation of $K_L{\cdot}a$ may cause error.

When the airflow rate was doubled, there was sufficient oxygen for optimum microbial growth. Theoretically under sufficient aeration conditions, the concentration of dissolved oxygen in the system should be constant; however, because of the reason as mentioned above, the dissolved oxygen curve showed a drop in the oxygen concentration from 24 to 30 hours. The dissolved oxygen was available at around 5–8 $mg{\cdot}l^{-1}$ during the aeration. The oxygen transfer coefficient $K_L{\cdot}a$ for the above system can be estimated by applying the following mathematical model. A graph of C_L against $(rX + dC_L/dt)$ was plotted as presented in Figure 3.6 for the 15 L aeration tank system with 5 and 10 litres/min limitation. The experimental data as presented in the Figure 3.6 show good agreement for 10 litres/min airflow rate. The oxygen transfer coefficient for 5 and 10 litres/min airflow rate was 0.0509 h^{-1} and 0.3918 h^{-1} respectively. The superficial gas velocity (v_g) for the turbulent flow region was predicted to be around 0.18 m s^{-1} and 1.3 m s^{-1} for the airflow rates of 5 and 10 litres/min for the correlation given in equation 10. The experimental data were compatible with the theoretical correlation.

$$\frac{dC_L}{dt} = K_L.a(C^* - C_L) - rX \qquad (3.13.3.1)$$

3.13.4 Conclusion

$K_L{\cdot}a$ and v_g for the 10 litres/min airflow rate for the 15 litre aeration system was 0.0509 h^{-1} and 1.3 m s^{-1}. From the experimental results, the microbial growth was not at the optimum stage for the reasons mentioned earlier. Nevertheless, a reduction of around 95% can be achieved for carbohydrate reduction. However, further studies should be carried out for optimisation of the treatment and to improve COD reduction for pharmaceutical wastewater treatment.

3.13.5 Nomenclature

C_o Initial concentration, $mg{\cdot}l^{-1}$
C Concentration, $kmo{\cdot}m^{-3}$
C_L Concentration in the bulk of liquid, $kmol{\cdot}m^{-3}$

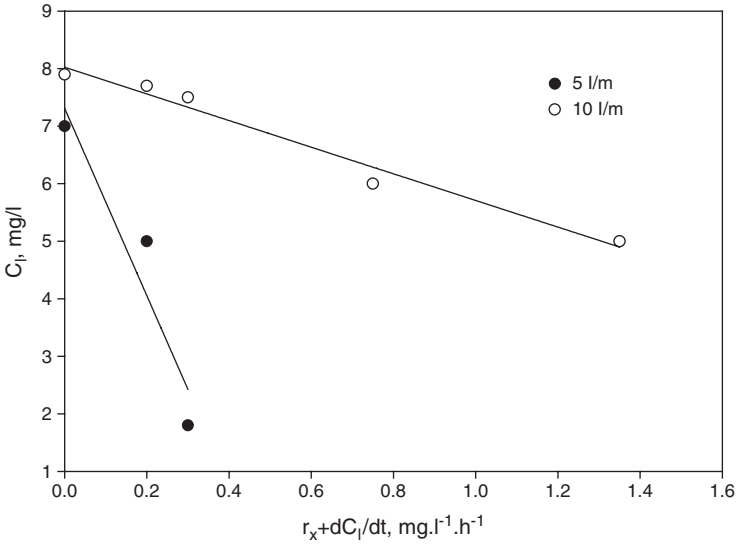

FIG. 3.6. Experimental data for dissolved oxygen concentration level in liquid phase at 5 and 10 l/m.

X	Biomass concentration, $g \cdot l^{-1}$
N_A	Molar flux, $kmol \cdot m^{-3} \cdot h^{-1}$
$K_L \cdot a$	Mass transfer coefficient in liquid phase, h^{-1}
C^*	Oxygen concentration in equilibrium with liquid phase at the interface, $kmol \cdot m^{-3}$
Q_{O_2}	Oxygen absorption rate, $mol \cdot l^{-1} \cdot h^{-1}$
P_g	Gassed power, W
V_L	Volume of liquid in the fermenter, m^3
$-r$	Consumption rate of substrate, $mol \cdot l^{-1} \cdot s^{-1}$
t	time, h

REFERENCES

1. Eckenfelder, W.W., "Industrial Water Pollution Control", 3rd edn. McGraw-Hill, New York, 2000, p. 341.
2. Scragg, A.H., "Bioreactors in Biotechnology". Ellis Horwood, New York, 1997.
3. Deronzier, G., Duchene, Ph. and Heduit, A., *Wat. Sci. Technol.*, **38** (3), 35 (1998).
4. Badino, Jr, C.A., Facciotti, M.C.R. and Schmidell, W.J., *Chem. Technol. Biotechnol*. **75**, 469 (2000).
5. Chern, J.-M. and Yu, C.-F., *Indust. Engng Chem. Res*. **36**, 5447 (1997).
6. Bailey, J. and Ollis, D.F., "Biochemical Engineering Fundamentals". McGraw-Hill, New York, 1986.
7. Greenberg, A.E., Clesceri, L.S. and Eaton, A.D., "Standard Methods for the Examination of Water and Wastewater", 18th edn. American Public Health Association, American Water and Wastewater Association, Water Environment Federation, Washington, DC., 1992.
8. Summers, J.B., *J. Biol. Chem*. **62**, 248 (1924).
9. Thomas, L.C. and Chamberlin G.J., "Colorimetric Chemical Analytical Methods". Tintometer Ltd. Salisbury, United Kingdom, 1980.

3.14 CASE STUDY: FUEL AND CHEMICAL PRODUCTION FROM THE WATER GAS SHIFT REACTION BY FERMENTATION PROCESSES

3.14.1 Introduction

Synthesis gas (syngas), a mixture of primarily CO, H_2, and CO_2, is a major building block in the production of fuels and chemicals. They are produced from several sources, including coal, oil shale, tar sands, heavy residual oil or low-grade natural gas. Catalytic processes are used to convert syngas components into a variety of fuels and chemicals such as hydrogen, methane, methanol, ethanol, acetic acid, etc.[1] Microorganisms are used as suitable biocatalysts to convert syngas into chemicals and fuels. Biological processes, although generally slower than chemical reaction, have several advantages over catalytic processes, such as higher specificity, higher yields, lower energy cost and generally greater resistance to catalyst poisoning. Furthermore, the irreversible character of biological reactions allows complete conversion and avoids thermodynamic equilibrium relations.[1]

Anaerobic bacteria are able to grow autotrophically on syngas components. They follow specific pathways to produce fuels and chemicals from inorganic waste gases.[2] The reaction occurs under mild conditions, ambient temperature and pressure with the formation of specific products. However, direct production of fuels and chemicals by gasification technology is economically unfavourable and requires very large plant.[3,4] Suitable microorganisms may be used for production of fuels and chemicals from bioconversion of syngas. Fermentation needs substrates such as CO or CO_2 to provide energy for bacterial growth, maintenance and by-products such as organic acid, alcohols, and hydrogen that result from microbial metabolism.[5,6] A recent investigation was conducted using suitable microorganisms to produce acetic acid and ethanol from H_2, CO and CO_2. The organism must be anaerobic and grow either chemolithotrophically on CO and H_2/CO_2, or chemoorganotrophically with carbon sources such as fructose, malate, glutamate or pyruvate. It was reported that CO, H_2 and CO_2 can be converted to acetate by several bacteria such as *Clostridium aceticum*, *Acetobacterium woodii*, *Clostridium ljungdahlii* and *Clostridium thermoaceticum*.[7,8]

Generally, bacteria in the fermentation process require substrates like glucose, sucrose, malate or acetate as carbon sources to obtain energy for growth and maintenance for synthesis of organic acids, alcohols and hydrogen, which are liberated in the course of microbial metabolism.[9,10] It is believed that for oxidation of CO, acetyl coenzyme A is required to enter CO into the citric acid cycle. *Rhodospirillum rubrum* is capable of producing carbon monoxide dehydrogenase (CODH) to facilitate the oxidation process.[11] It was stated that synthetic gases were converted to molecular hydrogen with the aid of several photosynthetic

---

This case study was contributed by:
Habibollah Younesi[1], Ghasem Najafpour[2], Mohamed Abdul Rahman[3]
[1]Department of Environmental Health, Faculty of Natural Resources and Marine Science, Tarbiat Modress University (TMU), Nour, Mazandaran, Iran.
[2]School of Chemical Engineering, Noshirvani Institute of Technology, University of Mazandaran, Babol, Iran.
[3]School of Chemical Engineering, Engineering Campus, Universiti Sains Malaysia Seri Ampangan, 14300 Nibong Tebal, S.P.S., Pulau Pinang, Malaysia.

bacteria, for instance *Clostridium aceticum*, *Acetobacterium woodii, Clostridium ljungdahlii* and *Clostridium thermoaceticum*, which are able to produce fuels and chemicals.[6,7]

Purple non-sulphur phototrophic anaerobic bacteria use light (photons) to produce hydrogen by a biological route. The metabolites of photosynthetic bacteria are organic acids or carbon monoxide as the energy source. Bacteria grown on carbon monoxide produce molecular hydrogen and carbon dioxide and generate no by-products. The carbon monoxide dehydrogenase (CODH) from methanogenic bacteria is the key enzyme in CO metabolism.[12] It has been reported that light and acetate are present during hydrogen formation, in which light is required for hydrogen evolution and acetate is not consumed during hydrogen production.[13] Reports in the literature state that *R. rubrum* is grown on organic components. Photoheterotrophic growth is based on most intermediate metabolites in the tri-carboxylic acid (TCA) cycle. The major pre-course in this pathway is an acetylating agent for the synthesis of other components and coenzyme A (CoA). Acetyl coenzyme A is the key component for entering the TCA cycle. In this cycle, molecular hydrogen and carbon dioxide are continuously evolved.[14]

In the past decade, an increasing interest in biological utilisation of gaseous substrates has developed in several bioprocesses for fuel synthesis.[12,15] Production of chemicals and fuels from gaseous substrates was demonstrated in biocatalytic processes. It was also reported that biological processes are used to convert gaseous substrates such as CO/H_2 or CO_2/H_2 to ethanol and acetate at ambient temperature and atmospheric pressure.[16] The reactions are generally carried out in the aqueous phase where microorganisms are suspended as free cells or in flocs. The advantages of microbial processes are stated as the product specificity, yielding few by-products, and high process yield. Also, the resistance of biocatalysts has been found to be higher than chemical catalysts. In industrial gas streams, chemical catalysts are easily inhibited by trace contaminants, such as H_2S and COS. Therefore, the economic attraction of biological processes in the development of suitable biocatalysts to ferment gaseous substrates to valuable products has been considered.[17,18]

In the present study, a strictly anaerobic bacterium, *Clostrdium ljungdahlii*, was used to investigate ethanol and acetate production by bioconversion of syngas with various total pressures of syngas in a series of batch bioreactors. The significant aspect of this fermentation was to investigate the bioconversion of syngas to commercial fuel. The effects of initial total pressure of syngas on microbial cell population, substrate and product inhibition in the culture media were also studied.

3.14.2 Kinetics of Growth in a Batch Bioreactor

When microbial cells are incubated into a batch culture containing fresh culture media, their increase in concentration can be monitored. It is common to use the cell dry weight as a measurement of cell concentration. The simplest relationships describing exponential cell growth are unstructured models. Unstructured models view the cell as an entity in solution, which interacts with the environment. One of the simplest models is that of Malthus:[19]

$$\frac{dx}{dt} = \mu x \tag{3.14.2.1}$$

where S is cell dry weight in $g \cdot l^{-1}$, μ is specific growth rate in h^{-1}, and t is time in hours. This model predicts unlimited growth with time. We can propose an inhibition term to provide limited growth which is dependent on cell concentration. We assume that the limiting substrate is consumed according to first-order kinetics:

$$\frac{dS}{dt} = -k_S S \tag{3.14.2.2}$$

where S is substrate concentration in $g \cdot l^{-1}$ and k_S is first-order rate constant in h^{-1}. We also assume that the substrate is converted with a fixed yield factor:

$$Y_{x/S} = -\frac{\Delta x}{\Delta S} = -\frac{x - x_o}{S - S_o} \tag{3.14.2.3}$$

where $Y_{x/S}$ is yield coefficient in g cell/g substrate, x_0 is inoculum concentration and S_0 is initial substrate concentration in $g \cdot l^{-1}$, respectively. Rearranging (3.14.2.3) gives:

$$S = \frac{x_o + Y_{x/S} S_o - x}{Y_{x/S}} \tag{3.14.2.4}$$

Maximum cell dry weight is inoculum size plus coefficient yield multiplied by inoculum concentration, with the assumption that substrate is converted to biomass:[19,20]

$$x_m = x_0 + Y_{x/S} S_0 \tag{3.14.2.5}$$

Inserting (3.14.2.5) into Equation (3.14.2.4) yields:

$$S = \frac{x_m - x}{Y_{x/S}} = \frac{x_m}{Y_{x/S}} \left(1 - \frac{x}{x_m} \right) \tag{3.14.2.6}$$

Applying the chain rule principle on the right-hand side of (3.14.2.2):

$$\frac{dS}{dx} \frac{dx}{dt} = -k_S S \tag{3.14.2.7}$$

Introducing yield coefficient into (3.14.2.7):

$$\frac{dx}{dt} = k_S Y_{x/S} S \tag{3.14.2.8}$$

Inserting Equation (3.14.2.6) into Equation (3.14.2.8) gives:

$$\frac{dx}{dt} = kx_m\left(1-\frac{x}{x_m}\right) \tag{3.14.2.9}$$

Equation (3.14.2.9) contributes to the postulated model which is induced by an inhibition factor for the population growth rate. Assuming that the inhibition is second-order with respect to cell dry weight (x^2), then the equation becomes:[19]

$$\frac{dx}{dt} = \mu_m x\left(1-\frac{x}{x_m}\right) \tag{3.14.2.10}$$

where μ_m is maximum specific growth rate in h^{-1}. This equation is known as the Riccati equation, which can be easily integrated to give the logistic equation:

$$x = \frac{x_o e^{\mu_m t}}{1-(x_o/x_m)(1-e^{\mu_m t})} \tag{3.14.2.11}$$

The logistic equation leads to a lag phase, an exponential initial growth rate and a stationary population of concentration (x_m). In a population, it is often the case that the birth rate decreases as the population itself increases. The reasons may vary from increased scientific or cultural sophistication to a limited food supply.

It is useful to develop a more general population model that accommodates birth and death rates that are not necessarily constant. Initially, living cells are inoculated into the batch bioreactor containing the nutrients to begin the growth process. Suppose that the population changes only by the occurrence of births and deaths, and there is no immigration from the outside environment under consideration. It is customary to track the growth or decline of population in terms of its birth rate and death rate. To describe the above discussion in mathematical form, the Malthus function can be written for the species that is growing after inoculation:

$$\frac{dx_1}{dt} = \mu x_1 \tag{3.14.2.12}$$

To include a linear decreasing function of the population size, the second-order cell population inhibition is considered:

$$\mu = \mu_m\left(1-\frac{x_1 x_2}{x_m^2}\right) \tag{3.14.2.13}$$

where x_1 is growing cells in $g\cdot l^{-1}$ and x_2 is declining cells as a result of either the toxic by-products or depletion of nutrient supply. Substituting (3.14.2.12) into (3.14.2.13), gives

$$\frac{dx_1}{dt} = \mu_m x_1\left(1-\frac{x_1 x_2}{x_m^2}\right) \tag{3.14.2.14}$$

The products that inhibit the cell population in the bioreactor and that promote the cell population gives:

$$\frac{\mathrm{d}x_2}{\mathrm{d}t} = kx_2 \tag{3.14.2.15}$$

where x_1 and x_2 are cell species in $g \cdot l^{-1}$, and k is the decline or promotion constant in h^{-1}. This means that k is negative when the cell population is inhibited by toxic chemicals, and k is positive when the cell population is promoted by nutrient. Integrating Equation (3.14.2.14) yields:

$$x_2 = x_{\mathrm{O}_2} \mathrm{e}^{kt} \tag{3.14.2.16}$$

Inserting (3.14.2.16) into (3.14.2.14) provides:

$$-\frac{\mathrm{d}x_1}{\mathrm{d}t} + \mu_m x_1 = x_1^2 \frac{x_{\mathrm{O}_2} \mu_m}{x_m^2} \mathrm{e}^{kt} \tag{3.14.2.17}$$

Equation (3.14.2.17) shows the form of the Bernoulli equation that is a first-order differential equation. By substituting (3.14.2.18)

$$u = \frac{1}{x_1}, \quad \text{and} \quad -\frac{\mathrm{d}x_1}{\mathrm{d}t} = x_1^2 \frac{\mathrm{d}u}{\mathrm{d}t} \tag{3.14.2.18}$$

u is new dependent variable. Transfer (3.14.2.17) into the linear equation:

$$\frac{\mathrm{d}u}{\mathrm{d}t} + \mu_m u = \frac{x_{\mathrm{O}_2} \mu_m}{x_m^2} \mathrm{e}^{kt} \tag{3.14.2.19}$$

which is a first-order linear differential equation of the form

$$\frac{\mathrm{d}y}{\mathrm{d}x} + P(x)y = Q(x) \tag{3.14.2.20}$$

By multiplying through with the integrating factor $e^{\int P(x)\mathrm{d}x}$ the solution is

$$y = \mathrm{e}^{-\int P(x)\mathrm{d}x} \left[\int Q(x) \mathrm{e}^{\int P(x)\mathrm{d}x} \mathrm{d}x + B \right] \tag{3.14.2.21}$$

Applying this general procedure to the integration of (3.14.2.19), gives

$$u = \mathrm{e}^{-\int \mu_m \mathrm{d}t} \left[\int e^{\int \mu_m dt} \left(\frac{x_{\mathrm{O}_2} \mu_m}{x_m^2} \right) \mathrm{e}^{kt} \mathrm{d}t + B \right] \tag{3.14.2.22}$$

Then,

$$u = \mathrm{e}^{-\mu_m t} \left[\left(\frac{x_{\mathrm{O}_2} \mu_m}{x_m^2} \right) \int \mathrm{e}^{(k+\mu_m)t} \mathrm{d}t + B \right] \tag{3.14.2.23}$$

By integrating (3.14.2.23),we obtain:

$$u = \left(\frac{x_{\mathrm{O}_2}}{x_m^2} \right) \left(\frac{\mu_m}{k+\mu_m} \right) \mathrm{e}^{kt} + B\mathrm{e}^{-\mu_m t} \tag{3.14.2.24}$$

Substituting (3.14.2.18) into (3.14.2.24) yields:

$$x_1 = \frac{1}{\left(\frac{x_{\mathrm{O}_2}}{x_m^2} \right) \left(\frac{\mu_m}{k+\mu_m} \right) \mathrm{e}^{kt} + B\mathrm{e}^{-\mu_m t}} \tag{3.14.2.25}$$

Solving (3.14.2.25) for initial value problems and applying pure culture media with a single species (x), gives:

$$x = \frac{x_0 \mathrm{e}^{\mu_m t}}{1 - \left(\frac{x_0}{x_m} \right)^2 \left(\frac{\mu_m}{k+\mu_m} \right) [1 - \mathrm{e}^{(k+\mu_m)t}]} \tag{3.14.2.26}$$

Equation (3.14.2.26) is the novel population equation, which describes the cell population with inhibition or promotion.[19,20]

3.14.3 Effect of Substrate Concentration on Microbial Growth

Equation (3.14.2.11) predicts the cell dry weight concentration with respect to time. The model shows the cell dry weight concentration (x) is independent of substrate concentration. However, the logistic model includes substrate inhibition, which is not clearly seen from Equation (3.14.2.11).

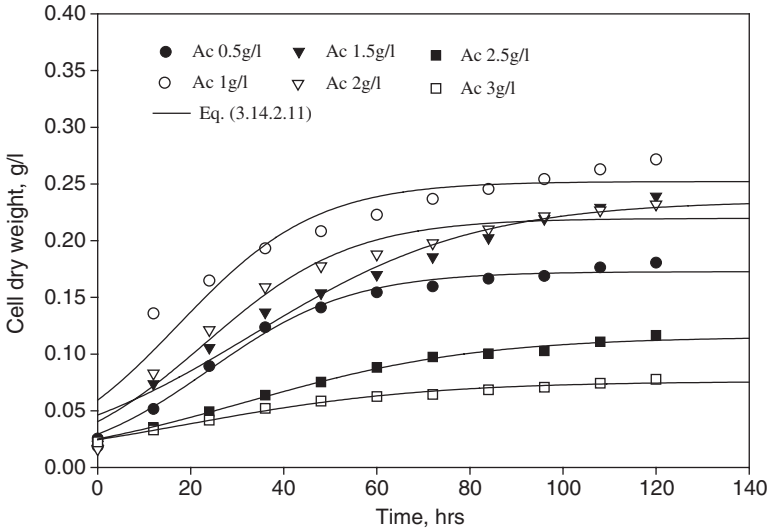

FIG. 3.7. Cell dry weight of *R. rubrum* grown on various acetate concentrations at an agitation speed of 200 rpm and light intensity of 1000 lux.

Figure 3.7 shows the growth of *R. rubrum* in a batch fermentation process using a gaseous carbon source (CO). The data shown follow the logistic model as fitted by (3.14.2.11) with the solid lines, which also represent an unstructured rate model without any lag phase. The software Sigma Plot was used to fit model (3.14.2.11) to the experimental data. An increase in concentration of acetate in the prepared culture media did not improve the cell dry weight at values of 2.5 and 3 $g \cdot l^{-1}$ acetate, as shown in Figure 3.7. However, the exponential growth rates were clearly observed with acetate concentrations of 0.5–2 $g \cdot l^{-1}$ in the culture media.

It was found that the substrate consumption rate followed first-order kinetics with respect to substrate concentration.[21,22] The expression of substrate consumption with time is written in a first-order differential equation:

$$-\frac{dS}{dt} = k_S S \tag{3.14.3.1}$$

where k_S is the substrate consumption rate constant in h^{-1}.

After separating the variables, (3.14.3.1) was solved by integration and the initial conditions were implemented ($t_0 = 0$, $S = S_0$). The resulting expression is

$$S = S_0 \exp(-k_S t) \tag{3.14.3.2}$$

where S_0 is initial substrate concentration in $g \cdot l^{-1}$.

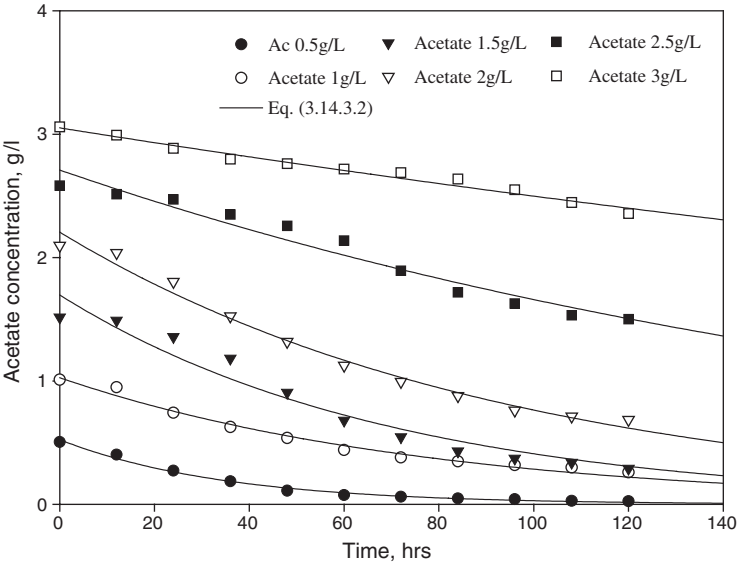

FIG. 3.8. Acetate reduction in batch cultivation of *R. rubrum* at an agitation speed of 200 rpm and light intensity of 1000 lux.

Figure 3.8 shows the time course consumption of varying acetate concentrations in batch culture for 120 h. An alternative way to describe substrate utilisation of microorganisms is to use first-order reaction kinetics, i.e. (3.14.3.2). The software Sigma Plot 5 was used to compare the fitted equation with the experimental data. Acetate concentration (3 $g \cdot l^{-1}$) was slightly decreased while the reduction of acetate concentration for 1–2 $g \cdot l^{-1}$ was significantly higher. Acetate conversion dropped from 73% to 23% when acetate concentration was doubled from 1.5 to 3 $g \cdot l^{-1}$. This indication may represent inhibition of substrate in the batch media to retard the microbial growth rate. The objective of variation in acetate concentration was to investigate and identify a suitable acetate concentration for desired cell population and hydrogen production from synthesis gas.

When microbial cells were incubated into a batch culture containing fresh culture media, an increase in cell concentration was observed. It is common to use cell dry weight as a measurement of cell concentration. The simplest relation describes the exponential growth as an unstructured model. Microbial cell growth is an autocatalytic reaction where the growth rate is proportional to the cell concentration initially present in the media.[23] In fact, the microbial populations in which there is increase in biomass are accompanied by an increase in the number of cells. The practicalities for growing bacteria in suitable culture depend on both the type of organisms and the system being employed, but the microbial growth theory is applied universally.[19] The batch system is a closed system, which would only maintain cell viability for a limited time, and the growth cycle changes progressively from one phase to another in the remaining media and environmental conditions.[24] The logistic equation leads to an exponential initial growth rate and a stationary population of

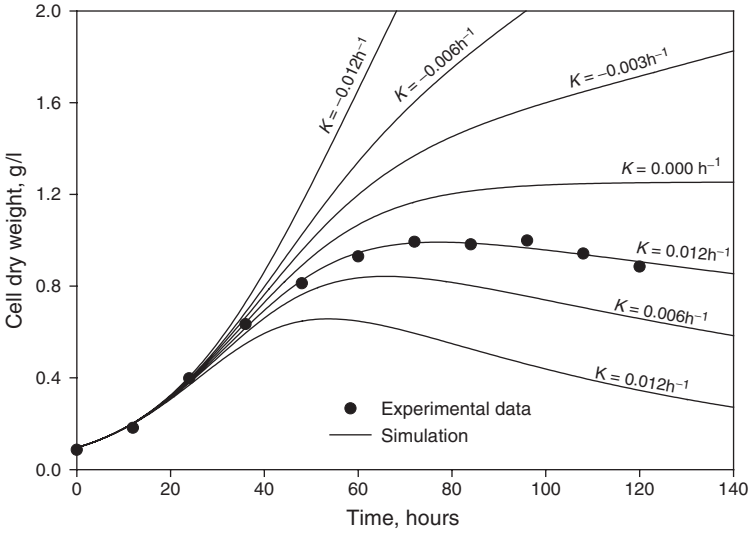

FIG. 3.9. Growth simulation of *C. ljungdahlii* on synthesis gas in batch bioreactor, the experimental data are average values.

concentration (x_m). But the logistic equation does not predict the death phase of microorganisms after the stationary phase. In this research, a modified equation was introduced which can predict the death phase of bacteria after the stationary phase. Figure 3.9 shows the simulation of the cell dry weight versus time. Equation (3.14.2.1) fitted fairly with experimental data. The simulated value was plotted with various values of k in Figure 3.9. k is a constant value, which is associated with the promotion or decline of the cell population in the batch system. On the other hand, the negative value of k shows the promotion of cell population whereas a positive value of k shows a decline in the cell population. The maximum cell dry weight concentration (x_m) was 1.2 g·l^{-1}, when the inhibition value was 0.003 h^{-1}. The maximum cell dry weight reached 1.5 g·l^{-1} when the growth inhibition ($k = 0$) was not observed. The determination coefficient of the fit (R^2) was 0.997.

3.14.4 Mass Transfer Phenomena

The simplest theory involved in mass transfer across an interface is film theory, as shown in Figure 3.10. In this model, the gas (CO) is transferred from the gas phase into the liquid phase and it must reach the surface of the growing cells. The rate equation for this case is similar to the slurry reactor as mentioned in Levenspiel.[20]

The rate of CO transport from the bulk gas into the gas and liquid films is as follows:

$$r'_{CO} = k_{CO,gas} a_i (P_{CO,gas} - P_{CO,i}) \tag{3.14.4.1}$$

$$r'_{CO} = k_{CO,liquid} a_i (C_{CO,i} - C_{CO,liquid}) \tag{3.14.4.2}$$

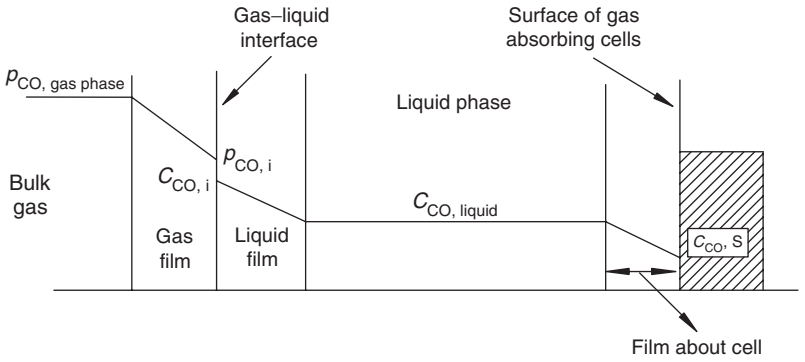

FIG. 3.10. The film theory for mass transfer.

where r'_{CO} is rate of mass transfer for component CO in $mol \cdot l^{-1} \cdot h^{-1}$; $k_{CO,gas}$ and $k_{CO,liquid}$ are the mass transfer coefficients in gas and liquid phases in m/h, respectively; a_i is the interfacial area in $m^2 \cdot m^{-3}$; $P_{CO,gas}$ and $P_{CO,i}$ are partial pressure of gaseous substrate CO at gas phase and interface in atm, respectively; and $C_{CO,i}$ and $C_{CO,liquid}$ are concentrations of component CO in the interface and liquid phase in mol/l, respectively.

Because the interface region is thin, the flux across a thin film will be at steady state. Therefore, the transfer rate to the gas–liquid interface is equal to its transfer rate through the liquid-side film. Thus,

$$k_{CO,gas} a_i (P_{CO,gas} - P_{CO,i}) = k_{CO,liquid} (C_{CO,i} - C_{CO,liquid}) \tag{3.14.4.3}$$

At the interface, the relation between $P_{CO,i}$ and $C_{CO,i}$ is given by the distribution coefficient, called Henry's constant (H) for gas–liquid systems. Thus,

$$P_{CO,i} = HC_{CO,i} \tag{3.14.4.4}$$

Substituting (3.14.4.4) into (3.14.4.3), gives

$$k_{CO,gas} a_i (P_{CO,gas} - P_{CO,i}) = k_{CO,liquid}\ a_i \left(\frac{P_{CO,i}}{H} - C_{CO,liquid} \right) \tag{3.14.4.5}$$

Rearranging (3.14.4.5) for $P_{CO,i}$, gives

$$P_{CO,i} = \frac{k_{CO,gas} a_i P_{CO,gas} + k_{CO,liquid} a_i C_{CO,liquid}}{\frac{k_{CO,liquid} a_i}{H} + k_{CO,gas} a_i} \tag{3.14.4.6}$$

Substituting (3.14.4.6) into (3.14.4.1), gives

$$r'_{CO} = \frac{k_{CO,gas} a_i k_{CO,liqiuid} a}{\frac{k_{CO,liquid} a}{H} + k_{CO,gas} a} \left(\frac{P_{CO,gas}}{H} - C_{CO,liquid} \right) \tag{3.14.4.7}$$

Rearranging (3.14.4.7), gives

$$r'_{CO} = \frac{1}{\frac{1}{k_{CO,liquid} a_i} + \frac{1}{H k_{CO,gas} a_i}} \left(\frac{P_{CO,gas}}{H} - C_{CO,liquid} \right) \tag{3.14.4.8}$$

which results in a relation between the overall mass transfer coefficient, $K_L a$ and the physical parameters of the two-film transport, k_{gas} and k_{liquid}.

$$\frac{1}{K_L a} = \frac{1}{k_{CO,liquid} a_i} + \frac{1}{H k_{CO,gas} a_i} \quad \text{and} \quad C^* = \frac{P_{CO,gas}}{H} \tag{3.14.4.9}$$

For slightly soluble gas, such as CO, Henry's constant is large.[19,20] Thus, $k_{CO,gas}$ is considerably larger than $k_{CO,liquid}$. That makes $K_L a$ equal to $k_{CO,liquid} a_i$. Thus, essentially, all the resistances to mass transfer lie on liquid-film side. Therefore,

$$r'_{CO} = K_L a (C^*_{CO} - C_{CO,liquid}) \tag{3.14.4.10}$$

where $K_L a$ is the overall volumetric mass transfer coefficient, C^* is concentration of CO in equilibrium with the bulk gas partial pressure (mol·l^{-1}) and $C_{CO,liquid}$ is the concentration of CO in the bulk liquid (mol·l^{-1}).

The reaction rate ($-r_{CO}$) for a constant volume batch reactor system is equal to the rate of mass transfer (r'_{CO}):

$$r'_{CO} = -r_{CO} = -\frac{1}{V_L} \frac{dN_{CO,gas}}{dt} = -\frac{dC_{CO,gas}}{dt} = \frac{dC_{CO,liquid}}{dt} \tag{3.14.4.11}$$

Then, substituting (3.14.4.11) into (3.14.4.8), yields

$$-r_{CO} = -\frac{1}{V_L} \frac{dN_{CO,gas}}{dt} = \frac{K_L a}{H} (P_{CO,gas} - P_{CO,liquid}) = \frac{K_L a}{H} \Delta p \tag{3.14.4.12}$$

where

$$\frac{H}{K_L a} = \frac{1}{H k_{CO,gas} a} + \frac{1}{k_{CO,liquid} a} \tag{3.14.4.13}$$

Henry's constant (H) for CO at 30 and 38 °C is 1.116 and 1.226 atm · l · mmol^{-1} CO.[19,20,25]

Based on assumption, the rate of reaction is absolutely controlled by the mass transfer process, the dissolved CO in liquid phase penetrates into the cell, then microorganisms rapidly utilise the transferred CO in the reaction centre. These phenomena may not be justified for the fresh inocula entering the culture media; however, once the culture is dominated by active organisms, the concentration of CO in gas phase decreases as the propagation of microorganisms increases. Therefore, the concentration of CO in the liquid phase decreases nearly to zero. That justifies making an assumption, i.e. $P_{\mathrm{CO,liquid}} = 0$. This means that the CO molecules available in the liquid phase are rapidly utilised by the microorganisms. Thus, the rate of mass transfer can be proportional to the partial pressure of CO in the gas phase as expected by (3.14.4.12). Therefore, (3.14.4.14) can be simplified in the regime of mass transfer control by the following expression:[15,17]

$$-\frac{1}{V_L}\frac{\mathrm{d}N_{\mathrm{CO,gas}}}{\mathrm{d}t} = \frac{K_L a}{H} P_{\mathrm{CO,gas}} \tag{3.14.4.14}$$

The plot of the rate of disappearance of CO per volume of liquid in the serum bottles versus partial pressure of CO in the gas phase based on (3.14.4.14) could give the constant slope value of $K_L a/H$. Henry's constant is independent of the acetate concentration but it is only dependent on temperature. The overall volumetric mass transfer coefficient can be calculated based on the above assumption. The data for various acetate concentrations and different parameters were plotted to calculate the mass transfer coefficient.

Figure 3.11 illustrates the mass transfer coefficient for batch-grown *R. rubrum* and was computed with various acetate concentrations at 200 rpm agitation speed, 500 lux light intensity, and 30 °C. As the experiment progressed, there was an increase in the rate of carbon monoxide uptake in the gas phase and a gradual decrease in the partial pressure of carbon monoxide. Also, a decrease in the partial pressure of carbon monoxide was affected by acetate concentration in the culture media. The value of the slope of the straight line increased with the decrease in acetate concentrations, i.e. 2.5 to 1 g·l^{-1}. The maximum mass transfer coefficient was obtained for 1 g·l^{-1} acetate concentration ($K_L a = 4.3 \cdot \mathrm{h}^{-1}$). The decrease in mass transfer coefficient was observed with the increase in acetate concentration. This was due to acetate inhibition on the microbial cell population as acetate concentration increased in the culture media. The minimum $K_L a$ was 1.2 h^{-1} at 3 g·l^{-1} acetate concentration.

3.14.5 Kinetic of Water Gas Shift Reaction

Since there are various specific growth rates and different values of rate constants while substrate concentration varies, therefore mix inhibition exists. Andrew[26] incorporated a substrate inhibition model[27] in the Monod equation; the modified Monod equations with second-order substrate inhibition are presented in (3.14.5.1) and (3.14.5.2).[16,17]

$$\mu = \frac{\mu_m P_{\mathrm{CO,liquid}}}{K_P + P_{\mathrm{CO,\,liquid}} + P^2_{\mathrm{CO,\,liquid}}/K_i} \tag{3.14.5.1}$$

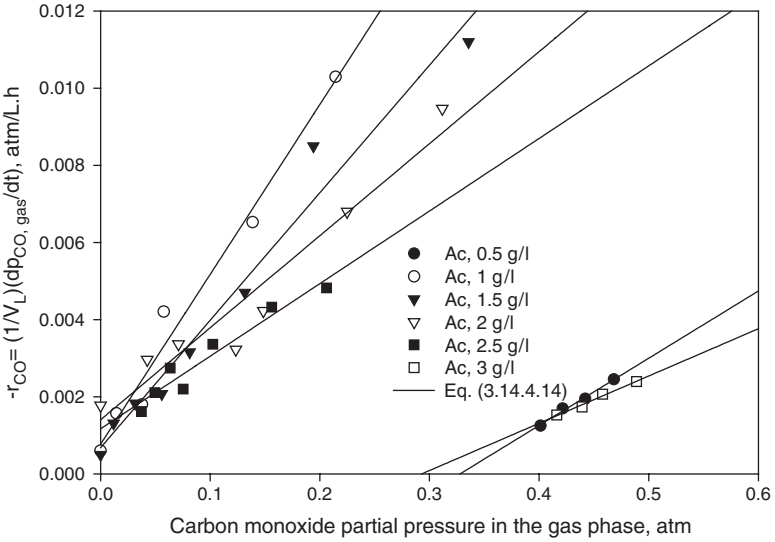

FIG. 3.11. Rate of CO uptake by *R. rubrum* with various acetate concentrations at an agitation speed of 200 rpm and light intensity of 500 lux.

$$q_{\mathrm{CO}} = \frac{q_m p_{\mathrm{CO,\,liquid}}}{K'_p + P_{\mathrm{CO,liquid}} + P^2_{\mathrm{CO,liquid}}/K'_i} \tag{3.14.5.2}$$

where K_i and K'_i are the substrate inhibition constants. To obtain the maximum specific growth rate and Monod constant, a linear model of $1/\mu$ versus $1/P_{\mathrm{CO,liquid}}$ was plotted to fit the experimental data in a linear regression model. Equations (3.14.5.2) and (3.14.5.3) are rearranged for the linearisation model to compute the substrate inhibition constants as shown below:[16,17]

$$\frac{P_{\mathrm{CO,liquid}}}{\mu} = \frac{K_p}{\mu_m} + \frac{P_{\mathrm{CO,liquid}}}{\mu_m} + \frac{P^2_{\mathrm{CO,liquid}}}{\mu_m K_i} \tag{3.14.5.3}$$

$$\frac{P_{\mathrm{CO,liquid}}}{q_{\mathrm{CO}}} = \frac{K'_p}{q_m} + \frac{P_{\mathrm{CO,liquid}}}{q_m} + \frac{P^2_{\mathrm{CO,liquid}}}{q_m K'_i} \tag{3.14.5.4}$$

The experimental data followed the predicted model and the line represents the above stated function. The presented data indicate that the range of concentrations in this study exhibited an observed substrate inhibition. The experimental data from the current studies were observed to be fit with the predicted model based on Andrew's modified equations.

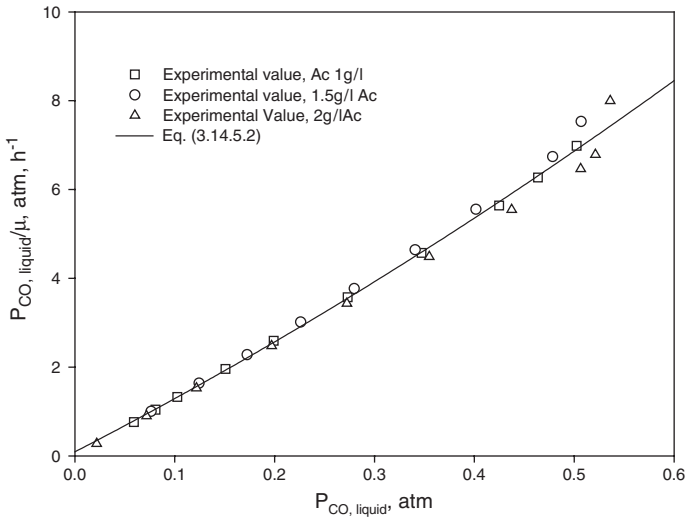

FIG. 3.12. Quadratic model based on (3.14.5.2) with substrate inhibition at an agitation speed of 200 rpm and light intensity of 500 lux.

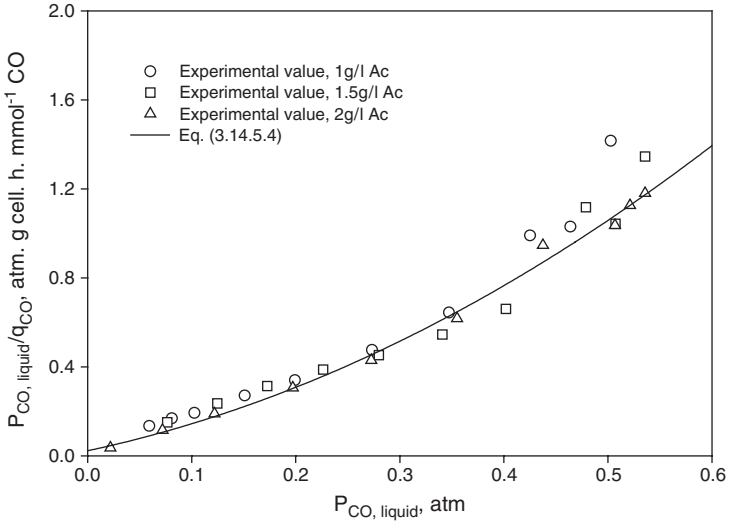

FIG. 3.13. Quadratic model based on (3.14.5.4) with substrate inhibition at agitation speed of 200 rpm and light intensity of 500 lux.

Figures 3.12 and 3.13 show the kinetic parameter evaluation of (3.14.5.2) and (3.14.5.4), i.e. μ_m, q_m, K_P, *and* K'_P. The inhibition phenomena were examined for the growth rate and the rate of CO uptake, respectively. The experimental data followed the quadratic manner as presented in the (3.14.5.2) and (3.14.5.4), respectively. The Sigma Plot 5 was used to

calculate coefficients of (3.14.5.2) and (3.14.5.4). The specific growth rate and CO uptake rate was considered at 1, 1.5 and 2 $g \cdot l^{-1}$ acetate concentrations, light intensity at 500 lux and 200 rpm agitation speed.

Table 3.1 shows the kinetic parameters for cell growth, rate models with or without inhibition and mass transfer coefficient calculation at various acetate concentrations in the culture media. The Monod constant value, K_M, in the liquid phase depends on some parameters such as temperature, initial concentration of the carbon source, presence of trace metals, vitamin B solution, light intensity and agitation speeds. The initial acetate concentrations in the liquid phase reflected the value of the Monod constants, K_P and K'_P. The average value for maximum specific growth rate (μ_m) was 0.01 h^{-1}. The value

TABLE 3.1. *Kinetic parameters and rate models with and without inhibition mass transfer coefficients*

Acetate concentration						
(g · l-1)	0.5	1.0	1.5	2.0	2.5	3.0
Growth kinetics						
x_0, g/l	0.029	0.059	0.046	0.040	0.025	0.025
μ_m, h^{-1}	0.066	0.068	0.042	0.064	0.040	0.040
x_m, g/l	0.173	0.252	0.235	0.220	0.115	0.076
R^2, %	99.3	92.7	97.2	97.0	99.3	99.0
Substrate consumption rate						
Ac_0, g/l	0.53	1.03	1.697	2.21	2.71	3.01
k_{A_c}, h^{-1}	0.029	0.128	0.142	0.011	0.005	0.002
R^2, %	99.1	98.4	95.4	98.6	96.0	97.6
Hydrogen yield						
$Y_{H_2/CO}$, %	—	83.0	85.7	70.4	—	—
R^2, %	—	97.0	99.6	99.1	—	—
Mass transfer						
K_La, h^{-1}	—	4.3	3.2	2.3	—	—
R^2, %	—	96.0	92.0	99.4	—	—
Monod equation						
μ_m, h^{-1}	—	0.057	0.095	0.125	—	—
K_p, atm	—	0.345	0.403	0.530	—	—
R^2, %	—	95.0	94.1	94.4	—	—
Andrew's equation						
K_p, atm	—	0.015	—	—	—	—
μ_m, h^{-1}	—	0.010	—	—	—	—
K_i, atm	—	10.3	—	—	—	—
R^2, %	—	99.7	—	—	—	—
K'_p, atm	—	0.032	—	—	—	—
q_m, mmol $CO \cdot g^{-1}$cell $\cdot h^{-1}$	—	1.10	—	—	—	—
K'_i, atm	—	13.0	—	—	—	—
R^2, %	—	99.5	—	—	—	—

of μ_m was double that of μ_m reported in the literature.[27] The CO uptake rate (q_m) was 1.1 mmol $\cdot$ g^{-1}cell $\cdot$ h^{-1} for 1 g $\cdot$ l^{-1} acetate. The CO uptake rates were a few times higher than the previous data cited in the literature.[27] The Monod saturation constant for growth (K_P) was exactly 0.015 atm. The K_P value was very small because of substrate depletion as a result of the fast microbial growth.

3.14.6 Growth Kinetics of CO Substrate on *Clostridium ljungdahlii*

Growth-dependence of microbial cells on CO was proposed by equation of Andrew, that substrate inhibition was included as:[26]

$$\mu = \frac{\mu_{\mathrm{m,CO}} C^*_{\mathrm{CO}}}{K_{\mathrm{CO}} + C^*_{\mathrm{CO}} + (C^*_{\mathrm{CO}})^2/K_{\mathrm{i}}} \tag{3.14.6.1}$$

where μ is the specific growth rate in h^{-1}, $\mu_{\mathrm{m,CO}}$ is the maximum specific growth rate for CO in h^{-1}, C^*_{CO} is carbon monoxide concentration in the gas phase in equilibrium with the liquid phase in mmol CO $\cdot$ l^{-1}, K_{CO} is the Monod constant for CO in mmol CO $\cdot$ l^{-1} and K_i is the inhibition constant in mmol CO $\cdot$ l^{-1}. C^*_{CO} in the gas phase was calculated based on Henry's law, which relates partial pressure of CO to Henry's law constant ($C^*_{\mathrm{CO}} = P_{\mathrm{CO,gas}}/H$). Using (3.14.6.1), modified to drive an equation to predict what CO concentration should be used at any cell dry weight to maintain maximum cell dry weight:

$$\frac{C^*_{\mathrm{CO}}}{\mu} = \frac{K_{\mathrm{CO}}}{\mu_{\mathrm{m,CO}}} + \frac{C^*_{\mathrm{CO}}}{\mu_{\mathrm{m,CO}}} + \frac{(C^*_{\mathrm{CO}})^2}{\mu_{\mathrm{m,CO}} K_i} \tag{3.14.6.2}$$

Figure 3.14 shows the quadratic equation of growth-dependence of CO by *C. ljungdahlii* with various initial pressures in experiments repeated three times . It was shown that CO transfer increased by augmentation of CO concentration (C_{CO}) and was easily used by *C. ljungdahlii* in the culture media. Cultures of *C. ljungdahlii* exhibited CO inhibition in batch cultivation. The inhibition constant was obtained at 2.0 mmol CO/l. The reason may be due to the formation of ethanol, which damages the functions of *C. ljungdahlii* in the culture media. The inhibition of ethanol may reduce by its removal through a continuous process because ethanol is a volatile product. The maximum specific growth rate and Monod constant for CO were 0.022 h^{-1} and 0.078 mmol CO $\cdot$ l^{-1}, respectively.

3.14.7 Acknowledgements

The present research was made possible through a long-term IRPA grant No. 01-02-05-3223EA011, sponsored by the Ministry of Science, Technology and Innovations

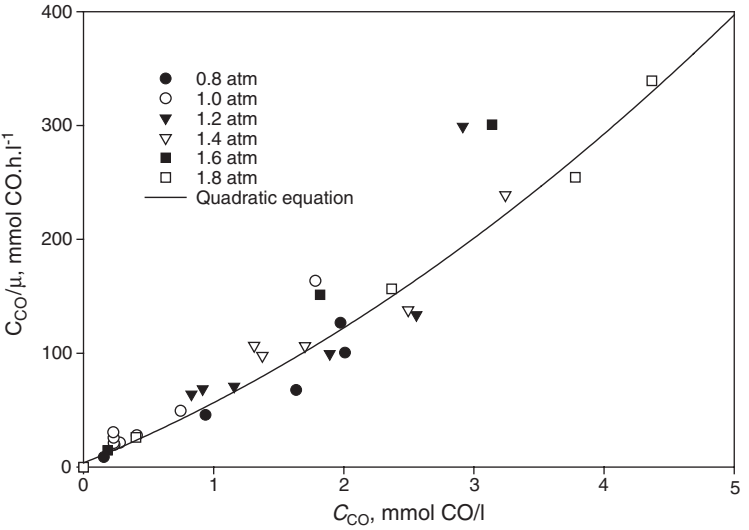

FIG. 3.14. Growth-dependence on CO concentration represented by the equation of Andrew with various syngas pressures.

(MOSTI), Malaysia, and Universiti Sains Malaysia (USM). The authors thank the RCMO and MOSTI scientific panels, Universiti Sains Malaysia and MOSTI for their financial support.

3.14.8 Nomenclature

a_i	Interfacial area per unit volume of liquid, m^{-1}
B	Integration constant
C^*_{CO}	CO concentration in gas phase equilibrium with liquid phase, mmol CO·l^{-1}
$C_{CO,liquid}$	CO concentration in the liquid phase, mol·l^{-1}
$C_{CO,i}$	CO concentration in the interface, mol·l^{-1}
CO	Carbon monoxide
CO_2	Carbon dioxide
H	Henry's law constant
H_2	Hydrogen
k	Decline or increase in growth constant by products, h^{-1}
$k_{CO,gas}$	Mass transfer coefficient in the gas phase, m·h^{-1}
$k_{CO,liquid}$	Mass transfer coefficient in the liquid phase, m·h^{-1}
K_i	Inhibition constant for CO, mmol CO·l^{-1}
K'_i	Substrate inhibition constant for uptake rate, atm
K_{CO}	Monod constant for CO, mmol CO·l^{-1}
K_S	First-order rate constant, h^{-1}
$N_{CO,gas}$	Number of moles of CO component in the gas phase, atm
K_La	Overall gas–liquid mass transfer coefficient, m·h^{-1}

K_P	Monod saturation constant for growth, atm
K'_P	Monod saturation constant for substrate uptake, atm
$P_{CO,i}$	Partial pressure of CO in interface, atm
$P_{CO,gas}$	Partial pressure of CO in the gas phase, atm
$P_{CO,liquid}$	Partial pressure of CO in the liquid phase, atm
q_{CO}	Substrate uptake rate per unit of cell weight, mmol $\cdot$ g^{-1} cell $\cdot$ h^{-1}
q_m	Maximum specific substrate uptake rate, mmol $\cdot$ g^{-1} cell $\cdot$ h^{-1}
S_0	Initial substrate concentration, g$\cdot$l^{-1}
S	Substrate concentration, g$\cdot$l^{-1}
t	Time, h
V_L	Volume of liquid phase, l
x_0	Initial cell dry weight concentration, g$\cdot$l^{-1}
x	Cell dry weight concentration, g$\cdot$l^{-1}
x_m	Maximum cell dry weight concentration, g$\cdot$l^{-1}
$Y_{x/S}$	Yield coefficient of cell substrate, g cell$\cdot$g^{-1} substrate
μ	Specific growth rate, h^{-1}
μ_m	Maximum specific growth rate, h^{-1}
$\mu_{m,CO}$	Maximum specific growth rate for CO, h^{-1}

REFERENCES

1. Klasson, K.T., Ackerson, M.D. and Clausen, E.C., *Enzyme Microb. Technol*. **14**, 602 (1922).
2. Braun, M., Mayer, F. and Gottschlk, G., *Arch. Microb*. **123**, 288 (1981).
3. Czerink, S., French, R., Feik, C. and Chorenet, E., In *Proceedings of the 2000 DOE Hydrogen Production Review*. NREL/CP-570-28890 (2000).
4. George, J.T. and Iacovos, A.V., *Ind. J. Chem. Res*. **37**, 1410 (1998).
5. Asada, Y. and Miyake, J., *J. Biosci. Bioengng* **88**, 1 (1991).
6. Gyoo, Y.J., Jung, R.K., Ji-Young, P. and Sunghoon, P., *Int. J. Hydrogen Energy*. **27**(66), 601 (2002).
7. Kellum, R. and Drake, H.L., *J. Bacteriol*. **160**(1), 466 (1984).
8. Klasson, K.T., Gupta, A., Clausen, E.C. and Gaddy, J.L., In *14th Symposium on Biotechnology for Fuels and Chemicals, May 11–15*, Gatlinburg, TN, USA (1992).
9. Ghirardi, M.L., Kosourov, S., Tsygankov, A. and Seibert, M., In *Proceedings of the 2000 DOE Hydrogen Production Review*. NREL/CP-570-28890 (2000).
10. Gonzalez, J.M. and Robb, F.T., *FEMS Microbiol. Lett*. **191**, 243 (2000).
11. Kerby, R.L., Hong, S.S., Ensign, S.A., Coppoc, L.J. and Ludden, R.G.P., *J. Bacteriol*. **174**(16), 5284 (1992).
12. Philips, J.R., Clausen, E.C. and Gaddy, J.L., *Appl. Biochem. Biotechnol.* **45/46**, 145 (1994).
13. Pin-Ching, M. and Weaver, P.F., In *Proceedings of the 2000 DOE Hydrogen Production Review*. NREL/CP-570-28890 (2000).
14. Tanisho, S., Kuromoto, M. and Kadokura, N., *Int. J. Hydrogen Energy* **23**(7), 559 (1998).
15. Vega, J.L., Clausen, E.C. and Gaddy, J.L., *Biotechnol. Bioengng* **34**, 774 (1989).
16. Vega, J.L., Clausen, E.C. and Gaddy, J.L., *Biotechnol. Bioengng* **34,** 785 (1989).
17. Vega, J.L., Holmberg, V.L., Clausen, E.C. and Gaddy, J.L., *Arch. Microbiol.* **151**, 65 (1989).
18. Pezacka, E. and Wood, H.G., *Arch. Microbiol*. **137**, 63–69.
19. Bailey, J.E. and Ollis, D.F., "Biochemical Engineering Fundamentals", 2nd edn. McGraw-Hill, New York, 1986.
20. Levenspiel, O., "Chemical Reaction Engineering". John Wiley, New York, 1999, pp. 523–535.

21. Koku, H., Eroglu. I., Gunduz, U., Yucel, M. and Turker, L., *Int. J. Hydrogen Energy* **27**, 1315 (2002).
22. Koku, H., Eroglu, I., Gunduz, U., Yucel, M. and Turker L., *Int. J. Hydrogen Energy* **28**, 381–388.
23. Scragg, A.H., "Bioreactors in biotechnology: a practical approach". New York: Ellis Horwood, 1991, pp. 26–109.
24. Nielsen, J. and Villadsen, J., "Bioreaction Engineering Principles". New York: Plenum Press, 1994, pp. 229–435.
25. Geankoplis, C.J., "Transport Processes and Separation Process Principles", 4th edn. Prentice Hall, New Jersey, 2003, p. 988.
26. Andrew, J.F., "*Biotechnol. Bioeng*ng **10**, 707 (1968).
27. Klasson, K.T., Lundback, K.M.O., Clausen E.C. and Gaddy J.L., *J. Biotechnol.* **29**, 177 (1993).

CHAPTER 4

Fermentation Process Control

4.1 INTRODUCTION

The growth of an organism in a bioreactor has to be controlled, so the operators must have sufficient information about the state of the organism and the bioreactor conditions. Monitoring a fermentation process may need basic knowledge of the bioprocess, and the running conditions should be recorded. Also any changes taking place must be reported. As most bioreactors operate under sterile conditions, information can be obtained by taking samples or by in situ measurements. There are direct and indirect measurements of microbial growth. The methods of direct growth measurement are cell optical density, total cell counters, Coulter counter, cell dry weight, packed cell volume and optical detectors. Growth is based on absorbance/light scattering. The absorbance of culture is generally measured with spectrophotometer at a wavelength of about 600 nm.[1] The indirect measurements of cell growth are based on cellular components, measurements of ATP, bioluminescence, substrate consumption and product formation, oxygen uptake rate, respiration quotient and heat evolution.

There are many types of bioreactor used in bioprocesses such as the continuous stirred tank reactor (CSTR), plug flow column, bubble column bioreactor, packed bed bioreactor, fluidized bed bioreactor, trickle bed bioreactor, tower fermenter, air lift bioreactor, and immobilized bioreactor. The most common form is the simple stirred tank bioreactor. This is a well-stirred tank designed for perfect mixing; under these conditions the fluid is uniform everywhere. The standard CSTR is normally operated under aerobic conditions. In the CSTR bioreactor, the routine measurement of temperature, pressure, pH and dissolved oxygen condition is carried out through a set of experimental runs. In equipped bioreactors, the basic instrumentation may provide sufficient information to determine the total mass or volume of the bioreactor contents, the agitation speed, power and torque, redox potential, dissolved carbon dioxide concentration, gas and liquid flow rates into the fermentation vessel, with analysis of oxygen and carbon dioxide contents of the exhaust gas. Basic control facilities normally consist of temperature control, pH and dissolved oxygen content, control foaming and level control for steady operation.[2] Figure 4.1 shows the usual instrumentation for a bioreactor with an agitating motor and all control units. The vessel is jacketed for cooling and heating, with a separate side unit of a temperature-controlled bath. Steam is used for sterilisation and elimination of contaminants.

Measurements and control of the fermentation conditions are very important for bioprocess control as they provide knowledge and hence a better understanding of the operation.

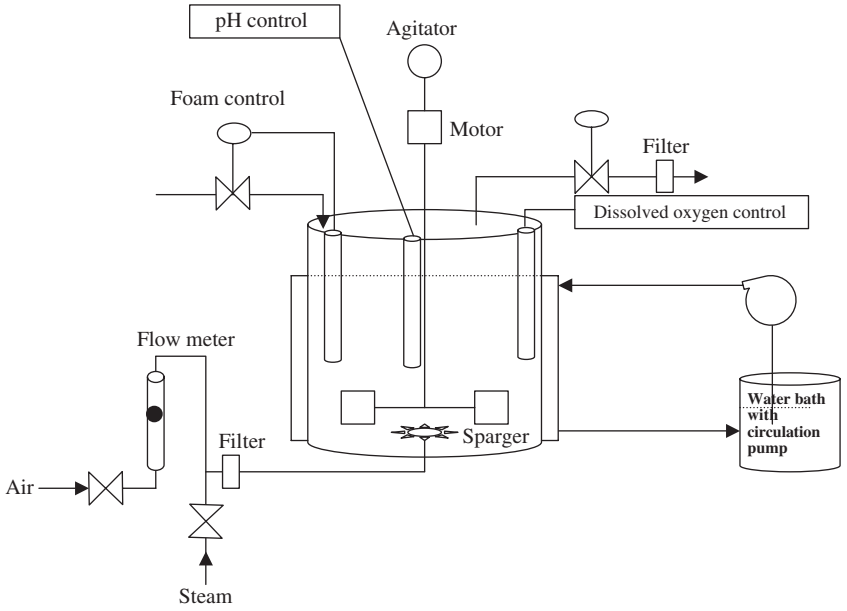

FIG. 4.1. Instrumentation control for continuous stirred tank (CSTR) bioreactor.

The recorded data can be used to improve the process. Controlling operating conditions is important for maintaining viable cells, and it makes the interpretation of fermentation data easier.

The growth of living organisms is a bioprocess, which is regulated by a complex interaction between the physical, chemical and biological conditions of the living environment of fermentation and the biochemical processes inside the cells. The most important part of the instrumentation is concerned with physical factors such as temperature, pressure, agitation rate, power input, flow rates and mass quantities. Such measurements are standard in all industrial bioprocesses. Chemical factors are utilised for measuring oxygen and carbon dioxide concentrations in the exit gas and by aqueous phase pH. However, for measurements of redox potential, dissolved oxygen and dissolved carbon dioxide concentration, dependability is more important in the instrumentation of controlled units.

Several different instruments are available for measuring flow rates of gases (the inlet air and the exhaust gas). The simplest instrument is a flow meter for measuring flow rates, such as a rotameter, which provides a visual readout or is fitted with a transducer to give an electrical output. Thermal mass flow meters are increasingly popular, especially for laboratory- and pilot-scale reactors. In these devices, gas flows through a heated section of tubing and the temperature differences across this heated section are directly related to the mass flow rate. The flow rate of the liquid can be monitored with electromagnetic flow meters, but it is very costly. Use of a normal rotameter for low flow rate may cause some error. Therefore a level sensor is used. As the liquid level reaches the probe, the conductivity of

TABLE 4.1. *Bioreactor operating parameters*

Physical	Chemical	Biological and cell properties
Time	pH	Respiratory quotient
Temperature	Redox potential	O_2 uptake rate
Pressure	Dissolved oxygen	CO_2 production rate
Agitation speed	Dissolved carbon dioxide	Optical density
Total mass	O_2 in gas phase	Cell concentration
Total volume	CO_2 in gas phase	Viability of cells
Volume feed rate	Lipid	Cell morphology
Viscosity of culture	Carbohydrates	Cellular composition
Power input	Enzyme activities	Protein, DNA, RNA
Foam	Nitrogen	ATP/ADP/AMP
Shear	Ammonia if present	NAD^+/NADH
Mixing time	Mineral ions	Activities of whole cells
Circulation time	Precursors	Specific growth rate
Gas holdup	Inducers	Specific oxygen uptake rate
Bubble size distribution	Growth stimulants	Specific substrate uptake rate
Impeller flooding	Effective mineral as catalysts	Metabolites
Broth Rheology	Products	Growth factors
Gas mixing patterns	Volatile products	Growth inhibitors
Liquid level	Conductivity	Biomass composition
Reactor weight	Off gas composition	Biomass concentration
Foam level		

the media surrounding the probe changes, so monitoring is based on the conductance of the liquid level. Such capacitance probes or conductance probes are used to detect foam on the surface of the bioreactor.

Table 4.1 summarises the physical, chemical and biological parameters that should be collected during fermentation. The lack of reliable biological sensors in most fermentation processes results in poor feedback of biological information. Biochemical engineers are able to sort out information using material balance to estimate quantities such as respiration quotient, oxygen uptake rate and carbon dioxide production rate. Analysis of bioreactor off-gas is very important for any material balance that leads us to biological activities of viable organisms in the bioprocess.

4.2 BIOREACTOR CONTROLLING PROBES

In bioprocess plant instrumentation and process control, variables are very important. Reading and processing the information about the biosystem and monitoring the cells are the major aims of the process instrumentation. Controlling pH, measuring the dissolved oxygen in the fermentation broth and controlling foam are all considered major parameters and necessary biological information for large-scale operations. The main objective is to

operate a bioreactor without any problems. To do so we need to be familiar with all the controlling facilities and process instrumentation. Application of biosensors in the bioreactors is very common, so it is good to know how the controlling unit operates.

4.3 CHARACTERISTICS OF BIOREACTOR SENSORS

The sensor in a bioreactor provides knowledge and information on the state of the process and also supplies suitable operational data for the process variables. Some of the physical and chemical effects on the bioreactor have to be translated to electrical signals, which can be amplified and then displayed on a monitor or recorder and used as an input signal for a controlling unit. In practice, the response of most of the processes follows a signoidal S-shaped curve. A similar response would be obtained if a dissolved oxygen probe were suddenly removed from a vessel with depleted oxygen levels, the probe transferred to a vessel with water maintained with supplied air passed through the aqueous phase, and the system agitated for sufficient oxygen transfer so that it is saturated in the liquid phase.[3] Air bubbles may interfere with sensor signals, and false readings can mislead the bioreactor operation.

The dynamics given by the instrument response signal comprise several processes taking place in series. Thus the transfer of oxygen from the air into the liquid causes reduction in the rate of mass transfer due to the reduction in concentration gradient as the existing driving forces. The rate of change of the oxygen concentration in the gas phase is determined by the magnitude of the time constant, which depends on the gas volume and the mass transfer coefficient $K_L a$. The rate of change in the dissolved oxygen with time is determined by the magnitude of the time constant for the liquid phase, which depends on the volume of the liquid and the mass transfer coefficient. Finally the time-varying liquid-phase concentration is registered by the dissolved oxygen electrode and is transmitted as an output signal. Again the signal is affected by the electrode time constant. Thus the process dynamics are determined by a combination of the time constants for gas phase, liquid phase and the electrode dynamics.

Figure 4.2 shows the computer simulation results of such a dynamic aeration experiment. The *y*-axis shows the response fraction with respect to time. The gas phase response is typically first-order, and the liquid phase shows some lag or delay on the signal. The electrode response is much more delayed for a slow-acting electrode.[4]

4.4 TEMPERATURE MEASUREMENT AND CONTROL

Control of temperature for fermentation vessels is required because of the narrow range of optimal temperature. Most fermenters operate around 30–36 °C, but certain fermentation may require control of the temperature in a range of 0.5 °C; this can easily be obtained in large bioreactors.[4,5] To maintain bioreactor temperature within the limited range, the system may require regulation of heating and cooling by the control system. Heat is generated in the fermenter by dissipation of power, resulting in an agitated system; heat is also generated by the exothermic biochemical reactions. In exothermic reactions, the fermentation

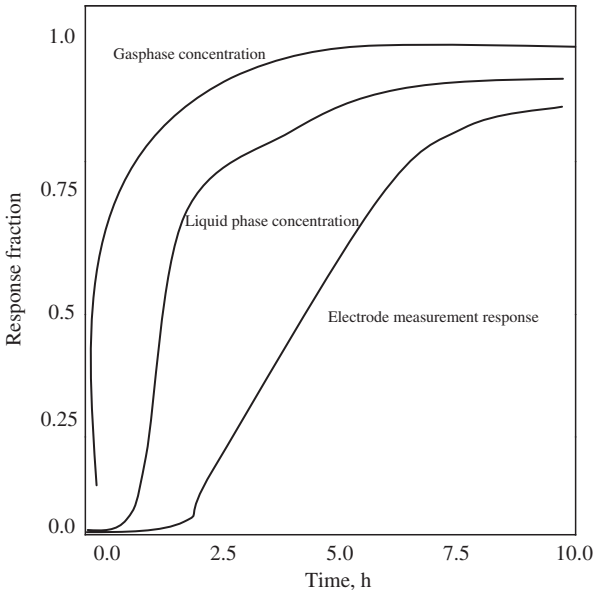

FIG. 4.2. Computer simulation of a dynamic aeration experiment with a slow DO electrode.

vessel requires cooling. At the start and end of the fermentation, the heat generation rate is very low, although the systems are normally heated to achieve the desired temperature. There are many alternatives for measuring and controlling the bioreactor temperature. These include glass thermometers, thermocouples, thermistors, resistance thermometers and miniature integrated circuit devices. Thermal units capable of giving direct electrical output signals are favoured for control purposes. Thermocouples are cheap and simple to use, but they are rather low in resolution and require a cold junction. Thermistors are semiconductors, which exhibit a change in electrical conductivity with temperature. They are very sensitive and inexpensive; they give a highly nonlinear output. Modern transistorised, integrated circuits combine the features, but they often display a more linear output. Platinum resistance thermometers are usually preferred as standard. To avoid contamination of the bioreactor the thermometers are usually fitted into thin-walled stainless-steel pockets, which project into the bioreactor. The pockets are filled with a heat-conducting liquid to provide good contact and to speed the instrument response. The resistance thermometer works on the principle that electrical resistance changes with temperature. It requires the passage of a current to develop a measurable voltage, which is proportional to the temperature. However, the current should not be so large that it causes heating effects. The changes in the electrical resistance of the electrical wires to the thermometer can be quite large, with their resistance being affected by changes in the ambient temperature. These effects can be eliminated by using separate wires to supply and sense the current. The advantages of platinum resistance detectors are their high accuracy, high stability and that the linear output signal can be obtained in normal temperature ranges. The high temperature

steam for sterilisation may require separate instrumentation within a temperature range of 50–150 ºC.[5]

The energy balance for the bioreactor is shown by the following equation. As the fermenter is used batch wise, the heat balance is mathematically expressed as stated in (4.4.1):

$$\mathrm{d}\left[\frac{MC_PT}{\mathrm{d}t}\right] = \mu X(-\Delta H_X)V - UA[T - T_j] \tag{4.4.1}$$

where M is the total mass of the reactor for batch system is constant in kg, C_P is the specific heat in $\mathrm{kJ{\cdot}kg^{-1}{\cdot}K^{-1}}$, T is the temperature of the fermentation in K and t is time in s. Also, the term μX is the rate of cell growth in $\mathrm{kg{\cdot}m^{-3}{\cdot}s^{-1}}$, V is the working volume of the bioreactor in $\mathrm{m^3}$, and $-\Delta H_x$ is the exothermic heat generated inside the fermenter in $\mathrm{kJ{\cdot}kg^{-1}}$ cell. Under steady-state conditions of controlled temperature, $\mathrm{d}T/\mathrm{d}t = 0$, the rate of heat accumulation is zero and the rate of heat production is equal to the heat transfer by the jacketed system. The rate of heat production is related to the rate of cell growth. The rate of heat transfer is the mean temperature gradient, $[T - T_j]$, multiplied by overall heat transfer coefficient (U) in $\mathrm{kJ{\cdot}m^{-2}{\cdot}s^{-1}{\cdot}K^{-1}}$. T_j is the temperature of the coolant in the jacket in Kelvins (K).

4.5 DO MEASUREMENT AND CONTROL

The dissolved oxygen content of the fermentation broth is also an important fermentation parameter, affecting cell growth and product formation. The rate of oxygen supply to the cell is often limited because the solubility of oxygen in fermentation is low. Unfortunately, measurement and control of dissolved oxygen under bioreactor conditions is a challenging problem. The low solubility of oxygen makes the measurements very difficult. There are several methods to determine the concentration of dissolved oxygen. Most DO probes use a membrane to separate the point of measurement from the broth; all probes require calibration before use. Three main methods are used: (1) the tubing method; (2) use of mass spectrometer probes; and (3) electrochemical detectors. In the tubing method, an inert gas flows through a coil of permeable silicon rubber tubing, which is immersed in the bioreactor. Oxygen diffuses from the broth, through the wall of the tubing and into a flow of inert gas passing through the tube. The concentration gradient exists because of the diffusion of oxygen into the inert gas. Then the concentration of oxygen gas in the inert gas is measured at the outlet of the coil by an oxygen gas analyser. This method has a relatively slow rate of response, of the order of several minutes. The advantages of this method are that it is simple and in situ sterilisation is easily carried out. In the second method, the membrane of a mass spectrometer probe is used to separate the fermenter contents from the high vacuum of the mass spectrometer. Measurement of oxygen in the mass spectrometer probe and the tubing method is based on the ability of the gas to diffuse across the surface membrane.

The most common method of measuring dissolved oxygen is based on electrochemical detector. Two types of detector are commercially available: galvanic and polarographic detectors. Both use membranes to separate electrochemical cell components from the broth. The membrane must be permeable only to oxygen and not to any other chemicals, which might interfere with the measurement. Oxygen diffuses from the broth, across the permeable membrane to the electrochemical cell of the detector, where it is reduced at the cathode to produce a measurable current or voltage, which is proportional to the rate of arrival of oxygen at the cathode. It is important to note that the measurement rate of oxygen arrival at the cathode depends on the rate of arrival at the outer membrane surface, the rate of transfer across the membrane and the rate of transport from the inner surface of the membrane to the cathode. The rate of arrival at the cathode is proportional to the rate of diffusion of oxygen across the membrane. The rate of diffusion is also proportional to the overall concentration driving force for oxygen mass transfer. We assume the oxygen concentration at the inner surface of the membrane is efficiently reduced to zero. The rate of diffusion is thus proportional to the oxygen concentration in the liquid only. The electrical signal produced by the probe is directly proportional to the dissolved oxygen concentration of the liquid. The probe has to be calibrated for accurate measurements.

In the galvanic detector, the electrochemical detector consists of a noble metal like silver (Ag) or platinum (Pt), and a base metal such as lead (Pb) or tin (Sn), which acts as anode. The well-defined galvanic detector is immersed in the electrolyte solution. Various electrolyte solutions can be used, but commonly they may be a buffered lead acetate, sodium acetate and acetic acid mixture. The chemical reaction in the cathode with electrons generated in the anode may generate a measurable electrical voltage, which is a detectable signal for measurements of DO. The lead is the anode in the electrolyte solution, which is oxidised. Therefore the probe life is dependent on the surface area of the anode. The series of chemical reactions occurring in the cathode and anode is:

$$\begin{aligned} \text{Cathode:} \quad & O_2 + 2H_2O + 4e^- \rightarrow 4OH^- \\ \text{Anode:} \quad & Pb \rightarrow Pb^{++} + 2e^- \\ \text{Overall:} \quad & O_2 + 2Pb + 2H_2O \rightarrow 2Pb(OH) \end{aligned} \tag{4.5.1}$$

Polarographic electrodes are different from the galvanic type. In this type of electrode the external negative base voltage is applied between the cathode (Au or Pt) and the anode (Ag/AgCl) so that oxygen is reduced at the cathode according to the sequential reactions stated below. The following reaction takes place at cathode and anode respectively:

$$\begin{aligned} \text{Cathode:} \quad & O_2 + 2H_2O + 2e^- \rightarrow H_2O_2 + 2OH^- \\ & H_2O_2 + 2e^- \rightarrow 2OH^- \end{aligned} \tag{4.5.2a}$$

$$\begin{aligned} \text{Anode:} \quad & Ag + Cl^- \rightarrow AgCl + e^- \\ \text{Overall reaction:} \quad & 4Ag + O_2 + 2H_2O + 4Cl^- \rightarrow 4AgCl + 4OH^- \end{aligned} \tag{4.5.2b}$$

An electrical output for a polarographic detector is produced according the above reactions. Again, various electrolytes can be used for this type of detector, but they are usually based on KCl or AgCl with additional high molecular mass compounds, which are added to prevent the loss of electrolyte during sterilisation.

4.6 pH/REDOX MEASUREMENT AND CONTROL

Fermenters are generally operated most efficiently. The fermentation process is normally carried out at a constant pH. The pH of a culture medium will change with the metabolic product of microorganisms, which are developed in the fermentation media. Therefore, pH control is required during the course of fermentation. The pH has a major effect on cell growth and product formation by influencing the breakdown of substrates and transport of both substrate and product through the cell wall. It is therefore a very important factor in fermentation. In fine chemicals, organic acids, amino acids and antibiotic fermentations, even a small change in the pH can cause a large fall in the productivity. Also, in animal-cell fermentations, the pH is strictly affected by the cell density.

Measurement of pH is based on the absolute standard of the electrochemical properties of the standard hydrogen electrode. The basic part of the electrode is a very thin glass membrane (0.2–0.5 mm), which reacts with water to form a hydrated gel layer of only 50–500 Å thicknesses. This layer exists on both sides of the membrane and is essential for the correct operation and maintenance of the electrode. Hydrogen ions, which exist within the layer, are mobile and any difference between the ionic activities on each side of the membrane will lead to the establishment of a pH-dependent potential. A constant potential is maintained at the inner surface of the glass membrane by filling the tube of the electrode with a buffered solution of accurately determined and stable composition, and with constant and accurate hydrogen ion activity. An Ag/AgCl electrode is generally used as the electrical outlet from this system. As the pH of the process fluid varies, it causes a change in the potential on the outer surface of the membrane. To measure this a reference electrode is necessary to complete the measurement circuit. In the combined electrode, this is constructed as an integrated part of the electrode assembly and consists of an $Ag/AgCl_2$ electrode in KCl electrolyte saturated with $AgCl_2$. The reference electrode must have direct contact with the process liquid to have an electrical continuity in the system. The overall potential measured by the electrode with respect to the hydrogen ions is given by the Nernst equation:

$$E = E_o + \frac{RT}{F} \ln[a_H^+] \tag{4.6.1}$$

where E is the measured potential in volt, E_o is the standard electrode potential in volts, R is the gas constant, F is the Faraday constant, T is the absolute temperature and a_H^+ is the hydrogen ion activity. The second term of (4.6.1) is related to pH, with a proportionality

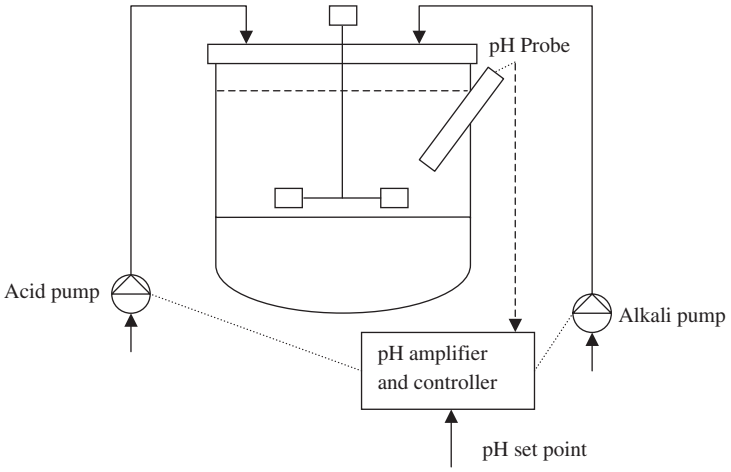

FIG. 4.3. Instrumentation for a pH control system in a bioreactor.

constant instead of ionic activity. The potential terms are translated to pH, leading to the following relation:

$$E = E_o - K[\mathrm{pH} - \mathrm{pH_o}] \tag{4.6.2}$$

where K is the proportionality constant, $\mathrm{pH_o}$ is the reference or base pH. At room temperature, 25 °C (298K), the value for K is 59.15 mV per unit pH. The calomel reference electrode can be prepared with a predictable and reproducible voltage of 0.28 V. The pH of a solution can be determined with an electrode. A typical pH control scheme for a pilot-plant fermenter is shown in Figure 4.3.

4.7 DETECTION AND PREVENTION OF THE FOAM

In a gas and liquid system, when gas is introduced into a culture medium, bubbles are formed. The bubbles rise rapidly through the medium and dispersion of the bubbles occurs at surface, forming froth. The froth collapses by coalescence, but in most cases the fermentation broth is viscous so this coalescence may be reduced to form stable froth. Any compounds in the broth, such as proteins, that reduce the surface tension may influence foam formation. The stability of preventing bubbles coalescing depends on the film elasticity, which is increased by the presence of peptides, proteins and soaps. On the other hand, the presence of alcohols and fatty acids will make the foam unstable.

Foaming of the bioreactor is a nuisance, reflects on the mass transfer process and must be prevented, for many reasons. The problems related to foaming are obvious if they are due to gas sparging. The problems are the loss of broth, clogging of the exhaust gas system

and possible contamination, a problem that is due to wetting of the gas filters. During fermentation, foaming may occur suddenly. Some foams are easy to destroy and can be removed by foam breaker; others are quite stable and are relatively hard to remove from the top of the bioreactor. The suppression of foam is usually accomplished by mechanical agitation such as a foam breaker. The mechanical devices operate on the centre of the shaft. They are generally blades or disks that are mounted on the same agitator shaft. Chemical anti-foams are used to regulate the foam and prevent any foaming on the surface of broth. The chemical anti-foams are expensive and minimal amounts must be used. Use of chemical anti-foam may complicate the microbial fermentation process, and some may act as an inhibitor. Therefore they have to be regulated to eliminate any side effect on the bioprocess. Chemical anti-foams are usually based on silicon and act by reducing the interfacial tension of the broth. Mechanical devices have advantages because expensive chemicals do not have to be added to the fermentation broth. However, the addition of an anti-foam may require the detection of foam. This requires the addition of the necessary amount of anti-foam to control any preventive foaming in the bioreactor. Also, ultrasonic waves may be an additional means of destroying foam.

Generally two main types of foam detector are used. They work by detecting either changes in electrical capacitance or changes in electrical resistance. Table 4.2 shows the application of foam detectors based on various principles, such as conductance, thermal conductivity, capacitance, ultrasonic rotating disks.

The capacitance foam detector is made of two electrodes, which are installed in the bioreactor. They measure the capacitance of the air space above the normal working liquid level in the bioreactor. If foaming occurs, the air space capacitance is reduced. Detection is by a change in the magnitude of a small alternating electrical current, which is applied between the two electrodes. This method is applicable in large-scale bioreactors. The change in electrical current is converted to an output signal from the detectors; the change in current is directly proportional to the amount of foam formed. From evaporation of the liquid media, fouling problems may occur on the electrode by the broth. This may cause some error in foam detection, so regular cleaning is needed to maintain the electrode.

The foam detector based on the resistance method acts on the conductivity of the probe. The length of the probe is coated with some electrically insulating material, leaving the tip

TABLE 4.2. *Types of foam detector, their features and functions*

Conductance	An insulated stainless steel electrode which forms one terminal in the circuit.
Thermal conductivity	Two thermistors mounted some distance apart. A current through the thermistors heats them above ambient; foam cool down.
Capacitance	A vertical tube with a central electrode. The height to liquid or foam alters the capacitance.
Ultrasonic	A transmitter and receiver mounted opposite each other in a bioreactor. At 25–40 kHz ultrasound is absorbed by the foam.
Rotating disk	This may double as a foam breaker; foam will slow down the rotation or need an increase in power to maintain speed.

of the probe exposed to the media. As the foam builds up, it contacts the tip of the probe, thus completing an electrical circuit and producing an output signal. In the fermentation medium, as the tip of the probe contacts the generated foam, an electrical circuit is generated, and an output signal is produced for foam detection.

Another type of probe is based on the principle of the sudden cooling of the heated element. When foam comes in contact with a heated electrical element, the hot surface detects sudden cooling, which is translated to an output signal. The major problem with the use of a heated element is fouling of the media: the sensitivity decreases while it is used, so such detectors may not be reliable in practice.

The two other foam sensors mentioned above are ultrasound and rotating disks. The ultrasound sensor is a transmitter and receiver mounted opposite to each other and operating at 25–40 kHz. In the bioreactor, the waves are absorbed by the foam and the signal is generated. The rotational disk foam sensor is a mechanical foam breaker which is used by increasing the rotational resistance.

The use of a chemical agent as an anti-foam is affected by an on–off algorithm with variable dosing time and time delay. If the presence of foam is detected, then the controller first activates a delay timer. This type of foam controller works with some delay and variable dosing time. If at the end of the delay period the foam is still present, then the dosing pump is activated and chemical agent is added to the bioreactor. If the foam is still detected at the end of this period, the combined system of delay and dosing is reactivated. With this method of controller, addition of any unnecessary anti-foam is prevented.

4.8 BIOSENSORS

The biochemical constituents of fermentation broth have been developed by a wide range of biosensors. A biosensor consists of two main elements. These two elements, the biocatalyst and a transducer, are combined as a single detecting probe, in which the transducer and biocatalyst are held together in a very close contact. The biosensor acts as a device as flow passes. It can detect penetration of flow through biocatalysts and measures the biochemical transformation of a given substance, for example change in pH. The function of the transducer is to detect such change and to produce an output signal, which is related to the concentration of the measured substance. In fact, a biosensor is a combination of biological sensor attached to transducer that is a simple device which acts specifically with a high sensitivity in measurements.

The application of biosensors in an operating bioreactor is usually based on whole cells or enzyme activities. The perfect function of a biosensor is very dependent on the biological activities of a system. The biocatalytic reaction produces some detectable change that must be converted to an output signal by the transducer. The transducers are usually amperometric and potentiometric devices. Such transducers are included in dissolved oxygen probes and pH electrodes, ion selective electrodes and gas-sensing devices. Amperometric detectors operate by measuring the flux of some electrochemical redox activities of the produced biosensor reaction. For example, a dissolved oxygen probe can be used to measure the rate of oxygen flux produced in an oxidised catalysed reaction. DO probes are a popular

form of biosensor transducer. They are used for microbial and enzymatic oxido-reductase reactions. Many enzymatic reactions are associated with the uptake or production of protons. The rate of proton flux can be measured by using a potentiometric detector, which is normally done in a pH probe.

Several biosensors are commercially available. One of the most useful is the glucose sensor. The standard sensor determines glucose concentration based on the glucose oxidase enzyme. The chemical reaction for oxidation of glucose is:

$$\text{Glucose} + O_2 + H_2O \rightarrow \text{Gluconic acid } (H^+) + H_2O_2 \tag{4.8.1}$$

A suitable biosensor can measure the amount of oxygen consumed in the above reaction. The biosensor is constructed by the surrounding tip of the DO probe, which is a glucose-permeable membrane and retaining glucose oxidase/electrolyte solution in direct contact with the membrane of the DO probe. Normally the DO probe can measure the rate of oxygen flux in the bulk liquid. The flux across the DO probe membrane to the cathode, where oxygen is reduced, is equal to the rate of oxygen flux reaching and reducing electrode. The reduced amount of oxygen is equivalent to the rate of glucose that is consumed in the glucose oxidase enzymatic conversion of glucose to gluconic acid.

The use of a catalyst with oxidase enzyme is an example of the use of a combined enzyme system, which illustrates the wide potential offered by multi-enzyme electrode systems. Various enzymes can be arranged to work sequentially to transform quite complex substances and eventually produce a measurable concentration-dependent change, which is detected by the output signal and recorded for analysis.

4.9 NOMENCLATURE

E Potential, V
E_o Standard electrode potential, V
R The gas constant
F Faraday constant
K Proportionality constant, mV per unit pH
T Absolute temperature

REFERENCES

1. Baily, J.E. and Ollis, D.F., "Biochemical Engineering Fundamentals", 2nd edn. McGraw-Hill, New York, 1986.
2. Scragg, A.H., "Bioreactors in Biotechnology, A Practical Approach". Ellis Horwood Series in Biochemistry and Biotechnology, New York, 1991.
3. Wang, D.I.C., Cooney, C.L., Deman, A.L., Dunnill, P., Humphrey, A.E. and Lilly, M.D., "Fermentation and Enzyme Technology". John Wiley & Sons, New York, 1979.
4. Doran, P.M., "Bioprocess Engineering Principles". Academic Press, New York, 1995.
5. Stanbury, P.F. and Whitaker, A., "Principles of Fermentation Technology". Pergamon Press, New York, 1987.

CHAPTER 5

Growth Kinetics

5.1 INTRODUCTION

Microbial growth is considered for the observation of the living cell activities. It is important to monitor cell growth and biological and biocatalytic activities in cell metabolism. A variety of methods are available to predict cell growth by direct or indirect measurements. Cell dry weight, cell optical density, cell turbidity, cell respiration, metabolic rate and metabolites are quite suitable for analysing cell growth, substrate utilisation and product formation. The rate of cell growth is described in this chapter. Various bioprocesses are modelled for substrate utilisation and product formation. Growth kinetics in batch and continuous culture is examined in detail.

5.2 CELL GROWTH IN BATCH CULTURE

Batch culture is a closed system without any inlet or outlet streams, as nutrients are prepared in a fixed volume of liquid media. The inocula are transferred and then the microorganisms gradually grow and replicate. As the cell propagates, the nutrients are depleted and end products are formed. The microbial growth is determined by cell dry weight ($g \cdot l^{-1}$) and cell optical density (absorbance at a defined wavelength, λ_{nm}). A growth curve can be divided into four phases, as shown in Figure 5.1. As inocula are transferred to the fermentation media, cell growth starts rapidly in the media. The lag phase shows almost no apparent cell growth. This is the duration of time represented for adaptation of microorganisms to the new environment, without much cell replication and with no sign of growth. The length of the lag phase depends on the size of the inocula. It is also results from the shock to the environment when there is no acclimation period. Even high concentrations of nutrients can cause a long lag phase. It has been observed that growth stimulants and trace metals can sharply reduce the lag phase. Figure 5.2 shows the influence of magnesium ions on the reduction of lag phase in a culture of *Aerobacter aerogenes*. The lag phase in the batch culture of *A. aerogenes* was drastically reduced from 10 hours to zero when the concentration of Mg^{2+} was increased from 2 to $10\,mg \cdot l^{-1}$. There are many other factors believed to affect the lag phase. These are discussed in more detail in microbiology textbooks.[1]

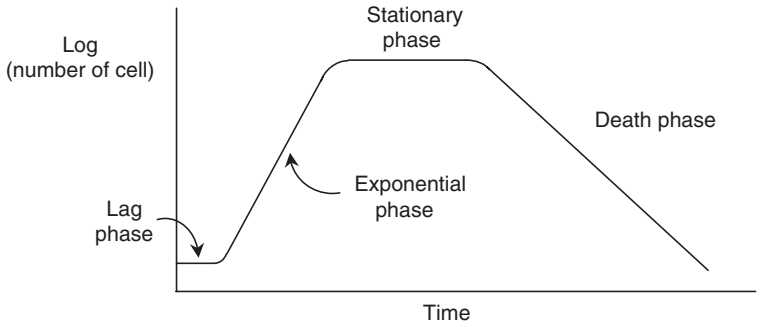

FIG. 5.1. Typical batch growth curve of a microbial culture.

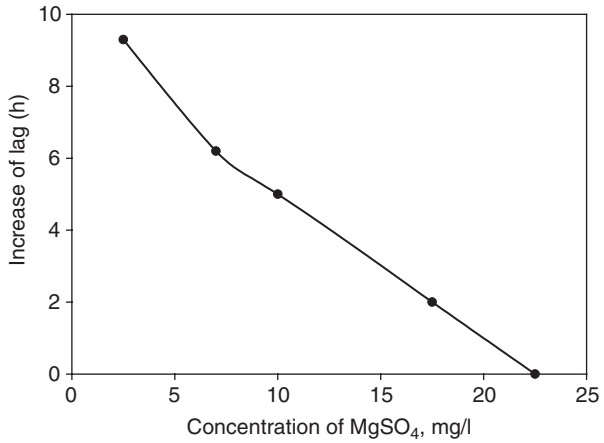

FIG. 5.2. Influence of $[Mg^{2+}]$ on the lag phase in *Aerobacter aerogenes* culture.

5.3 GROWTH PHASES

Once there is an appreciable amount of cells and they are growing very rapidly, the cell number exponentially increases. The optical cell density of a culture can then be easily detected; that phase is known as the exponential growth phase. The rate of cell synthesis sharply increases; the linear increase is shown in the semi-log graph with a constant slope representing a constant rate of cell population. At this stage carbon sources are utilised and products are formed. Finally, rapid utilisation of substrate and accumulation of products may lead to stationary phase where the cell density remains constant. In this phase, cell may start to die as the cell growth rate balances the death rate. It is well known that the biocatalytic activities of the cell may gradually decrease as they age, and finally autolysis may take place. The dead cells and cell metabolites in the fermentation broth may create

toxicity, so deactivating remaining cells. At this stage, a death phase develops while the cell density drastically drops if the toxic secondary metabolites are present. The death phase shows an exponential decrease in the number of living cells in the media while nutrients are depleted. In fact the changes are detected by monitoring the pH of the media.

5.4 KINETICS OF BATCH CULTURE

The batch culture is a simple, well-controlled vessel in which the concentration of nutrients, cells and products vary with time as the growth of the microorganism proceeds. Material balance in the reactor may assist in following the biochemical reactions occurring in the media. In batch fermentation, living cells propagate and many parameters of the media go through sequential changes with time as the cells grow. The following parameters are monitored while the batch process continues:

- Cells and cell by-product
- Concentration of nutrients
- Desirable and undesirable products
- Inhibition
- pH, temperature, substrate concentration

The objective of a good process design is to minimise the lag phase period and maximise the length of exponential growth phase.

The substrate balance in a batch culture for component i in the culture volume of V_R and change of molar concentration of C_i is equal to the rate of formation of product:

$$\frac{\mathrm{d}}{\mathrm{d}t}(V_R \cdot C_i) = V_R \cdot r_{fi} \tag{5.4.1}$$

where V_R is the culture volume, assumed to be constant while no liquid media is added or removed, C_i is the molar concentration of component i and r_{fi} is the rate of product formation. Then (5.4.1) is reduced to:

$$\frac{\mathrm{d}C_i}{\mathrm{d}t} = r_{fi} \tag{5.4.2}$$

The rate of product formation, r_{fi}, depends upon the state of the cell population, environmental condition, temperature, pH, media composition and morphology with cell age distribution of the microorganism.[2,3] A similar balance can be formulated for microbial biomass and cell concentration. The exponential phase of the microbial growth in a batch culture is defined by:

$$\frac{\mathrm{d}X}{\mathrm{d}t} = \mu X \tag{5.4.3}$$

There is no cell removal from the batch vessel and the cell propagation rate is proportional to specific growth rate, μ (h^{-1}), using the differential growth equation the cell concentration with respect to the time is:

$$X(t) = X_o e^{\mu t} \tag{5.4.4}$$

5.5 GROWTH KINETICS FOR CONTINUOUS CULTURE

The fermentation system can be conducted in a closed system as batch culture. The batch system growth kinetics and growth curve were explained in sections 5.2 and 5.3. The growth curve is the best representation of a batch system. Disadvantages exist in the batch system such as substrate depletion with limited nutrients or product inhibition growth curve. The growth environment in the batch system has to follow all the phases projected in the growth curve. Besides nutrient depletion, toxic by-products accumulate. Even the composition of media with exponential growth is continuously changing; therefore it will never be able to maintain any steady-state condition. The existing limitation and toxic product inhibition can be removed if the system is an open system and the growing culture is in a continuous mode of operation. In engineering, such a system is known as an open system. There would be an inlet medium as fresh medium is pumped into the culture vessel and the excess cells are washed out by the effluents, leaving the continuous culture from the fermentation vessel. The advantages of continuous culture are that the cell density, substrate and product concentrations remain constant while the culture is diluted with fresh media. The fresh media is sterilised or filtered and there are no cells in the inlet stream. If the flow rate of the fresh media gradually increases, the dilution rate also increases while the retention time decreases. At high flow rate, the culture is diluted and the cell population decreases; with the maximum flow rate when all the cells are washed out, the composition of the inlet and outlet conditions remain about the same. In this condition a washout phenomenon takes place. In continuous culture, the flow rate is adjusted in such a way that the growth rate and the cell density remain constant. There are two types of culture vessel: chemostat and biostat; both are open systems.[4,5] Detailed explanations are given below.

(i) Chemostat (growth rate controlled by dilution rate, D, (h^{-1})
(ii) Turbidostat (constant cell density that is controlled by the fresh medium)

1. Chemostat. The nutrients are supplied at a constant flow rate and the cell density is adjusted with the supplied essential nutrients for growth. In a chemostat, growth rate is determined by the utilisation of substrates like carbon, nitrogen and phosphorus. A simple chemostat with feed pump, oxygen probe, aeration and the pH controlling units is shown in Figure 5.3. The system is equipped with a gas flow meter. Agitation and aeration provided suitable mass transfer. The liquid level is controlled with an outlet pump.

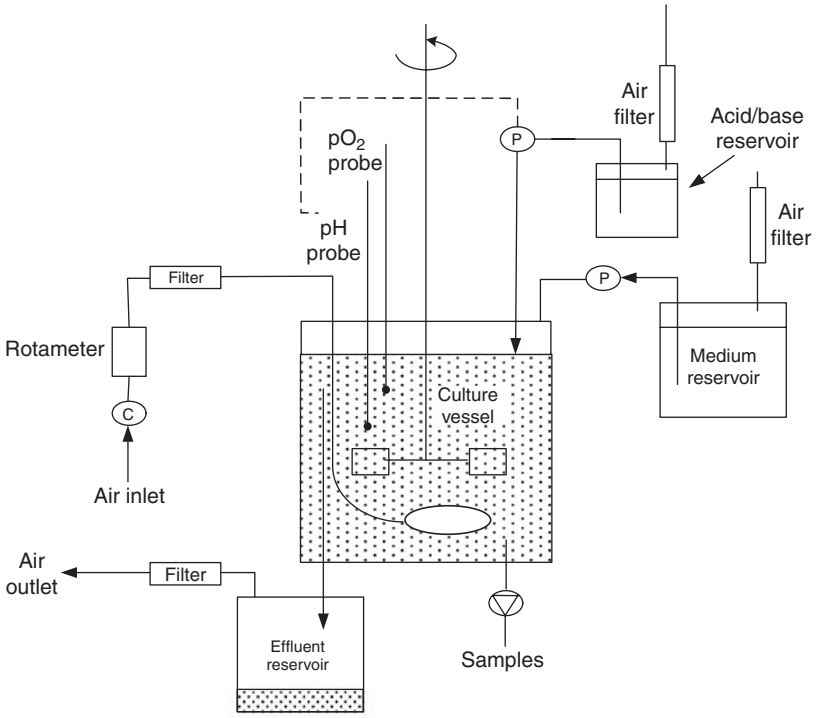

FIG. 5.3. Schematic diagram of continuous culture with control units in a constant volume chemostat.

Fresh medium is pumped into the culture vessel. The liquid level is controlled as the overflow is drained to a product reservoir.

For constant volume of the fermentation vessel, a liquid level controller is used. The system is also designed with an outlet overflow to keep the liquid level constant. Figures 5.4, 5.5 and 5.6 show various mechanisms for constant-volume bioreactors. An outlet pump is customarily used to maintain a constant flow rate. Complex systems are designed to control the mass of the generated cells; photocells or biosensors are used to monitor the optical density of the cells (Figure 5.7). Cell concentration is controlled by the supplied nutrients and the flow rate of fresh media. The substrate concentration and the retention time in the fermentation vessel may dictate the cell density. Besides the nutrients and the controlling dilution rate, there are several physiological and process variables involved in the kinetics and the design of a bioreactor.[6,7] These parameters are temperature, pH, redox (reduction and oxidation) potentials, dissolved oxygen, substrate concentration and many process variables. In a chemostat, cell growth rate is determined by an expression that is based on substrate utilisation, mainly C, N and P with trace amounts of metals and vitamins. The advantages of continuous culture are that the essential nutrients can be adjusted for maximum growth rate and to maintain steady-state conditions. There is a determined

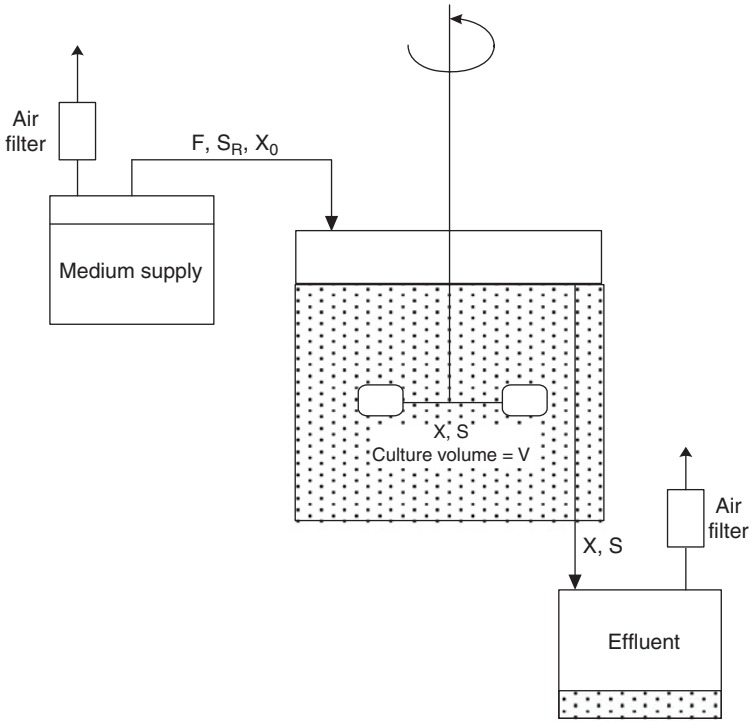

FIG. 5.4. Chemostat without pumps maintained at constant level.

relation between cell concentration and dilution rate. At steady state, cell concentration is maximised with optimum dilution rate. There is also a critical dilution rate where all the cells are washed out and there is no chance for the microorganisms to replicate; this is known as the maximum dilution rate.

2. Biostat. This is also known as a turbidostat. It is a system where cell growth is controlled and remains constant while the flow rate of fresh media does not remain constant. Cell density is controlled based on set value for turbidity, which is created by the cell population while fresh media is continuously supplied. A turbidostat is shown in Figure 5.8.

In a chemostat and biostat or turbidostat, even with differences in the supply of nutrients and/or fresh media, constant cell density is obtained. The utilisation of substrate and the kinetic expressions for all the fermentation vessels are quite similar. It is possibile to have slight differences in the kinetic constants and the specific rate constants.[3,4] Figure 5.9 shows a turbidostat with light sources. The system can be adapted for photosynthetic bacteria.

The continuous cultures of chemostat and biostat systems have the following criteria:

- Medium and cells are continuously changing
- The cell density (ρ_{cell}) is constant

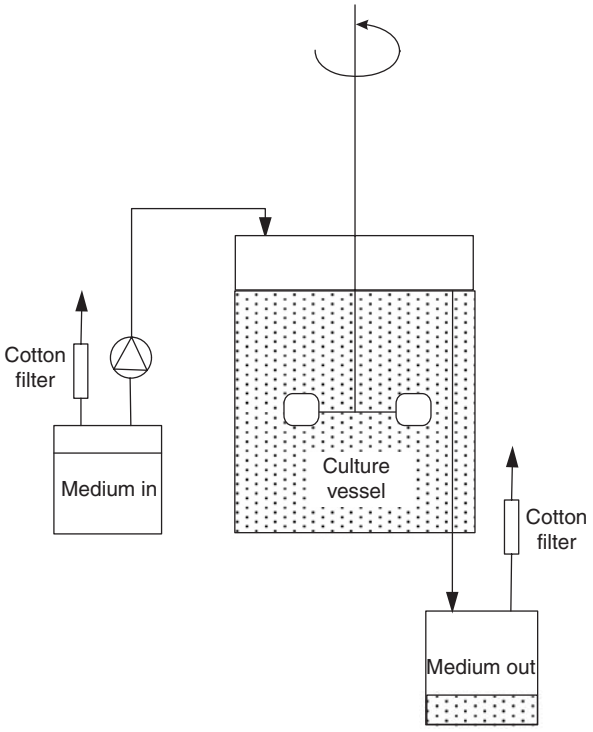

FIG. 5.5. Chemostat with feed pump overflow drainage maintained at constant level.

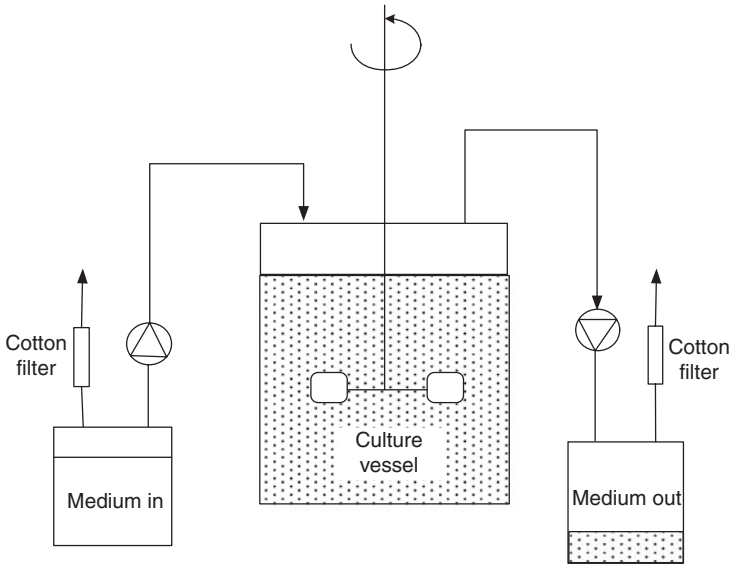

FIG. 5.6. Chemostat using single medium inlet feed and outlet pumps.

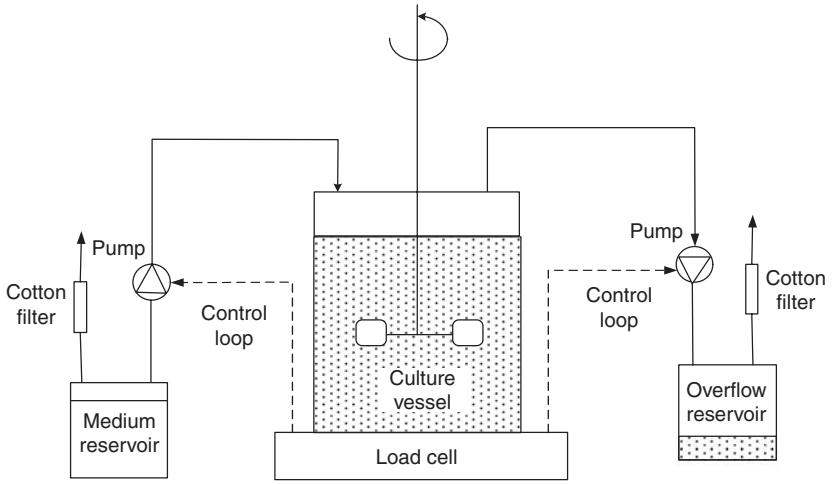

FIG. 5.7. Chemostat with inlet and outlet control loops, feed and product pump with cell loading and recycling.

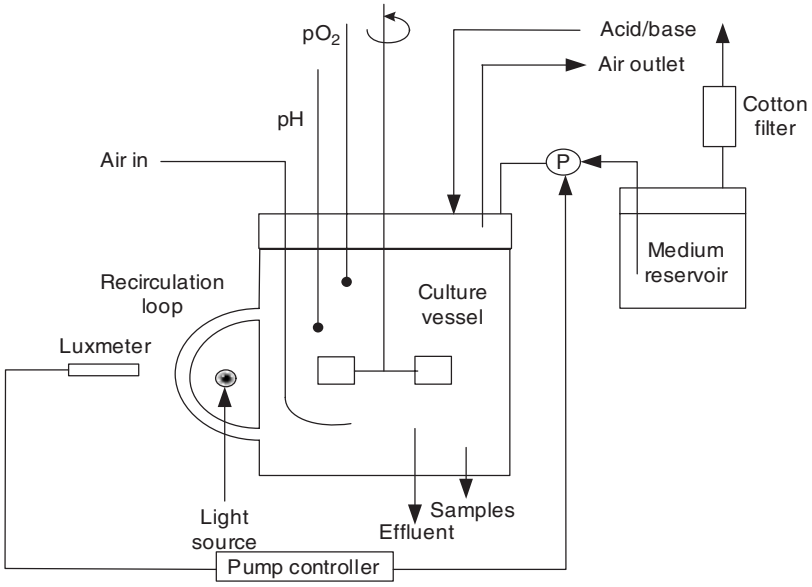

FIG. 5.8. Biostat with light source used detect cell turbidity and bacterial optical density.

- Steady-state growth
- Open system

The system is balanced for cell growth by removing old culture and replacing it with fresh medium at the same rate.

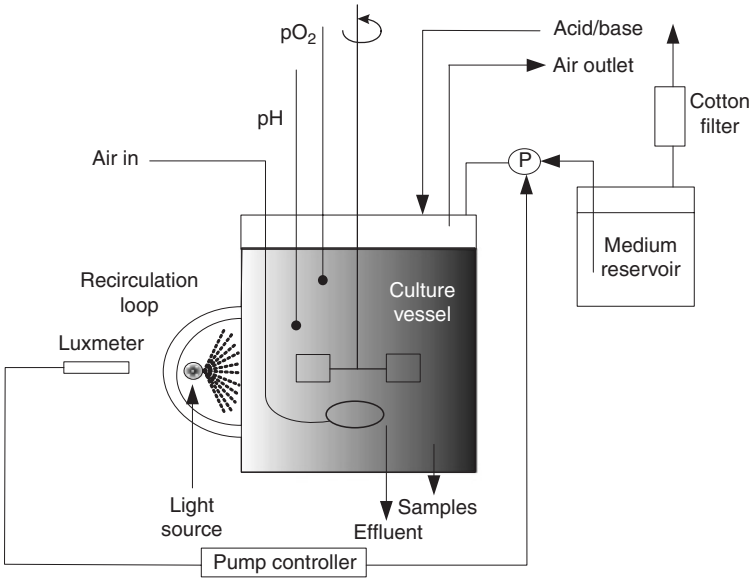

FIG. 5.9. Continuous culture with light source used for photosynthetic bacteria, turbidostat.

5.6 MATERIAL BALANCE FOR CSTR

At steady-state condition for chemostat operation, change of concentration is independent of time. Material balance for the fermentation vessel is:

$$\text{In} - \text{Out} + \text{Reaction rate} = \text{Accumulation}$$

At steady-state condition there is no accumulation, therefore the material balance is reduced to:

$$F(C_{if} - C_i) + V_R \cdot r_{fi}) = 0 \tag{5.6.1}$$

where C_{if} is the molar concentration in feed stream, C_i is the molar concentration in the outlet stream and $-r_{fi} = \dfrac{\mathrm{d}C_{fi}}{\mathrm{d}t}$ is the rate of feed stream or consumption rate

$$r_{fi} = \frac{F}{V_R}(C_i - C_{if}) = D(C_i - C_{if}) \tag{5.6.2}$$

The rate of formation of a product is easily evaluated at steady-state condition for inlet and outlet concentrations, where D is the dilution rate, defined as $D = \dfrac{F}{V_R}$, which characterises

the inverse retention time in the CSTR unit. The dilution rate is equal to the number of fermentation vessel volumes that pass through the vessel per unit time. D is the reciprocal of the mean residence time.

The kinetic of cell growth for prediction of growth rate is projected by the net growth rate, which is:

Rate of cell dry weight

$$\mathrm{d}X/\mathrm{d}t = \text{growth rate} - \text{cell removal rate} - \text{cell death rate}$$

In a continuous culture:

$$\mathrm{d}X/\mathrm{d}t = \mu X - DX - \alpha X \tag{5.6.3}$$

where α is the specific death-rate constant.

5.6.1 Rate of Product Formation

Similarly, the rate of product formation is defined as:

$$\frac{\mathrm{d}P}{\mathrm{d}t} = q_P X - DP - \beta P \tag{5.6.1.1}$$

where q_P is the specific growth rate for product formation, β is the denaturation of product coefficient and the specific rate of product formation. For a special case the specific growth rate for product formation is simplified and reduced to:

$$q_P = \frac{1}{X}\frac{\mathrm{d}P}{\mathrm{d}t} \tag{5.6.1.2}$$

If the cells are in the exponential growth period and there is no cell death rate, $\alpha \approx 0$. The net cell concentration is:

$$\frac{\mathrm{d}X}{\mathrm{d}t} = \text{growth} - \text{output} = \mu X - DX \tag{5.6.1.3}$$

At steady-state condition, the biomass concentration remains constant, that is, $\mathrm{d}X/\mathrm{d}t = 0$, and (5.6.1.3) concludes to $\mu = D$; therefore the specific growth rate is equal to the dilution rate.

5.6.2 Continuous Culture

Exponential growth in a batch culture may be prolonged by addition of fresh medium to the fermentation vessel. In a continuous culture the fresh medium has to be displaced by an equal volume of old culture, then continuous cell production can be achieved.

5.6.3 Disadvantages of Batch Culture

There are several disadvantages of batch culture. The nutrient in the working volume becomes depleted; the other major problem is the limitation and depletion of the substrate. Since there is no flow stream to take effluent out, as the system is closed, toxins form there. A disadvantage related to substrate depletion is that the growth pattern may reach the death phase quickly in an old culture. The long duration of the batch system for slow growth results in exhaustion of essential nutrients and an accumulation of metabolites as by-products. Exhaustion of nutrients and substrate may cause the system to become retarded. The technical problem resulting in changes to media composition may directly affect the microbial exponential growth phase. Inhibition is another factor affecting the bioprocess, which causes the reaction rate shift. As a result, inhibition may slow down bio-catalytic activities. Product inhibition may block enzyme activities, and the cells became poisoned by the by-product. One common disadvantage of the batch process is that one has to carry out a cycle for production: the product should be sent for downstream processing, then the system has to be cleaned and recharged with fresh feed, so the process is highly labour-intensive for downtime and cleaning.

5.6.4 Advantages of Continuous Culture

There are several advantages to continuous culture, where all the problems associated with the batch culture are solved. Firstly, the growth rate is controlled and the cells are well maintained, since fresh media is replaced by old culture while the dilution is taking place. As a result, the effect of physical and chemical parameters on growth and product formation can easily be examined. The biomass concentration in the cultured broth is well maintained at a constant dilution rate. The continuous process results in substrate-limited growth and cell-growth-limiting nutrients. The composition of the medium can be optimised for maximum productivity; in addition secondary metabolite production can also be controlled. The growth kinetics and kinetic constants are accurately determined. The process leads to reproducible results and reliable data. High productivity per unit volume is achieved. The continuous culture is less labour-intensive, and less downtime is needed. Finally, steady-state growth can be achieved, even if mixed cultures are implemented.

5.6.5 Growth Kinetics, Biomass and Product Yields, $Y_{X/S}$ and $Y_{P/S}$

The yield is defined as ratio of biomass to the mass of substrate.

The ethanol fermentation from sugar is simplified based on the following reaction:

$$C_6H_{12}O_6 \rightarrow 2C_2H_5OH + 2CO_2 \tag{5.6.5.1}$$

The rates of biomass production and product formation are:

$$\frac{dX}{dt} = \frac{dX}{ds}\frac{ds}{dt} = -Y_{X/S}\cdot\frac{dS}{dt} \quad \text{and} \quad \frac{dP}{dt} = -Y_{P/S}\cdot\frac{dS}{dt} \tag{5.6.5.2}$$

where the yields of biomass and product are:

$$Y_{X/S} = -\frac{\Delta X}{\Delta S} \quad \text{and} \quad Y_{P/S} = -\frac{\Delta P}{\Delta S} \tag{5.6.5.3}$$

For instance the theoretical yield of ethanol fermentation based on fermentation of glucose results in two moles of ethanol:

$$\frac{2 \text{ mol EtOH}}{\text{mol } C_6H_{12}O_6} = \frac{2 \times 46}{180} = 0.511 \frac{\text{g EtOH}}{\text{g } C_6H_{12}O_6}$$

The effect of substrate concentration on specific growth rate (μ) in a batch culture is related to the time and μ_{max}; the relation is known as the Monod rate equation. The cell density (ρ_{cell}) increases linearly in the exponential phase. When substrate (S) is depleted, the specific growth rate (μ) decreases. The Monod equation is described in the following equation:

$$\mu = \mu_m \frac{S}{K_S + S} \tag{5.6.5.4}$$

where μ is the specific growth rate, μ_m is the maximum specific growth rate in h^{-1}, K_S is saturation or Monod constant and S is substrate in $g \cdot l^{-1}$. The linearised form of the Monod equation is:

$$\frac{1}{\mu} = \left(\frac{K_S}{\mu_m}\right)\frac{1}{S} + \frac{1}{\mu_m} \tag{5.6.5.5}$$

The average biomass concentration is defined as the product of yield of biomass and change of substrate concentrations in inlet and outlet streams. The biomass balance is:

$$\overline{X} = Y_{X/S}(-\Delta S) = Y_{X/S}(S_i - S_o) \tag{5.6.5.6}$$

where, S_i and S_o are inlet and outlet concentrations in $mol \cdot l^{-1}$. Rate expression is based on the Monod equation for substrate utilisation, given by the rate equation (5.6.5.4):

$$\mu K_S + \mu S = \mu_{max} S \quad \text{or} \quad \mu K_S = (\mu_{max} - \mu) S \tag{5.6.5.7}$$

The rate equation was solved for substrate concentration in the product stream. Rearrangement of (5.6.5.7) results in an equation for substrate in terms of specific rate:

$$S = \frac{K_S \mu}{\mu_{\max} - \mu} \tag{5.6.5.8}$$

Finally, at steady-state condition, as has been stated above (5.6.1.3), the rate of substrate consumption is equal to the biomass generation, with the assumption of zero death rate:

$$\mu = D \Rightarrow S_o = \frac{K_S D}{\mu_{\max} - D} \tag{5.6.5.9}$$

5.6.6 Biomass Balances (Cells) in a Bioreactor

The material balance for cells in a continuous culture chemostat is defined as:

$$\text{cell accumulation} = \text{cell in} - \text{cell out} + \text{cell growth} - \text{cell death} \tag{5.6.6.1}$$

$$\frac{\mathrm{d}X}{\mathrm{d}t} = \left(\frac{F}{V}\right)(X_o - X) + \mu X - \alpha X \tag{5.6.6.2}$$

where F is the flow rate in l/h, V is the working volume of the bioreactor in l, X is the cell concentration in $\mathrm{g \cdot l^{-1}}$, μ is the specific growth rate in $\mathrm{h^{-1}}$, K_e or K_d equal α, known as the specific death rate in $\mathrm{h^{-1}}$ and D or F/V is the dilution rate in $\mathrm{h^{-1}}$. Since in the exponential phase steady-state growth has been achieved and the specific growth rate is much greater than the specific death rate, then (5.6.6.2) is simplified and reduced to a point where the specific growth rate is equal to the dilution rate:

$$\frac{\mathrm{d}X}{\mathrm{d}t} = -DX + \mu X \tag{5.6.6.3}$$

At steady-state condition:

$$\frac{\mathrm{d}X}{\mathrm{d}t} = 0$$

$$0 = X(\mu - D) \tag{5.6.6.4}$$

Then, $\mu = D$.

There is a specific dilution rate known as critical dilution rate where a washout phenomenon takes place. At the critical dilution rate there is not enough time for the microorganisms to replicate.

5.6.7 Material Balance in Terms of Substrate in a Chemostat

The substrate balance is given based on following equation:

$$-\frac{dS}{dt} = \left(\frac{F}{V}\right)(S_{in} - S_{out}) - \underbrace{\left(\frac{\mu}{Y_{X/S}}\right)X}_{\text{cell growing}} - \underbrace{\left(\frac{q_P}{Y_{P/S}}\right)X}_{\text{product formed}} - \underbrace{mX}_{\text{Maintenance} = 0} \tag{5.6.7.1}$$

In general, $\mu >> m$, so we can therefore neglect the last term.

For steady-state no product is formed which means there are no changes in substrate and product concentrations:

$$-\frac{dS}{dt} = 0 \quad \text{and} \quad \left(\frac{q_P}{Y_{P/S}}\right) = 0 \tag{5.6.7.2}$$

Also, $F/V = D$ then $\mu = D$

$$0 = D(S_{in} - S_{out}) - \frac{\mu X}{Y_{X/S}} \tag{5.6.7.3}$$

Rearranging the above equation:

$$\overline{X} = Y_{X/S}(S_{in} - S_{out}) \tag{5.6.7.4}$$

For steady-state condition:

$$D = \mu_m \frac{S}{K_S + S} \Rightarrow S_{out} = \frac{K_S D}{\mu_m - D} \tag{5.6.7.5}$$

Substituting equation (5.6.7.2) into equation (5.6.7.1):

$$\overline{X} = Y_{X/S}\left(S_{in} - \frac{K_S D}{\mu_m - D}\right) \tag{5.6.7.6}$$

For unsteady state:

$$\frac{dX}{dt} = X(\mu - D) \tag{5.6.7.7}$$

The equation with respect to substrate:

$$\frac{dX}{dt} = X\left(\mu_m \cdot \frac{S}{K_S + S} - D\right) \tag{5.6.7.8}$$

5.6.8 Modified Chemostat

With cell recycling, chemostat efficiency is improved. To maintain a high cell density the cells in the outlet stream are recycled back to the fermentation vessel. Figure 5.10 represents a chemostat unit with a cell harvesting system. The separation unit is used for harvesting the cells and recycling then to the culture vessel to increase the cell concentration.

The material balance in a constant volume chemostat is derived based on cell balance as shown in the following equations. Material balance in a chemostat with recycle, ρ_{cell}:

$$\frac{dX}{dt} = \left(\frac{F}{V}\right)[X_o - X(1+\tau)] + \mu X + \left(\frac{F}{V}\right) \cdot cX \tag{5.6.8.1}$$

where τ = recycle ratio

c = the factor by which the outlet stream is concentrated before return

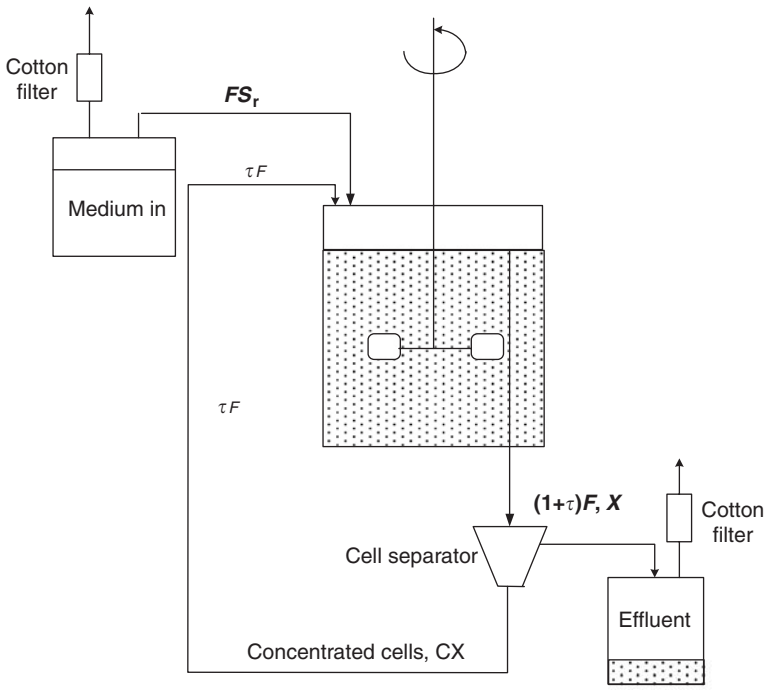

FIG. 5.10. Chemostat with a cell recycle stream.

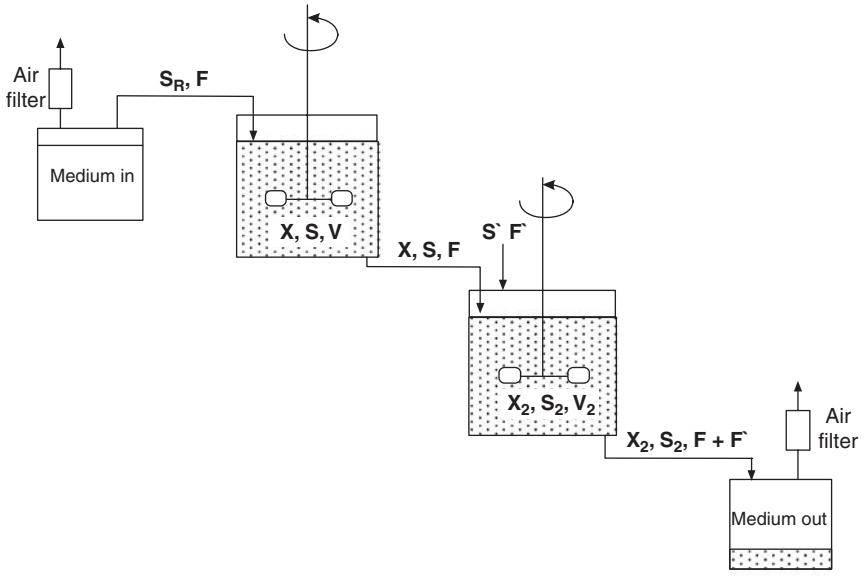

FIG. 5.11. Two stages of CSTR fermentation vessels in series.

For steady-state, $\frac{dX}{dt} = 0$

$$\mu = D(1+\tau-\tau c) \tag{5.6.8.2}$$

Multi-stages of continuous culture are designed to use the outlet of the first vessel as the inoculum for the next stage. If intermediate metabolites are used as feed for another microorganism, sequential continuous culture is useful. The dilution rate for each vessel may be different to the other vessel. It is also possible to supply different nutrients for each stage of fermentation vessel. It is common to operate earlier stages as aerobic and subsequent stages in an anaerobic condition. In addition, if unused substrate leaves the product stream, it can be used in the next stage even at low substrate concentration. The kinetic representation may show a slower rate and even drop to zero-order. Figure 5.11 shows two stages of a chemostat in operation.

5.6.9 Fed Batch Culture

Culture with continuous nutrient supply can be operated in two modes: (i) variable volume; (ii) fixed volume.

For variable volume, feed rate F_{in} is not the same as outflow when $F_{out} = 0$

$$\frac{d}{dt}(XV) = \mu XV - F_{out}X \tag{5.6.9.1}$$

$$\frac{dV}{dt} = F_{in} - F_{out} \tag{5.6.9.2}$$

and dilution rate,

$$D = \frac{F_{in}}{V} \tag{5.6.9.3}$$

Material balance for substrate:

$$\frac{dS}{dt} = \frac{F}{V}[S_i - (1+\tau)S_o + S_o] - \frac{\mu}{Y_{X/S}} \cdot S_o \tag{5.6.9.4}$$

For steady-state, $\frac{dS}{dt} = 0$

$$\overline{X} = \frac{D}{\mu} \cdot Y_{X/S}(S_i - S_o) \tag{5.6.9.5}$$

Substituting μ:

$$\overline{X} = Y_{X/S}(S_i - S_o)/(1+\tau-\tau c) \tag{5.6.9.6}$$

$$\frac{dX}{dt} = \left(\mu - \frac{F_{in}}{V}\right)X = (\mu - D)X \tag{5.6.9.7}$$

For quasi-steady state, the specific growth rate reaches the media dilution rate, $\mu \approx D$. If $F_{in} > F_{out}$, the specific growth rate may decrease.

- Fed batch is used to overcome substrate limitations, especially for the production of antibiotics.
- Avoid substrate inhibition, which can allow a periodic shift of the growth rate.

5.7 ENZYME REACTION KINETICS

Most enzymes catalyse reactions and follow Michaelis–Menten kinetics. The rate can be described on the basis of the concentration of the substrate and the enzymes. For a single enzyme and single substrate, the rate equation is:

$$E + S \leftrightarrow ES \tag{5.7.1}$$

$$ES \rightarrow E + P \tag{5.7.2}$$

$$v = -\frac{\mathrm{d}S}{\mathrm{d}t} = \frac{v_{\max} S}{K_M + S} \tag{5.7.3}$$

$$\frac{1}{v} = \frac{K_M}{v_{\max}} \frac{1}{S} + \frac{1}{\mu_{\max}} \tag{5.7.4}$$

where V is rate of substrate consumption in $\mathrm{mol \cdot l^{-1} \cdot h^{-1}}$, $V_{\max}$ is the maximum specific growth rate in $\mathrm{h^{-1}}$, S is substrate concentration in $\mathrm{g \cdot l^{-1}}$ and K_M is Michaelis–Menten constant in $\mathrm{g \cdot l^{-1}}$. A double reciprocal plot or a well know Lineweaver–Burk plot of $1/\mu$ versus $1/S$ is shown in Figure 5.12.

For batch reaction, there is no inlet or outlet stream

$$m_i = m_o = 0 \tag{5.7.5}$$

$$-r_A = -r_s = \frac{1}{V} \frac{\mathrm{d}(SV)}{\mathrm{d}\tau} = \frac{-v_{\max} S}{K_m + S} \tag{5.7.6}$$

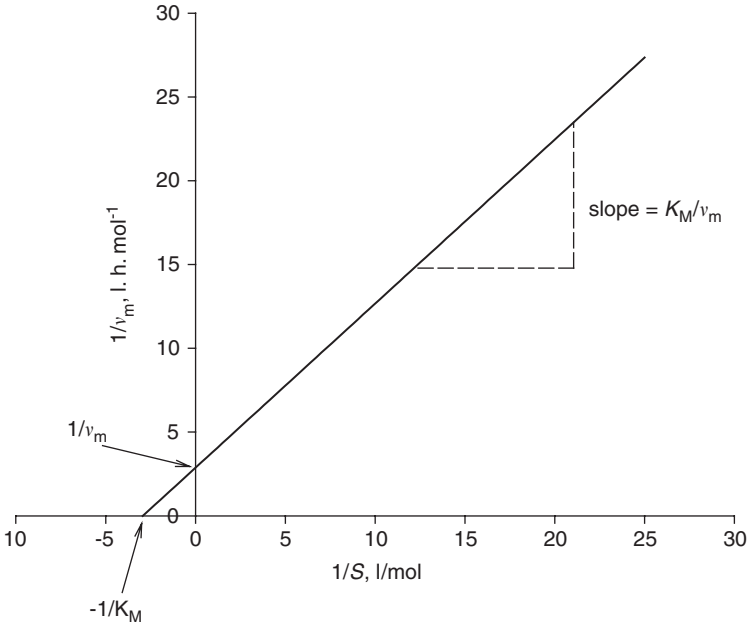

FIG. 5.12. Single enzyme with different substrates.

where V is the volume of batch reactor which is constant volume.

$$\frac{dS}{dt} = -\frac{v_{max} S}{K_m + S} \tag{5.7.7}$$

$$-\int_0^t dt = \int_{S_O}^{S_f} \frac{K_m + S}{v_{max} S} ds \tag{5.7.8}$$

$$-t = \frac{K_m}{v_{max}} \ln \frac{S_f}{S_o} + \frac{1}{v_{max}} (S_f - S_o) \tag{5.7.9}$$

$$t_{batch} = \frac{K_m}{v_{max}} \ln \frac{S_0}{S_f} + \frac{(S_0 - S_f)}{v_{max}} \tag{5.7.10}$$

where S_0 is the initial substrate concentration in $g \cdot l^{-1}$, and S_f is the final substrate concentration in $g \cdot l^{-1}$.

5.7.1 Mechanisms of Single Enzyme with Dual Substrates

The kinetics of double substrates with defined dissociation constants are given as:

$$E + S_1 \underset{k_{-1}}{\overset{k_1}{\longleftrightarrow}} ES_1, \; K_1 = \frac{k_-}{k} \tag{5.7.1.1}$$

where K_1 is the equilibrium or dissociation constant.

$$ES_1 \xrightarrow{k_1} E + P_1 \tag{5.7.1.2}$$

Similarly, for a second substrate, the reaction is carried out and the second product is formed.

$$E + S_2 \Leftrightarrow ES_2, K_2 \tag{5.7.1.3}$$

where K_2 is the equilibrium or dissociation constant.

$$ES_2 \xrightarrow{k_2} E + P_2 \tag{5.7.1.4}$$

Overall enzyme balance and equilibrium constants are defined for the intermediate substrate and enzyme complex. The total enzyme concentration is the sum of free and conjugated enzymes with the substrates.

$$e_o = E + ES_1 + ES_2 \tag{5.7.1.5}$$

The intermediates, complexes of ES_1 and ES_2, are defined based on equilibrium constants.

$$K_1 = \frac{[E][S_1]}{ES_1} \Rightarrow ES_1 = \frac{[E][S_1]}{K_1} \tag{5.7.1.6}$$

$$K_2 = \frac{[E][S_2]}{[ES_2]} \;\Rightarrow\; ES_2 = \frac{[E][S_2]}{K_2} \tag{5.7.1.7}$$

The initial and total enzyme concentrations are defined based on measurable components given below:

$$e_o = E\left(1 + \frac{S_1}{K_1} + \frac{S_2}{K_2}\right) \tag{5.7.1.8}$$

The free enzyme can also be defined based on the following equation:

$$E = \frac{e_o}{\left(1 + \frac{S_1}{K_1} + \frac{S_2}{K_2}\right)} \tag{5.7.1.9}$$

The rate equation for first substrate:

$$-\frac{\mathrm{d}s_1}{\mathrm{d}t} = \upsilon_1 = k_1[ES_1] = \frac{k_1[E][S_1]}{K_1} \tag{5.7.1.10}$$

The rate is defined with respect to dual substrates:

$$\upsilon_1 = \frac{k_1 e_o[S_1]}{K_1} \Bigg/ \left(1 + \frac{S_1}{K_1} + \frac{S_2}{K_2}\right) \tag{5.7.1.11}$$

The rate equation for the second substrate is:

$$-\frac{\mathrm{d}s_2}{\mathrm{d}t} = \upsilon_2 = k_2[ES_2] = \frac{k_2[E][S_2]}{K_2} \tag{5.7.1.12}$$

The second rate is also defined as follows:

$$\upsilon_2 = \frac{k_2 e_o [S_2]}{K_2} \Bigg/ \left(1 + \frac{S_1}{K_1} + \frac{S_2}{K_2}\right) \tag{5.7.1.13}$$

Overall reaction rates for dual substrates are the sum of the rates of dissociation of two substrates.

$$\upsilon_T = -\frac{\mathrm{d}S_T}{\mathrm{d}t} = -\left(\frac{\mathrm{d}S_1}{\mathrm{d}t} + \frac{\mathrm{d}S_2}{\mathrm{d}t}\right) = e_o \left(\frac{k_1 S_1}{K_1} + \frac{k_2 S_2}{K_2}\right) \Bigg/ \left(1 + \frac{S_1}{K_1} + \frac{S_2}{K_2}\right) \tag{5.7.1.14}$$

If one substrate vanishes then the rate is based on the concentration of the total substrate that is present in the reaction vessel; so if S_2 is zero, then the total substrate concentration S_{T_o} is the concentration of substrate involved in the reaction.

$$\upsilon_T = \frac{e_o k_1 S_{T_o}}{K_1 + S_{T_o}} \tag{5.7.1.15}$$

Otherwise if one of the substrate increases, the other substrate decreases. If S_2 increases then S_1 has to decrease. The simplified rate, which is very similar to that for a single substrate, is given as follows:

$$\upsilon_T = \frac{e_O k_2 S_{T_o}}{K_2 + S_{T_o}} \tag{5.7.1.16}$$

In general, enzymes are proteins and carry charges; the perfect assumption for enzyme reactions would be multiple active sites for binding substrates with a strong affinity to hold on to substrate. In an enzyme mechanism, the second substrate molecule can bind to the enzyme as well, which is based on the free sites available in the dimensional structure of the enzyme. Sometimes large amounts of substrate cause the enzyme-catalysed reaction to diminish; such a phenomenon is known as inhibition. It is good to concentrate on reaction mechanisms and define how the enzyme reaction may proceed in the presence of two different substrates. The reaction mechanisms with rate constants are defined as:

$$E + S \underset{k_{-1}}{\overset{k_1}{\longleftrightarrow}} ES \tag{5.7.1.17}$$

The dissociation constant is related to the equilibrium constant, given by $k_1 = \dfrac{k_{-1}}{k_1}$

$$ES + S \overset{K_2}{\longleftrightarrow} ESS \quad \text{or} \quad ES_2 \tag{5.7.1.18}$$

$$K_2 = \frac{k_{-2}}{k_2} = \frac{[ES][S]}{[ES_2]} \tag{5.7.1.19}$$

$$ES \xrightarrow{k} E + P \tag{5.7.1.20}$$

The total enzyme concentration is the sum of free and conjugated enzymes with substrates.

$$e_o = E + ES_1 + ES_2 \tag{5.7.1.21}$$

When the enzyme–substrate complex is stabilised, it may reach a fixed concentration, therefore there is no more change in *ES*:

$$-\frac{\mathrm{d}[ES]}{\mathrm{d}t} = k_2[ES][S] - k_2[ES_2] + k_{-1}[ES] - k_1[E][S] - k[ES] = 0 \tag{5.7.1.22}$$

The rate equation for the enzyme complex leads to product in (5.7.1.22) is defined as:

$$\upsilon = k[ES] \tag{5.7.1.23}$$

ES_2 was obtained from (5.7.1.19):

$$[ES_2] = \frac{[ES][S]}{k_2} \tag{5.7.1.24}$$

Incorporating (5.7.1.24) into (5.7.1.22), after simplification it is reduced to:

$$(k_{-1} - k_2)[ES] = k_1[E][S] \tag{5.7.1.25}$$

Substituting (5.7.1.24) into (5.7.1.22), the rate of enzymatic reaction with dual substrates is obtained:

$$\upsilon = \frac{k \;\; k_1[E][S]}{k_{-1} - k_2} \tag{5.7.1.26}$$

The reaction mechanisms may assist us in obtaining a suitable rate equation. Based on the enzyme reaction mechanism given by (5.7.1.18) for the intermediate enzyme–substrate complex, the following equations are derived for *ES*:

$$-\frac{\mathrm{d}(ES)}{\mathrm{d}t} = k_1[E][S] - k_{-1}[ES_1] - k_2[ES][S] + k_{-2}[ES_2] = 0 \tag{5.7.1.27}$$

From the equilibrium constant, the free enzyme concentration must be defined. We know the total enzyme concentration as the sum of the conjugated enzymes with substrates and the free enzymes.

$$e_o = E + ES + ES_2 \Rightarrow E = e_o - ES - ES_2 \tag{5.7.1.28}$$

Substituting (5.7.1.28) into (5.7.1.27), then solving for intermediate enzyme–substrate complex:

$$k_1[e_o][S] - (k_1 + k_{-1})[ES] + (k_{-2} - k_1)[ES_2] - k_2[ES][S] = 0 \tag{5.7.1.29}$$

$$k_1 e_o[S] = (k_1 + k_{-1})[ES] - \left[\left(\frac{k_{-2} - k_1}{k_2}\right) - k_2\right][ES][S] \tag{5.7.1.30}$$

The enzyme–substrate complex is used by substituting *ES* into (5.7.1.23):

$$v = k[ES] = \frac{ke_o[S]}{1 + K_1 - \left[\left(\frac{K_2}{k_1} - 1\right) - \frac{k_2}{k_1}\right][S]} \tag{5.7.1.31}$$

At equilibrium conditions the rate constant for (5.7.1.17) is:

$$K_1 = \frac{[E][S]}{[ES]} \tag{5.7.1.32}$$

The intermediate enzyme–substrate complex is defined:

$$[ES] = \frac{[E][S]}{K_1} = \frac{e_o S - ES_2 - ES_2 S}{K_1} \tag{5.7.1.33}$$

The second equilibrium constant for the (5.7.1.18) is also defined:

$$K_2 = \frac{[ES][S]}{[ES_2]} \tag{5.7.1.34}$$

where the total enzyme is $e_o = E + ES + ES_2$

$$E = e_o - ES - ES_2 \tag{5.7.1.35}$$

Let us eliminate ES_2 by substituting $ES_2 = e_o - E - ES$ into equation 5.7.1.27

Equation 5.7.1.34 gives:

$$K_2 e_o - K_2 E - K_2 [ES] = [ES][S] \tag{5.7.1.36}$$

Equation 5.7.1.32 leads to:

$$K_1 [ES] = [E][S] \tag{5.7.1.37}$$

The free enzyme concentration is:

$$[E] = \frac{K_1 [ES]}{[S]} \tag{5.7.1.38}$$

Substituting (5.7.1.38) into (5.7.1.36) results in:

$$K_2 e_o - K_2 \frac{K_1 [ES]}{[S]} - K_2 [ES] = [ES][S] \tag{5.7.1.39}$$

The intermediate complex *ES* is defined:

$$[ES] = K_2 e_o \Big/ \left[S + K_2 - \frac{K_2 K_1}{[S]} \right] \tag{5.7.1.40}$$

The enzyme rate equation with two dissociation relations at equilibrium yields:

$$\upsilon = k e_o \Big/ 1 + \frac{[S]}{K_2} + \frac{K_1}{[S]} \tag{5.7.1.41}$$

Now, maximise the rate at a specific substrate concentration:

$$\frac{\mathrm{d}\upsilon}{\mathrm{d}t} = 0 = -\frac{1}{K_2} + \frac{K_1}{S^2} \Rightarrow \frac{K_1}{S^2} = \frac{1}{K_2} \tag{5.7.1.42}$$

Maximum substrate concentration is defined by the square root of the dissociation constants

$$S_{\max} = \sqrt{K_1 K_2} \tag{5.7.1.43}$$

At a high substrate concentration, the rate can be simplified and a linearised model is obtained:

$$\frac{1}{\upsilon} = 1 + \frac{[S]}{K_2} \Big/ k e_o \tag{5.7.1.44}$$

A graph of $1/\upsilon$ versus S is plotted and the slope is $1/K_2ke_o$. There is an intercept in the graphical presentation to identify another constant. From the above equation, K_2 can be calculated, which is similar to S_{max}, where S_{max} means that the substrate concentration gives the maximum rate.

5.7.2 Kinetics of Reversible Reactions with Dual Substrate Reaction

The reaction mechanisms for reversible reactions are slightly different. In the above section, the second part of the reaction that leads to product was irreversible. However, if all the steps in enzyme reactions were reversible, the resulting rates may be affected.

$$S + E \underset{k_{-1}}{\overset{k_1}{\longleftrightarrow}} ES \tag{5.7.2.1}$$

where k_1 is the rate constant for forward and k_{-1} the rate constant for backward reactions. The second reaction is:

$$ES \Leftrightarrow P + E \tag{5.7.2.2}$$

where k_2 is the rate constant for forward and k_{-2} the rate constant for backward reactions. For dual substrates the reaction mechanisms may be complicated if the enzyme–substrate complex of the first substrate reacts with the second substrate; then the dissociation constant of K_{12} is defined to present the equilibrium, and vice versa the dissociation constant for the reaction of second substrate–enzyme complex with the first substrate is K_{21}.

$$e_o = e + ES_1 + ES_2 + ES_1S_2 \tag{5.7.2.3}$$

The rate equation for reversible reactions with two substrates is defined.

$$\upsilon = ke_o \Big/ 1 + \frac{K_{21}}{S_1} + \frac{K_{12}}{S_2} + \frac{K_2K_{21}}{S_1S_2} \tag{5.7.2.4}$$

Assume

$$K_1K_{12} = K_2K_{21} \tag{5.7.2.5}$$

$$\upsilon = \frac{ke_oS_2S_1}{S_1S_2 + K_{21}S_2 + K_{12}S_1 + K_2K_{21}} = \frac{ke_oS_2S_1}{(K_{12} + S_2)(K_1^* + S_1)} \tag{5.7.2.6}$$

For the special case the rates are simplified to more familiar rates and result in the following:

$$\upsilon = \frac{\upsilon^*_{max}\, S_1}{K_1^* + S_1} \tag{5.7.2.7}$$

where υ^*_{max} and K_1^* are the apparent maximum rate and Michaelis constant, respectively.

$$\upsilon^*_{max} = \frac{ke_o S_2}{K_{12} + S_2} \tag{5.7.2.8}$$

$$K_1^* = \frac{K_1 K_{12} + K_{12} S_2}{K_{12} + S_2} \tag{5.7.2.9}$$

If one substrate is in great excess, K_{12} is small or $S_2 >> K_{12}$ then $\upsilon_{max} = ke_o$ and $K_1^* \cong K_{21}$. In this case we can simplify the rate to:

$$\upsilon = \frac{ke_o S_1}{K_{21} + S_1} \tag{5.7.2.10}$$

5.7.3 Reaction Mechanism with Competitive Inhibition

Generally inhibitors are competitive or non-competitive with substrates. In competitive inhibition, the interaction of the enzyme with the substrate and competitive inhibitor instead of the substrate can be analysed with the sequence of reactions taking place; as a result, a complex of the enzyme–inhibitor (*EI*) is formed. The reaction sets at equilibrium and the final step shows the product is formed. The enzyme must get free, but the enzyme attached to the inhibitor does not have any chance to dissociate from the *EI* complex. The *EI* formed is not available for conversion of substrate; free enzymes are responsible for that conversion. The presence of inhibitor can cause the reaction rate to be slower than the ordinary reaction, in the absence of the inhibitor. The sequence of reaction mechanisms is:

$$E + S \Leftrightarrow ES, K_S \tag{5.7.3.1}$$

$$E + I \Leftrightarrow EI, K_i \tag{5.7.3.2}$$

where K_S and K_i are dissociations for the Michaelis–Menten rate constant and the inhibition constant, respectively:

$$ES \xrightarrow{k} E + P \tag{5.7.3.3}$$

The total enzyme concentration is the sum of all enzymes as free, and those conjugated as *ES* and *EI*:

$$e_o = E + ES + EI \tag{5.7.3.4}$$

The reaction rate model is based on total enzyme, substrate and inhibitor concentrations.

$$\upsilon = \frac{ke_o S}{S + K_S\left(1 + \dfrac{I}{K_i}\right)} \tag{5.7.3.5}$$

Comparison of the ordinary Michaelis–Menten relation with (5.108) shows that the inhibitor did not influence specific growth rate, $\upsilon_{\max}$, but the Michaelis–Menten constant was affected by the inhibitor and resulted in a constant, known as the apparent Michaelis constant.

$$K_m^{\text{app}} = K_S\left(1 + \frac{i}{K_i}\right) \tag{5.7.3.6}$$

where K_m^{app} is apparent Michaelis constant. The rate constant is increased by the presence of a competitive inhibitor. The inhibitor causes the reaction rate to slow down. The competitive inhibitor can be unaffected or eliminated by increasing the substrate concentration.

5.7.4 Non-competitive Inhibition Rate Model

The non-competitive inhibitor is defined by the following sequence of reactions:

$$EI + S \Leftrightarrow EIS, K_S \tag{5.7.4.1}$$

$$ES + I \Leftrightarrow ESI, K_i \tag{5.7.4.2}$$

In such inhibition, the inhibitor and the substrate can simultaneously bind to the enzyme. The nature of the enzyme–inhibitor–substrate binding has resulted in a ternary complex defined as *EIS*. The K_S and K_i are identical to the corresponding dissociation constants. It is also assumed that the *EIS* does not react further and is unable to deliver any product *P*. The rate equation for non-competitive inhibition, $u_{\max}$, is influenced:

$$\upsilon = \frac{ke_o S \Big/ \left(1 + \dfrac{i}{K_i}\right)}{S + K_S} \tag{5.7.4.3}$$

The maximum specific growth rate is retarded with non-competitive inhibitor. The apparent specific growth rate, $\upsilon_{\max}^{\text{app}}$, is smaller than the ordinary specific growth rate, $\upsilon_{\max}$.

$$\upsilon_{\max}^{\text{app}} = \frac{ke_o}{1 + \dfrac{i}{K_i}} \tag{5.7.4.4}$$

If the complex of *ESI* can be dissociated to product, the rate equation would result in mixed competitive and non-competitive inhibitors:

$$EIS \xrightarrow{k} EI + P \tag{5.7.4.5}$$

$$v = \frac{v_{\max}^{\text{app}} S}{S + K_m^{\text{app}}} \tag{5.7.4.6}$$

The competitive and non-competitive inhibitors are easily distinguished in a Lineweaver–Burk plot. The competitive inhibitor intercepts on the $1/v$ axis whereas the non-competitive inhibitor intercepts on the $1/S$ axis. The reaction of inhibitors with substrate can be assumed as a parallel reaction while the undesired product is formed along with desired product. The reactions are shown as:

$$A \xrightarrow{k_1} R \quad \text{desired} \tag{5.7.4.7}$$

$$A \xrightarrow{k_2} S \quad \text{undesired} \tag{5.7.4.8}$$

Since enzyme is not shown in the reaction we assume an elementary rate equation may explain the above reactions. The simple kinetics are discussed in most fermentation technology and chemical reaction engineering textbooks.[8–10]

Example 1

An enzyme is produced for manufacturing a sun protection lotion. Given kinetic data for the enzyme reaction with $v_{\max} = 2.5 \dfrac{\text{mmol}}{\text{m}^3\text{s}}$, $Km = 8.9$ mM and $S_O = 12$ mM, what would be the time required for 95% conversion in a batch bioreactor?

Solution

$$V_{\max} = \left(2.5 \frac{\text{mmol}}{\text{m}^3\text{s}}\right)\left(\frac{3600\ \text{s}}{\text{h}}\right)\left(\frac{1\ \text{m}^3}{1000\ \text{L}}\right) = 9 \frac{\text{mmol}}{\text{h L}}$$

$$t_{\text{batch}} = \frac{8.9\ \text{mM}}{9\ \text{mM/h}} \ln \frac{12}{0.6} + \frac{(0.95)(12)}{9} = 4.23\ \text{h}$$

Example 2

Calculate K_m and $V_{\max}$ for given substrate concentrations and rates. The inverse rate and substrate concentrations are calculated in Table E.2.1.

TABLE E.2.1. *Substrate concentration and reaction rate*

S (mol·l^{-1})	v (mol·l^{-1}·min^{-1})
4.10×10^{-3}	1.77×10^{-4}
9.50×10^{-4}	1.73×10^{-4}
5.20×10^{-4}	1.25×10^{-4}
1.03×10^{-4}	1.06×10^{-4}
4.90×10^{-5}	8.00×10^{-5}
1.06×10^{-5}	6.70×10^{-5}
5.10×10^{-6}	4.30×10^{-5}

TABLE E.2.2.

$1/S$, l·mol^{-1}	$1/v$, l·min·mol^{-1}
243.9	5650
1052.6	5780
1923.0	8000
9708.7	9434
20408.1	12500
94339.6	14925
196078.4	23256

Solution

Let us inverse the substrate concentration and reaction rate as shown in Table E.2.2.

In evaluation of kinetic parameters, the double reciprocal method is used for linearisation of the Michaelis–Menten equation (5.7.3).

(a) Use the Lineweaver–Burk plot as defined in the following relation:

$$\frac{1}{v} = \frac{1}{v_{\max}} + \frac{K_m}{v_{\max}} \frac{1}{S} \tag{E.2.1}$$

$$\text{Slope} = \frac{22500 - 10000}{1.875 \times 10^5 - 2.5 \times 10^4} = 0.077$$

$$v_{\max} = 1.25 \times 10^{-4} \text{ mol/l·min}$$

$$\frac{K_m}{v_{\max}} = 0.077 \tag{E.2.2}$$

$$K_m = 9.6 \times 10^{-5} \text{ mol/l}$$

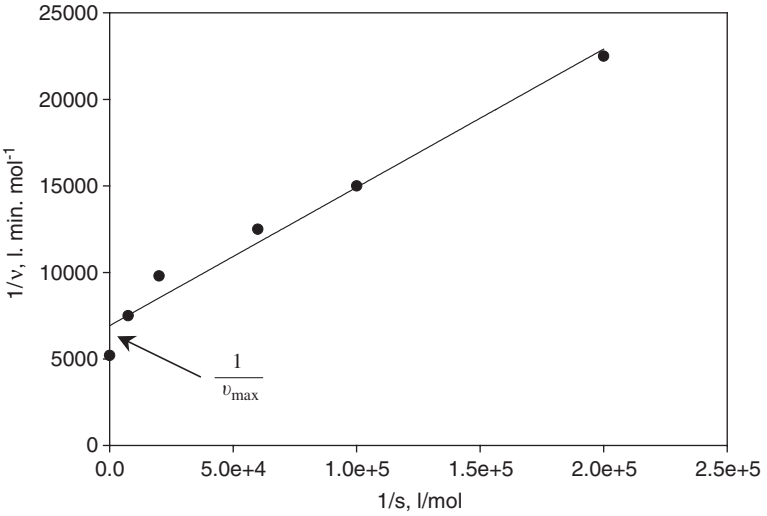

FIG. E.2.1. Lineweaver–Burk plot.

TABLE E.2.3. *Data collected and calculated for rate model*

S (mol·l^{-1})	v, mol·l^{-1}·min^{-1}	S/v, min	v/S, min^{-1}
4.10×10^{-3}	1.77×10^{-4}	23.00	0.044
9.50×10^{-4}	1.73×10^{-4}	5.50	0.182
5.20×10^{-4}	1.25×10^{-4}	4.20	0.240
1.03×10^{-4}	1.06×10^{-4}	0.97	1.030
4.90×10^{-5}	8.00×10^{-5}	0.60	1.670
1.06×10^{-5}	6.70×10^{-5}	0.16	6.250
5.10×10^{-6}	4.30×10^{-5}	0.12	8.330

(b) Use another form of linear graphical presentation to evaluate K_m and $V_{\max}$ based on the following relation:

$$\frac{S}{v} = \frac{K_m}{v_{\max}} + \frac{1}{v_{\max}} S \tag{E.2.3}$$

This method tends to create a cluster of data near the origin as shown in Figure E.2.2.

$$\text{Slope} = \frac{22.5 - 6.0}{3 \times 10^{-3}} = 5500$$

$$v_{\max} = 1.82 \times 10^{-4} \text{ mol/l·min}$$

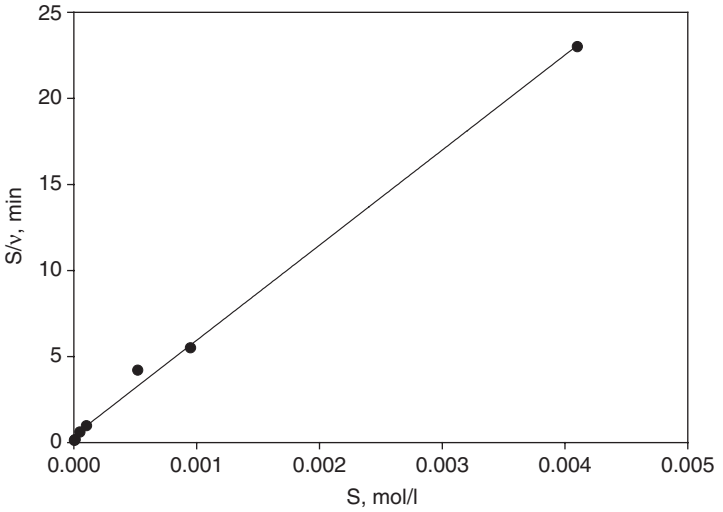

FIG. E.2.2. Linear model for the Monod rate equation with populated data at the origin.

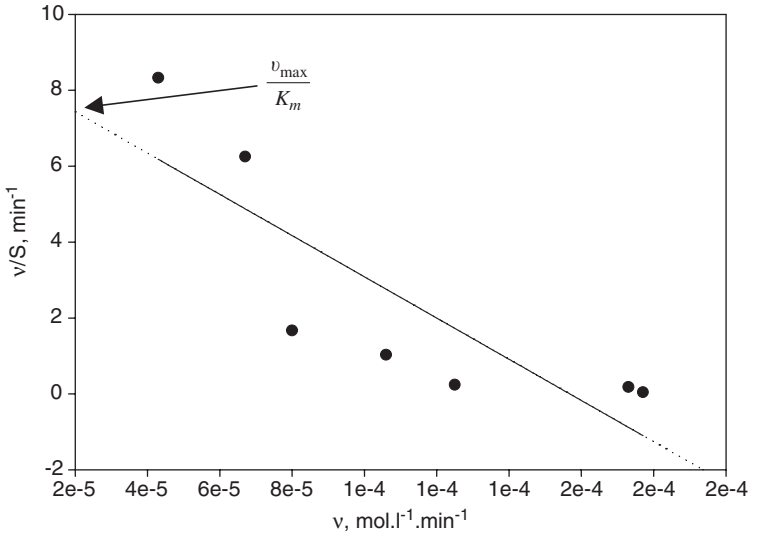

FIG. E.2.3. Eadie–Hofstee plot.

$$K_m = \frac{0.5}{5500} = 9.1 \times 10^{-5}\,\text{mo}$$

For the Eadie–Hofstee plot, both coordinates contain rates that are subjected to the greatest error, as indicated in Figure E.2.3.

$$v = v_{\max} - K_m \frac{v}{S} \tag{E.2.3}$$

A plot of *u/S* versus v is presented in Figure E.2.3 for defining slope and intercept, K_m and $v_{\max}$, respectively.

A linearisation model is used to explain the equation of a simple straight line:[9]

$$y = bx + a \tag{E.2.4}$$

where

$$b = \frac{\sum_{i}^{N} x_i y_i - N\bar{x}\bar{y}}{\sum x_i^2 - N\bar{x}^2} \tag{E.2.5}$$

$$a = \bar{y} - b\bar{x} \tag{E.2.6}$$

$\bar{x}, \bar{y}$ are average values of x_i and y_i

$$\text{Slope of the line} = \frac{1}{K_m}$$

$$K_m = 6.5 \times 10^{-5} \text{ mol}\cdot\text{l}^{-1}$$

$$v_{\max} = 18 \times 10^{-4} \text{ mol}\cdot\text{l}^{-1}\cdot\text{min}^{-1}$$

Example 3

In batch enzyme reaction kinetics, given $K_m = 10^{-3}$ M and substrate concentration $S_0 = 3 \times 10^{-5}$ M, after 2 min, 5% of the substrate was converted. How much of the substrate was consumed after 10, 20, 30 and 60 min?

Solution

For $S_o << K_m$, the rate model is reduced to a first-order rate equation:

The Michaelis–Menten rate equation is:

$$v = \frac{v_{\max} S}{K_m + S} \tag{E.3.1}$$

The simplified first-order rate is

$$-\frac{\mathrm{d}S}{\mathrm{d}t} = V_m^* S \tag{E.3.2}$$

Carry out integrations:

$$-\int_{S_o}^{S} \frac{\mathrm{d}S}{S} = V_m^* \int_0^t \mathrm{d}t \tag{E.3.3}$$

$$\ln \frac{S}{S_o} = -\nu_m t \tag{E.3.4}$$

The concentration profile is predicted by the following equation

$$S = S_0 e^{-V_m^* t} \tag{E.3.5}$$

At time equal to 2 min:

$$\frac{S}{S_o} = 1 - X_E \tag{E.3.6}$$

$$C_A = C_{A_o}(1 - X_A) \tag{E.3.7}$$

$$\frac{S}{S_o} = 0.95 \tag{E.3.8}$$

$$\mathrm{e}^{-2V_m^*} = 0.95 \tag{E.3.9}$$

$$\nu_m = -\frac{\ln 0.95}{2}$$

$$= 0.2565 \text{ min}^{-1}$$

$$\frac{S}{S_o} = \mathrm{e}^{-0.02565\, t} \tag{E.3.10}$$

Conversion

$$X_A = 1 - \frac{S}{S_o} = 1 - e^{-0.02565\,t} \tag{E.3.11}$$

For $t = 10$ min, $X_A = 1 - e^{-0.2565} = 0.226$ or 22.6%.
For $t = 20$ min, $X_A = 1 - e^{-0.02565(20)} = 0.401$ or 40.1%.
For $t = 30$ min, $X_A = 1 - e^{-0.02565(30)} = 0.5367$ or 53.67%.
For $t = 60$ min, $X_A = 1 - e^{-0.02565(60)} = 0.785$ or 78.5%.

Example 4

In a complex enzyme reaction, multiple substrate–enzyme complexes are formed. Assume the following reaction mechanisms are taking place in three consecutive stages:

$$S + E \xleftrightarrow{K_1} ES_1 \xleftrightarrow{K_2} ES_2 \xrightarrow{k_5} P + E \tag{E.4.1}$$

Develop a suitable rate expression using the Michaelis–Menten rate equation and the quasi-steady-state approximations for the intermediate complexes formed.

Solution

Equilibrium dissociation constants are defined as

$$K_1 = \frac{k_2}{k_1} = \frac{[E][S]}{[ES_1]} \tag{E.4.2}$$

$$K_2 = \frac{k_4}{k_3} = \frac{[ES_1]}{[ES_2]} \tag{E.4.3}$$

$$\upsilon = k_5[ES_2] \tag{E.4.4}$$

$$[ES_2] = \frac{[ES_1]}{K_2} \tag{E.4.5}$$

$$[ES_1]\frac{[E][S]}{K_1} \tag{E.4.6}$$

$$v = \frac{k_5}{K_2}[ES_1] = \frac{k_5}{K_1K_2}[E][S] \tag{E.4.7}$$

The total enzyme concentration is:

$$E_0 = E + ES_1 + ES_2 + E + \frac{[E][S]}{K_1} + \frac{[E][S]}{K_1 K_2} = E\left(1 + S\left[\frac{1}{K_1} + \frac{1}{K_1 K_2}\right]\right) \tag{E.4.8}$$

$$E = \frac{e_o}{1 + \left(\frac{K_2 + 1}{K_1 K_2}\right)[S]} \tag{E.4.9}$$

$$K_{\text{obs}} = k_{\text{apparent}} = \frac{K_1 K_2}{K_2 + 1} \tag{E.4.10}$$

$$\upsilon_{\max} = \frac{k_5 e_o}{K_2 + 1} \tag{E.4.11}$$

The final rate expression is:

$$\upsilon = \frac{e_o k_5}{K_1 K_2} \times \frac{[S]}{\left(1 + \left(\frac{K_2 + 1}{K_1 K_2}\right)[S]\right)} = \frac{k_5 e_o [S]}{K_1 K_2 + (K_2 + 1)[S]} = \frac{\left(\frac{k_5 e_o}{K_2 + 1}\right)[S]}{\left(\frac{K_1 K_2}{K_2 + 1}\right) + [S]} \tag{E.4.12}$$

Example 5

Pesticide inhibition on an active enzyme has been reported, which caused enzyme activities to reduce. The collected data with and without inhibition are presented in Table E.5.1. Determine the rate model with and without inhibitor (see Table E.5.1). Also define the type of inhibition.

TABLE E.5.1. *Substrate concentration and enzymatic rate calculation with and without inhibition*

S, mol·l^{-1}	υ (no inhibitor) mol·l^{-1}·min^{-1} × 10^6	υ^* (inhibitor) mol·l^{-1}·min^{-1} ×10^6
3.30×10^{-4}	56	37
5.00×10^{-4}	71	47
6.70×10^{-4}	88	61
1.65×10^{-3}	129	103
2.21×10^{-3}	149	125

TABLE E.5.2. *Inverse substrate concentration and inverse enzymatic rate calculation with and without inhibition*

$1/S$, $l \cdot mol^{-1}$	v (no inhibitor) $mol \cdot l^{-1} \cdot min^{-1} \times 10^6$	$1/v$	v^* (inhibitor) $mol \cdot l^{-1} \cdot min^{-1} \times 10^6$	$1/v^*$, $l \cdot min \cdot mol^{-1}$
3030	56	17857	37	27027
2000	71	14085	47	21277
1492	88	11363	61	16393
606	129	7752	103	9709
452	149	6711	125	8000

Solution

Plot both sets of data as a Lineweaver–Burk plot for competitive inhibition (see Fig. E.5.1):

$$v = \frac{k\, e_o\, S}{S + K_s\left(1 + \frac{i}{k_i}\right)} \tag{E.5.1}$$

The mechanism of the enzyme with substrate in the present of inhibitor is:

$$E + S \xleftrightarrow{K_S} ES \tag{E.5.2}$$

$$E + I \leftrightarrow EI \tag{E.5.3}$$

$$ES \rightarrow E + P \tag{E.5.4}$$

$$e_o = E + [ES] + [EI] \tag{E.5.5}$$

Without inhibition:

$$v = \frac{k\, e_o\, S}{S + K_s} = \frac{k\, e_o\, S}{S + 8.4 \times 10^{-3}} \tag{E.5.6}$$

$$K_s^{\text{app}} = K_s\left(1 + \frac{i}{k_i}\right) \tag{E.5.7}$$

$$1.5 \times 10^{-3} = 8.4 \times 10^{-4}\left(1 + \frac{i}{k_i}\right) \tag{E.5.8}$$

$$\frac{i}{k_i} = 0.786 \tag{E.5.9}$$

$$k_i\, \frac{i}{0.786} = \frac{10^{-5}}{0.786} = 1.73 \times 10^{-3}\, \mu \tag{E.5.10}$$

Plug in a number

$$88\times10^{-6} = \frac{k\,e_o \times 6.7\times10^{-4}}{6.7\times10^{-4} + 8.4\times10^{-3}} \tag{E.5.11}$$

$$k\,e_o = 1.2\times10^{-3}\ \text{min}^{-1}$$

$$61\times10^{-6} = \frac{1.2\times10^{-3}\times6.7\times10^{-4}}{6.7\times10^{-4} + 8.4\times10^{-3}\left(1+\dfrac{i}{k_i}\right)} \tag{E.5.12}$$

$$\frac{i}{k_i} = 0.49 \tag{E.5.13}$$

The reading from the plot for the rate without inhibition:

$$\text{Slope}\ \frac{(27-5)\times10^3}{3000} = 7.3$$

$$k_{\text{app}} = 1.5\times10^{-3}$$

For the data plotted with inhibition:

$$\text{Slope}\ \frac{(18-5)\times10^3}{3100} = 4.2$$

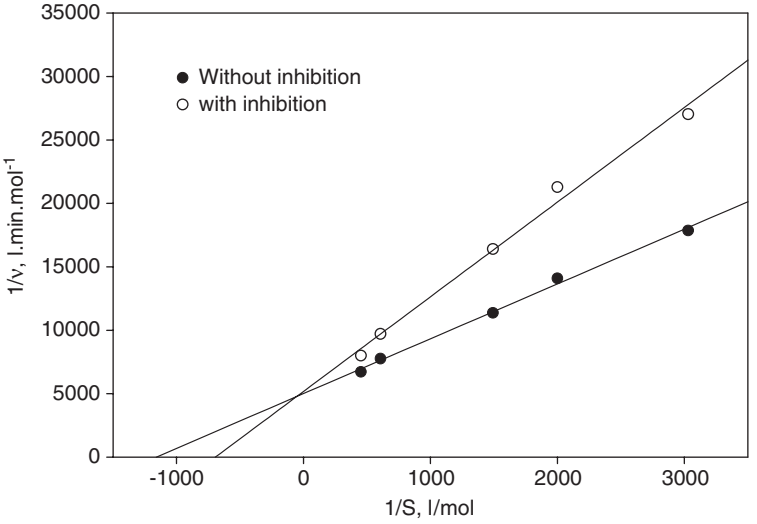

FIG. E 5.1. Competitive inhibition based on the Lineweaver-Burk model.

$$\frac{K_s}{\upsilon_{\max}} = 4.2$$

$$K_s = 8.4 \times 10^{-4} \text{ mol/L}$$

$$\upsilon_{\max} = 2 \times 10^{-4} \text{ mol/min}$$

Based on the graphical presentation, this is a competitive inhibition.

Example 6

The respiratory quotient (*RQ*) is often used to estimate metabolic stoichiometry. Using quasi-steady-state and by definition of *RQ*, develop a system of two linear equations with two unknowns by solving a matrix under the following conditions: the coefficient of the matrix with yeast growth ($\gamma = 4.14$), ammonia ($\gamma_N = 0$) and glucose ($\gamma_S = 4.0$), where the evolution of CO_2 and biosynthesis are very small ($\sigma = 0.095$). Calculate the stoichiometric coefficient for $RQ = 1.0$ for the above biological processes:

Solution

At quasi-steady-state condition:

$$\frac{\mathrm{d}[NADH + H^+]}{\mathrm{d}t} = \frac{\upsilon_s}{2} \times a - 2b - \frac{1}{2}\left[\upsilon_s - \upsilon_s(1+\sigma) - \frac{\delta}{n} \times \upsilon_N\right] = 0 \tag{E.6.1}$$

$$RQ = \frac{\text{moles of } CO_2}{\text{moles of } O_2} = \frac{a+\sigma}{b} \tag{E.6.2}$$

$$\begin{cases} \dfrac{\upsilon_s a}{2} - 2b = \dfrac{1}{2}\left[\upsilon_B - \upsilon_S\,(1+\delta) - \dfrac{\delta}{n}\upsilon_N\right] \\ a - b\,(RQ) = -\sigma \end{cases} \tag{E.6.3}$$

The mathematical solution for the above system is set as given by the following matrix:

$$\begin{bmatrix} \dfrac{\upsilon_S}{2} & -2 \\ 1 & -(RQ) \end{bmatrix} \begin{bmatrix} a \\ b \end{bmatrix} = \begin{bmatrix} \dfrac{1}{2} & \upsilon_B - \upsilon_S(1+\sigma) - \dfrac{\sigma}{n}\upsilon_N \\ -\sigma & \end{bmatrix} \tag{E.6.4}$$

At singular point, let

$$\begin{bmatrix} \dfrac{\upsilon_S}{2} & -2 \\ 1 & -(RQ) \end{bmatrix} = 0 \tag{E.6.5}$$

$$-(RQ)\left(\frac{\upsilon_S}{2}\right)-(-2)(1)=0 \tag{E.6.6}$$

$$RQ=\frac{4}{\upsilon_S} \tag{E.6.7}$$

For anaerobic fermentation, $\upsilon_S = 4$ then $RQ = 1.0$

$$\begin{bmatrix}2 & -2\\ 1 & -1.05\end{bmatrix}\begin{bmatrix}a\\ b\end{bmatrix}=\begin{bmatrix}\frac{1}{2}[4.14-4(1+0.095)-0]\\ -0.095\end{bmatrix}=\begin{bmatrix}-0.12\\ -0.095\end{bmatrix}$$

$$a=0.64,\ b=0.7 \tag{E.6.8}$$

$$\begin{bmatrix}2 & -2\\ 1 & -1.05\end{bmatrix}\begin{bmatrix}a\\ b\end{bmatrix}=\begin{bmatrix}-0.12\\ -0.095\end{bmatrix}$$

$$a=0.52,\ b=0.58 \tag{E.6.9}$$

Increasing RQ with very small changes causes the constants a and b to change in the reaction.

Example 7

For single- and multiple-substrate kinetics, single-substrate glucose, $30\,g\cdot l^{-1}$ and dual substrates glucose and lactose with each carbohydrate at a concentration of $15\ g\cdot l^{-1}$ or total

TABLE E.7.1. *Optical density for single and double substrates*

Time, h	OD, single	OD, double	Time, h	OD, single	OD, double
0.0	0.05	0.05	4.5	0.89	0.44
0.5	0.08	0.06	5.0	1.05	0.49
1.0	0.11	0.07	5.5	1.05	0.51
1.5	0.14	0.08	6.0	1.06	0.53
2.0	0.20	0.10	6.5	1.06	0.61
2.5	0.27	0.14	7.0	1.08	0.85
3.0	0.38	0.19	7.5	1.08	1.04
3.5	0.50	0.27	8.0	1.08	1.04
4.0	0.71	0.33	—	—	—

$t_{lag} = 1$ h for dual substrate.
$t_{lag} = 0$ for single substrate.

carbohydrate concentration of 30 $g \cdot l^{-1}$ were used in sterilised media (Table E.7.1). The cell optical density (*OD*) was measured at wavelength 420 nm. The following data for single and double substrates were obtained. If *OD* is linear in cell density with a value of 0.175 equal to 0.1 mg cell dry weight per millilitre, evaluate the specific growth rate, lag phase and yield of biomass.

Solution

$$\frac{1}{n}\frac{\mathrm{d}n}{\mathrm{d}t} = \mu \tag{E.7.1}$$

$$N(t) = No \;\; e^{\mu_m t} \tag{E.7.2}$$

For $t = 5$ h:

$$\left(\frac{0.1}{0.175}\right)(1.04) = N(S) = \left(\frac{0.05}{0.175}\right)\mathrm{e}^{5\mu_m}$$

$$N(0) = 0.05 \left(\frac{0.1 \text{ g dry cell}}{0.175}\right) = \frac{0.05}{0.175}$$

$$\mu_m = 0.5 \text{ h}^{-1} \text{ dual substrate (Fig. E.7.1)} \tag{E.7.3}$$

For $t = 8$ h:

$$\mu_m = \frac{\left[\ln\left(\frac{1.0}{0.05}\right)\right]}{8}$$

$$\mu_m = 0.57\ h^{-1} \text{ Single substrate}$$

Therefore, yield is:

$$Y = \frac{(1.04)\left[\frac{0.1}{0.175}\right]}{30} = 0.02$$

The shape of dual substrates with the same total concentration of sugar and lactic acid shows two stages like stepwise utilisation of dual substrates has taken place in the cells.

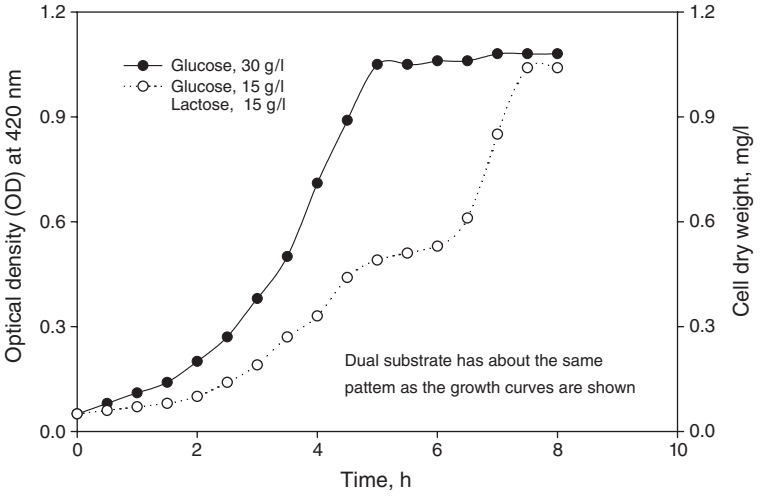

FIG. E.7.1. Single and double substrate growth model.

Example 8

Monod kinetics are considered in a CSTR with an organism growing with an initial substrate concentration of $50\,g{\cdot}l^{-1}$ and kinetic parameters of $K_s = 2\,g{\cdot}l^{-1}$ and $\mu_{max} = 0.5\,h^{-1}$. (a) What would be the maximum dilution rate for 100% yield of biomass with maximum rate? (b) If the same dilution is used, what would be number of CSTRs in series?

Solution

(a)
$$D_{max} = \mu_{max}\left[1 - \sqrt{\frac{K_s}{K_s + S_o}}\right] \tag{E.8.1}$$

$$= (0.5\ h^{-1}) \times \left[1 - \sqrt{\frac{2}{2+50}}\right]$$

$$= 0.402\,h^{-1} \tag{E.8.2}$$

(b) For the first tank, use (5.6.7.5), obtained from the steady-state condition, then solved for substrate concentration profile. The outlet substrate concentration was calculated as:

$$S_1 = \frac{DK_s}{\mu_{max} - D}$$

$$= \frac{(0.402)(2)}{0.5 - 0.402}$$

$$= 8.2\ g{\cdot}l^{-1} \tag{E.8.3}$$

Biomass concentration is obtained from definition as substrate is utilised; it is converted to cells or biomass:

$$X = Y_{X/S}(S_{\text{in}} - S_{\text{out}}) \tag{E.8.4}$$

Now substitute the outlet concentration of substrate, resulting in the following equation:

$$X_1 = Y\left[S_0 - \frac{DK_s}{\mu_{\max} - D}\right]$$

$$X_1 = (1)\left[50 - \frac{(0.402)(2)}{0.5 - 0.402}\right] = 41.8\,\text{g}\cdot\text{l}^{-1} \tag{E.8.5}$$

For the subsequent tanks, use the steady-state mass balance on substrate:

$$D(S_{\text{feed}} - S) - \frac{1}{Y_{X/S}}\mu X = 0 \tag{E.8.6}$$

$$D(S_1 - S_2) - \frac{\mu_{\max} S_2 X_2}{Y(S_2 + K_s)} = 0 \tag{E.8.7}$$

$$X_2 - X_1 = Y(S_1 - S_2) \tag{E.8.8}$$

$$X_2 = X_1 + Y(S_1 - S_2) \tag{E.8.9}$$

$$D(S_1 - S_2) - \frac{\mu_{\max} S_2[X_1 + Y(S_1 - S_2)]}{Y(S_2 + K_s)} = 0 \tag{E.8.10}$$

Solve for substrate concentration:

$$D(Y)(S_1 - S_2)(S_2 + K_S) = \mu_{\max}\, S_2[X_1 + Y(S_1 - S_2)] \tag{E.8.11}$$

$$(0.402)(1)(8.2 - S_2) = 0.5(S_2)[X_1 + Y(\,8.2 - S_2)] \tag{E.8.12}$$

$$0.5\,S_2^2 + 22.51\,S_2 - 6.6 = 0 \tag{E.8.13}$$

Solving the quadratic equation, the meaningful substrate concentration is:

$$S_2 = 0.29 \text{ g}\cdot\text{l}^{-1}$$

$$N = \text{two tanks}$$

Example 9

For the design of a CSTR with inhibition, consider the following rate is valid for a CSTR as a fermentation vessel.

Given the following data:
Initial substrate concentration, $S_o = 10\,\text{g}\cdot\text{l}^{-1}$
Inlet cell concentration for sterile media, $X_o = 0$
The rate constant, $K_S = 1\,\text{g}\cdot\text{l}^{-1}$
The inhibitory constant, $K_i = 0.01\,\text{g}\cdot\text{l}^{-1}$
The inhibitor concentration, $[I] = 0.05\,\text{g}\cdot\text{l}^{-1}$
The $\mu_{\max} = 0.5\ \text{h}^{-1}$ and Yield of biomass on substrate $Y_{X/S} = 0.1$ g cells/g substrate.

Solution

The rate model with inhibition is given by (5.7.3.5).

$$r_X = \frac{\mu_{\max} SX}{K_s + S + \dfrac{i}{K_i} K_s} \tag{E.9.1}$$

$$D = \mu = \frac{\mu_{\max} S}{S + K_s \left(1 + \dfrac{i}{K_i}\right)} \tag{E.9.2}$$

$X_0 = 0$ for sterile feed

$$X = Y_{X/S}\ (S_0 - S) \tag{E.9.3}$$

Rearrangement of the rate model and the equation is solved for substrate S:

$$S = \frac{DK_s + DK_s \left(\dfrac{i}{K_i}\right)}{\mu_{\max} - D} \tag{E.9.4}$$

With defined values of inhibition concentration, rate constant and given dilution rate, the substrate concentration is calculated based on (E.9.4). The tabulated data are given in Table E.9.1.

TABLE E.9.1. *Dilution rate, substrate concentration, cell dry weight and productivity in a CSTR with and without inhibition*

D, h^{-1}	$[I] = 0\ g \cdot l^{-1}$		$[I] = 0.05\ g \cdot l^{-1}$		XD, $g \cdot l^{-1} \cdot h^{-1}$	
	S ($g \cdot l^{-1}$)	X ($g \cdot l^{-1}$)	S ($g \cdot l^{-1}$)	X ($g \cdot l^{-1}$)	$i = 0$	$i = 0.05$
0.05	0.11	0.99	0.67	0.93	0.0495	0.0465
0.10	0.25	0.98	1.50	0.85	0.0980	0.0850
0.15	0.43	0.96	2.57	0.74	0.1290	0.1110
0.20	0.67	0.93	4.00	0.60	0.1860	0.1200
0.25	1.00	0.90	6.00	0.40	0.2250	0.1000
0.30	1.50	0.85	9.00	0.10	0.2550	0.0300
0.35	2.33	0.77	—	—	0.2700	—
0.40	4.00	0.60	—	—	0.2400	—
0.45	9.00	0.10	—	—	0.0450	—

For substrate ratio with no inhibition and with inhibition, the following equation is simplified.

$$\frac{S}{S_i} = \frac{\dfrac{DK_s}{(\mu_{\max} - D)}}{\dfrac{DK_s + DK_s\left(\dfrac{i}{K_i}\right)}{(\mu_{\max} - D)}} = \frac{1}{1 + \left(\dfrac{i}{K_i}\right)} \tag{E.9.5}$$

Cell productivity can be achieved by multiplying (E.9.2) to X:

$$DX = \mu X = \frac{\mu_{\max} S[Y_{X/S}(S_0 - S_i)]}{S_i + K_s\left(1 + \dfrac{I}{K_i}\right)} \tag{E.9.6}$$

The rate equation without inhibition is:

$$(DX)_i = \frac{\mu_{\max} S_i}{S_i + K_s} \tag{E.9.7}$$

$$\frac{XD}{(XD)_i} = \left(\frac{S}{S_i}\right)\left(\frac{S_0 - S}{S_0 - S_i}\right)\left(\frac{S_i + K_s\left(1 + \dfrac{I}{K_i}\right)}{K_s + S}\right) \tag{E.9.8}$$

For the special case the equation without any inhibition the maximum dilution rate is:

$$D_{\max} = \mu_{\max}\left[1-\sqrt{\frac{K_s}{S_0+K_s}}\right] \tag{E.9.9}$$

The maximum dilution rate with inhibition is:

$$D_{\max} = \mu_{\max}\left[1-\sqrt{\frac{K_s\left(1+\dfrac{I}{K_i}\right)}{S_0+K_s\left(1+\dfrac{I}{K_i}\right)}}\right] \tag{E.9.10}$$

Given inhibition concentration as $[I] = X/10$

Without inhibition (Figs. E.9.1–E.9.3):

$$D_{\max} = \frac{\mu_{\max}S_0}{S_0+K_s} \tag{E.9.11}$$

With inhibition (Figs. E.9.1–E.9.3):

$$D_{\max} = \frac{\mu_{\max}S_0}{S_0+K_s\left(1+\dfrac{I}{K_i}\right)} \tag{E.9.12}$$

$$D = \frac{\mu_{\max}S}{S+K_s\left(1+\dfrac{X}{10K_i}\right)} = \frac{\mu_{\max}S}{S+K_s\left(1+\dfrac{Y(S_0-S)}{10K_i}\right)} \tag{E.9.13}$$

$$S = \frac{DK_s\left(1+\dfrac{I}{K_i}\right)}{\mu_{\max}-D} = \frac{DK_s\left(1+\dfrac{Y(S_0-S)}{10K_i}\right)}{\mu_{\max}-D} \tag{E.9.14}$$

$$XD = DY(S_0-S) \tag{E.9.15}$$

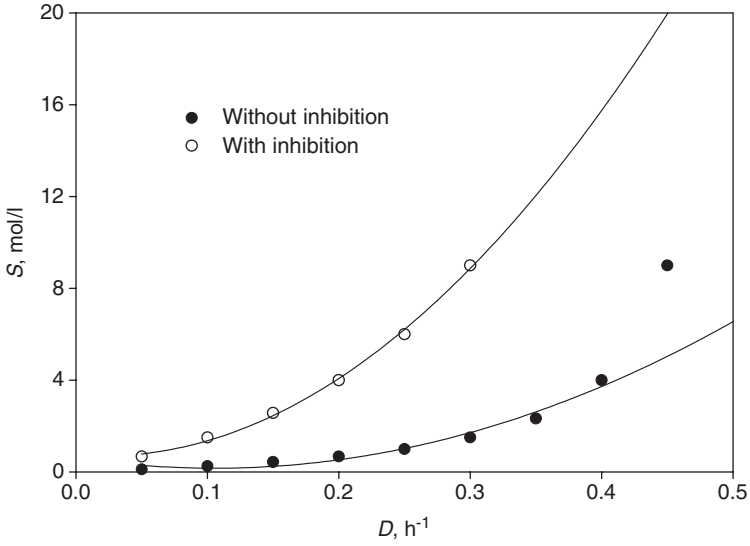

FIG. E.9.1. Substrate concentration versus dilution rate in a CSTR bioreactor.

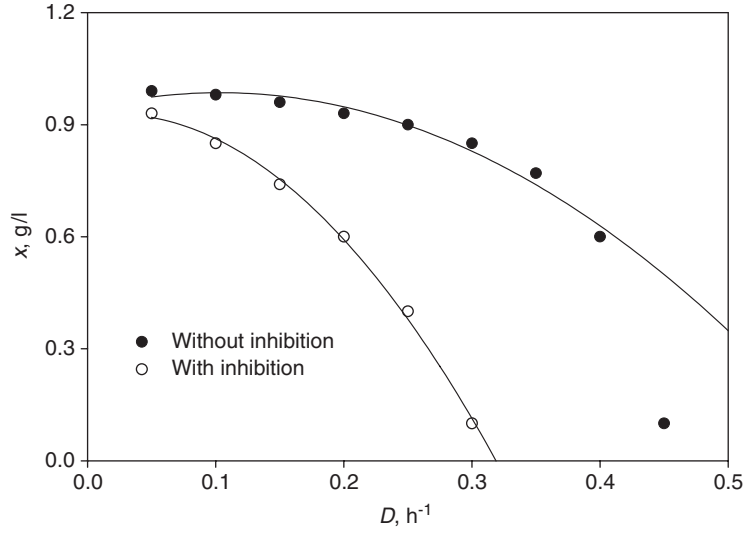

FIG. E.9.2. Cell dry weight concentration versus dilution rate in a CSTR bioreactor.

Example 10

Microbial growth was discovered with replication of each cell to three daughter cells. With the growth data define the mean time for the cell divisions. Table E.10.1 shows the cell dry weight increases with culture incubation time.

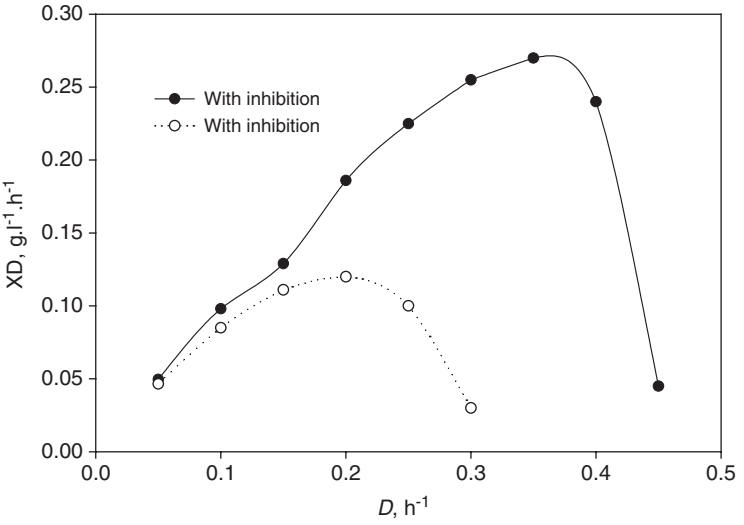

FIG. E.9.3. Productivity versus dilution rate in a CSTR bioreactor.

TABLE E.10.1. *Microbial growth in a batch fermentation bioreactor*

Time, h	0.00	0.50	1.00	1.50	2.0
Cell dry weight, $g \cdot l^{-1}$	0.09	0.15	0.25	0.35	0.55

Solution

$$\frac{1}{X}\frac{dX}{dt} = \mu \tag{E.10.1}$$

Since the population triples:

$$M_{cell} = 3M_{cell,0} \tag{E.10.2}$$

$$X = X_0 e^{-\mu t} \tag{E.10.3}$$

Then, generation time would be:

$$t = \frac{1}{\mu}\ln\frac{3X_0}{X_0} = \frac{\ln 3}{\mu} \tag{E.10.4}$$

TABLE E.10.2. *Natural logarithm of the cell dry weight concentration*

T	ln$X$
0.0	−2.303
0.5	−1.900
1.0	−1.470
1.5	−1.080
2.0	−0.670

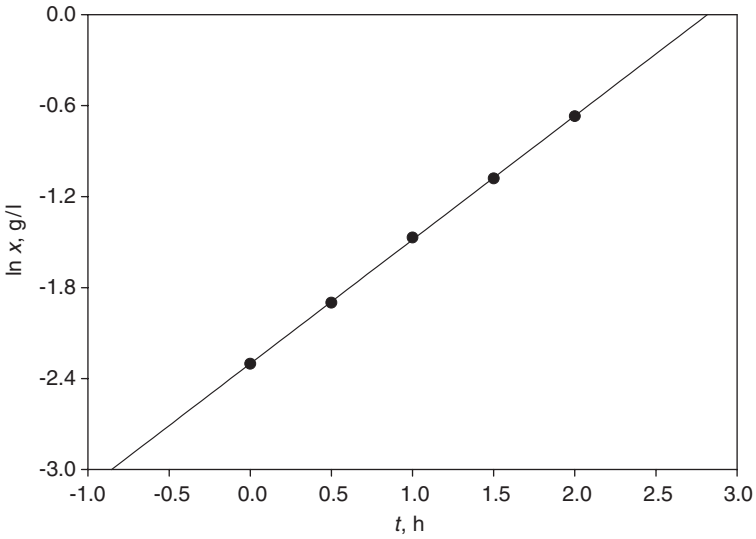

FIG. E.10.1. Plot of natural logarithm of the cell dry weight concentration versus time in the batch bioreactor fermentation.

Table E.10.2 gives natural logarithm of cell dry weight.

The above data are plotted in Figure E.10.1.

Thus, the generation time can be calculated from the slope of Figure E.10.1.

5.8 NOMENCLATURE

C_i Molar concentration of component i, g·l^{-1}

C_{if} Molar concentration in feed, g·l^{-1}

X	Biomass concentration, $g \cdot l^{-1}$
X_0	Initial biomass concentration, $g \cdot l^{-1}$
r_{fi}	Rate of product formation, $g \cdot l^{-1} \cdot h^{-1}$
μ	Specific growth rate, h^{-1}
μ_{max}	Maximum specific growth rate, h^{-1}
V_R	Culture volume, m^3
D	Dilution rate, h^{-1}
ρ_{cell}	Cell density, $g \cdot l^{-1}$
S	Substrate concentration, $g \cdot l^{-1}$
$Y_{X/S}$	Yield of biomass
$Y_{P/S}$	Yield of product
K_S	Saturation or Monod constant, $g \cdot l^{-1}$
K_m^{app}	Apparent Michaelis constant, $g \cdot l^{-1}$
υ_{max}^{app}	Apparent maximum specific growth rate constant, h^{-1}
υ	Specific growth rate constant, $g \cdot l^{-1}$. h^{-1}
i	Inhibition concentration, $g \cdot l^{-1}$
K_i	Inhibition constant, $g \cdot l^{-1}$ D or F/V as dilution rate in h^{-1}
F	Flow rate, h^{-1}
V	Working volume of the bioreactor, l
X	Cell concentration, $g \cdot l^{-1}$
K_d	Specific death rate, h^{-1}
k_2	Rate constant for forward, h^{-1}
k_{-2}	Rate constant for backward, h^{-1}

REFERENCES

1. Pelczar, M.J., Chan, E.C.S. and Krieg, N.R. “Microbiology”. McGraw-Hill, New York, 1986.
2. Baily, J.E. and Ollis, D.F. “Biochemical Engineering Fundamentals”, 2nd edn. McGraw-Hill, New York, 1986.
3. Wang, D.I.C., Cooney, C.L., Deman, A.L., Dunnill, P., Humphrey, A.E. and Lilly, M.D. “Fermentation and Enzyme Technology”. John Wiley & Sons, New York, 1979.
4. Scragg, A.H., “Bioreactor in Biotechnology, A practical Approach”. Ellis Horwood Series in Biochemistry and Biotechnology, New York, 1991.
5. Doran, P.M., “Bioprocess Engineering Principles”. Academic Press, New York, 1995.
6. Ghose, T.K., “Bioprocess Computation in Biotechnology”, vol. 1. Ellis Horwood Series in Biochemistry and Biotechnology, New York, 1990.
7. Shuler, M.L. and Kargi, F. “Bioprocess Engineering, Basic Concepts”. Prentice Hall, New Jersey, 1992.
8. Stanbury, P.F. and Whitaker, A. “Principles of Fermentation Technology”. Pergamon Press, Oxford, 1984.
9. Levenspiel, O., “Chemical Reaction Engineering”, 3rd edn. John Wiley & Sons, New York, 1999.
10. James, M.L., Smith, G.M. and Wolford, J.C. “Applied Numerical Methods for Digital Computation”. Harper & Row, New York, 1977.

5.9 CASE STUDY: ENZYME KINETIC MODELS FOR RESOLUTION OF RACEMIC IBUPROFEN ESTERS IN A MEMBRANE REACTOR

5.9.1 Introduction

In this case study, an enzymatic hydrolysis reaction, the racemic ibuprofen ester, i.e. (R)- and (S)-ibuprofen esters in equimolar mixture, undergoes a kinetic resolution in a biphasic enzymatic membrane reactor (EMR). In kinetic resolution, the two enantiomers react at different rates; lipase originated from *Candida rugosa* shows a greater stereopreference towards the (S)-enantiomer. The membrane module consisted of multiple bundles of polymeric hydrophilic hollow fibre. The membrane separated the two immiscible phases, i.e. organic in the shell side and aqueous in the lumen. Racemic substrate in the organic phase reacted with immobilised enzyme on the membrane where the hydrolysis reaction took place, and the product (S)-ibuprofen acid was extracted into the aqueous phase.

In this case study, the kinetic behaviour of the immobilised system was analysed while the following parameters were taken into account:

(a) the rate equations for native enzymes and immobilised enzymes are not necessarily the same because of microenvironment and shear stress effects;
(b) within the reaction layer, the substrate should diffuse, then mass transfer and enzymatic reaction occur simultaneously, giving rise to substrate concentration profiles at levels lower than the feed concentration;
(c) external mass transfer resistances have to be taken into account, depending on the operating conditions and the reactor configuration.

The values of the Michaelis–Menten kinetic parameters, $V_{\max}^{\text{app}}$ and K_m^{app} characterise the kinetic expression for the micro-environment within the porous structure. Kinetic analyses of the immobilised lipase in the membrane reactor were performed because the kinetic parameters cannot be assumed to be the same values as for the native enzymes.

The reaction under investigation is the enzymatic hydrolysis of racemic ethoxyethyl-ibuprofen ester. The (R)-ester is not active in the above reaction,[1–3], thus simplifying the reaction mechanism, as shown in Figure 5.13. Because both enantiomers are converted according to first-order kinetics, the conversion of one enantiomer is independent of the conversion of the other.[4]

5.9.2 Enzyme Kinetics

The initial reaction rate (v_o) obtained from each substrate concentration was fitted to Michaelis–Menten kinetics using *enzyme kinetics.* Pro (EKP) Software (ChemSW product,

---

This case study was contributed by:
Wei Sing Long[1], Azlina Harun Kamaruddin[1], Subash Bhatia[1], Ghasem Najafpour[2]
[1]School of Chemical Engineering, Engineering Campus, Universiti Sains Malaysia Seri Ampangan, 14300 Nibong Tebal, S.P.S., Pulau Pinang, Malaysia.
[2]School of Chemical Engineering, Noshirvani Institute of Technology, University of Mazandaran, Babol, Iran.

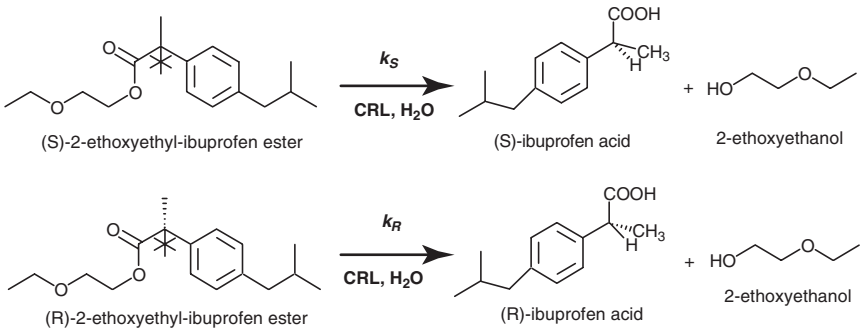

FIG. 5.13. Lipase-catalysed hydrolysis of racemic ibuprofen ester. CRL: *Candida rugosa* lipase.

Singapore) was obtained for estimates V_{max} and K_m of free lipase reaction and V_{max}^{app} and K_m^{app} and for immobilised lipase reaction. Hanes–Woolf and Simplex methods were used for the evaluation of kinetic parameters owing to their strength in error handling when experimental data are subject to random errors.[5]

5.9.2.1 Substrate and Product Inhibitions Analyses

Substrate and product inhibitions analyses involved considerations of competitive, uncompetitive, non-competitive and mixed inhibition models. The kinetic studies of the enantiomeric hydrolysis reaction in the membrane reactor included inhibition effects by substrate (ibuprofen ester) and product (2-ethoxyethanol) while varying substrate concentration (5–50 mmol·l^{-1}). The initial reaction rate obtained from experimental data was used in the primary (Hanes–Woolf plot) and secondary plots ($1/V_{max}$ versus inhibitor concentration), which gave estimates of substrate inhibition (K_{IS}) and product inhibition constants (K_{IP}). The inhibitor constant (K_{IS} or K_{IP}) is a measure of enzyme–inhibitor affinity. It is the dissociation constant of the enzyme–inhibitor complex.

Table 5.1 presents the intrinsic kinetic parameters (K_m and V_{max}) for the free lipase system and apparent kinetic parameters (K_m^{app} and V_{max}^{app}) for the immobilised lipase in the EMR using fixed 2 g·l^{-1} lipase concentration. The immobilised lipase showed higher maximum apparent reaction rate and greater enzyme–substrate (ES) affinity compared with free lipase.

5.9.2.2 Substrate Inhibition Study

The inhibition analyses were examined differently for free lipase in a batch and immobilised lipase in membrane reactor system. Figure 5.14 shows the kinetics plot for substrate inhibition of the free lipase in the batch system, where [*S*] is the concentration of (S)-ibuprofen ester in isooctane, and v_o is the initial reaction rate for (S)-ester conversion. The data for immobilised lipase are shown in Figure 5.15; that is, the kinetics plot for substrate inhibition for immobilised lipase in the EMR system. The Hanes–Woolf plots in both systems show similar trends for substrate inhibition. The graphical presentation of rate curves for immobilised lipase shows higher values compared with free enzymes. The value for the

TABLE 5.1. *Kinetic parameters for EMR and free lipase system*

EMR		Free lipase system	
V_{max}^{app} (mmol·l^{-1}·h^{-1})	K_m(mmol·l^{-1})	V_{max}(mmol·l^{-1} h^{-1})	K_m(mmol·l^{-1})
3.27	36.47	2.83	63.43

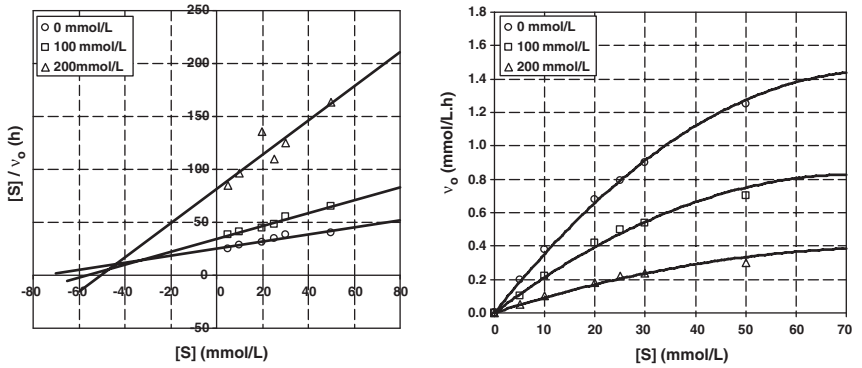

FIG. 5.14. Substrate inhibition plots for batch system with top left corner showing the concentration of substrate inhibitor designated by [*S**] (Left: Hanes-woolf; Right: Curve fit).

maximum specific growth rate in the immobilised enzyme reactor was 15% higher than the free enzyme system. The K_{IS} values calculated by EKP software are presented in the Table 5.2. The inhibition constant (K_{IS}) in EMR was 49.52 mmol·l^{-1}, higher than the value obtained in batch system (43.07 mmol·l^{-1}).

A possible substrate inhibition in the system was uncompetitive inhibition, as determined by EKP software. The mechanism of this kind of inhibition is presented in Figure 5.16. The reduction of K_m^{app} was caused by a possible uncompetitive inhibition, because excessive substrate binds to the enzyme–substrate complex forming the ternary ESS* complex, as depicted in Figure 5.16. This phenomenon showed an apparent increase in the affinity of the enzyme against the substrate as a result of more substrate being bound to the enzyme, i.e. the ESS* formation, thus leading to a reduction in V_{max}^{app}. This uncompetitive inhibition effect was in agreement with the literature that substrate inhibition in enzyme-catalysed reactions decreases the reaction rate for Michelis–Menten kinetics, resulting in the drop of racemate conversion.[3] Matson and Lopez, Xiu and Jiang, and Xiu *et al*.[4,6,7] found that when substrate inhibition took place, the conversion dropped and the enantiomeric reaction rate decreased, causing the optimal time for terminating the reaction for a racemic resolution to become longer. Uncompetitive inhibitor binds to the enzyme–substrate complex, hence pulling the equilibrium of the substrate binding reaction to the right (Figure 5.16), causing an apparent increase in the enzyme–substrate affinity and a decrease

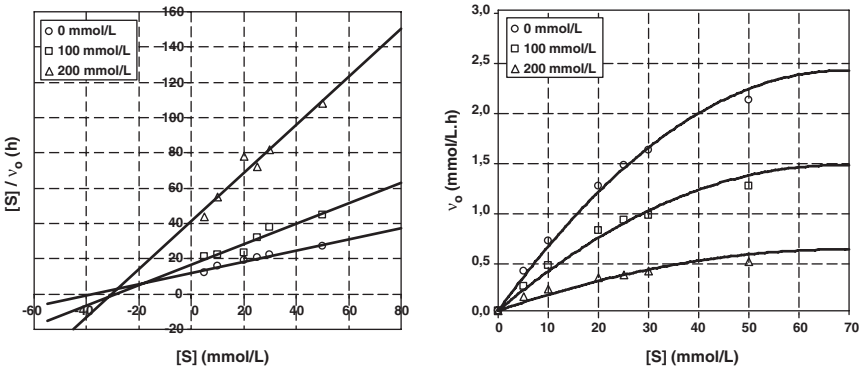

FIG. 5.15. Substrate inhibition plots for EMR system with top left corner showing the concentration of substrate inhibitor designated by [*S**] (Left: Hanes-woolf; Right: Curve fit).

TABLE 5.2. K_{IS} *value for free lipase and EMR*

	Inhibition	K_{IS} (mmol·l^{-1})
Free lipase	Uncompetitive	43.07
EMR	Uncompetitive	49.52

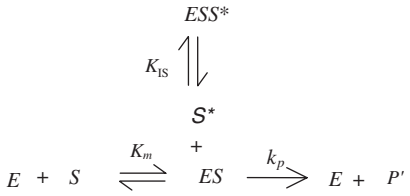

FIG. 5.16. Enzyme mechanism with uncompetitive substrate inhibition.

in the value of K_m^{app}. In other words, the inhibitor and substrate each bound to the enzyme independently.

5.9.2.3 Product Inhibition Study

The 2-ethoxyethanol was a by-product, as shown in Figure 5.13. The formation rate of 2-ethoxyethanol was the same as the conversion rate of the (S)- or (R)-ibuprofen ester: one mole of 2-ethoxyethanol was formed when one mole of ester was catalysed. A known concentration of 2-ethoxyethanol was added in the organic phase before the start of the reaction for product inhibition. The plots of the kinetics for the free lipase system are presented in Figure 5.17 and immobilised enzyme (EMR) in Figure 5.18, respectively. The K_{IP} value was 337.94 mmol·l^{-1} for the free lipase batch system and 354.20 mmol·l^{-1} for immobilised

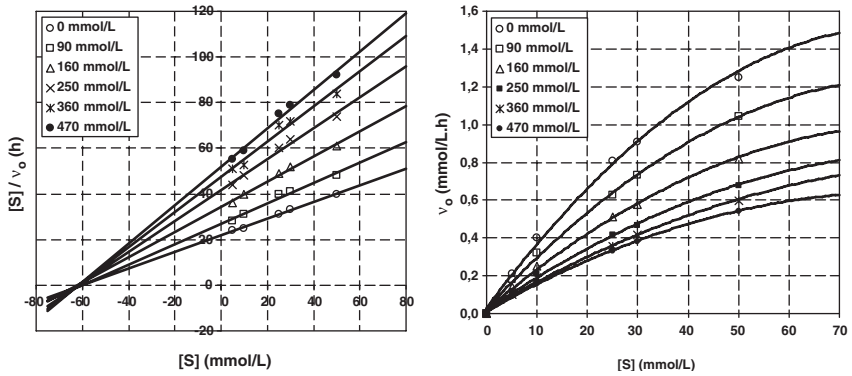

FIG. 5.17. Free lipase in batch system: Product inhibition plots (Left: Hanes-woolf; Right: Curve fit).

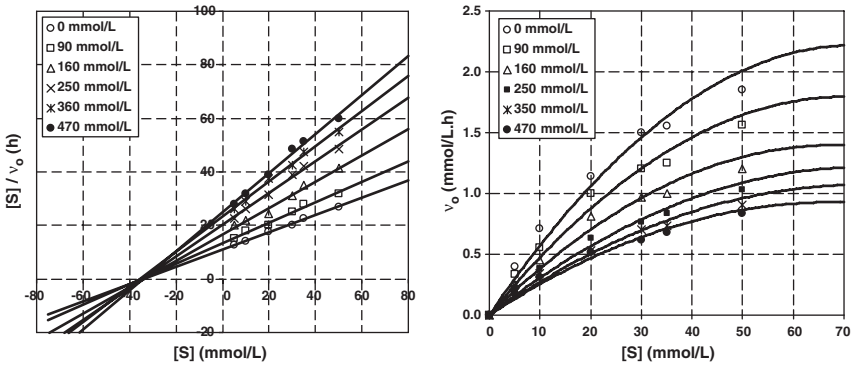

FIG. 5.18. Immobilised lipase in EMR: Product inhibition plots (Left: Hanes-woolf; Right: Curve fit).

lipase in the EMR. The product inhibition constants (K_{IP}) for the two systems are given in Table 5.3. The 2-ethoxyethanol was found to be a non-competitive inhibitor to the substrate as determined by the EKP software, with the mechanism shown in Figure 5.19.

In non-competitive inhibition, the substrate (S) and inhibitor (I) have equal potential to bind to the free enzyme (E). The inhibitor forms a ternary complex with enzyme–substrate (ES) whereas the substrate will form another ternary complex with enzyme–inhibitor (EI). Since the non-competitive inhibitor had no effect on the binding of substrate to the enzyme, the K_m value remained consistent (or unchanged). There are two different ways for the formation of ESI ternary complex; this complex would not form the product and therefore was decreased. Non-competitive inhibitor had no effect on substrate binding or the enzyme–substrate affinity, therefore the apparent rate constant (K_m^{app}) was unchanged.[5] A possible reason for product inhibition was because of the nature of 2-ethoxyethanol,

TABLE 5.3. *K_{IP} value for batch system and EMR*

	Product inhibition	K_{IP} (mmol·l^{-1})
Batch system	Non-competitive	337.94
EMR	Non-competitive	354.20

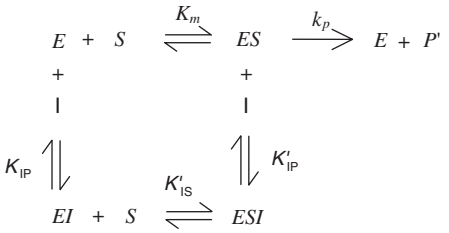

FIG. 5.19. Enzyme mechanism with non-competitive product inhibition.

which is miscible in both aqueous buffer and organic solvent. K_{IP} was larger than K_{IS} by an order of magnitude, i.e. K_{IP} was 337.94 mmol·l^{-1} for the free lipase system and 354.20 mmol·l^{-1} for EMR while K_{IS} was 43.07 mmol·l^{-1} for the batch system and 49.52 mmol·l^{-1} for EMR.

5.9.3 Enzyme Kinetics for Rapid Equilibrium System (quasi-equilibrium)

Enzyme reaction kinetics were modelled on the basis of rapid equilibrium assumption. Rapid equilibrium condition (also known as quasi-equilibrium) assumes that only the early components of the reaction are at equilibrium.[8–10] In rapid equilibrium conditions, the enzyme (E), substrate (S) and enzyme–substrate (ES), the central complex equilibrate rapidly compared with the dissociation rate of ES into E and product (P′). The combined inhibition effects by 2-ethoxyethanol as a non-competitive inhibitor and (S)-ibuprofen ester as an uncompetitive inhibition resulted in an overall mechanism, shown in Figure 5.20.

5.9.4 Derivation of Enzymatic Rate Equation from Rapid Equilibrium Assumption

The mechanism involved the overall conversion of [*S*] to [*P*]. The reverse reaction is insignificant because only the initial velocity in one of the forward direction is concerned. The mass balance equation expressing the distribution of the total enzyme is:

$$[E]_t = [E]+[ES]+[EI]+[ESI]+[ESS^*] \tag{5.9.4.1}$$

The rate-dependent equation was expressed in the form:

$$v = k_p[ES] \tag{5.9.4.2}$$

where v indicates the initial rate of the product-forming species. The rate equation was divided by $[E]_t$:

$$\frac{v}{[E]_t} = \frac{k_p[ES]}{[E]_t = [E]+[ES]+[EI]+[ESI]+[ESS^*]} \tag{5.9.4.3}$$

where $[E]_t$ contains a total of five enzyme species of one free and four complexes of enzyme, substrate and inhibitor. The concentration of each enzyme species was expressed in terms of free enzyme, E. This was accomplished by rearranging the expressions for the various equilibria. In this case, there are four equilibria:

$$K_m = \frac{[E][S]}{[ES]} \Rightarrow [ES] = \frac{[S]}{K_m}[E] \tag{5.9.4.4}$$

$$[EI] = \frac{[E][I]}{K_{\mathrm{IP}}} \tag{5.9.4.5}$$

$$[ESI] = \frac{[E][S][I]}{K_m K_{\mathrm{IP}}} \tag{5.9.4.6}$$

$$[ESS^*] = \frac{[E][S][S^*]}{K_m K_{\mathrm{IS}}} \tag{5.9.4.7}$$

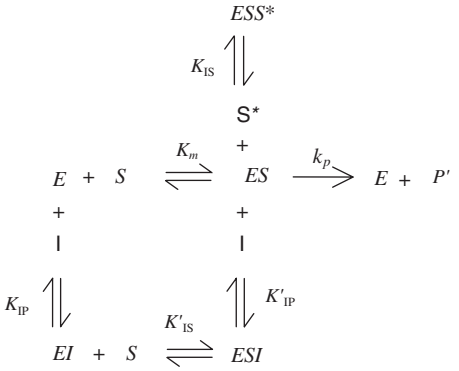

FIG. 5.20. Kinetics mechanism with uncompetitive substrate inhibition and non-competitive product inhibition.

Each enzyme complex in the rate-dependent equation was substituted by the above equations in terms of [*E*]. After cancelling [*E*] and substituting $k_p[E]_t = V_{\max}$ the following rate equation was obtained.

$$\frac{v}{V_{\max}} = \frac{\dfrac{[S]}{K_m}}{1+\dfrac{[I]}{K_{\mathrm{IP}}}+\dfrac{[S][I]}{K_m K_{\mathrm{IP}}}+\dfrac{[S]}{K_m}+\dfrac{[S][S^*]}{K_m K_{\mathrm{IS}}}} \tag{5.9.4.8}$$

The above equation can be transformed into the Michaelis–Menten equation by multiplying the numerator and denominator by K_m:

$$\frac{v}{V_{\max}} = \frac{[S]}{(K_m+[S])\left(1+\dfrac{[I]}{K_{\mathrm{IP}}}\right)+\dfrac{[S][S^*]}{K_{\mathrm{IS}}}} \tag{5.9.4.9}$$

In the present work, $[I] = [P]$ and $[S^*] = [S]$, so the equation becomes:

$$v = \frac{V_{\max}[S]}{(K_m+[S])\left(1+\dfrac{[P]}{K_{\mathrm{IP}}}\right)+\dfrac{[S]^2}{K_{\mathrm{IS}}}} \tag{5.9.4.10}$$

The above rate equation is in agreement with that reported by Madhav and Ching [3]. This rapid equilibrium treatment is a simple approach that allows the transformations of all complexes in terms of [*E*], [*S*], K_{IS} and K_{IP}, which only deal with equilibrium expressions for the binding of the substrate to the enzyme. In the absence of inhibition, the enzyme kinetics are reduced to the simplest Michaelis–Menten model, as shown in Figure 5.21. The rate equation for the Michaelis–Menten model is given in ordinary textbooks and is as follows:[11]

$$v = \frac{V_{\max}[S]}{[S]+K_m} \tag{5.9.4.11}$$

$$E + S \underset{}{\overset{K_m}{\rightleftharpoons}} ES \xrightarrow{k_p} E + P'$$

FIG. 5.21. First-order reaction kinetics mechanism without inhibitions.

5.9.5 Verification of Kinetic Mechanism

The velocity equation for rapid equilibrium system was easily derived by inversing the numerator and denominator of (5.9.4.10):

$$\frac{V_{\max}}{v} = \left(\frac{K_m + [S]}{[S]}\right)\left(1 + \frac{[P]}{K_{\mathrm{IP}}}\right) + \frac{[S]}{K_{\mathrm{IS}}} \tag{5.9.5.1}$$

$$\frac{1}{v} = \frac{1}{V_{\max}}\left(1 + \frac{K_m}{[S]}\right)\left(1 + \frac{[P]}{K_{\mathrm{IP}}}\right) + \frac{1}{V_{\max}}\frac{[S]}{K_{\mathrm{IS}}} \tag{5.9.5.2}$$

$$\frac{1}{v} = \frac{1}{V_{\max}}\frac{1}{K_{\mathrm{IP}}}\left(1 + \frac{K_m}{[S]}\right)[P] + \frac{1}{V_{\max}}\left(1 + \frac{K_m}{[S]} + \frac{[S]}{K_{\mathrm{IS}}}\right) \tag{5.9.5.3}$$

Plotting $1/\nu$ against $[P]$ will result in a Dixon plot, which is plotted at different fixed $[S]$ with the slope:

$$\frac{1}{V_{\max}}\frac{1}{K_{\mathrm{IP}}}\left(1 + \frac{K_m}{[S]}\right) \tag{5.9.5.4}$$

and the y-intersect:

$$\frac{1}{V_{\max}}\left(1 + \frac{K_m}{[S]} + \frac{[S]}{K_{\mathrm{IS}}}\right) \tag{5.9.5.5}$$

The plotting of Dixon plot and its slope re-plot (see 5.9.5.9) is a commonly used graphical method for verification of kinetics mechanisms in a particular enzymatic reaction.[9] The proposed kinetic mechanism for the system is valid if the experimental data fit the rate equation given by (5.9.4.4). In this attempt, different sets of experimental data for kinetic resolution of racemic ibuprofen ester by immobilised lipase in EMR were fitted into the rate equation of (5.7.5.6). The Dixon plot is presented in Figure 5.22.

Dixon Plot:

$$\frac{1}{v} = \frac{1}{V_{\max}^{\mathrm{app}}}\frac{1}{K_{\mathrm{IP}}}\left(1 + \frac{K_m^{\mathrm{app}}}{[S]}\right)[P] + \frac{1}{V_{\max}^{\mathrm{app}}}\left(1 + \frac{K_m^{\mathrm{app}}}{[S]} + \frac{[S]}{K_{\mathrm{IS}}}\right) \tag{5.9.5.6}$$

The slope and intersect of the illustrated plot were determined and compared with values calculated from (5.9.5.7) and (5.9.5.8):

$$\mathrm{Slope} = \frac{1}{V_{\max}^{\mathrm{app}}}\frac{1}{K_{\mathrm{IP}}}\left(1 + \frac{K_m^{\mathrm{app}}}{[S]}\right) \tag{5.9.5.7}$$

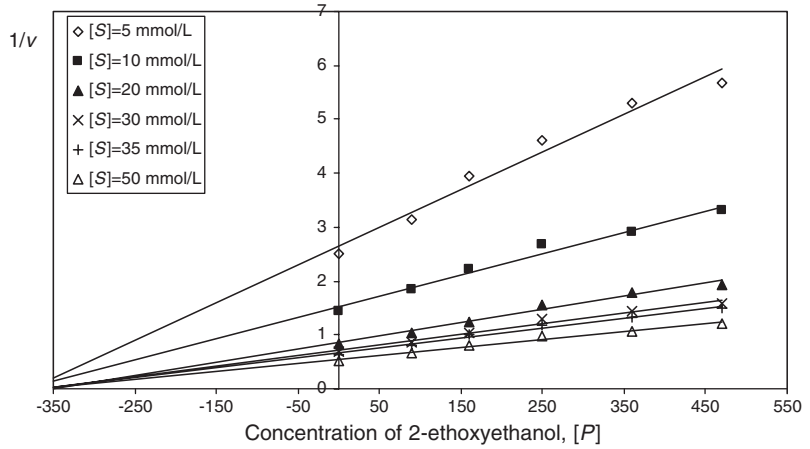

FIG. 5.22. Dixon plot: 1/*v* versus [P] at different initial substrate concentrations.

TABLE 5.4. *Comparison between graphical value (Figure 5.21) and calculated value*

[S] (mmol·1^{-1})	Slope			Intersect		
	From Figure 5.21	Calculated from (5.135)	Error (%)	From Figure 5.21	Calculated from (5.136)	Error (%)
5	0.0070	0.00720	2.7	2.6509	2.567	3.23
10	0.0039	0.00400	2.5	1.5292	1.4828	3.10
20	0.0024	0.00244	1.64	0.9360	0.9870	5.17
30	0.0020	0.00190	5.26	0.8140	0.8630	5.68
35	0.0018	0.00176	2.27	0.7911	0.8406	5.94
50	0.0015	0.00150	0.00	0.7852	0.8276	5.19

$$\text{Intersect} = \frac{1}{V_{\max}^{\text{app}}}\left(1+\frac{K_m^{\text{app}}}{[S]}+\frac{[S]}{K_{\text{IS}}}\right) \tag{5.9.5.8}$$

The experimental values fit the velocity equation with insignificant deviation in the slope and intersect values at maximum error of ±5.94 % (see Table 5.4). The corresponding slope re-plot given by (5.9.5.9) was plotted in Figure 5.23.

$$\text{Slope re-plot} = \frac{K_m^{\text{app}}}{V_{\max}^{\text{app}}K_{\text{IP}}}\left(\frac{1}{[S]}\right)+\frac{1}{V_{\max}^{\text{app}}K_{\text{IP}}} \tag{5.9.5.9}$$

$$\text{Slope} = \frac{K_m^{\text{app}}}{V_{\max}^{\text{app}}K_{\text{IP}}} \tag{5.9.5.10}$$

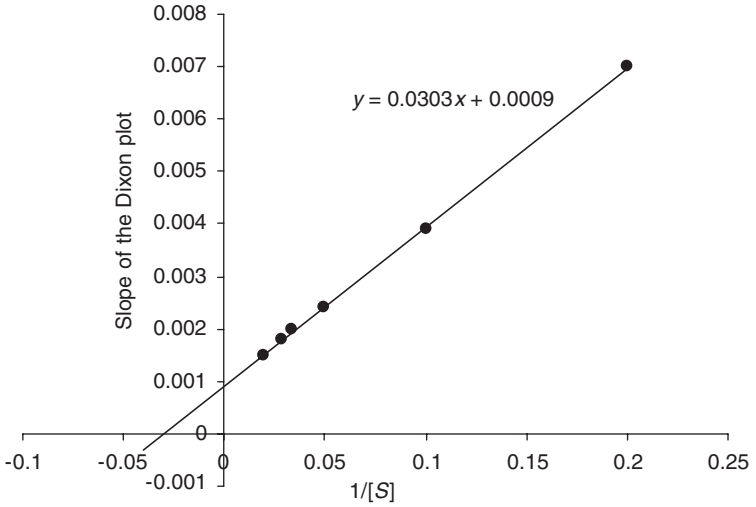

FIG. 5.23. Slope re-plot: the slope of the Dixon plot was plotted against 1/[S].

TABLE 5.5. *Slope re-plot (slope of Dixon plot versus 1/[S])*

	Slope		Intersect		
Slope re-plot (Figure 5.22)	Calculated from (5.138)	Error (%)	*Slope* re-plot (Figure 5.22)	Calculated from (5.139)	Error (%)
0.0303	0.0315	3.81	0.0009	0.00086	4.65

$$\text{Intersect} = \frac{1}{V_{\max}^{\text{app}} K_{\text{IP}}} \tag{5.9.5.11}$$

The values determined from Figure 5.23 agree well with the values calculated from the equations (Table 5.5), with an error of ±3.81% for the slope and ±4.65% for the intersect, respectively. The obtained experimental data were consistent with the proposed enzymatic reaction and the reaction mechanisms with uncompetitive substrate inhibition and the non-competitive product inhibition model.

REFERENCES

1. Battistel, E., Bianchi, D., Cesti, P. and Pina, C., *Biotechnol. Bioengng* **38**, 659 (1991).
2. Giorno, L., Molinari, R. Natoli, M. and Drioli, E., *J. Membr. Sci*. **125**, 177 (1997).
3. Madhav, M.V. and Ching, C.B., *J. Chem. Technol. Biotechnol*. **76**, 941 (2001).

4. Xiu, G.-H., Jiang, L. and Li, P., *Biotechnol. Bioengng* **74**, 29 (2001).
5. Chaplin, M.F. and Bucke, C., *In* "Enzyme Technology". Cambridge University Press, London, 1990.
6. Matson, S.L. and López, J.L., *In* "Frontiers in Bioprocessing". CRC Press, Florida, 1990.
7. Xiu, G.-H. and Jiang, L., *Ind. Eng. Chem. Res.* **39**, 4054 (2000).
8. Segel, I.H., "Enzyme Kinetics: Behavior and Analysis of Rapid Equilibrium and Steady-State Enzyme Systems". John Wiley & Sons, New York, 1975.
9. Long, W.S., Ph.D thesis. Universiti Sains Malaysia, Penang, Malaysia, 2004.
10. Long, W.S., Azlina Harun, K. and Bhatia, S., Chem. Eng. Sci. **60**, 4957 (2005).
11. Voet, D. and Voet, J.G., "Fundamentals of Biochemistry", 3rd edn. John Wiley, New York, 2004.

CHAPTER 6

Bioreactor Design

6.1 INTRODUCTION

To design a bioreactor, some objectives have to be defined. The decisions made in the design of the bioreactor might have a significant impact on overall process performance. Knowledge of reaction kinetics is essential for understanding how a biological reactor works. Other areas of bioprocess engineering such as mass and energy balances, mixing, mass transfer and heat transfer are also required.

The bioreactor is the heart of any biochemical process in which enzymes, microbial, mammalian or plant cell systems are used for manufacture of a wide range of useful biological products. The performance of any bioreactor depends on many functions, such as those listed below:

- Biomass concentration
- Sterile conditions
- Effective agitations
- Heat removal
- Correct shear conditions
- Nutrient supply
- Product removal
- Product inhibition
- Aeration
- Metabolisms/microbial activities

There are three groups of bioreactor currently in use for industrial production:

1. Non-stirred, non-aerated system: about 70% of bioreactors are in this category.
2. Non-stirred, aerated system: about 10% of bioreactors.
3. Stirred and aerated systems: about 20% of the bioreactors in industrial operation.

Non-stirred, aerated vessels are used in the process for traditional products such as wine, beer and cheese production. Most of the newly found bioprocesses require microbial growth in an aerated and agitated system. The percentage distribution of aerated and stirred vessels for bioreactor applications is shown in Table 6.1. The performances of various bioreactor systems are compared in Table 6.2. Since these processes are kinetically controlled, transport phenomena are of minor importance.

Non-stirred, non-aerated vessels are used for traditional products such as wine, beer and cheese. Most of the new products require growth of microorganisms in aerated, agitated vessels.

TABLE 6.1. *Percentage of distribution aerated and stirred vessel in bioreactor application*

Non-stirred, non-aerated	76%
Non-stirred, aerated	11%
Stirred, aerated	13%
Total	100%

TABLE 6.2. *Performances of bioreactors*

Concentration	Productive bioreactors		Wastewater treatment	
	10–50		Aerobic	Anaerobic
(kg/m^3)			5	50
	Moulds	Bacteria/yeast		Mixed Culture
Viscosity	High	Low	Low	Low
Oxygen consumption	High	High	Low	Absent
Mass transfer	Low	High	Low	Absent
Heat production metabolic (kW/m^3)	3–15	3–15	0.03–0.14	Negligible
Power consumption, hp	3–15	fewer than 5	0.02–05	Negligible

6.2 BACKGROUND TO BIOREACTORS

The main function of a properly designed bioreactor is to provide a controlled environment to achieve optimal growth and/or product formation in the particular cell system employed. Frequently the term "fermenter" is used in the literature to mean "bioreactor".[1–3] The performance of any bioreactor depends on many functions including:

- Biomass concentration must remain high enough to show high yield.
- Sterile conditions must be maintained for pure culture system.
- Effective agitation is required for uniform distribution of substrate and microbes in the working volume of the bioreactor.
- Heat transfer is needed to operate the bioreactor at constant temperature, as the desired optimal microbial growth temperature.
- Creation of the correct shear conditions. High shear rate may be harmful to the organism and disrupt the cell wall; low shear may also be undesirable because of unwanted flocculation and aggregation of the cells, or even growth of bacteria on the reactor wall and stirrer.

6.3 TYPE OF BIOREACTOR

Aerobic bioreactors are classified into four categories, depending on how the gas is distributed.

- Stirred tank reactor: the most common type of bioreactor used in industry. A draught is fitted which provides a defined circulation pattern.
- Airlift pressure cycle bioreactor: the gas is circulated by means of pressurised air.
- Loop bioreactor: a modified type of airlift system in which a pump transports the air and liquid through the vessel.
- Immobilized system: the air circulates over a film of microorganisms that grows on a solid surface. In an immobilized bioreactor, particulate biocatalysts for enzyme production and conversion of penicillin to 6-aminopenicillanic acid are used.
- Fluidized bed: when packed beds are operated in upflow mode, the bed expands at high flow rates; channelling and clogging of the bed are avoided. Normal application is wastewater treatment and the production of vinegar.
- Trickle bed: another variation of the packed bed, fluid is sprayed onto the top of the packing and trickles down through the bed. Air is introduced at the base, because liquid is not continuous throughout the column, so air moves easily around the packing. This type of bioreactor is widely used for aerobic wastewater treatment.
- Fed-batch mixed reactor: starting with a relatively dilute solution of substrate this provides control over the substrate concentration. High rates are avoided. Fed batch is used for baker's yeast to overcome catabolite repression and to control oxygen demand. It is also used routinely for production of Penicillin.
- Batch mixed reactor: There are three principal modes of bioreactor operation: (a) batch; (b) fed batch; (c) continuous.

Industrial bioreactors can withstand up to 3 atmospheres positive pressure. Large fermenters are equipped with a lit vertical sight glass for inspecting the contents of the reactor. Side parts for pH, temperature and dissolved oxygen sensors are a minimum requirement. A steam sterilisation sample port is provided. Mechanical agitators are installed on the top or bottom of the tank for adequate mixing.

Choice of operating strategy has a significant effect on substrate conversion, product susceptibility to contamination and process reliability.

Mass balance:
$$\frac{\mathrm{d}m}{\mathrm{d}t} = m_\mathrm{i} - m_\mathrm{o} + r_\mathrm{p} - r_\mathrm{s} \tag{6.3.1}$$

where r_p is the rate of product formation and $-r_\mathrm{s}$ is the rate of substrate consumption.

The design emphasis of this section will be on stirred tank bioreactors, which are the most common type used commercially in many bioprocess industries.

6.3.1 Airlift Bioreactors

In an airlift fermenter, mixing is accomplished without any mechanical agitation. Airlift bioreactors are used for tissue culture because the tissues are shear sensitive and normal mixing is not possible. There are many forms of airlift bioreactor. In the usual form, air is fed into the bottom of a central draught tube through a sparger ring, so reducing the apparent density of the liquid in the tube relative to the annular space within the bioreactor. The flow passes

up through the draught tube to the head space of the bioreactor, where the excess air and the by-product, CO_2, disengage. The degassed liquid then flows down the annular space outside the draft to the bottom of the bioreactor. Cooling can be provided by either making the draught tube an internal heat exchanger or with a heat exchanger in an external recirculation loop.

The advantages of airlift bioreactor are:

1. In low shear, there is low mixing which means the bioreactor can be used for growing plant and animal cells.
2. Since there is no agitation, sterility is easily maintained.
3. In a large vessel, the height of liquid can be as high as 60 m, the pressure at the bottom of the vessel will increase the oxygen solubility, and the value of $K_L a$ will increase.
4. Extremely large vessels can be constructed. In one single cell protein plant, the reactor had a total volume of 2300 m^3 (a column of 7 m diameter and 60 m height with a reactor working volume of 1560 m^3). Further, in this reactor the microorganisms were grown on methanol for SCP, the biochemical reaction resulting in an extremely large heat release. It was not possible to remove such a high exothermic heat of reaction with a conventional stirred-tank design.

In applications of airlift bioreactor there are various types of fermenter. The most common airlift bioreactors are pressure cycle, internal and external loop bioreactors.

6.3.2 Airlift Pressure Cycle Bioreactors

The gas is circulated by means of pressurised air. In airlift bioreactors, circulation is caused by the motion of injected gas through a central tube, with fluid recirculation through the annulus between the tube and the tower or vice versa. Figure 6.1 shows an airlift bioreactor with an internal loop cycle of fluid flow.

6.3.3 Loop Bioreactor

A modified type of airlift system with gas and liquid flow patterns in which a pump transports the air and liquid through the vessel. Here, an external loop is used, with a mechanical pump to remove the liquid. Gas and circulated liquid are injected into the tower through a nozzle. Figure 6.2 shows an airlift bioreactor that operates with an external recirculation pump.

6.4 STIRRED TANK BIOREACTORS

The most important bioreactor for industrial application is the conventional mixing vessel, which has the dual advantages of low capital and low operating costs. Figure 6.3 is a schematic diagram for such a reactor. Vessels for laboratory experiments of volume up to 20 litres are made of glass. For larger volumes, construction is made of stainless steel. The height:diameter ratio of the vessel can vary between 2:1 and 6:1, depending largely on the amount of the heat to be removed, and the stirrer may be top- or bottom driven. All tanks are fitted with baffles, which prevent a large central vortex being formed as well as improve

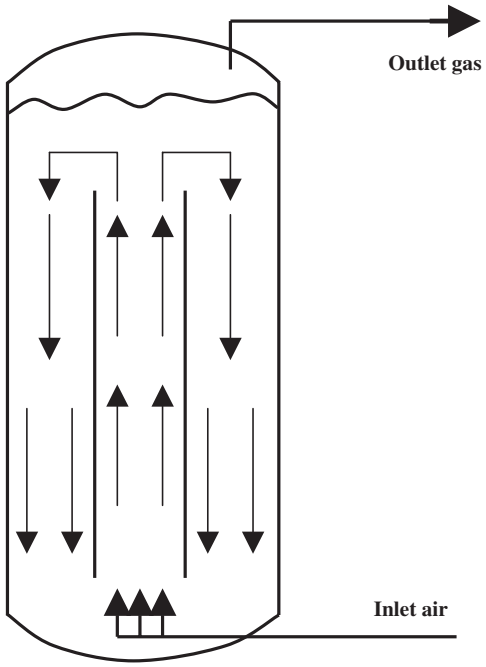

FIG. 6.1. Gas and liquid flow pattern with internal loop cycle.

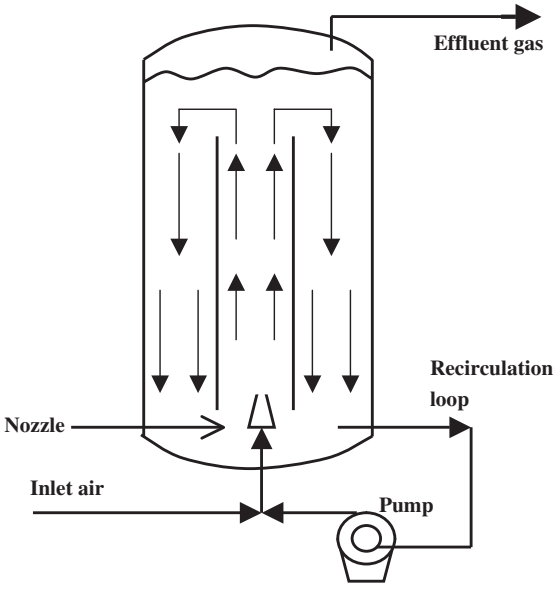

FIG. 6.2. Airlift bioreactor with external recirculation pump.

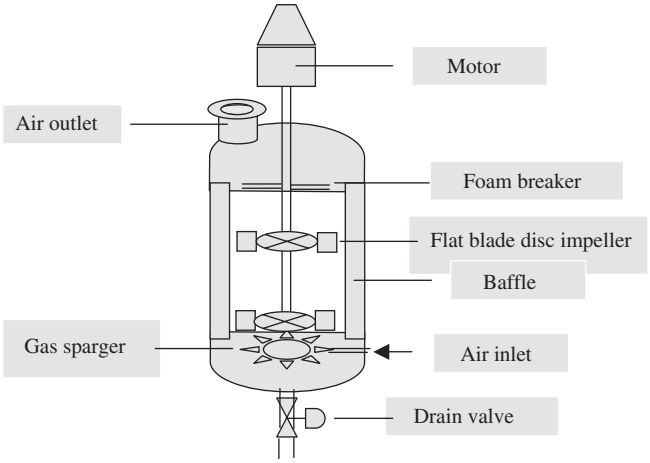

FIG. 6.3. Stirred tank bioreactor.

mixing. Four baffles are used for vessels less than 3 metres in diameter, and six to eight baffles are used in larger vessels. The width of the baffle is usually between $T/10$ and $T/12$, in which T is the tank diameter.[4,5]

Height of vessel to diameter:

$$\frac{H}{D_t} = 2{:}1 \quad \text{and} \quad 6{:}1 \tag{6.4.1}$$

Diameter of vessel to baffle:

$$10 < \frac{D_t}{D_b} < 12 \tag{6.4.2}$$

The diameter of the tank, D_{tank} is less than 3 m, four baffles of 6–8 inches may prevent a central vortex. Typically, 75% of the designed volume is used as working volume, in a fermentation vessel about 75% of the total CSTR volume is filled with liquid, the remaining 25% is used for gas space. If foaming takes place, there is no chance of immediate contamination. If the vessel height is equal to the diameter ($H = D$), one agitator is sufficient. If the vessel height is twice the diameter ($H = 2D$) or more, additional sets of agitators should be mounted on the shaft, separated by a distance φ. Installation of multiple sets of impellers improves mixing and mass transfer. Spargers should always be located near the bottom of the vessel with a distance $D_i/2$ below the agitator, where D_i is the diameter of the impellers. Power input per unit volume of fermentation vessel for a normal fermenter should be greater than 100 W/m^3, and the impeller tip speed ($\pi N D_i$) should be greater than

1.5 m/s. Let us define a dimensionless number that is known as the Froude number, *Fr*; the value of the stated dimensionless number has to be greater than 0.1:

$$Fr = \frac{N^2 D_i}{g} > 0.1 \tag{6.4.3}$$

High agitation and aeration cause major problems such as foaming, which may lead the fermentation vessel to unknown contamination. Antifoam cannot be always added for the reduction of foam: it may have inhibitory effects on the growth of microorganisms, so the simplest devices have rakes mounted on the stirrer shaft and located on the surface of the fluid.

If heat removal is a problem, as it can be in large bioreactors greater than 100 m^3, up to 12 baffles can be used, through which coolant passes.

Careful consideration has to be given to agitator design within a bioreactor because it controls the operation of the bioreactor.

The most common type of agitator used is the four-bladed disk turbine. However, research on the hydrodynamics of the system has shown that other disk turbine agitators with 12, 18 or concave blades have advantages.

Considerable research has been undertaken in gas/liquid systems with no solids present and where shear is not a problem. In systems that are shear-sensitive and where solids are present, there are advantages in using an inclined bladed turbine. The number of agitators mounted on the shaft will be dependent on the height of liquid in the vessel. For specification of the correct number of agitators on the shaft, the height of liquid in the vessel should be equal to the tank diameter, one agitator is required; if the height of liquid is two or three times of the tank diameter ($H = 2T$ or $3T$), additional agitators should be mounted on the shaft, separated by a distance φ; then $\varphi = T$, where T represents tank diameter. Installation of multi-sets of impellers improves mixing and enhances mass transfer.

High turbulence is required for efficient mixing; this is created by the vortex field which forms behind the blades. For all the gas to flow through this region it must enter the vessel close to and preferably underneath the disk; hence it is recommended that spargers should always be nearer, about a distance of $D_i/2$ below the agitator, where D_i is the impeller diameter.

The centrifugal force will draw the gas into the system, which ensures that sufficient turbulence is created. For this, a power input greater than 100 W/m^3 is required from the agitator.[6] Alternatively, a tip speed ($\pi N D_i$) greater than 1.5 m/s or a Froude number ($N^2 D_i/g$) greater than 0.1 are often used, where N is the agitator speed in Hz, and g is gravitational acceleration in m/s^2.

The design of the gas inlet device is of only secondary importance for the capture and dispersal of the gas by the agitator. For efficient mass transfer, a multiple-orifice ring sparger is generally used with a gas outflow diameter of $3D_i/4$. However, it is only slightly better than a single open-pipe sparging located centrally beneath the disk.

Foaming is often a problem in large-scale aerated systems. Antifoam cannot always be added for the reduction of foam because it may inhibit the growth of the microorganisms. However, there are several mechanical methods by which the foam can be broken up.

The simplest devices have rakes mounted on the stirrer shaft located on the surface of the liquid. A more sophisticated device is the 'Funda-foam system', in which the foam is destroyed by centrifugal forces. The nutrient solution held in the foam flows back into the bioreactor, and the air released from the foam leaves the vessel.

There should be a minimum number of openings in the bioreactor so that sterility can be maintained. Small openings must be made leak-proof with an O-ring, and larger openings fitted with gaskets. One of the most difficult areas to seal effectively is the point where the agitator shaft passes into the vessel; here a double mechanical shaft seal should be fitted. If possible the joints of all the parts connected within the sterile vessel as well as all of the pipes both inside and outside the bioreactor should be welded. There should not be any direct connection between the non-sterile and sterile area; that is, sampling devices and injection ports must be accommodated in steam-sterilisation closures.

6.5 BUBBLE COLUMN FERMENTER

For the production of baker's yeast, beer and vinegar, bubble column fermenters are used. They are also often used for sufficient aeration and treatment of wastewater. In designing such a bioreactor, the height of liquid to tank diameter (H:D) is about 2:1, a common ratio of H:D is also about 3:1; in bakers' yeast production the ratio of H:D is 6:1. In bubble columns the hydrodynamics and mass transfer depend on the size of the bubbles and how they are released from the sparger. The upward liquid velocity at the centre of the column, for the column diameter range 10 cm to 7.5 m ($0.1 < D < 7.5$ m) and the superficial gas velocity is in the range of $0 < u_{gas} < 0.4$ m/s.[7] The liquid velocity is correlated in the following equation:

$$u_{liquid} = 0.9\,[gDu_{gas}]^{0.33} \tag{6.5.1}$$

The gas superficial velocity is defined as the ratio of gas flow rate to column cross sectional area:

$$U_{gas} = \frac{Q_{gas}}{A} \tag{6.5.2}$$

The mixing time is calculated by:

$$t_{mixing} = 11\left(\frac{H}{D}\right)\left(\frac{gu_g}{D^2}\right)^{-0.33} \tag{6.5.3}$$

where H is the height of bubble column and D is the column diameter. Figure 6.4 shows a simple column with an air sparger installed at the bottom of the column which allows sufficient air to pass through the liquid.

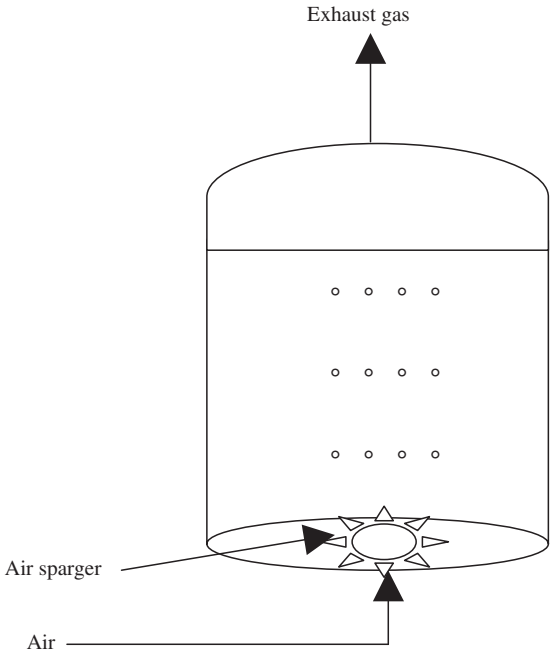

FIG. 6.4. Bubble column bioreactor.

6.6 AIRLIFT BIOREACTORS

In an airlift fermenter, mixing is accomplished without any mechanical agitation. An airlift fermenter is used for tissue culture, because the tissues are shear sensitive and normal mixing is not possible. With the airlift, because the shear levels are significantly lower than in stirred vessels, it is suitable for tissue culture. The gas is sparged only up to the part of the vessel cross section called the riser. Gas is held up, fluid density decreases causing liquid in the riser to move upwards and the bubble-free liquid to circulate through the down-comer. The liquid circulates in airlift reactors as a result of the density difference between riser and down-comer.

There are many forms of airlift bioreactor. In the usual form, air is fed into the bottom of a central draught tube through a sparger ring, so reducing the apparent density of the liquid in the tube relative to the annular space within the bioreactor. The flow passes up through the draught tube to the head space of the bioreactor, where the excess air and the by-product, CO_2, disengage. The degassed liquid then flows down the annular space outside the draft to the bottom of the bioreactor. In general, airlift bioreactors have the following features:

- Internal-loop vessels
- Draft tubes
- External loop or outer-loop

The cooling duty can be provided by either making the draught tube an internal heat exchanger or with a heat exchanger in an external circulation loop. The mass transfer coefficient for external loop airlift Fermenter is estimated as:[8]

$$K_L a < 0.32 u_g^{0.7} \tag{6.6.1}$$

The height of airlift reactors is typically about 10 times the diameter of the column ($H = 10D$). For deep-shaft systems the ratio of H:D is about 100. For large fermenters (500 m^3), a bubble column is an attractive choice, because it is simple and cheap to operate.

The main disadvantages of airlift reactors are:

1. High capital cost with large-scale vessels.
2. High energy costs. Although an agitator is not required, a greater air throughput is necessary, and the air has to be at a higher pressure, particularly on a large scale. Also, the efficiency of gas compression is low.
3. As the microorganisms circulate through the bioreactor, the conditions change, and it is impossible to maintain consistent levels of carbon source, nutrients and oxygen throughout the vessel.
4. The separation of gas from the liquid is not very efficient when foam is present. In the design of an airlift bioreactor, these disadvantages have to be minimised. If the feed comes in at only one location, the organism would experience continuous cycles of high growth, followed by starvation. This would result in the production of undesirable by-products, low yields and high death rates. Therefore, particularly on a large scale, multiple feed points should be used. Similarly, air should be admitted at various points up the column. However, the air must mainly enter from the bottom to circulate the fluid through the reactor.

6.7 HEAT TRANSFER

The temperature in a vessel can be controlled by removing heat by means of water circulating through a jacket on the outside of the vessel and/or by passing the water through hollow baffles situated in the vessel. With an airlift bioreactor the heat can be removed through the hollow draught tube. The rate at which heat is transferred is given by:

$$Q = UA\Delta T \tag{6.7.1}$$

where Q is heat transferred in W, U is the overall heat transfer coefficient in $W/m^2 \cdot K$, A is the surface area for heat transfer in m^2, and ΔT is the temperature difference between media and cooling water in K. The coefficient U represents the conductivity of the system, which depends on the system geometry, fluid properties, flow velocity, wall material and thickness. The overall resistance to heat transfer is the reciprocal of the overall heat transfer coefficient.

It is defined as the sum of the individual resistances to heat transfer as heat passes from one fluid to another, and can be written as:

$$\frac{1}{U} = \frac{1}{h_o} + \frac{1}{h_i} + \frac{1}{h_{of}} + \frac{1}{h_{if}} + \frac{1}{h_w} \tag{6.7.2}$$

where, h_o is the outside film coefficient, h_i is the inside film coefficient, h_{of} is the outside fouling film coefficient, h_{if} is the inside fouling film coefficient, h_w is the wall heat transfer coefficient (which is *k/x)*, k is the thermal conductivity of the wall, and x is the wall thickness in m. The units for all film coefficients are $W/m^2 \cdot K$. This equation is applicable for all cases except a thick-walled tube where a correction factor has to be used. The outside and inside film coefficients can be evaluated from semi-empirical correlations of the following form:

$$Nu = k(Re)^a (Pr)^b \tag{6.7.3}$$

where *Nu* is the Nusselt number, the ratio of convective to conductive heat transfer coefficients. The terms *k*, *a*, and *b* are constants. *Re* is the Reynolds number, which is the ratio of inertial over viscous forces, and *Pr* is the Prandtl number, which is the ratio of kinematic viscosity over the thermal diffusivity:

$$Nu = \frac{hD_t}{k} \tag{6.7.4}$$

$$Re = \frac{D_i V \rho}{\mu} \quad \text{or} \quad \frac{D_i^2 N_\rho}{\mu} \tag{6.7.5}$$

$$Pr = \frac{C_p \mu}{k} = \frac{\nu}{\alpha} \tag{6.7.6}$$

where D_t is the vessel diameter, D_i is the impeller diameter, all in m; ρ is the density in $kg \cdot m^{-3}$, μ is the viscosity in kg/m·s, ν the kinematic viscosity in m^2/s, k is the thermal conductivity in $W \cdot m^{-1} \cdot K^{-1}$, h is the convective heat transfer coefficient in $W \cdot m^{-2} \cdot K^{-1}$, C_p is the specific heat in $J \cdot kg^{-1} \cdot K^{-1}$, α is the thermal diffusivity in $m^2 \cdot s^{-1}$, V is the velocity in $m \cdot s^{-1}$ and N is the impeller speed in Hz. The above equation applies to turbulent conditions for Newtonian fluids. In stirred-tank bioreactors, normally turbulent conditions are attained. However, non-Newtonian behaviour can occur, especially if polysaccharides pass into the broth. An extensive literature survey of heat transfer correlations for both Newtonian and non-Newtonian single-phase systems has been done by many researchers. They have shown that for hold-ups of less than 15%, the rates of heat transfer with gas addition are very close to the values obtained without gas addition.[8,9] Gas hold-up is defined as the volume of gas in the vessel per vessel volume, and can be calculated from the equation

$$\varepsilon = K\left(\frac{P_g}{V_L}\right)^{0.48}(v_s)^{0.4} \tag{6.7.7}$$

where P_g is power consumed by gassed liquid in W, V_L is liquid volume without gassing, ν_s is the superficial gas velocity in m/s and K is a constant. Other correlations for gas hold-up are defined in the literature.[10,11]

The calculation of heat transfer film coefficients in an air-lift bioreactor is more complex, as small reactors may operate under laminar flow conditions whereas large-scale vessels operate under turbulent flow conditions. It has been found that under laminar flow conditions, the fermentation broths show non-Newtonian behaviour, so the heat transfer coefficient can be evaluated with a modified form of the equation known as the Graetz–Leveque equation:[9]

$$Nu = 1.75\delta^{0.33}Gz^{0.33} \tag{6.7.8}$$

where δ is correction for non-Newtonian behaviour equal to $(3n + 1)/4n$, where n is the flow behaviour index of power-law fluid. Gz is the Graetz number, a dimensionless number related to mass flow rate, heat capacity and conductive heat transfer coefficient.

$$Gz = \frac{\dot{m}C_p}{kL} \tag{6.7.9}$$

where $\dot{m}$ is the mass flow rate of fluid through the tube in kg/s, and C_p is specific heat in J/kg K, k is thermal conductivity in W/m·K, and L is the length along the tube in m. This equation is most accurately applied in the initial stages of the bioreactor. In later stages growing *Xanthmonas campestris*, the value of the film coefficients were up to 45% lower than predicted by the Graetz–Leveque equation, because of fouling of the heat transfer surface. However, with *Aspergillus niger*, values of up to four times those predicted by the non-Newtonian form of the Graetz–Leveque equation were observed. The enhancement was found to be dependent on cell concentration and morphology of the microorganisms, and was probably due to the increased turbulence of the boundary layer caused by the mycelial aggregates.

The overall heat transfer coefficient is dependent on the agitation rate in the vessel, throughput of the liquid and gas in an airlift bioreactor and the rate of circulation of cooling water in the jacket. The expected value of the overall heat transfer coefficient including all resistance for a non-fouling system should be in the range 500–1500 $W \cdot m^{-2} \cdot K^{-1}$. In case of any problems, for instance animal and plant cells, which are shear-sensitive the vessel side turbulence has to be reduced; consequently the heat transfer coefficient will be lowered. In such cases, the heat transfer will increase only by providing more heat transfer area. The additional effective surface area can be obtained by having a vessel with a large height:diameter ratio, because the volume of a vessel is proportional to the height multiplied by the cross-sectional area, whereas the surface area is the external area of the vessel that is αHD, where

α is the proportionality factor. Where the total heat transferred has to be calculated, the power of the agitator should be included, because a considerable amount of energy is converted to heat in the vessel.

Small temperature differences, ΔT, in a bioreactor are usually easily stabilised, unless refrigerated cooling water is used, which means that the product of overall heat transfer coefficient and the heat transfer area, '*UA*', has to be large. Therefore the heat transfer area can be maximised by having cooling water in the baffles as well as in the jacket of the bioreactor.

6.8 DESIGN EQUATIONS FOR CSTR FERMENTER

In designing a bioreactor, material balance is used for all the streams associated with the fermentation vessel. The biomass at inlet, outlet and the generated biomass must be balanced while the fermentation proceeds. The cell balance without any cell accumulation is shown in the following equation:

$$F(X_0 - X) + Vr_x = 0 \tag{6.8.1}$$

where X is viable cell in the effluent stream and X_0 is viable cell in the feed stream, F is the volumetric flow rate, V is the reactor working volume, and r_x is the rate of cell formation per unit volume. The rate equation is explained in detail by a Monod rate model. The Monod rate equation is well known in microbial growth kinetics:

$$\mu = \frac{\mu_{\max} S}{K_s + S} \tag{6.8.2}$$

where μ is the specific growth rate, $\mu_{\max}$ is the maximum specific growth rate, and K_s is the Monod constant.

6.8.1 Monod Model for a Chemostat

A Monod rate model is used to demonstrate the rate of biomass generation. We neglect the cell death rate. Let us denote the ratio of biomass rate of generation to biomass concentration, r_x/X, that is the specific growth rate; μ also denotes the dilution rate; D is defined as number of tank volumes passed through per unit time, F/V. After substitution of D and μ into (6.8.1), the following equation is obtained:

$$DX_o = (D - \mu)X \tag{6.8.1.1}$$

Substituting specific growth rate based on the Monod rate equation into (6.8.2), the rearranging results in:

$$\left(\frac{\mu_{\max} S}{K_s + S} - D\right) X + DX_0 = 0 \tag{6.8.1.2}$$

For sterile media with suitable nutrients in absence of any organisms,

$$X_{\mathrm{O}} = 0, \quad 0 = (D - \mu)X$$

Biomass generated is considered as $X \neq 0$, therefore $D - \mu = 0$

$$D = \mu \tag{6.8.1.3}$$

At steady state, substrate utilisation is balanced with a rate equation:

$$F(S_i - S) = \left(\frac{\mu_{\max} S}{K_m + S}\right) V \tag{6.8.1.4}$$

When the volume of the vessel is divided by the flow rate, retention time and dilution rate are defined in the following equation:

$$\frac{V}{F} = \tau = \frac{1}{D} \tag{6.8.1.5}$$

Plug in (6.8.1.5) to (6.8.1.4):

$$D(S_i - S) = \frac{\mu_{\max} S}{K_m + S} \tag{6.8.1.6}$$

Solve (6.8.1.6) for dilution rate or substrate concentration, as follows:

$$\frac{\mu_{\max} S}{K_s + S} = D \quad \text{or} \quad S = \frac{DK_s}{\mu_{\max} - D} \tag{6.8.1.7}$$

Material balance in terms of cell density is written as:

$$\frac{\mathrm{d}\rho_{\mathrm{cell}}}{\mathrm{d}t} = \frac{F}{V}(\rho_i - \rho_o) + (\mu - \alpha)\rho_{\mathrm{cell}} \tag{6.8.1.8}$$

At steady state, $\mathrm{d}\rho/\mathrm{d}t = 0$ for a sterile fermenter, $\rho_{\mathrm{i}} = 0$, (6.8.1.8) is simplified and reduced to dilution rate, which is similar to (6.8.1.3) above.

Substrate balance may also lead to the same results as the following relations:

$$\frac{\mathrm{d}S}{\mathrm{d}t} = \frac{F}{V}(S_i - S) - \frac{\mu\rho_{\text{cell}}}{\text{Yield of cell}} - m\rho_{\text{cell}} - \frac{q_p\rho_{\text{cell}}}{Y_{\text{p}/\text{s}}} \tag{6.8.1.9}$$

At steady-state condition, where $\mathrm{d}S/\mathrm{d}t = 0$ and $m\rho_{\text{cell}} << \mu\rho_{\text{cell}}/Y$, (6.8.1.9) can be simplified and leads to substrate balance with growth rate:

$$D(S_O - S) = \frac{\mu\rho_{\text{cell}}}{Y} \tag{6.8.1.10}$$

For the special case when $\mu = D$, the substrate balance equation reduces to yield of substrate to cell biomass:

$$\rho_{\text{cell}} = Y(S_i - S) \tag{6.8.1.11}$$

Let us define yield factor, Y:

$$Y = \frac{\text{mass of cell formed}}{\text{mass of substrate consumed}}$$

By rearrangement of (6.8.1.11) and when yield factor is inserted, it becomes the same equation as in (6.8.1.2):

$$DX_{\text{o}} + \left(\frac{\mu_{\max}S}{K_s + S} - D\right)X = 0$$

Substituting into the mass balance yields, the cell mass balance is arranged. At steady-state condition:

$$D(S_{\text{o}} - S) - \frac{\mu_{\max}SX}{Y(K_S + S)} = 0 \tag{6.8.1.12}$$

For sterile conditions X_o is zero, because no microbe is present in the feed stream and the feed is sterile without any contamination.

$$0 = (D - \mu)X \tag{6.8.1.13}$$

When the cell concentration is appreciable, the dilution rate must reach a specific rate ($X \neq 0$, $D = \mu$). The cell mass concentration is defined in (6.8.1.13) as the dilution rate approaches zero; the cell density is the product of yield and initial substrate concentration:

$$Y = \frac{X}{S_o - S} \tag{6.8.1.14}$$

Substituting (6.8.1.7) into (6.8.1.14), the biomass concentration is defined:

$$X = Y(S_o - S) = Y\left(S_o - \frac{DK_S}{\mu_{max} - D}\right) \tag{6.8.1.15}$$

As the dilution rate increases, the concentration level of final substrate will linearly increase with D, and D approaches μ_{max}. The result of a high dilution rate would cause the cell density to drop. When $D = \mu_{max}$, $X = 0$. This phenomenon is known as wash out.

$$D_{max} = \frac{\mu_{max} S_o}{K_s + S_o} = \mu_{max}\left(1 - \sqrt{\frac{K_s}{K_s + S_o}}\right) \tag{6.8.1.16}$$

Near the wash out, the reactor is very sensitive to variations of dilution rate D. A small change in D gives a relatively large shift in X and S. The rate of cell production per unit volume of reactor is DX. These quantities are shown in Figure 6.5, where there is a sharp maximum in the curve of DX. We can compute maximal cell rate by taking the derivative of DX with respect to D, then solving the equation. The derivative of DX with respect to D is defined as:

$$\frac{d(DX)}{dD} = 0 \tag{6.8.1.17}$$

$$\frac{d(XD)}{dD} = \frac{d}{dD}\left[YD\left(S_o - \frac{DK_s}{\mu_{max} - D}\right)\right] = 0 \tag{6.8.1.18}$$

After differentiation, the result is simplified for initial substrate concentration with respect to dilution rate:

$$S_o - \frac{DK_s}{\mu_{max} - D} - \frac{DK_s\,\mu_{max}}{(\mu_{max} - D)^2} = 0 \tag{6.8.1.19}$$

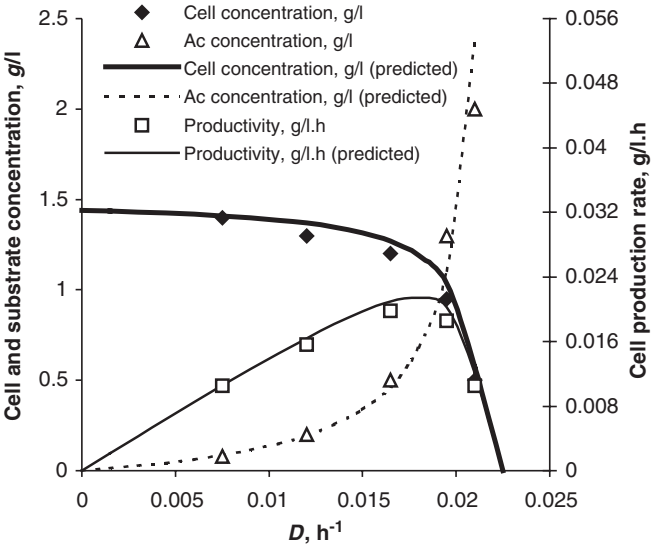

FIG. 6.5. Effect of dilution rate on cell density, substrate concentration and cell production rate.

Rearranging (6.8.1.19) gives a second-order equation with respect to D:

$$\left(\frac{D}{\mu_{\max}}\right)^2 (S_o + K_s) + S_o - 2\frac{D}{\mu_{\max}}(S_o + K_s) = 0 \qquad (6.8.1.20)$$

Solving the quadratic equation will lead to (6.8.1.21):

$$\frac{D}{\mu_{\max}} = \frac{(S_o + K_s) \pm \sqrt{(S_o + K_s)^2 - 4S_o(S_o + K_s)}}{2(S_o + K_s)} = 1 \pm \sqrt{1 - \frac{S_o}{S_o + K_s}}$$

$$\frac{D}{\mu_{\max}} = 1 - \sqrt{\frac{K_s}{K_s + S_o}} \qquad (6.8.1.21)$$

6.9 TEMPERATURE EFFECT ON RATE CONSTANT

Generally, in an equation of a chemical reaction rate, the rate constant often does not change with temperature. There are many biochemical reactions that may be influenced by temperature and the rate constant depends on temperature as well. The effect of temperature on

reaction rate constant may follow Arrhenius' law. The differential form of rate constant is shown as follows:

$$\frac{\mathrm{d}\ln k}{\mathrm{d}T} = \frac{E}{RT^2} \tag{6.9.1}$$

Integration may lead to a relation for rate constant with temperature dependency in the form of Arrhenius' law:

$$k = Ae^{-E/RT} \tag{6.9.2}$$

For a plug flow reactor, differential volume moves along the length. The following equation may express the material balance for a plug flow reactor:

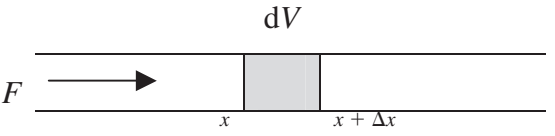

In = Out

$$FX + \mathrm{d}V\left(\frac{\mathrm{d}x}{\mathrm{d}t}\right)_{\text{growth}} = F(x + dx) \tag{6.9.3}$$

The integration may simply express the residence time for PFR:

$$t_p = \int_{x_1}^{x_2} \frac{\mathrm{d}x}{\left(\frac{\mathrm{d}x}{\mathrm{d}t}\right)_{\text{growth}}} = \int_0^{x_A} \frac{\mathrm{d}x_A}{-r_A}$$

$$\tau = \frac{V}{F} \tag{6.9.4}$$

The differentiation of (6.9.4) results in the following ratio:

$$\mathrm{d}t_p = \frac{\mathrm{d}V}{F} = \frac{\mathrm{d}x}{\left(\frac{\mathrm{d}x}{\mathrm{d}t}\right)_{\text{growth}}} \tag{6.9.5}$$

The result in (6.9.5) shows a discrete time, which is numerically used for a PFR bioreactor.

6.10 SCALE-UP OF STIRRED-TANK BIOREACTOR

A general rule, which is often applied in scale-up, is that of geometric similarity between the small and large vessels. However, as shown in Table 6.3, the relevant parameters that

TABLE 6.3. *Various parameters on scale-up using geometric similarities*

Property	Pilot scale (100 Litres)	Constant *P*/volume	Plant-scale constant ND_i^2	(125,000 litres) constant ND_i	Constant N_{Re}
Power, P (hp)	1.0	15.63	7800	6.25	0.005
P/Volume	1.0	1.00	6.25	0.005	4×10^{-6}
N, mixing time^{-1}	1.0	0.48	1.00	0.005	2×10^{-3}
D_i, m	1.0	2.50	2.50	2.50	2.50
Agitator flow Discharge, $Q\alpha ND_i^2$	1.0	7.50	15.63	6.25	2.50
ND_i	1.0	1.20	2.50	1.00	0.40
Reynolds number $\rho ND_i^2/\mu$	1.0	3.00	6.25	2.50	1.00
Froude number N^2D_i/g	1.0	0.60	2.50	1.00	0.0003

ND_i^2, impeller speed (Hz); $N^2D_i^3\alpha$, power; $ND_i\alpha$, average shear rate; Nα 1/mixing time.

affect mixing can vary widely between the two scales. The pilot scale is a base line; the parameters in the second column are given a numerical value of 1. Several strategies were used to observe the effect of design parameters on scale-up process. The third column considers the situation with geometric similarity and where constant power per unit volume was implemented in the design calculation. The new volume is 1250 times the old volume, and the linear dimension scale-up is 5:1.

The important parameters that affect mixing and growth of a microorganism are summarised as follows:

- Oxygen transfer rate (mass transfer coefficient).
- Power per unit volume, agitation and mixing.
- Volumetric flow rate of gas per unit volume of reactor.
- Maximum shear rate, average shear rate and mixing time, impeller tip velocity, ND_i.
- Pumping rate per unit volume, *N*.
- Heat transfer, Reynolds number and surface area of the vessel.

Referring to Table 6.3, it can be seen that with geometric similarities in self controls there is no mixing variable. In practice, we would select the important criterion that needs to be controlled and then size the vessel accordingly.

Let us summarise the results of Table 6.3. In column 2, constant power per unit volume is maintained, giving larger mixing times and maximum shear rates than in the pilot-scale vessel, but with a lower average shear rate. In column 3, a constant impeller speed and mixing time are maintained, which gives an increase in the power/unit volume of 6.25 times. This is not on scale-up as the maximum shear is also considerably increased. If constant tip velocity is maintained, as shown in column 4, the power per unit volume is drastically decreased and consequently the mass transfer rate of oxygen to microorganisms. In all of

these scale-up calculations, the Reynolds number is increased. In column 5, an attempt was made to maintain a constant Reynolds number, which resulted in a dramatic fall in the power requirement and an increase in mixing time. The extremely low Reynolds number caused very low agitation and low power input. This is usually not a practical situation, and generally the Reynolds number always increases in the scale-up process. The special criteria chosen for the scale-up process are based on three concepts:

- Constant power/unit volume.
- Constant gas flow rate/unit volume.
- Geometric similarity of the vessel.

These criteria have been found to give comparable growth and product rates compared with the pilot-scale operation. If we need to control maximum shear, the value of ND_i should be the same in both the pilot- and large-scale vessels.

Example 1

A bacterial fermentation was carried out in a reactor containing broth with average density $\bar{\rho} = 1200\,\text{kg/m}^3$ and viscosity $0.02\,\text{N}\cdot\text{s/m}^2$. The broth was agitated at 90 rpm and air was introduced through the sparger at a flow rate of 0.4 vvm. The fermenter was equipped with two sets of flat blade turbine impellers and four baffles. The dimensions of vessel, impellers and baffle width were:

tank diameter, $D_t = 4\,\text{m}$;
impeller diameter, $D_i = 2\,\text{m}$;
baffle width, $W_b = 0.4\,\text{m}$;
also the liquid depth was $H = 6.5\,\text{m}$.

Determine**:** (a) ungassed power, P; (b) gassed power, P_g; (c) K_La; (d) gas hold-up.

Solution

Let us define the ratio of tank diameter to impeller diameter:

$$\frac{D_t}{D_i} = \frac{4}{2} = 2 \tag{E.1.1}$$

Also, the ratio of the height of the liquid level to impeller diameter is:

$$\frac{H_L}{D_i} = \frac{6.5}{2} = 3.25 \tag{E.1.2}$$

$$n = \frac{90\ \text{rpm}}{60} = 1.5\ \text{rps} \tag{E.1.3}$$

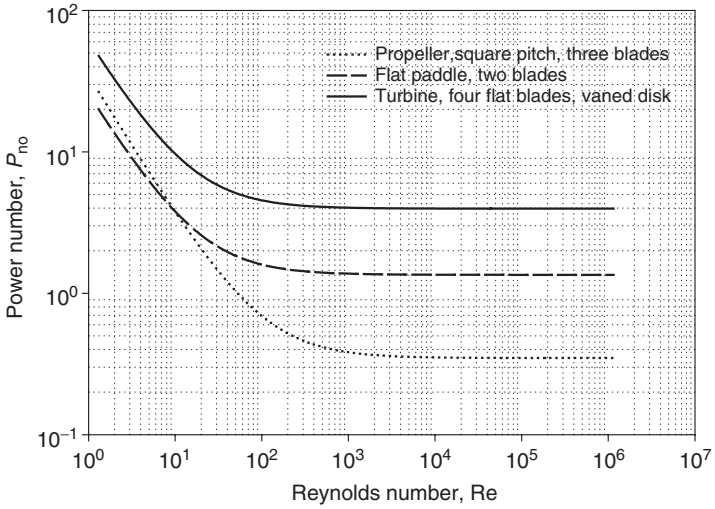

FIG. 6.6. Power number versus Reynolds number for various impellers (flat blades, turbine, vaned disk and marine propeller).

Now define the Reynolds number:

$$N_{Re} = \frac{ND_i^2\rho}{\mu} = \frac{(1.5)\,(2)^2(1200)}{0.02} = 3.6\times10^5 \tag{E.1.4}$$

Since the Reynolds number is greater than 10^4, therefore the flow is turbulent. Based on a power number defined in the turbulent regime, the power number is defined as about 6 (from Figure 6.6).

$$N_P = 6 = \frac{Pg_c}{\rho N^3 D_i^5} = \frac{P\times9.81}{(1200)(1.5)^3(2)^5} \tag{E.1.5}$$

Power is calculated as

$$P = \frac{(6)\,(1.5)^3(2)^5(1200)}{9.81} = 79266\ \frac{\text{kg m}}{\text{s}} = 106\ \text{hp} \tag{E.1.6}$$

Correction factors are used to define actual power

$$f_c = \sqrt{\frac{\left(\frac{D_t}{D_i}\right)^*\left(\frac{H_L}{D_i}\right)^*}{\left(\frac{D_t}{D_i}\right)\left(\frac{H_L}{D_i}\right)}} = \sqrt{\frac{3\times3.25}{3\times3}} = 0.85 \tag{E.1.7}$$

For two sets of impellers with application of a correction factor, ungassed power is

$$P = (2)(0.85)(106) = 180 \text{ hp} \tag{E.1.8}$$

Dimensionless aeration rate is defined as:

$$N_a = \frac{F_g}{N_i D_i^3} \tag{E.1.9}$$

$$F_g = 0.4 \text{ (volume)} = 0.4\,(4)2\left(\frac{\pi}{4}\right)(6.5) = 32.67\frac{\text{m}^3}{\text{min}} = 0.5445\frac{\text{m}^3}{\text{s}} \tag{E.1.10}$$

$$N_a = \frac{0.5445}{(1.5)(2)^3} = 4.5\times10^{-2} \tag{E.1.11}$$

Using the plot of P_g/P versus N_a (Figure 6.7), the ratio of gassed power to ungassed power is defined.

$$\frac{P_g}{P} = 0.74 \tag{E.1.12}$$

The gassed power is:

$$P_g = 0.74(180) = 133 \text{ hp} \tag{E.1.13}$$

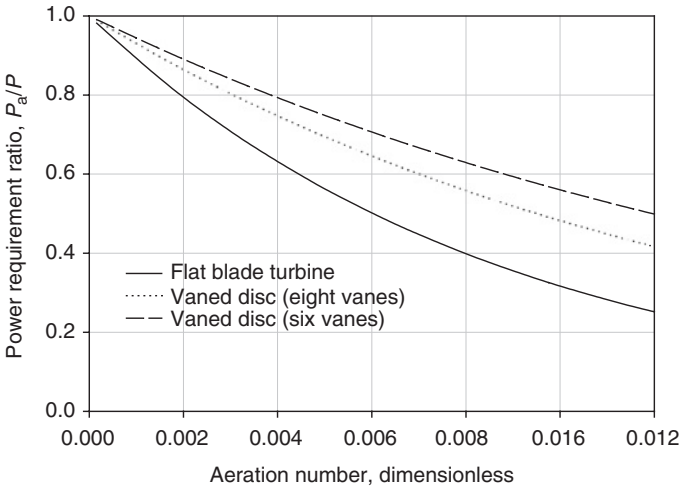

FIG. 6.7. Ratio of power requirement for aerated versus non-aerated systems.

The gas superficial velocity is:

$$V_s = \frac{32.67}{(4)^2\left(\frac{\pi}{4}\right)} = 2.6\frac{\text{m}}{\text{min}} \tag{E.1.14}$$

The mass transfer coefficient is defined as turbulent:

$$K_L a = 2\times10^{-3}\left(\frac{P_g}{V}\right)^{0.6} V_S^{0.667} = 10.97\,\text{s}^{-1} \tag{E.1.15}$$

$$\text{Gas hold-up,} \quad H_o = \frac{\text{Bubble volume}}{\text{Reactor volume}}$$

Gas hold-up is defined as volume of gas per unit volume of reactor. For air in water, Richard's data are by:

$$\left(\frac{P}{V}\right)^{0.4} (V_s)^{0.5} = 7.63H + 2.37 \tag{E.1.16}$$

$$\left(\frac{180}{81.68}\right)^{0.4}\left(2.6\times60\frac{\text{min}}{h}\right)^{0.5} = 7.63H + 2.37 \tag{E.1.17}$$

$H = 1.94$ m for aeration

$$H_o = \frac{V_g}{V_g + V_L} = \frac{1.94}{1.94 + 6.5} = 0.23 \tag{E.1.18}$$

Gas hold-up = 23%.

Example 2

The Monod rate model is valid for a CSTR bioreactor with maximum specific growth rate of 0.5 h^{-1} and K_s 2 $g\cdot l^{-1}$. What would be a suitable dilution rate at steady-state condition, where there is no cell death if initial substrate concentration is 50 $g\cdot l^{-1}$ and yield of biomass on substrate is 100%.

Solution

The Monod rate is

$$\mu = \frac{\mu_{\max} S}{K_S + S} \rightarrow D = \frac{\mu_{\max} S}{K_S + S}$$

$$S_{\text{out}} = \frac{K_S D}{\mu_{\max} - D} \tag{E.2.1}$$

$$Y_{x/s} = 1$$

$$S_o = 50 \text{ g.l}^{-1}$$

Substrate balance:

$$-\frac{\mathrm{d}S}{\mathrm{d}t} = \frac{F}{V}(S_{\text{in}} - S_{\text{out}}) - \left(\frac{\mu}{Y_{x/s}}\right)X - \left(\frac{q_p}{Y_{p/x}}\right)X$$

Assume no death rate,

$$\text{steady state} -\frac{\mathrm{d}S}{\mathrm{d}t} = 0, \quad \mu = D, \quad \frac{F}{V} = D$$

Use (6.34) and rearrange to get DX:

$$q_p = 0, \qquad \overline{X} = Y_{x/s}(S_{\text{in}} - S_{\text{out}})$$

$$D(S_{\text{in}} - S_{\text{out}}) = \left(\frac{\mu_{\max} S}{K_S + S}\right)\left(\frac{1}{Y_{x/s}}\right)X$$

$$\rightarrow D\overline{X} = Y_{x/s}\left(S_0 - \frac{K_S D}{\mu_m - D}\right)$$

Take derivative $\mathrm{d}(D\overline{X})/\mathrm{d}D = 0$ to obtain a value for maximum dilution rate:

$$D_{\max} = \mu_{\max}\left(1 - \sqrt{\frac{K_S}{K_S + S}}\right) = 0.5\left(1 - \sqrt{\frac{2}{52}}\right) = 0.4 \text{ h}^{-1}$$

$$\frac{\mathrm{d}(D\overline{X})}{\mathrm{d}D} = Y_{x/s}\left(S_{\text{o}} - \frac{K_S D}{\mu_m - D}\right) - \left[\frac{K_S(\mu_m - D) - K_S D}{(\mu_m - D)^2}\right]D$$

Get $$D_{\max} = \mu_{\max}\left(1 - \sqrt{\frac{K_S}{K_S + S}}\right)$$

Then calculate the substrate concentration at leaving stream:

$$S_{\text{out}} = \frac{K_S D}{\mu_{\max} - D} = \frac{2(0.4)}{0.5 - 0.4} = 8 \text{ g/l}$$

Example 3

A 20 m^3 working volume of a bioreactor is used for producting penicillin. What would be the sugar concentration (S_o) you choose if oxygen transfer rate is not the limiting reactant? Given data:

Impeller speed = 1.5 rps (90 rpm)
Number of blades = 8; flat, turbine types of blade
$\mu = 1$ mPa·s
$\rho = 1.2 \times 10^3$ kg/m^3
Aeration rate = 1 vvm
Ratio of gassed to ungassed power, $P_g/P = 0.4$
Driving force for OTR = 6×10^{-3} kg/m^3
Specific O_2 uptake = 0.65 mmol O_2/kg cell
Also, the kinetic data are given as $\nu_{\max} = 0.5\ h^{-1}$
Specific sugar consumption rate of cells = 1.0 kg/kg cell·h

Solution

Given data:

$D_{\text{tank}} = 2.4$ m

Data:

$D_{\text{tank}} = 2.4$ m
$D_i = D_{\text{tank}}/3 = 0.8$ m; for three sets of impellers

Impeller speed 150 rpm; assume broth viscosity is 1 cp and the specific gravity of the broth is 1.2; aeration rate is 1 vvm; given ratio of gassed power to un-gassed system is 0.4; specific oxygen uptake is 0.65 mmol O_2/kg cell; $OTR = 6 \times 10^{-3}$ kg/m^3.

$D_{\text{tank}}/D_i = 3$
$D_i = 0.8$ m, three sets of impellers are used.
$\mu = 1$ mpas
$\rho = 1200$ kg/m^3
$P_g/P = 0.4$, $\nu_{\max} = 0.5\ h^{-1}$
Specific sugar consumption rate of cells = 1.0 kg (kg cell)$^{-1}$·h^{-1}.

Mass transfer is calculated by the empirical correlation defined for non-Newtonian filamentous fermentation:

$$K_L a = 2\times 10^{-3}\left(\frac{P_g}{V}\right)^{0.6} V_S^{0.667}$$

$$K_L a = S^{-1}$$

$$\frac{P_g}{V} = \frac{\text{Gassed power}}{\text{volume}} = \frac{\text{hp}}{\text{m}^3}$$

$$V_s = \text{gas superficial velocity}, \frac{\text{cm}}{\text{min}}$$

Read power number versus Reynolds number in turbulent region is based on geometry of the impellers. The lowest power number is less than 1,for marine propellers. For flat bladed turbines in a turbulent region, the power number is equal to 6. The power graph is illustrated in Figure 6.6.

$$N_p = 6 = \frac{Pg_c}{N^3 D_i^5 \rho}$$

$$\text{Ungassed power}, P = \frac{6PN^3 D_i^5}{g_c} = \frac{6\times 1200\times (2.5)^3 (0.8)^5}{9.81} = 3758 \ \frac{\text{kg•m}}{\text{s}}$$

$$P = \frac{3758}{745.7} = 5\,\text{hp}$$

for three sets of impelers, 15 hp

$$P_g = 0.4(15) = 6 \text{ hp}$$

The Correction factor for non-geometrical similarity is:

$$f_c = \sqrt{\frac{\left(\frac{D_t}{D_i}\right)^* \left(\frac{H_L}{D_i}\right)^*}{\left(\frac{D_t}{D_i}\right)\left(\frac{H_L}{D_i}\right)}} = \sqrt{\frac{3\times 4.42}{3\times 3}} = 1.25$$

$$P = (\text{three sets})(1.25)(5.04) = 19 \text{ hp}$$

For the agitated and aerated vessel, the ratio of power requirements for aerated versus non-aerated systems is expressed by a dimensionless number known as the aeration rate; the value is obtained from Figure 6.7.

$$N_a = \frac{F_g}{N_i D_i^3}$$

$$N_a = \frac{0.333}{(2.5)(0.8)^3} = 0.26$$

$$F_g = 20\frac{m^3}{min} = 0.333\frac{m^3}{s}$$

$$P_g = 0.4(19) = 7.6 \text{ hp}$$

$$V_S = \frac{20\frac{m^3}{min}}{\frac{\pi}{4}(2.4)^2 m^2} = 4.42\frac{m}{min} = 7.4\times10^{-2}\frac{m}{s}$$

$$K_L a = 2\times10^{-3}\left(\frac{7.6}{20}\right)^{0.6}(4.42)^{0.667} = 6.7\times10^{-2}\frac{m}{s}$$

$$OTR = K_L a\ (C^* - C)$$

$$OTR = xq_{O_2} = (6.7\times10^{-2})(6\times10^{-3}) = 4.03\times10^{-4}\frac{kg}{m^3 s}$$

Maximum cell concentration, $OTR = x\ qO_2$

$$q_{O_2} = (0.65\times10^{-3})(32\times10^{-3}) = 2.08\times10^{-3}\frac{kg\ O_2}{kg\ cell\ s}$$

$$x_s = x = \frac{4.03\times10^{-4}}{2.08\times10^{-3}} = 19.375\frac{kg}{m^3}$$

$$x_s = x_o + \frac{\mu_m}{q_s}C_s = 0 + \frac{0.5}{1.0}C_s$$

$$C_s = \frac{19.375}{0.5} = 38.75\frac{kg}{m^3}$$

6.11 NOMENCLATURE

r_p	Rate of product formation, $g\cdot l^{-1}\cdot h^{-1}$
$-r_s$	Rate of substrate consumption, $g\cdot l^{-1}\cdot h^{-1}$
Fr	Froude number, dimensionless
g	gravity, m/s^2
N	rotational speed, Hz

D_i Impeller diameter, m
N_P Power number, dimensionless
V_S Gas superficial velocity, cm·min^{-1}
N_a Dimensionless aeration rate

REFERENCES

1. Demain, A.L. and Solomon, A.N., *Sci. Am.* **245**, 67 (1981).
2. Aiba, S. Humphrey, A.E. and Millis, N.F., "Biochemical Engineering", 2nd edn. Academic Press, New York, 1973.
3. Phaff, H.J., *Sci. Am.* **245**, 77 (1981).
4. McCabe, W., Smith, J. and Harriott, P., "Unit Operations of Chemical Engineering", 6th edn. McGraw-Hill, New York, 2000.
5. Wang, D.I.C., Cooney, C.L., Deman, A.L., Dunnill, P., Humphrey, A.E. and Lilly, M.D., "Fermentation and Enzyme Technology". John Wiley & Sons, New York, 1979.
6. Baily, J.E. and Ollis, D.F., "Biochemical Engineering Fundamentals," 2nd edn. McGraw-Hill, New York, 1986.
7. Doran, P.M., "Bioprocess Engineering Principles". Academic Press, New York, 1995.
8. Scragg, A.H., "Bioreactor in Biotechnology, A Practical Approach". Ellis Horwood Series in Biochemistry and Biotechnology, New York, 1991.
9. Blakebrough, N., McManamey, W.J. and Tart, K.R., *Trans. Inst. Chem. Eng* **56** 127 (1978).
10. Shuler, M.L. and Kargi, F., "Bioprocess Engineering, Basic Concepts". Prentice Hall, New Jersey, 1992.
11. Ghose, T.K., "Bioprocess Computation in Biotechnology," vol. 1. Ellis Horwood Series in Biochemistry and Biotechnology, New York, 1990.

CHAPTER 7

Downstream Processing

7.1 INTRODUCTION

Bioprocessing treats raw materials and generates useful products. Most bioprocesses involve one or more of the following processes: centrifugation, chromatography, cooling, crystallisation, dialysis, distillation, drying, evaporation, filtration, heating, humidification, membrane separation, milling, mixing, precipitation, centrifugation, solid handling and solvent extraction. A particular sequence of unit operations and bioprocesses is used for the manufacture of an extra pure pharmaceutical product.

Fermentation broths are complex, aqueous mixtures of cells, comprising soluble extracellular, intracellular products and any unconverted substrate or unconvertible components. Recovery and extraction of product is important in bioprocess engineering. In particular, separation is a useful technique; it depends on product, its solubility, size of the process, and product value. Purification of high-value pharmaceutical products using chromatography such as hormones, antibody and enzymes is expensive and difficult to scale up.[1] The necessary steps to follow a specific process depend on the nature of the product and the characteristics of the fermentation broth. There are a few steps for product recovery; the following processes are discussed, which are considered as an alternative for product recovery from fermentation broth.

Initially fermentation broth has to be characterised on the viscosity of the fluid. If the presence of the biomass or cells causes trouble, they have to be removed. The product is stored inside the cells, the cells must be ruptured and the product must be freed. Intracellular protein can easily be precipitated, settled or filtered. In fact the product in diluted broth may not be economical enough for efficient recovery. Enrichment of the product from the bioreactor effluents for increasing product concentration may reduce the cost of product recovery. There are several economical methods for pure product recovery, such as crystallisation of the product from the concentrated broth or liquid phase. Even small amounts of cellular proteins can be lyophilised or dried from crude solution of biological products such as hormone or enzymes.[2,3]

7.2 DOWNSTREAM PROCESSING

In downstream processing of a fermentation unit for enzyme production with a feed stream of sugar at a concentration of $35\ g \cdot l^{-1}$, the expected product to be recovered is α-amylase.

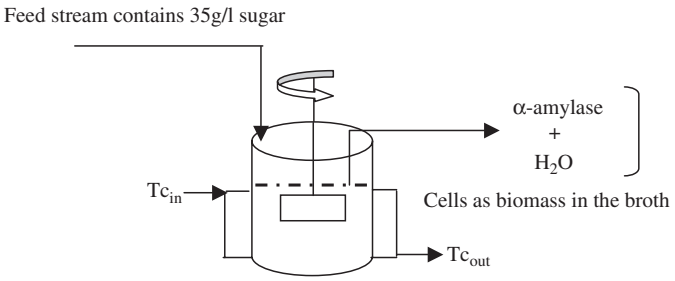

FIG. 7.1. Schematic of jacketed fermentation vessel.

The concentration of enzyme is very low, about several hundred milligrams per litre in the fermentation broth. Solvent extraction is a suitable process to recover a small amount of enzyme. The chance of some enzyme being intracellular is high, therefore cells are ruptured to liberate enzyme, which can then interact with organic solvents. Figure 7.1 shows a simple diagram for a jacketed fermentation vessel for operation at constant temperature.

Bioprocessing includes the bioreactor and a subsequent section for product recovery. The particular separation techniques useful for any given bioprocess depend not only on the size, charge and solubility of the product, but also on the size of the process and product value. For example, various forms of gel filtration, gel chromatography and ion exchanger are used to purify highly valuable pharmaceutical biological compounds such as hormones, antibiotics and enzymes. This chapter emphasises product recovery from fermentation products. Our discussion on separation and purification will cover several bioprocesses, such as solvent extraction and recovery of whole or part of the microbial products. The ultimate challenge is to select the best combination of substrate, enzyme or organism, bioreactor and separation of the specific product. Each separation needed depends on initial broth characteristics such as viscosity, product concentration, impurities and undesired particulates, and final product concentration needed for crystallisation, concentrated liquid product or dried powder.

It is often desirable to recover product and to choose a suitable strain of microorganism which produces extracellular rather than intracellular product. If the product stays inside the cells, the cells must be ruptured, so freeing intracellular enzyme, after which extraction or purification is performed to recover the valuable product. The fermentation broth has to be processed, and pass through several stages for separation and purification. The product requires a sequence of operations for high purification. The usual steps to follow are as follows.

(1) Removal of insoluble particulates using various separation techniques. Common operations are filtration, centrifugation and/or settling/sedimentation/decanting.
(2) Primary isolation is done to increase product concentration. Solvent extraction, absorption, precipitation and ultrafiltration are the best known. Ultrafiltration can discriminate at the molecular level. During primary isolation, desired product concentration increases considerably and substances of widely differing polarities are separated from the product.
(3) Product purification. For production of highly pure product the impurities have to be removed for further product concentration such as chromatography and adsorption.

These operations often select for impurity removal as well as further product concentration. Approaches include fractional precipitation. Other alternatives such as chromatography and adsorption are also considered as methods of process purification.

(4) Final product isolation and drying of the crystallised product are done by drum drying, spray drying or freeze drying. The last steps must provide the desired product in a form suitable for final formulation and blending, or for direct shipping. Processes of centrifugation, freeze drying/lyophilisation or organic solvent removal are commonly used.

For antibiotic production, the fermentation broth needs a pretreatment tank to produce crude and highly purified antibiotic products. The bioprocesses involved in producing antibiotics are spray or continuously dried crude solids and pure solid in the form of crystalline antibiotic.

Another case of bioprocessing is production of an alternative and renewable fuel from agricultural wastes. Lignocellulosic materials are an abundant and renewable source of energy; in acid hydrolysis, sugar is the desired product. The acid can be neutralised by adding sodium hydroxide or any bases; the sugar may not be fermentable in the presence of salts. Solvent extraction is normally performed to recover acid and reuse/recycle acid for hydrolysis process. Once fermentable sugar is obtained, it is useful to carry on fermentation for ethanol, organic acid, enzyme or antibiotic production. Figures 7.2 and 7.3 show the common

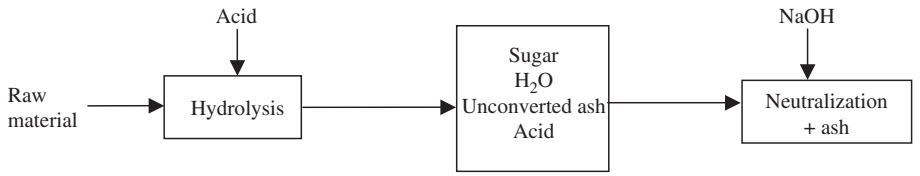

FIG. 7.2. Acid recovery by liquid–liquid extraction.

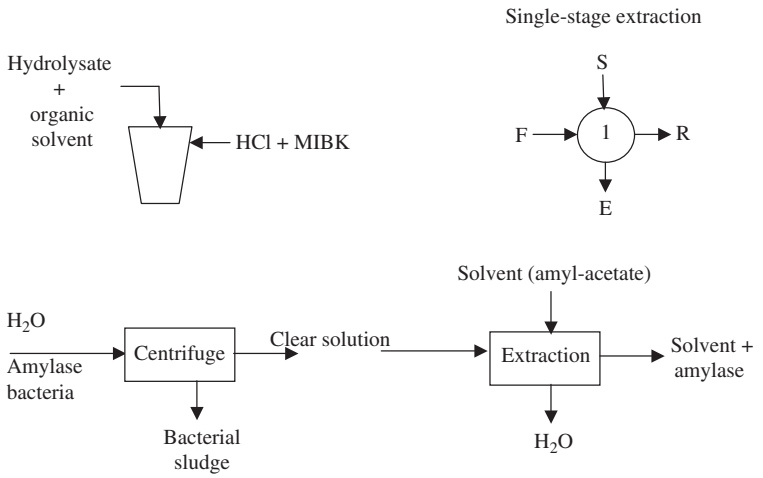

FIG. 7.3. Stages of unit operation for product recovery.

separation and extraction processes that are involved in purification of enzyme and fermentable sugar for related bioprocesses.

$$\text{Lignocellulosic material} + \text{Acid} \xrightarrow{\text{Hydrolysis}} \text{Sugar} + \text{Solid residues}$$

When the fermentation broth enters the downstream units, it has high viscosity and needs pretreatment. Addition of chemicals and coagulating aids for cell flocculation such as polyelectrolytes, $CaCl_2$ and colloidal clay are useful pretreatments to recover product downstream. Settling solids are often used in large-scale waste treatment processes as well as traditional fermentation industries. Generally, simple centrifugation produces a cell-concentrated stream of 15% w/v. Also, filtration produces more concentrated cell sludge of up to 20–35% w/v.[4]

7.3 FILTRATION

In filtration, solid particles are separated from a fluid–solid mixture by forcing the fluid through a filter medium or filter cloth, which retains the solid particles. As a result, solids are retained by filter media and the filtrate is obtained, which is a clear solution without any solid particles. The solid particles deposited on the filter form a layer, which is known as filter cake. The deposited solids create resistance which reduces filter flux. The depth of the filter cake gradually increases as more solids are retained. The filter cake may create more resistance to further filtration. Filtration can be performed using either vacuum or positive-pressure equipment. The exerting differential pressure across the filter separates fluid from solid and is called the filtration pressure drop. Ease of filtration depends on particle properties and fluid filtrates. The compaction of particles, either soft or hard, compressible or non-compressible, and the viscosity of the fluid may create different resistances. Fermentation broths are troublesome and hard to filter, because of the non-Newtonian behaviour of the broth. Most microbial filter cakes are compressible. When the filter pores are clogged by cell bodies, then the high pressure drop results in major problems in the filtration of fermentation broth. Then more pressure is created and gradually filtration rate drops.

Filter aids are widely used in the fermentation industry to improve the efficiency of filtration. It is a pre-coated filter medium to prevent blockage or blinding of the filter by solids, which would otherwise wedge themselves into the pores of the cloth. Filter aid can be added to the fermentation broth to increase the porosity of the cake as it formed. This is only recommended when fermentation product is extracellular. Filter aid adds to the cost of filtration. The minimum quantity needed to achieve the desired result must be established experimentally. Fermentation broths can be pretreated to improve filtration characteristics. Heating to denature proteins enhances the filterability of mycelial broths such as in penicillin production. Alternatively, electrolytes may be added to promote coagulation of colloids into larger, denser particles, which are easier to filter. The filtration process is affected by the viscosity and composition of the broth, and the cell cake.[5]

Plate filters are suitable for filtration of batch fermentation broth; accumulated biomass must be cleaned periodically. A rotary drum vacuum filter is used for a continuous system.

This type of filter can be used for removal of *Penicillium* and *Streptomyces* mycelia in the production of penicillin and streptomycin, respectively.[5] In these processes the rotary drum filter is used with a pre-coated cloth filter with filter aid; the filter cake is removed by a knife blade which scrapes the cake from the rotating drum.

7.3.1 Theory of Filtration

Assume laminar flow of filtrate of liquid through the filter cake. Rate of filtration is usually measured as the rate at which liquid filtrate is collected. The filtration rate depends on the area of the filter cloth, the viscosity of the liquid, the pressure drop across the filter and filter cake resistance. At any instant during filtration, the rate of filtration is given by the equation:

$$\frac{1}{A}\frac{\mathrm{d}V_\mathrm{f}}{\mathrm{d}t} = \frac{\Delta p}{\mu_\mathrm{c}\left[\alpha\left(\frac{W}{A}\right) + r_\mathrm{m}\right]} \tag{7.3.1.1}$$

where A is filter area, V_f is volume of filtrate, t is filtration time, ΔP is the pressure drop across the filter, μ_c is the fluid viscosity, and W is the mass of solids in the filter cake. W is defined as:

$$W = \text{mass of solids in the cake} = \left[\frac{\rho\varpi}{1-m\varpi}\right]V_\mathrm{f} = \frac{m\varpi}{1-m\varpi} \tag{7.3.1.2}$$

where m is the ratio of mass of wet cake over mass of dry cake and ϖ is the solid mass fraction.

Also from (7.3.1.1), r_m is the filter media resistance and α is the average specific cake resistance. If the filter cake is incompressible, α is constant; for compressible cake α is defined as:

$$\alpha = \alpha'(\Delta P)^S \tag{7.3.1.3}$$

where S is cake compressibility, α' is constant, depending on the size of particles in the cake. For incompressible solids, S is about zero; for highly compressible solids, S is about 1. For convenient integration, rewrite (7.3.1.1) in its reciprocal form:

$$A\frac{\mathrm{d}t}{\mathrm{d}V_\mathrm{f}} = \mu_\mathrm{f}\alpha\left(\frac{\rho\omega}{1-m\omega}\right)\frac{V_\mathrm{f}}{A\Delta P} + \frac{\mu_\mathrm{f} r}{\Delta P} \tag{7.3.1.4}$$

The separation of variables is used with suitable integrations, which result in the following equations:

$$A\int \mathrm{d}t = \left(\frac{\mu_\mathrm{f}\alpha\rho\omega}{1-m\omega}\right)\left(\frac{1}{A\Delta P}\right)\int V_\mathrm{f}\mathrm{d}V_\mathrm{f} + \frac{\mu_\mathrm{f} r}{\Delta P}\int \mathrm{d}V_\mathrm{f} \tag{7.3.1.5}$$

$$(A)(t) = \frac{\mu_f \alpha}{2A\Delta P}\left(\frac{\rho\omega}{1-m\omega}\right)V_f^{\,2} + \left(\frac{\mu_f r}{\Delta P}\right)V_f \tag{7.3.1.6}$$

Using an initial condition for calculation for defining integration constant at $t = 0$, $V_f = 0$, gives the integration constant to be zero. By division of the above equation with V_f we can obtain a linear model, which we can plot and obtain the slope and intercepts. The modified equation after division of (7.3.1.6) is:

$$\frac{t}{V_f/A} = \frac{\mu_f \alpha \rho \omega}{2\Delta P(1-m\omega)} \cdot \frac{V_f}{A} + \frac{\mu_f r}{\Delta P} \tag{7.3.1.7}$$

Now the (7.3.1.7) is linear as $\frac{t}{V_f / A}$ versus $\frac{V_f}{A}$ the linearised model is ($y = k_1 x + k_2$):

$$\frac{t}{V_f/A} = k_1\left(\frac{V_f}{A}\right) + k_2 \tag{7.3.1.8}$$

where, $k_1 = \frac{\mu_c \alpha \rho \omega}{2\Delta P(1-m\omega)}$ and $k_2 = \frac{\mu_c r_m}{\Delta P}$. The slopes of the above lines depend on physical properties of the fermentation broth such as viscosity, density, mass fraction and pressure drop. The pH for the filtration of fermentation broth in the production of streptomycin using *Streptomyces griseus* may show an additional effect; neutralising pH should eliminate such an effect.

In general, fungal mycelia are filtered relatively easily, because mycelia filter cake has sufficiently large porosity. Yeast and bacteria are much more difficult to handle because of their small size. Alternative filtration methods, which eliminate the filter cake, are becoming more acceptable for bacterial and yeast separation. Micro-filtration is achieved by developing large cross-flow fluid velocities across the filter surface while the velocity vector normal to the surface is relatively small. Build up of filter cake and problems of high cake resistance are therefore prevented. Micro-filtration is not discussed in this section.

7.4 CENTRIFUGATION

Centrifugation is used to separate materials of different densities when a force greater than gravity has been implemented, such as centrifugal forces. Centrifugation may be used to remove cells from fermentation broth; yeast, for example, is harvested in a centrifuge unit. For dilute suspensions each cell may be treated as a single particle in an infinite fluid. In the concentrated fluid with suspended solids, the particle's motion is influenced by neighbouring particles. A continuous process is commonly used in separation of solid particles from fermentation broth. The particle's velocity correlates with the hindered settling

particles (u_h), the single particle's velocity (u_o) and the volume fraction of particles (ϵ_p). The correlation is:

$$\frac{u_h}{u_o} = \frac{1}{1+\beta\varepsilon_p^{1/3}} \tag{7.4.1}$$

The empirical relations for β in the above equation derive for various ranges of ε_p are:

$$\beta = \begin{cases} 1+3.05\varepsilon_p^{2.84} & 0.15 < \varepsilon_p < 0.5, \quad \text{irregular particles} \\ 1+2.29\varepsilon_p^{3.43} & 0.2 < \varepsilon_p < 0.5, \quad \text{spherical particles} \\ 1-2 & \varepsilon_p < 0.15, \quad \text{dilute suspensions} \end{cases} \tag{7.4.2}$$

Another type of centrifuge is known as a scroll conveyer centrifuge. By comparing several types of continuous centrifuges, the scroll type of centrifuge has an important feature of the decanter, that is able to handle large solid particles without any clogging. The decanter centrifuge is used for recovery of large mould pellets and the large throughput capacity of the nozzle. The settled solid is easily removed with a scroll centrifuge.

7.4.1 Theory of Centrifugation

The particle's velocity in a particular centrifuge is compared with the settling velocity that occurs under the influence of gravity and the effectiveness of centrifugation. The terminal velocity during gravity settling of a small particle in dilute suspension is given by Stoke's law:

$$u_g = \left(\frac{\rho_p - \rho_f}{18\mu}\right) D_p^2 g \tag{7.4.1.1}$$

where u_g is the sedimentation velocity under gravity, ρ_p is the density of the particle, ρ_f is the density of fluid, μ is the viscosity of the fluid, D_p is the diameter of the solid particle, and g is gravitational acceleration. In (7.4.1.1) the centrifugal force is implemented to obtain terminal velocity in the centrifuge:

$$u_c = \left(\frac{\rho_p - \rho_f}{18\mu}\right) D_p^2 \omega^2 r \tag{7.4.1.2}$$

where u_c is the particle velocity in the centrifuge, ω is the angular velocity of the bowl in rad/s, and r is the radius of the bowl or centrifuge drum. The ratio of velocity in the centrifuge to velocity under gravity (u_c/u_g) is called the centrifuge effect or g-number, and is denoted as Z; therefore:

$$Z = \frac{\omega^2 r}{g} \tag{7.4.1.3}$$

The force developed in a centrifuge is Z times the force of gravity and is often expressed as so many g-forces. Industrial centrifuges have Z factors from 300 to 16,000. In a small laboratory centrifuge Z may be up to 500,000. The particle velocity in a given centrifuge can be increased by increasing the centrifuge angular velocity (ω); by increasing the particle diameter (D_p); by increasing the density differences between particle and liquid ($\Delta\rho = \rho_p - \rho_f$); and decreasing suspension viscosity (μ).

However, where the particles reach the walls of the bowl, the separation is also affected by the time of exposure to the centrifugal forces. In continuous flow and devices such as the disc-stack centrifuge, the residence time increases by decreasing the feed flow rate. Performance of centrifuges of different size can be compared by using a parameter known as the sigma factor (Σ). For a continuous centrifuge, the sigma factor is related to the feed flow rate:

$$\Sigma = \frac{Q}{2u_g} \tag{7.4.1.4}$$

where Q is the volumetric flow rate and u_g is the terminal velocity of the particles in a gravitational field. The sigma factor physically represents the cross-sectional area of a gravity settler with the same sedimentation characteristics as the centrifuge. For two centrifuges with equal particle velocities, the performance of their effectiveness is related by their flow rate:

$$\frac{Q_1}{\Sigma_1} = \frac{Q_2}{\Sigma_2} \tag{7.4.1.5}$$

where, subscripts 1 and 2 denote the two centrifuges. Equation (7.4.1.5) can be used to scale-up centrifuge equipment. The sigma factor depends on centrifuge design. Figure 7.4

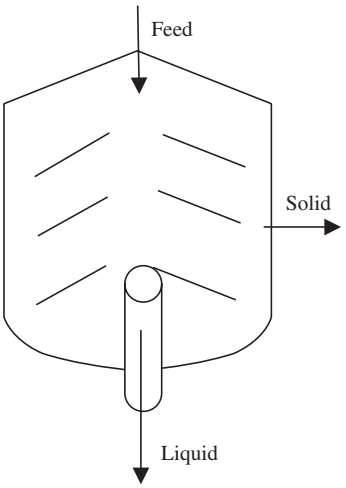

FIG. 7.4. Disc stack bowl centrifuge.

shows a simplified stack bowl centrifuge. For a disc-stack bowl centrifuge, Σ is defined as:

$$\Sigma = \frac{2\pi\omega^2(N-1)}{3g\tan\theta}(r_2^3 - r_1^3) \qquad (7.4.1.6)$$

where ω is the angular velocity in rads/s, N is the number of discs in the stacks, r_2 is the outer radius of the disc, r_1 is the inner radius of the disc, and θ is half of the cone angle of the disc. For a tubular bowl centrifuge the above equation has to be modified. Figure 7.4 shows the disc stack bowl centrifuge.

7.5 SEDIMENTATION

When cells have a high tendency to aggregate closely (coagulate) or to form multicellular flocs with the aid of polyvalent cations or extracellular polymers, the recovery of cell biomass becomes simple and easily applicable by the sedimentation process. Such aggregation provides cell recycle streams in activate sludge wastewater treatment; and several highly flocculent yeast strains are used in brewing beer and single-cell protein production. In fact, we need to remove cells from fermentation broth, so sedimentation is considered as a downstream processing method. Alum, lime and polyelectrolytes are commonly used to create macroflocs. There are several natural and chemical coagulants used for aggregating suspended cells in bioprocesses. Figure 7.5 shows that cells are removed from fermentation broth and the sludge of coagulants with biomass settles as sludge. The clear solution is analysed for enzyme activity and further process purification is needed for enzyme recovery.

$$\text{Cell removal} + \text{polyelectrolyte} \rightarrow \text{aggregated floc}$$

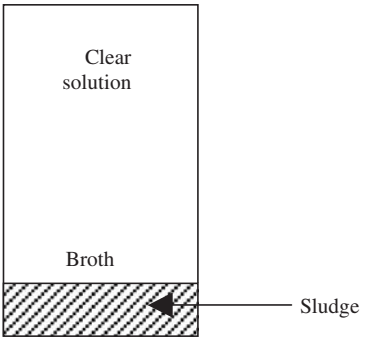

FIG. 7.5. Sedimentation and settled sludge.

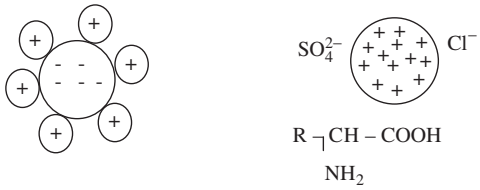

FIG. 7.6. Floc with positive or negative charges.

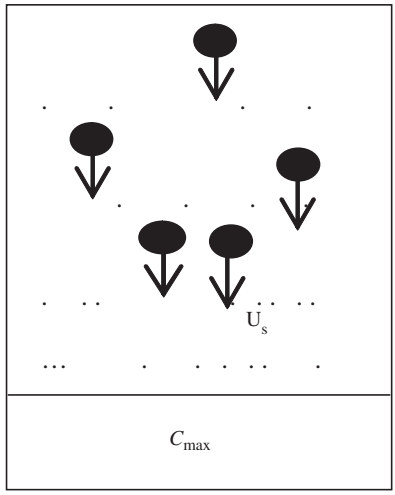

FIG. 7.7. Freely falling of solid particle.

The nature of chemical coagulants are such that the macrofloc may possess certain charges; for example lime (CaO), alum (Al_2O_3) and flocculating polyvalent cations carry positive charges, which interact with proteins. The interactions are simply illustrated in Figure 7.6.

It is necessary to define settleable solids and the settling velocity. Let us take barley and use the polysaccharide content of it with a well-known yeast for brewing beer. It is ideal to use a natural settling tank to have a clear solution; we can generate bioflocs that settle down the biomass faster. Figure 7.7 shows the free-falling solid particles in a fluid. When cells have a high tendency to aggregate, with the aid of polyvalent cations, cell biomass recovery becomes possible.

$$\text{Barley (starch)} \xrightarrow{\textit{Saccharomyces cerevisiae}} \text{brewing beer}$$

In brewing beer and SCP production, several highly flocculent yeast strains are used. The special yeast strains are easily separated without the use of any expensive separation process.[6] The settling velocity is defined by:

$$u_s = kC^{-m} \tag{7.5.1}$$

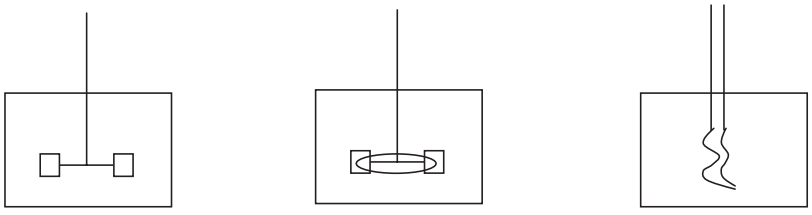

FIG. 7.8. Various impeller shapes.

where m is an empirical constant in the range 1.7–2.6. Once the cell concentration achieves a large value, C_{max}, further concentration occurs at a negligible rate as seen in an activated sludge process. The relative abilities of sedimentation, centrifugation, filtration and drying to achieve dewatering up to a desired level are important in determining which processes are appropriate. For example, centrifugation at $Z = 3000$ removes all the floc water, giving a pellet with 5% moisture; further dewatering may be required after cell lysis. Increased sedimentation rates may be possible in inclined tubes or narrow channels, leading to evolution of a clear fluid zone at the top of the channel or tube.

7.6 FLOTATION

Flotation is another method to remove solid (cells) from fermentation broth, using air bubbles to float protein. We may use different kinds of high shear-force devices to make homogeneous solutions for liberating intracellular enzymes. Figure 7.8 shows several types of impeller for homogenisation.

Non-mechanical methods are also used to break down the cell wall and to release intracellular enzymes or proteins. Listed below are several methods that fracture cell walls and release cell content:

- Osmotic shock
- Freezing
- Solvent
- Detergents
- Based on shear forces: high pressure homogeniser
- Manton Gaulin homogeniser works at high pressure, about 550 atm
- Lysis of cells for intracellular products
- Cell wall lysed with organic solvent extraction

7.7 EMERGING TECHNOLOGY FOR CELL RECOVERY

Particulates can be removed from aqueous suspension by attachment to rising air bubbles. This method is known as flotation, which is widely used for recovery of small particles

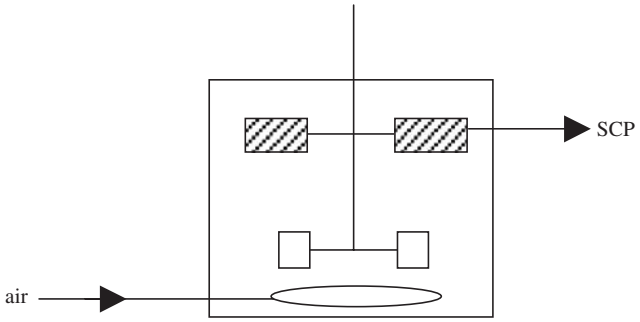

FIG. 7.9. Aeration vessel with foam breaker for SCP production.

from aqueous suspension minerals. This method is used in beer processing. A related technique, for flotation, uses air–water surface tension to strip out proteins from the broth solution and accumulate them in a high protein. English beer is prepared for cell separation by air flotation. Flotation is applied to concentrate *Acinetobacter cerificans* for production of SCP. *Acinetobacter cerificans* is a suitable microorganism used in the production of SCP. The synthesised protein is concentrated by aeration using the flotation method.[7,8] Figure 7.9 shows an aeration vessel with agitation and mechanical foam breakers.

Application of charges and filtration may separate protein very efficiently. Electrokinetic deposition uses voltage gradients of 1050 V/cm to produce solid biomass with densities of up to 40% w/v.

7.8 CELL DISRUPTION

Downstream processing of fermentation broths usually begins with separation of cells by filtration or centrifugation. In centrifugation, a vertical rotor, horizontal rotor or even disc types are used. Sedimentation or coagulation are used in downstream processing. A combination of bioprocesses is required for product recovery. Separation of products such as ethanol, citric acid and antibiotics is extracellular but isolation of enzymes inside the cells requires cell rupture. Cells are broken down by lysis of the cell wall. Cell disruption is used for downstream product recovery. Removal of biomass from the extracted product is necessary. The choice of process such as filtration, batch or continuous, vacuum filtration, cross flow, etc. is based on the nature of the product. Biomass separated from the liquid is discarded or sold as a by-product. For example the products of recombinant proteins, which remain inside the cells, must be ruptured to release the intracellular products. Two categories of well-defined methods for cell rupturing are: mechanical grinding with abrasives, high-speed agitation, high pressure pumping and ultrasound; non-mechanical methods such as osmotic shock, freezing and thawing, enzymatic digestion of cell walls and treatment with solvents and detergents.

A widely used technique for cell disruption is high-pressure homogenisation. Shear forces generated in this treatment are sufficient to completely disrupt many types of cell. A common

type is the Manton–Gaulin homogeniser.[9,10] In this system, a high-pressure pump incorporates an adjustable valve with a restricted orifice through which the cells are forced at a pressure of up to 550 atmospheres. The homogeniser is of general applicability for cell disruption. The homogenising valve can become blocked when used with highly filamentous organisms. Stages involved for product recovery are:

- Lysis of cells for intracellular product recovery
- Extraction of lysed or ground cells
- Removal of unconverted soluble substrate
- Removal of biomass from extracted product
- The choice of filtration (batch, continuous vacuum, cross flow, etc.)
- Centrifuge (vertical rotor, horizontal rotor)
- Sedimentation (and/or coagulation)

The process depends on broth conditions (temperature, pH, ionic strength), medium components and final state of the desired product.

7.9 SOLVENT EXTRACTION

Many antibiotics have excellent solubility in organic solvents and they are water immiscible. A multistage extraction separates the aqueous phase from the organic phase. Extraction can provide concentrated and purified products.

A typical penicillin broth contains 20–35 mg/l of antibiotic. Filtration is used to remove mycelial biomass from fermentation broth. The filtration may be subjected to filter aided polymers. Neutralisation of penicillin at pH 2–3 is required. Amyl acetate or butyl acetate is used as an organic solvent to remove most of the product from the fermentation broth. Finally, penicillin is removed as sodium penicillin and precipitated by a butanol–water mixture.

Extraction of penicillin from the fermentation broth is normally practised using organic solvents such as butyl acetate, amyl acetate methyl isobutyl ketone and methyl ethyl ketone (MEK). Isolation of erythromycin using pentyl or amyl acetate is another example of solvent extraction. For recovery of steroids, solvent extraction is used. Purification of vitamim B_{12} and isolation of alkaloids such as morphine and codeine from raw plant materials are used in solvent extraction methods. Two phases are formed: the separated organic and aqueous phases. Vigorous mixing requires perfect contact of liquid phases and turbulences to facilitate solute transfer from the aqueous phase to the organic phase. However, organic solvents are undesirable for the isolation of proteins. Two phases are produced when a particular polymer plus salt are dissolved in water above certain concentrations. When biomolecules and cell fragments are distributed in the aqueous phase, one phase contains protein and cell fragments are confined to other phase. The extracted phase goes to other unit for precipitation or crystallisation. The partition coefficient ($k = C_{Au}/C_{Al}$) is constant, where C_{Au} is the equilibrium concentration of component "A" in the upper phase and C_{Al} is the equilibrium concentration of "A" in the lower phase. If $k > 1$, component "A" favours the upper phase; if $k < 1$, component "A" favours the lower phase. For effective separation

in a single stage of extraction, $k \geqslant 3$ is required, for low k, a large volume of solute is also required. The yield is defined as the ratio solute extracted over the original amount of solute in the feed:

$$Y_u = \frac{C_{Au}}{V_o C_{Ao}} = \frac{V_u C_{Au}}{V_u C_{Au} + V_l C_{Al}} \tag{7.9.1}$$

where V_o is the original volume, V_u is the upper phase volume, and V_l is the lower phase volume.

7.9.1 Product Recovery by Liquid–Liquid Extraction

Solvent extraction is popular for recovery of fermentation products downstream. Antibiotics are dissolved in an organic solvent, which may be precipitated by converting antibiotic to salt form and separating it from the organic solvents. Simple alcohol (R-OH, CH_3OH, C_2H_5OH), propanol, butanol and ketones are used in pharmaceutical industries. A simple separation funnel to show the two phases are clearly separated is shown in Figure 7.10.

Two sequential stages of extraction with fresh solvent are shown in Figure 7.11.

$$S + F = R + E \tag{7.9.1.1}$$

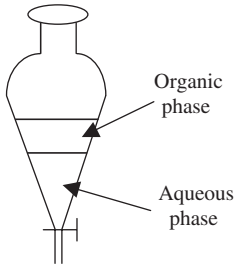

FIG. 7.10. Single-stage extraction in a separation funnel.

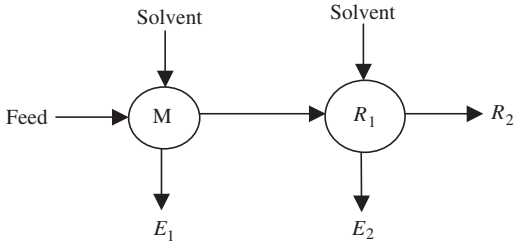

FIG. 7.11. Sequence of single stages of extraction with fresh solvent.

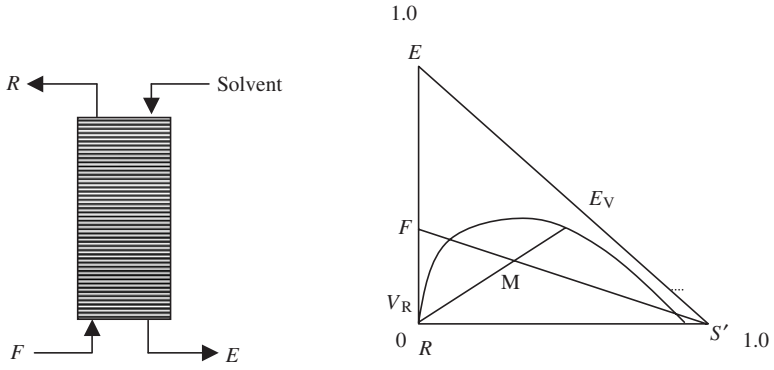

FIG. 7.12. Countercurrent extraction column with material balance in the ternary diagram.

7.9.2 Continuous Extraction Column Process, Rotating Disk Contactors

Organic solvents are used to extract antibiotics. The characteristics of antibiotics and product from extraction processes are summarized below:

- water immiscible
- multistage extraction
- purification, provides highly concentrated products

Stages of the extraction process using fermentation broth for product recovery are listed below:

- 20–35 g/l antibiotic
- filtration: to remove mycelia with addition of polymer to get clear filtrate
- neutralisation: penicillin, pH about 2–3
- solvent extraction: using suitable solvent such as amyl acetate, a salt solution of penicillin is obtained
- precipitation of antibiotics is done with butyl acetate, a isobutyl ketone and mineral ions such as Na^+
- crystallisation: solid product can easily be filtered

Erythromycin is extracted by an organic solvent such as pentyl acetate. Similarly, steroids, vitamin B_{12}, morphine and codeine are extracted with organic solvents.

Counter-current extraction columns are used. Figure 7.12 shows the counter-current extraction column with a ternary diagram for material balance and equilibrium curve.

The mixture of feed and solvent has been identified as the crossing lines of material balance and tie line connecting the desired product in organic and aqueous phases.

$$M = S + F \quad \text{and} \quad M' = \frac{S}{F} \tag{7.9.2.1}$$

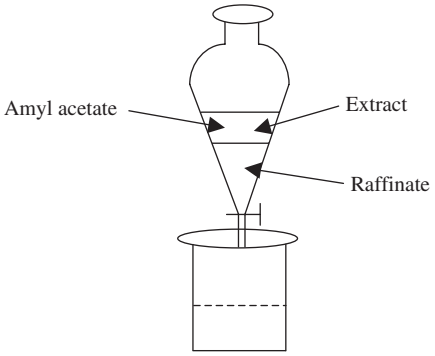

FIG. 7.13. Separation of extract and raffinate layers.

Equilibrium data must be obtained for material balance showing raffinate and extracted phases. A simple separation funnel for single-stage extraction using amyl acetate as organic solvent is shown in Figure 7.13.

The equilibrium constant is defined by K, $K = y/x$, and the portion coefficient is also defined by K as a ratio of C_{Au}/C_{Al} which is constant. Based on the value of K, single or multi-stage extractions are performed to do a perfect job in bioseparation.

Another parameter used to characterise two-phase partitioning is the purification factor, defined as:

$$\delta_c = \frac{\text{Concentration of product in the preferred phase}}{\text{Initial product concentration}} \qquad (7.9.2.2)$$

$\delta_c = C_{Al}/C_{Ao}$, where product is shown in the lower phase and $\delta_c = C_{Au}/C_{Ao}$, where product partitions to the upper phase. When single-stage extraction does not give sufficient recovery, repeated extraction can be carried out in a chain or cascade of contacting and separation units.

7.10 ADSORPTION

In general, adsorption is a surface phenomenon, where gas or liquid is concentrated on the surface of solid particles or fluid interfaces. There are many adsorption systems.

7.10.1 Ion-Exchange Adsorption

Adsorption beds of activated carbon for the purification of citric acid, and adsorption of organic chemicals by charcoal or porous polymers, are good examples of ion-exchange adsorption systems. Synthetic resins such as styrene, divinylbenzene, acrylamide polymers activated carbon are porous media with total surface area of 450–1800 $m^2 \cdot g^{-1}$. There are a few well-known adsorption systems such as isothermal adsorption systems. The best known adsorption model is Langmuir isotherm adsorption.

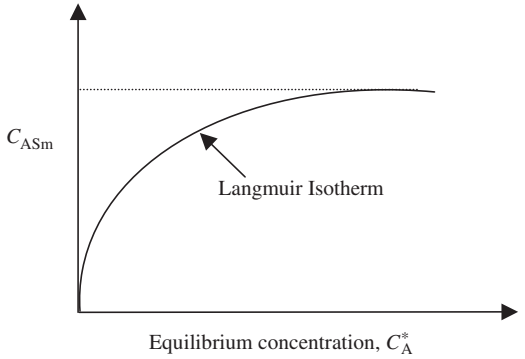

FIG. 7.14. Langmuir isotherm adsorption model.

7.10.2 Langmuir Isotherm Adsorption

Adsorption, like extraction, depends on equilibrium relationships. Isothermal adsorption is projected by Langmuir isotherms. The model is shown in Figure 7.14, which is based on the linear model of the following equation:

$$C_{As}^* = \frac{C_{ASm} k_A C_A^*}{1 + k_A C_A^*} \tag{7.10.2.1}$$

where, C_{As}^* is equilibrium concentration (kg solute/kg solid) and C_{ASm} is the maximum loading of adsobate.

7.10.3 Freundlich Isotherm Adsorption

Another useful model for isothermal adsorption is the Freundlich model, which is presented by the following equation.

$$C_{As}^* = k_F C_A^{*\,1/n} \tag{7.10.3.1}$$

where k_F and n are constants based on the characteristics of the particular adsorption system. If adsorption is favourable, the value of n is greater than 1. For n less than 1, the adsorption process is not favourable.

Figure 7.15 shows the adsorption of ion exchangers, downflow pattern. The bed has an adsorption zone with respect to time and is saturated with solute.

7.10.4 Fixed-Bed Adsorption

Fixed-bed adsorption may give a higher adsorption area per unit volume than any other type of adsorber. The point of saturation of the bed is called the breakthrough point. By knowing this point one can determine operation schedules. In designing fixed-bed adsorbers, the

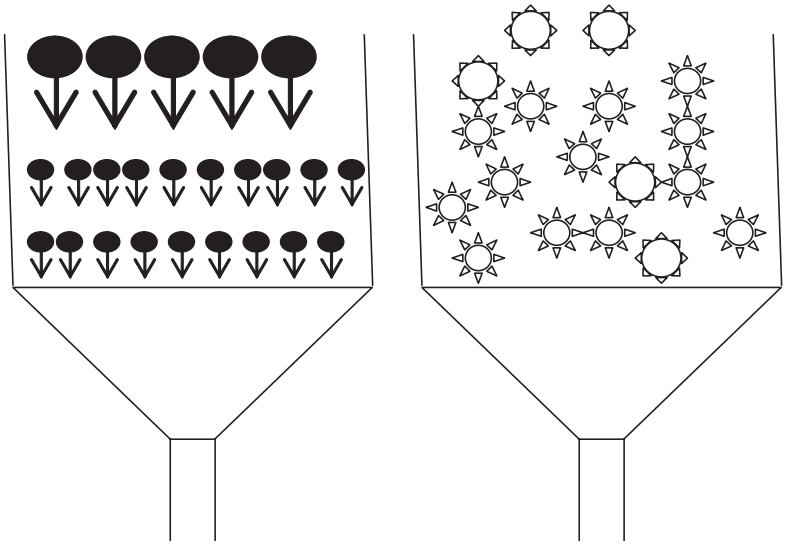

FIG. 7.15. Ion exchange adsorption bed.

quantity of resin and the time required for adsorption of a given quantity of solute must be estimated.

The overall rate of mass transfer from liquid to internal surface is given by

$$\frac{\partial C_{\mathrm{As}}}{\partial t} = \frac{K_L a}{1-\varepsilon}(C_{\mathrm{A}} - C_{\mathrm{A}}^*) \tag{7.10.4.1}$$

where C_{A}^* is the concentration of 'A' at equilibrium, and the void function is defined as a fractional volume, that is the ratio of the empty space volume in the bed and the total volume $\varepsilon = (V_{\mathrm{T}} - V_{\mathrm{S}})/V_{\mathrm{T}}$. V_{T} is the total volume and V_{S} the volume of resin in the packed bed.

7.11 CHROMATOGRAPHY

Chromatography is a separation procedure for resolving mixtures and isolating components. The basis of chromatography is differential migration, and the selective retardation of solute molecules during passage through the bed of resin particles. The fluid carrying the solutes through the column used for elution is known as the mobile phase. The material that stays inside the column and effects the separation is called the stationary phase. In gas chromatography (GC), the mobile phase is a gas. GC is widely used as an analytical tool to separate relatively volatile components. For instance, separation of three solutes from a mixture that is injected into a column would lead to three separate peaks identified by the detectors on the outlet analysis.

Chromatography is a high-resolution technique; therefore the method is suitable for recovery of high-purity therapeutics and pharmaceuticals. Different chromatographic methods are available for purification of proteins, amino acids, nucleic acids, alkaloids, vitamins, steroids and many other biological materials. These methods are adsorption chromatography, partition chromatography, ion-exchange chromatography, gel chromatography and affinity chromatography. These methods differ in the principal mechanism by which the molecules are retarded in the chromatography column. There are several distinct methods of chromatography:

- Adsorption chromatography
- Partition chromatography
- Ion-exchange chromatography such as carboxy methyl cellulose (CMC), agarose and/or dextrins
- Gel chromatography or molecular sieve chromatography such as polyacrylamide gels
- Affinity chromatography, which is the binding of bio-molecules with the matrix bed, often used for antibodies and antigens

In adsorption chromatography, the bed has special characteristics to adsorb solutes. The recommended beds for adsorption chromatography are silica gel, alumina and charcoal.

In ion-exchange chromatography agarose, dextrose and carboxy methyl cellulose (CMC) are used as the media beds for separation. In gel chromatography the bed is mainly molecular sieves such as polyacrylamide gels. In affinity chromatography, the separating bed is a binding biomolecular matrix which is able to attract antibodies or antigen, so there is good affinity for separating the product. The capacity of the column is given by:

$$k = \frac{V_e - V_o}{V_o} \tag{7.11.1}$$

where k is known as the capacity of the column, and the solvent volume for eluting the bed is defined with V_e; also V_o is the void volume, the free volume, outside of the bed particles; V_i is known as internal volume of liquid in the pores of the particles; and V_s is the volume of the gel itself. The relative retention, δ, is the ratio of two capacities known as selectivity. The total volume of the gel column is:

$$V_{total} = V_o + V_i + V_s$$
$$V_e = V_o + k_p V_i$$

where V_e is the volume of eluting solvent, V_o is the void volume outside the particles, V_i is the internal volume of liquid in the pores of the particles, and V_s is the volume of the gel itself.

The relative retention is $\delta = k_2/k_1$; k_1 and k_2 are called selectivity, and k_p is the gel partition coefficient, $k_P = (V_e - V_o)/V_i$, where V_i is the multiplication of mass of dry gel, 'a' with W_r.

$$V_i = aW_r = \frac{W_r \rho_g}{1 + W_r \rho_w}(V_T - V_o) \tag{7.11.2}$$

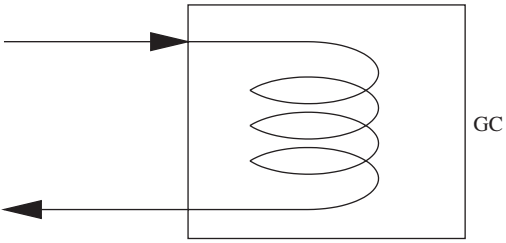

FIG. 7.16. GC column in an insulated box.

where W_r is the water regain value that is the volume of water taken up per mass of dry gel, ρ_g is the density of wet gel, and ρ_w is the density of water.

7.11.1 Principle of Chromatography

The basis of chromatography is in the differential migration of chemicals injected into a column. The carrier fluid takes the solutes through the bed used for elution (mobile phase). The bed is the stationary phase. Based on mobility, the retention-time detectors identify the fast and slow-moving molecules. Based on internal or external standards with defined concentration, all unknown molecules are calculated in a developed method by software. GC columns are installed in an oven which operates at a specified temperature. A diagram of an oven with GC column is shown in Figure 7.16.

Example 1

A 30 ml sample of broth from penicillin fermentation is filtered in the laboratory on a 3 cm^2 filter at a pressure drop of 5 psi. The filtration time is 4.5 minutes. Previous studies have shown that the filter cake of *Penicillium chrysogenum* is significantly compressible with $S = 0.5$. If 500 litres of fermentation broth from a pilot plant have to be filtered in 1 hour, what size of filter is required for a pressure drop of 10 psi and 5 psi? Neglect the resistance of the filter medium.

Solution

Since the filter resistance in the filter medium is neglected, the second part of equation (7.3.1.5) is neglected. Let us define a new constant, C, equal to the mass of solid deposited on the filter per volume of filtrate.

$$C = \frac{\rho\omega}{1 - m\omega} \tag{E.1.1}$$

Equation (7.3.1.5) was modified as the second part is neglected, so the filtration time per unit volume is:

$$\frac{t}{V_f} = \frac{\mu_c \alpha \rho \omega}{2\Delta P(1-m\omega)} \frac{V_f}{A^2} \tag{E.1.2}$$

The obtained equation is written with respect to pressure drop:

$$\frac{t}{V_f} = \frac{\mu_e \alpha' \Delta P^{S-1} c}{2A^2} \tag{E.1.3}$$

The area for a laboratory-scale filter is calculated by:

$$\begin{aligned}\mu_e \alpha' c &= \frac{2A^2 t}{(\Delta P)^{S-1} V_f^{\,2}} \\ &= \frac{2(3\ \text{cm}^2)^2 (4.5\ \text{min})}{(5\ \text{psi})^{0.5-1} (30\ \text{cm}^3)^2} \\ &= 0.20125 \frac{(\text{psi})^{0.5}\,\text{min}}{\text{cm}^2}\end{aligned}$$

The area for a pilot-scale filter is obtained by:

$$\begin{aligned}A^2 &= \frac{\mu_e \alpha' c (\Delta P)^{S-1} V_f^{\,2}}{2t} \\ &= \frac{(0.20125)(10)^{0.5-1} (500{,}000\ \text{cm}^3)^2}{120\ \text{min}} \\ &= 1.15 \times 10^4\ \text{cm}^2 \quad \text{or} \quad 1.15\ \text{m}^2\end{aligned}$$

The value for area A^2 is:

$$\begin{aligned}&\frac{(0.20125)(5)^{0.5-1} (500{,}000\ \text{cm}^3)^2}{120\ \text{min}} \\ &= 1.37\ \text{m}^2\end{aligned}$$

For a pressure drop of 5 psi the filter area is:

$$\begin{aligned}A^2 &= \frac{0.2(10)^{0.5-1} (500{,}000\ \text{cm}^3)^2}{120\ \text{min}} \\ A &= 1.37\ \text{m}^2\end{aligned}$$

Having a differential pressure in the above filtration process, and reducing the pressure drop from 10 to 5 psi, increases the filter area by 19%. The main reasons why an increase in the pressure drop results in less filter area are the compressed cake and the porosity of the filter cake.

Example 2

Filtration of 300 ml of fermentation broth was carried out in a laboratory-sized filter with a pressure drop of 10 psi. The filtration took 20 min. Based on previous studies, the filter cake obtained from *Penicillium chrysogenum* was compressible with the exponent '*s*' in the equation for calculation of filter area equal to 0.5.

(a) What size of filter is required to carry out filtration of 1 m^3 broth from a pilot plant in 20 hours and at a pressure drop of 20 psi?
(b) What is the percentage increase in filter area if the pressure drop is reduced to 10 psi?

Solution

$$\frac{t}{V_f} = \frac{\mu\alpha c}{2A^2\Delta P}\cdot V_f = \frac{\mu\alpha' c\Delta P^{S-1}}{2A^2}\cdot V_f$$

$$\alpha = \alpha'\Delta P^S$$

$$\mu\alpha' c = \frac{2A^2 t}{(\Delta P)^{S-1}V_f^2} = \frac{2(10)^2(20)}{(10)^{0.5-1}(300)^2} = 0.1405$$

$$A = \left[\frac{(\mu\alpha' c)\Delta P^{-0.5}V_f^2}{2t}\right]^{1/2} = \left[\frac{(\mu\alpha' c)\Delta P^{-0.5}}{2t}\right]^{1/2} V_f$$
$$= \left[\frac{0.1405(20)^{-0.5}}{2\times 2\times 60}\right]^{1/2} (10^6\,\text{cm}^3) = 1.14\times 10^4\,\text{cm}^2 = 1.14\ \text{m}^2$$

$$\frac{A_1}{A_2} = \left[\left(\frac{\Delta P_1}{\Delta P_2}\right)^{-0.5}\right]^{1/2} = \left(\frac{1}{2}\right)^{-0.25} = 1.189 \qquad \text{(E.2.1)}$$

An 18.9% increase in the area of filter was obtained.

$$\frac{A_1}{A_2} = \frac{(\mu\alpha' c/2t)_1^{0.5}\left[(20)^{-0.5}\right]^{1/2}}{(\mu\alpha' c/2t)_2^{0.5}\left[(20)^{-0.5}\right]^{1/2}} = \frac{0.473}{0.56} = 0.84$$

$$A_2 = \frac{A_1}{0.84} = \frac{1.14}{0.84} = 1.356\ \text{m}^2 \qquad \text{(E.2.2)}$$

The ratio of $\frac{A_2}{A_1} = \frac{1.356}{1.14} = 1.189$, which is approximately a 19% in filter surface area.

Example 3

In a batch production of penicillin, 40 m^3 capacity of the plant, sterile air is required to be supplied. The bioreactor requires 1 vvm (volume of air/volume of broth. min). The incoming air contains 3000 cells/m^3 of air, for 100 hours operation. Calculate the depth of filter, if the penetration of bacteria is 1 in 1 million.

Solution

Assume $D_{\text{filter}} = 60$ cm, based on availability of filter
Air flow rate, $F_{\text{air}} = (40\ \text{m}^3)(1\ \text{vvm})(60\ \text{min}\cdot\text{h}^{-1}) = 2400\ \text{m}^3\cdot\text{h}^{-1}$
Microbial load = $(3000\ \text{cells/m}^3)(2400) = 7.2 \times 10^8$ cells
Cross sectional area of filter, $A = (\pi/4)(0.6)^2 = 0.028\ \text{m}^2$
Air velocity = (2400)/(0.028) = 8488 m/h

$N_t = N_o\ e^{-kt}$, (E.3.1)

$\ln(N_1/N_2) = kL$ (E.3.2)

$\ln[(7.2 \times 10^8)/(10^{-6})] = kL$
$N_1 = 7.2 \times 10^8$ cells,
$N_2 = 1$ cell in 10^6 cells $= 10^{-6}$ cells
L represents the length of filter, and k is the rate constant based on filter bed material = 84
$L = (1/k)\ \ln 7.2 \times 10^{14} = (1/84)\ \ln 7.2 \times 10^{14} = 0.4$ m.

Example 4

Microbial cells are separated from a culture broth at a flow rate of $3.35 \times 10^{-3}\ \text{m}^3/\text{s}$. Assume the cells are spherical with average diameter of 1 μm. Select a centrifuge that can perform this separation. Given data: $\rho_{\text{cell}} = 1.1\ \rho_{\text{water}}$, $\rho_{\text{water}} = 997\ \text{kg}\cdot\text{m}^{-1}$ at 25 °C; $\rho_{\text{broth}} = 3\rho_{\text{water}}$, and the viscosity of water is $0.9 \times 10^{-3}\ \text{N}\cdot\text{s/m}^2$.

Solution

$$Z = \frac{\omega^2 r}{g} \qquad \text{(E.4.1)}$$

$$u_c = \left(\frac{\rho_p - \rho_f}{18\mu}\right) D_p^2 \omega^2 r = Zu \tag{E.4.2}$$

$$x = u_c t = Zu_g \left(\frac{V}{F}\right) \tag{E.4.3}$$

$$\frac{VZ}{x} = \frac{F}{u_g} = S$$

$$S = \frac{F}{u_g} = \frac{F(18\mu)}{D_p^2(\rho_{cell} - \rho_{water})}$$

$$S = \frac{(3.35\times10^{-3}\ \mathrm{m^3/s})(18\times0.9\times10^{-3}\times3\ \mathrm{N\cdot s/m^2})\left(\frac{\mathrm{kg-m/s^2}}{\mathrm{N}}\right)}{(1\times10^{-6}\ \mathrm{m})^2(1.1-1)(997\ \mathrm{kg/m^3})(9.81\ \mathrm{m/s^2})} = 1.65\times10^5\ \mathrm{m^2}$$

$$S = 2\Sigma$$

$$\Sigma = 83250\ \mathrm{m^2} \tag{E.4.4}$$

Example 5

Microbial cell recovery is carried out in a continuous disc-stack centrifuge. The centrifuge is operated at 5000 rpm for separation of baker's yeast. At a feed rate of 60 l/min, 50% of the cells are recovered. At constant speed, solid recovery is inversely proportional to flow rate.

(a) What flow rate is required to recover 90% of cells if the centrifuge speed is fixed at 5000 rpm?
(b) What operating speed is required to recover 90% of cells if the flow rate in the centrifuge is maintained at 60 l/min?

Solution

$$\frac{S_1\%}{S_2\%} = \frac{Q_2}{Q_1}$$

$$\frac{50}{90} = \frac{Q_2}{60},\ Q_2 = 33.33\ \mathrm{l/min}$$

$$\frac{Q_2}{Q_1}\frac{\Sigma_2}{\Sigma_1} = \frac{\omega_2^2}{\omega_1^2} = \frac{(5000)^2}{\omega_1^2} = \frac{60}{33.33}$$

$$\omega_2 = 6708\ \mathrm{rpm} \tag{E.5.1}$$

When we need to remove cells from fermentation broth, sedimentation is considered as a downstream processing method. Alum, lime, polyelectrolyte are commonly used.

Example 6: Enzyme Recovery Using Aqueous Extraction

Extraction for enzyme recovery is a common process. Polyethylene glycol-dextran mixture is used to recover α-amylase from fermentation broth. Given a partition coefficient of 4.2, calculate the maximum enzyme recovery when

$$\text{(a)} \quad \frac{V_u}{V_l} = 5$$

$$\text{(b)} \quad \frac{V_u}{V_l} = 0.5 \tag{E.6.1}$$

Solution

$$Y_u = \frac{V_u C_{Au}}{V_u C_{Au} + V_l C_{Al}} = \frac{V_u}{V_u + V_l (C_{Al}/C_{Au})} = \frac{V_u}{V_u + (V_l/K)} \tag{E.6.2}$$

$$\text{define} \quad K = \frac{C_{Au}}{C_{Al}}$$

$$\text{(a)} \quad Y_u = \frac{V_u/V_l}{\frac{V_u}{V_l} + \frac{1}{K}} = \frac{5}{5 + \frac{1}{4.2}} = 0.95 \quad \text{or 95\% yield}$$

$$\text{(b)} \quad Y_u = \frac{0.5}{0.5 + \frac{1}{4.2}} = 0.68, \quad \text{68\% yield for a lower value of upper phase volume}$$

Increase in the relative volume of the extracting phase enhanced the recovery.

Example 7: Antibody Recovery by the Adsorption Method

Cell-free fermentation broth contains 8×10^{-5} mol/l immunoglobulin C. Ninety per cent of antibody is recovered by adsorption on non-polar resin.

$$\text{Given} \quad C^*_{As} = 5.5 \times 10^{-5} C^{*\,0.35}_{A} \tag{E.7.1}$$

where C^*_{AS} is solute adsorbed/cm^3 and C^*_A is the liquid phase solute concentration in mol/l. What minimum quantity of resin is required to treat 2 m^3 of broth in a single-stage tank?

Solution

The minimum quantity of resin required when equilibrium occurs for 90% recovery. The rest is $0.1 \times 8 \times 10^{-5} = 8 \times 10^{-6}$ mol/l $= C_A^*$

$$\begin{aligned} C_{As}^* &= 5.5\times10^{-5}(8\times10^{-6})^{0.35} \\ &= 9.05\times10^{-7}\ \text{mol}/\text{cm}^3 \ \leftarrow\ \text{resin capacity} \end{aligned} \tag{E.7.2}$$

Amount of antibody adsorbed is

$$0.9(8\times10^{-5}\ \text{mol/l})(2\ \text{m}^3\times1000\,\text{l/m}^3) = 1.44\times10^{-1}\ \text{mol} \tag{E.7.3}$$

The volume of resin required is

$$\frac{0.144\ \text{mol}}{9.05\times10^{-7}\text{mol/cm}^3} = 1.59\times10^5\ \text{cm}^3 \approx 0.16\,\text{m}^3\ \text{resin required} \tag{E.7.4}$$

Example 8

Gel chromatography is used for hormone separation. A pilot-plant scale gel chromatography column packed with sephacryl resin is used to separate two hormones, A and B. The column is 5 cm in diameter and 30 cm in height; $V_o = 1.9 \times 10^{-4}\,\text{m}^3$, $\omega_r = 3 \times 10^{-3}\,\text{m}^3/\text{kg}$ dry sephacryl, $\rho_g = 1.25 \times 10^3$ kg/m^3. The partition coefficients are $k_{PA} = 0.38$ and $k_{PB} = 0.15$. If the eluting flow rate is 0.7 l/h, what is the retention time for each hormone?

Solution

$$V_T = \pi^2 h = \pi(2.5\times10^{-2}\text{m}^2)(0.3\ \text{m}) = 0.89\times10^{-8}\text{m}^3$$

$$V_i = \frac{(3\times10^{-3}\text{m}^3/\text{kg})(1.25\times10^3\text{kg/m}^3)}{1+(3\times10^{-3})(1000)}\times(5.89\times10^{-8} - 1.9\times10^{-4}) = 3.74\times10^{-4}\text{m}^3$$

$$V_{eA} = V_o + k_{PA}V_i = 1.94\times10^{-4} + 0.38(3.74\times10^{-4}) = 3.32\times10^{-4}\text{m}^3$$

$$V_{eB} = V_o + k_{PB}V_i = 1.94\times10^{-4} + 0.15(3.74\times10^{-4}) = 2.46\times10^{-4}\text{m}^3$$

$$\tau_A = \frac{3.32\times10^{-4}\text{m}^3}{(0.7\ \text{l/h})\left(\dfrac{\text{m}^3}{1000\ \text{L}}\right)\left(\dfrac{\text{h}}{60\ \text{min}}\right)} = 28\ \text{min}$$

$$\tau_B = \frac{2.46\times10^{-4}\text{m}^3}{(0.7\ \text{l/h})\left(\dfrac{\text{m}^3}{1000\ \text{L}}\right)\left(\dfrac{\text{h}}{60\ \text{min}}\right)} = 21\ \text{min} \tag{E.8.1}$$

Example 9: Cell Filtration of Fermentation Broth

A shake-flask broth was filtered with a filtration unit and all the process conditions and variables are defined in the following table.

Process variables	Values
Filter area, A	10 cm^2
Viscosity, μ_c	2 cp
Pressure drop, ΔP	0.3 atm
Density, ρ	1.1 g/cm^3
Solid mass fraction, ω	0.001
Ratio of masses of wet cake over dry cake, m	2.5

(a) Evaluate the specific cake concentration, α, and the resistance coefficient, r, of the filter, for two different filtration times and volumes of filtration solution [$t(s)$, V(ml)] = [(30, 38), (60, 52)].
(b) What size filter would be needed to process 100 m^3 broth in 10 min?

Solution

(a) Using the filtration equation (7.3.1.7)

$$\frac{t}{(V_f/A)} = \frac{\mu_c \alpha \rho V_f w}{2\Delta P(1-mw)A} + \frac{\mu_c r}{\Delta P}$$

$$\frac{t}{(V_f/10\ \text{cm}^2)} = \frac{(2\times10^{-2}\ \text{g/cm}\cdot\text{s})(\alpha)(1.1)(0.001)V_f}{2(0.3\ \text{atm})(1-2.5\times0.001)(10\ \text{cm}^2)} + \frac{(2\times10^{-2}\ \text{g/cm}\cdot\text{s})r}{(0.3\ \text{atm})}$$

$$\frac{t}{V_f} = \frac{2.2\times10^{-7}}{0.5985}\times V_f\alpha + 6.67\times10^{-3}r$$

$$\frac{30}{38} = 0.79 = 1.4\times10^{-5}\alpha + 6.67\times10^{-3}r$$

$$\Rightarrow \alpha = 7\times10^4\ \frac{\text{atm}\cdot\text{s}^2\cdot\text{cm}^2}{\text{g}^2}$$

$$\Rightarrow r = -\frac{0.187}{6.67}\times10^3$$

$$\frac{60}{52} = 1.15 = 1.91\times10^{-5}\alpha + 6.67\times10^{-3}r \qquad \text{(E.9.1)}$$

(b) Scale-up calculation:

$$\frac{t}{V_f}A = \frac{\mu_c \alpha \rho V_f w}{2\Delta P(1-mw)A} + \frac{\mu_c r}{\Delta P}$$

$$\frac{600\ \text{s}}{(10^5 \times 10^3\ \text{cm}^3)}A = \frac{2\times10^{-2}\times7\times10^4\times1.1\times0.001\times10^8}{2(0.3)(1-2.5\times0.001)A} + \frac{(2\times10^{-2})}{(0.3)}\times\frac{187}{20/3}$$

$$A = 1.8\times10^6\,\text{cm}^2 = 180\ \text{m}^2 \qquad \text{(E.9.2)}$$

7.12 NOMENCLATURE

r_m	Filter media resistance
α	Average specific cake resistance
m	Ratio of mass of wet cake over mass of dry cake
ϖ	Solid mass fraction.
A	Filter area, m^2
V_f	Volume of filtrate, ml
t	Filtration time, min
ΔP	pressure drop across the filter, Pa
μ_c	Fluid viscosity, cP
W	Mass of solids in the filter cake, kg
u_h	Hindered settling particles, m/s
u_o	Particles velocity, m/s
ϵ_p	Volume fraction of particles
u_g	Sedimentation velocity, m/s
u_c	Particle velocity in the centrifuge, m/s
ρ_p	Density of particle, $kg\cdot m^{-3}$
ρ_f	Density of fluid, $kg\cdot m^{-3}$
μ	Viscosity of fluid, cP
D_p	Diameter of solid particle, mm
g	Gravitational acceleration, $m\cdot s^{-2}$
ω	Angular velocity of the bowl, rad/s
Q	Volumetric flow rate, $ml\cdot h^{-1}$
u_g	Terminal velocity of the particles, m/s
Σ	Performance of centrifuge, sigma factor
N	Number of discs in stacks of centrifuge
r_1, r_2	Inner and outer radius of the discs, cm
θ	Half of the cone angel of the disc
C^*_{AS}	Equilibrium concentration (kg solute/kg solid)
C_{ASm}	Maximum loading of adsorbate, $g\cdot l^{-1}$
C_{Au}	Equilibrium concentration of A in upper phase, $g\cdot l^{-1}$
C_{Al}	Equilibrium concentration of A in lower phase, $g\cdot l^{-1}$

V_o Original volume, ml
V_u Upper phase volume, ml
V_l Lower phase volume, ml
W_r Water regain value, g
ρ_g Density of wet gel, $kg \cdot m^{-3}$
ρ_w Density of water, $kg \cdot m^{-3}$
V_T Total volume, m^3
V_S Volume of resin, m^3
C_A^* Concentration of A at equilibrium, $g \cdot l^{-1}$

REFERENCES

1. Aiba S., Humphrey, A.E. and Millis, N.F., "Biochemical Engineering", 2nd edn. Academic Press, New York, 1973.
2. Baily, J.E. and Ollis, D.F., "Biochemical Engineering Fundamentals", 2nd edn. McGraw-Hill, New York, 1986.
3. Bradford, M.M., *Analyt. Biochem.* **72**, 248 (1976).
4. Doran, P.M., "Bioprocess Engineering Principles". Academic Press, New York, 1995.
5. Dominguez, M., Mejia, A. and Gonzalez, J.B., *J. Biosci. Bioengng* **89**, 409 (2000).
6. Najafpour, G.D., Klasson, K.T., Ackerson, M.D., Clausen, E.C. and Gaddy, J.L., *Biores. Technol.* **48**, 65 (1994).
7. Driessen, F.M., Ubbels, J. and Stadhouders, J. *Biotech. Bioengng* **19**, 821 (1977).
8. Stanbury P.F. and Whitaker, A., "Principles of Fermentation Technology". Pergamon Press, Oxford, 1984.
9. Shuler, M.L. and Kargi, F., "Bioprocess Engineering, Basic Concepts". Prentice Hall, New Jersey, 1992.
10. Pelczar, M.J. Jr, Chan, E.C.S. and Krieg N.R., "Microbiology", 6th edn. McGraw-Hill, New York, 1993.

CHAPTER 8

Immobilisation of Microbial Cells for the Production of Organic Acid and Ethanol

8.1 INTRODUCTION

Microorganisms are biocatalysts actively used in the fermentation process where product and biomass are obtained from fermentable sugars. The cells are harvested and reused. The immobilisation of cells has been practised in the production of vinegar. Enzymes and whole cells can be bound to solid support, fixed in the form of an active layer. When substrate passes over the surface, enzymatic reactions change the substrate to the desired product. Enzymes and suitable microorganisms are used in manufacturing food flavours, additives, medicines, and other goods are produced by variety of microbial metabolites. Immobilised cells may perform differently to an equivalent mass of freely suspended cells.[1] They may produce extracellular polymers, which are usually lumped together with cells in dry biomass measurements, resulting in overestimation of the activity of immobilised biomass.[2] In addition, cell location in the form of biofilm can affect its quality and activity, because profiles of environmental conditions such as effect of substrate concentration often exit. However, in many studies results for freely suspended cultures have been used to model immobilised cell bioreactors, usually without a lot of attention in assessing the quality of the biomass in the system. Typically these models allow for the effect of difficult limitations in and around the biofilm, and assume that the immobilised cells have the same quality and activity as the suspended cell culture, regardless of the position in the biofilm.

In fact, significant substrate concentration gradients may exist for cells immobilised in biofilm. Cells located close to the nutrient supply are likely to maintain higher quality and activity compared with cells located relatively further away, leading to differentiation in the quality or activity of the immobilised cell population. This differentiation is more pronounced if there are starvation regions. In practice, zero substrate concentration may exist inside the biofilm, because in these regions the cell physiology may be markedly different from that of the freely suspended cells.

The cells' activities have been described based on a multi-species biofilm model, and the microbial kinetics by a mathematical model. Using this model predicts that the biomass on the external surface of the biofilm has higher activity than the biomass near the solid support surface, and that condition may occur, after the biofilm has reached a critical dept or formed

a thick multi-layers of the biofilm. The model was based on microbial growth kinetics determined by Wang *et al.*[2] However, no experimental results were presented in either of the immobilization studies to verify the model predictions, nor was the predicted immobilised biomass activity compared with that of freely suspended cells in a comprehensive way.

Wang *et al.*[2] and Najafpour *et al.*[3,4] worked with immobilised microbial cells of *Nitrobacer agilis, Saccharomyces cerevisiae* and *Pseudomonas aeruginosa* in gel beads, respectively. They found separately that the cells retained more than 90% of their activity after immobilisation by using specific oxygen uptake rate (SOUR) [mg $O_2 \cdot g^{-1}$ (dry biomass) h^{-1}] as the biomass activity indicator. Such differences in immobilised biomass and activity between free and immobilised biomass activities depend strongly on the particular characteristics of the microbial systems and their interaction with the support matrix.

8.2 IMMOBILISED MICROBIAL CELLS

Since 1978, several papers have examined the potential of using immobilised cells in fuel production. Microbial cells are used advantageously for industrial purposes, such as *Escherichia coli* for the continuous production of L-aspartic acid from ammonium furmarate.[5,6] Enzymes from microorganisms are classified as extracellular and intracellular. If whole microbial cells can be immobilised directly, procedures for extraction and purification can be omitted and the loss of intracellular enzyme activity can be kept to a minimum. Whole cells are used as a solid catalyst when they are immobilised onto a solid support.

There are three general methods available for the immobilisation of whole microbial cells: carrier binding, entrapment and cross-linking.

8.2.1 Carrier Binding

As shown in Figure 8.1a, the carrier binding method is based on binding microbial cells directly to water-insoluble carriers. The binding is due to ionic forces between the microbial cells and the water-insoluble carriers. This technique has rarely been used, however, because of lyses during the enzyme reactions. Microbial cells may leak from the carrier, thereby disrupting the immobilisation. Therefore, this method has not been applied successfully.[6]

8.2.2 Entrapping

In applying entrapment, microbial cells are directly entrapped into polymer matrices (Figure 8.1b). This method has been applied to several microorganism by using gelatin, agar, polyacrylamide gel, calcium alginate, etc., as the entrapping agents. The following matrices are used extensively to immobilise microbial cells:

- Collagen.
- Gelatin.
- Agar.
- Alginate.
- Carrageenan.

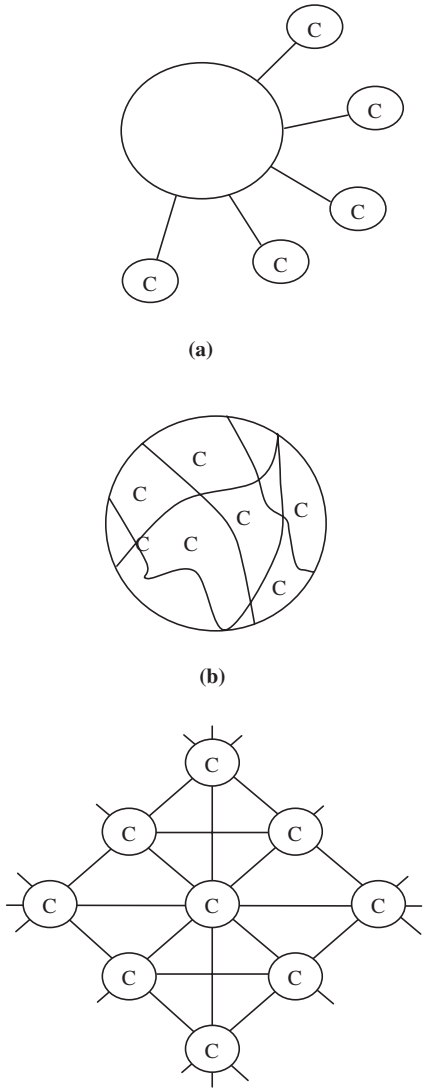

FIG. 8.1. Alternatives methods used to immobilise cells. (a) Carrier binding; (b) entrapment; (c) cross-linking.[3]

- Cellulose triacetate.
- Polyacrylamide.
- Polystyrene.

In this method, microbial cells are apparently lysed within the entrapping agent, but they retain the desired enzymatic activity. To prepare an efficient immobilisation, the type and

concentration of a bifunctional reagent for entrapment should be optimised. The advantage of this method is that cell leakage may act as a diffusion barrier, thus causing difficulty in transferring substrate and product through the matrix.[4,7,8]

8.2.3 Cross-Linking

Microbial cells immobilised by cross-linking with bi- or multifunctional reagents such as glutaraldehyde have been reported to be successful, but active immobilisations have not been obtained with other reagents such as toluenediisocyanate.[7] The microbial cell wall is composed of lipoproteins, with lipopolysaccharide extending from the cell membrane. Glutaraldehyde reacts with lysine within the protein in the lipid bilayer of the cell membrane. Furthermore, gelatin is physically absorbed on a solid support, which provides a covalent link between the microbial cells which is tightly bound to a solid support by absorption (Figure 8.1c).

Glutaraldehyde has been used as cross-linking reagent for ethanol production. Maximum achieving rates was reported as high as $7.4\ g \cdot l^{-1} \cdot h^{-1}$ ethanol produced from glucose.[9] The major advantage of the cross-linking method is that the immobilisation reagent does not act as diffusion barrier. Actually, a thin film of cells is provided in this system, making it ideal for many applications.[10,11]

8.2.4 Advantages and Disadvantages of Immobilised Cells

There are several advantages of an immobilised cell system over a batch or CSTR system. The first and most obvious benefit is the capability of recycling or reusing the microorganisms since they are retained inside the reactor as the product leaves the reactor. Secondly, immobilisation can be easily used for a continuous process maintaining high cell density, thus providing a high productivity.[12]

Thirdly, nutrient depletion and any inhibitory compounds do not, in general, have a large effect on the immobilised cells because the cells are fixed by immobilisation. In batch and CSTR fermentation, nutrient depletion, inhibition and accumulation of toxic by-products are major problems, but immobilised cells are usually unaffected by toxic by-products.

However, there are disadvantages to using immobilised cells. The cell may contain numerous catalytically active enzymes, which may catalyse unwanted side reactions. Also, the cell membrane itself may serve as a diffusion barrier, and may reduce productivity. The matrix may sharply reduce productivity if the microorganism is sensitive to product inhibition. One of the disadvantages of immobilised cell reactors is that the physiological state of the microorganism cannot be controlled.

8.3 IMMOBILISED CELL REACTOR EXPERIMENTS

The immobilised cell reactor (ICR) experiments were undertaken to determine the performance of immobilised *Propionibacterium acidipropionici* in a plug-flow tubular reactor. The

productivity of the ICR was evaluated by measuring glucose and xylose consumption, and propionic and acetic acid production, along the length of the reactor.[3]

The Rasching rings were sterilised and dip-coated in sterile 20% gelatin and 1.5% agar solution. The coated rings were randomly packed in the column. After the coated rings had dried, the packing was sprayed with a 2.5% glutaraldehyde solution. An alternative procedure to prepare the packing was also tested and proved to be satisfactory. In using the latter method, the reactor column was filled with clean Rasching rings. A hot gelatin agar solution was passed through the column, and allowed to wet the entire packing surface. When the coating was dried, the glutaraldehyde solution was passed through the column in a similar fashion. The column was allowed to stand for 24 hours and then washed with sterile, distilled water. The reactor was sterilised by passing ethylene oxide through the column. The ethylene oxide was allowed to stand in the column for eight hours before the system was purged with sterile nitrogen. The feed and product tubing were autoclaved by using steam at 15 psig.

After sterilisation a 24-hour-old seed culture was pumped through the column. An adaptation time of about 48 hours was allowed for the establishment of a film of microorganisms cross-linking to the Rashing rings. Feed media was then pumped into the reactor. An accurate calculation of the retention times in the reactor was difficult, owing to the fact that growth and carbon dioxide evolution may take a major fraction of void volume of the ICR, resulting in a false retention time. The microbial film thickness could be controlled by periodically passing sterile nitrogen or carbon dioxide through the column, to stop cell overgrowth.

A feed concentration of 15 g glucose and 15 g xylose per litre was used over a feed rate of 20–200 ml/hr. Samples were taken at successive points along the reactor length, and the usual analysis for glucose and xylose consumption, organic acid production and cell density were done. A kinetic model for the growth and fermentation of *P. acidipropionici* was obtained from these data.

Analytical procedures were set up to measure cell density, sugar concentration and organic acid concentration. The turbidity of the culture (optical density) was determined by reading the absorbance with spectrophotometer and cell counts. Sugar concentration as a single substrate was measured by an industrial digital analyser. Total sugar was evaluated by a reducing agent such as dinitrosalicylic acid in alkaline solution. An orange colour was produced which was read on a colourimeter at 540 nm. Organic acids were determined by a gas chromatograph, with a flame ionisation detector.

8.4 ICR RATE MODEL

Table 8.1 presents the results of the ICR retention time studies, sugar concentration (dual substrate) studies and cell density. The kinetic model for ICR was derived on the basis of a first order reaction, plug flow and steady-state behaviour.

$$r_A = kC_A \tag{8.4.1}$$

TABLE 8.1. *Continuous fermentation of dual substrate (glucose, xylose) in ICR at 36 °C*

Retention time (h)	Length of reactor (inches)	Substrate concentration ($g \cdot l^{-1}$)		Organic acid concentration ($g \cdot l^{-1}$)		Reaction rate of glucose ($g \cdot l^{-1} \cdot h^{-1}$)	Cell density (number of cells/ml)
		Glucose	Xylose	Propionic acid	Acetic acid		
28	0	15	15	—	—		
	6	6.28	10	1.3	7.78	0.31	9×10^{11}
	14	4.52	8.6	1.98	8.45	0.37	9×10^{11}
	24	2.13	7.2	2.7	12.4	0.46	9×10^{11}
	34	1.36	5.4	3.25	17.2	0.49	9×10^{11}
	44	1.14	3	3.95	19.1	0.495	9×10^{11}
20	0	15	15	—	—		
	6	7.1	11	1.2	6.45	0.395	9×10^{11}
	14	4.72	9.8	1.46	8.1	0.514	9.5×10^{11}
	24	2.21	7.9	1.87	12	0.64	9.5×10^{11}
	34	1.5	7.15	2.12	16.4	0.675	9.5×10^{11}
	44	1.2	5.8	2.4	18	0.69	9.5×10^{11}
12	0	15	15	—	—		
	6	9.3	14.5	2.59	1.33	0.475	1×10^{10}
	14	6.02	14	3.26	2.37	0.75	2×10^{10}
	24	3.62	13	4.5	2.45	0.95	3×10^{11}
	34	2.65	12	5.07	2.5	1.03	3×10^{11}
	44	2.3	10	5.36	2.54	1.06	5×10^{11}
5	0	15	15	—	—		
	6	9.8	15	0.5	0.58	1.04	6×10^{10}
	14	7.27	14.5	0.6	0.76	1.55	1.8×10^{10}
	24	6.05	14	0.65	1.2	1.79	5×10^{10}
	34	5.84	14	0.7	1.36	1.83	5×10^{10}
	44	5.2	13.5	0.8	1.65	1.96	6×10^{10}

$$u\frac{dC_A}{dz} = r_A \tag{8.4.2}$$

where r_A is the reaction rate, k is the rate constant, C_A is the sugar concentration, z is the axial reactor length, and u is the bulk fluid velocity. Substituting (8.4.1) into (8.4.2) yields

$$u\frac{dC_A}{dz} = kC_A \tag{8.4.3}$$

Equation (8.4.3) is a linear first-order differential equation of concentration and reactor length. Using the separation of variables technique to integrate (8.4.3) yields

$$\ln\left(\frac{C_A}{C_{A_o}}\right) = \frac{kz}{u} \tag{8.4.4}$$

Figure 8.2 shows a plot of $\ln C_A / C_{A_o}$ as a function of dimensionless reactor length for the fermentation data obtained at a feed concentration of $15\,g\cdot l^{-1}$ glucose and $15\,g\cdot l^{-1}$ xylose at different retention times. A straight line is obtained at each retention time. The value of the slope increased with increasing retention time owing to decreasing velocity through the column. Table 8.2 also indicates that the rate constant in the first-order reaction is fixed with different retention times.

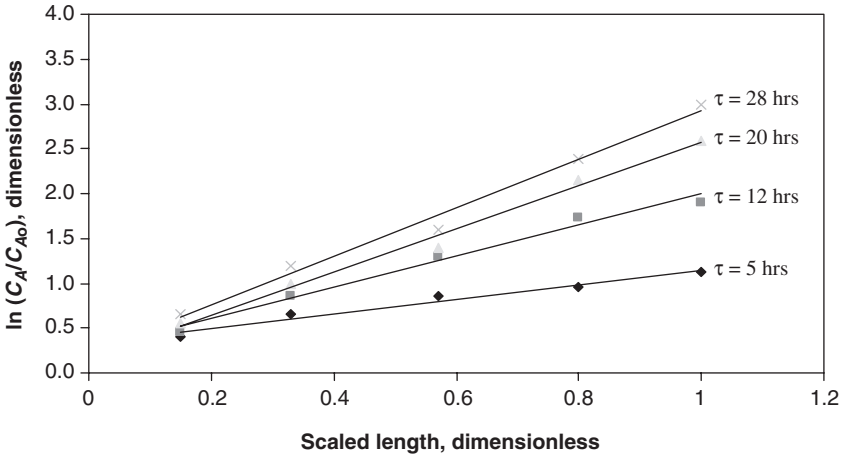

FIG. 8.2. Model test for ICR using *Propionibacterium acidipropionici*.

TABLE 8.2. *ICR kinetic model for immobilised Propionibacterium acidipropionici*

Retention time τ, hours	Flow rate ml/h	Rate constant h^{-1}
5	214	0.70
8	135	0.69
12	90	0.68
20	55	0.68
28	38	0.51

The ICR flow rate was five to eight times faster than the CSTR. The overall conversion of sugars in the ICR at a 12 hour retention time was 60%, At this retention time, the ICR was eight times faster than CSTR, but in the CSTR an overall conversion rate of 89% was obtained. At the washout rate for the chemostat, the ICR resulted in a 38% conversion of total sugars. Also, the organic acid production rate in the ICR was about four times that of the CSTR. At a higher retention time of 28 hours, the conversion of glucose in the ICR and CSTR are about the same, but the conversion of xylose reached 75% in the ICR and 86% in the CSTR.

8.5 NOMENCLATURE

r_A	Reaction rate, $g \cdot l^{-1} \cdot h^{-1}$
k	Rate constant, $l \cdot h^{-1}$
C_A	Sugar concentration, $g \cdot l^{-1}$
z	Axial reactor length, cm
u	Bulk fluid velocity, $cm \cdot h^{-1}$

REFERENCES

1. Gikas, P. and Livingston A.G., *Biotechnol. Bioengng* **55**, 660 (1997).
2. Wang, D.I.C., Cooney, CL., Demain, A.D.L., Dunnill, P., Humphrey, A.E. and Lilly, M.D., "Fermentation and Enzyme Technology". John Wiley & Sons, New York, 1979.
3. Najafpour, G.D., *J. Sci. I. R. Iran* **1**, 172 (1990).
4. Najafpour, G.D. and Younesi, H., *Biores. Technol*. **92**, 251 (2004).
5. Chibata, I., Immobilized Microbial Cells with Polyacrylamide Gel, Carrageenan and their Industrial Application, In "Immobilized Microbial Cells", chap. 3. American Chemical Society, Washington, D.C., 1979.
6. Chibata, I., *Microb. Technol*. **II**, 361 (1979).
7. Brodelius, P. and Mesback, K., *Adv. Appl. Microbiol*. **28**, 1 (1982).
8. Mark, R.R., Muzzio, F.J., Buettner, H.M. and Sebastian, C.R., *Biotechnol. Bioengng* **49**, 223 (1996).
9. Sitton, O.C. and Gaddy, J.L., *Biotechnol. Bioengng* **22**, 1735 (1980).
10. Najfpour, G.D., "Propionic and Acetic Acid Fermentation using *Propionibacterium acidipropionici* in Batch and Continuous Culture", Ph.D. thesis, University of Arkansas, Fayetteville, AR, 1983.
11. Najfpour G.D., *Resourc. Conserv*. **13**, 187 (1987).
12. Senthuran, A., Senthuran, V., Mattiasson, B. and Kaul, R., *Biotechnol. Bioengng* **55**, 841 (1997).

8.6 CASE STUDY: ETHANOL FERMENTATION IN AN IMMOBILISED CELL REACTOR USING *SACCHAROMYCES CEREVISIAE*

Abstract

Fermentation of sugar by *Saccharomyces cerevisiae*, for production of ethanol in an immobilised cell reactor (ICR), was successfully carried out to improve the performance of the

fermentation process. The fermentation set-up comprised a column packed with beads of immobilised cells. The immobilisation of *S. cerevisiae* was simply performed by the enriched cell culture harvested at exponential growth phase. The fixed-cell loaded ICR performed at an initial stage of operation and the cells were entrapped by calcium alginate. Production of ethanol was steady after 24 hours of operation. The concentration of ethanol was affected by the media flow rate and residence time distribution from 2 to 7 h. In addition, batch fermentation was carried out with a glucose concentration of 50 $g \cdot l^{-1}$. Subsequently, ethanol production and reactor productivities of batch fermentation and immobilised cells were compared. In batch fermentation, sugar consumption and ethanol production were 99.6% and 12.5 v/v after 27 hours, whereas in the immobilised cell reactor, 88.2% and 16.7 v/v were obtained with 6 hours' retention time, respectively. Nearly 5% ethanol production was achieved with a high glucose concentration (150 $g \cdot l^{-1}$) at 6 hours' retention time. A yield of 38% was obtained with 150 $g \cdot l^{-1}$ glucose. The yield was improved approximately 27% by ICR, and a 24 hour fermentation time was reduced to 7 hours. The cell growth rate was based on the Monod rate equation. The kinetic constants (K_m and μ_m) of batch fermentation were 2.3 $g \cdot l^{-1}$ and 0.35 h^{-1}, respectively. The maximum yield of biomass on substrate ($Y_{X/S}$) and the maximum yield of product on substrate ($Y_{P/S}$) in batch fermentation were 50.8 and 31.2%, respectively. Productivity of the ICR was 1.3, 2.3 and 2.8 $g \cdot l^{-1} \cdot h$ for 25, 35 and 50 $g \cdot l^{-1}$ of glucose, respectively. The productivity of ethanol in batch fermentation with 50 $g \cdot l^{-1}$ glucose was calculated as 0.29 $g \cdot l^{-1} \cdot h$. Maximum production of ethanol in the ICR compared with the batch reactor showed an approximate tenfold increase. The performance of the two reactors was compared and a respective rate model was proposed. The present research shows that a high sugar concentration (150 $g \cdot l^{-1}$) in the ICR column was successfully converted to ethanol. The achieved results in the ICR with a high substrate concentration are promising for scale-up operation. The proposed model can be used to design a larger-scale ICR column for the production of high ethanol concentrations.

Keywords: immobilised cell reactor (ICR); *Saccharomyces cerevisiae*; ethanol fermentation; encapsulated beads; calcium alginate

8.6.1 Introduction

Owing to diminishing fossil fuel reserves, alternative energy sources need to be renewable, sustainable, efficient, cost-effective, convenient and safe.[1] In recent decades, microbial production of ethanol has been considered as an alternative fuel for the future because fossil fuels are depleting. Several microorganisms, including *Clostridium* sp. and yeast, the well-known ethanol producers *Saccharomyces cerevisiae* and *Zymomonas mobilis,* are suitable candidates to produce ethanol.[2,3]

Microorganisms under anaerobic growth conditions have the ability to utilise glucose by the Embden–Mereyhof–Parnas pathway.[4] Carbohydrates are phosphorylated through the metabolic pathway; the end products are two moles of ethanol and carbon dioxide.[5]

During batch fermentation of *Saccharomyces cerevisiae*, other influential parameters can adversely influence the specific rate of growth, and inhibition can be caused either by

product or substrate concentration. The viability of the *Saccharomyces cerevisiae* population, its specific rate of fermentation and the sugar uptake rate are directly related to the desired medium condition.[6] It has been reported by Nagodawithana and Steinkraus,[7] that the addition of ethanol to the cultured media was less toxic for *Saccharomyces cerevisiae* than ethanol produced by cell bodies. This indicates that there are other metabolic by-products that can cause inhibition, and may show impurity of ethanol produced in the fermentation system. Also, the death rates were lower with addition of pure ethanol than the similar condition with the endogenously produced ethanol concentration.[7]

Use of biofilm reactors for ethanol production has been investigated to improve the economics and performance of fermentation processes.[8] Immobilisation of microbial cells for fermentation has been developed to eliminate inhibition caused by high concentrations of substrate and product, also to enhance productivity and yield of ethanol. Recent work on ethanol production in an immobilised cell reactor (ICR) showed that production of ethanol using *Zymomonas mobilis* was doubled.[9] The immobilised recombinant *Z. mobilis* was also successfully used with high concentrations of sugar (12%–15%).[10]

The potential use of immobilised cells in fermentation processes for fuel production has been described previously. If intact microbial cells are directly immobilised, the removal of microorganisms from downstream product can be omitted and the loss of intracellular enzyme activity can be kept to a minimum level.[11]

Recently, immobilised biomass activity has been given more attention, because it has been acknowledged to play a significant role in bioreactor performance.[12] Frequently, immobilised cells are subjected to limitations in the supply of nutrients. Thus, because of the presence of heterogeneous materials such as immobilised cells, there is no convective flow inside the beads and the cells can receive nutrients only by diffusion.[13] Immobilisation of cells to a solid matrix is an alternative means of high biomass retention. The cells divide within and on the core of the matrix.[14] Alginate is widely used in food, pharmaceutical, textile and paper products. Alginate is used in these products for thickening, stabilizing, gel and film forming. Sodium alginate is a linear polysaccharide, normally isolated from many strains of marine brown seaweed and algae, hence the name ‘alginate’. The copolymer consists of two uronic acids or polyuronic acid. It comprises primarily D-mannuronic acid (M) and L-glucuronic acid (G). Alginic acid can be either water-soluble or non-water soluble depending on the type of the associated salt. Interchange of sodium ions with calcium ions in the solution may follow solidification of sodium alginate in calcium chloride solution. The sodium salt, other alkaline metals and ammonia are soluble in water, whereas the polyvalent cations salts, e.g. calcium, are not water-soluble, except for magnesium ions.

The purpose of this research was to obtain high ethanol production with high yields of productivity and to lower the high operating costs. The ICR column fermenter was used-with *Saccharomyces cerevisiae* by an entrapment technique utilising alginate as a porous wall to retain the yeast cells. The effect of initial glucose concentration on the production of ethanol by *S. cerevisiae* was evaluated. The yield for large-scale ethanol production was compared with the ethanol produced in batch fermentation using the same microorganism.

8.6.2 Materials and Methods

8.6.2.1 Experimental Reactor System

The immobilised cell reactor was a plug flow tubular column, constructed with a nominal diameter of 5 cm, internal diameter of 4.6 cm, Plexiglas of 3 mm wall thickness and 85 cm length. The medium was fed to the ICR column from a feed tank located above the column. A variable-speed Masterflex pump, model L/S Easyload (Cole-Parmer, Vernon Hills, IL, USA) was used to transfer feed medium from a 20 litre polypropylene autoclaveable Nalgene carboy (Cole-Parmer, Vernon Hills, IL, USA), the carboy serving as reservoir. The effluent from the column was collected in a 20 litre polypropylene autoclaveable carboy serving as product reservoir. A flow breaker was installed between the column and feed pump, which prevented growth of microorganisms and contamination of feed line and feed tank. Samples from the ICR column were taken from the inlet and outlet compartments of the column. A 16 hour culture was harvested at exponential growth phase and mixed with 2% sodium alginate. The slurry of yeast culture was converted to droplet form while it was dripped into a 6% bath of calcium chloride using a 50 ml syringe. Once the slurry was added to the bath, beads of calcium alginate with entrapped cells were formed.[11] The bed consisted of uniformly packed 5 mm beads. The solidified beads were transferred to the column. About 70% of the column was packed. The extra space was counted for bed expansion by the fresh media. The void volume was measured by volume of distilled water pumped through the bed. The packed ICR column was used in continuous mode for the duration of fermentation. The fresh feed was pumped an in upflow manner, while sugar and ethanol concentration was monitored during the course of continuous fermentation. The working volume of ICR after random packing was 740 ml. The bed volume was about 660 ml. The experimental set up of the ICR is shown in Figure 8.3. There was no evidence of cell leakage from the beads to the surrounding media, the matrix was permeable to substrate and product, cell growth and glucose conversion were monitored in the ICR. Over-growth of beads after a few days of operation was controlled. Carbon dioxide was purged to eliminate over-growth of beads. The major over-growth occurred at the entrance region, in about the first 30 cm length of the column where the sugar concentration was very high. High sugar concentrations of 25, 35, 50 and 150 $g \cdot l^{-1}$ were used.

Microbial over-growth was controlled with carbon dioxide passed through the bed. There was a maximum 30% increase in the beads' diameter at the lower part of column, where the glucose concentration was maximum. The void volume was measured by passing sterilised water. In addition to the carbon source, the feeding media consisted of 1 $g \cdot l^{-1}$ yeast extract pumped from the bottom of the reactor, while the flow rate was constant for a minimum duration of 24 hours.

A seed culture of *S. cerevisiae* ATCC 24860 (American Type Culture Collection, Manassas, VA, USA) was grown in a media of 5 g glucose, and 0.5 g yeast extract, respectively, 1.5 g KH_2PO_4 and 2.25 g Na_2PO_4 phosphate buffer up to a total volume of distilled water, 500 ml. The media was sterilised at 121 °C for 15 min. The stock culture of the microorganisms was transferred to the broth media for preparation of seed culture.

Sodium alginate (Fisher Scientific, Manchester, UK) was prepared by dissolving 10 g of powder form in 500 ml of distilled water. A separate solution of 120 g of calcium chloride was dissolved in 2 l of distilled water. Sodium alginate and calcium chloride solution were

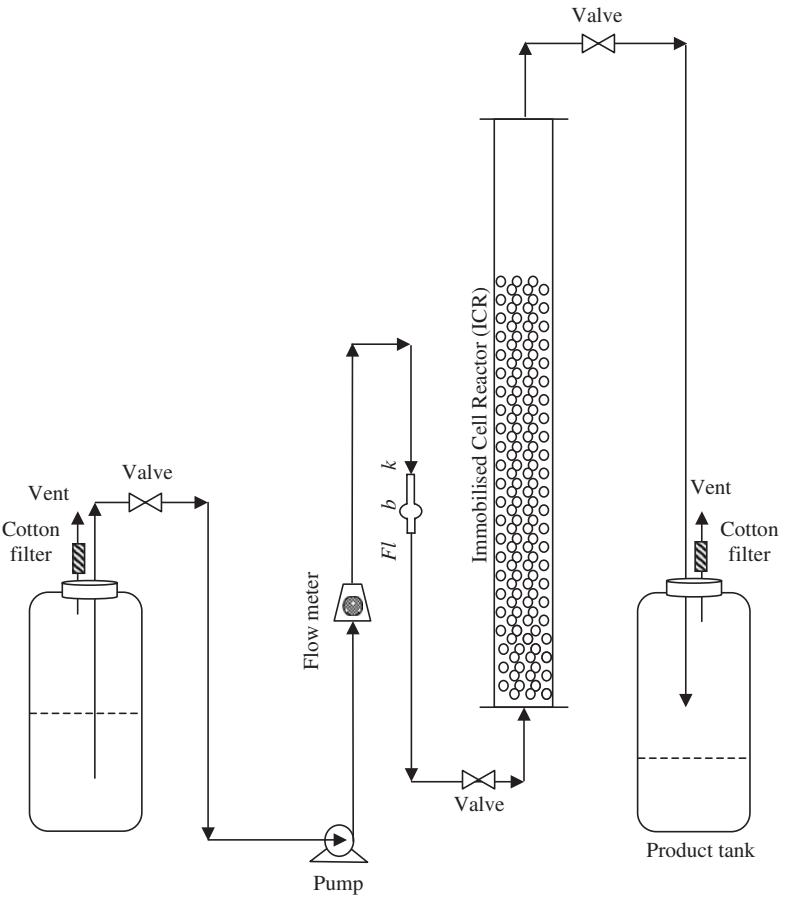

FIG. 8.3. Schematic diagram of ICR experimental setup. Reprinted from Najafpour *et al.* (2004).[18] Copyright with permission from Elsevier.

autoclaved at 121 ºC for 15 min. The sterilised sodium alginate solution and the high cell density of the grown seed culture were thoroughly mixed. Beads were prepared by droplet from pipette with about 5 mm diameter in a sterilised calcium chloride solution. The cell density of the seed culture for bead preparation was 3.1 $g \cdot l^{-1}$. The wet and dry weight of beads incubated for 16 hours were measured: 3.28 and 0.5 g, respectively. The moisture content of the beads was 85%. The physical properties and appearance of the *S. cerevisiae* beads are summarised in Table 8.3.

8.6.2.2 Determination of Glucose Concentration

To determine the concentration of inlet and outlet glucose in the ICR, a reducing chemical reagent, 3,5-dinitrosalicylic (DNS) acid 98% solution, was used. The DNS solution was

TABLE 8.3. *Physical properties and appearance of S. cerevisiae beads*

Alginate, wt %	1.5	2	3	6
Beads diameter, mm	5	4.9–5	4.8–4.9	4.5
Growth, diameter expansion after 72 h	50–60%	25–30%	20–25%	No expansion
Diffusion problem	Nil	Nil	Nil	May exists
Cell activity	Active	Fully active	Fully active	Partly active
Physical appearance	Easy to break	Flexible, hard enough to stand	Flexible and hard	Very hard
Stability	Not stable	Good stability	Stable and rigid	Very rigid

prepared by dissolving 10 g of 3,5-dinitrosalicylic acid in 2 M sodium hydroxide solution. A separate solution of 300 g sodium potassium tartrate solution was prepared in 300 ml of distilled water. The hot alkaline 3,5-dinitrosalisylate solutions were added to sodium potassium tartrate solution. The final volume of DNS solution was made up to 1 l with distilled water. A calibration curve was prepared with 2 $g \cdot l^{-1}$ glucose solution.[15,16]

8.6.2.3 Detection of Ethanol

Ethanol production in the fermentation process was detected with gas chromatography, HP 5890 series II (Hewlett-Packard, Avondale, PA, USA) equipped with a flame ionisation detector (FID) and GC column Porapak QS (Alltech Associates Inc., Deerfield, IL, USA) 100/120 mesh. The oven and detector temperature were 175 and 185 °C, respectively. Nitrogen gas was used as a carrier. Isopropanol was used as an internal standard.

8.6.2.4 Yeast Cell Dry Weight and Optical Density

In batch fermentation, approximately 2 ml sample was harvested every 2 hours. The absorbance of each sample during batch fermentation was measured at 620 nm using spectrophotometer, Cecil 1000 series (Cecil Instruments, Cambridge, England). The cells dry weight was obtained using a calibration curve. The cell dry weight was proportional to cell turbidity and absorbance at 620 nm. The cell concentration (dry weight) of 2.1 $g \cdot l^{-1}$ was obtained from the 24 hours culture broth, the free cell samples with absorbance of 1.6 at 620 nm.

8.6.2.5 Electronic Microscopic Scanning of Immobilised Cells

For electronic micrographs, samples were taken from fresh beads and 72 hour beads from the ICR column. The samples were dipped into liquid nitrogen for 10 minutes, then freeze dried for 7 hours (EMITECH, model IK750, Cambridge, UK). The sample was fixed on an aluminium stub and coated with gold–palladium by a Polaron machine model SD515

(EMITECH, Cambridge, UK) at 20 nm coating thickness. Finally the sample was examined under scanning electron microscope (SEM) by using a Stereoscan model S360 (SEM-Leica Cambridge, Cambridge, UK).

8.6.2.6 Statistical Analysis

The size of beads was uniform and consistent, the mean size of beads with 3% alginate and based on measurement of 20 samples; the mean value for the beads' diameter was 4.85 mm, with a standard deviation of 0.3 mm and calculated variance of 0.1 mm. The standard deviation was less than 5%. The data for the batch fermentation experiment with 50 $g \cdot l^{-1}$

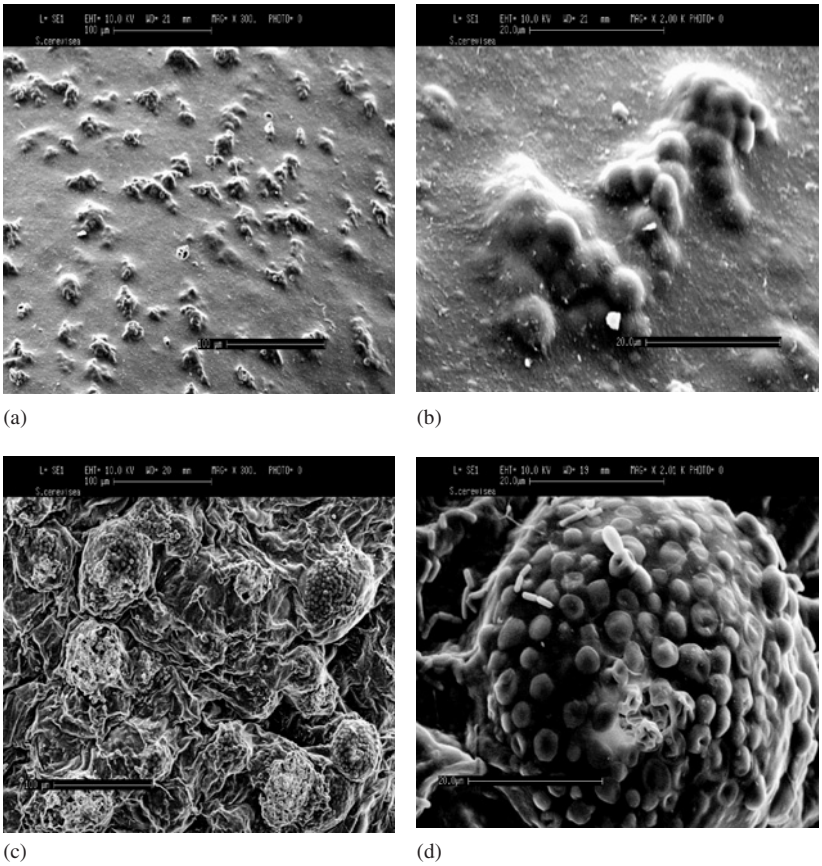

(a) (b)

(c) (d)

FIG. 8.4. Electron micrographs of the outer surface of immobilised *S. cerevisiae* beads. (a) Outer surface of the fresh beads with magnification of 300 μm. (b) Outer surface of the fresh beads with magnification of 2000 μm. (c) Outer surface of the used beads after 72 hours with magnification of 300 μm. (d) Outer surface of the used beads after 72 hours with magnification of 2000 μm. Reprinted from Najafpour *et al.* (2004). Copyright with permission from Elsevier.

glucose are presented in Figures 8.4–8.6; they were replicated three times. The data for ICR with 25, 35, 50 and 150 $g \cdot l^{-1}$ glucose that were conducted at a wide range of flow rates are shown in Figures 8.7–8.11, which were repeated in additional runs. The standard deviations of collected data for the batch experiments were approximately 5%, and the standard deviation for the ICR experimental data with a sugar concentration of 50 $g \cdot l^{-1}$ was approximately 10%. Data were analysed in a spreadsheet, Microsoft Excel 2000. The error analysis for the ICR data with a substrate concentration of 150 $g \cdot l^{-1}$ was slightly higher but it was in the range of 10–12%.

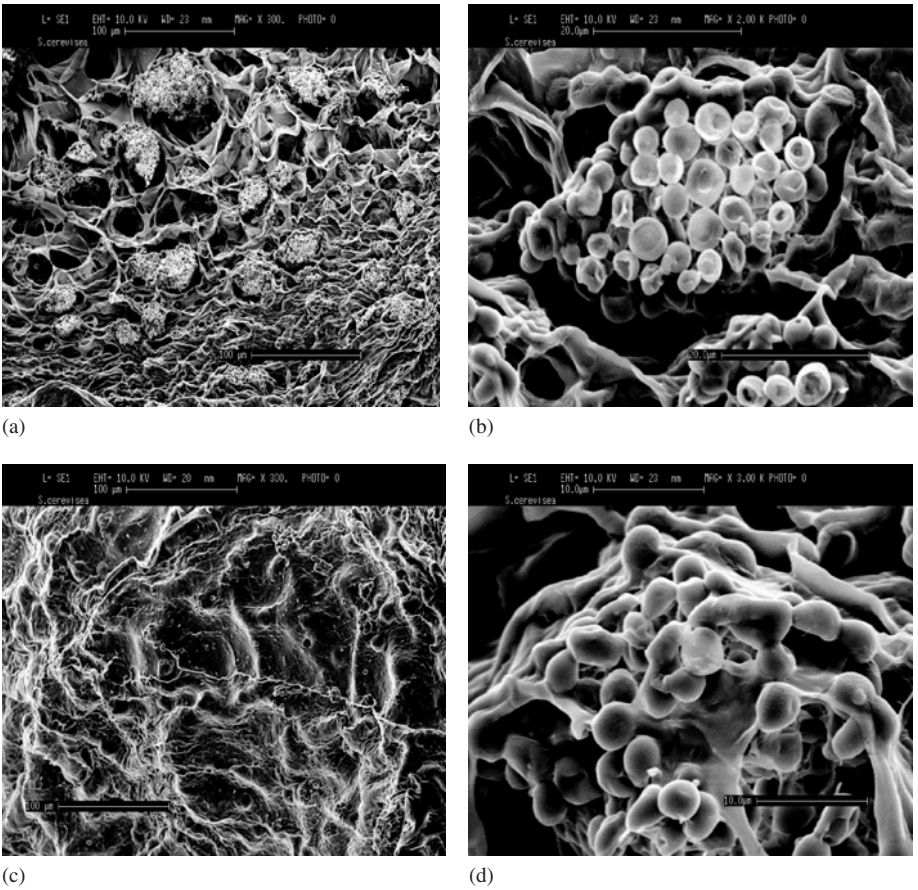

FIG. 8.5. Electron micrographs of the inner surface of immobilised *S. cerevisiae* beads. (a) Inner surface of the fresh beads with magnification of 300 μm. (b) Inner surface of the fresh beads with magnification of 2000 μm. (c) Inner surface of the used beads after 72 hours with magnification of 300 μm. (d) Inner surface of the used beads after 72 hours with magnification of 2000 μm. Reprinted from Najafpour *et al.* (2004).[18] Copyright with permission from Elsevier.

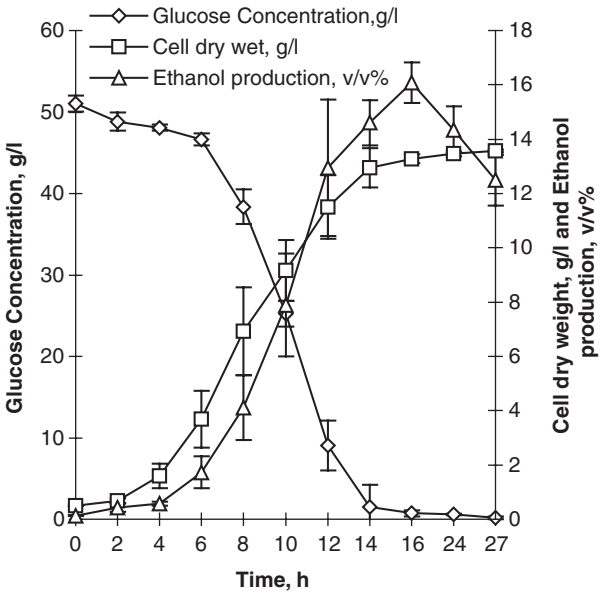

FIG. 8.6. Glucose concentration, cell density and production of ethanol in batch fermentation with initial concentration of 50 $g \cdot l^{-1}$ glucose versus time. Reprinted from Najafpour *et al*. (2004).[18] Copyright with permission from Elsevier.

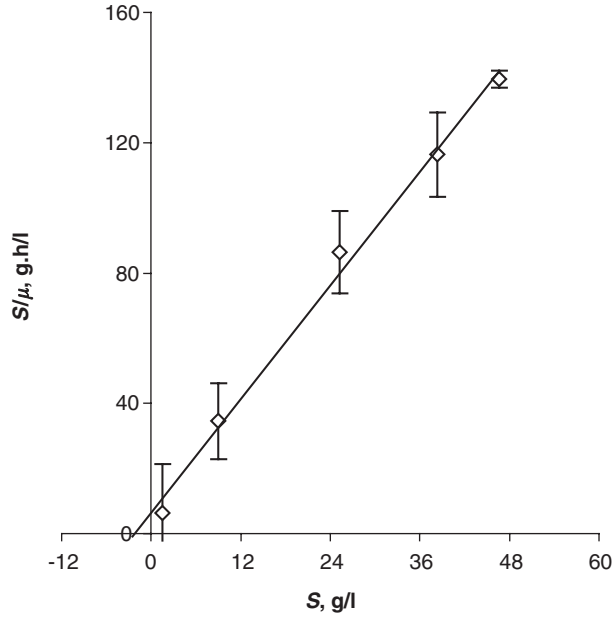

FIG. 8.7. Kinetic model for batch fermentation, Langmuir–Hanes plot. Reprinted from Najafpour *et al*. (2004).[18] Copyright with permission from Elsevier.

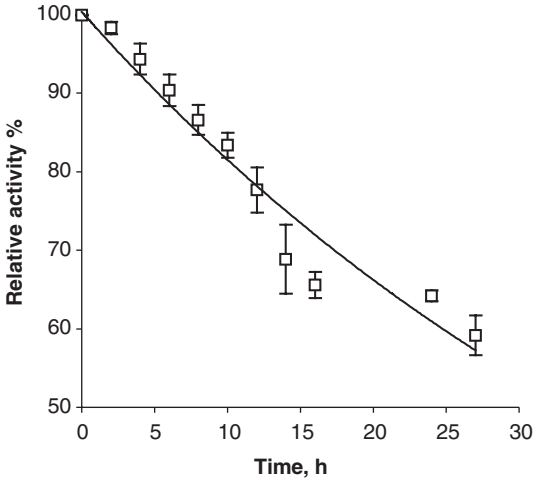

FIG. 8.8. Relative activities of *S. cerevisiae* in batch fermentation. Reprinted from Najafpour *et al*. 2004.[18] Copyright with permission from Elsevier.

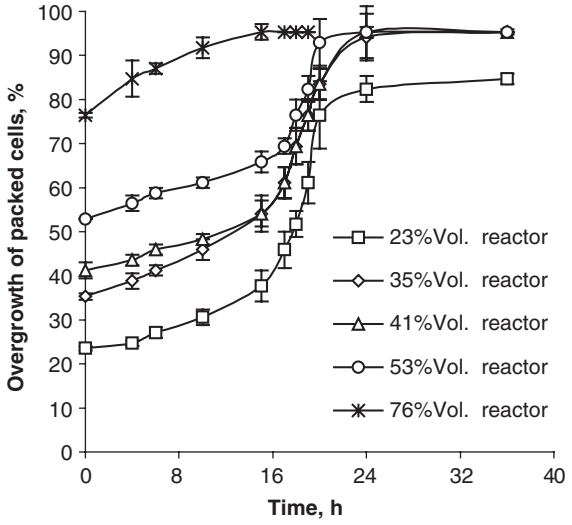

FIG. 8.9. Percentage, growth of immobilised cells with various initial beads loading. Reprinted from Najafpour *et al*. (2004).[18] Copyright with permission from Elsevier.

8.6.3 Results and Discussion

8.6.3.1 Evaluation of Immobilised Cells

In preparing immobilised cells, 1.5, 2, 3 and 6% alginate was used. By pressing them manually, the hardness and rigidity of the beads were tested. The physical criteria of the

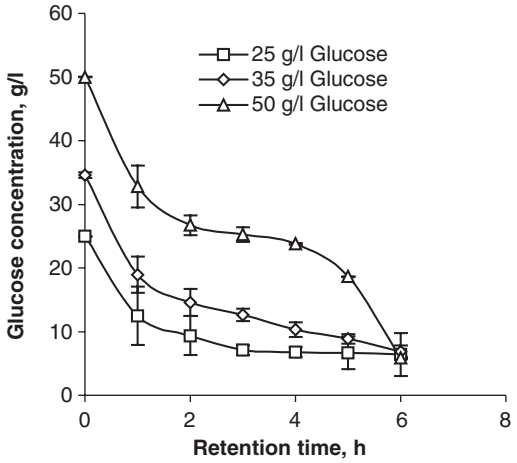

FIG. 8.10. Consumption of glucose in the immobilised cell column. Reprinted from Najafpour *et al*. (2004). Copyright with permission from Elsevier.

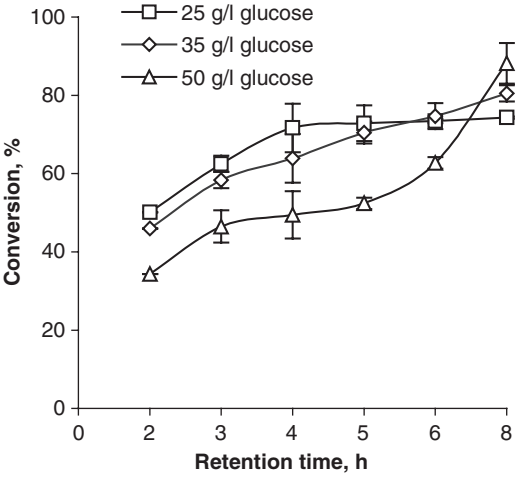

FIG. 8.11. Conversion versus retention time in the immobilised cell column. Reprinted from Najafpour *et al*. (2004).[18] Copyright with permission from Elsevier.

prepared beads are summarised in Table 8.1. The suitable alginate concentration based on activity of the beads for ethanol production was 2%. The weight percentage of alginate was related to substrate and product penetration into the beads and return to bulk of fluid. Beads with low alginate (1.5%) were too soft and easily breakable. The soft beads were

pressed once they were loaded in the ICR column. Therefore they were unable to be used successfully; also the soft beads faced problems such as overgrowth and expansion of their diameter when grown in sugar solution. The high alginate beads (6%) were very hard and almost unbreakable by pressing manually. They were very rigid, therefore diffusion was the most probable cause since ethanol production declined. The 2% alginate was used because the beads were strong enough to hold the weight of packing in the ICR column. The packed beads were used in the ICR column for 10 days. The prepared beads were refrigerated for 2 weeks and activated in sugar solution. The storage condition and ICR column were non-sterile; therefore, there was the possibility of contamination in the packing of the ICR and in the activation process.

A series of electron micrographs were taken from the fresh and 72 hour immobilised beads. The outer and inner surfaces of the beads are shown in Figures 8.4 and 8.5, respectively. These micrographs were used as a comparative indicator for yeast growth on the surface of the solid support (2% calcium alginate). There was no apparent leakage of cells from the beads into the bulk of the fluid. It was also apparent that by 72 hours in the ICR, the yeast was growing on the outer surface. Therefore the active sites were potentially available for ethanol production without diffusion problems. The outer surface of fresh and 72 hour immobilised cell beads at magnifications of 300 and 2000 are shown in Figure 8.4. A comparison between fresh and 72 hour beads indicates that the cells were present on the surface, with a few contaminants from a bacillus-type organism, as shown in Figure 8.4d. This may have occurred during the transfer stage.

The inner surface of the beads before and after use was compared. The cells were initially trapped inside the beads; after 72 hours the cells apparently migrated from the inner side to the surface. The micrographs of the inner sides of the beads before and after use, at magnifications of 300 and 2000, are shown in Figure 8.5. After 72 hours the cells appeared to have formed new colonies on the surface of the alginate layer. By contrast, the surfaces were completely covered with colonies after 72 hours of ethanol production in the ICR.

8.6.3.2 Batch Fermentation

Ethanol fermentation in batch experiments was carried out in triplicate with 50 $g \cdot l^{-1}$ glucose solution as the sole carbon source for *S. cerevisiae*. The purpose of the batch experiment was to compare the amount of glucose concentration and ethanol production in batch fermentation and the ICR. The concentration of glucose was gradually decreased while the cell density and ethanol production were increased for 27 hours, as shown in Figure 8.6. There was a lag phase of 4–6 hours; the glucose consumption was low at this stage. Subsequently the concentration profile drastically decreased during batch fermentation after 8–16 hours. Since the cell density was initially low, sugar consumption was also low. The resulting cell growth curve from the batch experiment was a typical sigmoidal (S-)shape. The maximum cell density of *S. cerevisiae* in batch fermentation was 13.7 $g \cdot l^{-1}$ with 50 $g \cdot l^{-1}$ glucose concentration. The average yield of biomass and product on substrates ($Y_{X/S}$ and $Y_{P/S}$) were 33 and 32%, respectively. The rate of ethanol productivity for 24 hours was 1.4 $g \cdot l^{-1} \cdot h^{-1}$.

A Langmuir–Hanes plot based on the Monod rate equation is presented in Figure 8.7. The Monod kinetic model can be used for microbial cell biocatalyst and is described as follows:

$$\frac{S}{\mu} = \frac{K_S}{\mu_m} + \frac{S}{\mu_m} \qquad (8.6.3.2.1)$$

The terms K_s and μ_m are defined as the Monod constant and maximum specific growth rate, respectively. The data generated in this study were linearly fitted with the model, as a function of concentration produced during the exponential phase versus time (Figure 8.7). From the plot, the maximum specific growth rate and Monod constant were determined to be 0.35 h^{-1} and 2.23 $g{\cdot}l^{-1}$, respectively. The large value of the Monod constant may suggest that at high concentrations of substrate, more influence on the cell–substrate complex [C.S] dissociation occurred than [C.S] formation.

8.6.3.3 Relative Activity

The economics of an immobilised cell process depend on the lifetime of the microorganism and a continued level of clean product delivered by the fixed cells. It is important to eliminate the free cells from the downstream product without the use of any units such as centrifuge or filtration processes. Since the cells are retained in the ICR, the activity of intracellular enzymes may play a major role. It is assumed that the deactivation of the enzyme at constant temperature follows a first-order equation as shown below:[17]

$$A_t = A_0 \exp(-k_d t) \qquad (8.6.3.3.1)$$

where A_t and A_0 are activities of enzymes at time, t and initial time zero, respectively. Also, k_d is the dissociation constant. The plot of relative activity versus time in batch fermentation with free cells is shown in Figure 8.8. The value of k_d was 0.36 h^{-1} (Figure 8.8). According to the first-order dissociation rate constant, the half-life of the *S. cerevisiae*, ($\tau_d = \ln 2/k_d$), in batch fermentation suspended cells with 50 $g{\cdot}l^{-1}$ of glucose was 1.95 h. The free cells were apparently completely deactivated after 60 hours in batch operation. The data indicate that the free cells were deactivated rapidly compared with immobilised cells when used in a continuous mode for more than 7 days.

8.6.3.4 Reactor Set-up

The volume of reactor without beads was 1.4 l. The column was loaded with the solidified uniform beads of *S. cerevisiae*. The void volume of the reactor was 660 ml when it was packed with immobilised beads. The growth of beads with different proportions of column packing is shown in Figure 8.9. A fresh feed of 10 $g{\cdot}l^{-1}$ glucose solution was pumped from the bottom of the reactor. The optimum amount of packing obtained was 65–70% of the reactor volume. The trend of the collected data resembles the growth curve of yeast in

suspended cell culture. The diameters of the beads increased with the increase in *S. cerevisiae* cell density, which indicates that *S. cerevisiae* was growing within the solid support. Under these circumstances substrate would be easily consumed at the solid surface coated with immobilised yeast cells. Thus, it was expected that substrate concentration at the surface would be less than the concentration of substrate in the bulk fluid. The main objective was to determine whether substrate penetrated into the beads. Since the matrix of beads was quite porous, it was assumed that the concentration gradient was the major force that influenced the mass transfer process in immobilised cells of *S. cerevisiae*. Therefore, the immobilised yeast system was preferred compared with free cells in the solution. Moreover, economic aspects of immobilised yeast must be considered as it eliminates the need for the extra unit for free-cell removal from the product stream. The other advantages of the immobilisation system are that the substrate may not accumulate on the surface of the beads and that there was no evidence of cell leakage from the beads.

8.6.3.5 Effect of High Concentration of Substrate on Immobilised cells

The fermentation was performed with various sugar concentrations to increase product concentrations. The initial sugar concentrations were 25, 35 and 50 $g \cdot l^{-1}$. The sugar consumption profile in the ICR is presented in Figure 8.10. The sugar consumption trends of various glucose concentrations were similar, with a sharp reduction of substrate occurring within the first 3 hours. A range of 55–75% of the sugars was reduced within a 3 hour retention time. A 6 hour retention time indicated that this was the most suitable time to achieve high sugar consumption. A longer retention time was required for higher sugar concentrations of up to 150 $g \cdot l^{-1}$ in the ICR column (7 hours) (Figure 8.13). The amount of cell immobilised with calcium alginate was determined by the cell dry weight of immobilised cells and the assumption that 98% of the beads were considered to be loaded with active cells. Beads were measured before loading in the ICR column.

Conversion of glucose versus dilution rate, used in the continuous fermentation process with immobilised *S. cerevisiae,* is shown in Figure 8.11. As the sugar concentration increased the conversion may have decreased. At very high sugar concentrations, the conversion of sugar decreased. The maximum sugar conversion at 6 hours' retention time was obtained from 74.3, 80.5 and 88.2% for 25, 35 and 50 $g \cdot l^{-1}$ glucose concentrations, respectively. At high concentrations of sugar, conversion was highly influenced by dilution rate. The conversion decreased to less than 10% once the dilution rate approached wash out. The sugar conversion at low sugar concentrations appeared to be much less sensitive to feed dilution rate. The conversion for 25 $g \cdot l^{-1}$ glucose was constant at 74% for a retention time of greater than 3 hours (Figure 8.11). The trend of the data with 50 $g \cdot l^{-1}$ sugar showed that conversion increased with retention time. At a higher sugar concentration, it required a longer retention time to achieve higher conversion.

Reactor productivity was obtained by dividing final ethanol concentration with respect to sugar concentration at a fixed retention time. It was found that the rates of 1.3, 2.3 and 2.8 $g \cdot l^{-1} \cdot h^{-1}$ for 25, 35 and 50 $g \cdot l^{-1}$ glucose concentrations were optimal. Ethanol productivities with various substrate concentrations were linearly dependent on retention time (Figure 8.12). The proportionality factor may have increased while the substrate

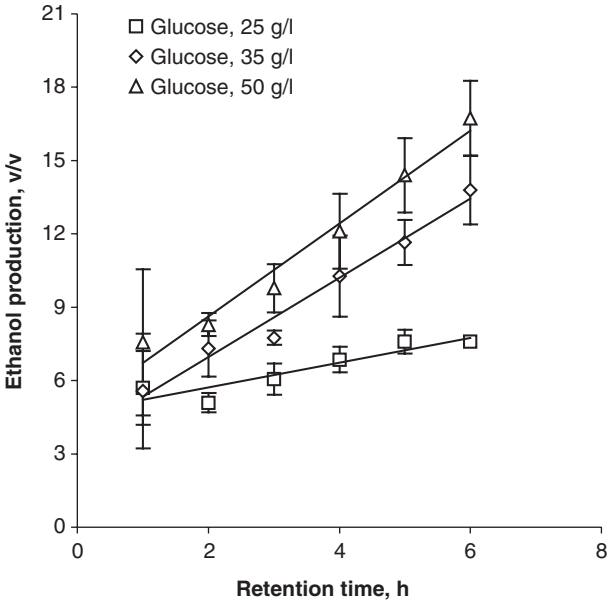

FIG. 8.12. Ethanol production versus retention time in the immobilised cell column. Reprinted from Najafpour *et al*. (2004).[18] Copyright with permission from Elsevier.

concentration increased. As the sugar concentration doubled, the slope of the line for ethanol productivity with 50 $g \cdot l^{-1}$ sugar increased fivefold. These results indicate that the ICR column has a high capacity to produce very high concentrations of ethanol. The final ethanol concentrations with 25 and 50 $g \cdot l^{-1}$ of glucose were 7.6 and 16.73 v/v, respectively.

A high glucose concentration of 150 $g \cdot l^{-1}$ was used in continuous fermentation with immobilised *S. cerevisiae*; the obtained data for sugar consumption and ethanol production with retention time are shown in Figure 8.13. As the retention time gradually increased the glucose concentration dropped, while the ethanol concentration profile showed an increase. The maximum ethanol concentration of 47 $g \cdot l^{-1}$ was obtained with a retention time of 7 hours. The yield of ethanol production was approximately 38% compared with batch data, where only an 8% improvement was achieved.

8.6.4 Conclusion

Continuous ethanol production in an ICR was successfully done with high sugar concentrations. In batch fermentation, when the concentration of glucose was 50 $g \cdot l^{-1}$, substantial substrate inhibition occurred. The advantage of the ICR was that the inhibition of substrate and product were not apparent even with a 150 $g \cdot l^{-1}$ glucose solution in the fresh feed (data not shown). The ICR system exhibited a higher yield of ethanol production (38%) than the batch system. The ICR column gave a high performance to processing feed with concentrated sugar. Most of ICR experimental runs resulted in a glucose consumption of 82–85%.

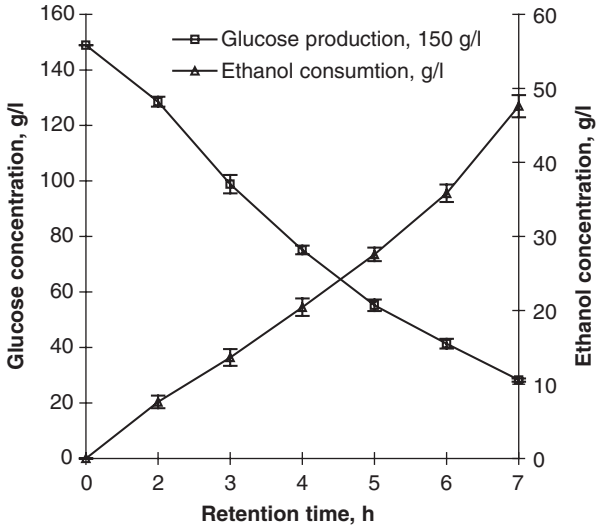

FIG. 8.13. Glucose concentration and ethanol production versus retention time in immobilised cell reactor with initial substrate concentration of 150 $g \cdot l^{-1}$ glucose. Reprinted from Najafpour *et al*. (2004).[18] Copyright with permission from Elsevier.

The results indicate that the immobilisation of *S. cerevisiae* possesses the capacity not only to utilise high concentrations of sugar but also to yield higher ethanol productivities during the course of continuous fermentation. Ethanol production in the ICR column increased by fivefold, as the glucose concentration was doubled from 25 to 50 $g \cdot l^{-1}$. It is clear: the new findings in the present investigation would be the application of concentrated feed with a higher rate of ethanol production, as the cell loaded into the gel matrices of sodium alginate shown in the SEM micrographs had eliminated the free cells from the ethanol product stream.

8.6.5 Acknowledgement

The present research was made possible through an IRPA grant No. 03-02-05-9016, sponsored by Universiti Sains Malaysia. We thank Research Creativity & Management Office, Universiti Sains Malaysia, Penang, Malaysia. Special thanks go to the Ministry of Science Technology and Environment (MOSTE), Kuala Lumpur, Malaysian government for their financial support for Intensive Research Priority Area (IRPA).

8.6.6 Nomenclature

S	Substrate concentration, $g \cdot l^{-1}$
C	Microorganisms cell concentration, $g \cdot l^{-1}$
K_s	Monod constant, $g \cdot l^{-1}$
μ	Specific growth rate, $g \cdot l^{-1} \cdot h^{-1}$

μ_m Maximum specific growth rate, h^{-1}.
T Time, h
A_t Activity of bacterium at time t, U/g cell.
A_o Initial activity of bacterium, U/g cell.
k_d Dissociation constant, h^{-1}

REFERENCES

1. Chum, L.H. and Overend, R.P., *Fuel Bioprocess Technol.* **17**, 187 (2001).
2. Flickinger, M.C. and Drew, S.W., *In* Encyclopedia of Bioprocess Technology: Fermentation, Biocatalysis, and Bioseparation, vol. 2, 939, 1999.
3. Gunasekaran, P. and Raj, K.C., 2001. Ethanol fermentation technology - *Zymomonas mobilis*, http://ces.iisc.ernet.in/curscinew/july10/articles14.htm.
4. Baily, J.E. and Ollis, D.F., "Biochemical Engineering Fundamentals", chapter 3. McGraw-Hill, New York, 1986.
5. Ingram, L.O., Gomez, P.F., Lai, X., Moniruzzaman, M. and Wood, B.E., *Biotechnol. Bioengng* **58**, 204 (1998).
6. Holzberg, I., Finn, R.K. and Steinkraus, K.H., *Biotechnol. Bioengng* **9**, 413 (1967).
7. Nagodawithana, T.W. and Steinkraus, K.H. *J. Appl. Env. Microbiol.* **31**, 158 (1976).
8. Vega, J.L., Clausen E.C. and Gaddy J.L., *J. Enzyme Microb. Technol.* **10**, 390 (1988).
9. Takamitsu, I., Izumida, H., Akagi, Y. and Sakamoto, M. *J. Fermentation Bioengng* **75**, 32 (1993).
10. Yamada, T., Fatigati, M.A. and Zhang M., *Appl. Biochem. Biotechnol.* **98**, 899 (2002).
11. Najafpour, G., "Organic Acids for Biomass by Continuous Fermentation", *Resour. Consern.* **17**, 187 (1987). (Riley, *et al*, 1996) (Senthuran, *et al*, 1997).
12. Gikas, P. and Livingston, A.G., *Biotechnol. Bioengng* **55**, 660 (1997).
13. Riley, M.R., Muzzio, F.J., Buettner, H.M. and Reyes, S.C., *Biotechnol. Bioengng* **49**, 223 (1996).
14. Senthuran, A., Senthuran, V., Mattiasson, B. and Kaul, R., *Biotechnol. Bioengng* **55**, 841 (1997).
15. Summers, J.B., *J. Biol Chem.* **62**, 248 (1924).
16. Miller, G.L. *Anal. Chem.* **31**, 426 (1959).
17. Yuan, Y.J., Wang, S.H., Song, Z.X. and Gao, R.C., *J. Chem. Technol. Biotechnol.* **77**, 602 (2002).
18. Najafpour, G.D., Younesi, H. and Ku Ismail, K.S., "Ethanol Fermentation in Immobilized Cell Reactor (ICR) Using Saccharomyces cerevisiae", Bioresource Technology, vol. 92/3, 2004, pp. 251–260.

8.7 FUNDAMENTALS OF IMMOBILISATION TECHNOLOGY, AND MATHEMATICAL MODEL FOR ICR PERFORMANCE

It is well known that pure enzymes change their behaviour and stability when they are immobilised. In the past two decades the immobilisation of microorganisms, cells and parts of cells has gradually been introduced into microbiology and biotechnology. The cell immobilisation techniques are modifications of the techniques developed for enzymes. However, the larger size of microbes has influenced the techniques. As for immobilised enzymes, two broad types of method have been used to immobilise microorganisms: attachment to a support and entrapment.

8.7.1 Immobilisation of Microorganisms by Covalent Bonds

By these methods microorganisms are cross linked by chemical substances, e.g. by glutardialdehyde. The surfaces (especially the proteins) of microorganisms are linked with the

surfaces of other microorganisms by aldehyde groups of glutardialdehyde. Yeast cells, for instant, react with free ε-amino group or N-terminal amino groups to form imines. Another reaction mechanism was proposed for a conjugated addition of amino groups to double linkages of α- and β-unsaturated oligomers, which are present in commercial aqueous solutions of glutardialdehyde. This mechanism may explain the stability of the linkages. By this chemical linking, growth inhibition and toxic influences on the microorganisms are very intensive. These reactions are only partly understood and can lead to decay or death of the microorganisms.

8.7.2 Oxygen Transfer to Immobilised Microorganisms

Availability of oxygen is one of the most important parameters that are different for immobilised and free microorganisms. Free organisms can get oxygen directly from the surrounding air or, in most technical processes, from the liquid, especially water, which contains dissolved oxygen. The molar transfer of oxygen with respect to time, dO_2/dt, can be described by the following equation:

$$\frac{dO_2}{dt} = K_L a(C_g - C_L) \tag{8.7.2.1}$$

$K_L a$ is the volumetric oxygen mass transfer coefficient, owing to the oxygen transfer from the gas phase or air, c_g, the surface of the cells, c_x or to the transfer of oxygen dissolved in water to the surface of the cells.

In principle, the same formula can be applied to immobilised microoraganisms, but here the conditions are quite different. The adsorbed cells form microbial films or varying thickness during a short incubation time. Oxygen has to be transferred into these microfilms, and because of this, zones of different oxygen concentration in the films exist, in which the growth of the microorganisms varies in direct relation to the oxygen concentration.

By using the unsteady-state model, the maximum oxygen penetration depth for highly packed immobilised cells has been reported to be in the range of 50–200 μm.

8.7.3 Substrate Transfer to Immobilised Microorganisms

In an immobilised cell bioreactor, significant substrate concentration gradients may exist. Cells are located close to the nutrient supply, which are likely to maintain higher quality and activity than cells located relatively further away, leading to differentiation in the quality or activity of the immobilised cell population. This differentiation is more pronounced if there are starvation regions (practically zero substrate concentration) inside the reactor.

Typical approaches for measuring diffusivities in immobilised cell systems include bead methods, diffusion chambers and holographic laser interferometry. These methods can be applied to various support materials, but they are time consuming, making it onerous to measure effective diffusivity (D_{eff}) over a wide range of cell fractions. Owing to the mathematical models involved, the deconvolution of diffusivities can be very sensitive to errors in concentration measurements. There are mathematical correlations developed to predict D_{eff} as

TABLE 8.4. *Methods of immobilisation*

Attachment	
Without support	Aggregation of floc for formation of cross-linking
With support	Covalent binding
	Adsorption to ion-exchangers or inorganic
	Biofilm formation
Entrapment	Organic polymer
	Inorganic polymer
	Semi-permeable membrane

a function of diffusivities in broth and inside the cells (D_0, D_c). The relation can also be used to extrapolate D_{eff} measurements from one cell fraction to any other cell fraction. Various values of D_0/D_c have been compiled in Table 8.4 for a variety of immobilised cell systems. These diffusivity ratios for specific systems (i.e. diffusing species, cell type and gel material) facilitate the prediction of D_{eff} values for a wide range of operating conditions. For a few systems, the diffusivity ratios are very large (∞). The infinite diffusivity ratio corresponds to a diffusing solute that does not enter the cells (i.e. $D_c = 0$); such cases were observed with large molecules of disaccharide (galactose), polysaccharides and cells of *Z. mobilis* (Table 8.5).

8.7.4 Growth and Colony Formation of Immobilised Microorganisms

It was pointed out by several scientists that immobilised microorganisms differ in their growth rates and show altered morphological forms of colonies. Adsorbed cells form micro- and macro-films in which the microorganisms in the outer region have a different morphology than in the inner region. These microfilms often show different colony forms in relation to their density. Thick films have a slimy character, thin film often show the presence of individual microorganisms. These characteristics can be observed with bacteria, yeast and with moulds. They are caused by differing oxygen concentrations and limited concentrations of nutrients.

By referring to our previous work on ICR,[1] a mathematical model for ICR performance may be obtained by applying a mass balance over a differential of the column:

$$\varepsilon \frac{\partial C_A}{\partial t} + u \frac{\partial C_A}{\partial z} = r_A \tag{8.7.4.1}$$

where ε is the void volume of the packed column (ml), C_A the substrate concentration ($g \cdot l^{-1}$), u the bulk fluid velocity ($cm \cdot h^{-1}$), z the axial reactor length (cm), and r_A the rate of substrate transfer to microbial film ($g \cdot l^{-1} \cdot h^{-1}$).

Assuming plug-flow and steady-state behaviour, (8.7.4.1) reduces to

$$u \frac{\partial C_A}{\partial z} = r_A \tag{8.7.4.2}$$

TABLE 8.5. *Microbial cells covalently linked to various supports*

Species	Support	Product
Actobacter	Metal hydroxides	Acetic acid
Aspergillus niger	Glycidyl methacrylate	Gluconic acid
Micrococcus luteus	CM-cellulose	Urocanic acid
Saccharomyces cerevisiae	Aminopropyl silica	Ethanol
Saccharomyces cerevisiae	Hydrocyalkyl methacrylate	Killer toxin
Saccharomyces cerevisiae	Cellulose	Ethanol
Zygosaccharomyces lactis	Hydroxyalkyl methacrylate	β-galactosidase

TABLE 8.6. *Experimental studies of diffusion in immobilised cell systems and their associated values of* D_0/D_c

Cell type	Immobilisation	Solute	D_0/D_c
Saccharomyces cerevisiae	Ca-alginate	glucose	0.1
Baker's yeast	Ca-alginate	glucose	10.6
Ehrlich ascites tumor	agar, collagen	glucose	2.4
Zymomonas mobilis	K-carrageenan, Ca-alginate	glucose	∞
Pseudomonas aeruginosa	Ca-alginate	glucose	2.3
Saccharomycess cerevisiae	Ca-alginate	glucose	2.8
Plant	Ca-alginate	sucrose	∞
Baker's yeast	Ca-alginate	galactose	15.8
Zymomonas mobilis	Ca-alginate	galactose	∞
Baker's yeast	Ca-alginate	lactose	∞
Ehrlich ascites tumor	agar, collagen	lactic acid	6.7
Clostridium butyricum	polyarylamide, agar collagen	hydrogen	3.2
Escherichia coli	natural aggregates	nitrous oxide	3.9
Saccharomyces cerevisiae	fermentation media	oxygen	2.3
Saccharomyces cerevisiae	Ca-alginate, Ba-alginate	oxygen	0.1
Escherichia coli	fermentation media	oxygen	2.2
Penicillium chrysogenum	fermentation media	oxygen	5.6
Bacillus amilaliquefaciens	Ca-alginate, PVA-SbQ gel	oxygen	1.8
Saccharomyces cerevisiae	Ca-alginate	ethanol	0.1
Baker's yeast	Ca-alginate	ethanol	∞

Plug-flow behaviour has been shown in this type of reactor by the use of tracer studies (Table 8.6).

The reaction rate for simple fermentation systems is normally given by the Monod equation. This model indicates that the specific conversion rate is constant when applied to an immobilised cell system (Table 8.7). If a first-order rate equation for sugar consumption is used, (8.7.4.2) yields:

$$u\frac{\partial C_A}{\partial z} = kC_A \tag{8.7.4.3}$$

TABLE 8.7. *Ethanol productivity from immobilised systems*

System	Feed sugar conc ($g \cdot l^{-1}$)	% of Feed sugar utilization	Dilution rate (h^{-1})	Max. ethanol productivity ($g \cdot l^{-1} \cdot h^{-1}$)
S. Cerevisiae Carrageenan	Glucose 100	86	1.0	43
S. Cerevisiae Ca-alginate	Glucose 127	63	4.6	53.8
S. Cerevisiae Ca-alginate	Molasses 175	83	0.3	21.3
S. Cerevisiae Carrier A	Molasses 197	74	0.35	25
Z. mobilis Ca-alginate	Glucose 150	75	0.85	44
Z. mobilis Ca-alginate	Glucose 100	87	2.4	102
Z. mobilis Carrageenan	Glucose 150	85	0.8	53
Z. mobilis Flocculation	Glucose 100			120
Z. mobilis Borosilicate	Glucose 50			85
Z. mobilis Carrageenan-locust bean gum	Whey-lactose 50	98		178

Equation (8.7.4.3) is a linear first-order differential equation for concentration and reactor length. After separation of variables, the equation can be integrated as

$$\int_{C_{A0}}^{C_A} \frac{dC_A}{C_A} = \int_0^z \frac{k dz}{u} \tag{8.7.4.4}$$

Integration of the above differential equation yields:

$$\ln(C_A/C_{A0}) = \frac{kz}{u} \tag{8.7.4.5}$$

Thus a linear relation between $\ln(C_A/C_{A0})$ and the reactor length should exist if the model accurately describes the immobilised cell reactor. The experimental data fitting the model was discussed earlier.

8.7.5 Immobilised Systems for Ethanol Production

The most significant advantage of immobilised cell systems is the ability to operate with high productivity at dilution rates exceeding the maximum specific growth rate (μ_{max}) of the microbe. Several theories have been proposed to explain the enhanced fermentation capacity of microorganisms as a result of immobilisation. A reduction in the ethanol concentration in the immediate microenvironment of the organism owing to the formation of a protective layer or specific adsorption of ethanol by the support may act to minimise end product inhibition. Alternatively, substrate inhibition may be diminished in the case of a gel matrix, if the rate of fermentation meets or exceeds the rate of glucose diffusion to the cell. A third possibility is that alteration of the cell membrane during immobilisation provides improved transfer of substrate into and product out of the microbe.

The effect of temperature on the rate of ethanol production is markedly different for free and immobilised systems. Thus while a constant increase in rate is observed with free *S. cerevisiae* as temperature is increased from 25 to 42 °C, a maximum occurs at 30 °C with cells immobilised in sodium alginate. The lower temperature optimum for immobilised systems may result from diffusional limitations of ethanol within the support matrix. At higher temperatures, ethanol production exceeds its rate of diffusion so that accumulation occurs within the beads. The achievement of inhibitory levels then causes the declines observed in the ethanol production rate.

Significant differences are also apparent for the effect of pH on the fermentation rate. The narrow pH optimum characteristic of a free cell system is replaced by an extremely broad range upon immobilisation. This effect stems from the gradient pH that exists within the bead.

REFERENCE

1. Najafpour G.D., *Resources Conserv.* **13**, 187 (1987).

CHAPTER 9

Material and Elemental Balance

9.1 INTRODUCTION

All microorganisms require nutrients for propagation and to produce metabolites as useful by-products. Medium is supplied to a system, products are leaving with effluent. Balancing individual elements assists us in understanding the biocatalytic activities and monitoring the downstream process. Nutrients in aqueous media with carbon, nitrogen and phosphorus sources are supplied. Mineral elements, vitamins and oxygen are also provided to enhance microbial growth. Once a system is selected, we shall observe and balance the inlet and outlet compositions. Knowledge of microbial elemental compositions such as C, H, N, S, P, Mg, Na and K is required for the solution of the elemental balance equation. Normally trace metals and minerals such as Fe, Cu, Zn, Co, Mn and Mo are required in small quantities, which act as growth stimulants with sufficient energy sources to provide ATP as needed to proceed and progress the biochemical reactions.[1] Carbohydrates as substrates are utilised in the cells to generate energy and carry biosynthesis. An adequate carbon source is essential for ensuring cell growth. Nutrients have frequently been added into media in substantially excessive amounts than are required by the cell, but the amounts of trace metals and minerals supplied are limited.[2–4]

For any viable microorganisms in a fermentation process, we should be able to respond to the following questions.

- What would the respiration quotient be? That is related to concentration of CO_2 generated in the fermentation process, known as off gas.
- What fraction of substrate is consumed and how much substrate is converted to biomass and end products?
- If the process is aerobic, how much O_2 is required?
- What would the oxygen transfer rate (OTR) be?

To answer these questions, at first mass balance is required to determine conversion and how much air to supply into the fermentation broth. The substrate consumption or production rates must be set as a start. To demonstrate suitable answers to the above statements, we may approach the questions by reviewing a few biological processes and illustrating all the assumptions and process conditions.

9.2 GROWTH OF STOICHIOMETRY AND ELEMENTAL BALANCES

Even though cell growth is a complex process, it has to follow the laws of conservation of mass and energy. Nutrients, organic compounds and other elements for life are involved in metabolic activities. As a result, cells grow, energy is generated, biosynthesis is accomplished and products are formed. From the above examples, the law of conservation of mass can be successfully used to determine unknown components. Cell growth also obeys the law of conservation of mass. Living matter mainly consists of four major elements: C, H, O and N. These are the four major elements in metabolic processes of cells. The biological products of aerobic growth are carbon dioxide and H_2O. Each element is balanced with the amount removed from the environment. In other words, the amount of metabolic product formed or the amount of heat released by cell growth is proportional to the amount of the substrate consumed and CO_2 formed. As metabolic products and organic compounds are different from the cell material released into the medium, nutrients and substrates are depleted from the medium; as a result, cell growth and products are formed. By considering the cell from a macroscopic point of view, consider it as a system in which cell growth is independent of biochemical reaction pathways. Employing the overall growth reaction, as substrate penetrates the system with a concentration gradient and products and additional biomass leave from the main system, cell growth is achieved.

Cell growth and metabolic activities are similarly described as a simple chemical reaction. It is also necessary to establish a definite formula for dry cell matter. The elemental composition of certain strains of microorganism is defined by an empirical formula $CH_\alpha O_\beta N_\delta$. The general biochemical reaction for biomass production is based on consumption of organic substrate, as shown below. Substrate oxidation is simplified in the following biochemical oxidation:

$$\underset{\text{substrate}}{C_wH_xO_yN_z} + a\underset{}{O_2} + \underset{\text{nitrogen source}}{bH_gO_hN_i} \longrightarrow \underset{\text{biomass}}{cCH_\alpha O_\beta N_\delta} + dCO_2 + eH_2O \tag{9.2.1}$$

About 95% of *Escherichia coli* is C, H, O and N. The chemical formula for cell composition and the stoichiometric coefficients in (9.2.1) depend on media composition and the environment surrounding the cell.[2,4] All the major elements in the above equation have to be balanced. Then the stoichiometric coefficients are identified by solving simultaneously the system of equations:

C balance: $w = c + d$
H balance: $x + bg = c\alpha + 2e$
O balance: $y + 2a + bh = c\beta + 2d + e$
N balance: $z + bi = c\delta$

Notice that we have five unknown coefficients (a, b, c, d and e) but four equations. This means we need an additional equation to solve a system of five equations with five unknowns. An important and measurable parameter in a living system is the respiration quotient (RQ), which is defined as moles of CO_2 produced per mole of O_2 uptake.[1,2]

$$\text{Respiratory quotient (RQ)} = \frac{\text{Moles of } CO_2 \text{ produced}}{\text{Moles of } O_2 \text{ consumed}} = \frac{d}{a} \tag{9.2.2}$$

The chemical composition of strains of microorganisms depends on the chemical composition of the media. Even for single strains of organisms such as *E. coli* grown in different media, the fractional composition of C, N, O and H are different if the media compositions are different.[2,5] There are a few environmental factors known as growth-rate limitations which affect cell growth and environmental condition. If a specific nutrient in the medium is suddenly increased, does the growth rate of the cell increase? At first, it is necessary to elaborate a brief discussion about sources needed for microbial growth, then respond directly to the points. Often the composition of the media is based on a single component that is growth-rate limited. This means changing the concentration of the specified nutrient may influence cell growth, and depletion of the specified nutrient may retard the growth pattern. Growth can also be inhibited by the product formed. On the other hand, changing concentrations of components of the medium causes relatively insignificant changes in the alteration of the growth rate. In reality this may not be true because cell growth does not depend on a single substrate; even growth of cells is extended on yeast extracts. Cell metabolism is not limited to carbohydrate catabolism: fats, lipids and proteins are involved in the generation of energy for biosynthesis. The elemental composition of selected microorganisms can be defined as:[2,4]

Escherichia coli: $CH_{1.77}O_{0.49}N_{0.24}$
Saccharomyces cerevisiae: $CH_{1.64}O_{0.52}N_{0.16}$
Candida utilis: $CH_{1.83}O_{0.54}N_{0.10}$

When RQ is given, the stoichiometric coefficients can be solved simultaneously.[4,6]

9.3 ENERGY BALANCE FOR CONTINUOUS ETHANOL FERMENTATION

Saccharomyces cerevisiae is anaerobically grown in a continuous culture at 30°C. Glucose is used as substrate and ammonia as nitrogen source. A mixture of glycerol and ethanol is produced. At steady-state condition mass the flow rate is stated. The following reaction is proposed for the related bioprocess:[4,6]

$$\text{Glucose} + NH_3 \rightarrow \text{Biomass} + \text{Glycerol} + \text{Ethanol} + CO_2 + H_2O \tag{9.3.1}$$

The basis of the calculation is operation for 1 hour. Necessary data are presented in Table 9.1.

The energy balance is based on first law of thermodynamics:

$$\sum n_{in} h_{in} - \sum n_{out} h_{out} + (-\Delta H_{rxn}) = \delta Q - \delta W \tag{9.3.2}$$

TABLE 9.1. *Heat of combustion in fermentation process for production of glycerol and alcohol*

Component	Δh_c^o, kJ/gmol	Molecular mass	kJ/kg
Glucose	−2805.0	180	-1.558×10^4
NH_3	−382.6	14	-2.251×10^4
Glycerol	−1655.4	92	-1.799×10^4
Ethanol	−1366.8	46	-2.971×10^4

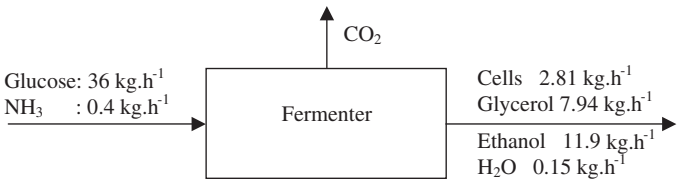

FIG. 9.1. Flow sheet for ethanol and glycerol fermentation.

Assume isothermal operation, and that no work done by the system. Then the first law simplifies to:

$$\delta Q = -\Delta H_{rxn} \tag{9.3.3}$$

Before energy balance is calculated, we need to make mass balance. Figure 9.1 shows the material balance for ethanol and glycerol fermentation. Put simply, mass into the system is equal to mass out of the system. The mass of carbon dioxide is calculated by adding mass of dry cell, mass of glycerol, mass of ethanol and mass of water at product stream and then subtracting the sum from the feed stream. As a result, the mass of carbon dioxide is defined. The heat of the reaction is calculated by the following equation:

$$\begin{aligned} -\Delta H_{rxn} &= \sum n_i h^o_{c,\text{products}} - \sum n_i h^o_{c,\text{reactants}} \\ -\Delta H_{rxn} &= 36(-1.558\times10^4) + 0.4\,(-2.251\times10^4) - 7.14\,(-1.799\times10^4) \\ &\quad -2.81(-2.12\times10^4) - 11.9(-2.971\times10^4) = -1.392\times10^4 \text{ kJ} \\ \text{Q} &= -1.392\times10^4 \text{ kJ} \end{aligned} \tag{9.3.4}$$

Since heat is generated as the system liberates energy, the above reaction is considered exothermic.

9.4 MASS BALANCE FOR PRODUCTION OF PENICILLIN

A batch process is customary for producing antibiotics. Submerged culture is used to propagate fungus with suitable carbohydrate resources. This assumption is based on simplicity in calculations and the normal use of penicillin in the pharmaceutical industry. Assume we

are required to produce antibiotic, one kilomole of penicillin G (334 kg) per batch. The general equation for the production of penicillin G and biomass is:

$$a\mathrm{C_6H_{12}O_6} + b\mathrm{H_2SO_4} + c\mathrm{NH_3} \rightarrow d\mathrm{C_{16}H_{18}O_4N_2S} + e\mathrm{CO_2} + f\mathrm{H_2O} + g\mathrm{C_4H_7O_3N} \quad (9.4.1)$$

Our next assumption is related to process yield: yields of product and biomass are 20% and 50%, respectively ($Y_{P/S} = 0.2$, $Y_{X/S} = 0.5$). Moles of penicillin G produced are based on a stoichiometric relation as given in (9.4.1).

$$d = \frac{334\ \text{kg}}{334\dfrac{\text{kg}}{\text{kmol}}} = 1\ \text{kmol}$$

Also, moles of glucose needed in penicillin production are based on a stoichiometric relation:

$$a = \frac{334\ \text{kg penicillin G}}{0.2\dfrac{\text{kg penicillin G}}{\text{kg glucose}} \times 180\dfrac{\text{kg}}{\text{kmol}}} = 9.28\ \text{kmol}$$

The third product is cell biomass. Moles of biomass produced is given by:

$$g = \frac{0.5 \times (9.28\ \text{kmol glucose}) \times 180\dfrac{\text{kg}}{\text{kmol}}}{117\dfrac{\text{kg}}{\text{kmol}}} = 7.14\ \text{kmol}$$

Moles of the remaining components are found using elemental balance. The method has been discussed, so now we make a balance for each element.

N balance: $c = (2 \times d) + (1 \times g)$
S balance: $b = 1 \times d$
C balance: $(6 \times a) = (16 \times d) + (1 \times e) + (4 \times g)$
Overall balance: $(180 \times a) + (98 \times b) + (17 \times c)$
$= (334 \times d) + (44 \times e) + (18 \times f) + (117 \times g)$

The known variables are substituted into the equations to get values for c, b, e and f. Upon solving the above equations simultaneously, the unknown coefficients are obtained.

Moles of ammonia required:

$$c = 9.14\ \text{kmol}$$

Moles of sulphuric acid required:

$$b = 1\ \text{kmol}$$

Moles of carbon dioxide released:

$$e = 11.12 \text{ kmol}$$

Moles of water produced:

$$f = 14.73 \text{ kmol}$$

Therefore, the stoichiometric coefficients for the projected equation in production of penicillin G are:

$$9.28C_6H_{12}O_6 + H_2SO_4 + 9.14NH_3 \rightarrow C_{16}H_{18}O_4N_2S + 11.12CO_2 + 14.73H_2O + 7.14C_4H_7O_3N$$

The error for calculations of mass balance is less than 1%, negligible in fact, so the method is reliable and useful for process design.

$$\text{Error} = \frac{2090.84 - 2079.18}{2090.84} \times 100\% = 0.56\%$$

Material balance is carried out at the inlet and outlet of the fermenter, which is summarised in Table 9.2. Also, the density and mass fraction of the inlet and outlet of the fermenter are shown in Table 9.3.

Example 1

In a continuous wastewater treatment plant, 10^5 kg of cellulose and 10^3 kg of bacteria enter into the digestion unit as feed stream on a daily basis, while 10^4 kg of cellulose and 1.5×10^4 kg of bacteria leave in the effluent. The rate of cellulose digestion is 7×10^4 kg·day^{-1}. The bacterial growth rate is 2×10^4 kg·day^{-1}. The cell death rate by cell autolysis is 5×10^2 kg·day^{-1}. Do the material balance for cellulose and bacteria based on the given data.

TABLE 9.2. *Summary of material balance for inlet and outlet of the fermenter*

Substance	Inlet (kg)	Outlet (kg)
Glucose	1670.40	0.00
H_2SO_4	98.00	0.00
NH_3	155.38	0.00
Penicillin G	0.00	334.00
CO_2	0.00	489.28
Water	167.04	432.18
Biomass	0.00	835.38
Total	2079.18	2090.84

TABLE 9.3. *Density and mass fraction of inlet and outlet of the fermenter*

Substance	Density, kg/m^3	Inlet (kg)	Outlet (kg)	Mass fraction	
				Inlet	Outlet
Glucose	1544	1670.40	0.00	0.80	—
H_2SO_4	1834	98.00	0.00	0.05	—
NH_3	597.1	155.38	0.00	0.07	—
Penicillin G	3420	0.00	334.00	—	0.16
CO_2	110.1	0.00	489.28	—	0.23
Water	1000	167.04	432.18	0.08	0.21
Biomass	1013	0.00	835.38	—	0.40
Total		2079.82	2090.84	1.00	1.00

Solution

Basis: 1 day operation

Cellulose Balance

Cellulose in the wastewater stream is not generated but it is consumed and biomass produced by the microbial population as a substrate for energy.

[Cellulose in] – [cellulose out] + [cellulose generation] − [cellulose consumption] = [cellulose accumulation]

$$10^5 - 10^4 + 0 - 7\times10^4 = 20{,}000 \text{ kg cellulose}$$
$$\text{In} - \text{Out} + \text{Generation} - \text{Consumption} = \text{Accumulated cellulose}$$

Biomass Balance

Applying the same concept for mass balance, the mass of sludge accumulated is:

Cell in – cell out + growth rate − death rate = cell accumulation

$$10^3 - 1.5\times10^4 + 2\times10^4 - 5\times10^2 = 5{,}500 \text{ kg bacteria}$$
$$\text{In} - \text{Out} + \text{Generation} - \text{Consumption} = \text{Accumulated cells}$$

9.5 CONSERVATION OF MASS PRINCIPLE

Based on the law of conservation of mass, mass is neither created nor destroyed, except in nuclear reactions. Therefore, in a definite system, mass in is equal to mass out.

Example 1

Humid air with O_2 is prepared for a gluconic acid fermentation. The humid air has been prepared by a special humidification chamber where 1.5 l/h of liquid water enters; at the same

time dry air and 15 mol/min dry O_2 enters the chamber. The exiting gas stream contains 1% (w/w) water. Draw and label the flow sheet and do the material balance for the humidifier.

Solution

The air humidification flow diagram for material balance is shown in Figure 9.2. The mass flow rate for water into the humidification unit is:

$$1.5\,\frac{\text{litre}}{\text{h}} \times \frac{10^3\ \text{g}}{1\ \text{litre}} \times \frac{1\ \text{h}}{60\ \text{min}} = 25\ \text{g/min}\ H_2O$$

The mass flow rate for dry oxygen is:

$$15\,\frac{\text{gmol}}{\text{min}} \times \frac{32\ \text{g}}{\text{gmol}} = 480\ \text{g/min}\ O_2$$

Basis of calculation: 1 min

Water Balance

Mass of water in is equal to mass of water out, since the enriched air with oxygen should have only 1% humidity. Therefore the mass of humid air can be calculated as tie element.

$$25 = 0.01 m_4$$
$$\Rightarrow m_4 = 2500\ \text{g Humid rich air with}\ O_2$$

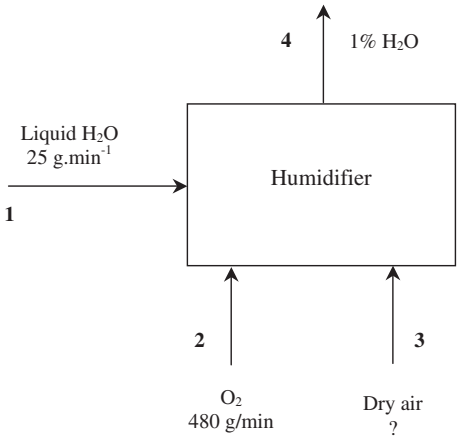

FIG. 9.2. Flow diagram for oxygen enrichment and air humidification.

Overall Material Balance

Total mass in is equal to total mass out.

$$m_1 + m_2 + m_3 = m_4$$
$$2500 = 25 + 480 + m_3$$
$$\Rightarrow m_3 = 1995 \text{ g}$$

The mass flow rate of dry air in is 1995 g/min.

Example 2

A fermentation broth containing *Streptomyces kanamyceticus* cells is filtered by a vacuum rotary filter. The feed rate is 120 kg·h^{-1}; each kilogram of broth contains 60 g of cells. To improve filtration, filter aids are added at a rate of 10 kg·h^{-1}. The concentration of kanamycin in the broth is 0.05%. The filtrate is collected at a rate of 112 kg·h^{-1}. The concentration of kanamycin in the filtrate is 0.045%. The filter cake contains cells, and filter aid is continuously removed from the filter cloth.

(a) What is the moisture content in the filter cake?
(b) If the concentration of kanamycin in the filter cake is the same as in the filtrate, how much kanamycin is absorbed per kilogram of filter aid?

Solution

Basis 1 hour operation.

The simplified flow diagram of continuous filtration with stream lines of material balance is shown in Figure 9.3. Mass in is equal to mass out.

$$120 + 10 = 112 + \text{M filter cake}$$
$$\text{M filter cake} = 18 \text{ kg·h}^{-1}$$

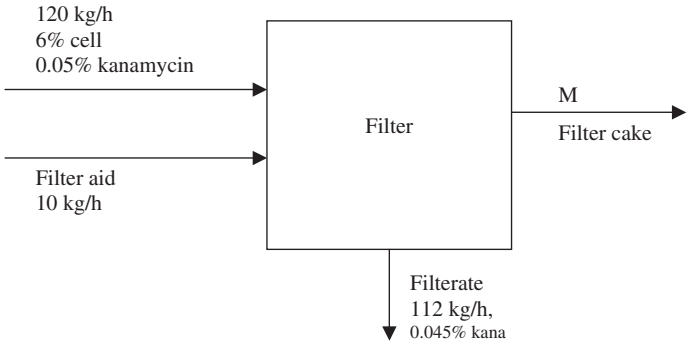

FIG. 9.3. Flow sheet for continuous filtration.

H_2O Balance

Mass of water at inlet streams is equal to mass of water at the filterate and filter cake.

$$120[(1-0.06)-0.0005] = 112.74 \text{ kg}$$
$$= 112\ (1-0.00045) + \text{cake moisture}$$

M (H_2O in the filter cake) = 0.79

The filter cake moisture content is calculated as:

$$\frac{0.79}{18} \times 100 = 4.4\% \text{ moisture}$$

The mass of water in the filtrate is $112 - 0.05 = 111.95$ kg
Amount of kanamycin in the moisture = 0.79 (0.00045)
$= 3.6 \times 10^{-4}$ kg

Kanamycin Balance

Mass of kanamycin in is equal to mass of kanamycin out.

$$0.0005 \times 120 = (112)(0.00045) + (0.79)(0.00045) + M_{\text{k.abs.}}$$
$$M_{\text{k.abs.}} = 0.06 - 0.05075 = 9.245 \times 10^{-3} \text{ kg}$$

Kanamycin absorbed per kilogram filter aid $= \dfrac{9.245}{10} = 9.245 \times 10^{-4}$ kg/kg

Various sources of carbohydrate are used in the fermentation processes. Molasses and corn steep are the most common carbon sources used to generate energy for biosynthesis. Having the correct composition and desired concentration is a necessary task in actual experimental work.

Example 3

Corn steep liquor contains 2.5% invert sugars and 50% water. The rest of the feed is considered as residual solids. Beet molasses containing 50% sucrose, 1% invert sugar, 18% water and remainder solids are mixed with corn steep liquor in a mixing tank. Water is added to produce a diluted mixture with 2% invert sugar, 125 kg corn steep liquor and 45 kg molasses, which is fed into an enzymatic hydrolysis tank.

(a) How much water is required?
(b) What is the concentration of sucrose in the final mixture?

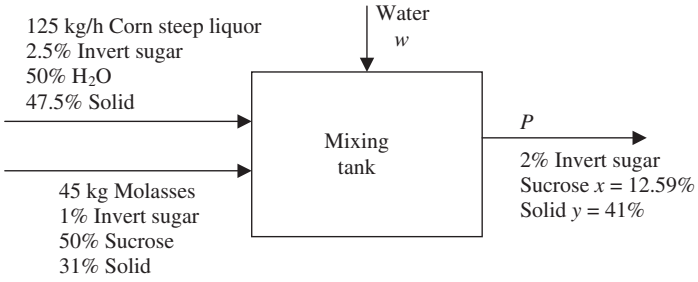

FIG. 9.4. Flow sheet for diluting sugar and mixing tank.

Solution

A flow diagram for diluting carbohydrates, corn steep liquor and molasses in the mixing tank is shown in Figure 9.4.

Mass Balance

Let us assume mass in is equal to mass out.

$$125 + 45 + W = P$$

Now we can balance the invert sugar:

$$(0.025 \times 125) + (0.01 \times 45) = 0.02\ P$$
$$P = 178.75\,\text{kg}$$
$$W = 8.75\,\text{kg}$$

The next step is to take sucrose into the balance:

$$(0.5)(45) = (x)(P)$$
$$(0.5)(45) = 178.75x$$

The concentration of sucrose in the product mixture is $x = 0.1259$ or 12.59% of product. The residual solids in corn steep, molasses and the diluted mixture are also balanced.

$$(0.31)(45) + (0.475)(125) = 178.75y$$
$$y = 0.41$$

The amount of solid in the product mixture is 41%.

9.5.1 Acetic Acid Fermentation Process

In fermentation for the production of acetic acid, ethyl alcohol is used in an aerobic process. In an ethanol oxidation process, the biocatalyst *Acetobacter aceti* was used to convert ethanol to acetic acid under aerobic conditions. A continuous fermentation for vinegar production was proposed for utilisation of non-viable *A. aceti* immobilised on the surface of alginate beads.

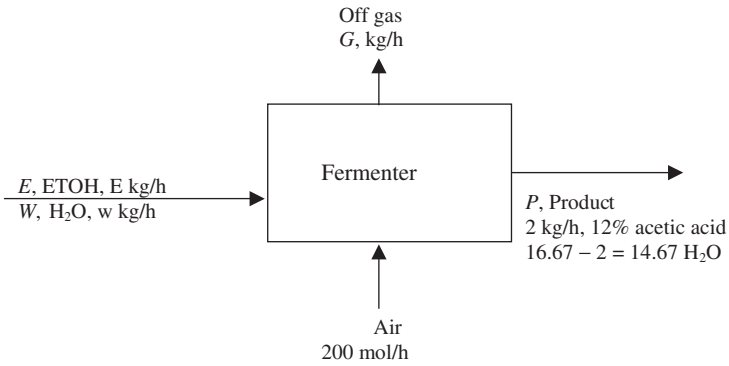

FIG. 9.5. Flow sheet for acetic acid production.

Example 1

The production rate of acetic acid was $2\,kg{\cdot}h^{-1}$, where the maximum acetic acid concentration was 12%. Air was pumped into the fermenter with a molar flow rate of $200\,mol{\cdot}h^{-1}$. The chemical reaction is presented in (E. 1.1) and flow diagram in Figure 9.5. Determine the minimum amount of ethanol intake and identify the required mass balance for the given flow sheet. The ethanol biochemical oxidation reaction using *A. aceti* is:

$$\underset{\text{Ethanol}}{C_2H_5OH + O_2} \xrightarrow[A.\ aceti]{} \underset{\text{Acetic acid}}{CH_3COOH + H_2O} \qquad \text{(E. 1.1)}$$

The process flow diagram for fermentation of ethyl alcohol is shown in Figure 9.5. Assuming steady-state condition and that the air intake has no moisture, volume and molar fractions are about the same, ethanol is not going to vapourize while fermentation is taking place. Assume the only biochemical reaction takes place is acetic acid production, which means ethanol is not used for maintenance or ATP generation. No side reactions occur. Relative molecular masses are: ethanol 46, acetic acid 60, oxygen 32, water 18 g/mol. Also, air consists of 21% oxygen and 79% nitrogen.

Solution

The basis for calculation is 1 hour operation and 2 kg acetic acid produced.

Mass flow rate of air: $(0.2\,kgmol/h)(28.84\,kg/kgmol) = 5.768\,kg{\cdot}h^{-1}$
Mass flow rate of O_2: $0.2 \times 0.21 \times 32 = 1.344\,kg{\cdot}h^{-1}$
Mass flow rate of N_2: $0.2 \times 0.79 \times 28 = 4.424\,kg{\cdot}h^{-1}$
Sum of $O_2 + N_2$: $1.344\,kg{\cdot}h^{-1} + 4.424\,kg{\cdot}h^{-1} = 5.768\,kg{\cdot}h^{-1}$

The product stream with 12% acetic acid has a mass flow rate of:

$$P = \frac{2}{0.12} = 16.67 \text{ kg}\cdot\text{h}^{-1}$$

Moles of acetic acid:

$$\frac{2 \text{ kg}}{60 \text{ kgmol/kg}} = 3.333 \times 10^{-2} \text{ kgmol}$$

From the reaction stoichiometry, for each mole of acetic acid one mole of oxygen was used. So the equal molar oxygen consumption is:

$$(3.333 \times 10^{-2})(32) = 1.067 \text{ kg } O_2 \text{ consumed}$$
$$\text{Excess amount of } O_2 = 1.344 - 1.067 = 0.277 \text{ kg}\cdot\text{h}^{-1}$$

The off gas stream consists of all inlet nitrogen plus excess oxygen.

Off gas, G is the sum of excess oxygen plus inert nitrogen.

$$G = N_2 + \text{excess } O_2 = 4.424 + 0.277 = 4.701 \text{ kg}$$
$$\text{Off gas composition is } 0.277/4.701 = 0.059, 5.9\% \ O_2 \text{ and } 94.1\% \ N_2$$

Water Balance

The sum of water at the inlet stream and water generated by the chemical reaction is equal to water at outlet stream.

$$H_2O \text{ in} + H_2O \text{ generated} = H_2O \text{ out}$$

Mass of H_2O generated: $(3.333 \times 10^{-2})(18 \text{ kg/kgmol}) = 0.6 \text{ kg}$
Water at inlet stream: $14.67 \text{ kg} - (0.6 \text{ kg}, H_2O \text{ generated}) = 14.07 \text{ kg}$

Ethanol Balance

Ethanol at concentration at the inlet plus ethanol generated is equal to ethanol in outlet stream as unreacted reactant plus ethanol consumed. For each mole of acetic acid, one mole of ethanol was utilised. The mass of ethanol used up is:

$$\text{Mass of ETOH consumed} = (3.333 \times 10^{-2})(46 \text{ kg/kgmol}) = 1.533 \text{ kg ETOH}$$

Assume all the ethanol (100%) was taken by the bacteria and that there was no ethanol generation or evaporation. This means ethanol in is equal to ethanol consumed in oxidation process.

$$\text{Ethanol in} = \text{ethanol consumed} = 1.533 \text{ kg ETOH}$$

9.5.2 Xanthan Gum Production

Example 1

Xanthan gum is produced using *Xanthomonas campestris* in a batch culture. Laboratory experiments have shown that for each gram of glucose utilised by the bacteria, 0.23 g oxygen and 0.01 g ammonia are consumed while 0.75 g gum, 0.09 g cells, 0.27 g gaseous CO_2 and 0.13 g H_2O are formed. Other components such as phosphate can be neglected. A medium containing glucose and ammonia dissolved in 20,000 litres of water is pumped into the CSTR fermenter and inoculated with *X. campestris*. Air is pumped; the off gas recovered during the entire batch is 1250 kg. The final gum concentration is 3.5 wt%. What is the percentage of excess air, and how much glucose and ammonia are required?

Reaction stoichiometry per unit mass of glucose:

$$1\text{ g glucose} + 0.23\text{ g } O_2 + 0.01\text{ g } NH_3 \rightarrow 0.75\text{ g gum} + 0.09\text{ g cells} + 0.27\text{ g } CO_2 + 0.13\text{ g } H_2O$$

Solution

Figure 9.6 shows the schematic diagram for production of xanthan gum with inlet and outlet streams.

Overall Mass Balance

$$F + A = 1250 + P$$

The amount of glucose required is:

$$1\text{ kg glucose} \times \left(\frac{0.035P}{0.75\text{ g gum}}\right) = 0.0467P\text{ kg glucose}$$

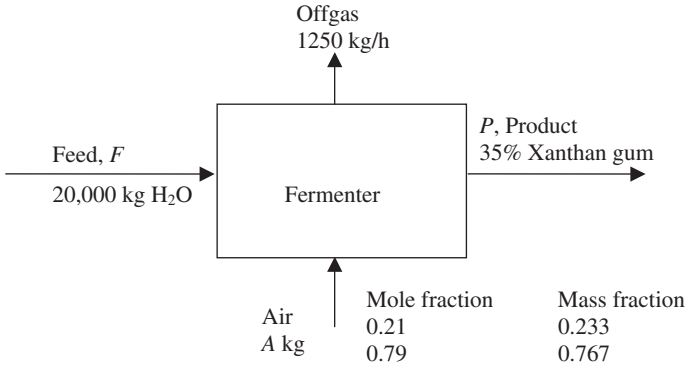

FIG. 9.6. Flow sheet for xanthan gum production.

The mass oxygen based on reaction stoichiometry is:

$$0.23 \text{ kg } O_2 \times \left(\frac{0.035P}{0.75 \text{ g gum}} \right) = 0.0107P \text{ kg } O_2$$

The amount of ammonia needed is:

$$0.01 \text{ kg } NH_3 \times \left(\frac{0.035P}{0.75 \text{ g gum}} \right) = 0.00047P \text{ kg } NH_3$$

Products

Mass of cell with respect to mass of product stream is:

$$0.09 \text{ kg cells} \times \left(\frac{0.035P}{0.75 \text{ g gum}} \right) = 0.0042P \text{ kg cells}$$

The mass of carbon dioxide generated is:

$$0.27 \text{ kg } CO_2 \times \left(\frac{0.035P}{0.75 \text{ g gum}} \right) = 0.0126P \text{ kg } CO_2$$

The amount of water according to reaction stoichiometry is:

$$0.13 \text{ kg } H_2O \times \left(\frac{0.035P}{0.75 \text{ g gum}} \right) = 0.00607P \text{ kg } H_2O$$

O_2 Balance

The mass of oxygen in the inlet air stream is equal to oxygen consumed and the excess oxygen leaving the outlet stream.

$$0.233A = O_2 \text{ out} + 0.0107PO_2 \text{ used}$$

The outlet stream

$$O_2 \text{ out} = 0.233A - 0.0107P$$

N_2 Balance

Mass of nitrogen at the inlet is equal to mass of nitrogen in the outlet steam.

$$0.707A = N_2 \text{ out}$$

Mass of carbon dioxide generated is equal to mass of CO_2 at the outlet stream.

CO_2 out = CO_2 generated = $0.0126P$

Off Gas Balance

$$1250 = (0.233A - 0.0107P) + 0.767A + 0.0126P$$
$$O_2 = N_2 - CO_2$$
$$1250 = A + 1.9 \times 10^{-3}P$$

Mass of air is:

$$A = 1250 - 0.0019P$$
$$\bar{m} = (0.0467 + 0.00047)/P + 20{,}000$$
$$20{,}000 + 0.04717P + A = 1250 + P$$

Substitute A into the above equation, then solve for P:

$$20{,}000 + (1250 - 0.0019P) = 0.9528P + 1250$$
$$P = 20{,}949\,\text{kg}$$

Now replace P in the above equation, then solve for A:

$$A = 1250 - 0.0019(20{,}949) = 1210.2\,\text{kg}$$

Now solve for $\bar{m}$:

$$\bar{m} = 20{,}988.2\ \text{kg}$$
$$P = 87.986\,\text{kg cells} + 263.96\,\text{kg } CO_2 + 127.1\,\text{kg } H_2O$$
$$\text{Off gas} = 57.8\,\text{kg } O_2 + 928.2\,\text{kg } N_2 + 263.96\,\text{kg } CO_2$$
$$\text{Excess air} = \frac{57.8}{224.15} \times 100 = 25.8\% = \frac{57.8}{0.0107(20949)} \times 100$$

9.5.3 Stoichiometric Coefficient for Cell Growth

Stoichiometric coefficients for cell growth for the production of SCP from hexadecane is given by the following reaction:

$$\underset{\text{Substrate}}{C_{16}H_{34} + aO_2 + bNH_3} \rightarrow \underset{\text{Biomass (SCP)}}{cCH_{1.66}O_{0.27}N_{0.2} + dCO_2 + eH_2O} \tag{9.9}$$

where $CH_{1.66}O_{0.27}N_{0.2}$ represents the chemical composition of cell biomass.

Example 1

Based on the stoichiometric relation of the above equation for SCP production, if RQ = 0.43, find the stoichiometric coefficients *a, b, c, d* and *e* in (9.9).

Solution

C balance: $16 = c + d \Rightarrow d = 16 - c$
H balance: $34 + 3b = 1.66c + 2e$
O balance: $2a = 0.27c + 2d + e$
N balance: $b = 0.2c$
RQ: $0.43 = d/a \Rightarrow d = 0.43a$
$d = 0.43a = 16 - c$

Substituting and Rearranging:

$$34 + 0.6c = 1.66c + 2e$$
$$2a = 0.27c + 2(16 - c) + e \quad 2a = 0.27c + 32 - 2c + e$$
$$74.4 - 4.65c + 2c - 0.27c = 32 + e$$
$$2\,(e + 2.92c = 42.4) \qquad c = 10.63$$
$$\Rightarrow$$
$$-\,(2e + 1.06c = 34) \qquad d = 5.37$$
$$a = 12.49$$
$$b = 2.13$$
$$e = 2\,(12.49) + 0.27\,(10.63) - 2\,(5.37) = 11.37$$

Therefore the exact stoichiometric coefficients for the above reaction are:

$$C_{16}H_{34} + 12.5O_2 + 2.13NH_3 \rightarrow 10.63CH_{1.66}O_{0.27}N_{0.2} + 5.37CO_2 + 11.4H_2O$$

9.6 EMBDEN–MEYERHOFF–PARNAS PATHWAY

The metabolic pathway for bacterial sugar fermentation proceeds through the Embden–Meyerhof–Paranas (EMP) pathway. The pathway involves many catalysed enzyme reactions which start with glucose, a six-carbon carbohydrate, and end with two moles of three carbon intermediates, pyruvate. The end pyruvate may go to lactate or be converted to acetyl CoA for the tricarboxylic acid (TCA) cycle. The fermentation pathways from pyruvate and the resulting end products are shown in Figures 9.7 and 9.8.

The overall reaction of glucose catabolism to lactate and acetate fermentation from 2 moles of glucose yields 2 moles of lactic acid, 3 moles of acetic acid and 5 moles of ATP, as shown below:

$$2C_6H_{12}O_6 \rightarrow 2 \text{ lactic acid} + 3 \text{ acetic acid} + 5 \text{ ATP} \qquad (9.6.1)$$

Reactions involve several enzymes, which have to follow in sequence for lactic acid and alcohol fermentation. This is known as the glucose catabolism pathway, with emphasis on energetic and energy carrier molecules such as ATP, ADP, NAD^+ and NADH. In this pathway the six-carbon substrate yields two three-carbon intermediates, each of which passes through a sequence of reactions to the stable end product of pyruvic acid.

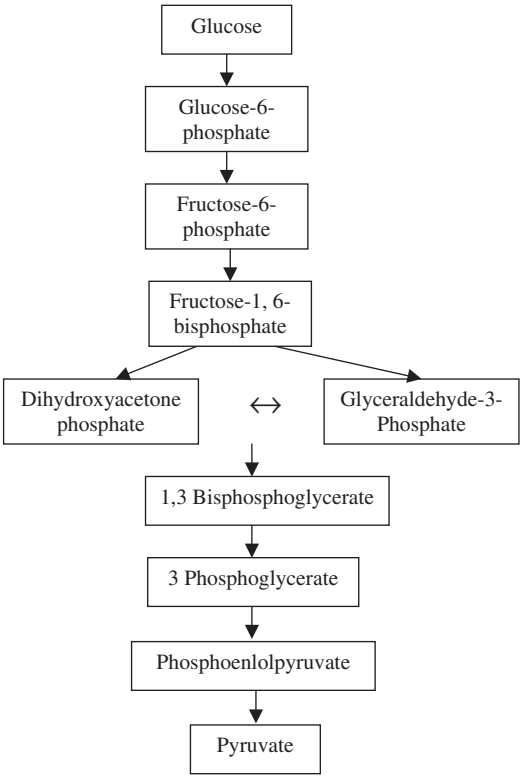

FIG. 9.7. Glyconeogenesis in the Embden–Meyerhoff–Parnas pathway.

Example 1

There was an old and outdated fermenter in our school warehouse. The dean of the school wished the equipment to be used for undergraduate students to learn about bioprocess concepts. The technician ran the equipment was experimentally but he forgot to weigh the glucose carbon source and did not analyse for ethanol. The product stream was analysed as follows: lactic acid 10 moles, acetic acid 5 moles, carbon dioxide 15 moles and hydrogen 10 moles. It was expected that sugar was oxidised, then converted to pyruvic acid, then proceeded though the Embden–Meyerhof–Parnas pathway. No other products except ethanol were formed. The problem was adjusted by pH control and restarting the process without any contamination. How many moles of ethanol were in the waste product stream? The overall biological reaction is summarised as:

$$a\mathrm{C_6H_{12}O_6} + b\mathrm{H_2O} \rightarrow c\mathrm{CH_3CH_2OH} + 10\mathrm{CH_3CH(OH)COOH} + 5\mathrm{CH_3COOH} + 15\mathrm{CO_2} + 10\,\mathbf{H_2} \quad \text{(E. 1.1)}$$

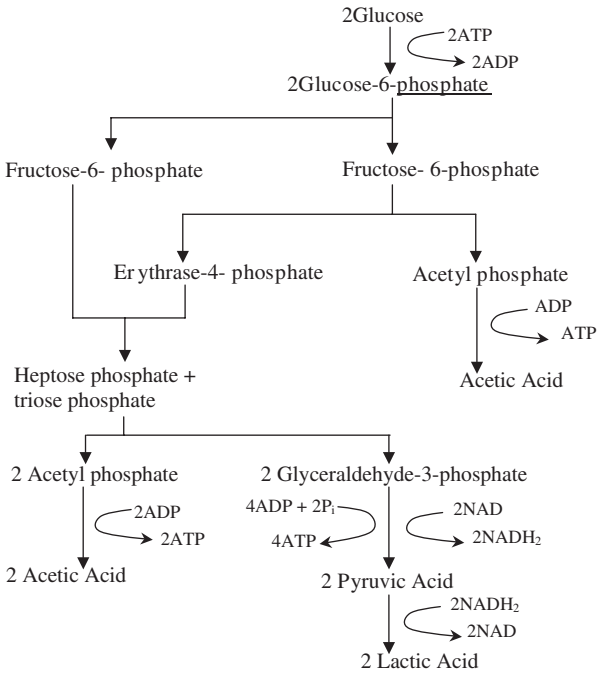

FIG. 9.8. Fermentation of glucose to acetate or lactate via the Embden–Meyerhoff–Parnas pathway.

Carbon balance: $6a = 2c + 30 + 10 + 15$
Hydrogen balance: $12a + 2b = 6c + 60 + 20 + 20$
Oxygen balance: $6a + b = c + 30 + 10 + 30$

$$\begin{cases} 6a - 2c = 55 \\ 12a + 2b - 2c = 100 \\ 6a + b - c = 70 \end{cases}$$

Multiplying the first equation with a negative sign gives:

$$\begin{cases} -2c = -6a + 55 \\ 12a + 2b - 2c = 100 \\ 6a + b - c = 70 \end{cases}$$

$$\begin{cases} 12a + 2b \;\; 3 \times 6a + 3 \times 55 = 100 \\ 12a + 2b \;\; 6a + 55 = 140 \end{cases}$$

$$\begin{cases} -6a + 2b = -65 \\ 6a + 2b = 85 \end{cases}$$

Solving the above equation for b, yields:

$$+4b = +2$$
$$b = 5$$
$$a = 12.5$$
$$c = \frac{6a - 55}{2}$$
$$c = 10$$

The defined equation is:

$$12.5C_6H_{12}O_6 + 5H_2O \rightarrow 10CH_3CH_2OH + 10CH_3CH(OH)COOH + 5CH_3COOH + 15CO_2 + 10H_2$$

Example 2

Assume that the cells can convert 67% of carbon source to biomass. Hexadecane and glucose are used as carbon sources. Calculate the stoichiometric coefficients of the following reactions:

$$C_{16}H_{34} + \alpha_1 O_2 + \alpha_2 NH_3 \rightarrow \beta_1(C_{4.4}H_{7.3}N_{0.86}O_{1.2}) + \beta_2 CO_2 + \beta_3 H_2O \quad \text{(E. 2.1)}$$

Solution

Figure 9.9 shows the flow sheet for stoichiometry and material balance in a cell. According to the problem, two thirds of the carbon source goes to biomass.

$$\frac{2}{3}(16) = 4.4\beta_1$$

Therefore:

$$\beta_1 = 2.424$$

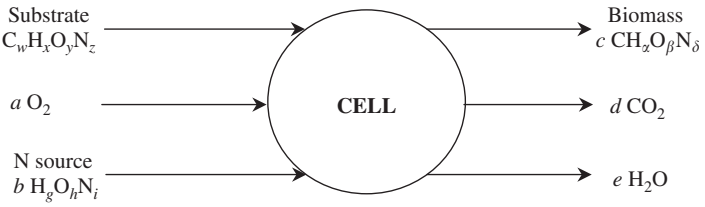

FIG. 9.9. Flow sheet for stoichiometry and material balance in a cell.

The reminder of carbon source, one third, goes to carbon dioxide

$$\frac{1}{3}(16) = \beta_2 = 5.333$$

Nitrogen balance: $\alpha_2 = 0.86\ \beta_1 = 2.085$
H_2 balance: $34 + 3\alpha_2 = 7.3\ \beta_1 + 2\beta_3$
$34 + 3(2.085) - 7.3(2.424) = 2\beta_3$
$\beta_3 = 11.28$

O_2 balance: $2\alpha_1 = 1.2\beta_1 + 2\beta_2 + \beta_3$
$= 1.2(2.424) + 2(5.333) + 11.28$
$\alpha_1 = 12.43$

Glucose oxidation to SCP:

$$C_6H_{12}O_6 + \alpha_1'O_2 + \alpha_2'NH_3 \rightarrow \beta_1'(C_{4.4}H_{7.3}N_{0.86}O_{1.2}) + \beta_2'CO_2 + \beta_3'H_2O \quad \text{(E. 2.2)}$$

$$\text{C balance: } \frac{2}{3}(6) = 4.4\beta_1$$

$$\beta_1' = 0.909$$

$$\frac{1}{3}(6) = \beta_{21} = 2.0$$

$$N_2 \text{ balance: } \alpha_2' = 0.86\beta_1' = 0.78$$

$$H_2 \text{ balance: } 12 + 3\alpha_1' = 7.3\beta_1' + 2\beta_3'$$

$$12 + 3(0.78) = 7.3\ (0.909) + 2\beta_3'$$

$$\beta_3' = 3.85$$

$$O_2 \text{ balance: } 6 + 2\alpha_1' = 1.2\beta_1' + 2\beta_2' + \beta_3'$$

$$2\alpha_1' = 1.2(0.909) + 2 \times 2 + 3.85 - 6$$

$$\alpha_1' = 1.47$$

Cells are able to utilise chemical energy very efficiently. Like any actual process, energy retained in the substrate is released as heat.

Example 3

From the above biomass production, calculate the yield coefficients. Based on definition, the yield of biomass on glucose means how much biomass is produced per gram of glucose utilised in a cell. The yield of biomass on glucose is calculated as follows:

$$Y_{X/S} = \frac{\text{Biomass}}{\text{Glucose}} \tag{E. 3.1}$$

$$Y_{X/S} = \frac{0.909(4.4\times12 + 7.3 + 0.86\times14 + 1.2\times16)}{180}$$

$$Y_{X/S} = \frac{83.03}{180} = 0.46 \text{ g cell/g glucose}$$

The yield of biomass produced per gram of oxygen consumed is:

$$Y_{X/O_2} = \frac{83.03}{2\times1.47\times16} = 1.76 \text{ g cells/g oxygen}$$

Cells utilise energy from substrate in an efficient way, like a real chemical process. Some of the energy is released as heat. The generated metabolic heat has to be removed from the bioreactor; the temperature must be controlled for optimal cell growth. Also, the liberated heat is proportional to cell growth. The yield factor Y_Δ is defined as grams of cell produced per kilocalorie of heat evolved. This is analogous to yield of biomass to substrate and heat combustion of substrate and cell, ΔH_s, and ΔH_c, respectively. The following equation relates the yield factor to the yield of biomass and the net heat evolved resulting from cell growth.

$$Y_\Delta = \frac{Y_{X/S}}{\Delta H_s - Y_{X/S}\Delta H_c} \tag{E. 3.2}$$

Given heat of combustion of sugar:

$$\Delta H_S = \frac{673 \text{ kcal/mol}}{180} = 3.74 \text{ kcal/g biomass}$$

Heat of combustion of cell:

$\Delta H_C = 5.8$ kcal/g dry cell mass

Now substitute the values into (E. 3.2) to obtain the yield factor.

$$Y_{\Delta} = \frac{0.46}{3.74 - 0.46 \times 5.8} = 0.43 \text{ kcal/g biomass}$$

The yield of biomass to substrate for hexadecane is obtained.

$$Y_{X/S} = \frac{2.424(91.34)}{226} = 0.988 \text{ g cell/g glucose}$$

The molecular mass of $C_{16}H_{34}$ is 226.

$$Y_{X/O_2} \frac{221.4}{12.43 \times 32} = 0.56 \text{ g cell/g } O_2$$

$$Y_{\Delta} = \frac{0.988}{11.2 - 0.988 \times 5.8} = 0.18 \text{ g cell/g glucose}$$

ΔH_S is the possible heat evolved from oxidation of hexadecane.

Example 4

Citric Acid Production in Solid State Fermentation

Citric acid is manufactured by submerged cultures of *Aspergillus niger* in a batch reactor operated at 30 °C. For an incubation period of 2 days, 2500 kg glucose and 860 kg oxygen were consumed to produced 1500 kg citric acid, 500 kg biomass and other by-products. Ammonia was used as nitrogen source. Power input to the system by mechanical agitation was about 15 kW. Approximately 100 kg of water evaporated during the 2 day operation. Estimate the energy for cooling requirements.

Solution

Figure 9.10 shows the flow diagram for production of citric acid in solid-state fermentation. The basis of calculation is 1500 kg citric acid.

$\Delta H_{\text{evap., } H_2O}$ at 30 °C, steam table = 2430.7 kJ/kg
Heat of reaction at 30 °C = −460 kJ/(mol O_2 used)

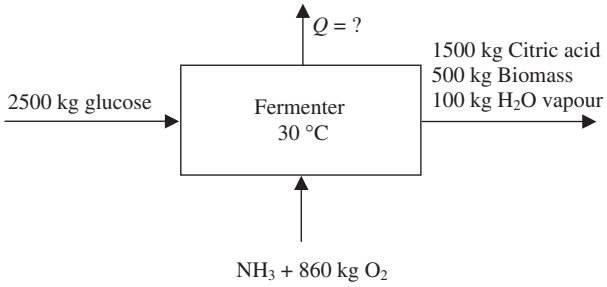

FIG. 9.10. Flow sheet for citric acid in solid-state fermentation.

Fermentation reaction:

$$\text{Glucose} + \text{NH}_3 + \text{O}_2 \rightarrow \text{Biomass} + \text{CO}_2 + \text{H}_2\text{O} + \text{Citric acid} \qquad \text{(E. 4.1)}$$

Mass is balanced at the beginning and the end of process. The evaporated water in solid-state fermentation may not be required for energy balance.

$$\text{Mass}_{\text{beginning}} = \text{Mass}_{\text{end}} + \text{H}_2\text{O}_{\text{vap}}$$

The first law of thermodynamics is valid for the energy balance.

$$-\Delta H_{rxn} - \text{m}_{\text{H}_2\text{O}}\,\Delta H_{\text{evap}} = \delta Q - \delta W \qquad \text{(E. 4.2)}$$

$$-\Delta H_{rxn} = (-460)(861\text{ kg})(1000\text{ g/kg})(1\text{ gmol}/32\text{ g}) = -1.24 \times 10^7\text{ kJ}$$

Heat lost by vaporisation of 100 kg H_2O

$$m_{\text{v}}\,\Delta H_{\text{evap}} = (100\text{ kg})(2430.7) = 2.43 \times 10^5\text{ kJ}$$

Mechanical work:

$$W_{\text{s}} = (15\text{ kW})(\text{kJ/s}/1\text{ kW})(2\text{ days})(24\text{ hours/day}) = 2.59 \times 10^6\text{ kJ}$$

$$\text{Q} = 1.24 \times 10^7 - 2.43 \times 10^5 + 2.59 \times 10^6 = 1.47 \times 10^7\text{ kJ (removed heat)}$$

REFERENCES

1. Aiba, S., Humphrey, A. E. and Millis, N. F., "Biochemical Engineering", 2nd edn. Academic Press, New York, 1973.
2. Baily, J.E. and Ollis, D.F., "Biochemical Engineering Fundamentals", 2nd edn. McGraw-Hill, New York, 1986.
3. Blanch, H.W. and Clark, S.D., "Biochemical Engineering". Marcel Dekker, New York, 1996.
4. Doran, P.M., "Bioprocess Engineering Principles". Academic Press, New York, 1995.
5. Shuler, M.L. and Kargi, F., "Bioprocess Engineering, Basic Concepts". Prentice-Hall, New Jersey, 1992.
6. Ghose, T.K., "Bioprocess Computation in Biotechnology", vol. 1. Ellis Horwood Series in Biochemistry and Biotechnology, New York, 1990.

CHAPTER 10

Application of Fermentation Processes

10.1 INTRODUCTION

In World War I, Germany needed to synthesise glycerol for manufacturing explosives. It was found that glycerol was generated in alcoholic fermentation. Nearberg discovered that the addition of sodium bisulphite to the fermentation broth was favoured and enhanced the production of glycerol at the expense of ethanol. German scientists quickly developed industrial-scale fermentation with a yield capacity of 1000 tons of glycerol per month.[1,2]

Ethanol is an essential chemical which is used as a raw material for a vast range of applications including chemicals, fuel (bioethanol), beverages, pharmaceuticals and cosmetics. The feedstock for ethanol generally comes from renewable sources such as starch (from wheat, barley, maize, potato, cassava, sweet potato, etc.) and molasses or syrups originating from sugar beet or sugar cane, etc. Bioethanol is produced by biological fermentation technology. The fermentation product stream is processed with subsequent enrichment by distillation/rectification and dehydration.

Bioethanol is becoming a viable solution as a source of renewable energy, as it is a non-fossil fuel. It may originate from renewable agricultural sources, resulting in cleaner combustion without any emissions to the air.

10.2 PRODUCTION OF ETHANOL BY FERMENTATION

Carbohydrates obtained from grains, potatoes or molasses are fermented by yeasts to produce ethanol in the production of beer, alcohols and distilled spirits. Fermentation of sugar using *Saccharomyces cerevisiae* produces ethanol under anaerobic conditions. The batch fermentation system is affected by high substrate and product inhibition. Glucose concentration plays the major role in increasing the concentration of ethanol and cell growth rate in the fermentation broth. Cell density, ethanol concentration and glucose concentration are measured. Industrial grade sugars and molasses are used for the production of bioethanol. Today, alcohol technologies are well developed. Many extraction and purification techniques have enhanced ethanol production and the process is considered economically feasible.

10.3 BENEFITS FROM BIOETHANOL FUEL

Alcoholic fermentation, ethanol production, has been best known for a few decades by *S. cerevisiae*. Many obligate aerobic fungi, such as common moulds of the genera *Aspergillus*, *Fusarium* and *Mucor* are also well known for their ability to produce ethanol.[2] The benefits are:

- renewable resources
- cleaner environment due to cleaner combustion
- lower net carbon dioxide emissions
- expanded market opportunities in agriculture
- less dependence on crude oil

10.4 STOICHIOMETRY OF BIOCHEMICAL REACTION

The following biochemical reaction represents sugar fermentation. Ethanol is the end product, which may be used as a useful bioprocess chemical.

$$\underset{\substack{\text{Glucose}\\ 180\ \text{g/mol}}}{C_6H_{12}O_6} \xrightarrow{\text{Yeast fermentation}} \underset{\substack{\text{Ethanol}\\ 46\ \text{g/mol}}}{2C_2H_5OH} + \underset{\substack{\text{carbon dioxide}\\ 44\ \text{g/mol}}}{2CO_2} \qquad (10.4.1)$$

There are two popular microorganisms that can produce high concentrations of alcohol. Their tolerance to high concentrations of ethanol and substrates are stated in the literature.[3–5] The most common are *Zymomonas mobilis* and *Saccharomyces cerevisiae*.

10.5 OPTICAL CELL DENSITY

Cell growth is defined with cell density. Cell concentration is an indication of viability of microorganism. Measure the optical cell density of *Saccharomyces cerevisiae* at a wavelength of 580 nm. Other wavelengths such as 600 nm or less may also be used, but one must be consistent. Draw a growth curve based on incubation time and cell dry weight. A standard calibration curve is needed before any actual experiment. Generate a calibration curve to relate the absorbance with cell dry weight. The usual rules of operating a spectrophotometer apply here, as well. For example, the accuracy of the method is greatest when the absorbance readings are in the range 0.1–1. For a given culture sample, a good spectrophotometer should yield a linear relation between the number of cells and the absorbance. However, optical density is also a function of cell morphology such as size and shape, because the amount of transmitted or scattered light depends strongly on these factors. Consequently, an independent calibration curve is required for each condition in accurate research work, as the cell size and shape depend on the specific growth rate and the nutrient composition. As a rule of thumb, an optical density of one unit corresponds to approximately 1 $g \cdot l^{-1}$ of dry cell. This is also commonly referred to as the turbidity measurement.

10.6 KINETICS OF GROWTH AND PRODUCT FORMATION

It has been suggested that fungi grow in filamentous form at an exponential rate with a constant specific growth rate (μ) until some substrate becomes growth limiting, according to the Monod equation:[4,6]

$$\mu = \frac{\mu_{max} S}{K_S + S} \tag{10.6.1}$$

where, μ_{max} is the specific growth rate of the organism in h^{-1}, K_S is the saturation constant in $kg \cdot m^{-3}$, and S is the concentration of the limiting substrate in $kg \cdot m^{-3}$. The ethanol fermentation performance and the bioprocess criteria are summarised below:

- High conversion yield
- High ethanol tolerance
- Resistance to inhibitors in hydrolysed product
- No oxygen requirement
- Low fermentation pH
- Broad substrate utilisation range

10.7 PREPARATION OF THE STOCK CULTURE

It is desirable to store organisms in pure culture for a long time without lack of nutrients. A nutrient broth may not last for weeks. Solid media nutrients with agar in slants are used. Normally the freeze-dried media obtained from ATCC is hydrated and grown in broth media, then transferred to a culture tube with slant agar.[7] Figure 10.1 shows that a stock culture on slant agar in a sealed tube can be kept in a refrigerator for a minimum duration of 4–6 months.

FIG. 10.1. Stock culture *Rhodospirillum rubrum* on slant agar (a hydrogen producer photosynthetic bacterium).

TABLE 10.1. *Data sheet for batch fermentation, at constant agitation, experimental run 1*

Time, h	Absorbance, $\lambda_{520\,nm}$	Cell concentration, g/l	Concentration of carbohydrates, g/l	Ethanol concentration, g/l
0	0.0	0.0	31.5	—
6	0.68	0.5	27.78	1.85
8	1.0	0.78	21.5	3.8
12	1.4	1.1	14.3	5.8
24	1.9	1.55	11.0	8.9

There are several steps for transferring pure culture from a broth cultured on slants. It should be an aseptic technique without transfer of any contaminants. An inoculating loop (Cole-Parmer) is flamed on a Bunsen burner until red hot. It is then cooled off on a corner of the media before entering the culture broth. A full loop of cultivated culture is taken in front of the flame and then transferred to the surface of the slanted agar with continuous streaking; it is incubated at 30 °C until growth is visible as colonies appear. The stock culture tube can then be kept in refrigerator and is good for 6 months. Renewal is necessary for a 6-month-old stock culture.

10.8 INOCULUM PREPARATION

To have stock culture in a slant, also find a single isolated colony of yeast on the Petri dish from which the culture can be transferred to the fermentation media. This technique may ensure you that the stock culture is not contaminated with other organisms.

Take a loop full of the creamy culture off the agar plate. Dip the loop into a 250 ml flask containing 100 ml of 5.0 $g \cdot l^{-1}$ glucose and 1 $g \cdot l^{-1}$ yeast extract. Swirl the loop in the nutrient solution to dislodge the selected culture from the loop.

Flame the neck of the flask and the cotton plug before inserting the plug back in the flask. Also, flame the loop to kill residual microorganisms.

Place the flask in a temperature-controlled shaker at 37 °C. The exponential growth phase will last from 2 to 24 hours after inoculation. The exact time and duration depend on the physiological condition of the inoculum. The data in Table 10.1 are plotted and a growth curve will be obtained for an exponentially growing culture. Figure 10.2 shows the typical growth curve obtained for a viable organism.

10.9 SEED CULTURE

Seed culture of *Saccharomyces cerevisiae* (ATCC 24860) is grown in a rich medium comprising of 1 g glucose, 0.1 g peptone and yeast extract, 0.33 g KH_2PO_4 and 0.03 g Na_2HPO_4 in 100 ml distilled water. The media will be autoclaved at 126 °C and 15 psig for 20 min. The stock culture from ATCC media is transferred to a prepared seed culture. The pH of

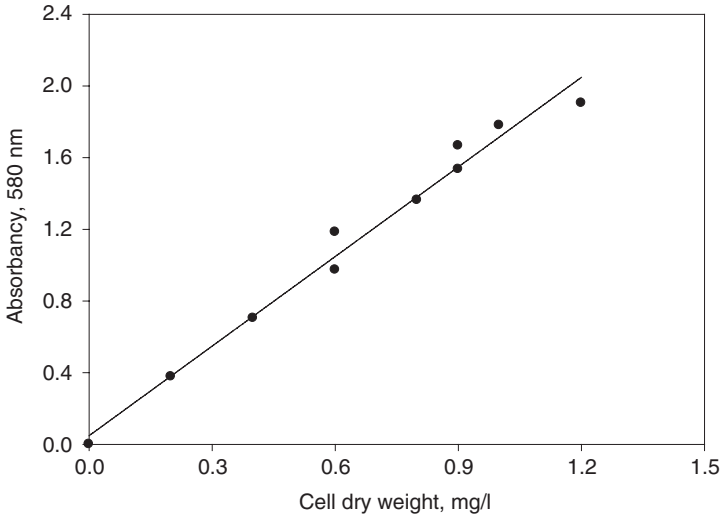

FIG. 10.2. Standard curve for cell density define based on growth of *Saccharomyces cerevisiae.*

FIG. 10.3. A 50 ml seed culture is used for inoculation of batch fermenter.

the medium is adjusted to 5.5, using 0.03 M phosphate buffer solution. A pH meter model WTW 82362 Weilheim, Germany, was used for the pH reading for the experiment in this chapter. Figure 10.3 shows a typical seed culture prepared for inoculation of batch fermentation. The transformation is carried out in front of a flame with a sterile syringe.

10.10 ANALYTICAL METHOD FOR SUGAR ANALYSIS

10.10.1 Quantitative Analysis

After the experiment is concluded, for each sample, measure the glucose concentration with the DNS reagent. DNS solution as a reducing sugar was prepared by dissolving 10 g 3,5-dinitrosalicylic acid in 200 ml of 2 M NaOH. A separate solution of 300 g sodium potassium tartrate was prepared in 500 ml of distilled water; mixing and heating were required. The hot salt solution was added to the DNS. The volume of the solution was made up to 1 litre by adding distilled water. A standard glucose solution ($2\,g{\cdot}l^{-1}$) is prepared in a day advance for any structural deformation or changes. A Calibration curve is prepared. A straight line can easily be obtained in the range 200–1600 $mg{\cdot}l^{-1}$ glucose.

10.11 ANALYTICAL METHOD DEVELOPED FOR ETHANOL ANALYSIS

Ethanol concentration in the fermentation broth is determined by using gas chromatography (HP 5890 series II with HP Chemstation data processing software, Hewlett-Packard, Avondale, PA) with a Poropak Q Column, and a Hewlett-Packard model 3380A integrator. A flame ionisation detector (FID) is used to determine ethanol. The oven temperature is maintained at 180 °C, and the injector and detector temperature are maintained at 240 °C. The sample taken from the fermentation media has to be filtered and any internal standard must be added for analysis based on internal standard methods; otherwise, the area under the peak must be compared with known standard samples for calculation based on external standard methods.

10.12 REFRACTIVE INDEX DETERMINATION

Refractive Index is used to analyse the sample. It can also be used to help determine the percentage of a chemical (such as ethanol) in an aqueous solution. Refractive index (RI) is always reported to four decimal places. An example of the RI scale is shown in Figure 10.4. The correct reading from the RI of the sample would be 1.3764.

10.13 MEASURING THE CELL DRY WEIGHT

About 5 ml of sample is withdrawn for every 4–6 hours. The absorbance reading of the sample at 580 nm was measured using a Hitachi U-2000 spectrophotometer. The sample is filtered in a vacuum through Whatman filter paper with a pore size of 2.5 μm and diameter of 47 mm. The dry weight of cells is measured to monitoring microbial cell population and cell density. A plot of optical density reading from the spectrophotometer against cell dry

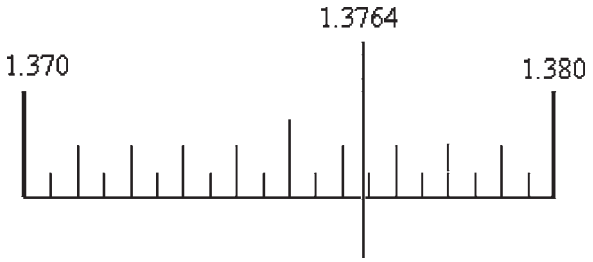

FIG. 10.4. Refractive index reading for ethanol solution.

weight can be obtained. The cell density, a standard calibration curve for *S. cerevisiae* at wavelength 580 nm, has been experimentally determined, which was shown earlier.

10.14 YIELD CALCULATION

To calculate percentage yield, one needs to know the theoretical value that can be obtained, based on material balance, and if 100% of the reactant(s) is converted to product. After obtaining the experimental value (actual yield), divide it by the theoretical value, then multiply by 100 to get percentage yield.[8]

$$\%\text{Yield} = \frac{\text{Experimental value}}{\text{Theoretical value}} \times 100 \tag{10.14.1}$$

10.15 BATCH FERMENTATION EXPERIMENT

It is very simple to perform batch fermentation in a small flask with a volume of say 200 ml. Now our target is to use a 2 litre B. Braun fermenter. All accessories are shown in Figure 10.5. The fermentation vessel only, as shown in Figure 10.6, with about 250 ml of media without any accessories but with some silicon tubing attached with a filter for ventilation is autoclaved at a 131 °C for 10 minutes at 15 psig.[9] After that, the system is handled with special care and all accessories attached. Media is separately sterilised and pumped into the vessel. Inoculum is transferred and the batch experiment is started right after the inoculation of seed culture. An initial sample is withdrawn for analysis.

10.16 CONTINUOUS FERMENTATION EXPERIMENT

The experiment is accomplished with a 2 litre B. Braun fermenter biostat (Germany) equipped with DO and pH meters. Temperature and level controllers are very sensitive, with highly accurate response from the sensors installed in the vessel. Figure 10.7 shows a perfect continuous fermentation set up used in photosynthetic production. A small modification of

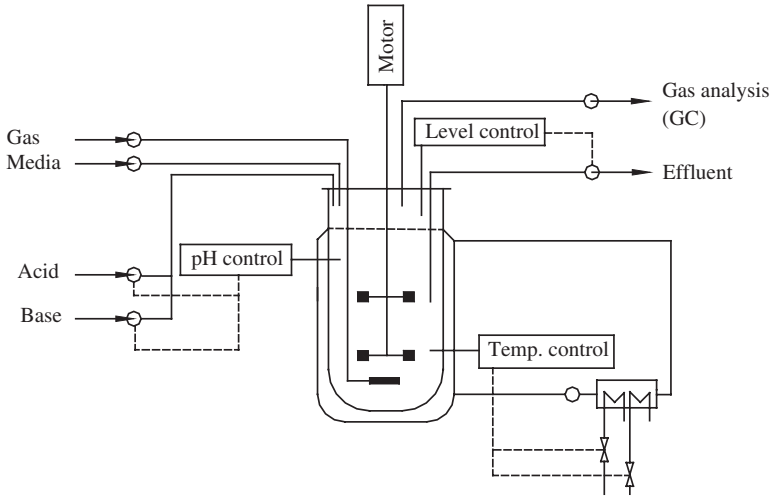

FIG. 10.5. Continuous stirred tank fermenter, experimental setup with instrumentations and controllers, effluent.

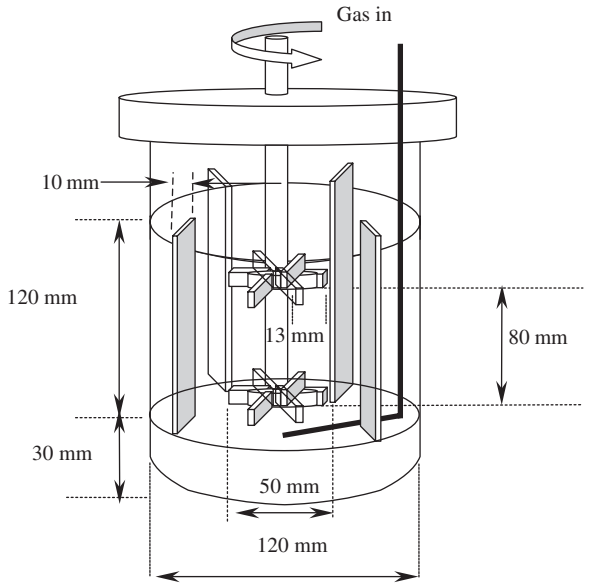

FIG. 10.6. Geometrical dimensions of B. Braun fermentation vessel.

the sampling port is necessary to change the sample jar with a stainless steel tube sample port connected with a rubber septum, which is gas tight. A simple syringe needle is used to take liquid samples aseptically. The original fabricated sampling jar must be attached to on-line steam to prevent any contamination while sampling liquid is withdrawn. The fermentation

FIG. 10.7. A complete laboratory set-up of biostat, B. Braun fermenter with external feed pumps and product reservoirs.

vessel is jacketed, and an external heating and cooling water bath is provided with the fermentation unit to control the temperature, set at 32 °C. Since ethanol fermentation does not require any oxygen, neither air nor pure oxygen is supplied. The CO_2 is vented from the carboy by installing a sterilised air filter.

Draw a sample at the time intervals proposed in Table 10.1. The fermentation should last for approximately 24 hours before the culture enters the stationary phase.

- A 5 ml sample is adequate to analyse optical density, glucose/sucrose concentration and ethanol concentration. For sugar analysis you may dilute 1 ml of sample and 9 ml of distilled water to have a suitable concentration range for DNS analysis.
- Save a drop of the sample on a slide for later microscopic examination of the purity of the culture.
- Initially, when the cell density is still low, the optical density of the sample can be measured without dilution with water. Perform this step quickly with a spectrophotometer at 580 nm. Then, filter out the cells from the sample. After the optical density is over, save 1 ml of the sample by pipetting it into a test tube for optical density measurement. Force the remaining sample through a filter. Normally a sterile syringe is used to withdraw the sample. A suitable filter case fitted on the tip of syringe is used for removing cells. The filtered sample is used for analysis by gas chromatography (GC). Ethanol is determined by GC. Otherwise, the refractive index method is easy to use but it may not be very accurate for research purposes.
- The clear filtrate is collected in a tightly capped sampling vial for later analysis. Freezing the filtrate will better preserve the existing condition.
- If a 1 ml sample is saved for the optical density measurement, dilute the sample with 5 ml of water. Record the optical density.

10.17 MEDIA STERILISATION

Next, the prepared nutrient must be sterilised. Usually, this is done by autoclaving. However, autoclaving is not a practical sterilisation method for the formulation used in this experiment. First, the heat of autoclaving may caramelise the sugar and darken the nutrient to a brown colour. Secondly, vitamins will be destroyed by the heat. Furthermore, the loss of liquid due to boiling during autoclaving will change the concentration of various nutrient components, including the rate-limiting carbon source. Evaporation loss is especially severe when ethanol is the designated carbon source. Even with all the disadvantages of an autoclave, it is still customary to use autoclave routine equipment with some modification such as for a fast programme or to sterilise sugar and media separately.

Instead, membrane filtration may be used to sterilise the nutrient in this experiment. This can be accomplished by drawing the nutrient from a mixing jar and forcing it through an in-line filter (0.2 μm pore size) either by gravity or with a peristaltic pump. The sterilised medium is fed into an autoclaved nutrient jar with a rubber stopper fitted with a filtered vent and a hooded sampling port.

For each run, calculate and plot the cell biomass concentration, glucose concentration, ethanol concentration, and pH as a function of time. Identify the major phases in batch fermentation: lag, exponential, stationary and death.

10.18 BATCH EXPERIMENT

10.18.1 Optical Cell Density, Ethanol and Carbohydrate Concentration

Measure the optical cell density of *S. cerevisiae* at a wavelength of 520 nm. Try to collect data based on information required in Table 10.1. Draw a growth curve based on incubation time and cell dry weight. The cell concentration is an indication of microorganism growth. A standard calibration curve is needed before any actual experiment.

10.18.2 Continuous Ethanol Fermentation Experiment

The batch experiment had neither incoming fresh media nor any product stream leaving the fermentation vessel. A complete experimental set up with a B. Braun Biostat, is shown in the above laboratory experimental set up. The continuous flow of media requires a feed tank and product reservoir. The batch process has many disadvantages such as substrate and product inhibition, whereas in the continuous process the fresh nutrients may remove any toxic by-product formed.

10.19 EXPECTED RESULTS

1. The parameters of the Monod cell growth model are needed: i.e. the maximum specific growth rate and the Michaelis–Menten constant are required for a suitable rate equation. Based on the data presented in Tables 10.1 and 10.2, obtain kinetic parameters for

TABLE 10.2. *Data sheet for continuous ethanol fermentation, experimental run 2, S_0=35 g/l*

Media flow rate, ml/h	Retention time, τ, h	Cell Density, g/l	Substrate concentration (S), g/l	1/*S*, l/g	$-r_A$, Rate of substrate uptake, g/l.h	$1/-r_A$	Ethanol concentration, g/l
83	24	2.30	8.3	0.12	1.11	0.90	8.9
125	16	1.95	9.5	0.105	1.59	0.63	6.9
167	12	1.45	13.0	0.077	1.83	0.55	5.2
250	8	1.03	20.5	0.049	1.81	0.55	3.8
500	4	0.38	27.5	0.036	1.88	0.53	1.5

the experimental data in ethanol production. It is customary to have a linear model and plot a double reciprocal model known as the Lineweaver–Burk plot.

2. Another parameter for living organisms is the media pH, which may change during the course of the fermentation. The cause of change in pH is due to product formation and metabolites from the cells being liberated. Here, the question is: did the change in pH coincide with the different batch growth phases? The answer may not be so clear, as it depends on the activity of the microorganisms and the media absorbing the metabolites.
3. Identification of the major elements of life for living organisms is a necessary step to have a deep understanding of the growth pattern, i.e. nutrient requirement, in a typical yeast cell. Trace metals and minerals act as cofactors in enzyme activities, so the amount of each element such as Zn, Cu, Co, Mg, Mn and Mo in a typical yeast cell may have major role. In fact, these essential elements or trace metals may need to be represented in very small amounts, even micrograms, in our synthetic medium formulation. From the relative ratios of the elements present in the media, we may be able to identify the limiting substrate. It is well known that the carbon source is the limiting substrate in application of kinetic models like the Monod rate model.

REFERENCES

1. Demain, A.L. and Solomon, A.N., *Sci. Am.* **245**, 67 (1981).
2. Phaff, H.J., *Sci. Am.* **245**, 77 (1981).
3. Aiba, S., Humphrey, A.E. and Millis, N.F., "Biochemical Engineering", 2nd edn. Academic Press, New York, 1973.
4. Baily, J.E. and Ollis, D.F., "Biochemical Engineering Fundamentals", 2nd edn. McGraw-Hill, New York, 1986.
5. Blanch, H.W. and Clark, S.D., "Biochemical Engineering". Marcel Dekker, New York, 1996.
6. Doran, P.M., "Bioprocess Engineering Principles". Academic Press, New York, 1995.
7. Pelczar, M.J., Chan, E.C.S. and Krieg, N.R., "Microbiology". McGraw-Hill, New York, 1986.
8. Scragg, A.H., "Bioreactors in Biotechnology, A Practical Approach". Ellis Horwood Series in Biochemistry and Biotechnology, New York, 1991.
9. Shuler, M.L. and Kargi, F., "Bioprocess Engineering, Basic Concepts". Prentice-Hall, New Jersey, 1992.

CHAPTER 11

Production of Antibiotics

11.1 INTRODUCTION

Antibiotics are produced by fermentation. The process may take a few days to obtain an extractable amount of product. Antibiotic production is done by the batch process. Oxygen transport is the major concern; therefore sufficient polymeric sugar and protein with a trace amount of elemental growth factors are used to enhance production. An anti-biogram test is used to observe the amount of antimicrobial agent in the fermentation broth. A bioassay determines the activity unit of the bactericides.

11.2 HERBAL MEDICINES AND CHEMICAL AGENTS

Herbal medicine was used in ancient treatment. Natural chemicals extracted from herbs were used. For seventeen centuries, natural quinine extracted from the bark of a particular tree known as "cinchona" was used to treat malaria. American Indians and southern Asians were able to fight malaria by chewing the bark of cinchona trees. Gradually, chemical agents were identified and used for treating patients. Toxic compounds, such as mercury, were used to treat syphilis for eighteen centuries. Even arsenic compounds were used to cure many diseases without great danger to the patient. Arsphenamine and neoarsphenamine were also used to treat patients with syphilis. Investigation of chemotherapy expanded into a wide range of compounds. Chemotherapy is known as treatment of a disease with chemicals called chemotherapy agents. Treatment with drugs has been practised for many centuries. In mid-1950s, the first generation of sulphonamide was successfully used against certain bacteria, which was a great victory in field of medicine. Antibiotics as chemotherapy agents were discovered. The action of drugs or chemical agents was to destroy germs and to control the growth of microorganisms, or to prevent microbial growth where the aim was to treat a patient. The chemical substances possessed selective toxicity, but over-dosage created complications for the host. The side-effects of chemicals were monitored based on observed symptoms during and after treatment. The drug targeted specific germs and parasites. In general, germicides were not selective in their mechanisms, and often interfered with the immune system. Inactivation of germs and parasites with antigen and antibody mechanisms played a major role in the development of germicides and

antiseptic agents. The action was similar to the inactivation of protein antigens, either by destroying, killing or deactivating any unknown bodies penetrating the host. The action of chemotherapeutic agents in a host can be summarised as follows.

- The antibiotic agents may destroy or prevent the germs or parasites, without creating any injury to the host cell, or with only minimum toxicity to the host.
- The chemical agents should contact the parasite by prevention, or diffusion through the cells and tissues of the host at suitable doses and effective concentrations.
- The action should not disturb the immune system, such as cell defence action known as phagocytosis and the production of antibody, which take place naturally in the presence of parasites.
- These agents profoundly prevent production of bacterial nucleic acids and inhibit genetic replication.

Sulphonamides are very useful in treating bacterial infections, especially infection agents of known microorganisms such as meningococci, shigella, respiratory infections caused by streptococci and staphylococci, and urinary tract infections resulting from Gram-negative microorganisms. Sulphonamide drugs are strongly recommended for rheumatic fever, endocarditis and urinary tract infections followed by any surgery.[1]

11.3 HISTORY OF PENICILLIN

The original organism for producting penicillin, *Penicillium notatum*, was isolated by Alexander Fleming in 1926 as a chance contaminant while culturing other organisms. However, all the penicillin-producing strains were isolated and purified from an infected cantaloupe melon obtained at a market in Peoria, Illinois, USA.[1] The infecting organism was *P. chrysogenum*. The original, wild strain of *Penicillium* produces a yellow pigment devoid of antibiotic properties which colours the final product. Production of antibiotics by mutants does not produce any pigment and yields a colourless end-product.

The chemotherapeutic agent extracted or obtained from secondary metabolites of living cells is known as ‘antibiotic’. The terms ‘antibiotic’ and ‘antibiosis’ were used in 20th century when Alexander Fleming in 1930s accidentally found a mould as a contaminated culture on Petri dish or plate agar while he was cultivating microorganisms. Fleming was culturing *Staphyloccus aureus* on plate or Petri dish with a thin agar layer. His cultured plate was contaminated with a mould. The amazing part of his work was that he found no microbial growth with in a radius of 3–5 cm of the mould.[2] Normally, any contaminated cultures are taken out of the investigation cycle, but Fleming was curious and decided to follow up his investigations. He wanted to know why there was no growth in presence of the mould. He needed to know what the toxic metabolite was that killed the organisms in the neighbourhood of the mould. He found that the cell metabolites were able to lyse and dissolve the cell wall of the microorganisms. He identified the contaminants as mould. Later mould was identified as *Penicillium* sp. Fleming named the drug penicillin, which was isolated from *Penicillium notatum*. Fleming had discovered a new antibiotic, and for his

great contribution he was awarded the Nobel Prize, in the field of medicine and physiology in 1945. His discovery was the answer to the question generated in his mind, which was why the colony of *Staphylococcus* did not grow in presence of *Penicillium notatum*.

The commercial production of penicillin and other antibiotics is the most dramatic example of industrial microbiology. The annual production of bulk penicillin is about 33 million pounds, with annual sales market of more than US$344 million.[1]

The mould isolated by Fleming was *Penicillium notatum*. He noted that it killed his culture of *Staphylococcus aureus*. Production of penicillin has been superceded by a better antibiotic-producing mould species, *Penicillium chrysogenum*. Development of submerged culture techniques has enhanced the cultivation of the mould in large-scale operations using sterile air supply.

- Streptomycin is produced by *Actinomycetes.*
- Molasses, corn steep liquor, waste product from the sugar industry and wet milling corn are used for the production of penicillin.
- *Penicillium chrysogenum* can produce 1000 times more penicillin than Fleming's original culture.[1,3,4]

The major steps in the commercial production of penicillin are as follows.

(1) Preparation of inoculum.
(2) Preparations and sterilisation of medium.
(3) Inoculation of the medium in the fermenter.
(4) Forced aeration with sterile air during incubation.
(5) Removal of mould mycelium after fermentation.
(6) Extraction and purification of the penicillin.

11.4 PRODUCTION OF PENICILLIN

There is only one choice for the antibiotic production process: the synthesis of benzylpenicillin (penicillin G, originally known as 'penicillin'). This, the most renowned antibiotic and the first one have been manufactured in bulk, is still universally prescribed.[5] Although originally made by surface liquid culture, penicillin G is now produced by air-lift fermentation under aerated conditions.

Penicillin G is not a typical fermentative antibiotic. It is made by a fungus, *Penicillium chrysogenum.* The number of antibiotics from fungal sources is few, though they do include penicillin G and V and cephalosporin C. These three antibiotics are the major starting materials for the semi-synthetic β-lactam antibiotics. The systemic antifungal antibiotic griseofulvine is also of fungal origin. Most antibiotics are produced by fermentation using bacteria, including streptomycin and the tetracycline family among numerous others. The manufacture of streptomycin from *Streptomyces griseus* will not be considered in this experiment. Streptomycin is the next important antibiotic after penicillin G to be made available to the clinician. It has played an important role in fighting tuberculosis.[1]

All of the above processes are operated as batch fermentations, in which a volume of sterile medium in a vessel is inoculated. The broth is fermented for a defined period. The tank is then emptied and the products are separated to obtain the antibiotic. The vessel is then recharged for batch operation with medium and the sequence repeated, as often as required. Continuous fermentation is not common practice in the antibiotics industry. The antibiotic concentration will rarely exceed $20\,g{\cdot}l^{-1}$ and may be as low as $0.5\,g{\cdot}l^{-1}$.

11.5 MICROORGANISMS AND MEDIA

A mutant strain of *Penicillium chrysogenum* ATCC 48271 is used for these experimental studies in a 2 lB. Braun air-lift fermenter. A complex growth medium for *P. chrysogenum* was prepared. The media contained: 20 g sucrose, 10 g lactose, 5 g peptone, 13 g $(NH_4)_2SO_4$, 3 g KH_2PO_4, 0.5 g Na_2SO_4, 0.55 g EDTA, 0.25 g $MgSO_4 \cdot 7H_2O$, 0.05 g $CaCl_2 \cdot 2H_2O$, 0.25 g $Fe_2SO_4 \cdot 7H_2O$, 0.02 g $MnSO_4 \cdot 4H_2O$, 0.02 g $ZnSO_4 \cdot 7H_2O$, 0.01 g $Na_2MoO_4 \cdot 2H_2O$ and 0.005 g $CuSO_4 \cdot 5H_2O$ in 1000 ml of distilled water. The media was sterilised in an autoclave at 121 °C for 30 min.

11.6 INOCULUM PREPARATION

Most fungi sporulate on suitable agar media but a large surface area is required to produce sufficient spores. A roll-bottle technique was used to produce spores of *Penicillium chrysogenum*, with 300 ml of media containing 3% agar sterilised in a 1 l cylindrical bottle. After autoclave, the media was cooled at 45 °C and rotated on a roller mill so that a layer of agar formed on the cylinder wall. The inoculum was of spore suspension incubated at 24 °C for 6–7 days. Submerged culture is common for sporulation of fungi such as *P. chrysogenum*. The sporulation is induced by inoculating 300 ml in a 1 l shaking flask with spores from a well-sporulated agar culture and incubated for sufficient time. At this stage, a 2 l fermenter was inoculated with a pure incoluum (300 ml) and harvested in the fast-growing (logarithmic) phase, so that in the culture media a high cell density could be obtained. The organism, *P. chrysogenum*, grows in a filamentous (hyphal) form, with branching occurring to a greater or lesser extent. The B. Braun airlift fermenter was used. Pressurised filter air was used to circulate the mycelia in the internal loop pattern. Air was continuously supplied. The bubbles lose oxygen as they rise up the column. At the same time, carbon dioxide and other gaseous metabolites diffuse into the media and are released in the overhead gas compartment. The production of penicillin G is very sensitive to temperature, the tolerance being less than 1 °C. Heat is generated by the metabolism of nutrients. It has to be removed by a well-controlled cooling system. Cooling coils are used for isothermal operation. The fermentation vessel is fitted with several probes to detect foaming, to monitor temperature, to control media level and to record parameters such as pH. The rate of air flow through the fermenter is measured, and the exhaust gases that emerge from the top of the vessel may also be analysed. Originally all penicillin G was manufactured using lactose in this way, and some manufacturers still prefer this technique.

Calcium, magnesium, phosphates and trace metals added initially are usually sufficient to last throughout the fermentation but the microorganism needs further supplies of nitrogen and sulphur to balance the carbon feed. Nitrogen is often supplied as ammonia gas. Ammonium ions can contribute to pH control, the carbon metabolism being acidogenic and balanced by the alkalinity of the ammonia. Sulphate is usually supplied in common with the sugar feed and the flow adjusted with suitable feed stream ratios.

All feed streams are sterilised before being metered into the fermentation vessel. Contaminants resistant to the antibiotic rarely find their way into the fermenter. When they find a way to contaminate media, their effects are so catastrophic that prevention is of paramount importance. A resistant, β-lactamase producing, fast-growing bacterial contaminant can destroy the penicillin.[5] The contaminants not only consume nutrients intended for the fungus, but also cause loss of pH control and interference with the subsequent extraction process.

The Petri dish culture of penicillin is shown in Figure 11.1(a). The action of antibiotic shows an 'overlay plate', in which a central colony of the fungus *Penicillium notatum* was allowed to grow on agar for 4–5 days. Then the plate was overlain with a thin film of molten agar containing cells of the yellow bacterium *Micrococcus luteus*. The production of penicillin by the fungus creates a clear zone free of free organisms, which means the antibiotic activities of penicillin create growth inhibition of the yellow bacterium. Figure 11.1(b)

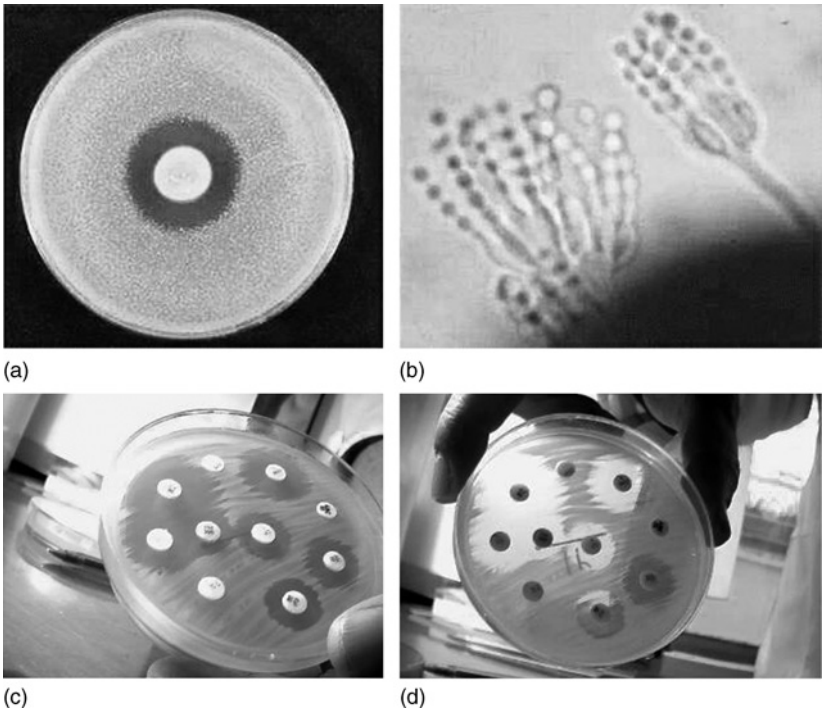

FIG. 11.1. (a) Action of penicillin; (b) structure of a species of *Penicillium.*

TABLE 11.1. *Clinically important antibiotics and the producing microorganism*[3]

Antibiotic	Producer organism	Activity	Site or mode of action
Penicillin	*Penicillium chrysogenum*	Gram-positive bacteria	Wall synthesis
Cephalosporin	*Cephalosporium acremonium*	Broad spectrum	Wall synthesis
Griseofulvin	*Penicillium griseofulvum*	Dermatophytic fungi	Microtubules
Bacitracin	*Bacillus subtilis*	Gram-positive bacteria	Wall synthesis
Polymyxin B	*Bacillus polymyxa*	Gram-negative bacteria	Cell membrane
Amphotericin B	*Streptomyces nodosus*	Fungi	Cell membrane
Erythromycin	*Streptomyces erythreus*	Gram-positive bacteria	Protein synthesis
Neomycin	*Streptomyces fradiae*	Broad spectrum	Protein synthesis
Streptomycin	*Streptomyces griseus*	Gram-negative bacteria	Protein synthesis
Tetracycline	*Streptomyces rimosus*	Broad spectrum	Protein synthesis
Vancomycin	*Streptomyces orientalis*	Gram-positive bacteria	Protein synthesis
Gentamicin	*Micromonospora purpurea*	Broad spectrum	Protein synthesis
Rifamycin	*Streptomyces mediterranei*	Tuberculosis	Protein synthesis

shows the typical asexual sporing structures of a species of *Penicillium*. The spores are produced in chains from flask-shaped cells (phialides), which are found at the tips of a brush-like aerial structure.[1]

Penicillin has an interesting mode of action: it prevents the cross-linking of small peptide chains in peptidoglycan, the main cell wall polymer of bacteria. Pre-existing cells are unaffected, but all newly produced cells are abnormally grown. The newborn cells are unable to maintain their wall rigidity, and they are susceptible to osmotic lysis.

The clinical aspects of several antibiotics such as penicillin G, cephalosporin and many other antibiotics are summarised in Table 11.1. The potential microorganisms for the production of various antibiotics and their activities on site or mode of action of the antibiotics are also listed.

11.7 FILTRATION AND EXTRACTION OF PENICILLIN

At harvesting time, the cells are removed. The penicillin G as the cell product is in the solution that is extracellular with a range of other metabolites and medium constituents. The first step is to remove the cells by filtration. This stage is done under conditions that avoid contamination of filtrate with enzyme, which may destroy antibiotic. The β-lactamase-producing microorganisms could react with the antibiotics, which would cause serious or total loss of product.[5] The next stage is to isolate the penicillin G. Solvent extraction is the generally accepted process. In aqueous solution at pH 2–2.5, there is a high partition coefficient in favour of certain organic solvents such as amyl acetate, butyl acetate and methyl *iso*-butyl ketone. The extraction has to be done quickly since penicillin G is very unstable at those low pH values. The penicillin is then extracted back into an aqueous buffer at pH 7.5. The partition coefficient now strongly favours the aqueous phase. The solvent is recovered by distillation for re-use.

11.8 EXPERIMENTAL PROCEDURE

The inoculate was prepared in 250 ml flasks containing 100 ml of growth medium, which is inoculated with 10 ml of spore suspension. The mixture was shaken at 250 rpm and the temperature was controlled at 26 °C for 48 h. Then, 110 ml of resulting mycelia suspension is used to inoculate a 1000 ml broth in the airlift fermenter. The sterilised media are slowly pumped into the bioreactor at a flow rate of about 100 ml·h^{-1} until 2 l working volume is fully utilised. Aeration rates of 0.5, 1 and 2 vvm (1, 2 and 4 l air/min) are used.[6,7] Samples were taken at 24 hour intervals and evaluated for biomass, sugars and antibiotic concentrations.

11.9 FERMENTER DESCRIPTION

A 2 lB. Braun airlift fermenter with a working volume of about 2000 ml was used. Sterile air is sparged through a sintered plate located near the bottom of the central concentric tube. There was no mechanical stirring; only the air nozzle was forced through the centred tube and the flow directed to the annulus tube side. Aeration causes circulation of media; the flow is gentle without serious shear forces. The temperature is maintained at 26 °C.

11.10 ANALYTICAL METHOD FOR BIOASSAY AND DETECTING ANTIBIOTIC

The extracted antibiotic was used in an antibiogram test. Petri dishes of *Bacillus subtilis* ATCC 6633 was cultured for bioassay of penicillin. Small circular paper filters (3–5mm) are placed at different positions on the surface of the agar. The small circular filters were sterilised earlier. A few drops of concentrated and extracted antibiotic were poured on the filter. The small circular filter will hold antibiotic after incubation for 24 hours. There will be a clear circle around the paper filter without any microbial growth. This bioassay is called antibiogram. Figure 11.2 shows an antibiogram test diffusion of antibiotic on an agar layer, which prevents microbial growth. Normally, an antibiogram is used for clinical purposes to identify a suitable antibiotic for infected patients. High-performance liquid chromatography (HPLC) is commonly used for quantitative analysis. The carbohydrate concentration is determined by the dinitrosalicylic acid method.[8] Biomass was evaluated by measuring the total solid concentration. Cell dry weight may represent the growth curve in the fermentation broth. The samples were centrifuged at 4500 rpm for 20 min and the sediment washed with distilled water and dried in an oven at 105 °C to determine cell dry weight.

11.11 ANTIBIOGRAM AND BIOLOGICAL ASSAY

Antibiotic activities are examined by transfer of seed culture of *Bacillus subtilis* on nutrient agar on a Petri dish. The seed culture for *Bacillus subtilis* is a simple basal media of

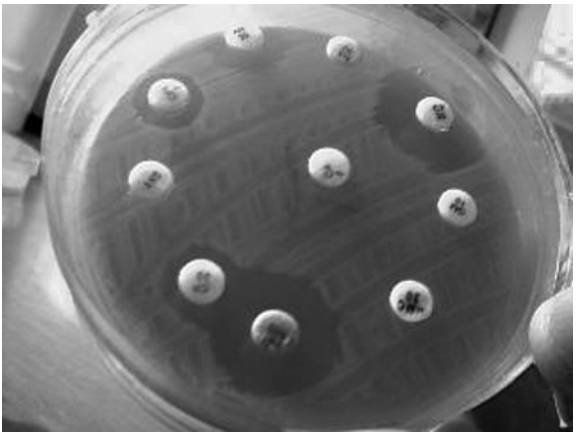

FIG. 11.2. Antibiogram test diffusion of antibiotic on agar layer, preventing microbial growth.

1 g glucose, 1 g peptone and 1 g yeast extract; it does not require a complex medium. The antibiogram test for diffusion of antibiotic product obtained with solvent extraction using amyl acetate or methyl *iso*-butyl ketone is then distilled and concentrated for bioassay. A few drops of antibiotic are tested according to the biogram test shown in Figure 11.1. The Petri dish media is a simple basal media with 3% agar. The Petri dishes are prepared in advance and stored in a refrigerator. They are ready to use for microbial growth tests. The inoculated Petri dishes with *B. subtilis* are incubated at 32 °C. The clear area around the antibiotic shows that *B. subtilis* is unable to grow near antibiotic. The activities are scaled from +1 to +4, based on the radius of the clear circle of 5–10 mm without any microbial growth.

11.12 SUBMERGED CULTURE

11.12.1 Growth Kinetics in Submerged Culture

The use of stirred fermenters with automatic control of the culture environment is the most suitable technique to evaluate bacterial or fungal kinetics. Cultures can be operated in discontinuous mode (batch cultures).

The growth curve in batch culture of a microorganism can be divided into six phases (Figure 11.3): log phase (I); accelerating growth phase (II); exponential growth phase (III); declining growth phase (IV); stationary phase (V); death phase or lytic decline phase (VI). The growth curve has been often represented by mathematical models.[9] In the case of media limitation, the Monod equation is most often used to describe growth rate.

$$\mu = \frac{\mu_m S}{K_S + S} \qquad (11.12.1.1)$$

where μ_m is the maximum specific growth rate in h^{-1}, K_S is the saturation constant in $g \cdot l^{-1}$. For special cases when $K_S << S$, then $S/(K_S + S) \approx 1$ and the growth is exponential. If the

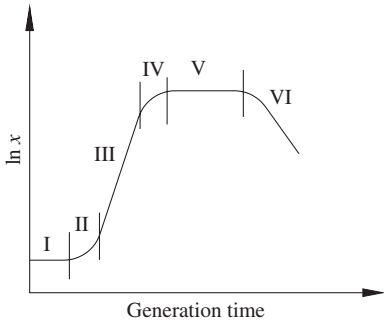

FIG. 11.3. Batch growth curve with various phases.

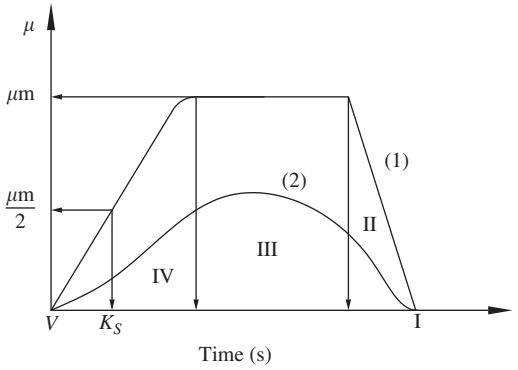

FIG. 11.4. Non-exponential growth curve in a batch culture.

value of K_S is relatively high compared with substrate concentration (S), when substrate concentration decreases, a decelerating growth phase is reached. Values of growth rate (μ) are dependent on a combination of media–fungus, but are most often the projected value is between 0.1 and 0.4 h^{-1}. Values of K_S can be determined by plotting $1/\mu_m$ against $1/S$. The linear rate equation becomes a Lineweaver–Burk plot:

$$\frac{1}{\mu} = \frac{K_S}{\mu_m}\frac{1}{S} + \frac{1}{\mu_m} \qquad (11.12.1.2)$$

Figure 11.4 shows the growth curve with lag, log, stationary and death phases for microorganism growth. In the case of non-exponential growth (Figure 11.4), the value of K_S can be approximated from the curve $\mu = f(S)$. Growth of fungi in batch culture is difficult to observe, because of exponential increases in biomass concentration for the organism with more than five doubling times. After a certain growth time, the fungus will eventually modify the physicochemical condition of its environment and correspondingly growth will slow down the process owing to low substrate concentration, limitation of nutrients, oxygen transfer rate, product inhibition

and accumulation of undesired products. Morphologically, linear growth can be correlated with a blockage of the branching, where branching of the mycelium or the fermentation of blastospores ('yeast-like cells') induces an exponential increase of the biomass.

11.13 BIOREACTOR DESIGN AND CONTROL

Incubation control necessitates the precise control of several influential parameters:

- Temperature
- pH
- Pressure
- Nutrients
- Agitation
- Dissolved oxygen
- Air flow
- Redox

These are the primary important process variables and growth conditions.[10]

The pH is typically controlled by acid/alkali feeds. Dissolved oxygen and redox loops are controlled as a cascade loop utilising air flow, agitation, pressure, auxiliary feed or a combination of these controllers.

The control of these and any other parameters is most usually done in fermenter vessels specifically designed for the purpose and accommodating various working volumes, depending on the yield and production requirements. Laboratory-scale vessels could have a capacity of just 10 litres or less whereas clinical trials and production vessels may be as large as several thousand litres.

The actual fermentation process is known as the incubation phase and is just part of the batch cycle. A complete fermentation cycle can typically include the following steps, most likely depending on bioreactor design:

- Empty vessel, sterilisation of vessel and piping using direct steam injection
- Charging medium
- Indirect sterilisation by steam injected into the vessel jacket
- Cooling and jacket drain
- Pre-inoculation vessel environment under control
- Inoculation, injection of a small sample of the monoculture
- Incubation of the fermentation process
- Harvesting the product, extraction process

A control system must therefore provide flexibility in such a way that the results are accurate and repeatable. Also, precise control of the fermentation environment is necessary, which includes:

- Precise loop control with set point profile programming
- Recipe management system for easy parameterisation
- Sequential control for vessel sterilisation and more complex control strategies
- Secure collection of online data from the bioreactor for analysis and evidence
- Local operator display with clear graphics and controlled access to parameters

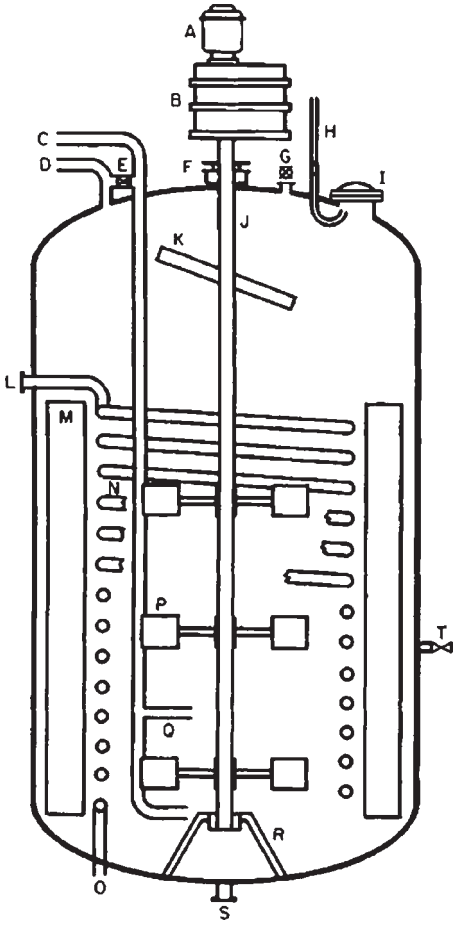

FIG. 11.5. Conventional batch fermenter. A, Agitator motor. B, Speed reduction unit. C, Air inlet. D, Air outlet. E, Air bypass valve. F, Shaft seal. G, Sight glass with light. H, Sight glass clean-off line. I, Manhole with sight glass. J, Agitator shaft. K, Paddle to break foam. L, Cooling water outlet. O, Cooling water inlet. P, Mixer. Q, Sparger. S, Outlet. T, Sample valve.

The conventional batch fermenter and the important parts of the fermentation vessel are shown in Figure 11.5.

11.14 ESTIMATION FOR THE DIMENSION OF THE FERMENTER

Fermenter working volume, $V_{\text{working}} = 10\,\text{m}^3$ with 20% over-design as a safety factor. The total volume is:

$$V = \frac{V_{\text{working}}}{0.8} = \frac{10\ \text{m}^3}{0.8} = 12.5\ \text{m}^3$$

Volume of fermenter, for a cylindrical system is defined as:

$$V = \frac{\pi}{4} \times D_t^2 \times H_L \tag{11.14.1}$$

where D_t is the diameter of the tank, in m; H_L is the height of fermentation vessel. Let us take the ratio liquid level to tank diameter H_L: D_t, 2:1, therefore,

$$V = \frac{\pi}{4} \times D_t^2 \times 2D_t \tag{11.14.2}$$

$$V = 0.5\pi \times D_t^3 = 12.5\ \mathrm{m}^3$$

Solving for tank diameter, D_t and liquid height:

$$D_t = 2.0\ \mathrm{m}$$

$$H_L = 2 \times D_t = 2 \times 2.0 = 4.0\ \mathrm{m}$$

Diameter of impeller is set one third of tank diameter:

$$D_i = \frac{D_t}{3} = \frac{2.0\ \mathrm{m}}{3} = 0.67\ \mathrm{m}$$

Let us take the required aeration as 1.0 vvm. The volumetric flow of air for a $12.5\ \mathrm{m}^3$ fermenter is defined:

$$F_g = 1.0\ \mathrm{vvm} \times 12.5\ \mathrm{m}^3 = 12.5 \frac{\mathrm{m}^3}{\mathrm{min}} \times \frac{1\ \mathrm{min}}{60\ \mathrm{s}} = 0.21 \frac{\mathrm{m}^3}{\mathrm{s}}$$

The gas superficial velocity is defined as the ratio of gas flow rate to vessel cross sectional area:

$$U_S = \frac{F_g}{A} = \frac{12.5 \dfrac{\mathrm{m}^3}{\mathrm{min}}}{\dfrac{\pi}{4}(2.0)^2\ \mathrm{m}^2} \times \frac{60\ \mathrm{min}}{1\ \mathrm{h}} = 238.73 \frac{\mathrm{m}}{\mathrm{h}}$$

11.15 DETERMINATION OF REYNOLDS NUMBER

Let us define an average density at inlet using weight fractions.

$$\rho_{ave,in} = (0.80 \times 1544) + (0.05 \times 1834) + (0.07 \times 597.1) + (0.08 \times 1000)$$

$$\rho_{ave,in} = 1448.70 \text{ kg/m}^3$$

Also the average density of outlet stream is:

$$\rho_{ave,out} = (0.16 \times 3420) + (0.23 \times 110.1) + (0.21 \times 1000) + (0.40 \times 1013)$$

$$\rho_{ave,out} = 1187.72 \text{ kg/m}^3$$

The highest density of the solution has been taken for the determination of the Reynolds number. The broth was viscous and the viscosity is assumed to be $\mu = 0.1$ Pa·s.

The rotational speed of impeller set at $N = 150$ rpm $= 2.5$ rps.

The Reynolds number is calculated based on provided data.

$$Re = \frac{\rho N D_i^2}{\mu} = \frac{\left(1448.70 \dfrac{\text{kg}}{\text{m}^3}\right) \times (2.5 \text{ rps}) \times (0.67 \text{ m})^2}{(0.1 \text{ Pa·s})}$$

$$Re = 16,258$$

The high Reynolds number represents the turbulent flow regime.

11.16 DETERMINATION OF POWER INPUT

At first it is necessary with knowledge of the flow regime to read the power number directly from a power graph, as discussed in Chapter 6 and illustrated in Figure 6.6: the reading for Reynolds numbers greater than 16,000 was $P_{no} = 5$. The equation for the power number is:

$$P_{no} = \frac{Pg}{\rho N_i^3 D_i^5} = 5 \tag{11.16.1}$$

Therefore, ungassed power is calculated as:

$$P = \frac{5 \times \left(1448.70 \frac{\text{kg}}{\text{m}^3}\right) \times (2.5 \text{ rps})^3 \times (0.67 \text{ m})^5}{9.81 \frac{\text{m}}{\text{s}^2}} = 1557.66 \frac{\text{kg} \cdot \text{m}}{\text{s}}$$

$$P = 1557.66 \frac{\text{kg} \cdot \text{m}}{\text{s}} \times \frac{1 \text{ hp}}{745.7 \frac{\text{kg} \cdot \text{m}}{\text{s}}} = 2.09 \text{ hp}$$

That is the input power required for one set of impellers. Correction factors for non-geometrical similarity are required to include the effect of known factors in precise calculations.

$$f_c = \sqrt{\frac{\left(\frac{D_\text{t}}{D_\text{i}}\right)^* \left(\frac{H_L}{D_\text{i}}\right)^*}{\left(\frac{D_\text{t}}{D_\text{i}}\right)\left(\frac{H_L}{D_\text{i}}\right)}} \tag{11.16.2}$$

where the parameter in design of bioreactor is set at $D_\text{t}/D_\text{i} = 3$ and $H_L/D_\text{i} = 3$. Upon substitution, for the above cases the correction factor is calculated.

$$f_c = \sqrt{\frac{\left(\frac{2.0}{0.67}\right)\left(\frac{4.0}{0.67}\right)}{3 \times 3}} = \sqrt{\frac{3 \times 6}{3 \times 3}} = 1.414$$

Therefore, the actual power with correction factor is:

$$P^* = 1.414 \times \text{P} = 1.414 \times 2.09 \text{ hp} = 2.96 \text{ hp}$$

Dimensionless aeration rate is defined by the following equation:

$$N_a = \frac{F_g}{N_\text{i} \, D_\text{i}^3} = \frac{0.21 \frac{\text{m}^3}{\text{s}}}{(2.5 \text{ rps}) \times (2.0 \text{ m})^3} = 0.0105 \tag{11.16.3}$$

Read the ratio of gassed power to ungassed power from Figure 6.7. The reading from graph is $P_g/P = 0.9$. The gassed power for the motor to rotate is:

$$P_g = 0.9 \times 2.96 \text{ hp} = 2.664 \text{ hp}$$

11.17 DETERMINATION OF OXYGEN TRANSFER RATE

The mass transfer coefficient for non-coalescing air bubbled in the fermentation broth in turbulent regime is frequently discussed in the literature.[6] The volumetric mass transfer coefficient is defined by the following correlation:

$$K_L a = 2 \times 10^{-3} \left(\frac{P_g}{V_L} \right)^{0.6} (V_S)^{0.667} \tag{11.17.1}$$

where the gas superficial for the above case is calculated as $V_S = 0.21\,\text{m}^3/s/4\pi\text{m}^2$ and the vessel working volume is

$$V_L = 4\pi \times 4 = 16\pi\text{m}^3$$

Substituting V_S and V_L into the above equation determines the volumetric mass transfer coefficient. Volumetric mass transfer coefficient is calculated as:

$$K_L a = 2 \times 10^{-3} \left(\frac{2.664}{16\pi} \right)^{0.6} \times \left(\frac{0.21}{4\pi} \right)^{0.667} = 2.24 \times 10^{-5}\text{s}^{-1}$$

The simple equation for oxygen transfer rate is based on driving forces existing for the equilibrium value for oxygen concentration and the dissolved oxygen available in the liquid phase. That is:

$$\text{OTR} = K_L a \, (C_1^* - C_1) \tag{11.17.2}$$

The assumption was made that the equilibrium value for oxygen was $C_1^* = 6\,\text{ppm}$ and all oxygen available in liquid phase was used by the microorganisms ($C_1 = 0$), which means the growth was mass-transfer-limited, the organisms were growing fast, and the limited oxygen transfer can retard the biological process. The oxygen transfer rate is calculated as:

$$\text{OTR} = 2.24 \times 10^{-5}(6 \times 10^{-3} - 0) = 1.344 \times 10^{-7} \frac{\text{kgO}_2}{\text{m}^3\text{s}}$$

TABLE 11.2. *Fermenter design specification sheet*

Fermenter				
Identification:	Item:	Fermenter	Date:	24-02-2005
			By:	Nicky Teoh
Function:	To produce Penicillin G from the raw materials fed			
Operation:	Batch			
Type:	Batch reactor			
Material handled:	Inlet		Outlet	
Quantity (kg)	2079.81		2090.84	
Composition:				
Penicillin G	—		334.0	
Water	167.04		432.18	
Glucose	1670.40		—	
H_2SO_4	98.00		—	
NH_3	155.38		—	
CO_2	—		489.28	
Biomass	—		835.38	
Pressure (bar)	1.00		1.00	
Temperature (°C)	25.00		25.00	
Design data:				
Tank		*Turbine*		
Height, m	4.0	Turbine impeller Diameter, m	0.67	
Diameter, m	2.0	Impeller Speed, rpm	150	
Capacity Safety factor, %	20.0			
Capacity, m^3	12.5	Ungassed power, hp	2.96	
Operating pressure, bar	1.0	Gassed power, hp	2.664	
Operating temperature, °C	32.0	Oxygen transfer rate, $kg \cdot m^{-3} \cdot s^{-1}$	1.344×10^{-7}	
Material of construction	Stainless Steel			
Utilities:	chilled water			
Tolerances:	rules of thumb and heuristics			

11.18 DESIGN SPECIFICATION SHEET FOR THE BIOREACTOR

The characteristics and design specification sheet for the bioreactor have been summarized; the specification sheet is shown in Table 11.2.

REFERENCES

1. Pelczar, M.J. Chan, E.C.S. and Krieg, N.R., "Microbiology", 6th edn. McGraw-Hill, New York, 1993.
2. Baily, J.E. and Ollis, D.F., "Biochemical Engineering Fundamentals", 2nd edn. McGraw-Hill, New York, 1986.

3. Stanbury P.F. and Whitaker, A., "Principles of Fermentation Technology". Pergamon Press, New York, 1987.
4. Demain A.L. and Solomon, N.A., *Sci. Am*. **245**, 67 (1981).
5. Voet, D. and Voet, J.G., "Biochemistry", 3rd edn. John Wiley, New York, 2004.
6. Scragg, A.H., "Bioreactors in Biotechnology, A Practical Approach". Ellis Horwood Series in Biochemistry and Biotechnology, New York, 1991.
7. Ghose, T.K., "Bioprocess Computation in Biotechnology", vol. 1. Ellis Horwood Series in Biochemistry and Biotechnology, New York, 1990.
8. Miller, G.L., *Anal. Chem*. **31**, 426 (1959).
9. Doran, P.M., "Bioprocess Engineering Principles". Academic Press, New York, 1995.
10. Shuler, M.L. and Kargi, F., "Bioprocess Engineering, Basic Concepts". Prentice-Hall, New Jersey, 1992.

CHAPTER 12

Production of Citric Acid

12.1 INTRODUCTION

Citric acid is an intermediate organic compound in the tricarboxylic acid (TCA) cycle, found naturally in citrus fruits, pineapples, pears and crystallised as calcium citrate. It is an important chemical used in medicines, flavouring extracts, food and candies, and the manufacture of ink and dyes. Citric acid is a six-carbon tricarboxylic acid, which was first isolated from lemon juice. It is used in the food and beverage industry for various purposes, as pharmaceuticals and for other industrial uses. It is an organic carboxylic acid, can be extracted from the juice of citrus fruits by adding calcium oxide (lime) to form calcium citrate, which is an insoluble precipitate that can be collected by filtration; the citric acid can be recovered from its calcium salt by adding sulphuric acid. Citric acid is mainly produced by fermentation. There are many potent microorganisms including fungi, yeast and bacteria that are able to produce citric acid by fermentation. It is obtained also by fermentation of glucose with the aid of the mould *Aspergillus niger.* Citric acid is used in soft drinks and food additives. Its salts, the citrates, have many uses: for example, ferric ammonium citrate is used in making blue print paper. Sour salt, used in cooking, is citric acid. Most citric acid is produced by fungal (*A. niger*) fermentation. Chemical synthesis of citric acid is possible but it is not cheaper than fungal fermentation. However, a small amount of citric acid is still produced from citrus fruits in Mexico and South America where they are available economically. There are basically three different types of batch fermentation process used in industry. There are two very common and practical fermentation processes used: the liquid surface culture and the submerged fermentation process. The second process, submerged culture fermentation, is more popular. Continuous fermentation has been studied at the laboratory scale.[1,2]

12.2 PRODUCTION OF CITRIC ACID IN BATCH BIOREACTOR

Citric acid fermentation of cane-molasses is by submerged fermentation in a 21 biostat (B. Braun) stirred fermenter. A strain of *Aspergillus niger* is the most widely used for commercial production. *A. niger* is also highly recommended in the present study, which can obtained from the American Type Culture Collection, Rockville, Maryland, USA. Molasses

from cane sugar are used with the addition of trace metals at the desired concentration. The sources of sugar and initial pH of the media play a major role in citric acid production. Submerged and surface cultures are customarily used with cheap but purified and high concentration sources of sugars.

12.2.1 Microorganism

Aspergillus niger ATCC 11414 can be used for citric acid fermentation. It should be ordered from the ATCC. The culture was maintained on 10.0% sterilised molasses obtained from Central Sugar SDN BHD, pH 5.8. The slant stock cultures of *A. niger* will be stored at 5 °C in the refrigerator. All the culture media, unless otherwise stated, is sterilised at 121 °C (15 psig pressure) for 15 minutes.

A. niger utilises beet molasses, fructose, glucose, and starch hydrolyzates as substrates for fermentation. Inoculation proceeds by introducing the active inoculum at its optimum stage. The substrate is used at a concentration of 10–15%. The production stage usually lasts for 5 days and takes place in stirred aerated fermenters at 30 °C. Agitation is in the middle range, about 200 rpm. Regulation of the dissolved oxygen concentration in the medium is done by the air supply, pressurized air and impeller speed, regulation of the pH value and regulation of the level of free potassium hexocyanoferrate in the medium. The trace metal potassium hexacyanoferrate is used for surface fermentation in citric acid production.[3]

Although *A. niger* has mainly been used in citric acid production, other strains of fungi, various kinds of yeast and some bacteria are known to accumulate citric acid in the medium. The reasons for choosing *A. niger* over other potential citrate-producing organisms are that cheap raw materials (molasses) can be used as substrate, and a high product yield can be obtained. There is general agreement in the literature that the pelleted form is desirable for acid production. An ideal pellet configuration, of 1.2–2.5 mm diameter after five days, is formed. The pellet form is a favourable spore. Pellet cultures have low viscosity, causing improved bulk mixing, aeration conditions and lower oxygen consumption than cultures composed mainly of filamentous forms. Furthermore, problems of wall growth and pipe blockage are reduced and separation of biomass from culture liquid by filtration is considerably enhanced by the pellet form.

12.3 FACTORS AFFECTING THE MOLD GROWTH AND FERMENTATION PROCESS

Trace element nutrition is one of the most important factors affecting the yields (grams of citric acid per gram of sugar) from citric acid fermentation. In particular, the levels of manganese, iron, copper and zinc are quite critical. If the levels of these trace elements are correct, other factors have less pronounced effects. Conversely, the medium will not allow high production unless the trace element content is controlled carefully. Manganese (Mn^{2+} ions) in the nutrient medium plays a key role in the accumulation of large amounts of citrate by *A. niger*. When the Mn^{2+} concentration is maintained below 0.02 mM (which does not affect growth rate or biomass yield), large amounts of citric acid are produced. It has been

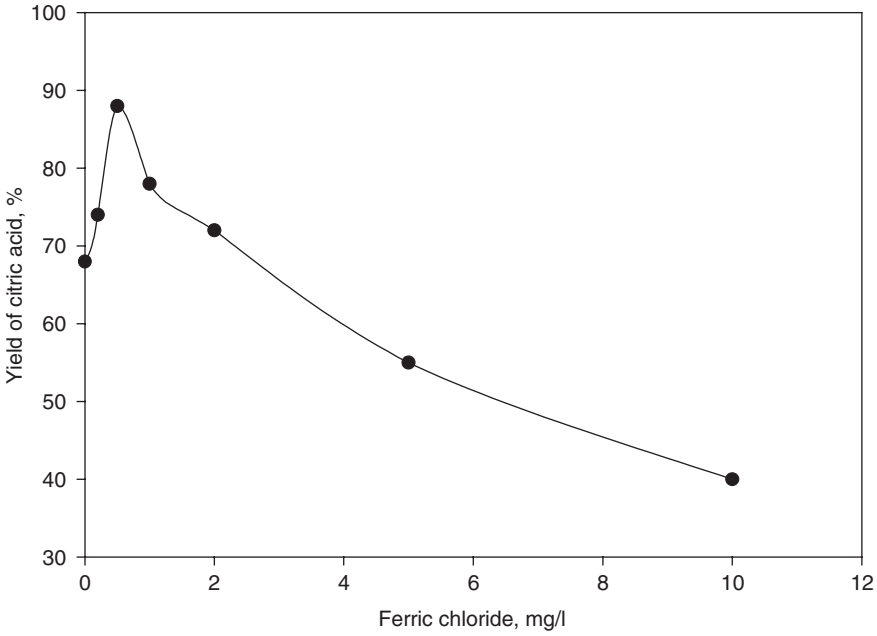

FIG. 12.1. Effect of iron concentration on yield of citric acid by *A. niger.*

found[1] that up to 0.5 mg iron per litre of medium is essential for high yields of citric acid by *A. niger* while the organism utilises sucrose in the submerged culture. The media with 40% sucrose was purified with an ion exchanger; resistance measured 3.5 MΩ, and it was diluted to 14.2% sugar content. The media composition was KH_2PO_4, 0.014%; $MgSO_4 \cdot 7H_2O$, 0.1%; $(NH_4)_2CO_3$, 0.2%; $FeCl_3$, 0.05% and add HCl to pH 2.6. Excess amounts of Fe^{3+} may drastically reduce the yield of citric acid from 88% to 39%. The effect of iron ions on yield of citric acid is shown in Figure 12.1.

A. niger normally produces many useful secondary metabolites; citric and oxalic acids are stated as the dominant products. Limitation of phosphate and certain metals such as copper, iron and manganese results in a predominant yield of citric acid. The additional iron may act as a cofactor for an enzyme that uses citric acid as a substrate in the TCA cycle; as a result, intermediates of the TCA cycle are formed.

The presence of excess iron favours the production of oxalic acid. Copper ions play an important role in reducing the deleterious effect of iron on citric acid production. It has also been reported that copper ions can successfully counteract addition of manganese to citric acid fermentation media and are inhibitors of cellular manganese uptake. It was found that copper is an essential requirement for citric acid production. An optimum concentration of Cu^{2+} is 40 ppm for high yields. Low concentrations of zinc in the fermentation medium are generally favoured in most media for citric acid production. It was reported that zinc deficiencies promote citric acid production. The zinc ion plays a role in the regulation of growth and citrate accumulation. At high zinc levels (about 2 μM) the cultures are maintained in

the growth phase, but when the medium becomes zinc deficient (below 0.2 μM), growth is terminated and citric acid accumulation begins. Addition of zinc to citrate-accumulating cultures results in their reversion to the growth phase. Since molasses (beet or cane) contains inhibitory amounts of metal ions like zinc, iron and copper, it is absolutely necessary either to remove these ions or to render them ineffective by pretreatment. The most commonly used methods of pretreatment are the addition of ferro or ferricyanide to precipitate iron, zinc, copper and manganese, decreasing the available manganese content to below 0.002 ppm or passing the medium over ion exchange resin.

12.4 STARTER OR SEEDING AN INOCULUM

From the beginning of the experiment Petri dishes of nutrients are prepared with a media composition of: glucose, 50 g; KH_2PO_4, 2 g; $MgSO_4 \cdot 7H_2O$, 1 g; peptone 8 g, yeast extract, 2 g; agar 20 g and distilled water 1000 ml. Media and Petri dishes are separately sterilised. It is recommended each Petri dish is separately wrapped in aluminum foil. Distribution of media must be done in the presence of a flame. The stock culture is transferred to the Petri dish for cultivation. The conidia are harvested then transferred to the defined media for *A. niger*. Also, cultivation can be done in a cotton-clogged head of a flask with desired media in a shaker for good aeration. After 18 hours of growth, mycelia in the form of short and fat hyphae known as small pellets develop. If Petri dishes are used, you should wait for 2 days for spore formation. The conidia are washed with 1% saline solution (NaCl 10 $g \cdot l^{-1}$) and collected in an Erlenmeyer flask in sterilised media. Aseptic transformation is required.

12.5 SEED CULTURE

A seed culture is prepared as sterile media, and the stock culture is induced for spore formation. Ferrocyanide [$K_4Fe(CN)_6$ 200 ppm] in a medium containing 100 $g \cdot l^{-1}$ sugar is employed as the basal fermentation medium. The sugar solution must be pretreated and filtered, and passed through a cation- and anion-exchange column. After determination of media, inoculate the sterile media. The culture conditions are typically: incubation temperature (30 °C), initial pH (6.0), air supply of 1–2 dm^3/min. (0.5 to 1.0 vvm), agitation intensity (200 rpm) and batch experiment time about 3–5 days. The yield of citric acid is about 67–70%. The pH gradually drops to an acidic condition, which causes the process to be retarded. Since it has been shown that the nature and quantity of trace metals, carbon and nitrogen source, air supply and media pH are very important for successful citric acid fermentation, all these factors are considered in the course of fermentation. Standard media for yeast and fungi are used. The composition is shown in Table 12.1.

12.6 CITRIC ACID PRODUCTION

Citric acid fermentation of cane-molasses by submerged fermentation in 21 B. Braun stirred fermenter (working volume 21) is performed. A strain of *A. niger* ATCC 11414 is

TABLE 12.1. *Initial media composition for seed culture preparation*

Media composition	Concentration, $mg \cdot l^{-1}$
$NH_4 4Cl$	50
KH_2PO_4	30
$MgSO_4 \cdot 7H_2O$	20
$FeSO_4 \cdot 7H_2O$	10
$ZnCl_2$	10
$CuSO_4 \cdot 5H_2O$	10
Distilled H_2O	1000 ml

used in the present study, obtained from the American Type Culture Collection. Ferrocyanide-treated molasses [$K_4Fe(CN)_6$ 200 ppm] medium containing $100\,g \cdot l^{-1}$ sugar is used as the basal fermentation medium. Different cultural conditions such as incubation temperature (30 °C), initial pH (6.0), air supply ($1.0\,l^{-1}\,l^{-1}$ min), agitation intensity (200 rpm) and incubation time (about 5 days) will be optimised for enhanced citric acid production. A maximum amount of anhydrous citric acid with $100\,g \cdot l^{-1}$ of substrate is in the range 71–88 $g \cdot l^{-1}$. If the product is removed as it is formed, the yield can be maximised. Final pH and cell dry weight are about 2.1 and $10\,g \cdot l^{-1}$, respectively.

A. niger remains the organism of choice for the production of citric acid. In a submerged fermentor, either purified compressed air or oxygen and agitation are used. Molasses are a desirable raw material for citric acid fermentation because of their availability and relatively low price.

Incubation temperature plays an important role in the production of citric acid. Temperatures between 25 and 30 °C are usually employed for culturing of *A. niger,* but above 35 °C citric acid formation is inhibited because of the increased production of by-product acids and the inhibition of culture development. Citric acid production by *A. niger* is sensitive to the initial pH of the fermentation medium. The maximum production of citric acid (6.5%) was obtained at pH 5.4 in the molasses medium. The appropriate pH is important for the progress and successful termination of fermentation. The citric acid produced by *A. niger* is extremely sensitive to trace metals present in the molasses. Trace metals such as iron, zinc, copper and manganese present a critical problem in submerged fermentation. The organisms need major elements such as carbon, nitrogen, phosphorus and sulphur in addition to various trace elements for growth and citric acid production.[4,5]

12.7 ANALYTICAL METHOD

12.7.1 Cell Dry Weight

Cells, spores and mycelia are filtered (0.45 μm), the filter is dried in an oven at 80 °C, and the cell dry weight is determined according to the procedure explained in the earlier bioprocess module.

TABLE 12.2. *Experimental run for production of citric acid*

Time, h	DO, $mg \cdot l^{-1}$	Citric acid concentration, $g \cdot l^{-1}$	Cell dry weight, $g \cdot l^{-1}$	Sugar concentration, $g \cdot l^{-1}$
0	8	0	0.1	10
12	7	0.4	0.3	9
24	7	0.9	0.5	8
36	6	1.35	0.7	7
48	6	2.1	1	6
60	5	2.9	1.1	4
72	5	3.6	1.2	2
84	4	3.9	1.3	1
96	4	4	1.3	1
108	6	4	1.3	1
120	7	4	1.3	1

12.7.2 Carbohydrates

Sugars are estimated with reducing DNS reagent, based on the colorimetric method developed in an earlier module. The samples are determined by colour developed, which is detected by a spectrophotometer at a wavelength of 540 nm. In large-scale operations, mycelia are separated by a rotary drum filter.

12.7.3 Citric Acid

The citric acid obtained from fermentation is removed from the culture by precipitation. The precipitation is formed by the addition of $Ca(OH)_2$ 200 $g \cdot l^{-1}$, at 70 °C. The pH of solution is adjusted to 7.2. Tri-calcium citrate tetrahydrate is collected by filtration. The tri-calcium citrate as filter cake is dissolved in H_2SO_4 at 60 °C with 0.1% excess, the solid retained is $CaSO_4$ and the free citric acid is obtained. The free concentration of citric acid is determined with an enzymatic kit available from Merck. GC/HPLC is recommended for high accuracy of any research work.[5]

12.8 EXPERIMENTAL RUN

Based on the above discussion we are now ready to start a real experiment. Molasses are transferred from the sugar industry and kept in a cool room. The ATCC culture order has arrived and hydrated. Stock culture was prepared and aseptic transfer successfully done.

Prepare spores, fungal conidia/small pellets in Petri dish or cotton-plugged flask, for 48 hours. Harvest the spore in separate flask with media for propagation. Once in the separated flask the concentration of spores has reached to about 3 million per litre. It is now ready to be transferred to a 21 B. Braun biostat fermenter. The minimum volume of harvested spores in the flask is 300 ml. Media must be prepared based on sufficient carbon source

with 10 $g \cdot l^{-1}$ sugar, nitrogen sources and trace metals, as explained before and defined in Table 12.1. Air or pure oxygen is supplied to ensure availability of oxygen for sufficient aeration. The experimental data obtained are reported in Table 12.2.

REFERENCES

1. Baily, J.E. and Ollis, D.F., "Biochemical Engineering Fundamentals", 2nd edn. McGraw-Hill, New York, 1986.
2. Doran, P.M., "Bioprocess Engineering Principles". Academic Press, New York, 1995.
3. Schmauder, H.P., (ed.) "Methods in Biotechnology". Taylor & Francis, UK, 1997.
4. Stanbury, P.F. and Whitaker, A., "Principles of Fermentation Technology". Pergamon Press, Oxford, 1984.
5. Matthews, R.F. and Braddock, R.J., *Food Technol*. **41**, 57 (1987).

CHAPTER 13

Bioprocess Scale-up

13.1 INTRODUCTION

Microbial processes are developed and implemented in many ways. These processes are operated at different scales, such as bench, pilot and plant scales. For economic reasons, large-scale bioprocesses should not be disturbed and any modification to the running processes may not be considered. For research, many small-scale processes are developed to screen and develop better strains, improve existing culture, use efficient media and handle the process more efficiently with maximum productivity. The role of biochemical engineers in microbial processes is well defined. First, they should have clear understanding of the bioprocess and know the action of biocatalysts to stimulate biochemical reactions. Secondly, they should maintain optimal growth and the environmental conditions required to obtain maximum production yield. The microbial environment involves substrate and product concentrations, media composition, pH and temperature. There are many physical and chemical parameters involved in the growth environment once the organisms are propagated in a well-advanced bioreactor with instrumentation control. The process parameters are the flow dynamics and chemical dynamics of the biochemical system such as mass transfer, mixing, shear generated by agitation, power input, dilution rate, nutrients and growth stimulants. The chemical para-meters of the process are well controlled and optimised for growth kinetics; physical factors are based on process design. The process design, geometric shape and the size of the bioreactor are affected by dilution rate and substrate consumption rate. The operating parameters are well controlled. Changing bioreactor size must follow certain rules to meet special criteria. Most bioprocess designers have attempted to follow only vessel geometric similarities and some dimensionless numbers. However, only increasing volume and dimensions by keeping some dimensionless number constant may not satisfy the needs of bioprocess design.

13.2 SCALE-UP PROCEDURE FROM LABORATORY SCALE TO PLANT SCALE

The usual procedure for scale-up of a fermenter based on concepts is well known. The following criteria are translated between two scales of operation. They are selected as a procedure for scale-up.

1. Similar Reynolds number or momentum factors.
2. Constant power consumption per unit volume of liquid, P_g/V.
3. Constant impeller tip velocity, ND_i.
4. Equal liquid mixing and recirculation times, t_m.
5. Constant volumetric of mass transfer coefficient, K_La.
6. Keep all environmental factors for the microorganism constant.

Based on the practical history of scale-up, most fermentation processes for alcohol and organic acid production have followed the concepts of geometric similarity and constant power per unit volume. From the above concept, and as a strong basis for translation of process criteria, only physical properties of the process were considered in the scale-up calculation. For power consumption in an agitated vessel, there is a fixed relation between impeller speed, N, and impeller diameter, D_i. The constant power per unit volume, for a mechanical agitated vessel is given by:

$$\frac{P}{V} = \frac{\rho N^3 D_i^5}{D_i^3} \quad \text{for } Re \geq 10^4 \tag{13.2.1}$$

The power per unit volume is constant. From power consumptions in a bench-scale bioreactor, the necessary agitation rate is calculated for the scale up ratio, using Equation (13.2.1). The choice of criterion is dependent on what type of fermentation process has been studied. The following equation expresses relations for the impeller size and agitation rate in small and large bioreactors.

$$N_1^3 D_{i,1}^2 = N_2^3 D_{i,2}^2 \tag{13.2.2}$$

The agitation rate is proportional to impeller diameter to the power of 2/3.

$$N_2 = N_1 \left(\frac{D_{i,1}}{D_{i,2}} \right)^{2/3} \tag{13.2.3}$$

Similarly, that is true for the rotational speed of large tank, which is related to a small tank with the ratio of impeller diameter of large and small tanks to the power of 2/3.

$$rpm_2 = rpm_1 \left(\frac{D_{i,1}}{D_{i,2}} \right)^{2/3} \tag{13.2.4}$$

The characteristics of an agitated vessel with impeller spacing are illustrated in Figure 13.1.

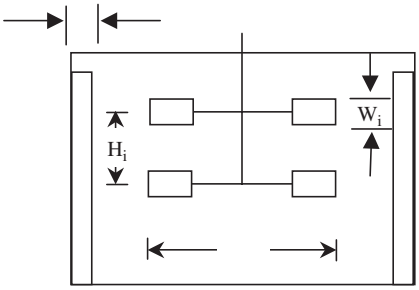

FIG. 13.1. Characteristics of agitated vessel with impeller spacing.

13.2.1 Scale-up for Constant K_La

The mass transfer coefficient K_La is constant; the general correlation is considered by many as proportional to the power per unit volume with constant exponent, and gas superficial velocity to another constant power as shown below:[1,2]

$$K_La = \alpha\left[\left(\frac{P_g}{V_L}\right)^a (V_S)^b\right] \tag{13.2.1.1}$$

There has to be a relation between k_La with aeration rate and agitation speed, and scale-up factor has to be determined. To eliminate the effect of viscous forces, the rheology of the media and broth for a large vessel have to be similar to that of a bench-scale vessel. For scale-up based on geometric similarity, the constant values a and b are proposed for the mass-transfer correlation in Table 13.1.

The oxygen transfer rate is calculated based on oxygen concentration gradient, by determination of the oxygen level in the liquid phase and the equilibrium value.

$$\text{OTR} = K_La(C^*_{AL} - C_{AL}) - XQ_{O_2} \tag{13.2.1.2}$$

At steady-state condition, change of oxygen concentration with time approaches zero. The value of K_La should be estimated by a correlation developed for various sizes of fermentation vessel.

$$K_La = \frac{XQ_{O_2}}{C^*_{AL} - C_{AL}} \tag{13.2.1.3}$$

where Q_{O_2} is oxygen transfer rate and X is biomass concentration.

TABLE 13.1. *Constants in mass transfer correlation for various fermenter size*

Fermentation vessel size, l	*a*	*b*
5	0.95	0.67
500	0.60–0.7	0.67
50,000	0.40–0.5	0.50

13.2.2 Scale-up Based on Shear Forces

Scale-up calculation is based on constant shear forces, where shear is directly related to impeller tip velocity. Shear forces are defined as

$$\tau = \mu \frac{\mathrm{d}u}{\mathrm{d}x} \tag{13.2.2.1}$$

where, τ is the shear stress, $\mathrm{d}u/\mathrm{d}x$ is the shear rate, and μ is the fluid viscosity. Since the shear is defined as S, which is proportional to $\pi N D_{\mathrm{i}}$, the concept of constant impeller tip velocity and constant power per unit volume were applied. Now introduce variable S for impeller tip velocity ND_{i} into Equation (13.2.2), then multiply both sides and divide by impeller diameter, so that the power equation is reduced to shear forces related to impeller diameter:

$$S_L = S_S \left(\frac{D_{\mathrm{i,L}}}{D_{\mathrm{i,S}}} \right)^{1/3} \tag{13.2.2.2}$$

The constant shear concept has been applied for bioreactor scale-up that utilises mycelia, where the fermentation process is shear sensitive and the broth is affected by shear rate of impeller tip velocity. For instance, in the production of novobicin, the yield of antibiotic production is dependent on impeller size and impeller tip velocity.

The impeller is a device where shear forces are transmitted to the fermentation broth. Since the process is sensitive to high agitation rate, it is necessary that the special bioreactor be scaled up, based on shear forces for maximising product yield such as antibiotics. This is the main reason for keeping impeller tip speed constant; in practice, it is recommended that this is in the range 0.25–0.5 $\mathrm{m \cdot s^{-1}}$. If the above conditions hold, it is not necessary to follow the geometric similarity constraint; however, it may violate the rule of power consumption per unit volume. Therefore keeping the impeller at a constant speed and keeping $K_L a$ constant may be required for special case studies for bioreactor design in antibiotic fermentation.

13.2.3 Scale-up for Constant Mixing Time

The problem associated with poor mixing in a large vessel was identified as low dissolved oxygen in the aerated vessel. The mixing time has been correlated with turbulent flow. In

a large-scale operation, the corrected function for mixing time incorporates the actual mixing time with impeller speed, tank diameter and liquid height. The function of mixing, f*(t)* is defined as constant mixing time:

$$\mathrm{f}(t) = t_{\mathrm{m}}(ND_{\mathrm{i}}^{\ 2})^{2/3} g^{1/6} D_{\mathrm{i}}^{\ 1/2} Y^{1/2} D_{\mathrm{t}}^{\ 3/2} \tag{13.2.3.1}$$

where, t_{m} is the mixing time, g is gravity, D_{t} is the tank diameter, and Y the depth of the liquid. Substitute (13.2.2) into (13.2.2.2) as power per unit volume is constant; the resulting equation is the mixing time:

$$\frac{t_{\mathrm{mL}}}{t_{\mathrm{mS}}} = \left[\left(\frac{N_{\mathrm{S}}}{N_{\mathrm{L}}} \right)^4 \left(\frac{D_{\mathrm{iL}}}{D_{\mathrm{iS}}} \right) \right]^{1/6} \tag{13.2.3.2}$$

That is proportional to impeller diameter to the power of 0.65. Then, solving for mixing time:

$$t_{\mathrm{mL}} = t_{\mathrm{mS}} \left(\frac{D_{\mathrm{iL}}}{D_{\mathrm{iS}}} \right)^{11/18} = t_{\mathrm{mS}} \left(\frac{D_{\mathrm{iL}}}{D_{\mathrm{iS}}} \right)^{0.65} \tag{13.2.3.3}$$

Equation 13.2.3.3 is used for geometric similarity, where t_{mS} and t_{mL} represent the mixing time for small and large fermentation vessels. Mixing and mixing time have been major concerns for several investigators, because large-scale vessels may not have uniform mixing whereas in small vessels mixing is not a problem. The mixing time in large vessels has been correlated based on dimensional analysis.

In 1953, Rushton proposed a dimensionless number that is used for scale-up calculation. The dimensionless group is proportional to N_{Re} as shown by the following equation:[2,3]

$$\psi = k(N_{Re})^a \tag{13.2.3.4}$$

where the Reynolds number for an agitated vessel was defined as:

$$Re = \frac{\rho N D_{\mathrm{i}}^{\ 2}}{\mu} \tag{13.2.3.5}$$

Since the process is more complex, the proposed method may not be valid for scale-up calculation. The combination of power and Reynolds number was the next step for correlating power and fluid-flow dimensionless number, which was to define power number as a function of the Reynolds number. In fact, the study by Rushton summarised various geometrics of impellers, as his findings were plotted as dimensionless power input versus impeller

Reynolds number; the plot is known as a power graph. The plot is presented in Figure 6.6, Chapter 6. Equation 13.2.3.6 correlates the power number as a function of Reynolds number.

$$N_p = k(\mathrm{Re})^{-m} \tag{13.2.3.6}$$

In fact, the power number is a dimensionless number that is the ratio of ungassed power to gassed power in a normal bioreactor.[3]

$$N_P = \frac{Pg_c}{\rho N^3 D_\mathrm{i}^5} \tag{13.2.3.7}$$

where P is ungassed power, in W or hp.

In a mixed agitated vessel with high agitation rate, at the centre of the vessel a vortex often forms. To prevent a central vortex in tanks less than 3 m in diameter, four baffles each with a baffle width of 15–20 cm are necessary. A basic assumption is to select a ratio of liquid height to tank diameter from 2:1 to 6:1.

$$\frac{H_\mathrm{L}}{D_\mathrm{t}} = 2{:}1\text{–}6{:}1 \tag{13.2.3.8}$$

It is common for an agitated vessel to have the tank diameter equal to the liquid working volume.

$$\frac{H_\mathrm{L}}{D_\mathrm{t}} = 1 \tag{13.2.3.9}$$

Also, select a ratio of tank diameter to baffle width from 10 to 12:

$$\frac{D_\mathrm{t}}{D_\mathrm{b}} = 10\text{–}12 \tag{13.2.3.10}$$

A suitable impeller interspacing (H_i) is preferred for good mixing that has to be in distance of less than $2D_\mathrm{i}$:

$$D_\mathrm{i} < H_\mathrm{i} < 2D_\mathrm{i} \tag{13.2.3.11}$$

It is well understood that mixing and mass transfer are affected by agitation and aeration rates. Typically, in an agitated vessel, the working volume is about 75% of nominal CSTR volume.

13.3 BIOREACTOR DESIGN CRITERIA

The Bioreactor is the major equipment used in biochemical processes. It differs totally from a simple chemical reaction vessel. To control physical operating parameters and microbial environmental conditions, there are several influential variables:

- Biomass concentration
- Sterile condition
- Effect of agitation and mass transfer
- Heat removal for temperature control
- pH control of the media
- Correct shear conditions

Bioreactors in terms of operation and specific criteria are well defined. The most useful and applied types of bioreactor are:

- CSTR
- Air lift: air is used for fluid circulation by pressurised air
- Loop reactor: modified air lift, pump transport the air and fluid through the vessel.
- Immobilised system: air and fluid circulate over a film of microorganisms grown on a solid support.
- Tower fermenter
- Membrane bioreactor

13.3.1 General Cases

If the height of liquid, $H_{L,}$ is equal to D_t, one set of agitators is enough to obtain sufficient mixing. For H_L equal to $2D_t$ or $3D_t$, additional sets of agitators separated by distance H_i are required, mounted on the same shaft. Spargers are placed at a distance $D_i/2$ from the bottom of the tank. Power input is greater than $100\,W\cdot m^{-3}$ and the tip impeller speed is πND_i greater than $1.5\,m\cdot s^{-1}$. Also, Froude number is $\frac{N^2 D_i}{g}$ greater than 1.0. H_i is impeller inter spacing.

Foam in the bioreactor is troublesome: it can reduce the oxygen transfer rate (OTR). Antifoam is use to prevent foam formation. However, excess antifoam may cause growth inhibition in the course of fermentation. The simplest device is known as a foam breaker, which is mounted on the stirrer shaft located on the surface of liquid. It is a flat blade.

13.3.2 Bubble Column

For production of baker's yeast, beer, vinegar, and in wastewater treatment, bubble columns are used. Generally these columns should be long enough so that bubbles are utilised as they rise while passing through the column. Column diameters range from 10 cm to 7.5 m. The height of column is three to six times greater than the diameter. The common height

and diameter ratio (*H/D*) is in the range 2–6. The H:D ratio that is commonly used is 3:1; the ratio especially used for baker's yeast production is 6:1.

Hydrodynamics and mass transfer in bubble columns are dependent on the bubble size and the bubble velocity. As the bubble is released from the sparger, it comes into contact with media and microorganisms in the column. In sugar fermentation, glucose is converted to ethanol and carbon dioxide:

$$C_6H_{12}O_6 \rightarrow 2C_2H_5OH + 2CO_2 \tag{13.3.2.1}$$

The superficial gas velocity is the air flow rate per unit cross sectional area of the column. The superficial gas velocity is less than $0.4\,m{\cdot}s^{-1}$ and media flow rate is based on liquid velocity. Then, the column may have a hydraulic retention time that is a function of fluid velocity and column diameter. The liquid velocity is given by:[4]

$$U_L = 0.9(gDU_g)^{0.33} \tag{13.3.2.2}$$

where, U_g is the upward gas bubble velocity at the centre of column, the gas superficial velocity is in the range of $0 < U_g < 0.4\,m{\cdot}s^{-1}$ and the column diameter is in the range $0.1 < D < 7.5\,m$. The hydraulic retention time is obtained by division of column height and the actual liquid velocity:

$$U_g = \frac{\text{Air flow rate}}{\text{Cross-sectional area}} = \frac{Q_g}{A} \tag{13.3.2.3}$$

The mixing time, t_m is given by:[2]

$$t_m = 11\left(\frac{H_L}{D}\right)\left(\frac{gU_g}{D^2}\right)^{-0.33} \tag{13.3.2.4}$$

where, H_L is the height of bubble column.

Example 1

Let us have a bubble column with an *H/D* ratio of 3, diameter 0.5 m and a gas flow rate of $0.1\,m^3{\cdot}h^{-1}$, which gives a superficial gas velocity of $0.25\,m{\cdot}s^{-1}$. What would be the liquid media flow rate?

Solution

Once superficial gas velocity is defined, then liquid velocity is given by (13.3.2.2).

$$U_g = \frac{Q_g}{A} = \frac{4(0.1)}{0.5\pi} = 0.255 \text{ m·s}^{-1}$$

$$U_L = 0.9\ [(9.81)(0.5)(0.255)]^{0.33} = 0.96 \text{ m·s}^{-1}$$

Equation (13.23) is used to calculate mixing time.

$$\tau_m = 11\left(\frac{1.5}{0.5}\right)\left(\frac{(9.81)(0.255)}{(0.5)^2}\right)^{-0.33} = 31 \text{ hours}$$

Based on mixing time, the liquid media flow rate is:

$$Q_L = \frac{V}{\tau} = \frac{(1.5)(0.25\pi)/4}{31} = 9.5\times10^{-3}\,\text{m}^3\text{·h}^{-1}$$

Example 2

Calculate the speed of an impeller and the power requirements of a production-scale bioreactor with 60 m^3 using two different methods. Also, match the volumetric mass transfer coefficient. The following optimum conditions were obtained with a small-scale fermenter of volume 0.3 m^3 and 60% of the vessel working. The density of broth, ρ_{broth}, 1200 $kg\cdot m^{-3}$, working volume 0.18 m^3, aeration rate of one volume of gas per volume of liquid (1 vvm), oxygen transfer rate 0.25 $kmol\cdot m^{-3}\cdot h^{-1}$, liquid height inside the vessel, H_L, $1.2D_t$. Two sets of standard, flat-blade turbine impellers were installed.

Solution

$$V_l = \frac{\pi}{4}\times D_t^{\,2}(1.2\,D_t) = 0.3\pi D_t^{\,3}$$

Diameter of the vessel:

$$D_t = \left(\frac{V_l}{0.3\pi}\right)^{1/3} = \left(\frac{0.18}{0.3\pi}\right)^{1/3} = 0.576 \text{ m}$$

Diameter of the impeller:

$$D_{i,1} = \frac{1}{3}\times D_t = \frac{0.576}{3} = 0.192 \text{ m}$$

Height of liquid media was assumed to be 1.2 times the diameter of the fermentation vessel.

$$H_{L1} = 1.2 \times 0.576 = 0.691 \text{ m}$$

Diameter of the larger vessel:

$$D_{t2} = \left(\frac{V_1}{0.3\pi} \right)^{1/3} = \left(\frac{60}{0.3\pi} \right)^{1/3} = 3.36 \text{ m}$$

The impeller size for the larger vessel is:

$$D_{i2} = \frac{3.36}{3} = 1.12 \text{ m}$$

and the liquid media height in the second fermenter is:

$$H_{L2} = 1.2 \times 3.36 = 4.03 \text{ m}$$

Assume the fermentation broth has the same viscosity as water:

$$\overline{\mu_1} = 1 \text{ cp}$$

Aeration rate for 1 vvm is:

$$F_1 = 1 \times 0.18 = 0.018 \text{ m}^3.\text{min}^{-1} = 3 \times 10^{-3} \text{ m}^3.\text{s}^{-1}$$

Gas superficial velocity is:

$$U_S = \frac{0.18 \times 60}{\frac{\pi}{4}(0.576)^2} = 41.45 \text{ m} \cdot \text{h}^{-1}$$

Let us take average values for the partial pressure of oxygen

$$\overline{P_{O_2}} = \frac{1 \text{ atm} + \left(1 + \frac{H_L \text{ m}}{10.3 \text{ m}} \cdot \text{atm} \right)}{2} \times 0.21 = 0.213 \text{ atm}$$

The oxygen transfer rate is

$$(Kv\,\overline{P_{O_2}}) = 0.25\ \text{kmol}\cdot\text{m}^{-3}\cdot\text{h}^{-1}$$

The mass transfer coefficient is

$$Kv_1 = \frac{0.25}{0.213} = 1.174\ \text{kmol}\cdot\text{m}^{-3}\cdot\text{h}^{-1}\cdot\text{atm}^{-1}$$

Use imperial correction based on the following equation for mass transfer in the bioreactors.[1,2] The general equation for evaluation of K_La is

$$K_La = x\left(\frac{P_g}{V}\right)^Y (U_s)^Z \tag{E.2.1}$$

where *x, y* and *z* are empirical constants. For Newtonian fluids, non-coalescing broth and gas bubbles, the following correlation is valid for a working volume of less than 4 m^3 and a power per unit volume of 500–10,000 $W\cdot m^{-3}$.

$$Kv = 0.002\left(\frac{P_g}{V}\right)^{0.7} Us^{0.5} \tag{E.2.2}$$

$$1.174 = 0.002\left(\frac{P_g}{V}\right)^{0.7} (41.45)^{0.5}$$

For the gassed power per unit volume $\left(\frac{P_g}{V}\right)$ is 630.7 W; the passed power, P_g, was 0.15 hp.

Since the flow regime is turbulent, the power number obtained from Figure 6.6, Power number versus Reynolds number, *Re*, reads $P_{no} = 6$. For two sets of impellers, $N_p = 2(6) = 12$.

$$N_P = \frac{P_1 g_C}{\rho N_1^{\,3} D_i^{\,5}} \tag{E.2.3}$$

$$P_1 = \frac{12\times 1200\times N_1^{\,3}\times (0.192)^5}{9.81} = 0.383\,N_1^{\,3}\ \text{W} = 5\times 10^{-4} N_1^{\,3}\,\text{hp}$$

Using Michel and Miller's correction factor for power calculation:[5,6]

$$P_{g1} = 0.5\left\{\frac{P_1^{\,2}\eta_1 D_{i1}^{\,3}}{\overline{\mu}_1^{\,0.56}}\right\}^{0.45} \tag{E.2.4}$$

Knowing the power input, we can calculate the rotational speed:

$$0.15 = 0.5\left\{\frac{(5\times10^{-4})^2(N_1{}^3)^2(0.192)^3}{(3\times10^{-3})^{0.56}}\right\}^{0.45}$$

$$N_1 = 10 \text{ rps}$$

$$N_1 = 600 \text{ rpm}$$

The power input for ungassed system is

$$P_1 = 5\times10^{-4} N_1{}^3 = 5\times10^{-4}(10)^3 = 0.5 \text{ hp}$$

$$\frac{P_g}{P} = \frac{0.15}{0.5} = 0.3$$

For constant power input based on geometric similarity of the vessels, agitation rate is calculated.

$$\frac{\rho N_1{}^3 D_{i1}{}^5}{V_1} = \frac{\rho N_2{}^3 D_{i2}{}^5}{V_2} \tag{E.2.5}$$

$$\left(\frac{N_2}{N_1}\right)^3 = \left(\frac{V_2}{V_1}\right)\left(\frac{D_{i1}}{D_{i2}}\right)^5 \tag{E.2.6}$$

$$N_2 = N_1\left(\frac{V_2}{V_1}\right)^{1/3}\left(\frac{D_{i1}}{D_{i2}}\right)^{5/3} = 600\left(\frac{60}{0.3}\right)^{1/3}\left(\frac{0.192}{1.12}\right)^{5/3} = 185 \text{ rpm} \leftarrow$$

For constant input velocity for a large system:

$$N_2 = N_1\left(\frac{D_{i1}}{D_{i2}}\right) = 600\left(\frac{0.192}{1.12}\right) = 103 \text{ rpm} \leftarrow$$

13.4 CSTR CHEMOSTAT VERSUS TUBULAR PLUG FLOW

The performance of a biochemical reactor is designed and evaluated based the reaction rate equation. The rate of biomass generation is based on the Monod rate model:

$$qx = \frac{kC_S x}{K_m + C_S} = \frac{kxS}{a+S} \tag{13.4.1}$$

where $S = \dfrac{C_s}{C_{sf}}$ and $a = \dfrac{K_m}{C_{sf}}$ are dimensionless, K_m is the Monod rate constant, $g \cdot l^{-1}$, and kx represents the maximum specific growth rate, $g \cdot l^{-1} \cdot h^{-1}$. The fresh media dilution rate for cell production is D, h^{-1}

$$D = \frac{qx}{x} = \frac{q_S}{C_{Sf} - C_S} \tag{13.4.2}$$

The substrate concentration is defined as:

$$S = (1 - S) Y_{X/S}\ C_{Sf} \tag{13.4.3}$$

The yield is incorporated into (13.4.1).

$$qx = \frac{kS}{a + S}(1 - S)\ \ Y_{X/S}\ C_{Sf} \tag{13.4.4}$$

Example 1

A special CSTR fermentation known as a chemostat bioreactor is used for microbial cell growth. The rate of biomass generation is given by:

$$q_x = \frac{4}{3}\frac{V_{SX}}{C_S + 4}\frac{\text{g cells}}{\text{m}^3 \cdot \text{h}} \tag{E.1.1}$$

We wish to compare the performance of two reactor types: plug flow versus CSTR with a substrate concentration of $C\text{s}_\text{f} = 60\,\text{g} \cdot \text{m}^{-3}$ and a biomass yield of $Y_{x/s} = 0.1$. In a plug flow bioreactor with volume of $1\,\text{m}^3$ and volumetric flow rate of $2.5\,\text{m}^3 \cdot \text{h}^{-1}$, what would be the recycle ratio for maximum q_x compared with corresponding results and rate models proposed for the chemostat?

Solution

To maximise q_x, we need to take the derivative of the following function, if $\dfrac{S(1-S)}{a+S}$ is maximum, then the derivative must be set to zero

$$\frac{\text{d}}{\text{d}S}\left[\frac{S(1-S)}{a+S}\right] = \frac{(1-2S)(a+S) - S(1-S)}{(a+S)^2} = 0 \tag{E.1.2}$$

$$(1-2S)(a+S)-S(1-S)=0 \tag{E.1.3}$$

$$S^2+2aS-a=0 \tag{E.1.4}$$

$$S=-a+\sqrt{a+a^2} \tag{E.1.5}$$

The quadratic equation is solved for a

$$a=\frac{1}{15}=\frac{K_m}{C_{Sf}}=\frac{4}{60}$$

$$Y_{X/S}=0.1$$

Maximum cell production is obtained in a chemostat at:

$$S=-a+\sqrt{a+a^2}=\frac{1}{15}+\sqrt{\frac{1}{15}+\left(\frac{1}{15}\right)^2}=\frac{1}{5}$$
$$\frac{1}{q_x}=\frac{4+C_S}{C_S\times x}\times\frac{3}{4} \tag{E.1.6}$$

Now, we can generate data by plug-in numbers in the above equation. We need to illustrate inverse rate versus substrate concentration. After the data are plotted we can justify a suitable type of bioreactor

$$x=Y_{X/s}(C_f-C_s)=0.1\,(60-3)=5.7$$

$$x=0.1\,(55)=5.5$$

The performance data for plug versus mix reactor were obtained. The data were collected as the inverse of q_x vs inverse of substrate concentration. Table E.1.1 shows the data based on obtained kinetic data. From the data plotted in Figure E.1.1, we can minimise the volume of the chemostat. A CSTR works better than a plug flow reactor for the production of biomass. Maximum q_x is obtained with a substrate concentration in the leaving stream of $12\,\mathrm{g\cdot m^{-3}}$.

$$S=\frac{1}{5}=\frac{C_S}{60}$$

Then, the substrate concentration is:

$$C_S=12\ \mathrm{g\cdot m^{-3}}$$

TABLE E.1.1. *Substrate concentration versus inverse biomass concentration*

Substrate concentration Cs, $g \cdot m^{-3}$	Inverse of biomass rate $1/q_x$, $m^3 \cdot g^{-1} \cdot h^{-1}$
3	0.310
5	0.250
10	0.210
15	0.210
20	0.225
25	0.250
30	0.280
35	0.330
40	0.410
45	0.540
50	0.810
55	1.610

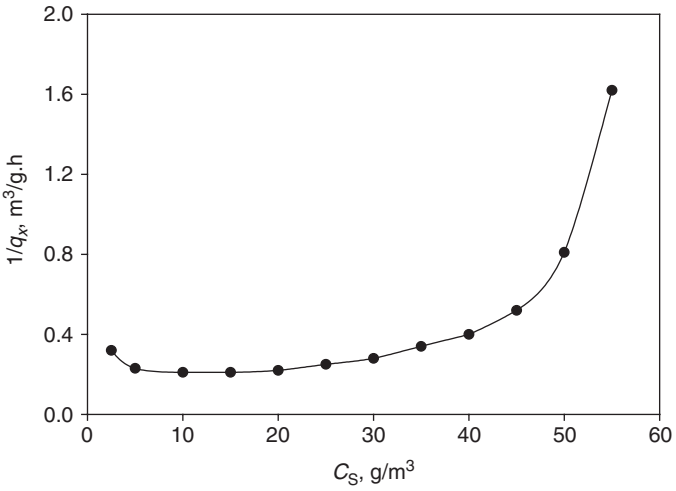

FIG. E.1.1. Performance plot for plug versus mix reactor.

A tubular bioreactor design with operational may lead to a CSTR, having sufficient recycle ratio for plug flow that behave like chemostat. The recirculation plug flow reactor is better than a chemostat, with maximum productivity at $C_s = 3\,g \cdot m^{-3}$. Combination of plug flow with CSTR which behave like chemostat was obtained from the illustration minimised curve with maximum rate at $C_{Sf} = 3\,g \cdot m^{-3}$.

In plug flow reactor the value for C_S is reduced from 12 to 3 g·m^{-3}, then the retention time and rate model with recycle ratio in a plug flow reactor can be written as:

$$\tau = \frac{C_{Sf}V}{\nu_O} = -(R+1)\int_{\frac{C_{Sf}+RC_S}{R+1}}^{C_S} \frac{dC_S}{\frac{4\nu_{SX}C_S}{3(C_S+4)}} \tag{E.1.7}$$

$$\frac{K_m}{S_f}\ln\left(\frac{C_{Sf}+RCs}{RCs}\right)+\ln\left(\frac{R+1}{R}\right)=\frac{R+1}{R}\times\frac{K_m}{f+R}+\frac{1}{R} \tag{E.1.8}$$

where S_f is the inlet to outlet substrate ratio, R is the recycle ratio, and f is the ratio of inlet to outlet substrate concentration. Solve R by trial and error, with calculation for right- and left-hand sides with the assumption of a value for R:

$$\frac{4/3}{60/3}\ln\left(\frac{60+2.5(3)}{2.5(3)}\right)+\ln\left(\frac{2.5+1}{2.5}\right)=\frac{2.5+1}{2.5}\times\frac{4/3}{20+2.5}+\frac{1}{2.5}$$

Let us plug in $f = 20$, $k_m = 4/3$ and $R = 2.5$ into (E.1.9), then calculate $k\tau$

$$k\tau = (R)\left[\ln\left(\frac{R+1}{R}\right)+\frac{K_m}{f}\ln\left(\frac{C_{Sf}+RC_S}{R}\right)\right] \tag{E.1.9}$$

$$k\tau = (2.5)\left[\ln\left(\frac{3.5}{2.5}\right)+\frac{4/3}{20}\ln\left(\frac{60+2.5(3)}{2.5}\right)\right]$$

$$k\tau = 1$$

Example 2: Applied Calculation Method for Scale-up

The bioreactor will be scaled up by a factor of 125. It is necessary to discuss the effect of operating variables resulting from constant power per unit volume, agitation rate, and speed tip velocity, N_{Re}. The data for a small-scale bioreactor are a 100 litres fermenter with 187.5 rpm and

$$V_1 \times 125 = V_2 = 12.5\ \text{m}^3$$

$$\frac{P}{V} = \text{constant} \tag{E.2.1}$$

$$N_i D_i = \text{constant} \tag{E.2.2}$$

Factoring for scale-up, we make some assumptions and may use a few known correlations to progress our calculations. Let us say $P\alpha V = D_i^3$, $H/D = 1$ and $D/D_i = 3$. Also, use constant power per unit volume for the small- and large-scale bioreactor.

$$\frac{P}{V} \approx (N_i^3 D_i^2)_{\text{Small}} = (N_i^3 D_i^2)_{\text{Large}} \tag{E.2.3}$$

Since we assumed power per unit volume is constant, it is possible $(N_i D_i)_1$ may not be equal with $(N_i D_i)_2$. Now calculate the agitation rate for a large vessel.

$$N_{i2} = N_{i1}\left(\frac{D_{i1}}{D_{i2}}\right)^{2/3} = 600\left(\frac{1}{5}\right)^{2/3} = 204 \text{ rpm}$$

$$\frac{H}{V}\alpha\frac{N_i D_i^3}{D_i^3}$$

$$V = HD^2\frac{\pi}{4} = \frac{\pi D^3}{4} = \frac{9}{4}\pi D_i^3$$

Now assume $H \approx D$, $D = 3D_i$ and bioreactor volume is proportional to impeller diameter to the power of $V \propto D_i^3$. The Reynolds number is written as:

$$Re_i = \frac{\rho N D_i}{\mu} \tag{E.2.4}$$

The power for laminar flow is proportional to agitation rate, N^2, and if the flow is turbulent the power is proportional to $\sim N^3 D_i^2$. Let us assume the mass transfer coefficients remain constant ($K_L a$ unchanged):

$$\frac{D_i}{D_t} = 0.33$$

$$ND_i = 0.5 \text{ m/s}$$

Also assume the height of liquid media is 1.2 times the tank diameter.

$$\frac{H}{D_t} = 1.2$$

$$V_s = 100\,1\frac{1.2}{4}\pi D_i^3$$

The diameter of small tank is 47.4 cm. Since the impeller is one third of the tank diameter, $D_i = 16\,\text{cm}$

$$Re_i = \frac{(1\ \text{g/cm}^3)(50\ \text{cm/s})(16)}{0.01} = 80{,}000\ \text{Tubulent flow} \tag{E.2.5}$$

Power is defined for a well-agitated vessel with a mechanical stirrer; then read power number for turbulent flow from Figure 6.6, Chapter 6:

$$P_{\text{no.}} = \frac{P \cdot g_C}{\rho N^3 D_i^5} = 6$$

$$ND_i = 0.5$$

$$N = \frac{0.5}{0.16} \tag{E.2.6}$$

Calculate power for a small-scale vessel:

$$P_{\text{Small}} = 6 \times \frac{(1000\ \text{kg/m}^3)(3.125)^3 (0.16)^5}{9.81} = 1.96\ \text{W} \tag{E.2.7}$$

The power for large vessel is based on scale factor, that is calculated as following:

$$P_{\text{Large}} = 125 \times 1.96 = 245\ \text{W} \tag{E.2.8}$$

For mass transfer calculation

$$K_L a = \text{constant}$$
$$V_s = 1001 \qquad D_i = 16\,\text{cm} \qquad D_t = 47.43\,\text{cm}$$
$$ND_i = 0.5$$
$$N_i = \frac{0.5}{0.16} = 3.125\ \text{rps} = 187.5\ \text{rpm} \tag{E.2.9}$$

When $Re = 80{,}000$ for turbulent flow, the power number versus Re, we can read

$$P_{\text{no}} = 6$$

$$P_{\text{NO}} = \frac{P \cdot g}{\rho N_i^3 D_i^5}$$

$$P_{\text{small}} = \frac{6 \times 1000 \times 3.125^3 \times 0.16^5}{9.81} = 1.96 \text{ W}$$

$$\frac{1.96}{0.1} = 19.6 \frac{\text{W}}{\text{m}^3} \tag{E.2.10}$$

Scale-up factor = 125

$$\frac{P_s}{P_L} = \frac{(N_i^3 D_i^5)s}{(N_i^3 D_i^5)_L} = \frac{1}{125} \tag{E.2.11}$$

The power required for a large vessel is:

$$P_L = 19.6 \times 125 = 2450 \text{ W} \tag{E.2.12}$$

The power per unit volume of small bioreactor is

$$P/V = 19.6/0.1 = 196 \text{ W.m}^{-3} \tag{E.2.13}$$

The volume of a large vessel is

$$V_L = 2450/196 = 12.5 \text{ m}^3$$

$$\left(\frac{D_{iL}}{D_{iS}}\right)^2 = 25$$

$$D_{iL} = (0.84 \text{ m})$$

$$\frac{\pi}{4} D_t^3 = \frac{\pi}{4} (2.515)^3 = 12.5 \text{ m}^3 \tag{E.2.14}$$

We have understood the following concepts are true; our calculations also support the fact that power per unit volume is constant.

$$ND_i \neq \text{constant} \qquad N^3 D_i^2 = \text{constant}$$

$$V_L = 12.5 V_s$$

$$D_{t,L} = \frac{4}{\pi} \sqrt[3]{12.5} \quad D_{tL} = 2.515 \text{ m}, D_{i,L} = 0.84 \text{ m}$$

$$N_{i,L} = N_{i,S}\left(\frac{D_{i,S}}{D_{i,L}}\right)^{2/3} = (3.125)\left(\frac{0.16}{0.8}\right)^{2/3} = 1 \text{ rps}$$

$$Re_{i,L} = \frac{\rho N_i D_i^2}{\mu} = \frac{(1000)(0.8)^2(1)}{0.001\frac{\text{kg}}{\text{m.s}}} = 6.2\times10^5$$

$$P_{no} = 6$$

$$\text{Power} = 0.3\,\text{hp} \qquad \text{(E.2.15)}$$

Example 3: Power Calculation

A 20 m^3 working volume of bioreactor is used for production of penicillin. What is the initial substrate concentration, S_o, that you choose when there is a limitation in sufficient oxygen transfer rate and there are no limiting reactants?

Bioreactor Characteristics and Given Data

D_{tank}	=	2.4 m	Turbine		
D_i	=	0.8 m	μ_{broth}	=	1 mPa.s
N_i	=	2.3 rps	P	=	1.2 ρ_{H_2O}
Number of blades	=	8	Aeration rate	=	1 vvm
P_g/P	=	0.4			

If you aerate a bioreactor, power consumption is much less than a non-aerated bioreactor.

Oxygen transfer rate, OTR: 6×10^{-3} kg·m^{-3}

Oxygen uptake rate, OUR: 0.65 mmol O_2·kg^{-1} cell

Specific growth rate, υ_{max}: 0.5 h^{-1}

Specific sugar consumption rate = 1.0 kg·kg^{-1} cell·h^{-1}

The mass transfer coefficient is calculated by the following correlation

$$K_L a\,(s^{-1}) = 2\times10^{-3}\left(\frac{P_g}{V}\right)^{0.6} V_S^{0.667} \qquad \text{(E.3.1)}$$

where P_g/V is the power per unit volume (hp·m^{-3}) and V_S is the gas superficial velocity (cm·min^{-1}).

Solution

The flow regime is turbulent as the Reynolds number is large.

$$N_{Re} = \frac{\rho D v}{\mu} = \frac{\rho D_i (N_i D_i)}{\mu} = \frac{1200(0.8)^2(2.3)}{0.1} = 1.92 \times 10^4$$

Read power number N_p from the graph $P_{no.}$ versus Re: $N_p = 6$

$$N_p = \frac{P g_c}{\rho N^3 {D_i}^5} \Rightarrow P = N_p \rho N^3 {D_i}^5 / g_c$$
$$= 6 \times 1200 \times (2.5)^3 \times (0.8)^5 / 9.81$$
$$= \frac{3758 \text{ kg.m/s hp}}{745.7 \text{ kg.m/s}} = 5.04 \text{ hp}$$

Correction factor for non-geometrical similarity,

$$f_c = \sqrt{\frac{(D_t/D_i)^* (H_L/D_i)^*}{(D_t/D_i)(H_L/D_i)}} = \sqrt{\frac{3 \times 4.42}{3 \times 3}} = 1.25$$

$$(D_t/D_i)^* = \frac{2.4}{0.8} = 3$$

$$(H_L/D_i)^* = \frac{20 \text{ m}^3}{(2.4)^2 \frac{\pi}{4} / 0.8} = 4.42$$

The power input for three sets of impellers in a single shaft is:

$$P = (5.04 \text{ hp})(1.25)(\text{three sets of impellers}) = 19 \text{ hp}$$

$$\text{Aeration rate} = N_a = \frac{F_g}{N_i {D_i}^3} \tag{E.3.2}$$

$$F_g = 20 \text{ m}^3.\text{min}^{-1} = 1 \text{ vvm} \times V_L = 0.333 \text{ m}^3 \cdot \text{s}^{-1}$$

Given gassed power is 40% of ungassed power,

$$P_g/P = 0.4 \qquad P_g = 0.4 \times 19 = 7.6\,\text{hp}$$

$$N_a \frac{F_g}{N_i D_i^3} = \frac{0.333}{2.5 \times (0.8)^3} = 0.26$$

$$V_S = \frac{20\ \text{m}^3/\text{min}}{\frac{\pi}{4} \times (2.4)^2\,\text{m}^2} = 4.42\ \text{m/min} = 7.4 \times 10^{-2}\ \text{m/s} \tag{E.3.3}$$

The mass transfer coefficient is calculated.

$$K_L a = 2 \times 10^{-3} \left(\frac{7.6 \times 754.7\ \text{W/hp}}{20} \right)^{0.6} (4.42)^{0.667} = 3.57\ \text{s}^{-1} \tag{E.3.4}$$

With an assumption of oxygen concentration at the interface, equilibrium with liquid phase is 6 ppm, the oxygen transfer rate is calculated.

$$OTR = K_L a (C^*_{O_2} - C_{O_2}) = (3.57)(6 \times 10^{-3}) = 0.02\ \text{kg/m}^3 \cdot \text{s}$$

$$OTR = x q_{O_2} = (0.65 \times 10^{-3})(32 \times 10^{-3}) x$$

$$OUR q_{O_2} = 2.08 \times 10^{-3}\ \text{kg O}_2\text{/kg cell.s}$$

$$x = \frac{0.02}{2.08 \times 10^{-3}} = 10.3\ \text{kg/m}^3 \tag{E.3.5}$$

Cell Balance

$$19.375 = x_S = x_0 + \overbrace{\frac{\mu_{max}}{q_S}}^{\text{Sugar to cell}} C_S = 0 + \frac{0.5}{1.0} C_S$$

$$C_S = \frac{10.3}{0.5} = 20.6\ \text{kg/m}^3 \tag{E.3.6}$$

Example 4: Scale-up Calculations

Calculate mass transfer, gas hold up, gassed and ungassed power for the fermenter with the given data:

$\rho_{broth} = 1200\,kg{\cdot}m^{-3}$ $\mu = 0.002\,N.s.m^{-2}$ $N_i = 90\,rpm$
$D_t = 4\,m$ $D_i = 2\,m$ $w_b = 0.4\,m$ $H_L = 6.5\,m$

Air is sparged with 0.4 vvm, it is equipped with two sets of impellers and a flat-blade turbine with four baffles.

Calculate: (a) power, P; (b) Power, P_g; (c) K_La; (d) gas holdup.

Solution

$$(D_t/D_i)^* = 2 \quad (H_L/D_i)^* = \frac{6.5}{2} = 3.25$$

$$N = 90\,rpm/60 = 1.5\,rps$$

$$N_{Re} = \frac{ND_i^2\rho}{\mu} = \frac{1.5\times 2^2\times 1200}{0.002} = 3.6\times 10^6$$

Read N_p from Figure 6.6, Chapter 6, power versus Re, for a turbulent regime, $N_p = 6$

$$6 = \frac{P\times 9.81}{(1.5)^3(2)^5(1200)} \Rightarrow P = 105\ hp$$

Correction factor for non-geometrical similarity,

$$f_c = \sqrt{\frac{(D_t/D_i)^*(H_L/D_i)^*}{(D_t/D_i)(H_L/D_i)}} = \sqrt{\frac{2\times 3.25}{3\times 3}} = 0.85 \qquad \text{(E.4.1)}$$

$$P = 2\times 0.8\times 105 = 168\,hp$$

The gas flow rate is

$$F_g = 0.4(4)^2\left(\frac{\pi}{4}\right)(6.5) = 32.67\ m^3/min = 0.5445\ m^3/s$$

The aeration number is

$$N_a \frac{F_g}{N_i D_i^3} = \frac{0.5445}{1.5 \times (2)^3} = 0.045$$

Reading gassed power to ungassed power ratio from the plot for the ratio of P_g/P, defined in Figure 6.6, Chapter 6.

$$\frac{P_g}{P} = \frac{P_a}{P} = 0.74$$

The gassed power is always less than the ungassed power.

$$P_g = 0.74P = 0.74(168) = 124.3\,\text{hp}$$

The mass transfer coefficient for turbulent flow is:

$$K_L a = 2 \times 10^{-3} \left(\frac{P_g}{V_L} \right)^{0.6} V_S^{0.667} \tag{E.4.2}$$

$$K_L a = 2 \times 10^{-3} \left(\frac{124.3 \times 754.7\ \text{W/hp}}{26\pi} \right)^{0.6} \left(\frac{0.54}{4\pi} \right)^{0.667} = 58.62\ \text{s}^{-1}$$

where the gas and liquid velocities are

$$V_S = \frac{0.5445\ \text{m}^3/\text{s}}{4\pi\ \text{m}^2} \quad V_L = 4\pi \times 6.5 = 26\pi\ \text{m}^3$$

Example 5

Calculate mass transfer coefficient in a $60\,\text{m}^3$ fermenter with a gas and liquid interfacial area of $a = 0.3\,\text{m}^2 \cdot \text{m}^{-3}$, given $\rho_{\text{broth}} = 1200\,\text{kg} \cdot \text{m}^{-3}$. The small reactor has working volume of $0.18\,\text{m}^3$, 1 vvm aeration rate. Oxygen transfer rate (OTR) is $0.25\,\text{kmol} \cdot \text{m}^{-3} \cdot \text{h}^{-1}$. There are two sets of impellers, and flat-blade turbine types of impeller were used, $H_L = 1.2D_t$.

Find the exact specifications of a large fermenter.

$$V_l = 0.18 = \frac{\pi}{4} D_t^2 (1.2D_t) = 0.3\pi D_t^3$$

The diameter of the tank is

$$D_t = \left(\frac{0.18}{0.3\pi}\right)^{1/3} = 0.576 \text{ m}$$

Also, the impeller diameter is

$$D_i = \frac{1}{3} D_t = 0.576/3 = 19.2 \text{ cm}$$

The liquid media height is

$$H_L = 1.2 \times 0.576 = 0.691 \text{ m}$$

The large tank diameter is

$$D_{t2} = \left(\frac{V_2}{0.3\pi}\right)^{1/3} = \left(\frac{60}{0.3\pi}\right)^{1/3} = 3.36 \text{ m}$$

and the impeller for the large tank is

$$D_{i2} = 3.36/3 = 1.12 \text{ m}$$

$$H_{L2} = 1.2 \times 3.36 = 4.03 \text{ m}$$

The air flow rate is

$$F_1 = 1 \times 0.18 \text{ m}^3/\text{min} = 3 \times 10^{-3} \text{ m}^3 \cdot \text{s}^{-1}$$

Gas superficial velocity,

$$U_s \frac{0.18 \times 60}{(\pi/4)(0.576)^2} = 41.45 \text{ m/h}$$

Oxygen partial pressure:

$$\overline{P_{O_2}} = 1 \text{ atm} + \left(1 + \frac{H_L m}{10.3 \text{ in}} \cdot \text{atm}\right) \times 0.21 = 0.213 \text{ atm}$$

$$OTR = K_L \cdot \overline{P}_{O_2} \Rightarrow K_{L1} = \frac{0.25 \text{ kmol/m}^3 \cdot \text{hr}}{0.213 \text{ atm}} = 1.174 \text{ kmol/m}^3 \cdot \text{h} \cdot \text{atm}$$

H:D = 3:1 = 6:1

The column diameter is in the range $0.1 < D < 7.5$ m.

The mass transfer for freely rising gas bubbles is governed by conservation of mass and momentum balance. When the distance, velocity and concentration of substances provide the major driving forces for fluid motion, three dimensionless numbers explain the mass transfer. The dimensionless numbers are the Schmidt number, Grashof number and Sherwood number. Schmidt number relates viscous forces with mass diffusivity. Grashof number deals with free convection and buoyant forces. The Rayleigh number results from the multiplication of the Schmidt number and the Grashof number. Finally, Sherwood number is the ratio of conductive forces and mass diffusivity. Based on analogy in mass transfer, the Sherwood number is similar to the Nusselt number in heat transfer. The Sherwood number can be correlated with Schmidt and Grashof numbers for calculating mass transfer coefficients in a mathematical expression.

$$Sc=\frac{\nu}{D_{O_2}} \tag{E.5.1}$$

$$Sh=\frac{k_l D}{D_{O_2}} \tag{E.5.2}$$

$$Gr=\frac{D^3\Delta\rho g}{18\mu_l^{\,2}} \tag{E.5.3}$$

And Rayleigh number

$$Gr\cdot Sc=Ra=\frac{D^3\Delta\rho g}{\mu_l D_{O_2}} \tag{E.5.4}$$

Calderbank's correlation for turbulent flow aeration shows mass transfer is proportional to D_i^2 and $Re^{3/4}$

$$Sh=0.13Sc^{1/3}Re^{3/4} \tag{E.5.5}$$

$$U_g=\frac{Q_g}{A} \tag{E.5.6}$$

13.5 DYNAMIC MODEL AND OXYGEN TRANSFER RATE IN ACTIVATED SLUDGE

The oxygen requirements for an activated sludge system with aeration and agitation for complete mixing are shown by mathematical model as the rate of oxygen transferred is

equal to the difference of inlet and outlet concentration plus the oxygen utilised for generation of biomass:

$$V\frac{dC_{O_2}}{dt} = a\cdot\bar{\mu}(C_{SO} - C_S) + b\,VX \tag{13.5.1}$$

where V is aeration tank volume in m^3, dC_{O_2}/dt is oxygen accumulation rate in kg $O_2\cdot m^{-3}\cdot day^{-1}$, a and b are empirical constants (kg $O_2\cdot kg^{-1}$ BOD) and (kg $O_2\cdot kg^{-1}$ MLSS$\cdot day^{-1}$), respectively. Also $\bar{\mu}$ is the flow rate of fresh wastewater ($m^3.day^{-1}$), MLSS stands for mixed liquor suspended solids, C_S is the BOD in effluent from aeration tank (kg BOD$\cdot m^{-3}$), C_{So} is BOD in fresh wastewater and X is the sludge concentration in the aeration tank (kg MLSS$\cdot m^{-3}$).

Example 1

In a specific activated sludge plant, the organic load is carried out at 0.8 kg BOD per kg MLSS$\cdot day^{-1}$ with an 80% BOD removal efficiency. Values for the above mathematical model are as follows.

Fresh feed flow rate 1 $m^3\cdot h^{-1}$, initial BOD concentration is 20,000 ppm and V is 10 m^3. The yield of biomass on substrate is 0.5 $g\cdot g^{-1}$ BOD.

$$a = 0.55\text{ kg } O_2\cdot kg^{-1}\text{ BOD}$$
$$b = 0.35\text{ kg } O_2\cdot kg^{-1}\text{ MLSS}\cdot day^{-1}$$

What is the oxygen requirement per kg BOD removal?

Solution

Making oxygen balance for the aeration tank, the dynamic transfer rate of oxygen is obtained:

$$V\frac{dC_{O_2}}{dt} = a.\bar{\mu}\ \ (C_{SO} - C_S) + b\,VX \tag{E.1.1}$$

Dividing the oxygen balance by the volume of the aeration tank and concentration of biomass, XV, the above equation will be simplified as follows:

$$\frac{1}{X}\frac{dC_{O_2}}{dt} = a\frac{\bar{\mu}}{VX}(C_{SO} - C_S) + b \tag{E.1.2}$$

$$\frac{\bar{\mu}\,C_{SO}}{VX} = \frac{\left(\dfrac{m^3}{day}\right)\left(\dfrac{\text{kg BOD}}{m^3}\right)}{(m^3)\left(\dfrac{\text{kg MLSS}}{m^3}\right)} \tag{E.1.3}$$

or

$$\frac{\text{kg BOD}}{\text{kg MLSS.day}} = 0.8 \leftarrow \text{BOD loading} \tag{E.1.4}$$

$$\frac{1}{X}\frac{\mathrm{d}CO_2}{\mathrm{d}t} = \frac{a\cdot\bar{\mu}\cdot C_{SO}}{VX}\left(1-\frac{C_S}{C_{SO}}\right) \tag{E.1.5}$$

The BOD removal is 80%

$$\frac{80}{100} = \frac{C_{SO}-C_S}{C_{SO}} = \left(1-\frac{C_S}{C_{SO}}\right) \tag{E.1.6}$$

$$0.8 = 1-\frac{C_S}{C_{SO}} \tag{E.1.7}$$

$$C_S = 0.2C_{SO} \tag{E.1.8}$$

$$\frac{1}{X}\frac{\mathrm{d}CO_2}{\mathrm{d}t} = 0.4\times 0.55(0.8)+0.35 = 0.526\frac{\text{kg } O_2}{\text{kg MLSS}-\text{day}} \tag{E.1.9}$$

Now we can increase the BOD removal efficiency with decreasing organic loading. What would be the amount of oxygen required per kg BOD removal, with 90% removal efficiency?

Given data for constant coefficient $a = 0.5$ and $b = 0.3$

$$\frac{1}{X}\frac{\mathrm{d}CO_2}{\mathrm{d}t} = a\left(\frac{F}{V}\right)\cdot\frac{1}{X}(C_{SO}-C_S)+b \tag{E.1.10}$$

Given *BOD loading*

$$\frac{FC_{SO}}{VX} = \frac{(\text{m}^3/\text{day})(\text{kg BOD/m}^3)}{(\text{m}^3)(\text{kg MLSS/m}^3)} = 0.4 \tag{E.1.11}$$

$$\frac{C_{SO}-C_S}{C_{SO}} = 0.9 \Rightarrow 1-\frac{C_S}{C_{SO}} = 0.9 \qquad C_S = 0.1C_{SO} \tag{E.1.12}$$

$$\frac{1}{X}\frac{\mathrm{d}CO_2}{\mathrm{d}t} = 0.5\times 0.4\times 0.9+0.3 = 0.48 \text{ kg of } O_2/\text{kg MLSS.day}$$

In fact, the more organic load there is, the more oxygen is needed in the treatment process.

Example 2

A bioreactor of $V = 20\,m^3$ working volume produces penicillin. What sugar concentration will you choose if OTR is not limited?

Hint: if you aerate a bioreactor, the power consumption is less than a non-aerated bioreactor and the specific sugar consumption rate is 1 $kg \cdot kg^{-1}$ cell$\cdot h^{-1}$.

Data given

D_t	= 2.4 m	Three sets of impellers		
D_i	= 0.8 m	M	=	*1* mPa.s
N_i	= 2.5 rps	P	=	1200 $kg \cdot m^{-3}$
Number of blades	= 8, turbine	Aeration rate	=	1 vvm
P_g/P	= 0.4	OTR	=	6×10^{-3} $kg \cdot m^{-3}$
Specific O_2 uptake	= 0.63 mmol $O_2 \cdot kg^{-1}$ cell	υ_m	=	0.5 h^{-1}

Solution

Let us find the Reynolds number

$$Re = \frac{\rho N D_i^2}{\mu} = \frac{1200 \times 0.8^2 \times 2.5}{0.1} = 1.9 \times 10^4$$

When flow is turbulent, the power number is obtained from Figure 6.6, Chapter 6, using *Re* from power curves.

$$N_P = P_{no} = 6$$

$$P_{no} = 6 = \frac{P \cdot g}{\rho N_i^3 D_i^5} \Rightarrow P = \frac{6\rho N_i^3 D_i^5}{g} = \frac{6 \times 1200 \times 2.5^3 \times 0.8^5}{9.81} = 5 \text{ hp}$$

Ungassed power = 5 × 3 sets of impellers = 15 hp

Correction factor for scale-up using non-geometry similarity,

$$f_c = \sqrt{\frac{(D_t/D_i)^* (H_L/D_i)^*}{(D_t/D_i)(H_L/D_i)}} = \sqrt{\frac{3 \times 4.42}{3 \times 3}} = 1.25$$

$$D_t/D_i = 3$$

$$H_L/D = 3$$

$$(H_L/D_i)^* = (20)/(2.4)^2(\pi/4) = 4.42$$

Gassed power, $P_g = 0.4\ (15) = 6$ hp $\Rightarrow$ for three sets of impellers using aeration

$$V_S = \frac{20\ \mathrm{m^3/min}}{(\pi/4)(2.4)^2\ \mathrm{m^2}} = 4.4\ \mathrm{m/min} = 7\times10^{-2}\ \mathrm{m\cdot s^{-1}}$$

The mass transfer coefficient for a turbulent regime is

$$K_L a = 2\times10^{-3}\left(\frac{6}{20}\right)^{0.6}(4.4)^{0.667} = 6\times10^{-2}\,\mathrm{s^{-1}}$$

The oxygen transfer rate is

$$OTR = K_L a(C_1^* - C_1) = 6\times10^{-2}(6\times10^{-3} - 0)$$

$$OTR = xq_{O_2} = 4\times10^{-4}\,\mathrm{kg\ O_2\cdot m^{-3}\cdot s^{-1}}$$

$$q_{O_2} = \left(6\times10^{-3}\,\frac{\mathrm{kg}}{\mathrm{m^3}}\times\frac{1}{32}\right)\mathrm{kg\ O_2\cdot kg^{-1}\ cell\cdot m^{-3}\cdot s^{-1}}$$

$$2.08\times10^{-3} = 0.65\times10^{-3}\,\frac{\text{mole } O_2}{\text{kg cell}}\times\frac{32\ \text{kg}}{\text{kmol}}$$

Biomass concentration is calculated.

$$x = \frac{6\times10^{-3}}{2.08\times10^{-4}} = 30\ \mathrm{kg\ cells\cdot m^{-3}}$$

What is your desired sugar concentration?

To answer the above question, we truly need to know the yield of biomass on substrate. Based on availability of oxygen, there is a good chance of sufficient biomass being generated, therefore nutrients and carbon sources must be available to carry on the process.

Example 3

Let us scale-up a small fermenter with volume (V) of 0.3 m^3. The scale-up factor is 200 fold. The large fermenter has a volume (V_2) of 60 m^3. The working volume is 60% of nominal volume, that is

$$V_L = 0.18\,\mathrm{m^3}$$

$$\text{Aeration rate} = 1\ \text{vvm}$$

$$\text{Density, } \rho = 1200\ \text{kg}\cdot\text{m}^{-3}$$

$$\text{Oxygen transfer rate, OTR} = 0.25\ \text{kmol}\cdot\text{m}^{-3}\cdot\text{h}^{-1}$$

$$H_L/D_t = 1.2$$

Two sets of impellers, turbine and flat blade.
The usual procedures for scaling up are summarised as following:

1. Reynolds number.
2. Power consumption per unit volume of liquid.
3. Tip velocity of an impeller, $N_i D_i$.
4. Liquid circulation time, mixing time.
5. Volumetric oxygen transfer coefficient.

Solution

$$V_1 = \frac{\pi}{4} D_t^2 (1.2 D_t) = 0.18\ \text{m}^3$$

$$D_t = \left(\frac{0.18}{0.3\pi}\right)^{1/3} = 0.576\ \text{m}$$

$$D_i = 1/3 D_t = 0.192\ \text{m}$$

$$H_{L1} = 1.2 \times 0.576 = 0.691\ \text{m}$$

Large reactor:

$$D_{t2} = \left(\frac{V_2}{0.3\pi}\right)^{1/3} = \left(\frac{60}{0.3\pi}\right)^{1/3} = 3.36\ \text{m}$$

and

$$D_i = 3.36/3 = 1.12\ \text{m}$$

$$H_{L2} = 1.2 \times 3.36 = 4.03\ \text{m}$$

Air flow rate

$$F_1 = 1 \times 0.18 \text{ m}^3/\text{min} = 3 \times 10^{-3} \text{ m}^3/\text{s}$$

Gas supply velocity,

$$U_S \frac{0.18 \times 60}{(\pi/4)(0.576)^2} = 41.45 \text{ m/h}$$

$$\overline{P}_{O_2} = \frac{1 \text{ atm} + \left(1 + \frac{H_L}{10.3}\right)}{2} = 0.213 \text{ atm}$$

$$OTR = K_v \cdot \overline{P}_{O_2}$$

$$K_v = \frac{0.25 \text{ kmol/m}^3 \cdot \text{h}}{0.213 \text{ atm}} = 1.174 \text{ kmol} \cdot \text{m}^{-3} \cdot \text{h}^{-1} \cdot \text{atm}^{-1}$$

$$K_v = 0.0318 \left(\frac{P_g}{V}\right)^{0.95} U_S^{0.67} = 1.174$$

$$P_g = 3.22V = 3.22 \times 0.18 = 0.58 \text{ hp}$$

For turbulent flow the power number is about 6 and for two sets of impellers is going to be doubled.

$$Re \rightarrow N_p = 6 \times 2 = 12$$

$$N_p = \frac{P_1 g}{\rho N_1^3 D_i^5} \Rightarrow P_1 = 12 \times 1200 \times N_1^3 (0.192)^5 / 9.81 = 0.383 N_1^3 \text{ hp}$$

If you have access to the graph P_g/P that is good, read gassed power to ungassed power ratio off of the graph.
Read aeration number (Na) from Figure 6.7, Chapter 6.
Now we make use of Miller's correlation for gassed power calculations:[5]

$$P_g = 0.5 \left(\frac{P_1^2 N_1 D_{i1}^3}{F^{0.56}}\right)^{0.43}$$

$$0.58 = 0.5\left(\frac{(0.383)^2 (N_1^3)^2 N_1 D_{i1}^3}{(3\times 10^{-3})^{0.56}}\right)^{0.43} \Rightarrow N_1 = 116 \text{ rpm}$$

$$P_1 = 0.383 N_1{}^3 = 0.383(116)^3 = 2.75 \text{ hp}$$

$$P_g/P = 0.58/2.75 = 0.21$$

Power input constant, geometric similarities

$$\frac{\rho N_1^3 D_{i1}^5}{V_1} = \frac{\rho N_2^3 D_{i2}^5}{V_2} \Rightarrow \left(\frac{N_2}{N_1}\right)^3 = \left(\frac{V_2}{V_1}\right)\left(\frac{D_{i1}}{D_{i2}}\right)^5$$

$$N_2 = N_1\left(\frac{V_2}{V_1}\right)^{1/3}\left(\frac{D_{i1}}{D_{i2}}\right)^{5/3} = 116\left(\frac{60}{0.3}\right)^{1/3}\left(\frac{0.192}{1.12}\right)^{5/3} = 35 \text{ rpm}$$

Constant impeller tip velocity:

$$N_1 D_{i1} = N_2 D_{i2}$$

$$N_2 = N_1\left(\frac{D_{i1}}{D_{i2}}\right) = 116\left(\frac{0.192}{1.12}\right) = 20 \text{ rpm}$$

$$P_g/V = 0.58/0.18 = 3.22 \text{ hp}$$

$$P_g = \left(\frac{0.58}{0.18}\right)\times(36 \text{ m}^3) = 116 \text{ hp}$$

$$P = 2.75\left(\frac{36}{0.18}\right) = 550 \text{ hp}$$

Example 4: Filter and Air Filtration

A batch production of penicillin of 40 m^3 capacity is required to supply sterile air through bioreactor at 1 volume of air per volume of culture per min (1 vvm). Incoming air contains

3000 bacteria per cubic metre of air, for 100 hours' operation. Calculate the filter depth, if the penetration of bacteria is 1 in 1 million.

Solution

Assuming:

$$D_{\text{filter}} = 60\,\text{cm based on availability}$$

Air flow rate,

$$F_{\text{air}} = (40\ \text{m}^3)(1\ \text{vvm})(60\ \text{min/h}) = 2400\ \text{m}^3\cdot\text{h}^{-1}$$

$$\text{Microbial load} = 3000\ \text{cells}\cdot\text{m}^{-3}$$

$$= 24000 \times 3000 = 7.2 \times 10^8\ \text{cells}$$

$$\text{Filter cross-sectional area} = (\pi/4)(0.6)^2 = 0.0283\ \text{m}^2$$

$$\text{Air velocity}\ \frac{\text{Vol. flow rate}}{A} = \frac{2400}{0.0283} = 8488\ \text{m}\cdot\text{h}^{-1}$$

Removal of organisms may follow the following exponential format of equation

$$\begin{aligned} N_t &= N_o e^{-kt} \\ \ln\frac{N_1}{N_2} &= kL \\ \ln\frac{7.2\times10^8}{10^{-6}} &= kL \end{aligned} \qquad \text{(E.4.1)}$$

$$N_1 = 7.2\times10^8\ \text{cells}$$
$$N_2 = 1\ \text{cell in}\ 10^6\ \text{cells} = 10^{-6}\ \text{cells}$$

where L is the length of filter and k is rate constant for bed materials $40\,\text{m}^{-1}$ and/or $84\,\text{m}^{-1}$. The length of filter is based on filter materials: for large k, a shorter length of filter was obtained.

$$L = \frac{1}{k}\ln(7.2\times10^{14}) = \frac{1}{40}\ln(7.2\times10^{14}) = 0.85\ \text{m}$$
$$L = \frac{1}{84}\ln(7.2\times10^{14}) = 0.41\ \text{m}$$

Example 5

In a batch fermentation of ethanol, kinetic data were collected as product formed. The data are shown in Table E.5.1. The data will be used to design a continuous bioreactor (CSTR) with a 100l working volume.

(a) If the feed rate, F, is 5×0^{-3} $m^3 \cdot h^{-1}$, calculate the ethanol concentration in the product stream. Keep in mind there was no ethanol in the feed stream.
(b) If the product yield is 45%, what would the sugar concentration in the feed stream be?

Experimental data are shown in Table E.5.1.

The data are plotted in Figure E.5.1.

TABLE E.5.1. *Ethanol production in batch fermentation with respect to inoculation time*

Time, h	Ethanol, $g \cdot l^{-1}$
0	0.0
10	2.0
15	4.0
18	6.2
21	10.0
27	16.0
33	30.0
42	56.5
48	75.7
51	85.0
54	96.0
57	103.5
60	107.3
66	110.5
72	113.0

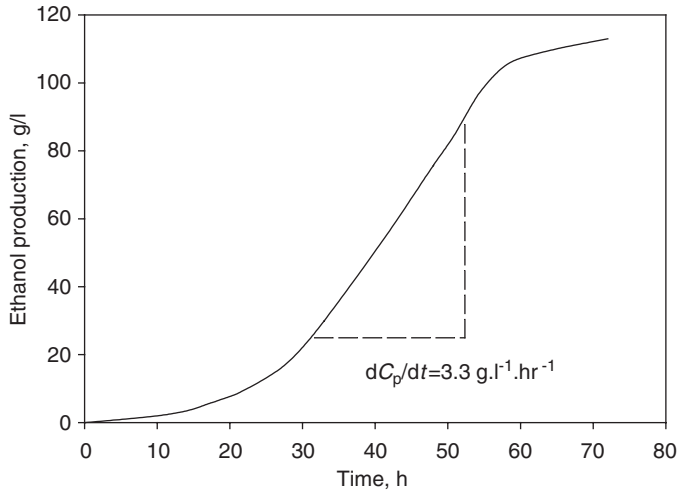

FIG. E.5.1. Ethanol concentration profile with respect to fermentation time in batch mode of operation.

Use material balance for ethanol production:

$$\frac{dC_p}{dt} = D(C_{po} - C_p) + r_p \tag{E.5.1}$$

At steady-state condition the product concentration remained constant, $dC_p/dt = 0$. Initially there was no ethanol in feed stream, $C_{po} = 0$; When there is no accumulation, the balance equation is reduced to:

$$D(-C_P) + r_P \tag{E.5.2}$$

$$r_p = DC_p = \frac{F}{V}C_p \tag{E.5.3}$$

$$C_P = \frac{V}{F}r_P \tag{E.5.4}$$

There is no wall temperature effect,

$$\left(\frac{\mu}{\mu_w}\right)^{0.14} = 1 \tag{E.5.5}$$

From plotted data

$$\frac{dC_P}{dt} = 3.3\,g{\cdot}l^{-1}{\cdot}h^{-1} \tag{E.5.6}$$

$$\frac{V}{F}r_p = \left(\frac{dC_p}{dt}\right)\frac{V}{F} = \frac{F}{V}C_p \tag{E.5.7}$$

$$C_p = \left(\frac{0.1\ m^3}{5\times10^{-3}}\right)(3.3) = \frac{330}{5} = 66\ kg{\cdot}m^{-3}$$

Ethanol concentration in the product stream is $66\,g{\cdot}l^{-1}$.

$$Y_{P/S} = 0.45$$

$$S_0 = \frac{C_P}{Y_{P/S}} = \frac{66}{0.45} = 147\ g{\cdot}l^{-1}$$

Example 6: Vinegar Production in a Jacketed Bioreactor

Ethanol is oxidised to acetic acid in the production of vinegar using *Acetobacter*. The reaction is exothermic:

$$C_2H_5OH + O_2 \xrightarrow{Acetobacter} CH_3COOH + H_2O \; \Delta H_{rxn} = -119 \text{ kcal} \cdot \text{mol}^{-1} \qquad \text{(E.6.1)}$$

The biochemical reaction rate followed the Monod rate model with a Monod rate constant of $k_S = 6.2 \times 10^{-6} \text{g} \cdot \text{cm}^{-3}$ and a specific growth rate of $\nu_{max} = 6.67 \times 10^{-7} \text{g} \cdot \text{cm}^{-3} \cdot \text{s}^{-1}$. Design the bioreactor with a suitable heat transfer area.
Given data

$N = 500 \text{ rpm} = 30000 \text{ rph}$
$D_i = 0.75 \text{ ft}$
$P = 62.4 \text{ lbm} \cdot \text{ft}^{-3}$
$M = 1 \text{ cp} = 2.42 \text{ lbm} \cdot \text{ft}^{-1} \cdot \text{h}^{-1}$
$T = 32 \text{ °C} = 90 \text{ °F}$
$k = 0.356 \text{ Btu.h}^{-1} \cdot \text{ft}^{-1} \cdot \text{°F}^{-1}$
$C_p = 1 \text{ Btu} \cdot \text{lb}^{-1} \cdot \text{°F}^{-1}$

Solution

$$-r_S = \frac{\nu_{max} S}{K_S + S} \qquad \text{(E.6.2)}$$

$K_s = 6.2 \times 10^{-6} \text{ g} \cdot \text{cm}^{-3}$ and $\upsilon_{max} = 6.67 \times 10^{-7} \text{ g} \cdot \text{cm}^{-3} \cdot \text{s}^{-1}$

Figure E.6.1 shows the jacketed bioreactor.

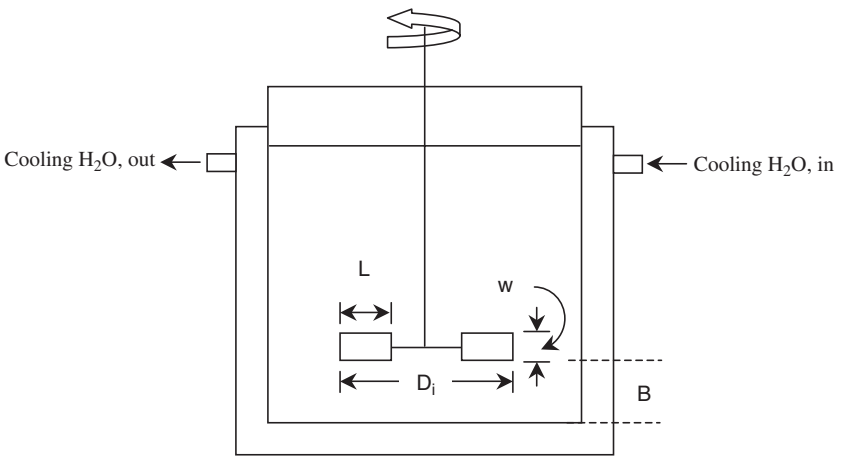

FIG. E.6.1. Diagram of jacketed vessel with impeller location.

From the graph, the overall heat transfer coefficient for jacketed vessel[7] is

$$U \approx 100 \text{ Btu}\cdot\text{h}^{-1}\cdot\text{ft}^{2^\circ}\text{F}^{1}$$

$$Re = \frac{\rho N D_i^2}{\mu} \tag{E.6.3}$$

$$Nu = \frac{hD_t}{k} = 0.36\, Re^{2/3} Pr^{1/3} \tag{E.6.4}$$

$$\frac{h_1}{h_2} = \left(\frac{D_1}{D_2}\right)^{1/2} \left(\frac{N_1}{N_2}\right) \tag{E.6.5}$$

The power for the fermentation vessel was projected by the following general equation

$$\text{Power(hp)} = 1.29\times10^{-4}\, D^{1.1} L^{2.72} N^{2.86} w^{0.3} H^{0.6} \mu^{0.14} \rho^{0.86} \tag{E.6.6}$$

$$Re = \frac{\rho N D_i^2}{\mu} = \frac{(62.4)(30{,}000)(0.75\, ft)^2}{2.42} = 4.3\times10^3$$

From Kern[7] page 718, with the given *Re*, read $hD/k \times 2000$

$$\frac{D_i}{D_t} = \frac{1}{3}$$

$$h = \frac{2000\times0.356}{3\times0.75} = 600 \text{ Btu/hr}\cdot\text{ft}^2\cdot{}^\circ\text{F}$$

Assuming the thickness of jacket = 1 in

$$h_{\text{cold water}} \approx 550 \text{ Btu/hr}\cdot\text{ft}^2\cdot{}^\circ\text{F}$$

$$U_c = \frac{h_i h_o}{h_i + h_o} = \frac{550\times600}{1150} = 300 \text{ Btu/hr}\cdot\text{ft}^2\cdot{}^\circ\text{F}$$

Dirt factor,

$$R_d = 0.005$$

$$\frac{1}{U_D} = \frac{1}{U_e} + R_d = \frac{1}{300} + 0.005 + 120 \text{ Btu/hr}\cdot\text{ft}^2\cdot{}^\circ\text{F}$$

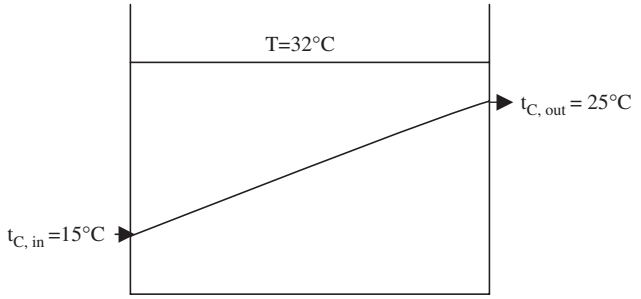

FIG. E.6.2. Temperature pattern in a jacketed bioreactor for log mean temperature.

The inlet and outlet temperature of the jacketed bioreactor is shown in Figure E.6.1. The log mean temperature is:

$$\Delta T_{\ln} = \frac{(32-15)-(32-25)}{\ln\left(\frac{17}{7}\right)} = 11.27\ ^{\circ}\mathrm{C}$$

Heat transfer based resistance theory for composite wall. The heat transfer overall coefficient is calculated.

$$\frac{1}{U} = \frac{1}{h_{\mathrm{i}}} + \frac{\Delta x}{k} + \frac{1}{h_{\mathrm{o}}} \tag{E.6.7}$$

Heat transfer area,

$$A = \pi[(D^2/4) + (DH_{\mathrm{L}})] = \pi[(2.25)^2/4 + 3(2.25)] = 24.25\,\mathrm{ft}^2 \tag{E.6.8}$$

$$Q = (24.45)(120)(1.8)(11.27) = 350{,}000\,\mathrm{Btu}\cdot\mathrm{h}^{-1}$$

$$Q = AU_{\mathrm{D}}\Delta T_{\ln} \tag{E.6.9}$$

Mass flow rate of cooling water = $35000\,\mathrm{lb_m}\cdot\mathrm{h}^{-1}$

13.6 AEROBIC WASTEWATER TREATMENT

The well-known aerobic downflow process is a trickled bed filter. Attached growth is used in the biological treatment of wastewater. Air passes through the bed while the liquid is forced to down by gravity. Figure 13.2 shows the liquid gas system for the mass transfer

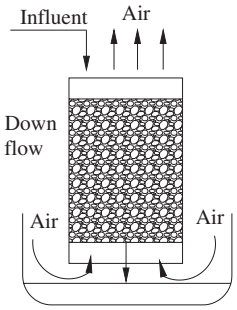

FIG. 13.2. Liquid gas mass transfer process in biological filter, attached growth system.

process in a biological filter. The system is known as attached growth. Modes of bioreactor operation are:

- Batch
- Fed batch
- Continuous

$$\frac{\mathrm{d}m}{\mathrm{d}t} = m_\mathrm{i} - m_\mathrm{o} + r_\mathrm{P} - r_\mathrm{S} \tag{13.6.1}$$

For batch operation

$$m_\mathrm{i} - m_\mathrm{o} = 0 \tag{13.6.2}$$

$$-r_\mathrm{S} = -r_\mathrm{A} = -\frac{1}{V}\frac{\mathrm{d}(SV)}{\mathrm{d}t} = \frac{n_\mathrm{max} S}{K_\mathrm{M} + S} \tag{13.6.3}$$

$$-r_\mathrm{A} = -\frac{\mathrm{d}C_\mathrm{A}}{\mathrm{d}t} \tag{13.6.4}$$

$$V = \text{constant}$$

$$\frac{\mathrm{d}S}{\mathrm{d}t} = -\frac{\nu_\mathrm{max} S}{K_\mathrm{M} + S} \tag{13.6.5}$$

$$-\int_0^t \mathrm{d}t = \int_{S_0}^{S} \left(\frac{K_\mathrm{M} + S}{\nu_\mathrm{max} S}\right) \mathrm{d}S \tag{13.6.6}$$

$$-t_\mathrm{batch} = \frac{K_\mathrm{M}}{n_\mathrm{max}} \ln \frac{S_\mathrm{f}}{S_\mathrm{o}} + \frac{1}{n_\mathrm{max}} (S_\mathrm{f} - S_0) \tag{13.6.7}$$

where, S_0 and S_f are initial and final substrate concentration in mol·l^{-1}.

13.6.1 Substrate Balance in a Continuous System

$$\frac{\mathrm{d}S}{\mathrm{d}t} = \frac{F}{V}(S_\mathrm{i} - S) - \underbrace{\frac{\mu P_\mathrm{cell}}{Y_{x/s}}}_{\text{Yield of cell}} - mP_\mathrm{cell} - \underbrace{\frac{q_p P_\mathrm{cell}}{Y_{p/s}}}_{\text{Nutrient maintenance}} \tag{13.6.1.1}$$

$$\text{Glucose} \xrightarrow[\text{ATP+P}_\mathrm{i} \rightarrow \text{ADP+7.8 kcal}]{} G6P \tag{13.6.1.2}$$

At steady-state condition

$$\frac{\mathrm{d}S}{\mathrm{d}t} = 0 \tag{13.6.1.3}$$

$$mP_\mathrm{cell} \leq \frac{\mu P_\mathrm{cell}}{Y_{s/x}} \tag{13.6.1.4}$$

$$\begin{aligned} D(S_i - S) &= \frac{\mu P_\mathrm{cell}}{Y_{x/s}} \quad \text{for SCP} \\ &= \frac{\mu P_\mathrm{cell}}{Y_{x/s}} + \frac{q_p P_\mathrm{cell}}{Y_{p/s}} \quad \text{for ethanol} \end{aligned} \tag{13.6.1.5}$$

when

$$\mu = D \tag{13.6.1.6}$$

$$\rho_\mathrm{cell} = Y_{x/s}(S_\mathrm{i} - S) \tag{13.6.1.7}$$

$$\begin{aligned} \frac{\mathrm{d}_{tank}}{\mathrm{d}t} &= \frac{E}{RT^2} \\ k &= k_o e^{-\frac{E}{RT}} \end{aligned} \tag{13.6.1.8}$$

Example 1

For production of an enzyme used for synthesis of a sun protection lotion, the required kinetic data and constants are:

$$\nu_\mathrm{max} = 2.3 \text{ mmol}\cdot\mathrm{m}^{-3}\cdot\mathrm{s}^{-1}$$

$$K_m = 8.9 \text{ mmol}\cdot\text{l}^{-1}$$

$$S_o = 12 \text{ mmol}\cdot\text{l}^{-1}$$

Find the reaction time for 95% conversion of raw materials.

$$t_{batch} = ? \text{ for } x_A = 0.95$$

Solution

$$\upsilon_{max} = \left(\frac{2.5 \text{ mmol}}{\text{m}^3\cdot\text{s}}\right)\left(\frac{3600 \text{ s}}{\text{h}}\right)\left(\frac{1 \text{ m}^3}{1000 \text{ L}}\right) = \frac{9 \text{ mmol}}{\text{L}\cdot\text{h}}$$

$$\begin{aligned} t_{batch} &= \frac{K_m}{\upsilon_{max}} \ln\frac{S_o}{S_f} + \frac{S_o - S_f}{\upsilon_{max}} \\ &= \frac{8.9}{9} \ln\frac{12}{(1-0.95)(12)} + \frac{0.95\times 12}{9} \\ &= 4.2 \text{ hours} \end{aligned}$$

13.6.2 Material Balance in Fed Batch

In fact, fed batch is a batch system operating without any outlet stream. The differences in substrate in and out are equal to the rate of product generation.

$$\frac{F}{V}(S_i - S) = \left(\frac{\upsilon_{max} S}{K_m + S}\right)\frac{V}{V} \tag{13.6.2.1}$$

The retention time:

$$\tau = \frac{1}{D} = \frac{V}{F} \tag{13.6.2.2}$$

$$D(S_i - S) = \frac{\upsilon_{max} S}{K_m + S} \tag{13.6.2.3}$$

$$\underbrace{\frac{d\rho_{cell}}{dt}}_{\text{steady state}=0} = \frac{F}{V}\left(\rho_i - \underbrace{\rho_o}_{\text{sterile system}}\right) + \left(\underbrace{\mu}_{\text{growth}} - \underbrace{\alpha}_{\text{death}}\right)\rho_{cell} \tag{13.6.2.4}$$

The simplified material balance would lead to growth rate

$$\mu = \frac{F}{V} \tag{13.6.2.5}$$

Example 1

A 10 m^3 bioreactor with $H/d = 2.5D$, 75% working volume, with two sets of standard flat-blade impellers was used for a baker's yeast production unit. The operating dilution rate was set at 0.5 h^{-1}. The rate equation satisfying the reactor design was a Monod model with $\mu_{max} = 0.65\,h^{-1}$and $k_S = 3\,kg{\cdot}m^{-3}$. The initial substrate concentration was 65 $g{\cdot}l^{-1}$ with 1vvm aeration, broth density 1200 $kg{\cdot}m^{-3}$ and viscosity $\mu = 0.02\,N{\cdot}s{\cdot}m^{-2}$. The yield of biomass on glucose was 0.5 g cell$\cdot g^{-1}$ glucose. Calculate power consumption for a 90 rpm agitation rate and OTR of 0.05 $g{\cdot}l^{-1}$. State the controlling resistance in the mass transfer process.

Solution

$$10 = \frac{\pi}{4}(2.5D)D^2$$
$$D_t = 1.7 \text{ m}$$
$$D_i = 0.57 \text{ m}$$

$$Re = \frac{(1.5 \text{ rps})(0.57)^2(1200)}{0.02\,\dfrac{\text{N}\cdot\text{s}}{\text{m}^2}} = 2.9\times10^4$$

The flow regime is turbulent flow. Read the value for the power number using Figure 6.6, Chapter 6.

$$N_p = 6$$

$$N_a = \frac{F_g}{\mu D_i^3} = \frac{7.5\,\text{m}^3/\text{min}}{(90 \text{ rpm})(0.57)^3} = 0.45$$

where N_a is known as the aeration number, then use Figure 6.7 in Chapter 6 to find the ratio of gassed power to ungassed power.

$$\frac{P_g}{\rho} = 0.95$$

$$N_p = \frac{Pg_c}{\rho n^3 D_i^3}$$

$$P = \frac{6 \times 1200(1.5)^3 (0.57)^5}{9.81} = 149 \frac{\text{kg·m}}{\text{s}}$$

$$= \frac{149}{745.7} = 0.2 \text{ hp}$$

Conversion factor:

$$1 \text{ hp} = 745.7 \text{ kg·m·s}^{-1}$$

$$P = 2 \times 0.2 = 0.4 \text{ hp}$$

$$P_g = 0.95(0.4) = 0.38 \text{ hp}$$

$$\frac{P_g}{V_L} = 0.051 \text{ w.l}^{-1}$$

Oxygen transfer rate

$$OTR = K_L a(C - C_L) = 7.9 \times 10^{-4}(0.03)$$
$$= 4 \times 10^{-5} \text{ kg.m}^{-3}\text{·s}^{-1}$$
$$K_L = 2 \times 10^{-3} V_s^{0.7} \left(\frac{P_g}{V_L} \right)^{0.2}$$

$$V_s = \frac{7.5 \text{ m}^3/\text{min}}{(\pi/4)(1.72)^2} = 3.23 \text{ m/min} = 194 \text{ m·h}^{-1}$$
$$K_L = 2 \times 10^{-3} (323 \text{ cm/min})^{0.7} (0.051)^{0.2} = 7.9 \times 10^{-4} \text{S}^{-1}$$

Liquid film was the controlling resistance.

13.7 NOMENCLATURE

N	Impeller speed, rpm
D_i	Impeller diameter, m
Q_{O_2}	Oxygen transfer rate, mmol·min^{-1}
X	Biomass concentration, g·l^{-1}
P_g/V	Power per unit volume, hp·m^{-3}

ND_i	Impeller tip velocity, $m \cdot s^{-1}$
t_m	Mixing time, min
K_La	Mass transfer coefficient, h^{-1}
τ	Shear stress, Pa
$\frac{du}{dx}$	Shear rate, s^{-1}
μ	Fluid viscosity, cp
$\frac{N^2 D_i}{g}$	Froude Number, dimensionless
H_i	Impeller interspacing, cm
U_g	Upward gas bubble velocity, $m \cdot s^{-1}$
g	Gravity, $m \cdot s^{-2}$
OTR	Oxygen transfer rate, $kmol.m^{-3} \cdot h^{-1}$
V_S, U_S	Gas superficial velocity, $m \cdot s^{-1}$
K_m	Monod rate constant, $g \cdot l^{-1}$
ν_{max}	Maximum specific growth rate, $mmol \cdot m^{-3} \cdot s^{-1}$
kx	Maximum specific growth rate., $g \cdot l^{-1} \cdot h^{-1}$
D	Fresh media dilution rate, h^{-1}
F	Flow rate, $ml \cdot min^{-1}$
V	Volume, m^3
$Y_{X/S}$	Yield of biomass on substrate
S_f	Inlet to outlet substrate ratio
R	Recycle ratio
f	Ratio inlet to outlet substrate concentration

REFERENCES

1. Scragg, A.H., "Bioreactors in Biotechnology, A Practical Approach". Ellis Horwood Series in Biochemistry and Biotechnology, New York, 1991.
2. Wang, D.I.C., Cooney, C.L., Deman, A.L., Dunnill, P., Humphrey, A.E. and Lilly, M.D., "Fermentation and Enzyme Technology". John Wiley & Sons, New York, 1979.
3. Baily, J.E. and Ollis, D.F., "Biochemical Engineering Fundamentals", 2nd edn. McGraw-Hill, New York, 1986.
4. Doran, P.M., "Bioprocess Engineering Principles". Academic Press, New York, 1995.
5. Michel, B.J. and Miller, S.A., *AIChE J.* **8**, 262 (1962).
6. Stanbury, P.F. and Whitaker, A., "Principles of Fermentation Technology". Pergamon Press, Oxford, 1984.
7. Kern, D., "Process Heat Transfer". McGraw Hill, New York, 1950, p. 717.

CHAPTER 14

Single-Cell Protein

14.1 INTRODUCTION

The term single-cell protein (SCP) is used to describe protein derived from cells of microorganisms such as yeast, fungi, algae and bacteria which are grown on various carbon sources for synthesis. The dried cells of microorganisms or the whole organism is harvested and consumed. This is a protein source for human food supplements and animal feeds. SCP production may have potential for feeding the ever-increasing world population. Massive quantities of SCP can be produced in a single day. As a source of protein it is very promising, with potential to satisfy the world shortage of food while population increases.

There are several carbon sources that are used as energy sources for microorganisms for growing and producing CSP. In some cases, raw material requires pretreatment or hydrolysis before use. Waste sources of carbon are customary and cheap to use. SCP technology is a suitable process for converting waste materials to useful biomass containing protein. The broth is concentrated protein which is then dried with limited moisture; it is stored for use as food or feed for humans and animals. Waste recycling has been advanced as a method for preventing environmental decay and increasing food supplies. It may be possible to convert waste streams into valuable products by separation and recovery or by biological conversion.[1–4] Many products are produced biologically from food process waste. The potential benefits of successful recycling of agricultural wastes are enormous. It may be the only method for large-scale protein production that does not require a concomitant increase in energy consumption. In addition, it may be the most effective method for producing animal and human food from lignocellulose materials that are otherwise of little nutritive value and are therefore used for fuel production. One advantage of the biological process is the flexibility of the microorganisms to adapt to different feedstocks. Therefore, when combined with the treatment of process waste streams, the biological conversion of these wastes to products can be both environmentally and economically favourable.

In the production of antibiotics, sufficient growth of fungi in submerged cultures has created potential sources of biomass as SCP and as flavour additives to replace mushrooms: the biomass contains 50–65% protein.[1,5] Production of mushroom from lignocellulosic waste seems to be a suitable and economical process since the raw material is inexpensive and available in most countries.

This chapter discusses the present status of microbial SCP production from agricultural wastes and describes some of the technical and economical problems related to the production processes that must be overcome for large-scale application to be possible.

14.2 SEPARATION OF MICROBIAL BIOMASS

Bacteria, yeast and algae are produced in massive quantities of protein sources as food for animals and humans.[1] SCP is considered a major source of feed for animals. The production of valuable biological products from industrial and agricultural wastes is considered through the bioconversion of solid wastes to added-value fermented product, which is easily marketable as animal feedstock. The waste streams that otherwise would cause pollution and threaten the environment can be considered raw material for CSP production using suitable strains of microorganisms.

14.3 BACKGROUND

It is evident that the conversion of photosynthetically produced organic compounds into human and animal food is the limiting process in human food production. The worldwide annual production of organic material by photosynthesis has been estimated to be between 25 and 50 tons.[5,6] Any practical method capable of converting a small fraction of this yield into human food should find wide application and go a long way to reducing chronic food shortages.

The growth of microorganisms, more rapid than that of the higher plants, makes them very attractive as high-protein crops; whereas only one or two grain crops can be grown per year, a crop of yeasts or moulds may be harvested weekly, and bacteria may be harvested daily. The use of microorganisms as a source of protein for human and animal food is not a new development. Traditional foods and feeds such as cheese, sauerkraut, miso and silage have a high content of microorganisms to which their nutritional properties are due in part. The high-quality proteins synthesised during the growth of these microorganisms compare favourably with those derived from the better grains.[1,3] There are many convincing reports on the availability of essential amino acids and the protein quality of SCP. Although there are few data on animal feeding trials using SCP produced from lignocellulose wastes, there is a large and growing body of information about SCP from petroleum and methanol. This information should be applicable to SCP from agricultural wastes with proper allowance for the undesirable contaminants in the sources. In petroleum, there has been concern about accumulation of carcinogenic hydrocarbons. In agricultural wastes, there is concern about accumulation of pesticides and herbicides. The guidelines for testing SCP as a major supplement in animal diets and should be consulted for further details on feeding trials. Many more feeding trials will be needed before SCP from lignocellulose wastes is accepted for routine feeding.

The main carbon source for production of SCP is petroleum. It has been practised in many companies around the world. Other potential substrates for SCP include bagasse, citrus wastes, sulphite waste liquor from pulp and paper, molasses, animal manure, whey, starch, sewage and agricultural wastes.

14.4 PRODUCTION METHODS

Some of the proposed methods for conversion of agricultural wastes into animal feed are presented in Table 14.1. These methods will be briefly evaluated in the following. First, a distinction should be made between the production of SCP from the lignocellulose parts of the plant and the production of SCP from the soluble carbohydrates of many agricultural wastes. At present, there are many plants around the world that operate for the production of SCP. The Ceres Ecology Corporation of Chino, California, in the USA will process waste from over 100,000 dairy cattle for feed recycling and for control of salt in groundwater. Other plants in Toulouse (France), Zacantecos (Mexico) and Sterling (Colorado, USA) use processes that depend upon an anaerobic fermentation in a silo or covered ditch. The manure undergoes a lactic acid fermentation due to the action of anaerobic bacteria (chiefly streptococci and lactobacilli), and a typical silage odour results in place of the odour of manure. The processing of poultry for production of prepared food generates waste containing fats and starchy materials. The waste is used in a biological process to be converted to SCP using several microorganisms.[3,4] These short-time anaerobic fermentation processes do not utilise the fibre, and are therefore a partial solution to the waste problem. The fibrous residue may be used as a soil conditioner before or after composting. Figure 14.1 shows the various types of waste produced annually.

TABLE 14.1. *Methods for conversion of cellulosic agricultural wastes into animal feed*

Treatment	Microorganism	Substrate	Protein produced	Fibre utilised
Dilute alkali	None	Straw	No	Yes
Aerobic mesophiles, 25 °C	*Cellulomonas*	Bagasse	Yes	Yes
Mould growth, 25 °C	*Trichoderma viride*	Waste paper	Yes	Yes
Aerobic thermophiles, 55 °C	*Thermoactinomyces*	Fermented livestock wastes	Yes	Yes

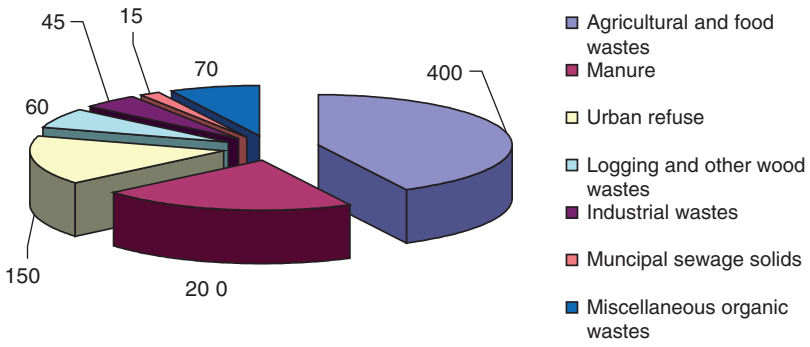

FIG. 14.1. Solid wastes in the USA in units of tons per year.

Rates of soluble sugar utilisation of 10–30 grams per litre per hour have been reported for SCP production by yeast. Rates of 5–15 grams per litre per hour have been claimed for utilisation of selected hydrocarbons. For the process of SCP production under present market conditions to be an economical, the rate of utilisation of cellulose must be at least 1–5 grams per litre per hour. As no pilot plants have been operated, it is not possible to report commercial rates, but laboratory-scale fermenters have been run at 1 gram per litre per hour on pretreated wastes. It has been reported that Gram-negative aerobic bacteria, *Cellulomonas* sp., grow rapidly on cellulose at 25–30 °C, but cannot utilise lignin or lignocellulose. Therefore extensive pretreatment of lignocellulosic material such as rice husks with hot alkali is required.[5,7] The microorganism must be harvested by centrifugation. Amino-acid analysis and animal feeding trials have shown that a high-quality SCP can be produced. Enzymes produced by the mould *Trichoderma viride* are used for production of soluble sugars from waste paper cellulose. Yeasts or bacteria for SCP production can then ferment these sugars. The enzyme reaction takes place in four steps:

1. Pretreatment of waste by ball milling or hot alkali.
2. Enzyme production by growth of *T. viride* on pretreated cellulose.
3. Depolymerization of cellulose by *T. viride* enzymes.
4. SCP production by yeast or bacteria.

Several potential and mutant strains of *T. viride* have been identified in SCP production. Their capacity for amyloletic enzyme production was enhanced severalfold in SCP from lingnocellulosic resources. The process of bioconversion of agricultural wastes to SCP appeared to be too complex to find an economic application for agricultural waste.

14.5 MEDIA PREPARATION FOR SCP PRODUCTION

Sago starch in Malaysia is abundant, inexpensive and common as raw material for SCP production. Fifty grams of sago starch is dissolved in one litre of 0.1 M NaOH solution. The mixture is heated treated until it is absolutely dissolved in deionised water with 4 g of NaOH, then the pH is adjusted to 7. Supplementary nutrients are added: 3.3 g KH_2PO_4, 0.3 g Na_2HPO_4 and 1 g yeast extract; autoclave the media, and use it as feed for a fermenter. One hundred millilitres of seed culture are prepared a day in advance for inoculation of fermentation. *Saccharomycopsis fibuligera* ATCC 9947 or ATCC 9266 is grown in a media comprising of 0.33 g KH_2PO_4, 0.03 g Na_2HPO_4, 0.1 g yeast extract and 1 g glucose in 100 ml distilled water. The seed culture is harvested after 24 hours of incubation at 32 °C. The microorganism is purchased from ATCC, and after hydration is kept in stock culture of YM media (Difco, USA) slants. The inoculum for seed culture is the organism transferred from the prepared slant media.

Culture medium used for growth of *Penicillium javanicum* has been reported by Burrel and his coworkers.[8] The recommended medium for cultivation of the fungi without any alteration contains the following chemical composition in one litre solution: Fumaric acid, 2.0 g, $(NH_4)_2SO_4$, 2.5 g; $KH_2PO_4{\cdot}2H_2O$, 1.0 g; $MgSO_4$, 0.5 g; $(NH_4)\ Fe(SO_4)_2{\cdot}12H_2O$,

0.2 mg; $ZnSO_4 \cdot 7H_20$, 0.2 mg; $MnSO_4 \cdot H_2O$:, 0.1 mg; thiamine hydro-chloride 0.1 mg, and add a suitable carbon source.

14.6 ANALYTICAL METHODS

Protein concentration can be determined by using method of Bradford,[9] which utilises Pierce reagent 23200 (Pierce Chemical Company, Rockford, IL, USA) in combination with an acidic Coomassie Brilliant Blue G-20 solution to absorb at 595 nm when reagent binds to the protein. A 20 mg/l bovine serum albumin (Pierce Chemical) solution was used as the standard. Starch concentration was measured by the orcinol method[4,9–11] using synthetic starch as the reference. A yellow to orange colour is obtained and measured at 420 nm when orcinol reacts with carbohydrates. Absorbance is determined by spectrometry.

14.6.1 Coomassie–Protein Reaction Scheme

This protein assay works by forming a complex between the protein and the Coomassie dye. When bound to the protein, the absorbance of the dye shifts from a wavelength of 465 nm to 595 nm (λ_{595}). The reagent generates a stronger blue colour which is detected at the specified wavelength. You will first generate a standard curve using the protein bovine serum albumin (BSA) by measuring the absorbance at 595 nm of a series of standards of known concentration. Next, you will measure the absorbance at wavelength of λ_{595} for all of your samples and determine its concentration by comparison with the standard curve.

$$\text{Protein} + \text{Coomassie G-250 in acidic medium} \rightarrow \text{protein–dye complex (blue; measured at 595 nm)}$$

14.6.2 Preparation of Diluted BSA Standards

Prepare a fresh set of protein standards by diluting the 2.0 mg per ml BSA stock standard (stock solution) as shown in Table 14.2. There will be sufficient volume for three replications of each diluted BSA standard, if necessary.

TABLE 14.2. *Preparation of BSA concentration for standard calibration curve*

Volume of BSA to add	Volume of diluents (buffer) to add	Final BSA concentration
300 μL of Stock	0 μL	**Stock** – 2000 μg/mL
375 μL of Stock	125 μL	**A** – 1500 μg/mL
325 μL of Stock	325 μL	**B** – 1000 μg/mL
175 μL of A	175 μL	**C** – 750 μg/mL
325 μL of B	325 μL	**D** – 500 μg/mL
325 μL of D	325 μL	**E** – 250 μg/mL
325 μL of E	325 μL	**F** – 125 μg/mL
100 μL of F	400 μL	**G** – 25 μg/mL

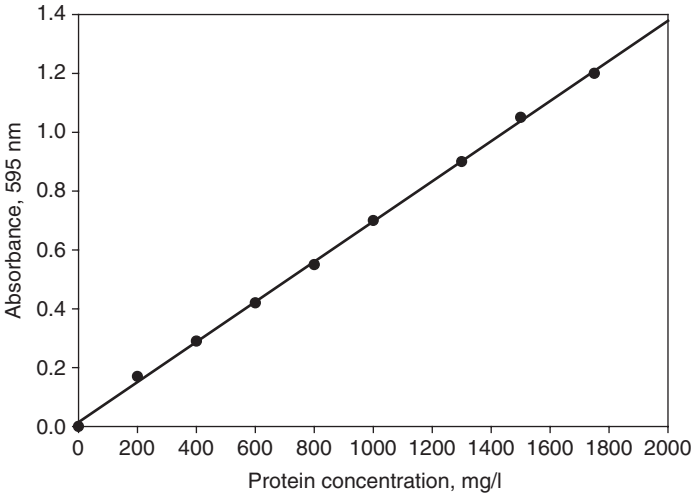

FIG. 14.2. Calibration curve for BSA standard solution.

14.6.3 Mixing of the Coomassie Plus Protein Assay Reagent

Allow the Coomassie Plus reagent to come to room temperature. Mix the Coomassie Plus reagent solution just before use by gently inverting the bottle several times. Do not shake.

14.6.4 Standard Calibration Curve

Prepare a standard curve by plotting the average blank corrected 595 nm reading for each BSA standard versus its concentration in mg/l, using the standard curve; determine the protein concentration for each unknown sample. Calibration curve for BSA standard is prepared using standard albumin, 50 ml Pierce 23210 with concentration of 2 g/l, diluted with 1 M NaOH solution. Add 1 ml of 1 M NaOH with 0.1 ml of diluted sample plus 5 ml of reagent, protein assay 23200 Pierce, stirred with a vortex mixer. Read the absorbance with a spectrophotometer at 595 nm. The resulting data for the calibration curve are shown in Figure 14.2.

14.6.5 Standard Calibration Curve for Starch

A standard solution of soluble strach, 2 g/l well dissolved in an alkali solution was prepared. With heating, the powder becomes a clear solution. A diluted solution from 200 to 2000 mg/l was prepared. Dissolved 0.4 g of orcinol (3, 5 dihydroxy toluene) in 99.6 g of H_2SO_4 (66% acid). Prepare 500 ml orcinol reagent, 170 ml water with 330 ml acid. Add acid to distilled water and gradually dissolve 3.115 g orcinol in the diluted acid solution. Take 0.1 ml of the diluted starch sample with 0.9 ml of distilled water, and then add 2 ml of the prepared orcinol reagent, heated in a boiling water bath for 15 min, stop the reaction by cooling it in an ice water bath. Add 7 ml of distilled water, read the absorbance at 420 nm. Plotting the data can find the given results as projected in Figure 14.3.

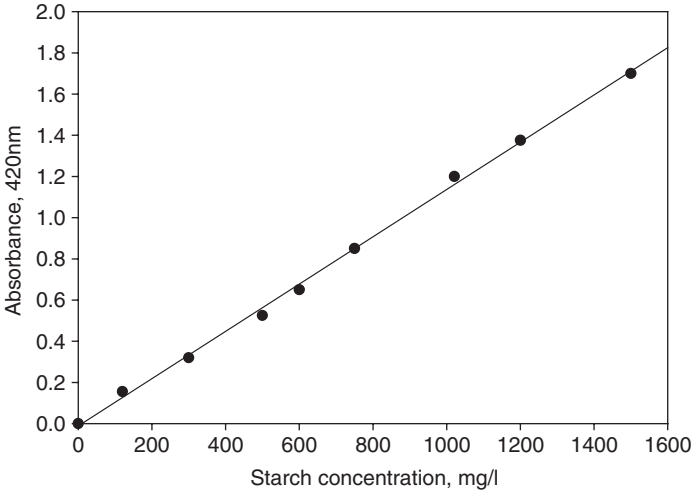

FIG. 14.3. Standard calibration curve for starch solution.

14.7 SCP PROCESSES

Using Brewer's yeast, *Saccharomyces cerevisiae*, the process was developed for the large-scale production of food. During World War I, a large-scale process for production of SCP was developed in Germany. About 60% of food was replaced by massive brewing of yeast, *S. cerevisiae*. In World War II, the yeast-based food had an important contribution in the German diet. The yeast was incorporated mainly into soup and sausages. Special strains of yeast, *Candida arborea* and *C. utilis*, were predominantly used. In the 1960s, several large-scale plants for the production of SCP were developed by British Petroleum (BP), as the organisms were able to utilise the aliphatic compounds of petroleum. *Candida lipolytica* was able to convert carbon sources originating from petroleum to protein. *C. lipolytica* was grown on alkanes, a yeast based food. Other strains and *Candia* also are used for CSP production. For the CSP produced by BP from distilled *n*-alkanes, the cells were separated, salted, dried and used as animal feed.[1]

In the process developed by BP, the protein was named 'Toprina'. BP planned to go for large-scale production, and the protein was proved toxicologically safe. The rising price of petroleum initiated the plan, but it was unable to contribute to reducing shortages of food and feed sources for humans and animals.[1,5] Production of SCP named 'Pruteen' from methanol by bio-oxidation of methane was another a successful case in CSP process development using *Methylophilus methylotrophus*. However, the whole project of SCP has been a victim of political or economic issues in Europe and Japan. Methane is an abundant and cheap carbon source without any toxicity; it is the main constituent of natural gas and is also produced from anaerobic digestion tanks. There are many biocatalysts involved in methane bio-oxidation using stable mixed cultures. This mixed culture is one of the best examples of symbiosis. At first, methane in the gas phase is bubbled into media then biologically oxidised to methanol. The Gram-negative bacilli (rod shapes) are used, while methanol is

produced in the presence of biocatalysts. Methane is a pure carbon source; it is easily utilised by several microorganisms such as *Methylomonas* and *Methylococcus*. Another species that has been extensively studied is *Methylomonas methanica*. Supplements of nitrogen, trace metals and minerals are required for optimal growth. Mixed cultures of Gram-negative rod-shaped bacilli have the potential to oxidise methane and produce methanol, whereas other organisms present utilise methanol as a carbon source to produce SCP. This is an example of symbiosis in mixed culture, where an intermediate product is formed, which is then used by the second organism. *Acinetobacter* and *Flavobacterium* are often used in mixed culture for producting SCP from methane. The fermentation of methanol to SCP was done in an airlift fermenter with sufficient aeration and without any mechanical agitation, using *Methylophilus methylotropha*. The SCP known as 'Pruteen' contained 72% crude protein.[1] The product was marketed for feed as a source of energy, vitamins and minerals with sufficient protein content. The amino-acid analysis was satisfactory as the methionine and lysine content of Pruteen were compared to the protein content of white fish meal.

14.8 NUTRITIONAL VALUE OF SCP

The nutritional value of SCP depends on the composition of its amino acids, vitamins and nucleic acids. The nutrient value of SCP may have a positive and negative impact. The rigid cell wall, the high content of nucleic acids, allergies and the gastrointestinal effect should be considered as a negative impact. However, with special treatment, it is possible to eliminate these from the product. A long-term use of SCP is required to consider and remove any toxicological effects and carcinogenesis. The positive point of view for SCP is the high content of protein with sufficient enzymes, minerals and vitamins.[12]

The protein content of SCP is very high. Dried cells of *Pseudomonas* sp. grown on normal petroleum-based liquid paraffin contain 69% protein. Algae normally possess about 40% protein.[1,5] The protein content of SCP is absolutely dependent on the raw material used as a carbon source and the microorganisms grown on the media. The proteins of the microorganisms contain all the essential amino acids. Table 14.3 presents the average protein contents of bacteria, yeast, fungi and algae.

Microorganisms such yeast and bacteria have a short doubling time, normally in the range of 5–15 minutes; mould and algae are 2–4 hours. The fast brewing of microorganisms compared with plant cells is a promising point for food replacement and shortage in the new millennium.

In terms of amino acids bacterial protein is similar to fish protein. The yeast's protein is almost identical to soya protein; fungal protein is lower than yeast protein. In addition, SCP is deficient in amino acids with a sulphur bridge, such as cystine, cysteine and methionine. SCP as a food may require supplements of cysteine and methionine; whereas they have high levels of lysine vitamins and other amino acids. The vitamins of microorganisms are primarily of the B type. Vitamin B_{12} occurs mostly in bacteria, whereas algae are usually rich in vitamin A. The most common vitamins in SCP are thiamine, riboflavin, niacin, pyridoxine, pantothenic acid, choline, folic acid, inositol, biotin, B_{12} and P-aminobenzoic acid. Table 14.4 shows the essential amino acid analysis of SCP compared with several sources of protein.

TABLE 14.3. *Cellular composition of SCP from various microorganisms (dry weight per cent)*[13]

	Yeast	Bacteria	Fungi	Algae
Protein	45–55	50–65	30–45	40–60
Nucleic acid	6–12	8–12	7–10	3–8
Fat	2–6	1.5–3	2–8	7–20
Ash	5–9.5	3–7	9–14	8–10

TABLE 14.4. *Essential amino acid content of the cell protein in comparison with other reference proteins (weight %)*[14]

Amino acid	*Cellulomonas*	*Saccharomyces cerevisiae*	*Penicillium notatum*	SCP (BP)	Egg	Cow milk
Lysine	7.6	7.7	3.9	7.0	6.3	7.8
Threonine	5.4	4.8	—	4.9	5.0	4.6
Methionine	2.0	1.7	1.0	1.8	3.2	2.4
Cysteine	—	—	—	—	2.4	—
Tryptophane	—	1.0	1.25	—	1.6	—
Isoleucine	5.3	4.6	3.2	4.5	6.8	6.4
Leucine	7.3	7.0	5.5	7.0	9.0	9.9
Valine	7.1	5.3	3.9	5.4	7.4	6.9
Phenyalanine	4.6	4.1	2.8	4.4	6.3	4.9
Histidine	7.8	2.7	—	2.0	—	—
Arginine	6.4	2.4	—	4.8	—	—

14.9 ADVANTAGES AND DISADVANTAGES OF SCP

Addition of SCP to the diet of a milking cow increases milk production and production efficiency by 15%.[1,7] Microorganisms such as bacteria and yeasts grow rapidly and contain more uric acid than slower-growing plants and animals. Although the uric acid limits the daily intake of SCP for humans and monogastric animals such as pigs and chickens, ruminants such as cattle, sheep and goats can tolerate higher levels of uric acid or break down urea and excrete it as ammonia.

About 80% of the total cell nitrogen is amino acids whereas the remaining 20% is possibly fat, ash and nucleic acids. The concentration of nucleic acids in SCP is higher than in conventional proteins. That is the characteristic of all fast-growing organisms. The problem occurs with the consumption of proteins, roughly 10% of nucleic acids. The high nucleic acid content of SCP results in an increase in uric acid in serum and urine.[15] Uric acid is the final product of purine degradation in humans. Most mammals, reptiles and molluscs possess the enzyme uricase, and they are able to oxidise uric acid to allantoic acid. High uric acid in humans causes ‘gout’. That disease results from the elevation of uric acid in body fluid. Its manifestation is painful inflammation of arthritic joints. In animals with urease

and allantoicase, the biodegradation of uric acid is accelerated, and the end product is ammonia. In the human body lack of such enzymes causes the catabolism of uric acid to be terminated, and uric acid has to be excreted in urine through the kidneys.[16]

The removal and reduction of the nucleic acid content of various SCPs is achieved by chemical treatment with sodium hydroxide solution or high salt solution (10%). As a result, crystals of sodium urate form and are removed from the SCP solution.[16,17] The quality of SCP can be upgraded by the destruction of cell walls. That may enhance the digestibility of SCP. With chemical treatment the nucleic acid content of SCP is reduced.

The presence of uricase assists the uric acid to be hydrolysed, and the end product of purine degradation is completed with the addition of uricase.

14.10 PREPARATION FOR EXPERIMENTAL RUN

1. Prepare seed culture and use it for inoculation of 21 airlift and 21 B. Braun biostat B using soluble starch or glucose.
2. Perform fermentation for 24 hours in a batch system.
3. Monitor DO level and control pH at 6.7–7 by using 0.2 M phosphate buffer solution.
4. Measure SCP based on standard methods and analysis explained above.
5. Determine yield of SCP-based carbon sources.
6. Take usual samples at intervals of 4–6 hours.
7. Measure carbon sources remaining.

REFERENCES

1. Rose, A.H., *Sci. Am.* **245**, 127 (1981).
2. Tamime, A.Y. and Deeth, H.C., *J. Food Protection* **43**, 939 (1980).
3. Driessen, F. M., Ubbels, J. and Stadhouders, J., *Biotechnol. Bioengng.* **19**, 821 (1977).
4. Najafpour, G.D., Klasson, K.T., Ackerson, M.D., Clausen, E.C. and Gaddy, J.L., *Biores. Technol.* **48**, 65 (1994).
5. Pelczar, M.J. Jr, Chan, E.C.S. and Krieg, N.R., "Microbiology", 6th edn. McGraw-Hill, New York, 1993.
6. Stanbury, P.F. and Whitaker, A., "Principles of Fermentation Technology". Pergamon Press, Oxford, 1984.
7. Yakoub Khan, M., Umar Dahot, M. and Yousuf Khan, M., *J. Islam. Acad. Sci.* **5**, 39 (1992).
8. Burrel, R.G., Clayton, C.W., Gallegly, M.E. and Lilly, V.G., *Phytopathol.* **6**, 422 (1966).
9. Bradford, M.M., *Analyt. Biochem.* **72**, 248 (1976).
10. Thomas, L.C. and Chamberlin, G.L., "Colorimetric Chemical Analytical Methods". Tintometer Ltd, Salisbury, UK, 1980, p. 31.
11. Miller, G.L., *Anal. Chem.* **31**, 426 (1959).
12. Lichtfield, J.H., "The Production of Fungi. Single-cell Protein I" (Mateles and Tannenbaum, eds.). M.I.T. Press, Cambridge, MA, 1968.
13. Miller, M.B. and Litsky, W., "Single Cell Protein in Industrial Microbiology". McGraw-Hill, New York, 1976.
14. Han, Y.W., Duhlap, C.E. and Callihan, C.D., *Food Technol.* **25**, 130 (1971).
15. White, P.S., Handler. and Smith, E.L., "Principles of Biochemistry", 4th edn. McGraw-Hill, New York, 1968.
16. Voet, D. and Voet, J.G., "Biochemistry", 3rd edn. John Wiley, New York, 2004.
17. Zee, J.A. and Simard, R.E., *Appl. Microbiol.* **29**, 59 (1974).

CHAPTER 15

Sterilisation

15.1 INTRODUCTION

Sterilisation is the action of eliminating microorganisms from a medium. Sterility is the absence of any detectable and viable microbes in a culture medium or in the gas phase. Sterilisation is a process that destroys all living organisms, spores and viruses in a pressurised vessel at high temperature. In the food and dairy industries, sterilisation is commonly used to preserve food products. At the laboratory scale, huge steel vessels with live stream at 105 kPa (15 psig) are commonly used for 20–30 minutes. This is a closed system known as an autoclave; therefore it is batch sterilisation. The temperature is raised to 121 °C when air is initially flashed out and all live streams are replaced. Wet steam is usually used for effective autoclaving. The high temperature and long duration may kill all living microorganisms, spores and viruses. When media is prepared, to eliminate bacterial and fungal contaminants it must be heat treated at high pressure. Even at high temperatures the fungal spores may survive if only heat is used. Therefore, media is autoclaved at 121 °C and 105 kPa (15 psig). In fact, an autoclave is used like a pressure cooker, which is convenient and economic autoclaving equipment.

Overheating the prepared media may have negative impact, causing the media pH to be unstable. Acid pH is very sensitive to overheating. Overheating in media containing sugars causes the carbohydrate to be caramelised. This media may have reverse impact, reducing bacteriological performance. Gelatinous media or any nutrient agar at acidic pH is hydrolysed. This is due to the acidic condition of catalytic activities or excess amounts of protons breaking down the solid media and extra sugars forming. This may cause substrate inhibition on growth of organisms on solid slant media.

15.2 BATCH STERILISATION

Batch sterilisation uses steam to eliminate living organisms. Heat losses, heating and cooling are major steps, and it is a time-consuming process. It requires air to be evacuated replaced with steam. At first the chamber is flashed with pressurised steam. With this technique we should get rid of the existing air. Steam sterilisation is performed in a jacketed vessel by supplying steam and maintaining the set pressure and temperature at a constant level for

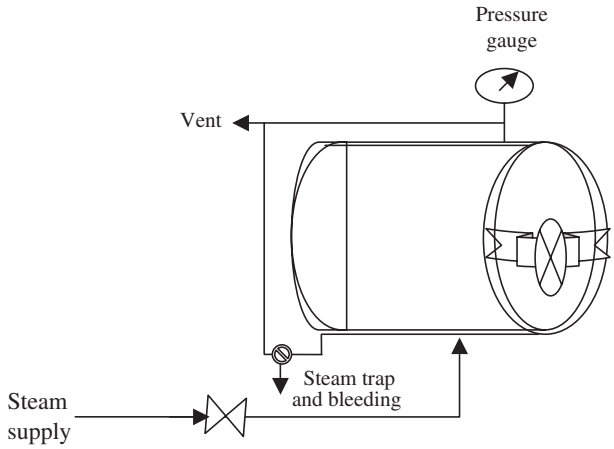

FIG. 15.1. Pressure steam steriliser (autoclave).

a fixed duration. Batch sterilisation wastes energy and overcooks the medium. There is no conservation of energy; therefore the process may not be economical for implementation at a large scale. Batch sterilisation is common at bench and laboratory scales as the diagram shows in Figure 15.1.

Batch media sterilisation is done in an autoclave. Basically, it is a huge steam cooker. Steam enters the jacket of the surrounding chamber. When the pressure from the steam has been built up in the jacket, a venting valve for the outlet of chamber air is closed and the inlet valve allows the steam to enter the chamber. The pressure of the chamber is increased to 105 kPa (15 psig). At this point the sterilisation time begins to count down. Usually 15–30 minutes are used, depending on the type and volume of media. For instance, sterilisation of one litre of media at 121 °C requires 20 minutes. Larger volumes may require longer retention times for sterilisation. There are recommended holding times of 20, 10 and 3 minutes for 121, 126 and 134 °C, respectively. The high pressure in a closed container allows the temperature to exceed 121 °C.

15.3 CONTINUOUS STERILISATION

One of the methods for continuous sterilisation of medium for fermentation is the direct use of live steam by injection of steam into the medium. The heat exchanger is eliminated. The medium stays in a loop for a predetermined holding time until the entire medium is sterile. The problem with directly injecting steam is dilution of media since it is initially cold. However, it has better heat economy, since it comes from substituting heat exchangers for direct steam injection. To utilise all the supplied heat, preheaters or heat economisers are used. Instead of having a cold water stream to cool the sterile media, the lower temperature, unsterile media stream takes the primary heat from the warm stream, cooling the sterile media. Continuous sterilisation has a holding coil for detention long enough to kill all the

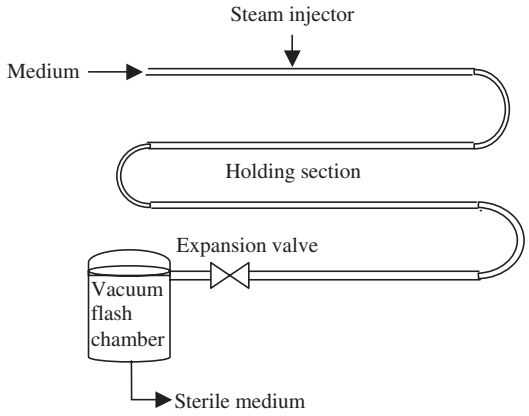

FIG. 15.2. Continuous sterilisation.

microorganisms. The medium from a make-up vessel flowing through the exchanger is held in the coil, and then goes through the heat exchanger, heating more unsterile medium while become cool itself, as it is collected in a sterile fermenter. Figure 15.2 presents the sequence of piping media goes through, along with steam. Finally, the media is collected in a vacuum flash drum.

Heat economisers are important for large-scale plant unit in continuous sterilisation. For a small-scale bioreactor use of direct steam injection is much simpler to operate. A heat exchanger is then needed with cooling water to bring the medium back to ambient temperature. Therefore jacketed vessels are commonly used with cooling water. There are advantages and disadvantages to batch and continuous sterilisation. The energy savings are related to the use of an economiser and direct stream or indirect sterilisation. In a large-scale system economy and role decide which one is the most suitable process to be implemented. For each case the specific design needs to be evaluated in terms of the thermal efficiency and fixed costs involved.

15.4 HOT PLATES

In directing steam heating, continuous sterilisation is preferable. The medium passed through a preheater may reach about 90 °C; then quite fast sterilisation may take at 140 °C. Figure 15.3 shows a counter-current hot-plate heat exchanger is normally used for continuous sterilisation. Hot-plate heat exchangers are extremely efficient and easily maintained if any fouling or scale deposition takes place. Normally fouling is serious problem, occuring by deposition of proteins on the hot surface of the exchanger, which causes reduction in the overall heat transfer coefficient. Plate exchangers are easily separated and cleaned. Special care must be taken when the media contains any agglomerated particles. Correlation is required to calculate the suitable residence time for sterilisation. The choice of a

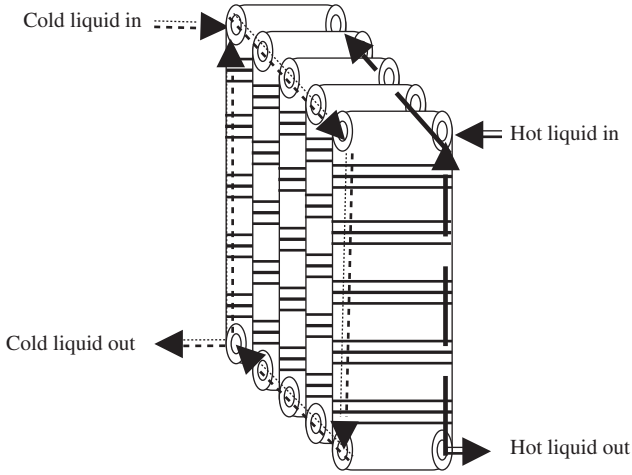

FIG. 15.3. Counter current hot plate heat exchanger.

suitable sterilisation process is based on economics and cost of the heat exchangers to reduce energy consumption. In a suitable exchanger, the larger the heat transfer coefficient, the greater the energy recovery.

15.5 HIGH TEMPERATURE STERILISATION

Fast sterilisation is performed at high temperature. High-temperature sterilisation requires short holding times. This technique is used in the fast preparation of nutrient media for industrial bioprocesses and in pasteurising milk. A short retention time may favour media with heat-sensitive proteins and cause less damage to the biochemical composition of the media than more prolonged times at lower temperatures. The ability of high temperatures to perform rapid sterilisation is related to activation energies. That is affected by how fast bacteria are killed in an elevated temperature. On the other hand, long sterilisation at high temperatures may destroy the protein and biochemical composition of the media. Short-duration sterilisation at high-temperatures are more lethal to organisms and less chemically damaging than are longer sterilisation processes at lower temperatures. Sterilisation at high temperature is recommended for 3 minutes at 134 °C. It is preferable to 20 minutes at 115 °C in conventional operation.

15.6 STERILISED MEDIA FOR MICROBIOLOGY

Sterile media are used for pure culture. The media used to culture microorganisms depend on the living conditions of the microorganisms. Media compositions must be identified

based on the needs of the organisms for carbon, nitrogen and phosphorus. Nutrients such as protein and sugars are added at wide ranges of pH. The acidic, neutral and alkaline conditions are defined based on differentiation of microbes in their biochemical reactions. Colour indicators are used to observe any transition of pH. Buffer is used in the media to maintain constant pH. Growth factors and growth stimulants are also used to accelerate microbial growth and to maintain exponential growth. The most common media in the liquid phase is nutrient broth; in the solid phase, nutrient agar is used to propagate microorganisms.

When microbiological media is prepared, it has to be sterilised before any inoculation of organisms. Sterilisation is used to eliminate any microbial contamination that may originate from air, glassware or hands. Microbes propagate quite quickly: within a few hours there will be thousands of organisms reproduced in the media. To control the growth of unwanted organisms, the media has to be sterilised quickly before any microbes start to utilise the nutrients. The sterilisation process makes the media absolutely free of contaminants and guarantees that the medium will stay sterile, so that is used only for the desired organisms.

The kinetics of culture media sterilisation describe the rate of destruction of microorganisms by steam using a first-order chemical reaction rate model. As the population of microorganisms (N) decreases with time, the rate is defined by the following equation:

$$-\frac{dN}{dt} = k_d N \tag{15.6.1}$$

where N is the number of viable organisms present in the culture media, t is the retention time or sterilisation time, and k_d is the reaction rate constant as it is known for a specific death rate. Using separation of variables and integrating with initial condition, the following useful expression is obtained:

$$N(t) = N_o e^{-k_d t} \tag{15.6.2}$$

where N_o is the number of viable organisms present in the media at the starting point before sterilisation. Now take the natural log of (15.6.2); it is reduced to a linear model:

$$\ln \frac{N(t)}{N_o} = -k_d t \tag{15.6.3}$$

The graphical presentation of the equation shows a straight line with a negative slope for k_d. As the death rate constant follows Arrhenius' law,[1] the death rate constant is temperature dependent. The value of k_d is about 0.02 min^{-1} at 100 °C, the death rate constant increases by 10-fold at 110 °C and 100-fold at 120 °C.[2]

$$k_d = k_o e^{-E/RT}$$

where k_o is the death rate constant at a reference temperature also known as Arrhenius' constant, R is the gas constant, T is the absolute temperature, E is the activation energy,

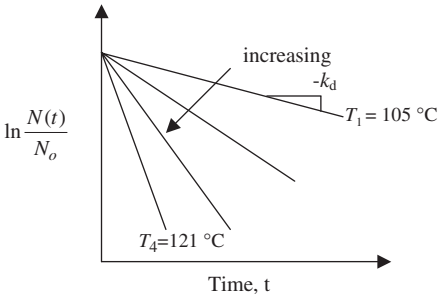

FIG. 15.4. The loss of cell viability at various temperatures.

which is 60–70 kcal per mole for microorganisms, 100–150 kcal per mole for spores, and 30–40 kcal per mole for media with vitamins and protein solution.[2]

Figure 15.4 shows the linear model for (15.6.3), the loss of cell viability at various temperatures. As the temperature increases from 105 to 121 °C, the value for the slope of the line increases. This means that the number of viable cells at a fixed time of sterilisation will drastically decrease as the temperature increases by 16 °C.

15.6.1 Sterilisation of Media for Stoke Cultures

To clear slant tubes, culture agar solution is prepared. To have clear agar solution, it has to boil. Agar is a polysaccharide. It is not soluble in cold water, so heating helps to dissolve it in water. Once the solution is dispensed in the tube, it goes for sterilisation. Agar is in the solid state at room temperature, about 35 °C.

15.6.2 Sterilisation of Bacterial Media

Often, sterilisation of culture media is done in an autoclave at temperatures between 121 and 134 °C. It is good to know the damage caused to the medium by heating it. Heating the culture media, which contains peptides, sugars, vitamins, minerals and metals, results in nutrient destruction, either thermal degradation or reaction between the components of the media. Protein in the media is denatured by high temperature, or sugars are easily caramelised. During the heat treatment, toxic compounds are formed, which may retard or inhibit the microbial growth. For minimal damage to the ingredients of the media, it is important to optimise and minimise the heating and holding time of the sterilisation process, respectively.

15.6.3 Sterilise Petri Dishes

There are several ways to handle Petri dishes. The standard dishes are 15–20 mm deep and 12–15 cm in diameter. They are normally available in glass and also transparent plastic. Petri dishes are individually wrapped. The media is separately sterilised while we add the sterilised media to the Petri dishes in front of a flame. It is recommended to use 20–25 ml

of medium in each Petri dish. These are all called culture dishes. The media contains about 1.5–2% agar. After the media cools off it solidifies. The Petri dishes with the nutrient agar should be sterilised and stored in a refridgerator.

It is common to sterilise the media and Petri dishes separately. When the medium is cooled to about 55 °C, in front of a flame or in a laminar flow chamber, lift the lid of the dish enough to pour about 25 ml of the medium to the desired depth and lower the lid in place. It is best to gently move the Petri dish in way that spreads a thin layer of agar uniformly without any air bubbles. Distribution of media in the Petri dishes should be done in front of a flame. Most plastic Petri dishes are made of polystyrene and are not autoclaveable. Plastic Petri dishes are easily deformed during sterilisation at high temperature. Some plastic dishes can be autoclaved, but they are more expensive. Please follow the instructions given by the manufacturer or obtain information from catalogues.

It is recommended to autoclave glass dishes and medium separately. If your dishes are autoclaveable, you may dispense the agar into the dish and then autoclave it. In this case it is best to cool the dishes in the autoclave or in the pressure cooker to reduce the amount of water that will condense on the cover of the dish.

15.7 DRY HEAT STERILISATION

Dry heat sterilisation is used for equipment that can withstand high temperature and dry heat but cannot withstand wet or steam autoclave. This method is often used for glassware as it dries and sterilises in one operation. The pipets must be wrapped in dustproof aluminum foil or placed in metal pipette cans. The can lids are removed during heating and replaced after sterilisation, that is before any dust can get in the can. Disposable items are not recommended for dry heat sterilisation. This method may only be good for permanent reusable glass pipettes.

Normal laboratory glassware must first be washed and cleaned. It has to be rinsed with deionised water. The clean glassware is sterilised in an oven set at 200 °C for 1–4 hours. It is suitable to cover glassware with aluminum foil to maintain aseptic conditions after removing the glassware from the oven. If aluminum foil is not available, special heat-resistant wrap paper can be used. The sterile glassware must be protected from the air, which has micro-flora, or any contaminants. Avoid the use of any plastic caps and papers. Detach any labelling tape or other flammable materials, as they are fire hazards.

15.8 STERILISATION WITH FILTRATION

Certain media components are susceptible to heat; it is going to be denatured if it is heated. Therefore they must be added to the media after autoclaving. To do so, it is necessary to carry out filtration, the components using a 0.22 μm pore size filter that is appropriate to the solvent used. Filters are normally available from Whatman, or Fisher Scientific. It is recommended you consult filter experts or suppliers about the solvent and the special application you are intending to implement for the desired filters for the process. Normally filtration of

media is used instead of sterilised media with an autoclave. To filter sterilised media, filter the water using a 0.45 μm pore size filter, before using a 0.22 μm pore size filter for final sterilisation.

15.9 MICROWAVE STERILISATION

Rapid sterilisation of media is achieved by using microwave ovens. Most plant tissue culture media can be sterilised using a microwave, although it may not be suitable with a medium containing complex additives like oatmeal.

15.10 ELECTRON BEAM STERILISATION

Electron beam sterilisation is a high-voltage potential established between a cathode and an anode in an evacuated tube. The cathode emits electrons, as a cathodic ray or electron beam. A high intensity of electrons is produced. These electrons are accelerated to extremely high velocities. These accelerated electron intensities have great potential as a bacteriocide. Most electron beams operate in a vacuum. As a result the unwanted organisms in the media vanish and the media is sterilised.

The electron accelerator equipment producing the high-voltage beam also has various applications in the medical field and surgical supplies. Electron beam sterilisation is a successful technology used for sterilisation of disposable medical appliances and devices with a wide range of densities. The electron beam inactivates microorganisms that cause destruction of biomolecules, and results in death of microbes by an indirect chemical reaction. Irradiation by gamma rays is a similar mechanism. Advanced electronics precisely control the use of electron beams in the sterilisation of medical devices. Electron beam sterilisation results in less material degradation than with gamma irradiation. Medical products are sterilised in the original shipping containers, saving lots of time and maintaining integrity of the original package.

15.11 CHEMICAL STERILISATION

Chemical agents are used to sterilise heat-sensitive equipment. Chemical solutions are used as a suitable method for sterilising long pipettes and glassware. Normally at pilot scale in the absence of life, steam and chemical agents are often used. Application of an oxidising agent such as 10% chlorox for 20 minutes or longer proves the system operates without any contamination. Excess amounts of chemical agent have to be removed; otherwise organisms are able to grow in a toxic environment. The bleach (sodium hypochlorite) then needs to be removed by rinsing with sterile water or rubbing with ethyl alcohol, 70% ethanol–water (pH = 2) or an alcohol solution of 70% *iso*-propanol without recontaminating the glassware or tools. Ethanol is commonly used for cleaning surfaces. Use of bleach on metal devices is not suitable as it corrodes metals rapidly. Ethylene oxide in the gas phase is commonly used.

This is a special chemical effectively used for column bioreactors. It is a volatile compound and strong oxidising agent. It boils at ambient temperature, therefore the solution of ethylene oxide (liquid phase) must be stored in a refrigerator (4 °C). An excellent oxidising agent such as a 3% sodium hypochlorite is used for chemical sterilisation of equipment.

REFERENCES

1. Pelczar, M.J., Chan, E.C.S. and Krieg, N.R., "Microbiology". McGraw-Hill, New York, 1986.
2. Scragg, A.H., "Bioreactors in Biotechnology, A Practical Approach". Ellis Horwood Series in Biochemistry and Biotechnology, New York, 1991.
3. Doran, P.M., "Bioprocess Engineering Principles". Academic Press, New York, 1995.
4. Shuler, M.L. and Kargi, F., "Bioprocess Engineering, Basic Concepts". Prentice-Hall, New Jersey, 1992.
5. Baily, J.E. and Ollis, D.F., "Biochemical Engineering Fundamentals", 2nd edn. McGraw-Hill, New York, 1986.
6. Matthews, I.P., Gibson, C. and Samuel, A.H., *J Biomed. Mat. Res.* **23**, 143 (1989).

CHAPTER 16

Membrane Separation Processes

16.1 INTRODUCTION

Membranes have gained an important place in chemical technology and are used in a broad range of applications ranging from pharmaceuticals to water treatment. Industrial applications are divided into six main subgroups: reverse osmosis, nanofiltration, ultrafiltration, microfiltration, gas separation, pervaporation and electrodialysis.[1] The key property that is exploited is the ability of a membrane to control the permeation rate of a chemical species through the membrane.[2] In controlled drug delivery, the goal is to moderate the permeation rate of a drug from a reservoir to the body. In separation applications, the goal is to allow one component of a mixture to permeate the membrane freely, while hindering permeation of other components.[3] This chapter provides a general introduction to membrane science and technology.

16.2 TYPES OF MEMBRANE

This chapter is limited to synthetic membranes, excluding all biological structures, but the topic is still large enough to include a wide variety of membranes that differ in chemical and physical composition and in the way they operate. In essence, a membrane is nothing more than a discrete, thin interface that moderates the permeation of chemical species in contact with it. This interface may be molecularly homogeneous, i.e., completely uniform in composition and structure; or the interface may be chemically or physically heterogeneous, e.g., containing holes or pores of finite dimensions or consisting of some form of layered structure. A normal filter meets this definition of a membrane, but, by convention, the term 'filter' is usually limited to structures that separate particulate suspensions larger than 1–10 μm.[3,4] The

---

This case study was contributed by:
Ghasem Najafpour,[1] Nidal Hilal,[2] and Abdul Latif Ahmad[3]
[1]Biochemical Engineering, Program Chairman of Biotechnology, Faculty of Chemical Engineering, Noshirvani Institute of Technology, University of Mazandaran, Babol, Iran.
[2]Reader in Chemical Engineering, Director of Centre for Clean Water Technologies, University of Nottingham, Deputy Director of Research/School of Chemical, Environmental and Mining Engineering, University Park, Nottingham, NG7 2NR, United Kingdom.
[3]Membrane Technology, School of Chemical Engineering, Engineering Campus, Universiti Sains Malaysia, Seri Ampangan, 14300 Nibong Tebal, S.P.S., Pulau Pinang, Malaysia.

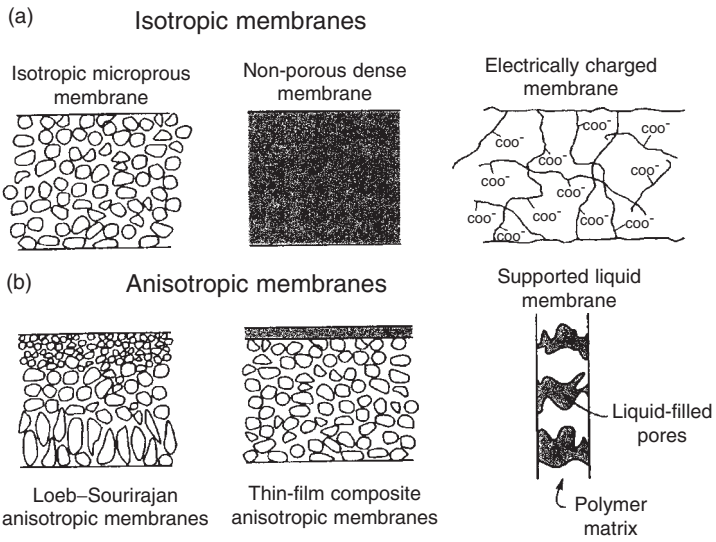

FIG. 16.1. Schematic diagrams of the principal types of membrane.

principal types of membrane are shown schematically in Figure 16.1 and are described briefly in the following pages.

16.2.1 Isotropic Membranes

16.2.1.1 Microporous Membranes

A microporous membrane is very similar in structure and function to a conventional filter. It has a grid, highly voided structure with randomly distributed, interconnected pores. However, these pores differ from those in a conventional filter by being extremely small, of the order of 0.01–10 μm in diameter. All particles larger than the largest pores are completely rejected by the membrane. According to the pore size distribution of the membrane, the particles smaller than the largest pores and the particles larger than the smallest pores are partly rejected. Particles much smaller than the smallest pores are absolutely passed through the membrane. Thus, separation of solutes by microporous membranes is mainly a function of molecular size and pore size distribution. In general, only molecules that differ considerably in size can be separated effectively by microporous membranes, e.g., in ultrafiltration and microfiltration.[5,6] Isotropic membranes are shown in Figure 16.1a.

16.2.1.2 Non-porous, Dense Membranes

Non-porous, dense membranes consist of a dense film through which permeats are transported by diffusion under the driving force of a pressure, concentration or electrical potential gradient. The separation of various components of a mixture is related directly to their relative transport rates within the membrane, which are determined by their diffusivity and solubility in the membrane material. Thus, non-porous, dense membranes can separate permeats of similar

size if their concentration in the membrane material (i.e. their solubility) differs significantly. Most gas separation, pervaporation and reverse osmosis membranes use dense membranes to perform the separation. Usually these membranes have an anisotropic structure to improve the flux.

16.2.1.3 Electrically Charged Membranes

Electrically charged membranes are dense or microporous. Most commonly these membranes are very fine microporous, with the pore walls carrying fixed positively or negatively charged ions. A membrane with fixed positively charged ions is referred to as an anion-membrane because it binds anions in the surrounding fluid. Similarly, a membrane containing fixed negatively charged ions is called a cation-exchange membrane. Separation with charged membranes is achieved mainly by exclusion of ions of the same charge as the fixed ions of the membrane structure, and to a much lesser extent by the pore size. The separation is affected by the charge and concentration of the ions in solution. For example, monovalent ions are excluded less effectively than divalent ions, and in solutions of high ionic strength, selectivity decreases. Electrically charged membranes are used for processing electrolyte solutions in electrodialysis.[7,8]

16.2.2 Anisotropic Membranes

The transport rate of a species through a membrane is inversely proportional to the membrane thickness. High transport rates are desirable in membrane separation processes for economic reasons; therefore, the membrane should be as thin as possible. Conventional film fabrication technology limits manufacture of mechanically strong, defect-free films to about 20 μm thickness.[2,9] The development of novel membrane fabrication techniques to produce anisotropic membrane structures has been one of the major breakthroughs of membrane technology during the past 30 years. Anisotropic membranes consist of an extremely thin surface layer supported on a much thicker, porous structure. The surface layer and its structure may be formed in a single operation or separately. In composite membranes, the layers are usually made from different polymers. The separation properties of permeation rates of the membrane are determined exclusively by the surface layer; the substructure functions as a mechanical support. The advantages of the higher fluxes provided by anisotropic membranes are so great that almost all commercial processes use such membranes.

16.2.3 Ceramic, Metal and Liquid Membranes

The discussion so far implies that membrane materials are organic polymers, and in fact most membranes used commercially are polymer-based. However, in recent years, interest in membranes made of less conventional materials has increased. Ceramic membranes, a special class of microporous membranes, are being used in ultrafiltration and microfiltration applications for which solvent resistance and thermal stability are required. Dense, metal membranes, particularly palladium membranes, are being considered for the separation of hydrogen from gas mixtures, and supported liquid films are being developed for carrier-facilitated transport processes.

TABLE 16.1. *Classification of membrane separation processes for liquid systems*

Process	Driving force	Separation size range	Examples of materials separated
Microfiltration	Pressure gradient	0.1–10 μm	Small particles, large colloids, microbial cells
Ultrafiltration	Pressure gradient	< 0.1 μm–5 nm	Emulsions, colloids, macromolecules, proteins
Reverse osmosis	Pressure gradient	< 5 nm	Dissolved salts, small organics
Electrodialysis	Electric field gradient	< 5 nm	Dissolved salts
Dialysis	Concentration gradient	< 5 nm	Treatment of renal failure

16.3 MEMBRANE PROCESSES

Industrial membrane processes may be classified according to the size range of materials that they are to separate and the driving force used in separation. There is always a degree of arbitrariness about such classifications, and the distinctions that are typically drawn. Table 16.1 presents classification of membrane separation processes for liquid systems.

The four developed industrial membrane separation processes are microfiltration (MF), ultrafiltration (UF), reverse osmosis (RO) and electrodialysis. These processes are well-established large-scale industrial processes. The range of application of the three pressure driven membrane water separation processes, reverse osmosis, ultrafiltration and microfiltration is illustrated in Figure 16.2. Microfiltration membranes filter colloidal particles and bacteria from 0.1 to 10 μm in diameter. Ultrafiltration membranes can be used to filter dissolved macromolecules, such as proteins, from solutions. The mechanism of separation by reverse osmosis membranes is quite different. In reverse osmosis membranes, the membrane pores are so small, from 3 to 5 angstroms (1 angstrom = 10^{-10} m) in diameter that they are within the range of thermal motion of the polymer chains that form the membrane.[4,10] The accepted mechanism of transport through these membranes is called the solution-diffusion model. According to this model, solutes permeate the membrane by dissolving in the membrane material and diffusing down to concentration gradient. Separation occurs because of the difference in solubilities and mobilities of different solutes in the membrane. The principal application of reverse osmosis is the desalination of brackish groundwater or seawater.

Figure 16.2 show the reverse osmosis, ultrafiltration, microfiltration and conventional filtration processes, which are related but differ principally in the average pore diameter of the membrane filter. Reverse osmosis membranes are so dense that discrete pores do not exist; transport occurs by statistically distributed free volume areas. The relative size of different solutes removed by each class of membrane is illustrated in the schematic.

The fourth fully developed membrane process is electrodialysis, in which charged membranes are used to separate ions from aqueous solutions under the driving force of an electrical potential difference. The process utilises an electrodialysis stack, built on the filter press principle and containing several hundred individual cells, each formed by a pair of anion and

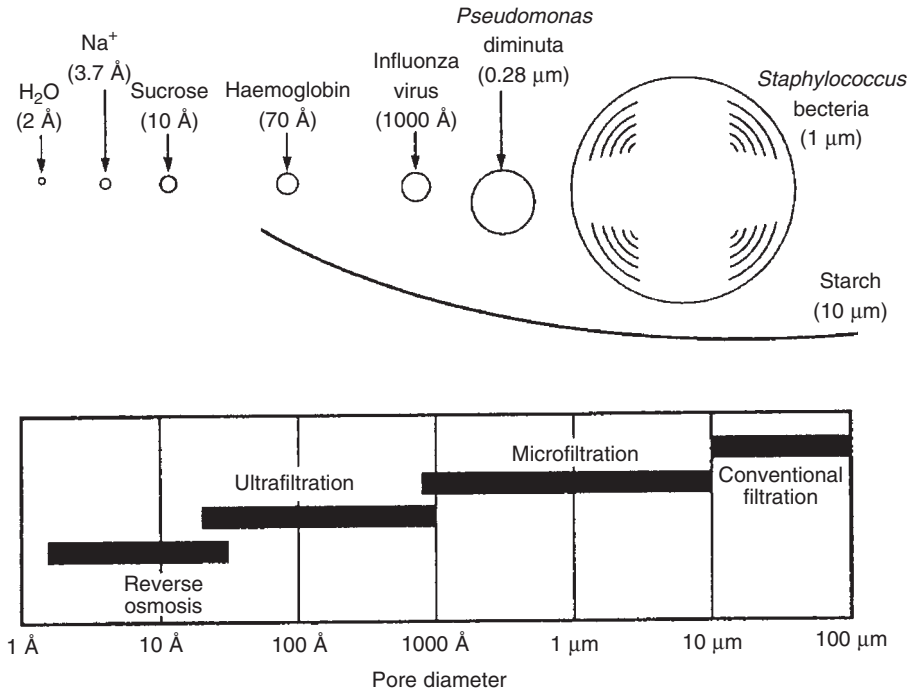

FIG. 16.2. Reverse osmosis, ultrafiltration, microfiltration and conventional filtration with distinct pore size.

cation exchange membranes. The principal application of electrodialysis is the de-salting of brackish groundwater. However, industrial use of the process in the food industry, e.g., to deionise cheese whey, is growing, as is its use in pollution control applications. A schematic of the process is shown in Figure 16.3.

In gas separation with membranes, a gas mixture at an elevated pressure is passed across the surface of a membrane that is selectively permeable to one component of the mixture. The basic process is illustrated in Figure 16.4. Major current applications of gas separation membranes include the separation of hydrogen from nitrogen, argon and methane in ammonia plants; the production of nitrogen from air; and the separation of carbon dioxide from methane in natural gas operations. Membrane gas separation is an area of considerable research interest and the number of applications is expanding rapidly.

Pervaporation is a relatively new process that has elements in common with reverse osmosis and gas separation. In pervaporation, a liquid mixture contacts one side of a membrane, and the driving force for the process is low vapour pressure on the permeate side of the membrane generated by cooling and condensing the permeate vapour. The attraction of pervaporation is that the separation obtained is proportional to the rate of permeation of the components of the liquid mixture through the selective membrane. Therefore, pervaporation offers the possibility of separating closely boiling mixtures or azeotropes that are difficult to separate by distillation

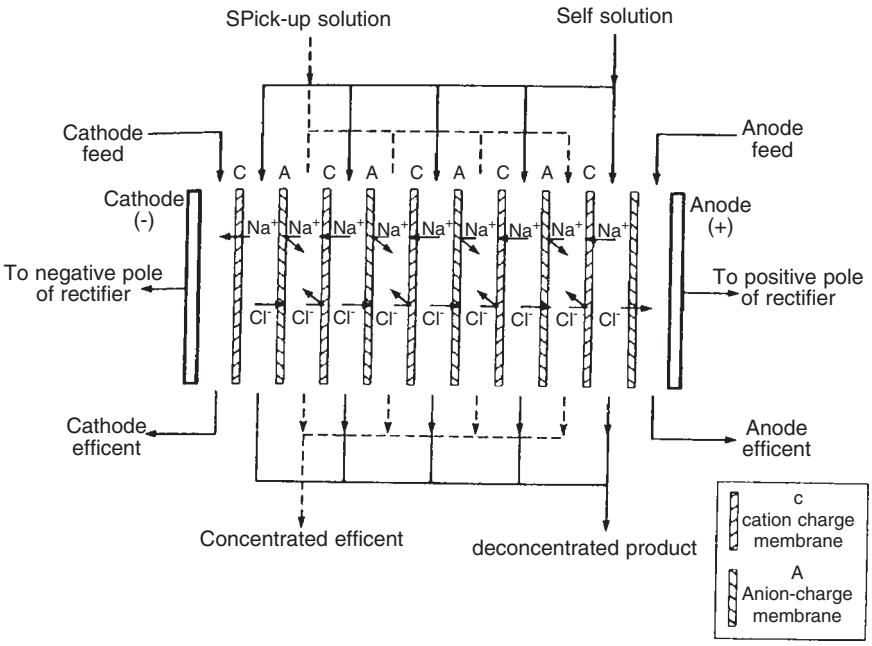

FIG. 16.3. Schematic diagram of an electrodialysis.

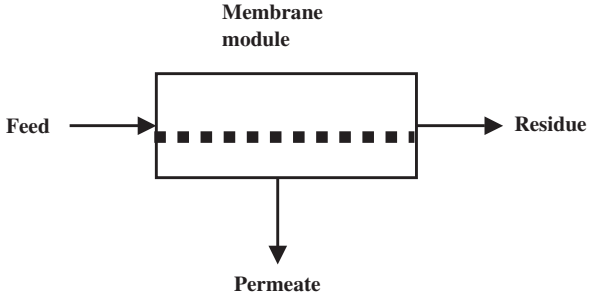

FIG. 16.4. Schematic diagram of the basic membrane gas separation process.

or other means. A schematic of a simple pervaporation process using a condenser to generate the permeate vacuum is shown in Figure 16.5. Currently, the main industrial application of pervaporation is in the dehydration of organic solvents, in particular, the dehydration of 90–95% ethanol solutions, a difficult separation problem because of the ethanol–water azeotrope at 95% ethanol. Pervaporation membranes can produce more than 99% ethanol from a 90% ethanol feed solution. Pervaporation processes are also being developed for the removal of dissolved organics from water and for the separation of organic mixtures.

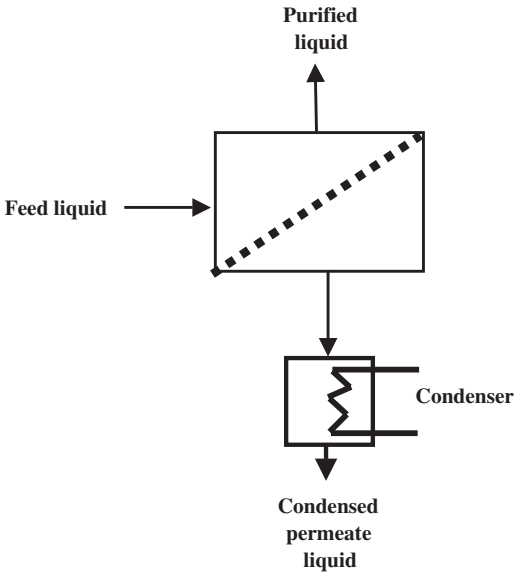

FIG. 16.5. Schematic diagram of the basic pervaporation process.

16.4 NATURE OF SYNTHETIC MEMBRANES

Membranes used for the pressure driven separation processes, microfiltration (MF), ultrafiltration (UF) and reverse osmosis (RO), as well as those used for dialysis, are most commonly made of polymeric materials. Initially most such membranes were cellulosic in nature. These are now being replaced by polyamide, polysulphone, polycarbonate and several other advanced polymers. These synthetic polymers have improved chemical stability and better resistance to microbial degradation. Membranes have most commonly been produced by a form of phase inversion known as immersion precipitation.[11] This process has four main steps:

(1) the polymer is dissolved in a solvent to 10–30% by weight;
(2) the resulting solution is cast on a suitable support as a film of thickness of about 100 μm;
(3) the film is quenched by immersion in a non-solvent bath, typically water or an aqueous solution;
(4) the resulting membrane is annealed by heating.

The third step gives a polymer-rich phase forming the membrane, and a polymer-depleted phase forming the pores. The ultimate membrane structure results as a combination of phase separation and mass transfer, variation of the production conditions giving membranes with different separation characteristics. Most MF membranes have a systematic pore structure, and they can have porosity as high as 80%.[11,12] Figure 16.6 shows an atomic force microscope

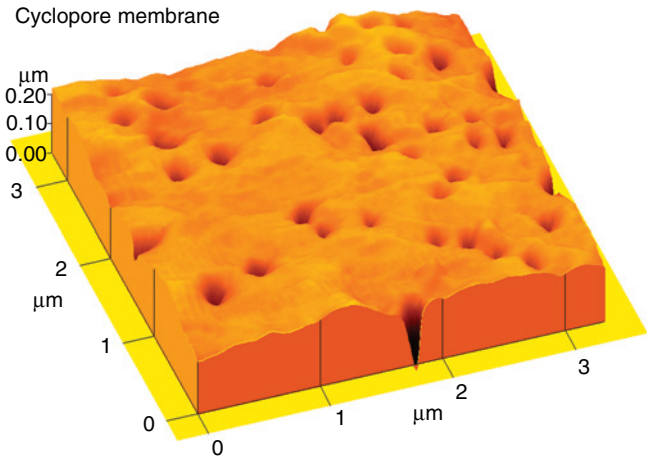

FIG. 16.6. Atomic force microscope image of a polycarbonate microfiltration membrane (cyclopore), 0.2 µm pore size.

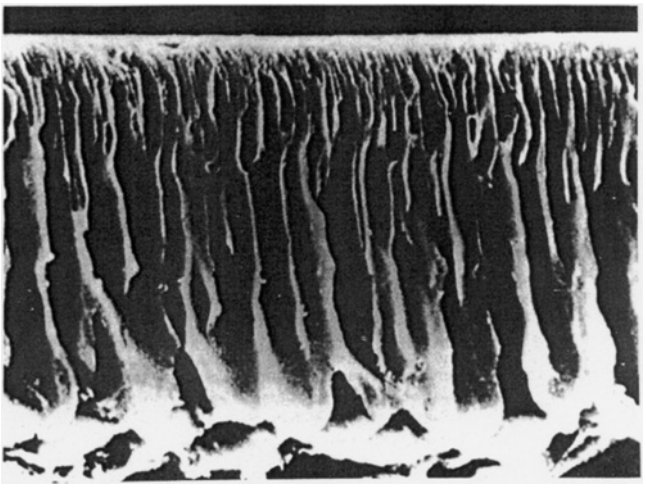

FIG. 16.7. Scanning electron micrograph of a section of an asymmetric polyamine ultrafiltration membrane showing finely porous 'skin' layer on more openly porous supporting matrix.

image of polycarbonate MF membrane (0.2 µm mean pore size). UF and RO membranes have an asymmetric structure comprising a 1–2 µm thick top layer of finest pore size supported by a approximately 100 µm thick more openly porous matrix (Figure 16.7). Such an asymmetric structure is essential if reasonable membrane permeation rates are to be obtained. Another important type of polymeric membrane is the thin-film composite membrane. This consists of an extremely thin layer, typically about 1 µm, of finest pore structure deposited

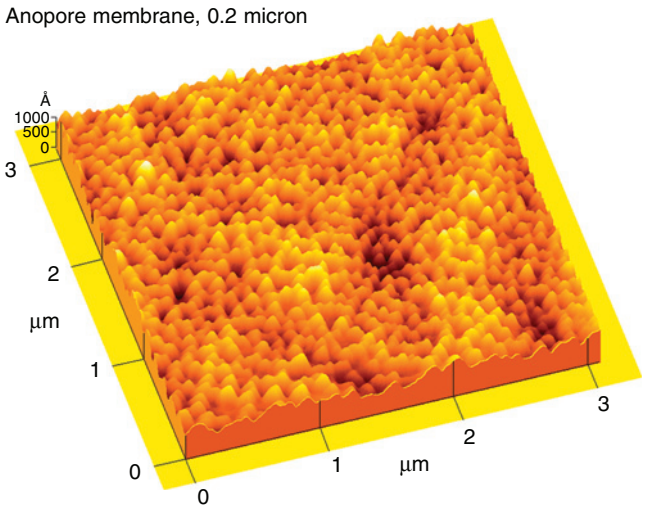

FIG. 16.8. Atomic force microscope image of anodisc microfiltration membrane, 0.2 µm pore size.

on a more openly porous matrix.[13,14] The main layer is formed by phase inversion or interfacial polymerisation on to an existing microporous structure.

Polymeric membranes are most commonly produced in the form of flat sheets, but they are also widely produced as tubes of diameter 10–25 mm and in the form of hollow fibres of diameter 0.1–2 mm.

A significant recent advance has been the development of MF and UF membranes composed of inorganic oxides.[11,13] These are currently produced by two main techniques:

(1) deposition of colloidal metal oxide on to a supporting material such as carbon;
(2) as purely ceramic materials by high temperature sintering of spray-dried oxide microspheres.

Other innovative production techniques lead to the formation of membranes with very regular pore structures, as shown in Figure 16.8. The main advantages of inorganic membranes compared with the polymeric types are their higher temperature stability, allowing steam sterilisation in biotechnological and food applications, increased resistance to fouling, and a narrower pore size distribution.[14]

The physical characterisation of membrane structure is important if the correct membrane is to be selected for a given application. The pore structure of microfiltration membranes is relatively easy to characterise, SEM and AFM being the most convenient method and allowing three-dimensional structure of the membrane to be determined. Other techniques such as the bubble point, mercury intrusion or permeability methods use measurements of the permeability of membranes to fluids. Both the maximum pore size and the pore size distribution may be determined.[13,15] A parameter often quoted in manufacturer's literature is the nominal

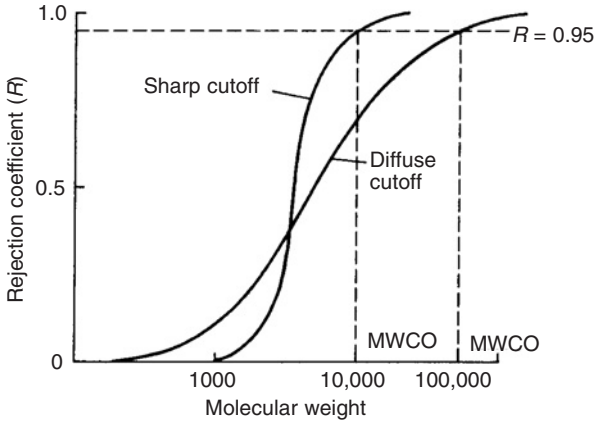

FIG. 16.9. Dependence of rejection coefficient on molecular weight for ultrafiltration membranes.

molecular weight cut-off (MWCO) of a membrane.[13,14] This is based on studies of how solute molecules are rejected by membranes. A solute will pass through a membrane if it is sufficiently small to pass through a pore, if it does not significantly interact with the membrane and if it does not interact with other (larger) solutes. It is possible to define a solute rejection coefficient R by:

$$R = 1 - (C_p/C_f) \tag{16.4.1}$$

where C_f is the concentration of solute in the feed stream and C_p is the concentration of solute in the permeate. For a given UF membrane with a distribution of pore sizes there is a relation between R and the solute molecular weight, as shown in Figure 16.9.

The nominal molecular weight cut-off is normally defined as the molecular weight of a solute for which $R = 0.95$. Values of MWCO typically lie in the range 2000–100,000, with values of the order of 10,000 being most common. Figure 16.10 shows an AFM scan of 30,000 MWCO membrane.

16.5 GENERAL MEMBRANE EQUATION

It is not possible at present to provide an equation, or set of equations, that allows the prediction from first principles of the membrane permeation rate and solute rejection for a given real separation. Research attempting such prediction for model systems is underway, but the physical properties of real systems, both the membrane and the solute, are too complex for such analysis. An analogous situation exists for conventional filtration processes. The general

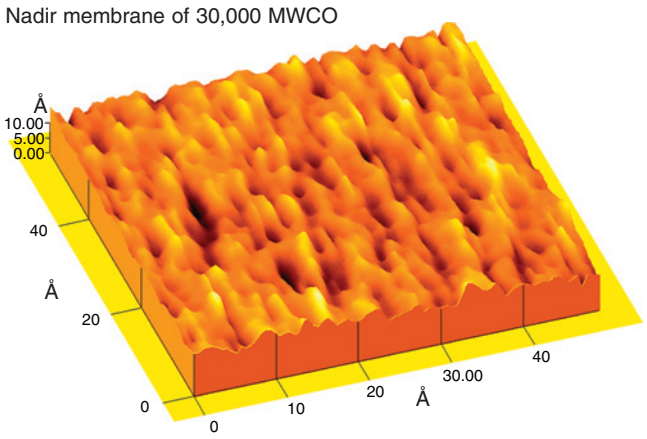

FIG. 16.10. Atomic force microscope image of 30,000 MWCO ultrafiltration membrane.

membrane equation is an attempt to state the factors that may be important in determining the membrane permeation rate for pressure driven processes.[1,4] This takes the form:

$$J = \frac{|\Delta P| - |\Delta \Pi|}{(R_m + R_c + R'_f)\mu} \tag{16.5.1}$$

where J is the membrane permeation rate (flux expressed as volumetric ate per unit area), $|\Delta P|$ is the pressure difference applied across the membrane (transmembrane pressure), $\Delta\Pi$ is the difference in osmotic pressure across the membrane, R_m is the resistance of the membrane, R_c is the resistance of layers deposited on the membrane (filter cake, gel solution) and R'_f is the 'resistance' of the film layer. If the membrane is only exposed to pure solvent, say water, then (16.5.1) reduces to $J = |\Delta P|/R_m\mu$. Knowledge of such water fluxes is useful for characterising new membranes and for assessing the effectiveness of membrane cleaning procedures. In the processing of solutes, (16.5.1) shows that the transmembrane pressure must exceed osmotic pressure for flow to occur. It is generally assumed that the osmotic pressure of most retained solutes is likely to be negligible in the formation of a gel when the concentration of macromolecules at the membrane surface exceeds their solubility giving rise to a precipitation, or due to materials in the process feed that adsorb on the membrane surface producing an additional barrier to solvent flow. The separation of a solute by a membrane gives rise to an increased concentration of that solute at the membrane surface, an effect known as 'concentration polarisation'. This may be described in terms of an additional "resistance," R'_f. The limitation of (16.5.1) is that the resistances are not readily calculable. However, it is within the framework of this equation that the factors influencing membrane permeation rate will be discussed in the following section.

16.6 CROSS-FLOW MICROFILTRATION

The solid–liquid separation of slurries containing particles below 10 μm is difficult by conventional filtration techniques. A conventional approach would be to use a slurry thickener in which the formation of a filter cake is restricted and the product is discharged continuously as concentrated slurry. Such filters use filter cloths as the filtration medium and are limited to concentrating particles above 5 μm in size. Dead end membrane microfiltration, in which the particle-containing fluid is pumped directly through a polymeric membrane, is used for the industrial clarification and sterilisation of liquids. Such process allows the removal of particles down to 0.1 μm or less, but is only suitable for feeds containing very low concentrations of particles as otherwise the membrane becomes too rapidly clogged.[2,4,8]

The concept of cross-flow microfiltration is shown in Figure 16.11, which represents a cross-section through a rectangular or tubular membrane module. The particle-containing fluid to be filtered is pumped at a velocity in the range 1–8 m/s parallel to the face of the membrane and with a pressure difference of 0.1–0.5 MN/m^2 (MPa) across the membrane. The liquid permeates through the membrane and the feed emerges in a more concentrated form at the exit of the module.[16,17] All of the membrane processes are listed in Table 16.2. Membrane processes are operated with such a cross-flow of the process feed.

The advantages of cross-flow filtration over conventional filtration are:

(1) A higher overall liquid removal rate is achieved by prevention of the formation of an extensive filter cake.
(2) The process feed remains in the form of mobile slurry suitable for further processing.
(3) The solids content of the product slurry may be varied over a wide range.
(4) It may be possible to fractionate particles of different sizes.

A flow diagram of a simple cross-flow system is shown in Figure 16.12. This is the system likely to be used for batch processing or development rigs; it is in essence a basic pump recirculation loop. The process feed is concentrated by pumping it from the tank and across the membrane in the module at an appropriate velocity. The partly concentrated retentate is recycled into the tank for further processing while the permeate is stored or discarded as required. In cross-flow filtration applications, product washing is frequently necessary and

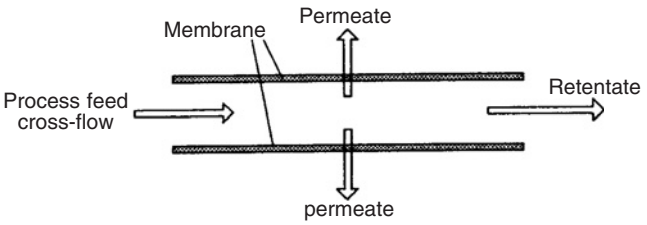

FIG. 16.11. The concept of cross-flow filtration.

is achieved by a process known as diafiltration in which wash water is added to the tank at a rate equal to the permeation rate.

In practice, the membrane permeation rate falls with time owing to membrane fouling; that is, blocking of the membrane surface and pores by particulate materials (Figure 16.13). The rate of fouling depends on the nature of the materials being processed, the nature of the membrane, the cross-flow velocity and the applied pressure. For example, increasing the cross-flow velocity results in a decreased rate of fouling. Backflushing the membrane using permeate is often used to control fouling (Figure 16.13c). Further means of controlling membrane fouling are discussed later.

Ideally, cross-flow microfiltration would be the pressure-driven removal of the process liquid through a porous medium without the deposition of particulate material. The flux decrease occurring during cross-flow microfiltration shows that this is not the case. If the

TABLE 16.2. *Module designs most commonly used in major separation processes*

Application	Module type
Reverse osmosis: seawater	Both hollow-fibres and spiral-wound modules
Reverse osmosis: industrial and brackish water	Spiral-wound modules used almost exclusively; fine fibres too susceptible to scaling and fouling
Ultrafiltration	Tubular, capillary and spiral-wound modules all used. Tubular generally limited to highly fouling feeds (automotive paint), spiral-wound to clean feeds (ultrapure water).
Gas separation	Hollow-fibre for high-volume applications with low-flux, low-selectivity membranes in which concentration polarisation is easily controlled (nitrogen from air)
	Spiral-wound when fluxes are higher, feed gases more contaminated, and concentration polarisation a problem (natural gas separations, vapour permeation).
Pervaporation	Most pervaporation systems are small so plate-and-frame systems were used in the first systems. Spiral-wound and capillary modules are being introduced.

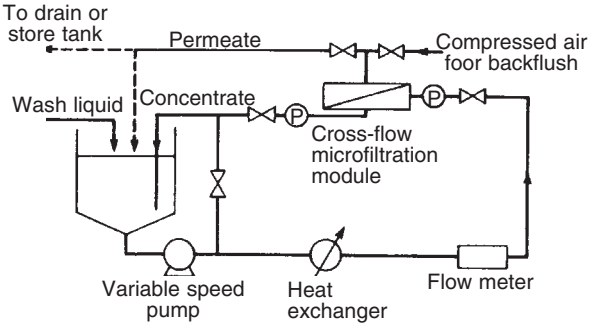

FIG. 16.12. Flow diagram for a simple cross-flow system.

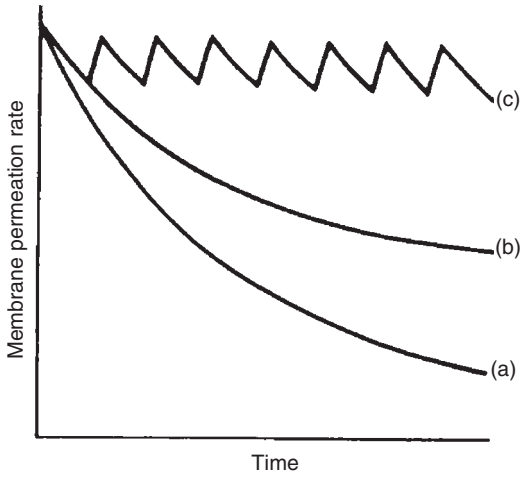

FIG. 16.13. Time dependence of membrane permeation rate during cross-flow filtration: (a) low cross-flow velocity, (b) increased cross-flow velocity, (c) back flushing at the bottom of each 'saw-tooth'.

decrease is due to particle deposition resulting from incomplete removal by the cross-flow liquid, then (16.5.1) may be written as:

$$J = \frac{|\Delta P|}{(R_m + R_c)\mu} \tag{16.6.1}$$

where R_c now represents the resistance of the cake, which if all filtered particles remain in the cake, may be written as:

$$R_c = \frac{rVC_b}{A_m} = \frac{rV_s}{A_m} \tag{16.6.2}$$

where r is the specific resistance of the deposit, V is the total volume filtered, V_s the volume of *particles* deposited, C_b the bulk concentration of particles in the feed (particle volume/feed volume) and A_m the membrane area. The specific resistance can be related to the properties for spherical particles by the Carman relation as:

$$r = 180\frac{1-e}{e^3}\frac{1}{d_s^2} \tag{16.6.3}$$

where e is the void volume of the cake and d_s the mean particle diameter.

Combining (16.6.1) and (16.6.2) gives:

$$J = \frac{1}{A_m}\frac{dV}{dt} = \frac{|\Delta P|}{(R_m + rVC_b/A_m)\mu} \tag{16.6.4}$$

Solution of (16.6.4) for V at constant pressure gives:

$$\frac{t}{V} = \frac{R_m \mu}{|\Delta P| A_m} + \frac{C_b r \mu V}{2 \Delta P A_m^2} \tag{16.6.5}$$

yielding a straight line on plotting t/V versus V.

The early stages of cross-flow microfiltration often follow such a pattern. However, the growth of the cake is limited by the cross-flow of the process liquid. There are several ways of accounting for the control of cake growth. A useful method is to rewrite (16.6.1) as:

$$J = \frac{1}{A_m}\frac{dV}{dt} = \frac{|\Delta P|}{(R_m + R_{sd} - R_{sr})\mu} \tag{16.6.6}$$

where R_{sd} is the resistance that would be caused by deposition of all particles and R_{sr} is the resistance removed by cross-flow. Assuming the removal of solute by cross-flow to be constant and equal to the convective particle transport at steady-state ($= J_{ss} C_b$), then,

$$\frac{1}{A_m}\frac{dV}{dt} = \frac{|\Delta P|}{(R_m + (V/A_m - J_{ss} t) r C_b)\mu} \tag{16.6.7}$$

where J_{ss} can be obtained experimentally or from the film-model (16.7.5).

In several cases, a steady rate of filtration in never achieved. In such cases it is possible to describe the time dependence of filtration by introducing an efficiency factor β representing the fraction of filtered particles remaining in the filter cake rather than being swept along by the bulk flow. Equation 16.7.4 then becomes

$$R_c = \frac{\beta r V C_b}{A_m} \tag{16.6.8}$$

where $0 < \beta < 1$. The layers deposited on the membrane during cross-flow microfiltration are sometimes considered to constitute dynamically formed membranes with their own rejection and permeation characteristics.

Film and gel-polarisation models are developed for ultrafiltration. These models are also widely applied to cross-flow microfiltration.

16.7 ULTRAFILTRATION

Ultrafiltration is one of the most widely used of the pressure-driven membrane separation processes. The solute retained or rejected by ultrafiltration membranes are those with

molecular weights of 1000 or greater, depending mostly on the MWCO of the membrane chosen. The process liquid, dissolved salts and low molecular weight organic molecules (molecular weight 500–1000) generally pass through the membrane. The pressure difference applied across the membrane is usually in the range 0.1–0.7 MN/m^2 (MPa) and membrane permeation rates are typically 0.01–0.2 m^3/m^2 h. In industry, ultrafiltration is always operated in the cross-flow mode.[4,8,11,18]

The separation of process liquid and solute that takes place at the membrane during ultrafiltration gives rise to an increase in solute concentration close to the membrane surface (Figure 16.14). This is termed 'concentration polarisation' and takes place within the boundary film generated by the applied cross-flow. With a greater concentration at the membrane, there will be a tendency for solute to diffuse back into the bulk feed according Fick's law. At steady-state, the rate of back-diffusion will be equal to the rate of removal of solute at the membrane, minus the rate of solute leakage through the membrane:

$$J(C - C_p) = -D\frac{dC}{dy} \tag{16.7.1}$$

Here solute concentration C and C_p (in permeate) are expressed as mass fractions, D is the diffusion coefficient of the solute and y is the distance from the membrane. Rearranging and integrating from $C = C_f$ when $y = l$ the thickness of the film, to $C = C_w$, the concentration of solute at the membrane wall, when y=0, gives:

$$-\int_{C_w}^{C_f} \frac{dC}{C - C_p} = \frac{J}{D}\int_0^l dy \tag{16.7.2}$$

$$\frac{C_w - C_p}{C_f - C_p} = \exp\left(\frac{Jl}{D}\right) \tag{16.7.3}$$

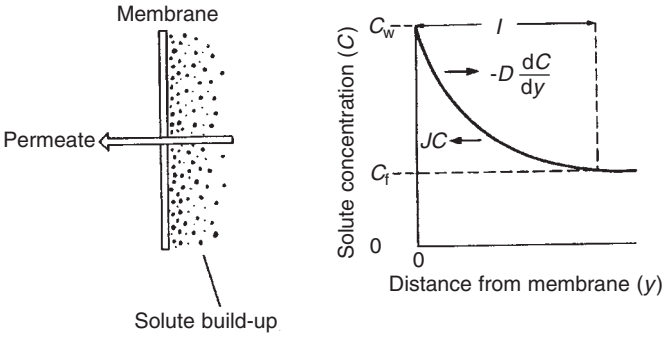

FIG. 16.14. Concentration polarisation at a membrane surface.

If it is further assumed that the membrane completely rejects the solute, that is, $R = 1$ and $C_p = 0$, then:

$$\frac{C_w}{C_f} = \exp\left(\frac{Jl}{D}\right) \tag{16.7.4}$$

where the ratio C_w/C_f is known as the polarisation modulus. Note that it has been assumed that l is independent of J and that D is constant over the whole range of C at the interface. The film thickness is usually incorporated in an overall mass transfer coefficient h_D, where $h_D = D/l$, giving:

$$J = h_D \ln\left(\frac{C_w}{C_f}\right) \tag{16.7.5}$$

The mass transfer coefficient is usually obtained from correlations for flow in non-porous ducts.

Process patterns diagnostic of gel-polarisation type behaviour are shown in Figure 16.15. The dependence of membrane permeation rate on the applied pressure is shown in Figure 16.15a. There is an initial pressure-dependence region followed by a pressure-independent region. The convergence of plots of the membrane permeation rate against C_f (Figure 16.15b) is a test of (16.7.5).

The basic features of the flux-pressure profiles (Figure 16.15a) are:

(1) at low $|\Delta P|$ the slope is similar to that for pure solvent flow;
(2) as $|\Delta P|$ increases, the slope declines and approaches zero at high pressure.

16.8 REVERSE OSMOSIS

A classic demonstration of osmosis is to stretch a parchment membrane over the mouth of a tube, fill the tube with a sugar solution, and then hold it in a beaker of water. The level of solution in the tube rises gradually until it reaches a steady level. The static head developed would be equivalent to the osmotic pressure of the solution if the parchment were a perfect semipermeable membrane, such a membrane having the property of allowing the solvent to pass through but preventing the solute from passing through. The pure solvent has a higher chemical potential than the solvent in the solution and so diffuses through until the difference is cancelled out by the pressure head. If an additional pressure is applied to the liquid column on the solution side of the membrane then it is possible to force water back through the membrane. This pressure driven transport of water from solution through membrane is known as 'reverse osmosis'. Note that it is not quite the reverse of osmosis because, for all real membranes, there is always a certain transport of the solute along its chemical potential gradient, and this is not reversed. This phenomenon of reverse osmosis has been extensively developed

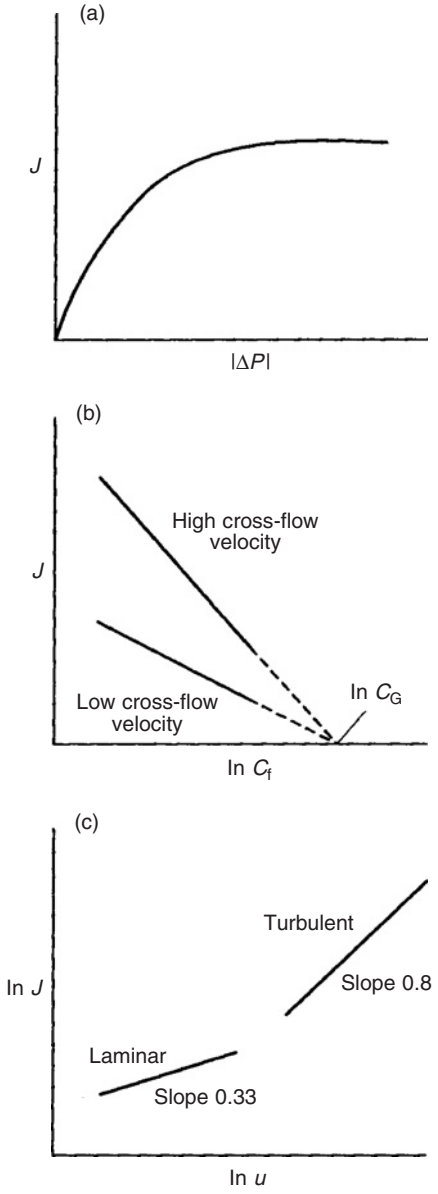

FIG. 16.15. Dependence of membrane permeation rate J on (a) applied pressure difference, (b) feed solute concentration C_f and (c) cross-flow velocity (u) for ultrafiltration.

as an industrial process for the concentration of low molecular weight solutes and especially for the desalination, or more generally demineralisation, of water.[3,4,11,15]

Typically, a membrane that rejects 93% of Na^+ or Cl^- will reject 98% of Ca^{2+} or SO_4^{2-} when rejections are measured on solutions of a single salt. With mixtures of salts in solution,

the rejection of a single ion is influenced by its relative proportion in the mixture. Thus for 0.1 kg/m^3 Cl^- in the presence of 1 kg/m^3 SO_4^{2-} there would be only 50–70% rejection compared with 93% for solutions of a single salt. The rejection of organic molecules depends on molecular weight. The molecular weights less than 100 are usually not rejected, those with molecular weights of about 150 have about the same rejection as NaCl, and those with molecular weights greater than 300 are effectively entirely rejected.

16.9 MEMBRANE MODULES

Industrial membrane plants often require hundreds of thousands of square metres of membrane to perform the separation required on a useful scale. Before a membrane separation can be used industrially, therefore, methods of economically and efficiently packaging large areas of membrane are required. These packages are called membrane modules. The areas of membrane contained in these basic modules are in the range 1–20 m^2. The modules may be connected together in series or in parallel to form a plant of the required performance. The four most common types of membrane module are tubular, spiral, wound and hollow fibre.

Despite the importance of membrane module technology, many researchers are astonishingly uninformed about module design issues. In part this is because module technology has been developed within companies, and many developments are only found in patents, which are ignored by many academics. An overview of the principal module types are given below, followed by a summary of the factors governing selection of particular types for different membrane processes. Cost is always important, but perhaps the most important issues are membrane fouling and concentration polarisation. This is particularly true for reverse osmosis and ultrafiltration systems, but concentration polarisation issues also affect the design of gas separation and pervaporation modules.[9,18]

16.9.1 Tubular Modules

Tubular modules are widely used where it is advantageous to have a turbulent flow regime; for example, in the concentration of high solids content feeds. The membrane is cast on the inside of a porous support tube which is often housed in a perforated stainless steel pipe (Figure 16.16). Individual modules contain a cluster of tubes in series held within a stainless steel permeate shroud. The tubes are generally 10–25 mm in diameter and 1–6 m in length. The feed is pumped through the tubes at Reynolds numbers greater than 10,000. Tubular modules are easily cleaned and a good deal of operating data exist for them. Their main disadvantages are the relatively low membrane surface area contained in a module of given overall dimensions and their high volumetric hold-up.

16.9.2 Flat-Sheet Modules

Flat-sheet modules are similar in some ways to conventional filter presses. An example is shown in Figure 16.17. This consists of a series of annular membrane discs of outer diameter 0.3 m placed on either side of polysulphone support plates which also provide

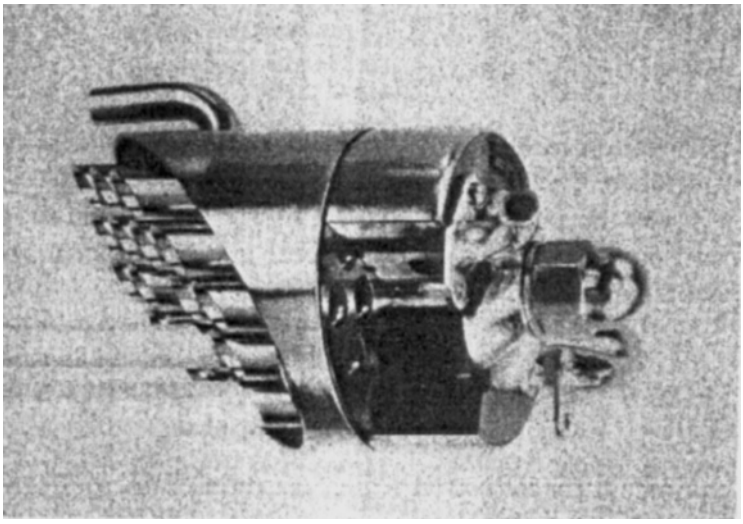

FIG. 16.16. Tubular membrane module.

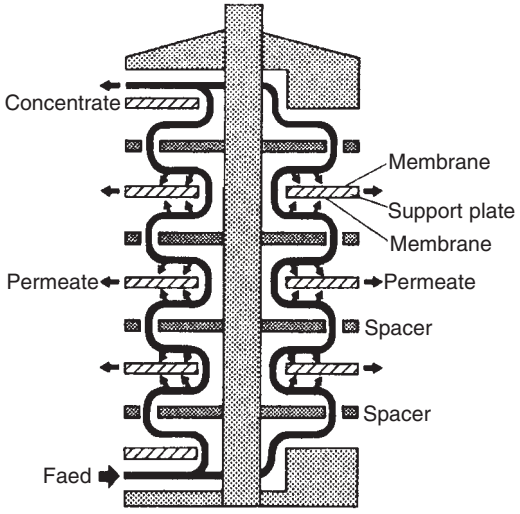

FIG. 16.17. Schematic diagram of a flat-sheet module.

channels through which permeate can be withdrawn. The sandwiches of membrane and support plate are separated from one another by spacer plates which have central and peripheral holes, through which the feed liquor is directed over the surface of the membranes, the flow is laminar. A single module contains 19 m^2 of membrane area. Permeate is

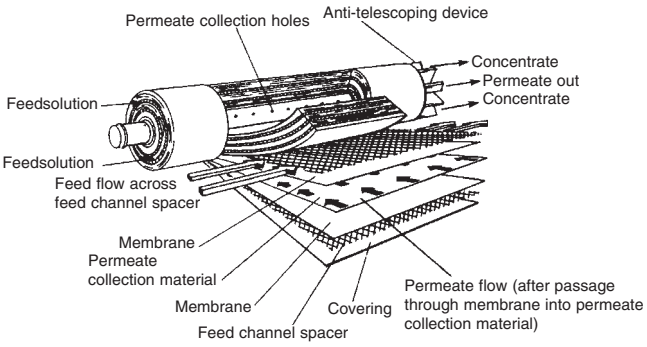

FIG. 16.18. Schematic diagram of spiral-wound module.

collected from each membrane pair so that damaged membranes can be easily identified, though replacement of membranes requires dismantling the whole stack.

16.9.3 Spiral-Wound Modules

Spiral-wound modules consist of several flat membranes separated by turbulence-promoting mesh separators and formed into a Swiss roll (Figure 16.18). The edges of the membranes are sealed to each other and to a central perforated tube. This produces a cylindrical module which can be installed within a pressure tube. The process feed enters at one end of the pressure tube and encounters a number of narrow, parallel feed channels formed between adjacent sheets of membrane. Permeate spirals roward the perforated central tube for collection. A standard size spiral-wound module has a diameter of about 0.1 m, a length of about 0.9 m and contains about 5 m^2 of membrane area. Up to six such modules may be installed in series in a single pressure tube. These modules make better use of space than tubular or flat sheet types, but they are rather prone to fouling and difficult to clean.

16.9.4 Hollow-Fibre Modules (Figure 16.19)

Hollow fibre modules consist of bundles of fine fibres, 0.1–2.0 mm in diameter, sealed in a tube. For reverse osmosis desalination applications, the feed flow is usually around the outside of the unsupported fibres with permeation radially inward, as the fibers cannot withstand high pressure differences in the opposite direction. This gives very compact units capable of high pressure operation. However, the flow channels are less than 0.1 mm wide and are therefore readily fouled yet difficult to clean. The flow is usually reversed for biotechnological applications so that the feed passes down the centre of the fibres giving better controlled laminar flow and easier cleaning. However, this limits the operating pressure to less than 0.2 MN/m^2 (MPa), that is, to microfiltration and ultrafiltration applications. A single ultrafiltration module will typically contain up to 3000 fibres and be 1 m long. Reverse osmosis modules will contain larger numbers of finer fibres. This is a very effective means of incorporating a large membrane surface area in a small volume.

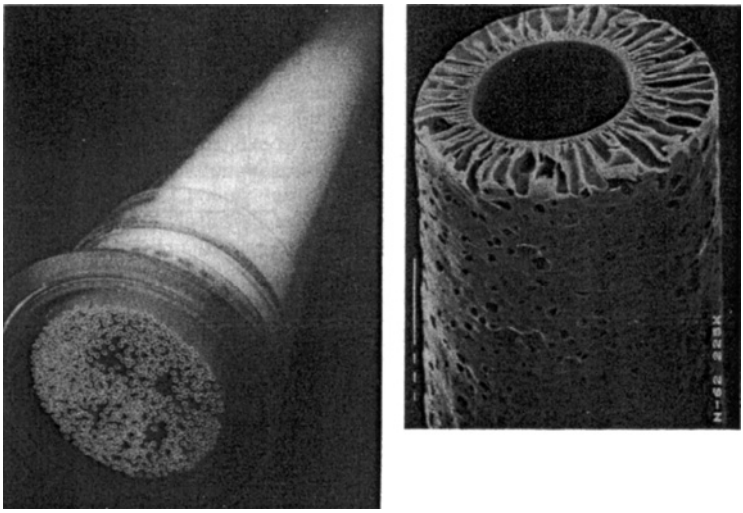

FIG. 16.19. Hollow-fibre module and, inset, a single fibre.

Membrane modules can be configured in various ways to produce a plant of the required separation capability. A simple batch recirculation system has already been described in cross-flow filtration. Such an arrangement is most suitable for small-scale batch operation, but larger scale plants will operate as 'feed and bleed' or 'continuous single pass' operation (Figure 16.20).

(a) Feed and bleed. Such a system is shown in Figure 16.20a. The start up is similar to a batch system in that the retentate is initially totally recycled. When the final required solute concentration is reached within the loop, a fraction of the loop is continuously bled off. Feed into the loop is controlled at a rate equal to the permeate plus concentrate flow rates. The main advantage is that the final connection is then continuously available as feed is pumped into the loop. The main disadvantage is that the loop is operating continuously at a concentration equivalent to the final concentration in the batch system and the flux is therefore lower than the average flux in the batch mode, with a correspondingly higher membrane area required.

Large-scale plants usually use multiple stages operated in series to overcome the low-flux disadvantage of the feed and bleed operation and yet to maintain its continuous nature (Figure 16.20b). Only the final stage is operating at the highest concentration and lowest flux, while the other stages are operating at lower concentrations with higher flux. Thus, the total membrane area is less than that required for a single stage operation. Usually a minimum of three stages is required, and seven to ten stages are quite common. The residence time, volume hold-up and tankage required are much less than for the same duty in batch operation. Feed and bleed systems also require less frequent sterilisation than batch processes in biotechnological applications, allowing longer effective operating times.

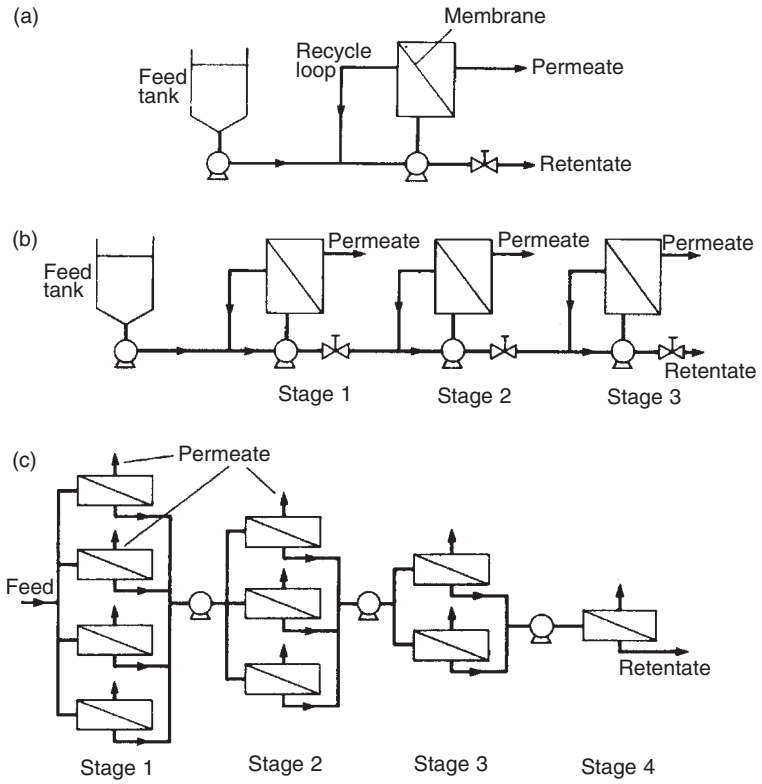

FIG. 16.20. Schematic flow diagrams of (a) single-stage 'feed and bleed', (b) multiple-stage 'feed and bleed' and (c) continuous single-pass membrane plants.

(b) Continuous single pass. In such a system the concentration of the feed stream increases gradually along the length of several stages of membrane modules arranged in series (Figure 16.20c). The feed only reaches its final concentration at the last stage. There is no recycle and the system has a low residence time. However, such systems must either be applied on a very large scale or have only a low velocities to control concentration polarisation. The smallest possible single-pass system will have a single module in the final stage, with a typical feed flow rate of about 0.1 m^3/min. Such systems are used in large-scale reverse osmosis desalination plants but are unlikely to be used in biotechnological applications.

16.10 MODULE SELECTION

The choice of the most suitable membrane module type for a particular membrane separation must balance several factors. The principal module design parameters that enter into the decision are summarised in Table 16.3.

TABLE 16.3. *Parameters for membrane module design*

Parameter	Hollow fine fibres	Capillary fibres	Spiral-wound	Plate-and-frame	Tubular
Manufacturing cost ($/m^2)	2–10	5–50	5–50	50–200	50–200
Concentration polarisation fouling control	Poor	Good	Moderate	Good	Very good
Permeate-side pressure drop	High	Moderate	Moderate	Low	Low
Suitability for high-pressure operation	Yes	No	Yes	Marginal	Marginal
Limitation to specific types of membrane material	Yes	Yes	No	No	No

Cost, always important, is difficult to quantify because the actual selling price of the same module design varies widely, depending on the application. Generally, high-pressure modules are more expensive than low-pressure or vacuum modules. Hollow fibre modules are significantly cheaper per square metre of membrane than spiral-wound or plate-and-frame modules but can only be economically produced for very-high-volume applications that justify the expense of developing and building the spinning and module fabrication equipment. An estimate of module manufacturing cost is given in Table 16.2; the selling price is typically two to five times higher.

Two other major factors determining module selection are concentration polarisation control and resistance to fouling. Concentration polarisation control is a particularly important issue in liquid separations such as reverse osmosis and ultrafiltration. Hollow-fine-fibre modules are notoriously prone to fouling and concentration polarisation and can be used in reverse osmosis applications only when extensive, costly feed solution pretreatment removes all particulates. These fibres cannot be used in ultrafiltration applications at all.

Another factor is the ease with which various membrane materials can be fabricated into a particular module design.[16,18] Almost all membranes can be formed into plate-and-frame, spiral-wound and tubular modules, but many membrane materials cannot be fabricated into hollow fine fibres or capillary fibres. Finally, the suitability of the module design for high-pressure operation and the relative magnitude of pressure drops on the feed and permeate sides of the membrane can be important factors.[4,11] The types of module generally used in some of the major membrane processes are listed in Table 16.2.

Example

An ultrafiltration plant is required to treat 50 m^3/day of protein-containing waste stream. The waste contains 0.05% by weight of protein which has to be concentrated to 2% to allow recycling to the main process stream. The tubular membranes to be used are

available as 30 m^2 modules. Pilot-plant studies show that the flux J through these membranes is given by:

$$J = 0.02 \ln\left(\frac{30}{C_f}\right)$$

where C_f is the concentration of protein in kg/m^3. However, owing to fouling the flux never exceeds 0.04 m/h.

Estimate the minimum number of membrane modules required for the operation of this process (a) as a single feed and bleed stage and (b) as two feed and bleed stages in series. Assume operation for 20 hours each day.

Solution

(a) As a single feed and bleed stage:

- Let Q_0 be the volumetric flow rate of feed, Q_2 the volumetric flow rate of concentrate, C_0 the solute concentration in the feed, C_2 the solute concentration in the concentrate, F the volumetric flow rate of membrane permeate, and A the required membrane area.
- We assume there is no loss of solute through the membrane.
- First we check the concentration (C_1) at which the flux becomes fouling-limited:

$$0.04 = 0.02 \ln\left(\frac{30}{C_1}\right) \Rightarrow C_1 \approx 4 \text{ kg/m}^3$$

That is, below this concentration the membrane flux is 0.04 m/h.

This does not pose a constraint for the single stage, as the concentration of solute (C_2) will be that of the final concentrate (20 kg/m^3).

Conservation of solute gives:

$$Q_0 C_0 = Q_2 C_2 \tag{a}$$

A fluid balance gives:

$$Q_0 = F + Q_2 \tag{b}$$

Combining these equations and substituting known values:

$$2.438 = A0.02 \ln\left(\frac{20}{30}\right) \Rightarrow A = 301 \text{ m}^2$$

Thus, 10 modules will almost meet the specification for a single-stage process.

As two feed and bleed stage in series:

In addtition to the symbols previously defined, let Q_1 be the volumetric flow rate of retentate at the intermediate point, C_1 be the concentration of solute in the retentate at this

point, F_1 and F_2 be the volumetric flow rate of membrane permeate in the first and second stages respectively, and A_1 and A_2 the required membrane area in these respective stages.

Conservation of solute now gives:

$$Q_0C_0 = Q_1C_1 = Q_2C_2 \tag{c}$$

A fluid balance on stage 1 gives:

$$Q_0 = Q_1 + F_1 \tag{d}$$

A fluid balance on stage 2 gives:

$$Q_1 = Q_2 + F_2 \tag{e}$$

Substituting given values in equations (d) and (e):

$$2.5 = \frac{1.25}{C_1} + 0.02A_1 \ln\left(\frac{30}{C_1}\right) \tag{f}$$

$$\frac{1.25}{C_1} = 0.0625 + 0.00811A_1 \tag{g}$$

The procedure now is to use trial and error to estimate the value of C_1 that gives the optimum values of A_1 and A_2.

- If $C_1 = 5\,\text{kg/m}^3$, the $A_1 = 63\,\text{m}^2$ and $A_2 = 23\,\text{m}^2$. That is, an arrangement of three modules – one module is required.
- If $C_1 = 4\,\text{kg/m}^3$, the $A_1 = 55\,\text{m}^2$ and $A_2 = 31\,\text{m}^2$. That is, an arrangement of two modules – one module is almost sufficient.
- If $C_1 = 4.5\,\text{kg/m}^3$, the $A_1 = 59\,\text{m}^2$ and $A_2 = 27\,\text{m}^2$. That is, an arrangement of two modules – one module meets the requirement. This arrangement is that requiring the minimum number of modules.

16.11 MEMBRANE FOULING

A limitation to the more widespread use of membrane separation processes is membrane fouling, as would be expected in the industrial application of such finely porous materials. Fouling results in a continuous decline in membrane permeation rate, an increased rejection of low molecular weight solutes and eventually blocking of flow channels. On start-up of a process, a reduction in membrane permeation rate to 30–10% of the pure water permeation rate after a few minutes of operation is common for ultrafiltration. Such a rapid decrease may be even more extreme for microfiltration. This is often followed by a more gradual

decrease throughout processing. Fouling is partly due to blocking or reduction in effective diameter of membrane pores, and partly due to the formation of a slowly thickening layer on the membrane surface.[16,17]

The extent of membrane fouling depends on the nature of the membrane used and on the properties of the process feed. The first means of control is therefore careful choice of membrane type. Secondly, a module design that provides suitable hydrodynamic conditions for the particular application should be chosen. Process feed pretreatment is also important. In biological applications pretreatment might include prefiltration, pasteurisation to destroy bacteria, or adjustment of pH or ionic strength to prevent protein precipitation. When membrane fouling has occurred, back-flushing of the membrane may substantially restore the permeation rate. However, this is seldom totally effective so that chemical cleaning is eventually required. This involves interruption of the separation process, and possibly quite substantial time losses due to the extensive nature of cleaning required. Thus, a typical cleaning procedure would involve: flushing with filtered water at 35–50 °C to displace residual retentate; recirculation or back-flushing with cleaning agent, possibly at elevated temperature; and rinsing with water to remove sterilising solution. More recent approaches to the control of membrane fouling include the use of more sophisticated hydrodynamic control affected by pulsated feed flows or non-planar membrane surfaces, and the application of further perturbations at the membrane surface such as continuous or pulsated electric fields.

16.12 NOMENCLATURE

C_f	Concentration of solute in feed stream, $mg \cdot l^{-1}$
C_p	Concentration of solute in permeate, $mg \cdot l^{-1}$
C	Solute concentration, $mg \cdot l^{-1}$
J	Membrane permeation rate, $mg \cdot l^{-1} \cdot h^{-1}$
ΔP	Pressure difference applied across the membrane
$\Delta \Pi$	Difference in osmotic pressure across the membrane
R_m	Resistance of the membrane
R_c	Resistance of layers deposited on the membrane
R'_f	Resistance of the film layer
R_c	Resistance of the cake
e	Void volume of the cake
d_s	Mean particle diameter
r	Specific resistance of the deposit
V	Total volume filtered
V_s	Volume of particles deposited
C_b	Bulk concentration of particles in the feed
A_m	Membrane area
R_{sd}	Resistance of all particles deposition
R_{sr}	Resistance removed by cross-flow
J_{ss}	Flux obtained experimentally or from the film-model
β	Fraction of filtered particles remained in the filter cake

REFERENCES

1. Coulson, J.M. and Richardson, J.F., "Chemical Engineering", vol. 2, 5th edn. Butterworth-Heinemann, 2002.
2. Strathmann, H., *J. Membr. Sci*. **9**, 121 (1981).
3. Lonsdale, H.K., *J. Membr. Sci*. **10**, 81 (1982).
4. Backer, R.W., "Membrane Technology and Applications", McGraw-Hill, 2000.
5. Rautenbach, R. and Albrecht, R., "Membrane Processes", John Wiley, Chichester, 1989.
6. Mulder, M., "Basic Principles of Membrane Technology", 2nd edn. Kluwer Academic Publishers, 2000.
7. Larcy, R.E., "Hanion Techniques for Chemical Engineers" (P.A. Schweitzer, ed.), 2nd edn. McGraw-Hill, New York, 1988.
8. Belfort, G., *In* "Advanced Biochemical Engineering" (H.R. Bungay and G. Belfort eds). John Wiley, New York, 1987.
9. Frankenfeild, J.W. and Li, N.N., *In* "Handbook of Separation Technology" (R.W. Rousseau ed.). Wiley, New York, 1987.
10. Bowen, W.R., Hilal, N., Lovitt, R.W. and Williams, P.M., *J. Membr. Sci*. **110**, 233 (1996).
11. Bowen, W.R., Hilal, N., Lovitt, R.W. and Williams, P.M., *J. Membr. Sci.* **110**, 229 (1996).
12. Bowen, W.R., Hilal, N., Lovitt, R.W. and Williams, P.M., *Colloid Interface Sci.* **180**, 350 (1996).
13. Bowen, W.R., Mohammed, A.W. and Hilal, N., *J. Membr. Sci.* **126**, 91 (1997).
14. Hilal, N., Bowen, R.W., Lovitt, R.W. and Wright, C.J., *J. Engng Life Sci.* **2** (5), 131 (2002).
15. Hilal, N., Al-Zoubi, H., Darwish, N.A., Mohammed, A.W. and Abu Arabi, M., *Desalination* **170**, 281 (2004).
16. Hilal, N., Ogunbiyi, O., Miles, N.J. and Nigmatullin, R., *Separation Sci. Technol.* **40**, 1957 (2005).
17. Bowen, W.R., Hilal, N., Lovitt, R.W. and Wright, C.J., *In* "Surface Chemistry and Electrochemistry of Membrane Surfaces", vol. 79, (T.S. Sørensen, ed.). Surfactant Science Series, Marcel Dekker, USA, 1999.
18. Bowen, W.R., Hilal, N., Jain, M., Lovitt, R.W., Mohammad, A.W., Sharif, A.O., Williams, P.M. and Wright, C.J., *In* "Comprehensive Chemical Kinetics", vol. 37, "Application of Kinetic Modelling" (R.G. Compton and G. Hancock, eds). Elsevier Science B.V., 1999.

16.13 CASE STUDY: INORGANIC ZIRCONIA γ-ALUMINA-COATED MEMBRANE ON CERAMIC SUPPORT

Abstract

Sol–gel is one of the most useful techniques for preparation of inorganic membranes with fine pores in the nanometer range (1–5 nm). The sol is a stable suspension of colloidal solid particles within soft uniform solution. The gel was obtained by hydrolysis with open reflux in 24 hours at 85–90 °C. The advantage of sol–gel technology is the ability to produce

---

This case study was contributed by:
Nidal Hilal,[1] Ghasem Najafpour,[2] Abdul Latif Ahmad[3]
[1]Reader in Chemical Engineering, Director of Centre for Clean Water Technologies, University of Nottingham, Deputy Director of Research/School of Chemical, Environmental and Mining Engineering, University Park, Nottingham, NG7 2NR, United Kingdom.
[2]Biochemical Engineering, Program Chairman of Biotechnology, Faculty of Chemical Engineering, Noshirvani Institute of Technology, University of Mazandaran, Babol, Iran.
[3]Membrane Technology, School of Chemical Engineering, Engineering Campus, Universiti Sains Malaysia, Seri Ampangan, 14300 Nibong Tebal, S.P.S., Pulau Pinang, Malaysia.

highly pure γ-alumina and zirconia membranes at medium temperatures of about 700 °C with uniform pore size distribution in a thin film. However, the major disadvantage of this process is that the membrane is sensitive to heat treatment, resulting in cracking on the film layer. Successful crack-free products were produced, but they needed special care and time for suitable heat curing. Only γ-alumina membranes have the disadvantage of poor chemical and thermal stability. There was no opportunity to carry heat treatment at very high temperatures above 700 °C, where at 900 °C it was expected the transformation of γ-aluminium from γ→θ→α-alumina may take place. Successful coating on supported membrane products was obtained using ZrO_2. Suitable supported and unsupported zirconia alumina membranes were developed and fabricated using the sol–gel technique. More than 100 samples of successful and unsuccessful membranes for demonstration were fabricated. The successful results are presented and discussed. In this project, the porous ceramic supports and the metal-oxide-coated membranes were fabricated in the research laboratory at the Universiti Sains Malaysia.

16.13.1 Introduction

Membrane separations represent a new type of unit operation, which, ultimately, is expected to be replaced by significant proportions of conventional separation processes. The advantage of membrane separation lies in its relatively low energy requirements. The reason for low energy consumption is that, unlike conventional processes such as distillation, extraction and crystallisation, it generally does not feature phase transition. The rapid development of membranes in wastewater treatment encourages the development and fabrication of an inorganic membrane. The results expand knowledge and produce various types of ceramic membrane.[1]

The ceramic membrane has a great potential and market. It represents a distinct class of inorganic membrane. In particular, metallic coated membranes have many industrial applications. The potential of ceramic membranes in separation, filtration and catalytic reactions has favoured research on synthesis, characterisation and property improvement of inorganic membranes because of their unique features compared with other types of membrane. Much attention has focused on inorganic membranes, which are superior to organic ones in thermal, chemical and mechanical stability and resistance to microbial degradation.

Alumina membranes have recently received considerable attention for their use in a wide range of applications. Alumina is the most cost effective and widely used material in the family of engineering ceramics. The raw materials from which this high-performance technical grade ceramic is made are readily available and reasonably priced, resulting in good value for the cost in fabricated alumina shapes, with an excellent combination of properties and an attractive price. For commercial membrane applications, α-Al_2O_3 and γ-Al_2O_3 are the most common membranes. α-Al_2O_3 membranes are well known for their thermal and hydrothermal stabilities beyond 1000 °C.

An inorganic membrane can be prepared by various methods such as sol–gel, phase separation and leaching.[2,3] The sol–gel process is considered the most practical method among those used to prepare inorganic membrane. Sol–gel processing is a simple technology in principle but requires considerable effort to become of practical use. The advantage of this

technology is the ability to produce high-purity γ-alumina membranes at low temperatures (400–600 °C). The pore size distribution is very narrow and additional elements can be added.[4,5] However, only γ-alumina membranes have the disadvantage of a poor chemical and thermal stability. Below pH 4, they dissolve to form Al^{3+} ions; above pH 12, the membrane will form $Al(OH)^{-}_{4}$. γ-Al_2O_3 has a highly detective spinal structure and can be considered as an AlO_xH_y species, which dissolves more slowly, in low and high pH of the aqueous phase as strong hydroxides behave.

Meanwhile, at higher temperatures (600–900 °C), pore growth occurs. Above 850 °C, the transformation of γ-alumina upon heating: γ→θ→α-alumina. The stable α-Al_2O_3 phase forms above 1000 °C by nucleation and growth.[6] In the transition of alumina derived from boehmite gels, the pores are as large as the grains. These pores are unable to stop grain boundary migration when α-Al_2O_3 forms above 1100 °C. Hao *et al.*[7] stated that the phase transformation from γ-Al_2O_3 to θ-Al_2O_3 occurred at 900 °C for pure alumina membranes. With further heat treatment, 1200 °C and higher, a complete transformation of the θ-Al_2O_3 to the high temperature α-Al_2O_3 phase is observed.

Foreign additives can affect the phase transformation as well as the pore structure at high temperatures. To inhibit dissolution of alumina species or pore growth, the particles are coated with an inert component such as zirconia, titania and lanthana.[1] It has been reported that the effect of zirconia addition in alumina retarded the grain growth behaviour of the alumina membrane. It was found that the ZrO_2 prevents abnormal growth of Al_2O_3 during heat treatment.[1,3] The effect of zirconia on the phase transformation could be explained by

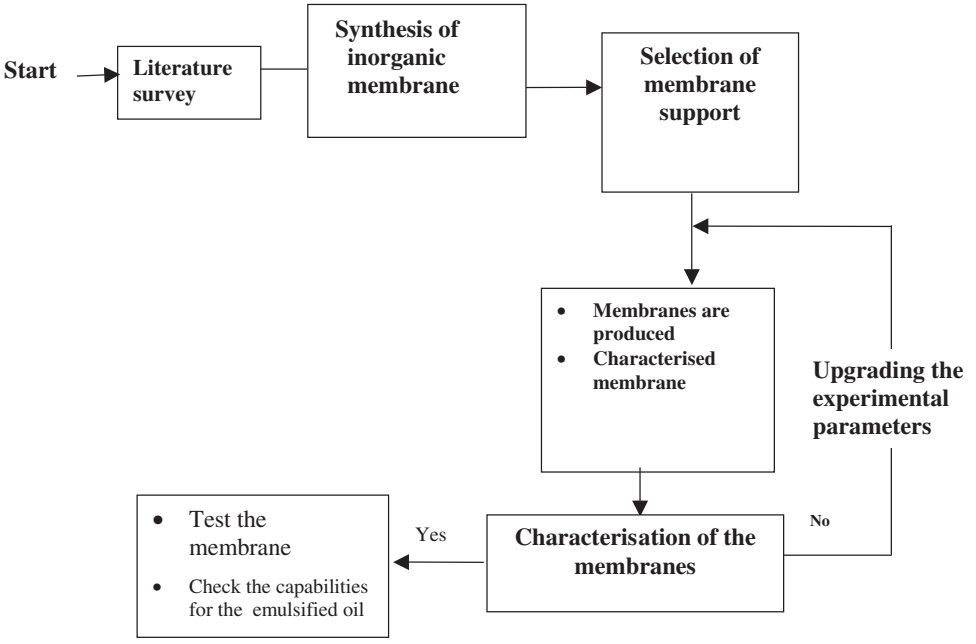

FIG. 16.21. Overall scheme and stages involved for fabrication of inorganic membrane.

the fact the presence of the zirconia on the γ-alumina surface may reduce the possibility of the nucleation of α-alumina, thus raising the phase transformation temperature.

In this case study, a zirconia–alumina membrane has been developed using the sol–gel technique with and without support.[6,7] The porous ceramic was prepared to fabricate the membrane support. A thin film of aluminum and zirconium were formed on the porous ceramic support. Unsupported membrane was also prepared. The unsupported membrane was not strong enough to hold a high-pressure gradient; it was very fragile and not useful

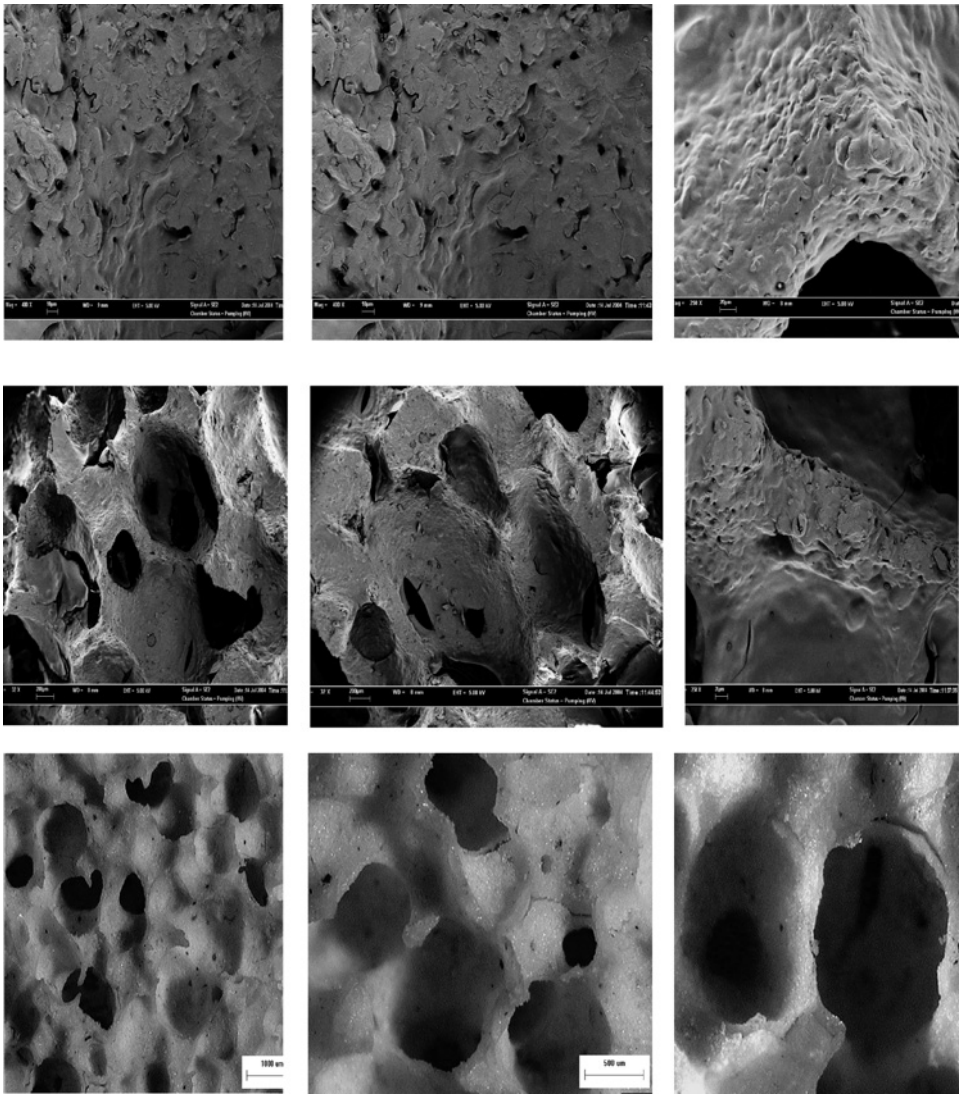

FIG. 16.22. Non-uniform porous media of the ceramic membrane support.

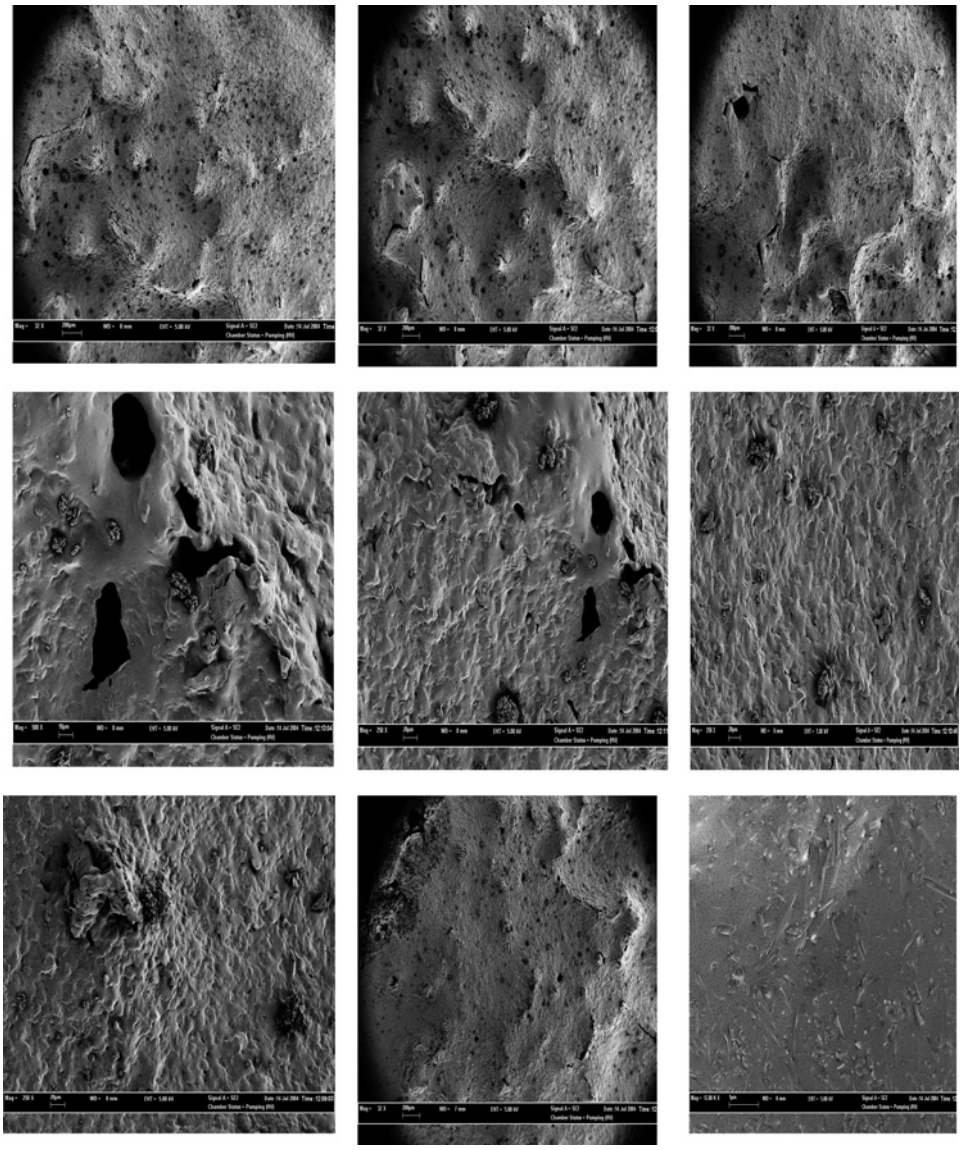

FIG. 16.23. Alumina coated on the ceramic membrane.

for independent use. The supported membrane on a highly porous ceramic was quite strong, but the coating covered the solid surface. The ceramic support was strong enough to hold any mechanical forces. Apart from the ceramic support, poly-vinyl alcohol (PVA) was prepared to be used as a binder in the preparation of zirconia-alumina membranes to avoid the formation of cracks on the membrane surface. The overall process in the fabrication of membranes

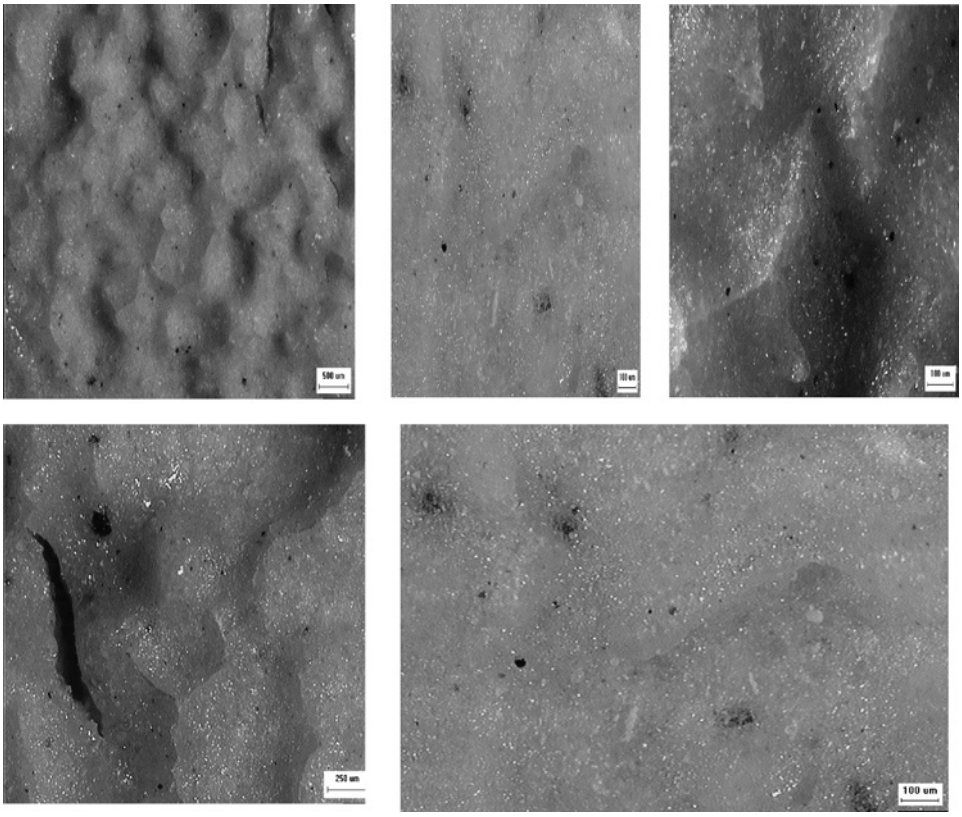

FIG. 16.24. Zirconia coated on the ceramic membrane.

is shown in Figure 16.21. The uniform coating and crack-free membranes were examined by scanning electron microscopy (SEM) and light microscop (LM) photographs shown in Figures 16.22–16.25. The main part of the research activities was the preparation and development of an inorganic membrane with and without support (zirconia-coated on γ-alumina). The membrane surface was characterised by SEM and LM.

In preparing the membrane, a clear sol was obtained by the addition of acid into the aluminum sec-butoxide sol to peptise the sol and obtain a stable colloid solution. Aluminum monohydroxides formed by the hydrolysis of aluminum alkoxides, which are peptisable to a clear sol. Peptisation was performed by the addition of acid and heat treatment for a sufficient time. It was found that stable sols cannot be obtained when the concentration of the peptisation acid is too low. The critical range for inorganic acids such as nitric, hydrochloric and perchloric acids is 0.03–0.1 mole/mole of hydroxide. In this study, nitric acid was used as the peptising agent. The resulting sols are poured into Petri dishes and dried in an oven at a controlled drying rate to obtain a gel layer. The molar ratio of zirconia salt

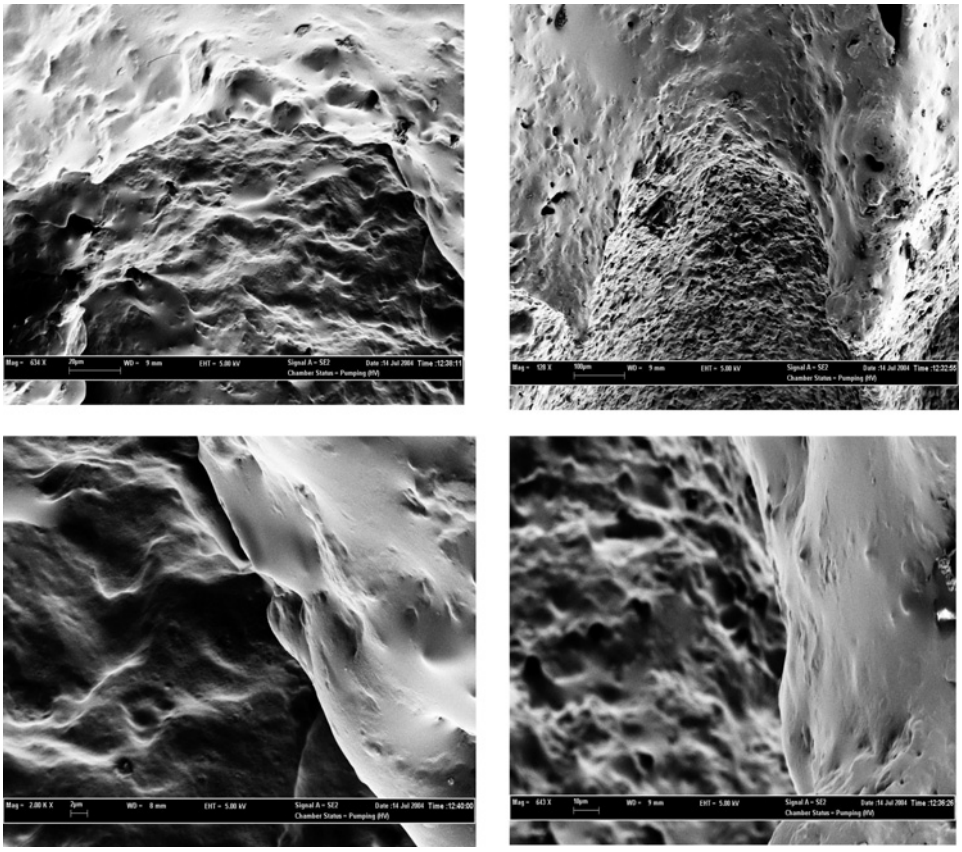

FIG. 16.25. Mixture of zirconia and alumina coated on the ceramic membrane.

to alumina was a controlling variable in obtaining crack-free zirconia-coated γ-alumina membranes.[10,11] Finally, the dried gel is sintered and heat treated at 500 °C for 3 hours.

Support materials were prepared by blending the fine power as stated in the later part of this case study. PVA was used as the binder. The organic macromolecule was used to create sufficient pores in the material when burned out after a solid strong support was formed. Drying was performed in a high-temperature furnace. The shape and thickness of the support were based on the mass of the material and the way it was moulded.

Once the membrane was successfully produced, it was analysed for characterisation and scanning. The sol–gel technique was successfully used to obtain a crack-free unsupported membrane, which was expected to have pore size of 1–2 nm. The development of the crack-free membrane may not have the same strength without strong, solid support. The next stage of this work was to characterise the fabricated membrane. The objectives of this study were to develop a zirconia-coated γ-alumina membrane with inorganic porous support by the sol–gel method and to characterise the surface morphology of the membrane and ceramic support.

16.13.2 Materials and Methods

The fabricated membrane consists of inorganic ceramic material with a fine coating. The support materials were prepared by tape casting or slip casting.[6] Slips were prepared by dispersing the alumina powder in water with the dispersing agent. The slips were homogenized by ball milling for 12–18 h or by ultrasonification for 20 min. The starch was added during vigorous stirring. The addition of starch to the slip created pores[10] in the material when burned out after forming. Then the binder was added while gently stirring the suspension. PVA has been used for a long time as the organic binder of choice in many ceramics applications. The high binding strength, ease of plasticisation, water solubility and cost effectiveness of this polymer have made it a reliable performer.[10] Drying was provided by application of heat from underneath the tape and by a controlled passage of air over the surface of the tape. Square supports were cut from the tapes and several tapes laminated together in a press at 60 MPa at room temperature to build up the desired thickness of about 1 mm.

Finally, to evaluate the membranes, analysis such as X-ray diffraction (XRD), SEM, TEM and light scattering were performed at the School of Mineral and Material Engineering, Universiti Sains Malaysia. The last part of the work, testing the produced membrane to remove emulsifier oil from domestic wastewater, was accomplished on a limited budget. An experimental rig and membrane module were required. Also the need for experimental data for the application of the supported membrane may show the real success of this project.

16.13.2.1 Preparation of PVA Solution

PVA was used as a temporary binder owing to its water solubility, excellent binding strength and clean burning characteristics. To prepare the PVA solution, 4 g of PVA were added to 100 ml distillated water. The mixture was heated and stirred vigorously until all the PVA was dissolved in the water. This took about half an hour. Peptisation was done by addition of 5 ml 1M HNO_3 to the solution. Finally, the solution was refluxed for 4 hours. The PVA solution was used in the preparation of the zirconia-alumina sol–gel solution. The preparation of the PVA solution can be summarised as follows:

(i) 4 g PVA were added into a 250 ml beaker;
(ii) 100 ml of double distilled water was stirred vigorously until all the PVA was dissolved;
(iii) The solution was boiled until all the PVA was dissolved. This step took at least 0.5–1 h;
(iv) 5 ml of 1M HNO_3 was added into the solution;
(v) the solution was reflexed for 4 h.

16.13.2.2 Preparation of Zirconia-Coated Alumina Membrane

The supported and unsupported membranes were produced by a sol–gel dipping technique. The sol–gel solution was made by using aluminium tri-sec-butoxide and zirconium (IV) oxide. Compared with the pure alumina membrane, the zirconia-coated alumina membrane had high chemical resistances, which allowed steam sterilisation and cleaning procedures in the pH range of 0–14. It possessed good pure-heating permeability and high membrane flux in separation and filtration. It had high thermal stability, which was an attractive criterion

for catalytic membrane reactors used at high temperatures. The molar ratio of Al^{3+}:H^+:Zr:H_2O was 1:0.07:0.15:100, whereas the volumetric ratio on the basis of 100 ml of H_2O is Al^{3+}:H^+:Zr:H_2O = 1:3.88 ml:1.0275 g:100 ml. The 100 ml of double-distilled water was heated on a hot plate between 80 and 85 °C to ensure the formation of γ-AlOOH. Aluminium tri-sec-butoxide (14.25 ml) was added to the double-distillated water. The solution was vigorously stirred with a magnetic stirrer until a homogeneous mixture was obtained. HNO_3 (1M) (3.88 ml) was added to the sol for peptisation, and the mixture was again stirred for an additional 15 minutes. After that, 1.0275 g of ZrO_3 was added into the mixture. The sol was kept at boiling condition in the open flask for 1 h. The PVA solution was added to the mixture according to a PVA: sol ratio of 1:20, and stirred in the mixture continuously. The product was refluxed under continuous stirring at 90 °C for 16–20 h to ensure complete mixing and hydrolysis. The sol was cooled down slowly and left for a few hours. The above steps were repeated with different amounts of ZrO_3. The sol was dried under ambient conditions until gelation and viscous gel was obtained. The sol was transferred to the support by the dip-coating method to prepare a thin layer of gel on the support. The membrane thickness firstly increased linearly with the dipping time, until it may reach a limit. It was noted that a thicker and non-uniform gel layer was more liable to crack than a thinner one. A uniform gel layer was obtained by heating and calcination. After dip coating the sol on the surface of the support, the membrane was heated in the furnace. The furnace temperature started at 30 °C and was raised to 300 °C at a rate of 0.5 °C/min. The furnace temperature was kept at 300 °C for 0.5 h for relaxation of the gel and to avoid the stress exceeding the elastic strength of the gel. The temperature was raised from 300 °C to 700 °C at a rate of 0.5 °C/min. Sintering of the inorganic membrane was done at 700 °C for 5 h. Cooling was conducted at a rate of 1 °C/min, to ambient temperature, 30 °C.

16.13.2.3 Preparation of Porous Ceramic Support

The preparation of porous ceramic support is summarised in the following sections.

16.13.2.3.1 Raw material

(i) Feldspar potash
(ii) Ball clay
(iii) Kaolin
(iv) Silica power
(v) Sodium hexametaphosphate flake
(vi) Distilled water
(vii) PVA 3% solution

16.13.2.3.2 Preparation of the PVA solution

(i) 7.5 g of PVA was gradually added to 250 ml to double-deionised water at ambient temperature.
(ii) Stir the solution until all the PVA distributed equally.
(iii) Boil the solution until all PVA is dissolved and stir the solution carefully. The step should take at least 40 minutes.

(iv) After that, 10 ml of 1M HNO_3 is added to the solution.
(v) Reflux the solution for 4 hours.

16.13.2.3.3 Sieve all the feldspar potash, ball clay, kaolin and silica powder by mesh, size 90 μm.

16.13.2.3.4 All the powders were mixed according to mass ratio given below:

(i) 25% feldspar potash
(ii) 25% ball clay
(iii) 25% kaolin
(iv) 25% silica powder

16.13.2.3.5 Mix 20 g of mixed powder and 25 ml PVA solution to form the concentrated slurry support. A different composition of mixed powder and PVA solution was used.

16.13.2.3.6 Dip the sponge in the mixture. After that put the sponge inside the furnace with the starting temperature at 30 °C, raise the temperature at 1 °C/min up to 1200 °C. Maintain the temperature for 2 h. After heating, decrease the furnace temperature by 1 °C/min back to 30 °C.

Some experience is needed to perform the last step efficiently. From our previous work, the strength of the ceramic support will increase with a decrease in the amount of dispersion solution.

The advantage of sol–gel technology is the ability to produce a highly pure γ-alumina and zirconia membrane at medium temperatures, about 700 °C, with a uniform pore size distribution in a thin film. However, the membrane is sensitive to heat treatment, resulting in cracking on the film layer. A successful crack-free product was produced, but it needed special care and time for suitable heat curing. Only γ-alumina membrane have the disadvantage of poor chemical and thermal stability.

16.13.3 Results and Discussion

The vast increase in the application of membranes has expanded our knowledge of fabrication of various types of membrane, such as organic and inorganic membranes. The inorganic membrane is frequently called a ceramic membrane. To fulfil the need of the market, ceramic membranes represent a distinct class of inorganic membrane. There are a few important parameters involved in ceramic membrane materials, in terms of porous structure, chemical composition and shape of the filter in use. In this research, zirconia-coated γ-alumina membranes have been developed using the sol–gel technique.

Finally, analytical equipment was used for characterisation, such as XRD, SEM, TEM, LM and light scattering. These were available either in the School of Chemical Engineering or other departments and research centres in the Universiti Sains Malaysia. However, owing to limited access to the high-end analytical equipment to analyse the membrane, the surface morphology of the membrane and the porous ceramic support was only characterised with SEM and LM.

More than 50 samples of successful and unsuccessful membranes for demonstration were fabricated. The successful results are discussed and presented in Figures 16.22–16.25. The porous ceramic supports were fabricated in our research lab.

Figure 16.22 shows SEM micrographs for the porous media of ceramic support at different magnifications. The non-uniformity resulted from the synthetic foam used as a base to absorb the ceramic solution before vaporising any water from the inorganic mixture. Uniform porous media as a solid support for the membrane was obtained.

Figure 16.23 presents the alumina-coated ceramic membrane. There were opportunities to fabricate a crack-free ceramic membrane coated with γ-alumina. The supported zirconia-alumina membrane on the ceramic support shows an irregular surface. The non-uniform surface of ceramic support causes the irregular surface on the top layer of the membrane. Some of the membrane sol was trapped in the porous ceramic support during coating, and caused the irregularity of the membrane surface.

The zirconia membrane was obtained in a unique manner. Figure 16.24 shows light micrographs of the zirconia-alumina membrane coated on the ceramic support. The non-unifomity and crater-filled surface of the ceramic support was covered by the zirconia-alumina membrane layer. Zirconia was mounted by very thin or nano-layers on the ceramic membrane.

A combination of alumina and zirconia was used as a strong nano-film on the ceramic membrane. SEM micrographs are shown in Figure 16.25. Observation by SEM shows that the zirconia–alumina membrane layer was properly adhered and could stand on the top of the porous ceramic support.

16.13.4 Conclusion

We have successfully developed a new inorganic ceramic membrane coated with zirconium and alumina. A thin film of alumina and zirconia unsupported membrane was also fabricated. The successful method developed was the sol–gel technique.

16.13.5 Acknowledgements

The present research was made possible through an IRPA grant No. 703574, through Universiti Sains Malaysia (USM). We thank USM's Research Creativity and Management Office (RCMO) and the School of Chemical Engineering, Universiti Sains Malaysia, for their support.

REFERENCES

1. Anderson, M.A., Gielselmann, M.J. and Xu, Quinyin, *J. Membr. Sci.* **39**, 243 (1988).
2. Annika, K. and Elis, C., *J. Europ. Ceram. Soc.* **17**, 289 (1997).
3. Moreno, R., *Am. Ceram. Soc. Bull.* **71**, 1647 (1992).
4. Gamze, G.A., Zulal, M. and Volcan, G., *Ceram. Int.* **22**, 23 (1996).
5. Gu, Y.F. and Meng, G.Y., *J. Europ. Ceram. Soc.* **19**, 1961 (1999).

6. Brinker, C.J. and Schere, G.W., The Physics and Chemistry of Sol-Gel Processing. Academic Press, Amesterdam, 1990.
7. Hao, W., Pan, F., Wang, T. and Zheng, S., *J. Mat. Sci*. (Shanyang, china) **20**, 472–474 (2004).
8. Huang, X.R., Meng, G.L., Hunag, Z.T. and Geng, J.E., *J. Membr. Sci.* **133**, 145 (1997).
9. Karin, L. and Eva, L., *J. Europ. Ceram. Soc.*, **17**, 359 (1997).
10. Lambert, C.K. and Gonzalez, R.D., *Mat. Lett.* **38**, 145 (1999).
11. Leenars, A.F.M., Keizer K. and Burggraaf, A.J., *J. Mat. Sci.* **19**, 1077 (1984).
12. Larbot, A., Fabre, J.P. Guizard, C. and Cot, L., *J. Membr. Sci.* **39**, 203 (1988).
13. Pierre A.C., *J. Am. Ceram. Soc.* **70** 28 (1987).
14. Yoldas, B.E., *Ceram. Bull.* **54**, 289 (1975).

CHAPTER 17

Advanced Downstream Processing in Biotechnology

17.1 INTRODUCTION

In recent decades, advances in biotechnology have increased the potential usage of biologically based products. The emergence of new and promising research activities in molecular biology and immunology is promoting a continuous increase in the number of proteins that need to be purified and characterised. A wide variety of proteins are used as diagnostic reagents such as vaccines, monoclonal antibodies, enzymes and regulatory factors. The development of simplified and cost-effective bioseparation schemes to purify these products in a highly purified form is a constant major challenge for the continued success and commercialisation of biotechnological industries. The series of separation processes used for the purification of bio-based products can be collectively described by the general term 'downstream processing'.[1,2] The objective is to establish a sequence of operations that will transform the starting material to a state defined by the specification and end use of the desired product. Individual steps should be based on molecular-based knowledge of how individual proteins will behave during purification, to appropriately establish an efficient and economic process. Technologies applicable in such bioprocesses must also accommodate particulate-containing feedstock such as microbial fermentation broths, animal or plant cell cultures and cell disruptive. It is important that the recovery in these processes is done rapidly to maintain the native conformation and activity of highly sensitive protein molecules.[3] Therefore, the main objectives for the biochemical engineer must encompass the design of an optimal process that: (i) provides the desired quality of final product; (ii) minimises the total process time and cost through improved operational efficiency; and (iii) falls within the constraints of acceptable market entry.

This chapter was contributed by:
Mohsen Jahanshahi and Ghasem Najafpour
Faculty of Chemical Engineering, Noshirvani Institute of Technology, University of Mazandaran (UMZ), P.O. Box: 484, Babol, Iran.

17.2 PROTEIN PRODUCTS

Advances in biotechnology have enabled the development and use of protein products as pharmaceutical reagents as well as in applications in industrial and domestic spheres.[4] The domestic market represented by the food and beverage industries requires protein products of low value, but with a high volume demand where purity of the protein is a lesser consideration when compared with cost.[5] This is in contrast to those protein products with high value in the market such as therapeutic enzymes, where high purity is essential.[6] Proteins commonly exhibit narrow stability ranges, outside of which denaturation occurs. In addition, degradative enzymes such as proteases and lipases can make small alterations to the protein structure, which may lead to substantial changes in their activity and antigenic properties.

A generalised sequence of the discrete unit operations involved in standard downstream processing is depicted in Figure 17.1. In the case of an intracellular product, cell disruption is the first step in the sequence after harvesting the cells (for example by centrifugation). Here, the cell boundary is permeablised, punctured or disintegrated to release the product into the surrounding medium. The cell disruption step is unnecessary in the case of extracellular products, since the products are synthesised within the cells and subsequently excreted naturally into the broth. Each individual technique employed in the purification of proteins

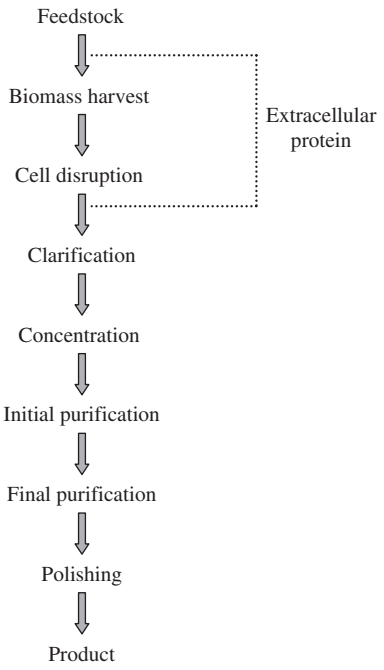

FIG. 17.1. Conventional downstream processing scheme for the purification of proteins.

has its own advantages and disadvantages. However, a diverse combination of separation steps is commonly required based on the various physical and chemical characteristics of the proteins.

Figure 17.1 shows a typical conventional approach adopted for purification of intracellular and extracellular proteins.

17.3 CELL DISRUPTION

Cell disruption is an essential initial preparative step for the purification of intracellular protein products. Different methods of cell disruption have been reviewed by several researchers[7] particularly focusing on large-scale operations.[8] Different methods of cell disruption that are currently available can be conveniently divided into two main groups: (i) mechanical; and (ii) non-mechanical. Complete destruction of the cell wall in a non-specific manner is usually achieved by mechanical means exploiting solid-shear (bead mill) and liquid-shear forces (high-pressure homogeniser or micro-fluidiser). Non-mechanical methods are judged to be more benign and often only perforate or permeabilise cells rather than tearing them apart. For example, chemical and enzymatic methods rely on selective interaction of a substance, or an enzyme, respectively with components of the cell wall or the membrane which modify the cell boundary and allow product to seep out. However, such treatment at a large scale may be costly and the waste disposal of process additives may also cause problems. As a result, mechanical methods such as high-pressure homogenisers (HPHs) or bead mills are preferred for large-scale applications.[9] Homogenisation involves the single or multiple passing of a cell suspension at a constant flow rate through an adjustable, restricted orifice discharge valve. As the cells are forced at high pressure through the orifice they are subjected to a combination of cavitation and liquid shear where operating pressure, cell concentration and temperature are influential upon disruption efficiency.[10,11]

Mechanical cell disruption in a bead mill has many attractive process characteristics including high disruption efficiency in single-pass operations, high throughput and biomass loading, good temperature control and commercially available equipment applicable from laboratory to industrial scale.[12] In addition, the single-pass and continuous operating characteristics of the bead mill has recommended it as the ideal feedstock generator for immediate and direct sequestration of released products in a fluidised bed.[13,14] Bead mills consist of a mostly horizontally positioned, closed grinding chamber. Upon a motor-driven agitator shaft, different impellers can be employed in the form of discs, rings or pins (Figure 17.2). These can be mounted concentrically or eccentrically and impart kinetic energy from the rotating parts to the grinding elements which are suspended in the cell suspension. Cells are disrupted by shear forces generated by the radial acceleration of these elements (typically ballotini glass or zirconia beads) as well as by bead collisions. Virtually all of the energy input is dissipated as heat, necessitating an efficient cooling of the chamber, which is achieved by a cooling jacket. The rate of disruption is dependent on several operational parameters such as agitator speed, suspension throughput, bead size, bead loading and cell concentration. Many of these parameters have been exhaustively studied using different types and sizes of horizontal bead mill.[8]

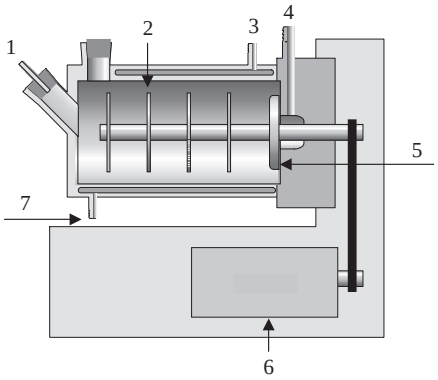

FIG. 17.2. Sketch of the Dyno Mill KDL-I. 1. Cell suspension inlet; 2. agitator disks; 3. coolant 4. disruptate outlet; 5. gap separator; 6. motor; 7. Coolant.

17.4 PROTEIN PURIFICATION

17.4.1 Overview of the Strategies

The initial stages of protein purification stages can be done by exploiting a variety of techniques such as membrane separation, aqueous two-phase partition and batch adsorption.[15] Membrane separation covers a wide range of fundamentally different processes from microfiltration through to electrodialysis.[16] The common features of these processes include separation occurring between two fluids that are separated by an interphase constituted by a membrane. This allows the selective transport of components of the two phases and thus some materials to pass through while others may be retained. Aqueous two-phase partition is a method used for protein separation based on the partition of proteins between two water-rich phases, which are obtained by dissolving two hydrophilic polymers in water or one polymer and salt above a defined concentration.[17] Batch adsorption is performed by contacting adsorbent particles with biological feedstocks in stirred tanks.[18] After product capture, the adsorbent is separated from the broth by decantation washing and thereupon the product is eluted. Batch adsorption is a process which is characterised by a single equilibrium stage and thus lacks high resolution compared with classical process chromatography. In addition, the problem of separating the protein-loaded adsorbent from the biomass has to be solved.

Primary and final protein purification steps are commonly done by liquid chromatography to achieve further purification of the desired proteins.[19] These techniques have been developed to separate protein products from each other by exploiting their difference with respect to molecular characteristics.[4] Ion exchange and hydrophobic interaction chromatography is most commonly applied in downstream processing for primary capture of protein products. The proteins are separated by ion exchange chromatography based upon the reversible adsorption of charged groups of the adsorbent phase. In contrast, the basis for hydrophobic chromatography is the interaction between hydrophobic domains of protein

and the hydrophobic groups of the adsorbent phase. The principal application of affinity chromatography, which facilitates the selective adsorption of target proteins to biological specific ligands (for example protein A and antibodies) immoblised on and within the adsorbent phase, makes it well suited for the final stages of purification of protein products.[20] However, recent developments[21] have suggested that the adoption of this high-resolution chromatography system in the earlier stage of downstream processing can facilitate the overall recovery performance (for example reduce working and processing time). The robust and inexpensive synthetic ligands (for example triazine dyes) are well suited to such applications (see the following section).

17.4.2 Dye-Ligand Pseudo-Affinity Adsorption

Historically, chlorotriazine dyes such as Cibacron Blue 3GA, Procion Red H-E7B, Procion Green H-4G and Yellow H-E3G were designed as cheap chemicals for use in the textile and printing industries. The chlorotriazine dyes are known to show affinities for several classes of proteins such as dehydrogenase, phosphatransferases and plasma proteins by virtue of an approximate mimic of the structure of various cofactor nicotinamide adenine dinucleotide (NAD) and flavin adenine dinucleotide (FAD).[22] As a result, the chlorotriazine dyes have been widely exploited as ligands in affinity chromatography for the purification of protein products. In general, dye ligands that tend to show affinities for specific classes of protein (i.e. dehydrogenases, phosphotransferases, plasma proteins, etc.) include reactive dyes belonging to the chlorotriazine group.[23] The dyes provide interactions with enzymes that mimic interactions provided by natural ligands or their chemical analogues and, because these dyes have no biological relationship with the macromolecules, the terms ‘pseudo-ligand’ or ‘pseudo-affinity’ are commonly used to describe them or their interactions.[24] Dissociation constants, K_d, of dye ligands are commonly in the range 10^{-6} to 10^{-7} M , which lies intermediate between ion exchange, 10^{-4} to 10^{-6} M and truly biospecific ligands, 10^{-6} to 10^{-8} M.[25] The dyes are particularly promising pseudo-affinity ligands because they offer several advantages over biospecific ligands including ease of coupling to support matrices, low cost, wide availability and high stability operational and sanitisation operations.[24]

17.5 GENERAL PROBLEMS ASSOCIATED WITH CONVENTIONAL TECHNIQUES

From an economic point of view, the number of sequential operations necessary to achieve the desired purity of a protein product contributes significantly to the overall cost of the downstream process. This is due to the capital investment and amount of consumables needed for each step as well as the individual time required for each operation. Additionally, the overall yield of the purification is reduced with each additional process step as a result of inherent handling losses of product and/or product activity. It has been estimated that the overall cost of the downstream process is closely correlated with the number of purification steps involved and that cost may account for up to 80% of the final process investment.[26]

Traditional techniques employed both for harvesting biomass and feedstock clarification are centrifugation and filtration.[27] Centrifugation might need to be undertaken twice, while an additional depth or microfiltration step is commonly included to ensure a particle-free (99–99.9% in terms of cell clearance) solution which can be fractionated by traditional packed-bed chromatography. Although filtration has been applied successfully in numerous solid–liquid operations, performance is usually diminished as a result of membrane fouling (for example by cells, cell debris, lipids and nucleic acids) during operation.[28] In addition, combined centrifugation and filtration operations often result in long processing times. Furthermore, it has been noted that the presence of large amounts of insoluble and highly viscous materials (for example cells, cells debris and long chain genomic DNA) in the process feedstock can further restrict the clarification performance. This problem is especially critical in the case of a cell disruptate, which results in the generation of cell debris, colloidal materials and the release of large amounts of intracellular products.[29] A rapid method of product capture of the target protein is therefore preferred because the time taken to remove particulates can promote denaturation due to process conditions that are detrimental to structural integrity, for example the action of proteases, carbohydrates or oxidising conditions. Thus, it is obvious that the development of fast and cost-effective primary recovery steps form the basis for a successful downstream process, especially in the production of intracellular proteins.

17.6 FLUIDISED BED ADSORPTION

Fluidised bed adsorption (FBA) has emerged as an efficient recovery method proven to have significant advantages over conventional procedural sequences, for example discrete feedstock clarification followed by fixed-bed adsorption of the product. In fluidised beds, liquid is pumped upwards through a bed of adsorbent beads which, in contrast to a packed bed, are not constrained by an upper flow adapter. Thus, the bed can expand and spaces open up between the adsorbent beads. The increased voidage of the bed allows particulates in the feed to pass freely through the spaces without entrapment (see Figure 17.3). Thus, the need for prior removal of cells and/or debris is eliminated. After the adsorption stage, the remaining feedstock and particulates are washed from the adsorbent bed and the product is subsequently eluted either in fluidised or packed-bed mode. As a consequence, clarification, concentration and initial fractionation are combined in one unit operation and thus fluidised beds exhibit great potential for simplifying downstream processes with concomitant savings in capital and operating costs.

Fluidised beds have been used previously for the industrial-scale recovery of the antibiotics streptomycin and novobiocin.[30] However, more recently, considerable interest has been shown in the use of fluidised beds for the direct extraction of proteins from whole fermentation broths.[31] In a packed bed, the adsorbent particles are packed within the contactor. The voidage, that is, the inter-particle space, is minimal and thus feedstock clarification is mandatory to avoid clogging of the bed. In a fluidised/expanded bed, the adsorbent bed is allowed to expand by irrigation with feedstock. Bed voidage is increased, allowing the passage of particulates in the feed. The diameters of the adsorbent beads are exaggerated for illustrative clarity.

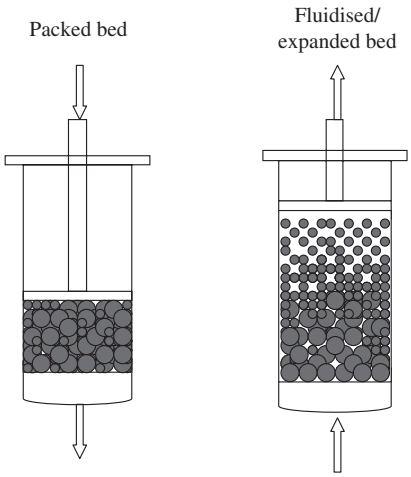

FIG. 17.3. Adsorbent particles in a packed and a fluidised bed.

17.6.1 Mixing Behaviour in Fluidised/Expanded Beds

The conventional chemical engineering view of a fluidised bed is one in which there is a significant degree of mixing, in both the solid and fluid phases, for example in gas-fluidised systems.[32] In many applications, mixing of the solid phase is desirable, for example to obtain high rates of heat transfer and a uniform temperature within the bed. Gas fluidised beds are characterised by an 'aggregative' behaviour in which bubbles of gas pass through a bed of particles which are just fluidised resulting in considerable mixing of the solid phase as well as distinct bypassing of the gas phase. In general, mixing in liquid fluidised systems is not as severe as in gas fluidised systems. Here, the density differences between the solid and the fluid phase are comparatively small, and thus the bed shows a 'particulate' behaviour in which the bed retains a uniform character.[31]

In a packed bed, the adsorbent beads are stationary and liquid flow through the bed approximates plug flow. Thus, the number of theoretical equilibrium stages (referred to as plates) is maximised, which results in good adsorption and chromatographic performance. As a consequence of the absence of plug flow in the liquid phase, compounded by the mixing of the adsorbent, a fluidised bed would be expected to show an inferior adsorption performance compared with that of a packed bed. Thus, for protein recovery in liquid fluidised beds, it is highly desirable to minimise the degree of mixing so as to mimic the adsorption characteristics found in a packed bed contactor with respect to capacity and resolution.

Several strategies have been reported to limit the mixing of adsorbent particles within liquid fluidised beds. One approach is to divide the bed into sections by the introduction of baffles into the contactor. Other approaches seek to keep the adsorbent beads in a fixed position or at least localise their movement to achieve a stable fluidised bed which subsequently behaves like a packed bed, but with a greater voidage. For example, by using magnetically susceptible adsorbent particles, a fluidised bed can be stabilised by subjecting it to a magnetic

field. Such beds are claimed to exhibit little or no back-mixing and can be operated continuously.[33] The practical benefit of this approach, i.e. restricted movement of adsorbent particles and associated uncoupling of the bed expansion from fluidisation velocity has subsequently been demonstrated by Zhang.[34] In this work, magnetically stabilised fluidised beds (MSFBs) were exploited for: (i) the direct recovery of the intracellular enzyme glyceraldehydes-3-phosphate dehydrogenase (G3PDH) from unclarified yeast disruptates; and (ii) for the recovery of antibody fragments from *Escherichia coli* fermentation broths. However, this technique requires complicated and relatively expensive equipment, particularly at large scale.

A simpler approach has been designed for the physical properties of the solid phases in such a way that they generate an inherently stable fluidised bed. If the adsorbent beads have an appropriate distribution of sizes and/or densities, grading or classification of the adsorbent occurs within the bed, with the larger/denser particles being located near the bottom of the bed and the smaller/lighter particles nearer the top. The segregation behaviour restricts the local mobility of the fluidised particles. Such a bed exhibits dispersion characteristics similar to a packed bed.[36] Thus, the hydrodynamic properties of a fluidised bed are combined with the chromatographic properties of a packed bed. The degree of classification is dependent on the ratio of the size of the largest and smallest particle within the bed. This ratio has been claimed to be at least 2.2.[37]

To account for the difference in the dispersion characteristics of the classified, stable fluidised bed and the conventional, well-mixed fluidised bed, the term ‘expanded bed’ has been used by several authors and the leading manufacture of chromatography media and equipment.[38] In the work presented here, the term ‘fluidised bed’ will be used synonymously with ‘expanded bed’ to refer to adsorbents fluidised under conditions that seek to minimise particle mixing.

17.7 DESIGN AND OPERATION OF LIQUID FLUIDISED BEDS

17.7.1 Hydrodynamic Characterisation of Flow in Fluidised/Expanded Beds and Bed Voidage

The voidage (ε) of a bed of particles is the fraction of the bed volume occupied by the interstitial space between the particles. Its value depends upon the geometrical configuration of the beads, the pattern in which they are arranged within bed, the size distribution of the particles and the ratio of mean particle and contactor diameter. The bed voidage can be calculated using the following equation:

$$\text{Voidage } (\varepsilon) = 1 - \frac{V_P}{V_b} \tag{17.7.1.1}$$

where V_p is the volume of the particles and V_b is the volume of the bed. The voidage of a packed bed is related to the sphericity of the particles, with a sphericity value of 1 for fully spherical particles. The bed voidage values can typically range from 0.32 for a densely packed adsorbent to 0.43 for a loosely packed adsorbent.[39] However, the voidage of a bed containing a range of particle sizes and geometrical shapes cannot be predicted accurately.

Therefore, an assumed value for ε_o of 0.40 for a perfectly packed adsorbent bed is commonly found in chromatographic studies.[40] This value has also been applied throughout this study for all the materials used.

17.7.2 Minimum Fluidisation Velocity of Particles

The minimum fluidisation velocity of the particles is achieved when the adsorbent becomes suspended in the liquid. This occurs when the drag forces exerted by the upward flow of the liquid phase are equal to the weight of particles in the liquid. Therefore, at minimum fluidising conditions, it can be described by the following expression:

drag by upward liquid flow = weight of the particles − buoyancy of the particles

This expression can be also presented as:

pressure drop across the bed × cross section area of the bed = volume of the bed × fraction of the particles × specific weight of the particles

or

$$\Delta P \times A_c = A_c \times H_{mf} \times (1-\varepsilon_{mf}) \times [(\rho_P - \rho) \times g] \tag{17.7.2.1}$$

where ΔP is the pressure drop, A_c is the cross-sectional of the column area, H_{mf} and ε_{mf} are the bed height and bed voidage at the minimum fluidisation velocity (U_{mf}), respectively, ρ_p is the density of the particles, ρ is the density of liquid phase and g is acceleration due to gravity. Rearranging (17.7.2.1) gives:

$$\frac{\Delta P}{H_{mf}} = (1-\varepsilon_{mf}) \times (\rho_P - \rho) \times g \tag{17.7.2.2}$$

However, on the basis of the relation between pressure drop and the minimum fluidisation velocity of particles, the point of transition between a packed bed and a fluidised bed has been correlated by Ergun[41] using (17.7.2.3). This is obtained by summing the pressure drop terms for laminar and turbulent flow regions.

$$\frac{\Delta P}{H_{mf}} = 150 \times \frac{(1-\varepsilon_{mf})^2}{\varepsilon_{mf}^3} \times \frac{\mu \times U_{mf}}{d_P^2} + 1.75 \times \frac{(1-\varepsilon_{mf})}{\varepsilon_{mf}^3} \times \frac{\rho \times U^2}{d_P^2} \tag{17.7.2.3}$$

where μ is the viscosity of the liquid and d_p is the diameter of the particle. The first term of the Ergun equation is linear with respect of velocity and this will be dominant when the flow in the voids is laminar. Hence, (17.7.2.3) can be simplified to:

$$\frac{\Delta P}{H_{mf}} = 150 \times \frac{(1-\varepsilon_{mf})^2}{\varepsilon_{mf}^3} \times \frac{\mu \times U_{mf}}{d_P^2} \quad \text{when} \quad Re_P = \frac{d_P \times \rho \times U_{mf}}{\mu} < 20 \tag{17.7.2.4}$$

The second term relates to turbulence. Therefore, (17.7.2.3) can be simplified to:

$$\frac{\Delta P}{H_{\mathrm{mf}}} = 1.75 \times \frac{(1-\varepsilon_{\mathrm{mf}})}{\varepsilon_{\mathrm{mf}}^3} \times \frac{\rho \times U^2}{d_{\mathrm{P}}^2} \quad \text{when} \quad Re_{\mathrm{P}} = \frac{d_{\mathrm{P}} \times \rho \times U_{\mathrm{mf}}}{\mu} > 1000 \qquad (17.7.2.5)$$

In the intermediate region both terms have to be used. Therefore, the superficial velocity at minimum fluidising conditions can be found by combining (17.7.2.2) and (17.7.2.3) and multiplying both sides by $\rho d_{\mathrm{p}}^3/\mu^2$ $(1 - \varepsilon_{\mathrm{mf}})$ to yield:

$$150\frac{(1-\varepsilon_{\mathrm{mf}})}{\varepsilon_{\mathrm{mf}}^3} \times \frac{d_{\mathrm{P}} \times U_{\mathrm{mf}} \times \rho}{\mu} + \frac{1.75}{\varepsilon_{\mathrm{mf}}^3} \times \left(\frac{\rho \times U_{\mathrm{mf}} d_{\mathrm{P}}}{\mu} \right)^2 = \frac{\rho \times (\rho_{\mathrm{P}} - \rho) \times \mathrm{g} \times d_{\mathrm{P}}^2}{\mu^2} \qquad (17.7.2.6)$$

If $\varepsilon_{\mathrm{mf}}$ is unknown, the following equation suggested by Wen and Yu[41] can be used to determine the minimum fluidisation velocity for the whole range of Reynolds numbers by assuming:

$$\frac{(1-\varepsilon_{\mathrm{mf}})}{\varepsilon_{\mathrm{mf}}^3} \cong 11 \quad \text{and} \quad \frac{1}{\varepsilon_{\mathrm{mf}}^3} \cong 14 \qquad (17.7.2.7)$$

Hence, solving explicitly for U_{mf}

$$U_{\mathrm{mf}} = \frac{\mu}{\rho \times d_{\mathrm{P}}} \times \left[(33.7)^2 + 0.0408 \times \frac{\rho \times (\rho_{\mathrm{P}} - \rho) \times g \times d_{\mathrm{P}}^2}{\mu^2} \right]^{1/2} - 33.7 \qquad (17.7.2.8)$$

Thus, at low particle Reynolds numbers (Re_{p}), (17.7.2.8) can be simplified to:

$$U_{\mathrm{mf}} = \frac{d_{\mathrm{P}}^2 \times (\rho_{\mathrm{P}} - \rho) \times g}{1650 \times \mu} \qquad (17.7.2.9)$$

Equation (17.7.2.9) was originally used to correlate the minimum fluidisation velocity for gas–solid fluidisation beds but has been successfully employed by Lan and his co-workers[42] for adsorbents in the field of direct recovery using liquid–solid systems (Figure 17.4).

17.7.3 Terminal Settling Velocity of Particles

If a single particle is falling freely under gravity in an infinitely dilute suspension, it will accelerate until it reaches a steady-state velocity. This final velocity is known as the terminal settling velocity (U_{t}) and represents the maximum useful superficial velocity achievable in a fluidised bed. Thus, the contained particles will be elutriated from the column if the superficial velocity is above U_{t}, the value of which can be predicted using the Stokes equation

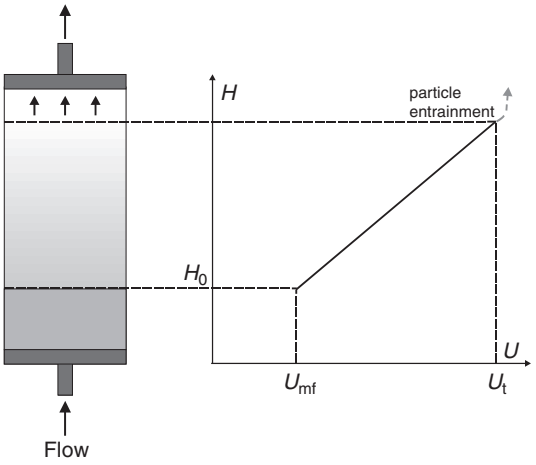

FIG. 17.4. Operational window of fluidisation velocities.

(17.7.3.1). A wide range of particle terminal velocities for various Reynolds numbers have been investigated by Kunii and Levenspiel.[43] They suggested that if the particles were assumed to be spherical and operated at low particle Reynolds number ($Re_p < 0.4$), the Stokes equation was found to be acceptable (see Figure 17.4). Therefore, the terminal velocity U_t can be expressed as:

$$U_t = \frac{d_P^2 \times (\rho_P - \rho) \times g}{18 \times \mu} \tag{17.7.3.1}$$

where d_p is the diameter of the particle, ρ_p and ρ are the density of the particle and liquid phase respectively, μ is the velocity of liquid phase and g is acceleration due to gravity. The Stokes equation has been reported in the literature as being successfully used to predict terminal settling velocities of fluidised/expanded bed adsorbents.[44,45]

Alternatively, the model of Shiller and Naumann is commonly used for the prediction of terminal velocity of a spherical particle:

$$Ga = 18Re_t + 2.7\ Re_t^{1.687} \quad 3.6 < Ga < 10^5 \tag{17.7.3.2}$$

where

$$Ga = \frac{\rho \times (\rho_P - \rho) \times g \times d_P^3}{\mu^2} \tag{17.7.3.3}$$

and

$$Re_t = \frac{\rho \times d_P \times U_t}{\mu} \tag{17.7.3.4}$$

where Ga is the Galileo number, Re_t represents the terminal Reynolds number and d is the particle diameter. The model of Shiller and Naumann has been successfully used to estimate the particle terminal velocity by Thomas and Yates,[46] and Jahanshahi and his co-workers.[47]

17.7.4 Degree of Bed Expansion

The degree of bed expansion contributes to the efficiency of fluidised bed/expanded bed adsorption as a composite function of liquid distribution, liquid and particle properties (size, shape and density) and process conditions. Besides being an important design feature, the degree of bed expansion may be used as a quick and simple measure of bed stability.[48]

The relation between superficial velocity (U) and bed voidage (ε) in a fluidised bed can be described by the classical correlation first postulated by Richardson and Zaki:[49]

$$U = U_t \varepsilon^n \tag{17.7.4.1}$$

where ε is the fluidised voidage and n is the Richardson–Zaki coefficient. It allows the calculation of the particle terminal velocity of any given suspension of uniformly dispersed spheres together with the liquid velocity required to perform a given expansion of a fluidised bed by the logarithmic plot of linear velocity against fluidised voidage. Thus:

$$\log U = \log U_t + n \times \log \varepsilon \tag{17.7.4.2}$$

The void fraction (ε) is estimated from the measured height of the expanded bed (H) and is a function of superficial liquid velocity. Thus:

$$\varepsilon = 1 - \frac{M}{\rho_P \times A_c \times H} \tag{17.7.4.3}$$

where M is the mass of particles. Also, the fluidised voidage can be determined as the total volume of particles (for a given bed) is constant in both packed bed and fluidised bed configurations. Therefore:

$$A_c H_o (1 - \varepsilon_o) = A_c H (1 - \varepsilon) \tag{17.7.4.4}$$

where H_o and ε_o are the packed bed height and voidage respectively. Hence, by rearranging (17.7.4.4), the bed voidage at any fluidised bed height can be estimated using the equation:

$$\varepsilon = 1 - \frac{(1 - \varepsilon_o) \times H_o}{H} \tag{17.7.4.5}$$

The Richardson–Zaki coefficient (n) can be calculated from the following correlations:

$$n = 4.65 + 20\frac{d}{D} \quad Re_t < 0.2 \tag{17.7.4.6}$$

$$n = \left(4.4 + 18\frac{d}{D}\right) Re_t^{-0.03} \quad 0.2 < Re_t < 1 \tag{17.7.4.7}$$

$$n = \left(4.4 + 18\frac{d}{D}\right) Re_t^{-0.1} \quad 1 < Re_t < 200 \tag{17.7.4.8}$$

$$n = 4.4\ Re_t^{-0.1} \quad 200 < Re_t < 500 \tag{17.7.4.9}$$

$$n = 2.4 \quad Re_t > 500 \tag{17.7.4.10}$$

where D is the column diameter and Re_t is the particle Reynolds number based on the terminal velocity. The popularity of the Richardson–Zaki correlation in this field of study arises from its simplicity and good agreement with experimental data.[48,50]

The operational window of a fluidised bed process is defined by the minimum fluidisation velocity, U_{mf}, at which a settled bed of adsorbent beads starts to fluidise and the terminal velocity (U_t) at which the bed stabilises and adsorbent beads are entrained from the bed.

17.7.5 Matrices for Fluidised Bed Adsorption

Early work exploiting extensively cross-linked agarose adsorbents originally designed for conventional, packed bed processes demonstrated the principal of operation and the potential of fluidised bed adsorption for processing particulate feedstocks.[31] However, it was found that these materials were not optimally suited because the combination of particle diameter and density allowed only at low flow rates (for example 10–30 cm.h^{-1}) which resulted in low overall productivities. Denser particles such as silica were more appropriate in this respect.[51] However, a drawback of silica-containing material is the limited stability at high pH values, which makes it less suitable for biopharmaceutical production where alkaline conditions are commonly used for cleaning-in-place and sanitisation-in-place procedures.

The development of denser adsorbents enabled the use of higher flow rates and improved the stability of operation of expanded beds. Tailor-made adsorbents were produced using hydrophilic natural polymers such as cellulose, agarose or synthetic trisacrylate-based materials. To enhance the particle density, heavy, inert filler materials have been incorporated during assembly. The resulting composite materials included cellulose-titanium dioxide and dextran-silica.[52] Other materials reported for the fabrication of denser adsorbents were glass and zirconia. For example, Thömmes and his co-workers[53] exploited custom-derived controlled pore glass particles for the purification of monoclonal antibodies. Zirconia-based

materials exhibit a significantly higher density than silica. It has been demonstrated that even small particles (for example less than 50 μm in diameter) may be fluidised at linear flow rates similar to those used for silica or density-enhanced agarose particles having a greater diameter.[54] In another approach, McCreath and colleagues developed perfluoropolymer particles which were derived with dye ligands for the affinity purification of dehydrogenases from disrupted baker's yeast.[55] The increased density of the support (2.20 $g \cdot ml^{-1}$) also allowed the use of comparatively small particles (50–80 μm) at an acceptable linear flow rate of 120 $cm \cdot h^{-1}$.

Agarose-based materials have been commercialised specifically for fluidised bed adsorption by increasing their specific weight with incorporated quartz or steel particles (STREAMLINE™).[37] The densities so achieved have been exploited at 1.15 $g \cdot ml^{-1}$ for agarose-quartz and 1.3 $g \cdot ml^{-1}$ for agarose-steel composites. These materials are available with a range of ligand functionalities such as anion exchange (DEAE, Q), cation exchange (SP), chelating ligand (iminodiacetic acid for immobilised metal affinity chromatography, IMAC), protein A (affinity purification of antibodies) and phenyl groups (hydrophobic interaction chromatography, HIC). More recently, so-called pellicular adsorbents were defined as suitable for fluidised bed adsorption. These adsorbents are characterised by a dense core such as glass or stainless steel[47,56] coated with a layer of porous material, such as agarose. Such matrices promise high rates of adsorption/desorption owing to the absence of deep convective pores and the short diffusion distances within the thin porous layer that comprises the pellicle.

17.7.6 Column Design for Fluidised Bed Adsorption

To achieve a stable fluidised bed, the column has to fulfil some simple but important demands. A suitable liquid distribution is crucial to accomplish plug flow conditions within the bed and thus minimise particle dispersion. A prerequisite for the generation of an even velocity profile across the cross section of a column is an evenly distributed pressure drop across the distributor at the column inlet. Pressure drop fluctuations lead to the development of channels which are the most important influence upon homogeneity in an adsorption process. Flow distribution can be achieved by using sieve plates, meshes or a bed of glass ballotini.[43] Bascoul and his colleagues[57] have investigated bed stability as a function of the distributor design, showing that channelling in the lower part of a fluidised bed due to uneven flow distribution is reduced with increasing column length. This has led to the conclusion that the fluidised bed itself serves as an effective flow distribution system. More recently, a novel distributor design was introduced which uses a stirrer in the bottom of the contactor to distribute the incoming feedstock. This configuration divides the fluidised bed in a limited, well-mixed zone at the bottom and a stable fluidised bed above it. Such contactors were included in the study presented here. Besides the demand for an even flow distribution, the distributor has to enable the unhindered passage of particulates without becoming blocked or damaging shear sensitive cells. Partial blockage of a distributor will cause channelling in the fluidised bed. Cell breakage in the flow distributor can lead to the unwanted release of intracellular compounds which may impair the purification process of an extracellular product for whole broths.

Another important factor that bears upon bed stability is the column verticality. Van der Meer and his colleagues[58] have demonstrated that even small deviations from vertical alignment lead to significant inhomogeneity of liquid flow. These findings were confirmed by Bruce and his co-workers[59] who found that this effect is more pronounced in small-diameter contactors. In their work, the dynamic capacity of a 1 cm column, used for the capture of glucose-6-phosphate dehydrogenase (G6PDH) from unclarified yeast homogenate, was reduced by approximately 30% when misaligned by 0.185°. However, a 5 cm contactor operated under similar conditions appeared to be unaffected.

17.8 EXPERIMENTAL PROCEDURE

In principle, the experimental protocol of fluidised bed adsorption does not deviate from packed-bed operations, but the main difference is the direction of the liquid flow. The sequence of steps of equilibration, sample application, wash, elution and cleaning (CIP) is performed in an upward direction although the last two might be undertaken in fixed-bed mode. During equilibration, the matrix is fluidised and a stabilised, fluidised bed is developed. Here, the classification within the bed with regard to particle size of the adsorbent particles may be detected by visual observation. At the same time, the matrix is primed for adsorption by the selection of a suitable buffer for product-adsorbent interactions. Subsequently, the feedstock is applied to the fluidised bed. Target proteins are adsorbed while cells, debris and other particulates and contaminants pass through the bed. After sample application, residual biomass and unbound proteins are removed from the bed in a washing procedure. Elution may be performed either in packed bed or in fluidised bed mode. A common procedure has been to allow the adsorbent to settle and reverse the flow for elution. Here, the upper adapter is lowered to the top of the settled bed. On the other hand, maintaining a fluidised bed during elution prevents particle aggregation and thus facilitates subsequent cleaning of the adsorbent.[60] However, owing to the greater interstitial volume of the fluidised bed, the elution volume is increased comparison with fixed-bed elution. After elution, the adsorbent is subjected to cleaning-in-place (CIP) procedures. These are important because the application of whole broth increases the contact of the adsorbent with nucleic acids, lipids and cellular compounds, which are commonly removed or reduced in conventional primary recovery steps before fixed-bed column chromatography. Commonly used agents in CIP protocols are NaCl, NaOH, ethanol, acetic acid, urea and guanidine hydrochloride.[48]

17.9 PROCESS INTEGRATION IN PROTEIN RECOVERY

There is much current interest aimed at the implementation of processes that integrate the upstream and downstream operation for protein recovery.[13,14,19] Although adsorption in fluidised beds provides a considerable saving in cost and time over conventional purification techniques, it still deploys a discrete operation with which the desired protein is captured at termination of fermentation or once a cell suspension has been disrupted. The main

disadvantage of this discrete recovery operation is the risk of detrimental effects on unstable product associated during hold-up periods.[13] This may be defined as the duration when the feedstock is harvested, preconditioned and stored before being subjected to fluidised-bed processing. The hold-up period risks time-dependent product modification and/or inactivation by system antagonists including proteases, carbohydrates, harsh physical conditions[3] or product losses associated with protein–debris interaction. Additionally, it has been reported that protein products are usually stabilised and less susceptible to protease degradation when they are adsorbed upon a chromatography solid phase. Therefore, a logical physical coupling of fluidised-bed adsorption with upstream operations of fermentation or cell disruption might be predicted to gain additional benefits of product yield and quality by virtue of the immediate and direct sequestration of products from process feedstocks at source.[14,61] However, the application of a multi-fluidised bed system (MFBS), where each bed is sequentially operated online to the fermenter or disrupter to achieve a repetitive operation of this cycle, could decrease the adsorbent inventory and increase the maximum batch size.

17.9.1 Interfaced and Integrated Fluidised Bed/Expanded Bed System

Fluidised bed recovery of protein from particulate-containing feedstock can be achieved using two possible methods, defined as an interfaced or an integrated system.[62] The interfaced system exploits a fluidised bed to capture the desired protein either at termination of fermentation or once a cell suspension has been disrupted. In this system, the fluidised bed is normally operated in single-pass chromatography mode to achieve high adsorption efficiency. In contrast, the integrated fluidised bed system achieves the direct sequestration of target product from process feedstock at source, for example productive fermentation or immediate upon cell disruptate.[52]

The direct product sequestration (DPS) is designed to minimise product degradation, which leads to higher product yield and improved molecular integrity.[63] An early application of DPS of protein products was demonstrated, wherein an extracellular acid protease produced by the oleagious yeast *Yarrowia lipolytica* was continuously captured from a productive fermentation. Here, the authors reported that the development of such a technique increased product yield through a reduction in the processing time and the imposition of a pseudo-constitutive state upon the yeast. Similar advantages were noted with the DPS of α-amylase from fermentations of *Bacillus amyloliquifaciens* exploiting a manifold of fluidised beds.[64] Additionally, Carmichael and his co-workers[65] demonstrated the application of DPS in the recovery of tPA from animal cell cultures (Chinese hamster ovary cells). The work of Hamilton and his colleagues[62] addressed the development of process intensification of direct product sequestration of acid protease produced by *Y. lipolytica.* Hamilton and his co-workers,[61] subsequently performed further investigations into the recovery of similar enzymes successfully from feedstock characterised with a high ionic condition without prior preconditioning (for example dilution or dialysis). This exploited mixed-mode chemical ligands, and as a result, the processing time was further shortened and overall operational efficiency increased.

During the purification of intracellular proteins, cell disruption by mechanical or biochemical means is the first step required in the process. However, it commonly initiates cellular and

molecular degradation processes, analogous to those of natural cell death and lysis, owing to the disintegration of intracellular compartments which confine lytic enzymes.[3,8] In addition, the generation of fine cell debris may promote electrostatic and/or hydrophobic product–debris interactions. Such adverse effects will compromise the yield and molecular fidelity of protein products, particularly when feedstocks are accumulated and processed in time-dependent batch operations. Proteolytic activity may be restrained by the addition of specific inhibitors. However, owing to the complexity and diversity of different host organisms, such measures are haphazard. Consequently, rapid processing (for example by the direct product sequestration at cell disruption) should minimise such degradation and enhance the yield and quality of even the most labile products.[13,14] Here, instead of accumulating a disruptate in a holding tank, the product remains in its physiological environment, i.e. the intact cell, as long as possible and is exposed to the adsorbent immediately after its release from the cell in the disrupter. Contact times between the target molecule and the disruptate are thus minimal. Mechanical cell breakage in a bead-mill has many attractive process characteristics including high disruption efficiency, high throughput and biomass loading, good temperature control and unlimited scale-up for most bioprocesses. As a result of the operational characteristics of single-pass and continuous operation, the use of a bead mill is recommended as the ideal feedstock generator for direct sequestration of released products in a fluidised bed.

Baker's yeast suspension (20% ww/v original cells) was pumped to the bead mill at a flow rate of 280 $cm \cdot h^{-1}$ within the BRG 4.5 cm inner diameter contactor. Then, the disruptate from the mill was directly introduced to the pre-equilibrated fluidised bed containing ZSA II-CB and Macrosorb K4AX-CB.

The experimental rig and process configuration for integrated bead milling and fluidised bed adsorption is shown in Figure 17.5.

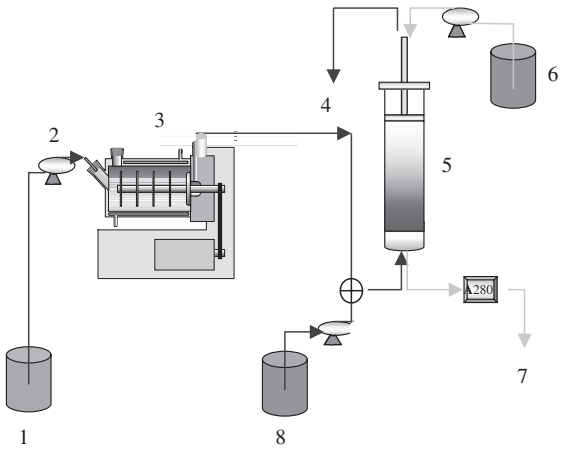

FIG. 17.5. Experimental configuration for integrated bead milling and fluidised bed adsorption 1. Feedstock; 2. peristaltic pump; 3. bead mill; 4. flow through/waste; 5. fluidised bed contactor; 6. elution buffer; 7. fraction collector/waste; 8. loading buffer.

17.10 NOMENCLATURE

ε	Voidage
V_p	Volume of the particles
V_b	Volume of the bed
A_c	Cross-sectional of the column area
ΔP	Pressure drop
U_t	Terminal settling velocity
U_{mf}	Minimum fluidisation velocity
H_{mf}	Bed height at minimum fluidisation velocity
ε_{mf}	Bed voidage at minimum fluidisation velocity
ρ_p	Density of the particles
ρ	Density of liquid phase
g	Acceleration of gravity
μ	Viscosity of the liquid
d_p	Diameter of the particle
Ga	Galileo number
Re_t	Terminal Reynolds number
U	Fluid superficial velocity
H	Expanded bed
M	Mass of particles
D	Column diameter

REFERENCES

1. Wheelwright, S.M., *Bio/Technology* **5**, 789 (1987).
2. Asenjo, J.A. and Patrick, I., *In* "Protein Purification Applications" (E.L.V. Harris and S. Angal, eds). Oxford University Press, Oxford, 1990.
3. Kaufmann, M., *J. Chromatogr. B* **699**, 347 (1997).
4. Harris, E.L.V., "Protein purification methods: A Practical Approach". IRL Press, Oxford, 1989.
5. Gilchrist, G.R., "Direct fluidised bed adsorption of protein products from complex particulate feedstocks". PhD thesis, University of Birmingham, 1996.
6. Walsh, G. and Headson, D., "Protein Biotechnology". John Wiley and Sons, New York, 1994.
7. Hughes, D.E., Wimpenny, J.W.T. and Lloyd, D., *In* "Methods in Microbiology", vol. 5B (J.R. Norris and D.W. Ribbons, eds). Academic, New York, 1971.
8. Middelberg, A.P.J., *Biotechnol. Adv*. **13**, 491 (1995).
9. Agerkvist, I. and Enfors, S.-O., *Biotechnol. Bioengng* **36**, 1083 (1990).
10. Vogels, G. and Kula, M.-R., *Chem. Engng Sci*. **47**, 123 (1991).
11. Kula, M.-R. and Schütte, H., *Biotechnol. Progr.* **3**, 31 (1987).
12. Schütte, H., Kroner, K.H., Hustedt, H. and Kula, M.-R., *Enzyme Microb. Technol*. **5**, 143 (1983).
13. Bierau, H., Zhang, Z. and Lyddiatt, A., *J. Chem. Technol. Biotechnol*. **74**, 208 (1999).
14. Jahanshahi, M., Sun, Y., Santos, E., Pacek, A.W., Franco, T.T., Nienow, A.W. and Lyddiatt, A., *Biotechnol. Bioengng* **80**, 201 (2002).
15. Lee, S-M., *J. Biotechnol*. **11**, 103 (1989).
16. Bell, G. and Cousins, R.B., *In* "Engineering Process for Bioseparation" (L.R. Weatherley ed.). Butterworth-Heinemann, UK, 1994.
17. Kula, M.-R., *Bioseparation* **1**, 181 (1990).

18. Roe, S.D., *In* "Separations for Biotechnology" (M.S. Verral and M.J. Hudson, eds). Ellis Horwood, Chichester, 1987.
19. Lyddiatt, A., *Curr. Opin. Biotechnol.* **13**, 95 (2002).
20. Chase, H.A., *J. Chromatogr*. **297**, 179 (1984).
21. Kumar, A., Galaev, I. Yu. and Mattiasson, B., *J. Chromatogr*. B **741**, 103 (2000).
22. Denizli, A. and Piskin, E., *J. Biochem. Biophys. Meth.* **49**, 391 (2001).
23. Kopperschläger, G., Bohme, H.J. and Hofmann, E., *Adv. Biochem. Engng* **25**, 101 (1982).
24. Haff, L.A. and Easterday, R.L., *In* "Theory and Practice in Affinity Chromatography" (F. Eckstein and P.V. Sundaram, eds). Academic Press, New York, 1978.
25. Skidmore, G.L., Horstmann, B.J. and Chase, H.A., *J. Chromatogr*. **498**, 113 (1990).
26. Spalding, B.J., *Bio/Technology* **9**, 229 (1991).
27. Van Reis, R., Leonard, L.C., Hsu, C.C. and Builder, S.E., *Biotechnol. Bioengng* **38**, 413 (1991).
28. Anspach, F.B., Curbelo, D., Hartmann, R., Garke, G. and Deckwer, W.-D., *J. Chromatogr*. *A* **865**, 129 (1999).
29. Datar, R.V. and Rosen, C.G., *In* "Bioprocessing" (G. Stephanopoulos, ed.). VCH, Weinheim, 1996.
30. Belter, P.A., Cunningham, F.L. and Chen, J.W., *Biotechnol. Bioengng* **15**, 533 (1973).
31. Chase, H.A., *Trends Biotechnol*. **12**, 296 (1994).
32. Levenspiel, O., "Chemical Reaction Engineering". Wiley & Sons, New York, 1999.
33. Burns, M.A. and Graves, D.J., *Biotechnol. Progr*. **1**, 95 (1985).
34. Zhang, Z., O'Sullivan, D. and Lyddiatt, A., *J. Chem. Technol. Biotechnol*. **74**, 270 (1999).
35. Thömmes, J., Halfar, M., Lenz, S. and Kula, M.-R., *Biotechnol. Bioengng* **45**, 205 (1995).
36. Karau, A., Benken, J., Thömmes, J. and Kula, M.-R., *Biotechnol. Bioengng* **55**, 54 (1997).
37. Hjorth, R., *Trends Biotechnol*. **15**, 230 (1997).
38. Brown, G.G., "Unit Operation". John Wiley and Sons, New York, 1950.
39. Draeger, N.M. and Chase, H.A., *Bioseparation* **2**, 67 (1991).
40. Ergun, S., *Chem. Enginng Prog*. **48**, 89 (1952).
41. Wen, C.Y. and Yu, Y.H., *AICHE J*. **12**, 610 (1966).
42. Lan, J.C.-W., Hamilton, G.E. and Lyddiatt, A., *Bioseparation* **8**, 43 (1999).
43. Kunii, D. and Levenspiel, O., "Fluidisation Engineering". John Wiley and Sons, New York, 1969.
44. Sun, Y., Pacek, A.W., Nienow, A.W. and Lyddiatt, A., *Biotechnol. Bioprocess Engng* **6**, 1 (2001).
45. Thomas, C.R. and Yates, J.G., *Chem. Eng. Res. Des*. **63**, 67 (1985).
46. Jahanshahi, M., Pacek, A.W., Nienow, A.W. and Lyddiatt, A., *J. Chem. Technol. Biotechnol*. **78**, 1111 (2002).
47. Chang, Y.K., McCreath, G.E. and Chase, H.A., *Biotechnol. Bioengng* **48**, 355 (1995).
48. Richardson, J.E. and Zaki, W.W., *Trans. Inst. Chem. Engng* **32**, 35 (1954).
49. Tong, X.-D. and Sun, Y., *J. Chromatogr. A* **943**, 63 (2002).
50. Finette, G.M.S., Mao, Q.M. and Hearn, M.T.W., *J. Chromatogr. A* **743**, 57 (1996).
51. Morton, P.H. and Lyddiatt, A., *In* "Ion Exchanger Advances" (M.J. Slater, ed.). Elsevier Applied Science, 1992.
52. Thömmes, J., Weiher, M., Karau, A. and Kula, M.-R., *Biotechnol. Bioengng* **48**, 367 (1995).
53. Morris, J.E., Tolppi, C.G., Carr, P.W. and Flickinger, M.C., *Abstr. Papers Am. Chem. Soc*. 207 (1994).
54. McCreath, G.E., Chase, H.A. and Lowe, C.R., *J. Chromatogr*. **659**, 275 (1994).
55. Palsson, E., Gustavsson, P.E. and Larsson, P.O., *J. Chromatogr. A* **878**, 17 (2000).
56. Bascoul, A., Delmas, H. and Couderc, J.P., *Chem. Engng J. and Biochem. Engng J.* **37**, 11 (1988).
57. Van Der Meer, A.P., Blanchard, C.M.R.J.P. and Wesselingh, J.A., *Chem. Engng Res. Des*. **62**, 214 (1984).
58. Bruce, L.J., Clemmitt, R.H., Nash, D.C. and Chase, H.A., *Chem. Technol. Biotechnol*. **74**, 264 (1999).
59. Hjorth, R., *Bioseparation* **8**, 1 (1999).
60. Hamilton, G.E., Luechau, F., Burton, S.C. and Lyddiatt, A., *J. Biotechnol*. **79**, 103 (2000).
61. Hamilton, G.E., Morton, P.H., Young, T.W. and Lyddiatt, A., *Biotechnol. Bioengng* **64**, 310 (1999).
62. Morton, P. and Lyddiatt, A., *J. Chem. Technol. Biotechnol*. **59**, 106 (1994).
63. Burns, M. and Lyddiatt, A., "Controlled fluidised bed protein recovery using hydrophobic matrices". The IChemE Research Event, IChemE, Rugby, UK, 1996.
64. Carmichael, I.A., Al-Rubeai, M. and Lyddiatt, A., *In* "New Developments and New Applications in Animal Cell Technology". ESACT, Kluwer Academic Publishers, 1998.

17.11 CASE STUDY: PROCESS INTEGRATION OF CELL DISRUPTION AND FLUIDISED BED ADSORPTION FOR THE RECOVERY OF LABILE INTRACELLULAR ENZYMES

Abstract

An integrated process for the primary recovery of an intracellular enzyme, where cell disruption is directly coupled with fluidised bed adsorption of the product, was proposed as a generic approach to benefit the yield and molecular integrity of labile protein products. The purification of glyceraldeyde 3-phophate dehydrogenase (G3PDH) from baker's yeast was selected for the demonstration of this principle. Cell disruption by bead milling was combined with direct adsorption of the enzyme on a Cibacron Blue derivative of a zirconia–silica pellicular adsorbent in a fluidised bed contactor, which enables proteins to be recovered directly from particulate-containing feedstock such as fermentation broths and preparations of disrupted cells without the need for prior removal of the suspended solids, operated immediately downstream of the cell disruption. The short process time and immediate sequestration of product from the hostile disruptate environment facilitated the recovery of partly purified preparation of this labile enzyme. The purification factor of this primary recovery was more than 3-fold with a 99% yield of bound activity. However, purification of the clinical therapeutic enzyme L-asparaginase from unclarified *Erwinia chrysanthemi* was selected as a step towards the implementation of realistic systems. The recovery of such labile enzyme exploiting this novel approach yielded an interim product which rivalled or bettered that produced by the current commercial process employing discrete operations of alkaline lysis, centrifugal clarification and batch adsorption. In addition to improved yield and quality of product, the process time during primary stages of purification was greatly diminished. Ready scale-up of the integration processes and encouraging performances in the present work recommend future application of such a novel method in the fast purification of labile enzymes.

Keywords: cell disruption; process integration; fluidised bed adsorption; intracellular enzymes; protein recovery

17.11.1 Introduction

Adsorption in expanded or fluidised beds is now widely adopted for the direct recovery of protein products from particulate feedstocks. As an integrative protein recovery operation it circumvents process bottlenecks encountered with the solid liquid separation required upstream of fixed bed adsorption, while achieving considerable concentration and primary

---

This case study was contributed by:
Mohsen Jahanshahi and Ghasem Najafpour
Faculty of Chemical Engineering, Noshirvani Institute of Technology, University of Mazandaran (UMZ), P.O. Box: 484, Babol, Iran.

purification of products.[1,2] However, such technology still uses discrete upstream operations of fermentation or cell disruption, and is commonly characterised by potentially detrimental hold-up periods while batches of feedstock are accumulated and/or conditioned before fluidised bed processing.[3] Hold-up risks product modification, inactivation or degradation by system antagonists such as proteases, carbohydrases and drifting physical conditions of temperature, pH and ionic strength.[4] Furthermore, cell disruption commonly initiates cellular and molecular degradation processes, analogous to those of natural cell death and lysis, due to the disintegration of intracellular compartments which confine lytic enzymes. In addition, the generation of fine cell debris may promote electrostatic and/or hydrophobic product-debris interactions. Consequently, rapid processing for example by the direct product sequestration at cell disruption should minimise such degradation and enhance the yield and quality of even the most labile products. Here, instead of accumulating a disruptate in a holding tank, the product remains in its physiological environment, i.e. the intact cell, as long as possible and is exposed to the adsorbent immediately after its release from the cell in the disrupter and contact times between the target molecule and the disruptate are thus minimal.[5] This paper summarises experiments that seek to demonstrate the feasibility of the integration of cell disruption by bead milling with product capture by fluidised bed adsorption. In the first place, a study of the primary purification of the cytoplasmic enzyme glyceraldehyde 3-phosphate dehydrogenase (G3PDH) from baker's yeast exploiting Cibacron Blue zirconia–silica agarose is reported. Subsequently, the integrated primary purification of the labile enzyme L-asparaginase sourced as an intracellular product in *Erwinia chrysanthemi* disruptates exploiting cation exchange adsorbents is investigated.

17.11.2 Materials and Methods

The bead mill was a DYNO MILL KDL-I model (Willi A. Bachofen AG, Switzerland) consisting of a glass chamber cooled by re-circulating iced water (0 °C) from a reservoir. The chamber was loaded with glass beads (0.2–0.5 mm) to 83% settled volume occupancy. The agitator speed was 3200 rpm corresponding to a peripheral speed of the agitating discs of 10.5 m s^{-1}. Baker's yeast was thawed overnight below 4 °C in buffer A (10 mM Tris/HCl, pH 7.5 containing 1 mM EDTA). In integrated experiments, cell suspension (20% ww/v herein) was fed to the mill by a peristaltic pump at a flow rate of 4.05 $l \cdot h^{-1}$. To achieve an experimental steady-state condition for effluent protein and G3PDH concentrations, the first five chamber volumes of effluent were discarded before switching the disruptate to the contactor. However, *Erwinia chrysanthemi* frozen cells were thawed and resuspended in equilibration buffer (buffer A, 20 mM citric acid/tri-sodium citrate, pH 5.5). The cell suspension was adjusted to a pH of 5.5 (20 mM citric acid) and a biomass concentration of 15% wet weight per volume (ww/v). In both cases, the disruptates were fed from the bead mill into the fluidised bed contactor. The custom-built BRG contactor comprised a hemispherical inlet port which was clamped to the glass column. This configuration allowed the inclusion of a mesh (for example stainless steel, 98 μm) between the inlet and the column for the support of the settled adsorbent bed and distribution of the incoming flow. As an alternative method for flow distribution, a short bed of glass beads (710–1180 μm, 2.5 $g \cdot ml^{-1}$) could be used filling the hemispherical inlet and the column (2 cm height).

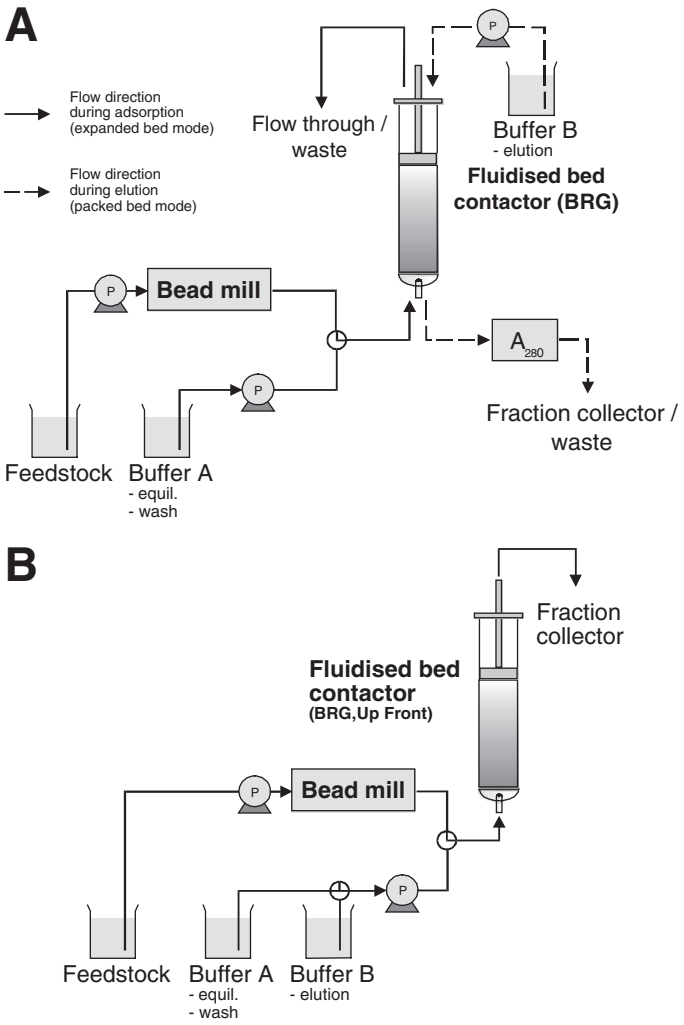

FIG. 17.6. Experimental configuration for the integrated, primary purification of intracellular proteins from unclarified disruptates. Panel A: configuration employed for the purification of G3PDH from baker's yeast. Elution was performed in packed bed mode under reversed flow. Panel B: configuration for loading, wash and elution in fluidised bed mode (employed for the purification of L-asparaginase from *Erwinia chrysanthemi*).

17.11.3 Results and Discussion

The primary purification of the enzyme G3PDH was exploited herein as a preliminary study to investigate and demonstrate the feasibility of the integrated operation of cell disruption by bead milling and immediate product capture by fluidised bed adsorption (panel A in Figure 17.6). Yeast G3PDH binds nicotinamide adenine dinucleotide (NAD) as a cofactor,

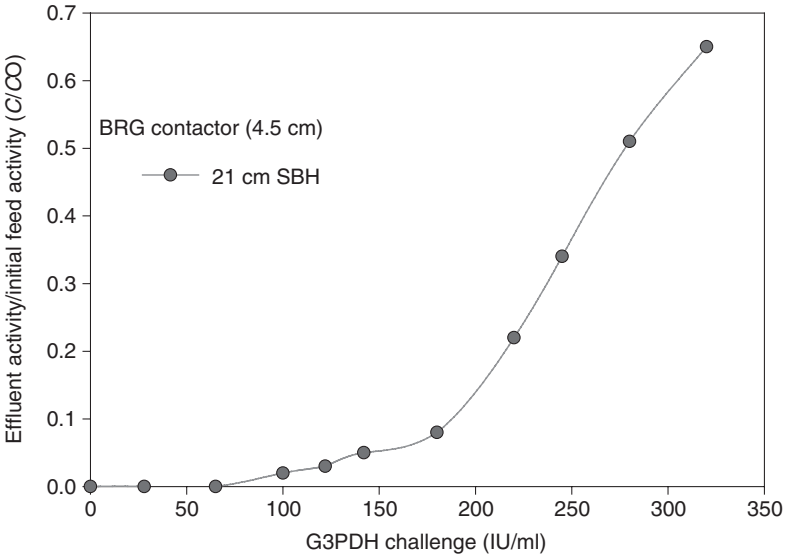

FIG. 17.7. Fluidised bed adsorption of G3PDH from milled yeast homogenate onto zirconia–silica Cibacron Blue. The feedstock (20% w/v) was fed to the bead mill at a rate 4.05 $dm^3 \cdot h^{-1}$, which corresponded to a linear flow velocity of 250 $cm \cdot h^{-1}$ within the BRG contactor with a settled bed height of 21 cm. The disrupted baker's yeast homogenate from the bead mill was applied to the integrated fluidised bed directly and terminated when $C/C_O = 0.65$.

which enables the use of the triazene dye Cibacron Blue 3GA as a pseudo-affinity ligand for its purification. Therefore, this dye was immobilised onto zirconia–silica adsorbent to prepare a fluidisable adsorbent for the purification of G3PDH. During adsorption, disruptate was applied to the bed until apparent of the adsorbent capacity for G3PDH had been achieved (Figure 17.7). Scouting experiments were conducted to establish efficacy of wet-milling alone for protein release and temperature rises, exploiting a range of biomass concentrations (15–50% ww/v) and feedstock flow rates. For total protein or G3PDH release, the data indicated that total cell disruption was effectively achieved over a wide range of feed rates from 5 to 25 $l \cdot h^{-1}$ (data not shown). A typical mass balance of G3PDH purification is documented in Table 17.1. Specific activities were higher than those previously recorded from wet-milling and fluidised bed adsorption operated as discrete processes over longer time scales.[6] This was encouraging given the low starting activity of yeast, which had been stored at −20 °C for 9 months. The purification factor of this primary recovery was more than 3-fold with a 99% yield of bound activity.

However, Figure 17.6 (panel B) depicts a revised process of product release and primary purification of L-asparaginase. A cation exchanger, CM Hyper D LS (a prototype material from Biosepra/Life Technology), was used as a medium in fluidised bed adsorption. A wash volume of five settled volumes was generally sufficient to reduce the concentration of contaminating proteins by more than 90%. Step elution resulted in sharp peak of enzyme, which could be collected in about two to three settled bed volumes (Figure 17.8). SDS–PAGE electrophoresis identified and purified the protein. A comparison of the purity of samples collected from key stages of conventional commercial process and the integrated

TABLE 17.1. *Mass balance of G3PDH recovery from baker's yeast in direct process integration*

Stage	Volume (ml)	Total activity (IU)	Total protein (mg)	Specific activity (IU/mg)	Purification factor	Bound yield (%)
Feedstock	1000	150000	12300	12.19	1	—
Flow through	1000	34400	4800	—	—	—
Washing	4000	20000	3620	—	—	—
Elution	700	94920	2240	42.37	3.48	99.2

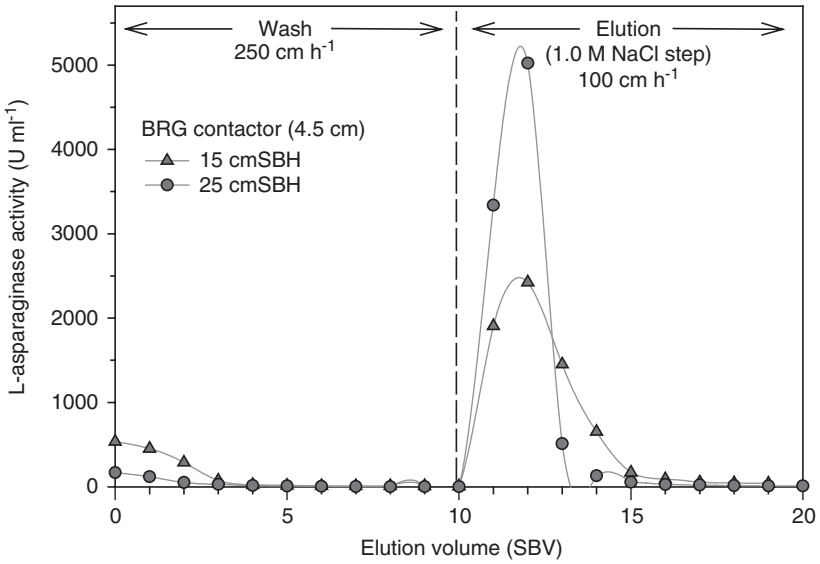

FIG. 17.8. Elution of L-asparaginase from CM HyperD LS in fluidised beds. The beds were washed with five settled bed volumes (SBVs) of buffer A at the loading flow velocity (BRG contactor 250 cm/h). Elution was achieved in fluidised bed mode at a linear flow velocity of 100 cm/h by a step of 1.0 M NaCl in buffer A.

cell disruption/fluidised bed adsorption is depicted in Figure 17.9. Fluidised bed eluate (lanes 2 and 6) appear to be more pure than the equivalent interim product of the current purification process (lanes 7 and 8) which applied CM cellulose in fixed bed. Eluates from fluidised bed adsorption show a strongly stained band of a low molecular weight contaminant (less than 14.4 kDa) which is either absent or not pronounced in the CM cellulose eluate. Further processing of the fluidised bed adsorption eluate (lane 2) revealed that a diafiltration step (lane 3) and another adsorption step confirmed its separation from the product (lane 4).

17.11.4 Conclusion

Experiments investigated the integration of cell disruption by bead milling and product capture by fluidised bed adsorption. By using fluidised bed adsorption, the clarification of the broth would be incorporated with the capture of the product which would result in a considerably

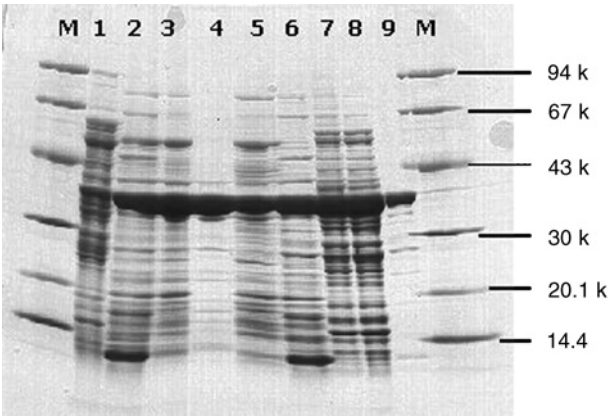

FIG. 17.9. Purity comparison (SDS–PAGE) of the conventional purification process and integrated cell disruption/fluidised bed adsorption.The numbers given in the flow sheet indicate the origin of samples and correspond to their respective lane numbers. Lanes: M, low molecular weight markers; 1, *Erwinia* disruptate, 15% biomass ww/v; 2, eluate CM HyperD LS, fluidised bed; 3, desalted eluate (after dia/ultrafiltration, 30 K MWCO membrane); 4, flow-through, DEAE fixed bed; 5, elution, DEAE fixed bed; 6, eluate CM HyperD LS; 7, CM cellulose eluate; 8, CM cellulose eluate, final; 9, final commercial product.

shortened overall process time. Here, the feasibility of the concept of performing cell disruption and product capture simultaneously was demonstrated for the purification of the G3PDH from *Saccharomyces cerevisiae* and L-asparaginase from *E. chrysanthemi.* From a stage comparison of conventional purification routes of the respective enzymes with the integrated approach, it is evident that there is a considerable reduction in the number of consecutive unit operations in line with operating time-frames and concomitant product losses (in particular due to the elimination of disruptate accumulation and discrete solid–liquid separation steps). Because proteins are generally stabilised when adsorbed onto a solid support, it is advantageous to place an adsorptive step as far upstream as possible. It has been demonstrated earlier that fluidised bed adsorption is a scaleable operation. In the same way, bead mills are commercially available from laboratory to industrial scale. Thus, integrated bead milling and fluidised bed adsorption is a scalable and generic approach to the efficient recovery of intracellular proteins.

17.11.5 Acknowledgement

We are grateful to Professor Andrew. Lyddiatt, Dr Horst Bierau and the University of Birmingham, UK, for various aspects of this collaborative work.

REFERENCES

1. Chase, H.A. and Draeger, N.M., *J. Chromatogr*. **597**, 129 (1992).
2. Hjorth, R., *Trends Biotechnol*. **15**, 230 (1997).

3. Thommes, J., Halfar, M., Lenz, S. and Kula, M.-R., *Biotechnol. Bioengng* **45**, 205 (1995).
4. Kaufmann, M., Unstable proteins: how to subject them to chromatographic separations for purification procedures. *J. Chromatogr. B* **699**, 347 (1997).
5. Jahanshahi M., Sun, Y., Santos, E., Pacek, A., Teixera, F.T., Nienow, A. and Lyddiatt, A., *Biotechnol. Bioengng J*. **80**, 201 (2002).
6. Zhang, Z. and Lyddiatt, A., *J. Chem. Technol. Biotechnol*. **74**, 270 (1999).

Appendix

Constants and conversion factors

Power	W	cal/s	kcal/h	Btu/s	Btu/h	lb_f·ft/s	hp
1 W	1	0.239	0.8604	9.478×10^{-4}	3.412	0.7376	1.341×10^{-3}
1 cal/s	4.18	1	3.6	3.966×10^{-3}	14.276	3.086	5.611×10^{-3}
1 kcal/h	1.1622	0.2778	1	1.102×10^{-3}	3.966	0.857	1.559×10^{-3}
1 Btu/s	1055	252	907.78	1	3600	778	1.415
1 Btu/h	0.293	0.07	0.252	2.78×10^{-4}	1	0.216	3.93×10^{-4}
1 lb_f·ft/s	1.356	0.324	1,167	1.285×10^{-3}	4.63	1	1.818×10^{-3}
1 hp	746	178.2	642	0.707	2540	550	1

Energy	J	cal	Btu	lb_f·ft	Kw·h	hp·h	erg
1 J	1	0.239	9.478×10^{-4}	0.738	2.778×10^{-7}	3.725×10^{-7}	1×10^{7}
1 cal	4.184	1	3.966×10^{-3}	3.086	1.162×10^{-4}	1.559×10^{-6}	4.18×10^{7}
1 Btu	1055	252	1	778	2.93×10^{-4}	3.93×10^{-4}	1.055×10^{10}
1 lb_f·ft	1.356	0.324	1.285×10^{-3}	1	3.766×10^{-7}	5.05×10^{-7}	1.356×10^{7}
1 kw·h	3.6×10^{6}	8.6×10^{5}	3412	2.655×10^{6}	1	1.341	3.6×10^{13}
1 hp·h	2.68×10^{6}	6.42×10^{6}	2.54×10^{3}	1.98×10^{6}	0.7457	1	2.6845×10^{13}
1 erg	1×10^{-7}	2.39×10^{-8}	9.478×10^{-11}	7.376×10^{-8}	2540	3.72×10^{-4}	1

Physical constants and conversion factors

Ideal gas law constant, R	8.314 J·mol^{-1}·K
	1.987 cal·mol^{-1}·K
	82.058 cm^3·atm·mol^{-1}·K

Given a quantity	Multiply by	To get quantity
US gallons	3.785	Litres
Cubic feet	28.316	Litres
Metres	39.37	Inches
Kilograms	2.2046	Pounds
Ponds	453.59	Grams
Poise	0.1	$g \cdot cm^{-1} \cdot s^{-1}$
Centipoise	0.01	poise
Centipoise	0.001	$kg \cdot m^{-1} \cdot s^{-1}$
Centipoise	2.42	$lb \cdot ft^{-1} \cdot h^{-1}$

Index

This page intentionally left blank